

Yapeng Fang  
Hongbin Zhang  
Katsuyoshi Nishinari *Editors*

# Food Hydrocolloids

Functionalities and Applications

 Springer

# Food Hydrocolloids

Yapeng Fang • Hongbin Zhang •  
Katsuyoshi Nishinari

Editors

# Food Hydrocolloids

Functionalities and Applications

 Springer

*Editors*

Yapeng Fang  
School of Agriculture and Biology  
Shanghai Jiao Tong University  
Shanghai, China

Hongbin Zhang  
School of Chemistry and Chemical Engineering  
Shanghai Jiao Tong University  
Shanghai, China

Katsuyoshi Nishinari  
School of Food and Biological  
Engineering  
Hubei University of Technology  
Wuhan, China

ISBN 978-981-16-0319-8      ISBN 978-981-16-0320-4 (eBook)  
<https://doi.org/10.1007/978-981-16-0320-4>

© Springer Nature Singapore Pte Ltd. 2021

This work is subject to copyright. All rights are reserved by the Publisher, whether the whole or part of the material is concerned, specifically the rights of translation, reprinting, reuse of illustrations, recitation, broadcasting, reproduction on microfilms or in any other physical way, and transmission or information storage and retrieval, electronic adaptation, computer software, or by similar or dissimilar methodology now known or hereafter developed.

The use of general descriptive names, registered names, trademarks, service marks, etc. in this publication does not imply, even in the absence of a specific statement, that such names are exempt from the relevant protective laws and regulations and therefore free for general use.

The publisher, the authors, and the editors are safe to assume that the advice and information in this book are believed to be true and accurate at the date of publication. Neither the publisher nor the authors or the editors give a warranty, expressed or implied, with respect to the material contained herein or for any errors or omissions that may have been made. The publisher remains neutral with regard to jurisdictional claims in published maps and institutional affiliations.

This Springer imprint is published by the registered company Springer Nature Singapore Pte Ltd.  
The registered company address is: 152 Beach Road, #21-01/04 Gateway East, Singapore 189721, Singapore



*We would like to dedicate this book to Professor Glyn Owen Phillips, who passed away in July 2020. He has been the Founding Executive Principal of North East Wales Institute (presently, the Glyndwr University Wrexham), the Founding Editor of the journal Food Hydrocolloids, and the leading organizer of the Gums and Stabilisers Conference for the Food Industry and the International Hydrocolloids Conference. He established an international network of scientific communication and collaboration based on two Hydrocolloids Research Centres, one in Wrexham and the other in Wuhan, bearing his name. He was a man of fidelity and a friend and guide with paternal affection. It was a pity that the meeting to celebrate his 90th birthday planned at St Tropez in 2017 was cancelled, but instead a special issue of Food Hydrocolloids was published. His influence on many scientists was profound and worldwide and will be greatly missed.*

# Preface

Food hydrocolloids encompass a wide range of hydrophilic biopolymers such as proteins, polysaccharides and their derivatives. They are indispensable for the formulation and processing of our daily food products, e.g., drinks, jams, dressings, cakes, noodles, hams and more complex functional foods. The importance of hydrocolloids to the food industry, in our view, has not been fully recognized and explored. Albeit often used as minor components in foods, hydrocolloids always perform crucial functions. They not only confer desired structure, stability and palatability to food products, but also provide with bioactivity and health benefit that the consumer persistently pursues for. There is a big gap to be connected between the structures stabilized by food hydrocolloids and the resulting functions, particularly, the nutritional and health outcomes. The scientific concept of the “food hydrocolloids” has been consequently expanded from the hydrophilic materials themselves to the various colloidal structures and functions formed thereby.

In this context, we think it necessary to introduce hydrocolloid knowledge in a more systematic framework by categorizing into different functionalities and highlighting the food-related applications. This book aims to be a textbook or reference tool for undergraduate/graduate students or professionals working in the field of food science and technology or biopolymer science. It is our purpose that it can benefit to bridge the divide between fundamental research and industrial applications. We also hope that it can add to the excellent book *Handbook of Hydrocolloids* edited by Glyn O. Phillips and Peter A. Williams, which has received great welcome and will be even more popular with its upcoming third edition. The handbook however differs in organizing knowledge according to each individual hydrocolloid and aiming to be a technological reference.

This book is the result of long friendship and close collaborations between the three editors. Y.F. and H.Z. both had stayed in the laboratory of K. N. at Osaka City University, where Y. F. completed his PhD study and H. Z. conducted his postdoctoral research under the kind supervision of K. N. A stronger international collaboration network on food hydrocolloids has been set up in China since K. N. joined the Hubei University of Technology Wuhan in 2013 as a Specially Appointed

Professor. The book is an initiative of the research network and involves many excellent contributors who are young yet active and creative in the frontline of hydrocolloid research. Sincere thanks are due to all the chapter contributors whose efforts make this book a very worthwhile undertaking.

Shanghai, China  
Shanghai, China  
Wuhan, China

Yapeng Fang  
Hongbin Zhang  
Katsuyoshi Nishinari

# Contents

<b>1</b>	<b>Introduction to Food Hydrocolloids</b> . . . . .	<b>1</b>
	Wei Lu, Xiaobei Li, and Yapeng Fang	
<b>2</b>	<b>Solution Properties</b> . . . . .	<b>29</b>
	Hongbin Zhang and Ruiqi Li	
<b>3</b>	<b>Rheological and Thickening Properties</b> . . . . .	<b>75</b>
	Katsuyoshi Nishinari	
<b>4</b>	<b>Gelling Properties</b> . . . . .	<b>119</b>
	Katsuyoshi Nishinari	
<b>5</b>	<b>Emulsifying Properties</b> . . . . .	<b>171</b>
	Hui Zhang and Lingli Deng	
<b>6</b>	<b>Liquid Foaming Properties</b> . . . . .	<b>207</b>
	Yongguang Guan	
<b>7</b>	<b>Tribological and Sensory Properties</b> . . . . .	<b>245</b>
	Sandip Panda and Jianshe Chen	
<b>8</b>	<b>Coating and Film-Forming Properties</b> . . . . .	<b>267</b>
	Qian Xiao	
<b>9</b>	<b>Self-assembling Properties</b> . . . . .	<b>307</b>
	Huiyan Zeng	
<b>10</b>	<b>Flavour Delivery</b> . . . . .	<b>335</b>
	Matthias Schultz	
<b>11</b>	<b>Encapsulation and Targeted Release</b> . . . . .	<b>369</b>
	Bin Liu, Lulu Jiao, Jingjing Chai, Cheng Bao, Ping Jiang, and Yuan Li	
<b>12</b>	<b>Replacement of Fat or Starch</b> . . . . .	<b>409</b>
	Cuixia Sun and Yapeng Fang	

**13 Structuring for Elderly Foods** . . . . . 445  
Makoto Nakauma and Takahiro Funami

**14 Bioactivities** . . . . . 473  
Kang Liu, Xue-Ying Li, Jian-Ping Luo, and Xue-Qiang Zha

**15 Dietary Fibers: Structural Aspects and Nutritional Implications** . . . 505  
Bin Zhang, Shaokang Wang, Santad Wichienchot, Qiang Huang,  
and Sushil Dhital

## About the Editors

**Yapeng Fang** is a Distinguished Professor at the School of Agriculture and Biology, Shanghai Jiao Tong University. He holds a bachelor and master degree in polymer physics and chemistry from Shanghai Jiao Tong University, and a PhD degree in Food Science and Health from Osaka City University. His research interest is focused on the structure-function relationship of hydrocolloids, and the design of future foods based on hydrocolloid technologies. He currently serves as an Associate Editor of the journal *Food Hydrocolloids*.

**Hongbin Zhang** is a full professor with tenure at the Department of Polymer Science and Engineering, School of Chemistry and Chemical Engineering, Shanghai Jiao Tong University (SJTU). He holds a master degree in applied chemistry and a PhD degree in polymer materials from SJTU. His research interest is focused on the interdisciplinary of polymer physicochemistry, rheology, colloid chemistry, and food science, involving polysaccharide, solution, hydrogel and emulsification.

**Katsuyoshi Nishinari** is currently a specially appointed professor at Glyn O. Phillips Hydrocolloids Research Centre, Hubei University of Technology. He worked for National Food Research Institute and then Osaka City University (OCU), and now is an emeritus professor of OCU. He is also visiting professors at Glyndwr, ESPCI, SJTU, Osaka, Keio, and other universities. His research interest includes food hydrocolloids, and rheology applied in food (oral) processing. He currently serves as the editors of several colloids and rheology related journals.

# Chapter 1

## Introduction to Food Hydrocolloids



Wei Lu, Xiaobei Li, and Yapeng Fang

**Abstract** This introductory chapter provides an overview of the definition, classification, structure, market, regulation, and functional aspects of food hydrocolloids. The narrow and wide definition of hydrocolloids is compared. A detailed classification based on the source of hydrocolloids is summarized and the molecular structure of typical hydrocolloids, such as polysaccharides and proteins, is introduced. Food hydrocolloids show diverse potentials in the application of food, nutrition, and biomedicine industries. They can act as thickening agents, and form gels with controlled physical properties and functionalities. They can also be employed as stabilizers for various dispersions, and delivery carriers for bioactive ingredients. Besides, many hydrocolloids, e.g., whey proteins, or dietary fibers, possess potential health benefits and can provide basic and essential nutrients for maintaining human life activity. Furthermore, food hydrocolloids can be tailored into functional materials with advanced applications in food packaging, biomedical materials, bionanomaterials, polymer electrolytes, synthesis of inorganic nanoparticles, and removal of organic pollutants. The market and regulatory aspects of food hydrocolloids are also briefly reviewed.

**Keywords** Hydrocolloids · Definition · Classification · Structure · Functionality · Regulation · Safety

---

W. Lu · Y. Fang (✉)

School of Agriculture and Biology, Shanghai Jiao Tong University, Shanghai, China

e-mail: [ypfang@sjtu.edu.cn](mailto:ypfang@sjtu.edu.cn)

X. Li

DuPont Nutrition and Health, Shanghai, China

## 1 History of the Term

The colloidal gels were first investigated by Thomas Graham (1861), who is widely regarded as the founder of colloid chemistry. He proposed a definition of substances based on their diffusive behaviors. According to his definition, colloids are slowly diffusing substances with very high molecular weight and specific structure. Between these colloidal substances, there exist “feeble forces” that holds them together in a solution. Graham also defined the colloidal state as a dynamical state of matter which may change into a crystalloidal status.

About half a century behind the foundation of colloid chemistry, Freundlich, Ostwald, and Weimarn proposed a new definition of colloids (Mokrushin 1962), which is different from that given by Graham. They defined colloids as any substances which are in the dispersed colloidal state. The molecular weight has no relation to the colloidal state by this definition. For example, the fine suspensions of gold, silver chloride, or sulfur can also be classified as colloidal solutions according to this definition. The cognition process on the rationality and limitation of these two definitions may be also considered as the development process of modern colloid chemistry.

It was reported that the term “hydrocolloid” derived from the Greek *hydro* “water” and *Kolla* “glue” (Wüstenberg 2015). First known use of *hydrocolloid* can be dated back to 1916, which was used to describe a substance that yields a gel with water. Hydrocolloids are now defined as various long-chain polymers which can form viscous dispersions and/or gels when dispersed in water. These polymers can be found in extracts from seaweeds, exudates from trees, flours from grains, products from fermentations, and many other natural products. They contain many hydroxyl groups, which significantly increase their hydrophilicity making them hydrophilic compounds. Furthermore, they can create a dispersion, which is between a true solution and a suspension and show colloidal properties. In consideration of these two properties, they are termed as “hydrophilic colloids” or “hydrocolloids.”

## 2 Definition

A narrow definition of hydrocolloids refers to a series of polysaccharides and proteins that are widely used in different industrial sectors to perform various functions including thickening and gelling agents, stabilizers of food dispersions (e.g., foams or emulsions), encapsulation and delivery carriers of functional ingredients and their controlled release (Phillips and Williams 2009). Besides, all soluble starches, which chemically belong to the polysaccharide family, can also be considered as a class of hydrocolloids with many potential applications in the food sector.

Hydrocolloids can also be broadly defined as a variety of biopolymers, biopolymer-stabilized dispersions, and biopolymer-based gels and particles, such as polysaccharides, proteins, lipids, protein/polysaccharide aqueous dispersions,



emulsions (including Pickering emulsions), foams, bubbles, protein/polysaccharide-based hydrogels and micro/nanoparticles, solid lipid nanoparticles, liposome, and oleogels.

### 3 Classification

Hydrocolloids are widely used in a variety of industries to perform different functions as described above (Williams and Phillips 2009; Lin et al. 2012). The frequently used hydrocolloids and their origins are given in Table 1.1.

Some of the plant hydrocolloids come from trees and tree gum exudates (e.g., cellulose, gum Arabic, gum karaya, gum ghatti, gum tragacanth) while some of them come from plant (cellulose pectin, and starch), seeds (locust bean gum, guar gum, tara gum, tamarind gum, soybean proteins, zein, rice protein, and gluten), and tubers (konjac glucomannan). Algal hydrocolloids are mainly derived from red seaweeds (agar, carrageenan, and furcelleran) and brown seaweeds (alginate).

Microbial hydrocolloids can be produced from simple sugars (glucose or sucrose) or starch using a microbial fermentation process. Species of bacteria and fungus that have been used to produce these hydrocolloids by fermentation include *Xanthomonas campestris* (xanthan gum), *Leuconostoc mesenteroides* and *Streptococcus mutans* (dextran), *Agrobacterium* (curdlan), *Athelia rolfsii* (scleroglucan), *Sphingomonas elodea* (gellan), and *Aureobasidium pullulans* (pullulan).

Animal-sourced hydrocolloids mainly are proteins coming from collagen taken from bones, skin, and tendons of animals, and skins of fish (gelatin), milk (caseinate and whey proteins), eggs (egg white proteins), and chitin shells of shrimps and other Crustaceans (chitosan).

**Table 1.1** Source of frequently used hydrocolloids

Source	Hydrocolloids
Plant	<p><i>Polysaccharides</i></p> <p>Starches, pectins, cellulose, larch gum, guar gum, locust bean gum, tara gum, tamarind seed gum, acacia gum/gum, Arabic gum, tragacanth, karaya gum, ghatti gum, inulin, and konjac glucomannan</p> <p><i>Proteins</i></p> <p>Soy proteins, zein, rice proteins, and gluten (wheat protein)</p>
Algal	Alginate, carrageenan, agar, and furcelleran
Animal	Gelatin, caseinate, whey proteins, egg white proteins, glycogen, and chitosan
Microbial	Dextran, xanthan, scleroglucan, curdlan, pullulan, and gellan
Modified	Modified starches, propylene glycol alginate, microcrystalline cellulose (MCC), amidated pectin, methylcellulose (MC), ethylcellulose (EC), hydroxypropylmethylcellulose (HPMC), hydroxypropyl cellulose (HPC), and carboxymethylcellulose (CMC)

## 4 Structures

### 4.1 Polysaccharides

The primary molecular chain structure of polysaccharides is monosaccharide units (Table 1.2) bound together by glycosidic bond, which is formed between the hemiacetal or hemiketal group of a monosaccharide and the hydroxyl group of neighboring monosaccharide, known as O-glycosidic bonds. Besides, S-, N-, or C-glycosidic bonds also exist, where the oxygen of the glycosidic bond is replaced with sulfur, nitrogen, or carbon, respectively. In addition,  $\alpha$ - or  $\beta$ -glycosidic bonds can be distinguished by the relative stereochemistry (R or S) of the groups of C5 and C1 in the pyranose ring. If groups connected to these two carbons have the same stereochemistry, the glycosidic bond is defined as  $\alpha$  type, whereas a  $\beta$ -glycosidic bond is formed when the groups show different stereochemistry.

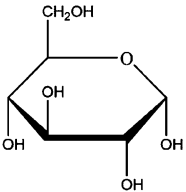
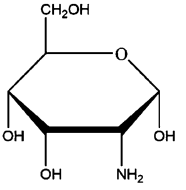
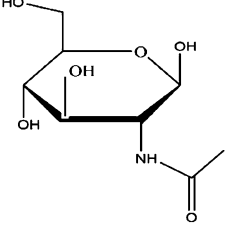
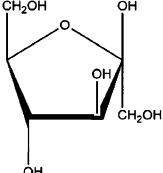
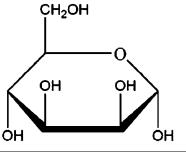
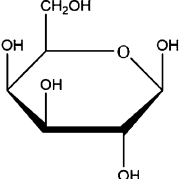
Therefore, glycosidic bonds in the backbone of polysaccharides mainly include  $\alpha$ -1,4 (e.g., amylose, glycogen, amylopectin),  $\beta$ -1,4 (e.g., pectin, alginate, cellulose, guar gum, xanthan, konjac glucomannan, xylan),  $\alpha$ -1,6 (e.g., dextran),  $\beta$ -1,3 (e.g., Arabic gum, laminarin), and  $\beta$ -1,2 (e.g., inulin) glycosidic bonds (Fig. 1.1). The backbone of some polysaccharides also shows a mixture of the different glycosidic bonds. For example, carrageenan is composed of repeating sulfated and/or non-sulfated galactose and 3,6-anhydrogalactose units. The units are linked by alternating  $\alpha$ -1,3 and  $\beta$ -1,4 glycosidic bonds. A similar chain structure can be observed for gellan gum, which is made up of repeating tetra-saccharides consisting of two glucose and one of each residue of rhamnose and glucuronic acid.

Polysaccharides composed of the same monosaccharide are called homopolysaccharides such as starches and glucan while those composed of more than one type of monosaccharides are called heteropolysaccharides. Some polysaccharides show a segmented chain structure. Alginic acid (Fig. 1.2), for example, is a linear biopolymer composed of  $\beta$ -1,4 linked D-mannuronate (M) and L-guluronate (G) residues. G and M residues are covalently linked together in different sequences or blocks. They can appear in consecutive M-residues (M-blocks), consecutive G-residues (G-blocks), or alternating M and G-residues (MG-blocks).

Besides, several polysaccharides show a crystalline zone in their chain structure, e.g., cellulose, or starch. The crystalline fractions of these polysaccharides with different structures and properties can be collected by physical or chemical processing such as microcrystalline cellulose (MCC), microfibrillated cellulose (MFC), and nanocrystalline cellulose (NCC). Furthermore, the chemical structure of natural polysaccharide is modified to improve its water solubility or functionalities. Examples include modified starch, propylene glycol alginate, amidated pectin, methylcellulose, ethylcellulose, or carboxymethylcellulose.

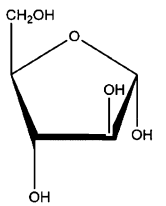
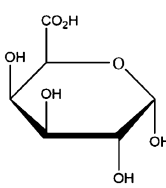
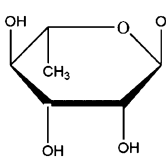
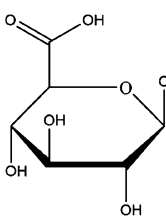
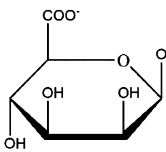
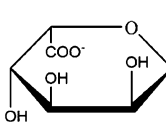
In direct analogy with proteins, polysaccharides can also have several levels of structures. The primary structure of a polysaccharide is defined as the sequence of monosaccharides. The intramolecular single helices with different persistence lengths are considered as secondary structures of a polysaccharide while tertiary

**Table 1.2** Examples of common monosaccharides and corresponding polysaccharides

Monosaccharide	Molecular structure	Representative polysaccharides
Glucose		Starch, cellulose, $\beta$ -glucan, konjac glucomannan, gellan, dextran, pullulan, xanthan, xyloglucan
Glucosamine		Chitosan
Acetyl-glucose		Chitosan Poly-N-acetyl- $\beta$ -D-glucosamine
Fructose		Inulin
Mannose		Konjac glucomannan, guar gum, tara gum, fenugreek gum, locust bean gum, xanthan
Galactose		Arabic gum, guar gum, carrageenan, agar, tara gum, fenugreek gum, acacia gum, karaya gum, xyloglucan, locust bean gum

(continued)

**Table 1.2** (continued)

Monosaccharide	Molecular structure	Representative polysaccharides
Arabinose		Arabic gum
Galacturonic acid		Pectin
Rhamnose		Gellan
Glucuronic acid		Gellan, xanthan
Mannuronate		Alginate
Guluronate		Alginate

structures always exhibit as tight or loosely supercoiled helices. Tightly or loosely intertwined chains with tertiary structures form the intermolecular quaternary structures of polysaccharides (Fig. 1.3).

Diener et al (2019) demonstrated several structural levels using carrageenan as model polysaccharides. In the presence of potassium, a disorder to order the transition from random coil to single helix (secondary structure) was first observed,

	Cellulose	Starch		Glycogen
		Amylose	Amylopectin	
Source	Plant	Plant	Plant	Animal
Monose	$\beta$ -glucose	$\alpha$ -glucose	$\alpha$ -glucose	$\alpha$ -glucose
Glycosidic bonds	1-4	1-4	1-4 and 1-6	1-4 and 1-6
Diagram				
Shape				

Fig. 1.1 Examples of molecular chain structure of polysaccharides

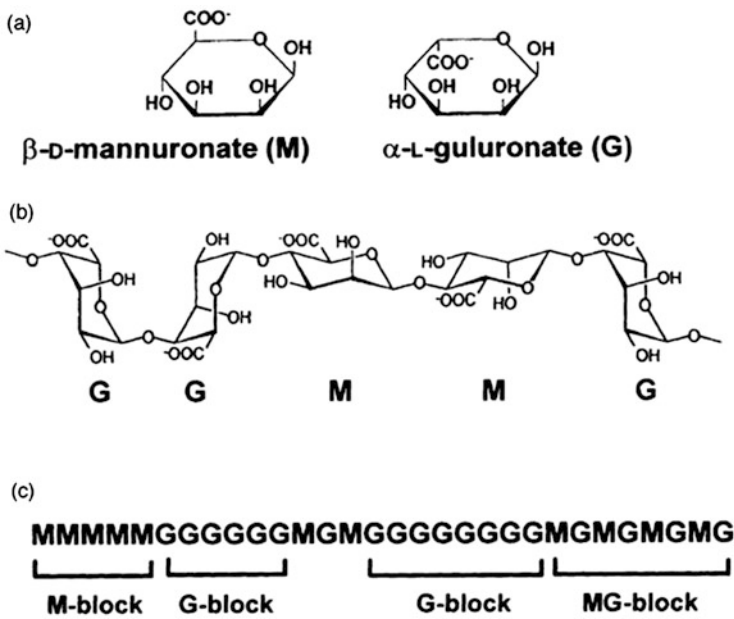
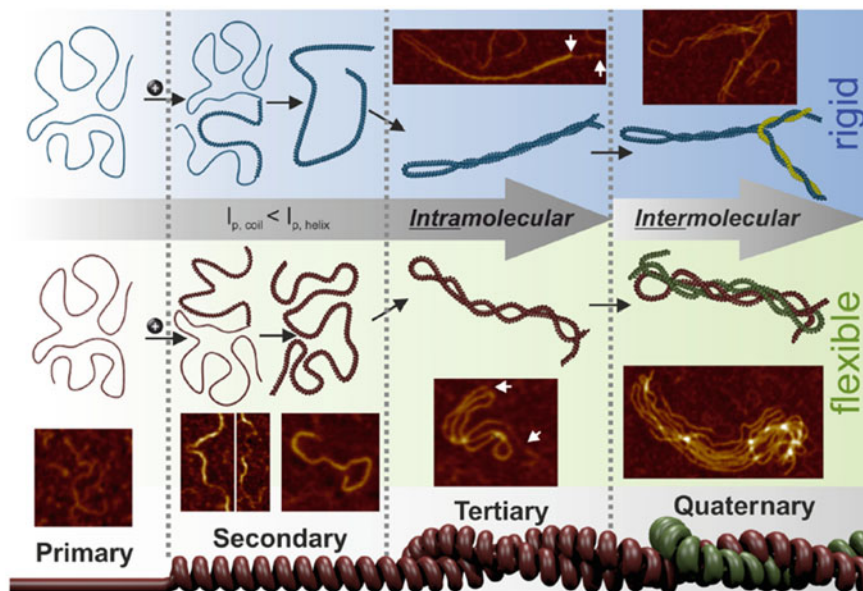


Fig. 1.2 Structural characteristics of alginates: (a) monosaccharide composition (b) chain conformation, (c) block distribution (Draget and Taylor 2011). The permission for reproduction of the figure was obtained from Elsevier



**Fig. 1.3** Schematic elucidation of the multilevel structure of polysaccharide chains: An example from carrageenan (Diener et al. 2019). The permission for reproduction of the figure was obtained from ACS Publications

followed by intrachain supercoiling events (tertiary structure) and macroscopic anisotropic domains, which are part of a network (quaternary structure) with tunable elasticity up to  $\sim 10^3$  Pa. Loosely intertwined helices were also observed as tertiary structure.

## 4.2 Proteins

Proteins are biopolymers comprised of one or more chains of amino acid residues. The amino acid residues in protein chains are linked together by peptide bonds, which is an amide-type of the covalent chemical bond linking C1 of one  $\alpha$ -amino acid and N2 of another adjacent amino acid (Fig. 1.4).

Protein structure mainly refers to four distinct aspects (Finkelstein and Ptitsyn 2016): (1) primary structure, the amino acid sequence; (2) secondary structure, repeating structures formed by hydrogen bonds, mainly including  $\alpha$ -helix,  $\beta$ -sheet, and  $\beta$ -turns; (3) tertiary structure, the spatial shape of a polypeptide chain or the spatial arrangement of the secondary structures. Tertiary structure is mainly stabilized by hydrophobic interactions, but also involving disulfide bonds, hydrogen bonds, salt bridges, or post-translational modifications; and (4) quaternary structures,

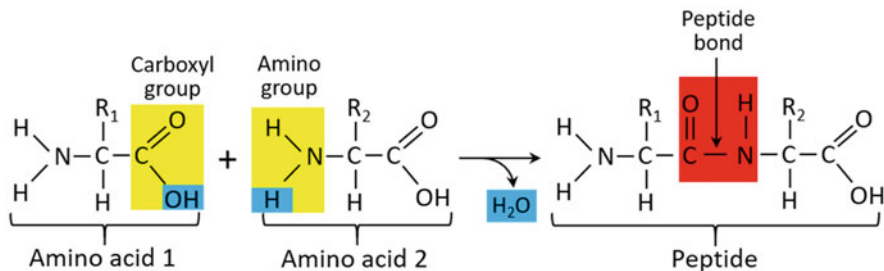


**Fig. 1.4** Diagram of the formation and structure of peptide bond

the structure formed by several polypeptide chains (technically termed as protein subunits) (Robert et al. 2009).

Proteins are not completely rigid molecules. Proteins may transform between the above-mentioned structures while they perform their functions. Generally, the tertiary or quaternary structure of proteins is regarded as their conformation, which is defined as the spatial arrangements of atoms. The conversion between different conformations generally does not refer to the breakage or formation of covalent bonds. For example, the structure of protein molecules can be altered by thermal vibration (thermal denaturation) or the collision with other molecules (Christopher et al. 2013). Thermal denaturation is also one of the mechanisms that induce the gelling of protein molecules in solutions. Conformation is different from another relevant term named configuration, which mainly refers to the fixed three-dimensional relationship of the atoms in a molecule, defined by the bonds between them. The change of configuration of proteins may involve the break or formation of covalent bonds, e.g., the change of primary and/or secondary structure of proteins (Finkelstein and Ptitsyn 2016).

## 5 Marketing

The lifestyle changes, the increasing awareness of the association between diet and health, and emerging new processing technologies contribute to a rapid increase in the consumption of food hydrocolloids-based ready-made, functional, and healthy food products, which consequently leads to an increase in the market demand of hydrocolloids. The market demand for hydrocolloids is estimated at \$ 8.8 billion in 2018 and is predicted to grow at a compound annual growth rate (CAGR) of 5.3% from 2018 to 2023, to reach \$ 11.4 billion by 2023 (Singh 2019). North American is predicted to be the fastest-growing market in these 5 years (Fig. 1.5).

The rising demands for convenient food products in the countries of the Asia Pacific, South America, and the Middle East & African regions promote the development of the processed food industry worldwide, which accordingly leads to a growth in the hydrocolloids market. In addition, manufacturers always focus on the

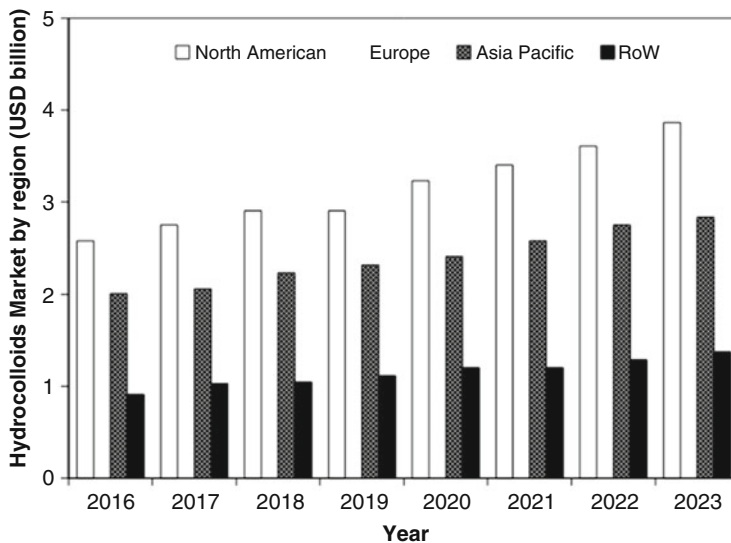


**Fig. 1.5** Hydrocolloids market by region. RoW indicates the rest of the world (Singh 2019). The data from 2019 to 2023 is predicted based on the estimated growth rate

product innovation and multifunctionality of hydrocolloids with the objective of offering high-quality hydrocolloids for the end-users. Thus, manufactures perform various research and development (R&D) activities and these activities accordingly contribute to the rapid growth of the hydrocolloids market. One of the major factors that restrict the development of the hydrocolloids market is the international regulations and quality standards of food additives (e.g., stabilizers). The fluctuations in the price of raw materials for producing hydrocolloids can also affect the market.

In 2018, the thickeners sector, animal sector, food & beverage and gelatin sector are estimated to account for the largest share based on functions, sources, applications, and types of hydrocolloids, respectively. Take gelatin as an example, gelatin has wide applications in food products such as desserts, candies, ice creams, and marshmallows. In Europe, gelatin is classified as food and is not subjected to food additive legislation, which creates a lucrative opportunity for manufacturers in the next few years.

## 6 Legislation and Safety

### 6.1 Background

Food hydrocolloids, such as pectin, agar, starch, and gelatin, have been used for centuries, and consumers are quite familiar with these hydrocolloids. Many hydrocolloids in use today were developed long before regulatory approvals, and their use



level and use in specific applications were restricted. For instance, carrageenan, agar, or alginate extracted from seaweeds are eaten as basic foods. These edible polymers from seaweeds are thus considered safe for use in food products. This principle of “generally recognized as safe” (GRAS) is still in use today but under a more rigorous review. For example, carrageenan can be classified into  $\lambda$ -,  $\kappa$ -, and  $\iota$ -, carrageenan. Some of the modified carrageenan, e.g., semi-refined version, found its way of being used as food texturizing agent only since the 1980s and 1990s while refined carrageenan has been used for more than 60 years (Imeson 2010). However, intentional acid-hydrolyzed carrageenan, like poligeenan, cannot form gels and even have been proved to cause *in vivo* gastrointestinal ulceration and tumors via food, water, or oral route. Poligeenan has been also reported to show immune system toxicity and potentially suppress the immune response (McKim et al. 2018). These results suggested that degraded fractions of nature hydrocolloids which can be safely used as food additives need strict safety evaluation before being used in the food industry.

## 6.2 Legislation

Regulatory approval of a food ingredient is necessary because the additives would have no function or market without approval by the governments. Food hydrocolloids are generally regulated either as a food additive or as a food ingredient. Except for gelatin, most of the food hydrocolloids are currently regulated as food additives.

Regulatory authorities strictly control the approval of food additives (Imeson 2010). Chemical modifications are generally not allowed except for cellulose derivatives, starches, and propylene glycol alginate. Physical and enzymatic modifications are allowed, e.g., physically modified pectin (Slendid™, CP Kelco Division of JM Huber). Some new hydrocolloids are brought to the market under the “generally recognized as safe” principle, such as konjac, tara gum, and pullulan. Gellan gum is the last hydrocolloid that completely goes through a food additive petition in the global market. It took many years and cost tens of millions of dollars to get the approval of gellan gum. The total profit earned by gellan gum over the next 20 years after its approval is still lower than the cost for its approval. These probably suggest that it is almost impossible for a new hydrocolloid to accomplish a full approval process in the global market in the foreseeable future. Cassia gum has recently been approved in France (August 2008) and it is expected to be approved in the EU market soon.

### 6.2.1 International System

The Food and Agriculture Organization (FAO) and the World Health Organization (WHO) established the Codex Alimentarius Commission (CAC) in 1962. CAC is an intergovernmental organization consisting of delegations from FAO and WHO

member countries that take part in developing the food standards. Another organization, the Joint FAO/WHO Expert Committee on Food Additives (JECFA) was established before the CAC in 1956 (Magnuson et al. 2013), which is considered as the oldest and most active body in doing a similar job.

The main task of CAC is to address the safety and nutritional quality of food products and to develop international standards for promoting trade of foods, such as setting standards for approved food additives, determining its limits of addition and safety indexes (e.g., limits for contaminants and toxins, and residue limits for pesticides), and establishing hygiene and technological function practice codes. These standards, guidelines, practice codes, and recommendations constitute the Codex Alimentarius.

### **6.2.2 European System**

European Commission first cleared food hydrocolloids in 1995 based on the Directive 95/2/EU for Food Additives, which is known as the Miscellaneous Additives Directive (MAD). MAD authorized a large number of food hydrocolloids (including alginates, starches, celluloses, and most gums) for their utilization in food products at suitable levels (Phillips and Williams 2009). Since the adoption of the Directive, the Commission proposed several modifications by considering the development of the market. A second modification was made in 1998 and the Member States of the EU were required to put into effect this updated version in 2000. The new regulation in this Directive (98/72/EC) came into force in all EU Member States and it affected many hydrocolloids, mainly including potassium alginate, sodium alginate, konjac, carrageenan, guar, and pectin.

### **6.2.3 US and Japan Systems**

Since the CAC is the final regulation and can provide for worldwide approvals, countries (outside the EU) are free to adopt their standards. In United States (USA), the Food and Nutrition Board of the Institute of Medicine (funded by the United States Food and Drug Administration, FDA) published the Food Chemicals Codex (FCC), and the regulation about hydrocolloids can be found in the Fourth Edition pressed in 1996. Japan also has its own regulation system, including many food additives specific to Japan (Dai and Chau 2017).

### **6.2.4 China Systems**

In China, except for starch, the usage of hydrocolloids in foods is regulated by “National standards for food safety: standards for the use of food additives (GB2760),” which was first established in 2011 (GB2760-2011), and then modified in 2014 (GB2760-2014). It stipulates the type of hydrocolloids that can be used in

China and their levels in the products. Based on GB2760-2014, around 40 hydrocolloids are allowed to be used in the China market. For example, the most widely used hydrocolloids in meat and fish products include carrageenan, xanthan gum, guar gum, agar, gelatin, alginate, locust bean gum, curdlan, and konjac glucomannan. These frequently used hydrocolloids are all naturally derived.

Generally, these edible hydrocolloids are used at a low level, mainly functioning as thickening agents, stabilizers, and gelling agents. Many hydrocolloids can also be considered as dietary fibers, which have many potential health benefits. Thus, a low level of using edible hydrocolloids in food products is always safe or even good for health. However, some manufacturers use a high level of hydrocolloids for specific purposes (cost, stability, etc.), leading to a potential safety issue of the products. In addition, many hydrocolloids can also be used in industrial products, and industrial-grade hydrocolloids are much cheaper than food grade, but potentially contain various harmful ingredients, which can threaten human health. Therefore, it is illegal to use industrial-grade hydrocolloids in food products but it still can happen that some producers illegally add them into foods due to their low cost.

### **6.3 Consumer Concerns**

No matter what the scientific facts are, it is the consumers' approval that decides the market future of a food ingredient, and hydrocolloids are no exception. In terms of perception, a label is very important. A friendly label always can reduce people's perception of too much chemical connotation, and thus feel they are safe. For example, label-friendly carbohydrate gum and vegetable gum are used to describe methylcellulose and hydroxypropylmethylcellulose in the USA, respectively. Another example, carboxymethyl cellulose (CMC) is a very chemical name, whereas cellulose gum, a synonym of CMC, sounds much more acceptable. Therefore, EU authorities allow the use of cellulose gum on the label.

Another main concern is genetic engineering and relevant genetically derived hydrocolloids. For example, seeds, seaweed, or other plants could be genetically modified to yield a higher production of relevant hydrocolloids; kelp could be edited to produce more alginates; the mature time of a carob tree that can produce a commercial scale of bean gum could be significantly shortened as compared with the normal 12–15 years. However, the safety of these genetically derived hydrocolloids is not conclusive, and their application is still constrained by consumer concerns (Imeson 2010).

**Table 1.3** Hydrocolloids commonly used in food applications

Applications		Hydrocolloids
Structuring agents	Thickening agents	Xanthan, methyl cellulose (MC), carboxymethyl cellulose (CMC), guar gum, hydroxypropylmethyl cellulose (HPMC), locust bean gum, konjac glucomannan, tara gum, and xyloglucan
	Gelling agents	Amylose, agar, carrageenan, gellan gum, pectin, alginate, casein, soybean proteins, gelatin, xanthan, MC, HPMC, locust bean gum, konjac glucomannan, xyloglucan, and curdlan
Stabilizers	Emulsifiers	Gum Arabic, modified starch, modified cellulose, crystalline cellulose, pectins, galactomannans, casein/caseinate, whey proteins, and soy proteins
	Foaming agents	Casein, whey proteins, zein, gelatin, pectins, modified cellulose, chitin, and chitosan
Delivery carriers	Nanoparticles, films, fibrils, microcapsules, hydrogels particles	Whey proteins, casein, gelatin, zein/gliadin, agar, carrageenan, alginate, chitosan, guar gum, cellulose, pectin, xanthan gum, and starch
Bioactive ingredients	Dietary fibers, antimicrobial, anti-virus, anti-coagulant, antioxidant, anti-cancer, reducing blood lipids, enhancing the immune system and bone health, anti-cardiovascular disease, lowering blood pressure, losing weight, satiating effect	Resistant starch, cellulose, hemicellulose, guar gum, pectins, $\beta$ -glucans, psyllium; sulfated polysaccharides from marine algae (e.g., sulfated fucoidan, carrageenan, galactans, fucoidan, sulfated rhamnogalactans, laminaran, and alginic acid), and whey proteins
Advanced materials	Food packaging, biomedical materials, scaffolds, biomimetic materials, nano-structured membranes, electrolytes, decontamination materials	Starch, modified cellulose, chitin/chitosan, pectin, gluten, soy proteins, gelatin, zein, crystalline cellulose, and crystalline starch

## 7 Functionality and Application

Hydrocolloids can be functionally used as the thickening and gelling agents, stabilizers for emulsions and foams, and delivery carriers for bioactive components. They can be also tailored into advanced nanomaterials with various specific applications in both food and biomedical industries. Besides, hydrocolloids and their derivate show diverse health benefits and are considered as a class of bioactive ingredients. In this section, these main functionalities of hydrocolloids are summarized (Table 1.3).

## 7.1 Structuring Agents

Hydrocolloids have been used in a variety of food formulas to improve their quality and shelf-life. The two major applications of hydrocolloids are thickening and gelling agents. Regarding the thickening, they have been used in many food systems, such as gravies, soups, sauces, salad dressings, and toppings. In terms of gelling, hydrocolloids can be used in products like jelly, jam, marmalade, low-calorie gels, or restructured foods.

### 7.1.1 Thickening Agents

The process of thickening refers to the entanglement of polymer chains, leading to a significant increase in the viscosity of the system. Thickening occurs above a critical polymer concentration (overlap concentration,  $C^*$ ), which refers to the transition from the “dilute region,” where the polymers can move freely without entanglement in solution, to the “semi-dilute region,” where molecules crowding promotes the overlap of polymer coils and thus leads to the entanglement. Below  $C^*$ , the polymer dispersions exhibit Newtonian behavior whereas shows a non-Newtonian behavior above this concentration (Phillips and Williams 2009).

The viscosity of the polymer solution is significantly affected by the molecular mass of the polymer. The dependency of viscosity on the shear rate increases with the increasing molecular mass. When the molecular mass of the polymer increases, the shear thinning of the polymer dispersion occurs at a lower shear rate value. In addition, the hydrodynamic size of polymers can be obviously influenced by their molecular structures. Linear and stiff molecules always show a larger hydrodynamic size than that with a branched and flexible structure and thus yield a much higher viscosity (Phillips and Williams 2009).

Hydrocolloids that have been applied as thickening agents include starch, gum Arabic or acacia gum, modified starch, xanthan, gum tragacanth, galactomannans, gum karaya, and CMC (Saha and Bhattacharya 2010) (Table 1.4). The thickening effect of hydrocolloids can be influenced by many factors, including the type of hydrocolloids used, concentration, pH, temperature, or the food system in which they are used.

### 7.1.2 Gelling Agents

Gels are a form of matter intermediate between solid and liquid states, showing both elastic (mechanical rigidity) and flow (liquid) properties (Aguilera 1992). A sol (liquid) to gel (solid) transition occurs when gels are formed. Gelation is the process that the polymer chains crosslink to form a three-dimensional (3D) network that entraps water within it (Oakenfull and Glicksman 2009). Food hydrocolloids are widely employed as gelling agents to produce food gels with acceptable properties,

**Table 1.4** Hydrocolloids used as thickeners in foods

Hydrocolloids	Properties	Applications
Xanthan	Highly shear thinning; keeps viscous at high temperature and wide pH ranges	Soups and gravies, ketchup, beverages, toppings, desserts, and fillings
CMC	High viscosity; decreased viscosity by adding electrolytes and at low pH	Gravies, salad dressings, ketchup, and fruit pie fillings
MC and HPMC	Viscosity increases with increasing temperature; viscosity is independent of pH and electrolytes	Cake batters, beverages, salad dressings, and whipped toppings
Gum Arabic	Low viscosity; shear thinning dispersion at low shear rates (<10/s); near Newtonian behavior above the shear rate of 100/s	Soft drinks and fruit juice based beverages
Galactomannans (guar gum, locust bean gum and tara gum)	High viscosity at low shear rate; highly shear thinning; the viscosity is independent of electrolytes; decreased viscosity at very high and very low pH, and high temperatures	Dairy products, i.e., ice cream, ketchup, fruit juices, pudding powder, and cake batter
Konjac glucomannan	Highly viscosity independent of salts; forms thermally irreversible gels in the presence of alkali	Noodles, jelly desserts, surimi, meat products
Xyloglucan	Heat, acid, salt resistant, short texture (non-thread forming)	Sauce for grilled eat, cutlet
Gum tragacanth	Rehydrates fast in cold or hot water to produce highly viscous dispersion, up to 4000 mPas at 1 w/w%	Salad dressing, bakery emulsion, fruit beverage, and sauce

especially the texture properties (Table 1.5). Food gels are 3D network structures of high moisture. Food gels can resist flow under pressure and retain their distinct shape. They are viscoelastic systems with a storage modulus ( $G'$ ) larger than the loss modulus ( $G''$ ) (de-Vries 2004).

Many classifications can be done for gels (See Chap. 4). Gels formed by covalent bonds are called chemical gels, and those formed by secondary bonds such as hydrogen bonds, electrostatic and hydrophobic interactions, and/or van der Waals forces are called physical gels (Djabourov et al. 2013). Gels can be formed by physical (e.g., heat or pressure), chemical (e.g., pH), or biological treatments (e.g., enzymes). For example, milk gels can be formed by acid or by rennet, while KGM gelation is induced by alkali. However, some physically induced gels, for example by heating, can make covalent bonds and thus lead to the formation of chemical gels. The gel formation always depends on several physicochemical factors, including temperature, pressure, ionic strength, pH, presence of enzyme, solvent quality, the concentration of gelling agents, selection of different biopolymers and their molecular weight (Banerjee and Bhattacharya 2012). Selection and control of these factors result in the formation of different kinds of gels, such as hydrogels, organogels, xerogels, aerogels, emulsion gels, oleo gels, weak gels, fluid gels, or temperature-sensitive gels (thermoreversible or thermo-irreversible) (Graham et al. 2019). Gels

**Table 1.5** Hydrocolloids used as gelling agents

Hydrocolloids as a gelling agent	Properties	Applications
Modified starch	Cold-set gel; thermal irreversible and opaque	Dairy desserts
Agar	Cold-set gels; thermoreversible	Bakery products, jellies
$\kappa$ -, and $\iota$ -Carrageenan	Cold-set gels; thermoreversible	Puddings, milk shakes, tofu
Low methoxy pectin	Cold-set gels at low pH; thermoreversible	Jams, glazes, jellies, milk-based desserts
High methoxy pectin	Cold-set gels at low pH; thermal irreversible	Jams, jellies
Gellan gum	Cold-set gels; thermoreversible; highly transparent	Jellies with different flavors
Alginate	Thermal irreversible gels; stable when being heated	Restructured foods, bakery creams
Methyl and hydroxypropylmethyl cellulose	Thermoreversible gels; unstable when being chilled	Cake batters, beverages, whipped toppings, salad dressings
Curdlan	Thermoreversible and thermal irreversible gels	Surimi, sausage

with a wide range of properties can be obtained depending on the conditions that are employed for gel formation. Some gels are brittle, i.e., fractures at a small deformation, while the others are deformable and would not break even at very large deformation. They can be transparent or also be opaque.

## 7.2 Stabilizers

Hydrocolloids are widely used as stabilizers of food dispersions such as emulsions and foams, which can be used to design a variety of functional food structures with desired properties in texture, stability, flavor release, or nutrition.

### 7.2.1 Emulsifier

Hydrocolloids-based emulsifiers can be seen in many food products include carbonated ice cream, soft drinks, and sauces. Many hydrocolloids are able to act as stabilizers (stabilizing agents) of oil-in-water (O/W) emulsions, whereas only a few of them can act as emulsifiers (emulsifying agents). Emulsifying agents are required to have surface activity at the oil–water interface, and thus the ability to adsorb to the surface of newly formed oil droplets during homogenization, leading to

the formation of stable O/W emulsions (Dickinson 2009). Emulsifying activity and emulsion stability should be briefly described here as is done for foaming ability later.

The commonly used polysaccharide-based emulsifiers are Arabic gum, sugar beet pectin, modified starches, galactomannans, and modified celluloses. The emulsifying ability of these polymers has their chemical structure bases in either (1) the non-polar chemical groups attached to the molecular backbone (e.g., propylene glycol alginate, or hydrophobically modified starch/cellulose) or (2) the presence of a protein component covalently-, or physically linked to the polysaccharide (e.g., Arabic gum, sugar beet pectin, or guar gum).

Bovine milk and egg proteins are the most widely used protein-sourced emulsifiers such as casein and whey protein. Casein is a group of amphiphilic proteins which can be classified into  $\alpha_{s1}$ -,  $\alpha_{s2}$ -,  $\beta$ -, and  $\kappa$ -casein dependent on their sensibility to free calcium ion. Whey protein contains a family of globular proteins with rigid structures, mainly including  $\alpha$ -lactalbumin,  $\beta$ -lactoglobulin, bovine serum albumin (BSA), and immunoglobulins. Animal-sourced gelatins (bovine, pig, or fish) also have amphiphilic characters, and show surface activity, but they typically exhibit a poor stabilization effect towards emulsions. Recently, the development of plant-sourced protein-based emulsifiers is receiving more and more attention, which is mainly driven by the vegetarian's will of replacing animal proteins to reduce the consumption of animal proteins, as well as to promote food sustainability and security. Some plant proteins are promising emulsifiers, including lupin proteins, pea proteins, corn germ proteins, and soy proteins (Ozturk and McClements 2016).

### 7.2.2 Foaming Agent

Foam is a dispersion where a high-volume of gas is dispersed in a liquid. The stabilization of foams requires an interfacial barrier to prevent coalescence of neighboring gas bubbles, e.g., the protein layer at the air–water interface. Food particles at the air–water interface can also stabilize or destabilize foams, depending on their properties (e.g., wettability or spreading). Foaming properties generally refer to the foaming capacity and foam stability. Foaming capacity (or foamability) is the capacity for the continuous phase to embed gas while the foam stability is defined as the ability to maintain the gas for a certain time. Many food-derived hydrocolloids have been widely used as stabilizers of foams, including casein, whey proteins, zein, gelatin, pectin, cellulose, chitin, and chitosan (Dickinson 2017). The foaming properties of hydrocolloids, e.g., proteins, depend on the intrinsic factors (e.g., chemical structure, size, hydrophobicity, or surface chemistry) and external factors (e.g., concentration, pH, temperature, and the presence of other components).



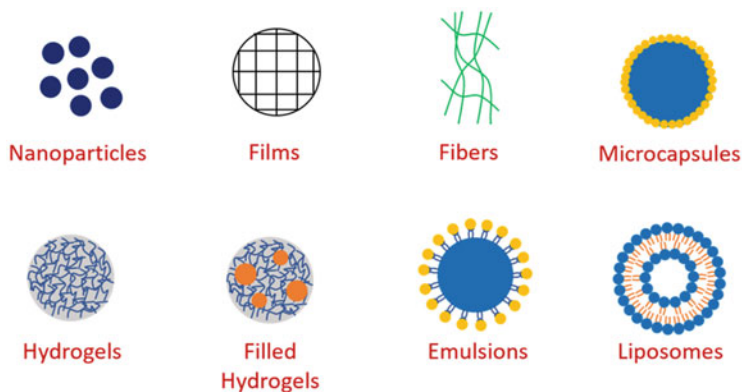


**Fig. 1.6** Summarized functional delivery systems based on hydrocolloids

### 7.3 *Delivery Carriers*

Proteins and polysaccharides are two important kinds of biopolymers employed to fabricate food-grade delivery systems. They are biocompatible, biodegradable, and non-toxic polymers, which makes them attractive building units for delivery systems in food, biology, and medicine applications. In addition, the diversity of molecular structures exhibited by proteins or polysaccharides (e.g., molecular weight, branched or linear structure, charges, polarities, amphiphilicity, dimensions, or reactivities) offers researchers the opportunity to build delivery carriers with desired specifications (McClements 2016). These protein- or polysaccharide-based delivery carriers can be prepared by bottom-up methods that involve self-assembly of individual molecules into large particles, or top-down methods that involve breaking-down of large biopolymers into small fragments. Multiple intermolecular forces usually take part in the formation and stabilization of these carriers for bioactive components including electrostatic interaction, hydrophobic effect, hydrogen bond, steric repulsion, and/or van der Waals attractive force.

Proteins and polysaccharides commonly used to fabricate delivery carriers can be classified into water-soluble and water-insoluble ones. Water-soluble proteins and polysaccharides include casein, whey protein, agar, gelatin, carrageenan, alginate, pectin, guar gum, and xanthan gum while water-insoluble ones have zein, chitosan, gliadin, starch, or cellulose. Functional delivery carriers developed based on these biopolymers exhibited different structures, e.g., nanoparticles, films, fibers, hollow microcapsules, emulsions, or hydrogel particles (Fig. 1.6), through which a variety of nutraceuticals were delivered, such as polyphenols, vitamins, carotenoids, unsaturated fatty acids, fish oils, or essential oils (Abd El-Salam and El-Shibiny 2012; Ezhilarasi et al. 2012; Fathi et al. 2014).

## 7.4 Bioactive Ingredients

Except for the above-mentioned functionalities, many food hydrocolloids also show potential health benefits. For example, whey proteins and their derivate show a variety of health benefits, including antimicrobial and antiviral properties, and enhance immune defense and bone health, and protect against cancer and cardiovascular disease, and reduce oxidative stress and increase levels of glutathione, and lower blood pressure, and potentially decrease the low-density lipoprotein (LDL) and blood cholesterol level, moderate blood sugar and increase both the level of insulin and the sensitivity of its effects, reduce inflammation, have beneficial effects on inflammatory bowel disease, and induce satiety and reduce hunger, and potentially help to lose weight (Birsen Bulut and Nihat 2012). Many of these health benefits can be attributed to bioactive peptides released by intestinal hydrolysis of whey proteins, e.g., antimicrobial peptides, angiotensin-converting enzyme (ACE) inhibition peptides, antioxidant peptides, or blood-sugar-control peptides.

Polysaccharides have been also reported to possess a variety of health benefits. One of their major health benefits is being considered as dietary fibers, which can positively generate a series of biological activity (Fig. 1.7), including but not limited to eliminating constipation or stimulating colonic muscular activity, encouraging stool expulsion, promoting the level of short-chain fatty acids (SCFAs), gastrointestinal peristalsis, inhibiting the population of pathogenic bacteria (*Clostridia*), acting as prebiotics (diet fibers) and antimicrobial agents, and reducing the lipid absorption (Mudgil and Barak 2013; Makki et al. 2018). Dietary fibers are a family of polysaccharides, and can be further divided into insoluble and soluble forms (Deehan et al. 2017). The definition of “soluble” and “insoluble” is different in the nutritionist community and physicochemical community. This is a serious problem. KGM is usually classified as a soluble dietary fiber by nutritionists, but physicochemists struggle to dissolve KGM. It depends on the acetyl content. If the acetyl group is introduced artificially, the solubility is improved. But some natural KGM is not so soluble. Water-insoluble dietary fibers such as cellulose and hemicellulose have a fecal bulking effect and are hard to be digested by the gut bacteria. However, water-soluble fibers can be fermented by the gut bacteria and release health-beneficial metabolites such as SCFAs. Furthermore, many soluble non-starch polysaccharides such as guar gum, pectin,  $\beta$ -glucans, and psyllium, can form a gel structure in the intestinal tract which can delay the absorption of glucose and lipids (Deehan et al. 2017).

In addition to dietary fibers, polysaccharides also show a variety of potential health benefits. Sulfated polysaccharides derived from marine algae, for example, are reported to possess many biological activities, including anti-coagulant, anti-virus, antioxidant, immunomodulation, inducing osteoblastic cell differentiation, protecting gastric mucosa against acid and pepsin, inhibiting UV-B induced matrix metalloproteinase-1 activity in human skin, and reducing cholesterol and triglycerides (TG) levels (Wijesekara et al. 2011). These health benefits of sulfated

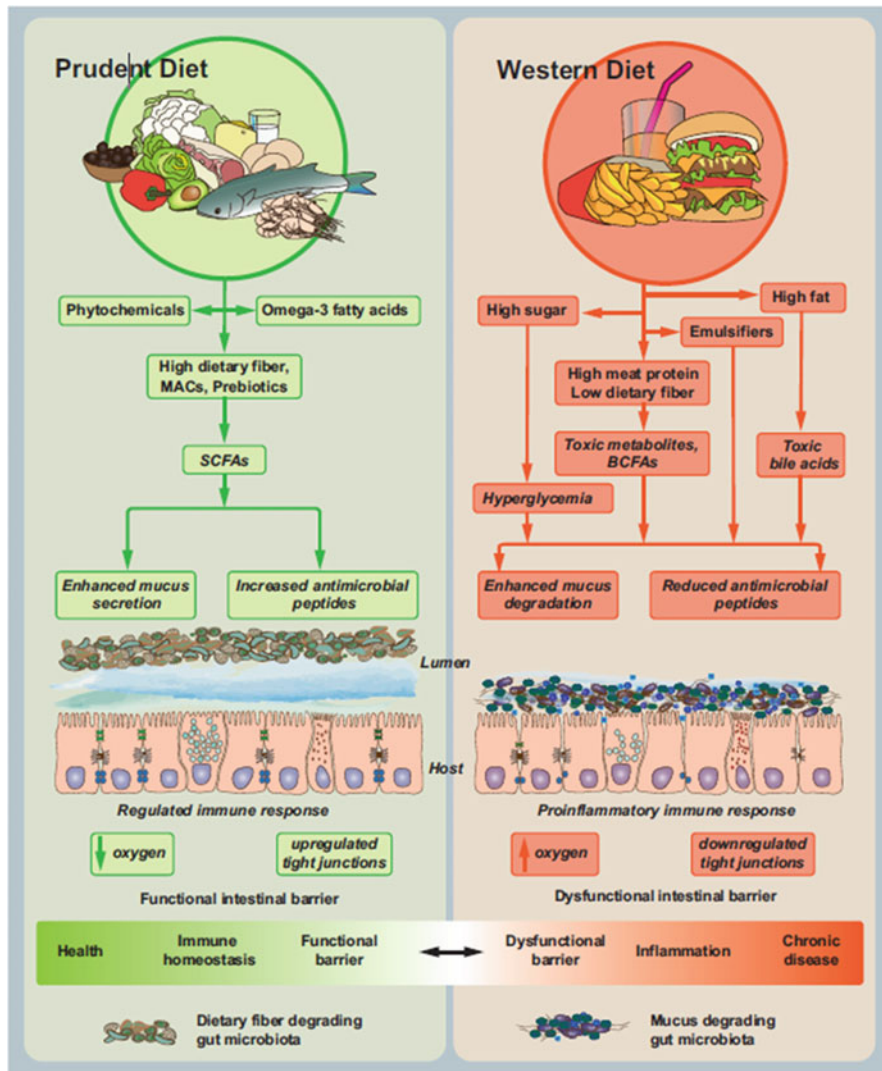


**Fig. 1.7** Influence of low- and high-fiber diet on the composition, diversity, and function of gut microbiota (Makki et al. 2018). The permission for reproduction of the figure was obtained from Cell Press

polysaccharides are always correlated to their molecular structure, such as molecular weight.

Another attractive health benefit of polysaccharides is their great potential in reducing the risk of cancer. Many studies, mainly observational, have investigated the correlation between fiber intake and the risk of colon or rectum cancers. Intervention studies have confirmed the impact of dietary fiber on the recurrence

of adenoma, which are often considered an early marker of colorectal cancer. Nevertheless, there is no hard evidence that can prove the reducing-effect of fiber intake on the risk of colorectal cancer. Thus, the guideline on dietary fiber intake aiming to reduce the colorectal cancer risk seems to be lacking enough evidence but individuals with a low level of fiber intakes potentially have an increased cancer risk (Mudgil and Barak 2013).

## 7.5 *Functional Materials*

In addition to the above-mentioned functionalities, many food hydrocolloids can also be tailored into a variety of functional materials, such as food-packaging film, artificial joint prosthesis, bone tissue engineering materials, and cartilage tissue engineering (Kapoor and Kundu 2016).

### 7.5.1 **Food-Packaging Materials**

Foods are generally packaged to extend their shelf-life and to illustrate the composition and nutrition information to the consumers. With the increasing concern on the environmental and food safety requirements, the development of renewable biodegradable food-packaging materials raises more and more attention over the last few years, and a class of natural biopolymer-based materials has been developed as promising food-packaging materials. The food-derived biopolymers that were used to develop food-packaging materials can be classified into two major groups, polysaccharides and proteins. Polysaccharide-based packaging materials include starch, cellulose, chitin/chitosan, konjac glucomannan, and pectin while protein-based materials mainly have soy protein, wheat gluten, corn zein, gelatin, whey proteins, and casein (Tang et al. 2012).

Polysaccharide-based food-packaging films have different characteristics depending on the materials (Cazón et al. 2017): (1) Starch-based food-packaging materials always have moderate oxygen barrier properties but poor moisture barrier and mechanical properties; (2) Chemically modified cellulose derived packaging materials always show good moisture barrier properties, and are suitable for baked goods, fresh products (e.g., meat, fish, vegetables, fruits), processed meats, cheese, and candy. Esterified cellulose-based materials are excellent for high moisture foods as it allows respiration and reduces fogging; (3) Chitin/chitosan-based materials have clear, tough, flexible, and good oxygen barriers properties but poor long-term stability and low water vapor barrier properties; (4) Pectin based packaging material possesses high water vapor permeability, which limits its use in food packaging.

Different protein-based packaging materials also have their specific properties: (1) Gluten-based materials show good oxygen barrier properties but poor carbon dioxide (CO<sub>2</sub>) barrier properties, which makes them possible to act as packaging materials for specific applications, e.g., mushrooms; (2) Soy protein-based materials

are always brittle and show poor water resistance; (3) Films formed by gelatin do not have good mechanical properties, even reinforced by several techniques, which thus limits their application as a packaging material; (4) Zein films always showed similar tensile strength but higher oxygen permeability as compared with gluten films. This is attributed to an easier diffusion of oxygen across the helical structure of zein as compared with the highly cross-linked structure of wheat gluten (Cazón et al. 2017).

Furthermore, nanocomposites based on the above-mentioned polysaccharides and proteins have also been developed as food-packaging materials, including starch-kaolin, starch-clay, cellulose acetate-clay, pectin-montmorillonite (MMT), gluten-MTT, gelatin-MMT, and SPI-MMT. These nanocomposites based packaging materials show improved tensile strength, thermal stability, and water/oxygen barrier capacity as compared with those produced by sole polysaccharides or proteins (Tang et al. 2012).

### 7.5.2 Biomedical Materials

Inorganic particle based biomedical nanomaterials can cause cytotoxicity owing to their accumulation, aggregation, decomposition, and/or generating reactive oxygen

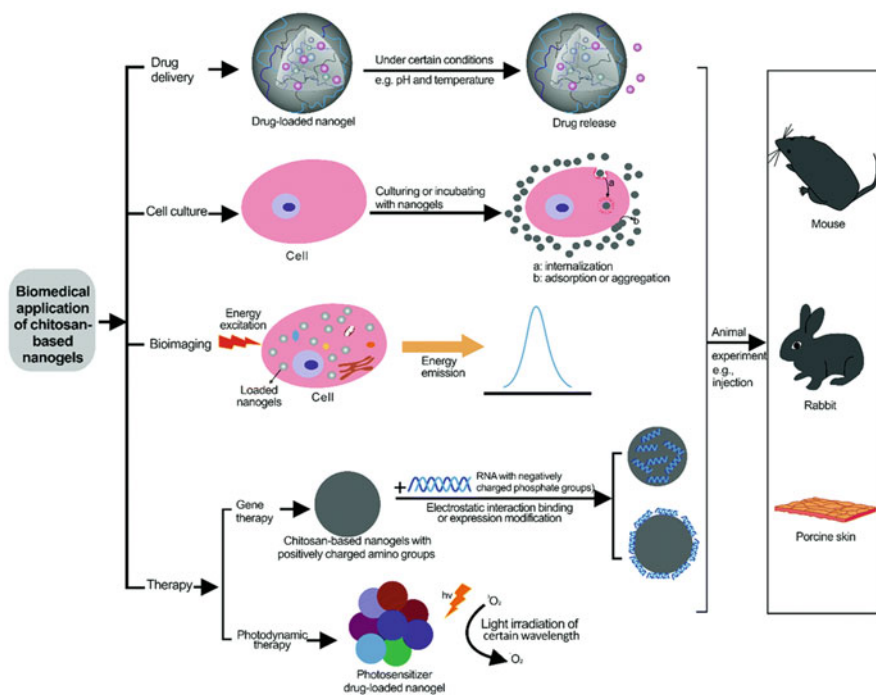


**Fig. 1.8** Biomedical applications of chitosan-based nanogels (Wang et al. 2017). The permission for reproduction of the figure was obtained from Royal Society of Chemistry

species inside the cell. However, natural biopolymers, such as food polysaccharides and proteins, always have good biocompatibility and biodegradability, and they can be developed as functional and eco-friendly advanced materials. Food-derived biopolymers can be developed into diverse kinds of biomedical materials (Fig. 1.8). The biopolymers that have been employed to produce these advanced biomedical materials include chitin/chitosan, cellulose/nanocrystals, hyaluronan, gelatin, silk proteins, and whey proteins.

For example, polysaccharides nanocrystal can be developed into a variety of biomedical materials, such as electrolytes, nanoscaffolds, nanosponges, various biomimetic materials, cellular bioimaging materials, permselective membranes, and templates for the synthesis of inorganic nanoparticles (Lin et al. 2012). Natural polysaccharide nanocrystals potentially have prolonged retention in the circulation

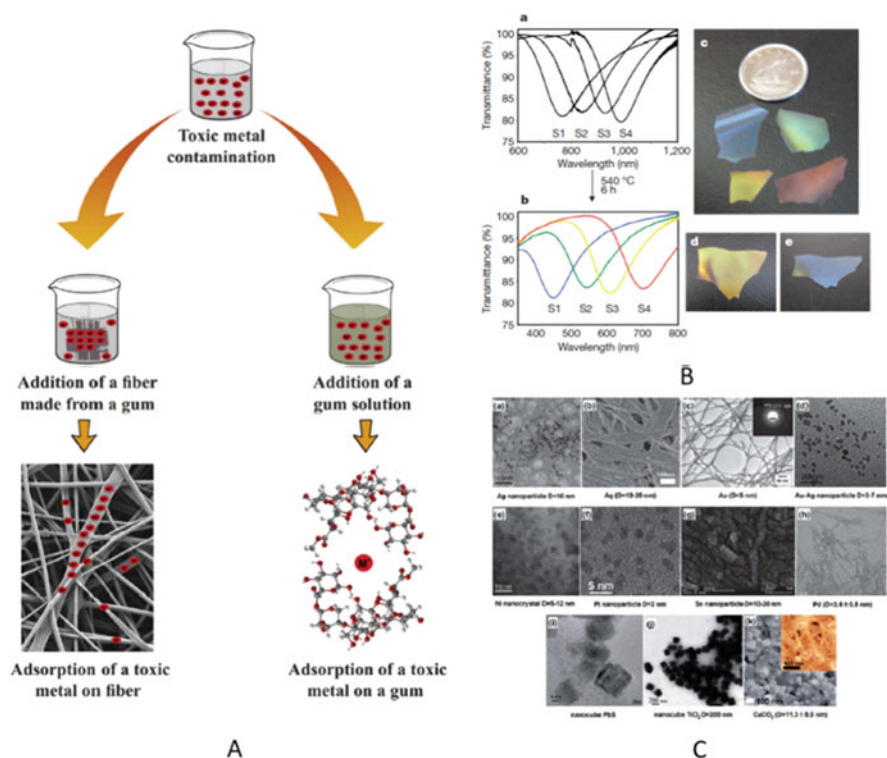


**Fig. 1.9** Several hydrocolloids-based advanced materials (a) adsorption of toxic metal on gum fibers (right) and gum (left) (Padil et al. 2018). The permission for reproduction of the figure was obtained from Elsevier. (b) nanocrystalline cellulose-based biomimetic optical nanomaterials with a peak reflected wavelength of covering the entire visible spectrum (Shopsowitz et al. 2010). The permission for reproduction of the figure was obtained from Springer Nature. (c) morphology observation of inorganic nanoparticles prepared using cellulose nanocrystal as the template (Lin et al. 2012). The permission for reproduction of the figure was obtained from Royal Society of Chemistry

system, rendering them a promising biomedical material that is biodegradable and safe for the environment and human health.

### 7.5.3 Template for Synthesizing Inorganic Nanoparticles

Many hydrocolloids, e.g., cellulose nanocrystal (Fig 1.9c), can act as a template or scaffold of synthesizing inorganic nanoparticles. For example, mesoporous silica nanoparticles can be successfully fabricated by using rod-like cellulose nanocrystal as the template (Dujardin et al. 2003; Gruber et al. 2011). The cellulose crystalline based materials have also been used as the template for producing gold (Au), silver (Ag), uranium (U), palladium (Pd), platinum (Pt), selenium (Se), Au-Ag, Ag-Pd, cadmium sulfide (CdS), zinc sulfide (ZnS), lead sulfide (PbS), and titania (TiO<sub>2</sub>) nanoparticles. The reduction reaction between the template and metal ions is the main mechanism for producing these nanoparticles, and the utilization of cellulose nanocrystal as the template can produce stable and high-density particles with a controlled size distribution, and significantly improve their chemical properties.

### 7.5.4 Other Types of Functional Materials

Food hydrocolloids can also be developed into many other types of advanced materials, such as mesoporous biomimetic optical nanomaterials with a peak reflected wavelength of covering the whole visible spectrum or even into the near-infrared by simple modification (Shopsowitz et al. 2010) (Fig 1.9b), bio-inspired mechanically adaptive nanomaterials used as adaptive substrates of intracortical microelectrodes (Shanmuganathan et al. 2010), nanostructured membranes with potential permselective function to differently charged substances (Thielemans et al. 2009), reinforced polymer electrolytes with high ionic conductivity and good stability (My Ahmed Said Azizi Samir et al. 2004), and decontamination materials of removing organic pollutants (Namazi and Dadkhah 2010) or toxic metal (Padil et al. 2018) (Fig 1.9a).

## 8 The Future Trends

Over the last half a century, great progress in the science and technology of food hydrocolloids was gained along with the rapid development of the food industry. Food hydrocolloids carry the flavor, texture, processing, nutrition, and health characteristics of foods and thus play an essential role in the food industry. In view of an increasing concern of consumers in a healthy way of life, both scientists and consumers pay more and more attention to the functionality of food products. The health benefits of food hydrocolloids have been revealed one after another. Nevertheless, the physiological activities of many emerging natural polysaccharides or



proteins have not been clarified. Furthermore, food hydrocolloids can potentially contribute to the future food structure design due to their ability in acting as structuring agents, e.g., elderly food, special diet food for diabetics, and low-salt foods, controlled-textured-flavored-foods for dysphagia. Moreover, excellent plasticity and mechanical properties of food hydrocolloids-based advanced materials make them possible to have promising applications in food, chemical, and biomedical industries, such as controlled or target delivery carriers of bioactive nutrients and drugs, meat analogue, artificial muscles, artificial joints or cartilage, or electronic elements. All in all, the food hydrocolloids market continues to see robust growth and the prospect of the future is worth to be expected.

## References

- Abd El-Salam MH, El-Shibiny S (2012) Formation and potential uses of milk proteins as nano delivery vehicles for nutraceuticals: a review. *Int J Dairy Technol* 65(1):13–21. <https://doi.org/10.1111/j.1471-0307.2011.00737.x>
- Aguilera J (1992) Generation of engineered structures in gels. In: Schwartzberg HG, Hartel RN (eds) *Physical chemistry of foods*. Marcel Dekker, New York, pp 387–421
- Banerjee S, Bhattacharya S (2012) Food gels: gelling process and new applications. *Crit Rev Food Sci Nutr* 52(4):334–346. <https://doi.org/10.1080/10408398.2010.500234>
- Birsan Bulut S, Nihat A (2012) Health benefits of whey protein: a review. *J Food Sci Eng* 2 (3):129–137. <https://doi.org/10.17265/2159-5828/2012.03.001>
- Cazón P, Velazquez G, Ramírez JA, Vázquez M (2017) Polysaccharide-based films and coatings for food packaging: a review. *Food Hydrocoll* 68:136–148. <https://doi.org/10.1016/j.foodhyd.2016.09.009>
- Christopher K, Mathews KEH, Appling DR, Anthony-Cahill SJ (2013) *Biochemistry*, 4th edn. Pearson, London
- Dai FJ, Chau CF (2017) Classification and regulatory perspectives of dietary fiber. *J Food Drug Anal* 25(1):37–42. <https://doi.org/10.1016/j.jfda.2016.09.006>
- Deehan EC, Duar RM, Armet AM, Perez-Muñoz ME, Jin M, Walter J (2017) Modulation of the gastrointestinal microbiome with nondigestible fermentable carbohydrates to improve human health. *Microbiol Spectr* 5:1–24
- de-Vries J (2004) Hydrocolloid gelling agents and their applications. In: Philips GOWP (ed) *Gums and stabilizers for the food industry*, vol 12. RSC, Oxford, pp 22–30
- Dickinson E (2009) Hydrocolloids as emulsifiers and emulsion stabilizers. *Food Hydrocoll* 23 (6):1473–1482. <https://doi.org/10.1016/j.foodhyd.2008.08.005>
- Dickinson E (2017) Biopolymer-based particles as stabilizing agents for emulsions and foams. *Food Hydrocoll* 68:219–231. <https://doi.org/10.1016/j.foodhyd.2016.06.024>
- Diener M, Adamcik J, Sanchez-Ferrer A, Jaedig F, Schefer L, Mezzenga R (2019) Primary, secondary, tertiary and quaternary structure levels in linear polysaccharides: from random coil, to single helix to supramolecular assembly. *Biomacromolecules* 20(4):1731–1739. <https://doi.org/10.1021/acs.biomac.9b00087>
- Djabourov M, Nishinari K, Ross-Murphy SB (2013) *Physical gels from biological and synthetic polymers*. Cambridge University Press, Cambridge
- Dragnet KI, Taylor C (2011) Chemical, physical and biological properties of alginates and their biomedical implications. *Food Hydrocoll* 25(2):251–256. <https://doi.org/10.1016/j.foodhyd.2009.10.007>



- Dujardin E, Blaseby M, Mann S (2003) Synthesis of mesoporous silica by sol–gel mineralisation of cellulose nanorod nematic suspensions. *J Mater Chem* 13(4):696–699. <https://doi.org/10.1039/b212689c>
- Ezhilarasi PN, Karthik P, Chhanwal N, Anandharamakrishnan C (2012) Nanoencapsulation techniques for food bioactive components: a review. *Food Bioprocess Technol* 6(3):628–647. <https://doi.org/10.1007/s11947-012-0944-0>
- Fathi M, Martín Á, McClements DJ (2014) Nanoencapsulation of food ingredients using carbohydrate based delivery systems. *Trends Food Sci Technol* 39(1):18–39. <https://doi.org/10.1016/j.tifs.2014.06.007>
- Finkelstein AV, Ptitsyn O (2016) Protein physics: a course of lectures. Elsevier, Amsterdam
- Graham T (1861) X. Liquid diffusion applied to analysis. *Philos Trans R Soc Lond* 151:183–224
- Graham S, Marina PF, Blencowe A (2019) Thermoresponsive polysaccharides and their thermoreversible physical hydrogel networks. *Carbohydr Polym* 207:143–159. <https://doi.org/10.1016/j.carbpol.2018.11.053>
- Gruber S, Taylor RNK, Scheel H, Greil P, Zollfrank C (2011) Cellulose-biotemplated silica nanowires coated with a dense gold nanoparticle layer. *Mater Chem Phys* 129(1–2):19–22. <https://doi.org/10.1016/j.matchemphys.2011.04.027>
- Imeson A (2010) Food stabilisers, thickeners and gelling agents. Black Well, West Sussex
- Kapoor S, Kundu SC (2016) Silk protein-based hydrogels: promising advanced materials for biomedical applications. *Acta Biomater* 31:17–32. <https://doi.org/10.1016/j.actbio.2015.11.034>
- Lin N, Huang J, Dufresne A (2012) Preparation, properties and applications of polysaccharide nanocrystals in advanced functional nanomaterials: a review. *Nanoscale* 4(11):3274–3294. <https://doi.org/10.1039/c2nr30260h>
- Magnuson B, Munro I, Abbot P, Baldwin N, Lopez-Garcia R, Ly K, McGirr L, Roberts A, Socolovsky S (2013) Review of the regulation and safety assessment of food substances in various countries and jurisdictions. *Food Addit Contam Part A Chem Anal Control Expo Risk Assess* 30(7):1147–1220. <https://doi.org/10.1080/19440049.2013.795293>
- Makki K, Deehan EC, Walter J, Backhed F (2018) The impact of dietary fiber on gut microbiota in host health and disease. *Cell Host Microbe* 23(6):705–715. <https://doi.org/10.1016/j.chom.2018.05.012>
- McClements IJJDJ (2016) Biopolymer-based delivery systems challenges and opportunities. *Curr Top Med Chem* 16:1026–1039
- McKim JM, Willoughby JA, Blakemore WR, Weiner ML (2018) Clarifying the confusion between polygeenan, degraded carrageenan, and carrageenan: a review of the chemistry, nomenclature, and in vivo toxicology by the oral route. *Crit Rev Food Sci Nutr* 59(19):3054–3073. <https://doi.org/10.1080/10408398.2018.1481822>
- Mokrushin SG (1962) Thomas Graham and the definition of colloids. *Nature* 195:861
- Mudgil D, Barak S (2013) Composition, properties and health benefits of indigestible carbohydrate polymers as dietary fiber: a review. *Int J Biol Macromol* 61:1–6. <https://doi.org/10.1016/j.ijbiomac.2013.06.044>
- My Ahmed Said Azizi Samir FA, Gorecki W, Sanchez J-Y, Dufresne A (2004) Nanocomposite polymer electrolytes based on poly(oxyethylene) and cellulose nanocrystals. *J Phys Chem B* 108:10845–10852
- Namazi H, Dadkhah A (2010) Convenient method for preparation of hydrophobically modified starch nanocrystals with using fatty acids. *Carbohydr Polym* 79(3):731–737. <https://doi.org/10.1016/j.carbpol.2009.09.033>
- Oakenfull D, Glicksman M (2009) Gelling agents. *C R C Crit Rev Food Sci Nutr* 26(1):1–25. <https://doi.org/10.1080/10408398709527460>
- Ozturk B, McClements DJ (2016) Progress in natural emulsifiers for utilization in food emulsions. *Curr Opin Food Sci* 7:1–6. <https://doi.org/10.1016/j.cofs.2015.07.008>
- Padil VVT, Waclawek S, Cernik M, Varma RS (2018) Tree gum-based renewable materials: sustainable applications in nanotechnology, biomedical and environmental fields. *Biotechnol Adv* 36(7):1984–2016. <https://doi.org/10.1016/j.biotechadv.2018.08.008>

- Phillips GO, Williams PA (2009) Handbook of hydrocolloids. Woodhead Publishing, Cambridge
- Robert K, Murray DAB, Notham KM, Kennelly PJ, Rodwell VW, Weil PA (2009) Harper's illustrated biochemistry, 28th edn. McGraw-Hill Medical, Toronto
- Saha D, Bhattacharya S (2010) Hydrocolloids as thickening and gelling agents in food: a critical review. *J Food Sci Technol* 47(6):587–597. <https://doi.org/10.1007/s13197-010-0162-6>
- Shanmuganathan K, Capadona JR, Rowan SJ, Weder C (2010) Biomimetic mechanically adaptive nanocomposites. *Prog Polym Sci* 35(1–2):212–222. <https://doi.org/10.1016/j.progpolymsci.2009.10.005>
- Shopsowitz KE, Qi H, Hamad WY, MacLachlan MJ (2010) Free-standing mesoporous silica films with tunable chiral nematic structures. *Nature* 468(7322):422–425. <https://doi.org/10.1038/nature09540>
- Singh S (2019) Hydrocolloids market. Market research reports. MarketsandMarkets™ INC, Northbrook
- Tang XZ, Kumar P, Alavi S, Sandeep KP (2012) Recent advances in biopolymers and biopolymer-based nanocomposites for food packaging materials. *Crit Rev Food Sci Nutr* 52(5):426–442. <https://doi.org/10.1080/10408398.2010.500508>
- Thielemans W, Warbey CR, Walsh DA (2009) Permselective nanostructured membranes based on cellulose nanowhiskers. *Green Chem* 11(4):531. <https://doi.org/10.1039/b818056c>
- Wang H, Qian J, Ding F (2017) Recent advances in engineered chitosan-based nanogels for biomedical applications. *J Mater Chem B* 5(34):6986–7007. <https://doi.org/10.1039/c7tb01624g>
- Wijesekara I, Pangestuti R, Kim S-K (2011) Biological activities and potential health benefits of sulfated polysaccharides derived from marine algae. *Carbohydr Polym* 84(1):14–21. <https://doi.org/10.1016/j.carbpol.2010.10.062>
- Williams PA, Phillips GO (2009) Introduction to food hydrocolloids. In: Phillips GO, Williams PA (eds) Handbook of hydrocolloids, 2nd edn. Woodhead Publishing, Cambridge, pp 1–22. <https://doi.org/10.1533/9781845695873.1>
- Wüstenberg T (2015) General overview of food hydrocolloids. In: Cellulose and cellulose derivatives in the food industry fundamentals and applications. Wiley, Weinheim, pp 1–68

# Chapter 2

## Solution Properties



Hongbin Zhang and Ruiqi Li

**Abstract** Solution properties are important physicochemical properties of food hydrocolloids. A number of critical molecular and conformation parameters such as the molecular weight, intrinsic viscosity, radius of gyration, persistence length, etc. are deduced from dilute solutions. The main functionalities of food hydrocolloids, such as viscoelasticity, physical stabilization, emulsification, suspension, mouthfeel, texture modification, delivery of actives, essentially rely on their solution properties. Various hydrocolloids have been widely used in aqueous solution to provide a variety of structures and functionalities to diverse food or non-food products. This chapter starts a brief survey of the main features of the chemical constitution and molecular structures of food hydrocolloids, and then an introduction into the conformation of single chains in solution, using examples for the explanation. After discussing the single chain behavior, the collective properties of polymers, mainly polysaccharides, in bulk are introduced and discussed based on the relevant dilute and semi-dilute solution theory. The impact of molecular parameters and chain conformation of polysaccharides on their solution properties is emphasized, while several molecular and conformation parameters are summarized. The utilization of the solution properties of food hydrocolloids is also described. A series of common polysaccharide liquid crystals are also briefly discussed.

**Keywords** Polysaccharide · Thermodynamics · Hydrodynamic parameter · Scaling law · Chain conformation

---

H. Zhang (✉) · R. Li

Advanced Rheology Institute, Department of Polymer Science and Engineering, School of Chemistry and Chemical Engineering, Frontiers Science Center for Transformative Molecules, Shanghai, R. P. China

e-mail: [hbzhang@sjtu.edu.cn](mailto:hbzhang@sjtu.edu.cn)

## 1 Introduction

Natural polymers such as polysaccharides and proteins have attracted much attention because of their great importance as functional food hydrocolloids as well as renewable resources and biodegradable materials, dealing with sustainable development and environmental conservation. These biopolymers have been widely used in aqueous solutions or in hydrogels to provide structure and function, e.g., viscoelasticity, physical stabilization, delivery of actives, emulsification, mouthfeel, texturizing, to a variety of food or non-food products.

Since many important properties of polymer solutions, such as viscosity, viscoelasticity, and phase behavior, are mainly dominated by the polymer chain conformation and dimension, for a comprehensive understanding of molecular interactions, along with for many technical applications, a knowledge of the polymer chain shape in solution is essentially important. Only by understanding their chain conformation and solution properties, establishing new characterization methods, and improving the theory of natural polymer solutions, it will be possible to clarify the relationship between their performances and structures, and to design more rational molecules and build functional materials with good performance to achieve added application value.

It should be noted at first that the structure of biopolymers, especially natural polysaccharides is far more complicated than the general synthetic polymers, typically, such as polyolefins (polyethylene, polypropylene, polystyrene, and so on), which have only very simple repeating units. However, even for the simplest polysaccharide family of glucans, their repeating unit is glucose residue sterically connected by several glycosidic linkages, and only the difference in glycosidic linkages yields a number of different glucans, for instance, starch (amylose, amylopectin) ( $\alpha$ -(1 $\rightarrow$ 4) linkage in backbone), cellulose ( $\beta$ -(1 $\rightarrow$ 4) linkage), curdlan ( $\beta$ -(1 $\rightarrow$ 3) linkage), and so on. These glucans are of varying chemical structures, and thereby result in various chain conformations in solution, and diverse solution properties. Second, very different from small molecule solution, polymer solution has its unique properties due to the high molecular weight of the polymer ( $M_w$ ), such as the slow dissolution process and high viscosity. The properties of the polymer solution are  $M_w$  dependent, and the polymer has the character of molecular weight polydispersity. And third, a polymer solution refers to a homogeneous system consisting of two or more components dispersed in a solvent in a molecular state. Polymer dissolution in solvent needs to go through two stages, first swelling, and then dissolution. The molecular diffusion in the solvent at first causes the movement of the polymer chain segment. After that, the molecular diffusion of polymer into the solvent starts, and the mixture becomes a homogeneous system. Due to the huge  $M_w$  of the polymer, the diffusion rate of the polymer is less than that of small molecules. The crosslinked polymer can only swell and do not dissolve.

Polymer solutions can be divided into dilute, semi-dilute, and concentrated solutions. The properties of the solutions can vary greatly with the polymer concentration. When the concentrations are small (generally less than 1%), there is no

contact between the polymer chains, and the solution viscosities are very low. Many important physical quantities are measured in dilute solution conditions. In semi-dilute solutions, the polymer chains contact and may be entangled with each other, and the solutions have high viscosities. In concentrated solutions, the polymer chains display entanglement; meanwhile, the viscosities are very high.

This chapter starts a brief survey of the thermodynamics (mainly free energy and osmotic pressure) of polymer solutions at equilibrium, including the introduction to the Flory–Huggins mean-field theory and Flory–Krigbaum dilute theory, to introduce some important physical parameters such as the Flory–Huggins interaction parameter ( $\chi$ ) and the second virial coefficient ( $A_2$ ). Then, the concentration regimes of polymer solutions, and the viscosity and scaling of some polysaccharides in solutions are discussed, and some important molecular and conformation parameters such as polymer  $M_w$  and its distribution ( $M_w/M_n$ ), intrinsic viscosity  $[\eta]$ , the mean square radius of gyration ( $R_g$ ), persistence length ( $L_p$ ), and chain stiffness parameter ( $B$ ) are summarized. Finally, some polysaccharide liquid crystals are also briefly introduced.

Here, the relevant measurement methods of the physical parameters are not emphasized as can be easily found in textbooks. Rheology, an important aspect of the polymer solution, which is not included in this chapter, will be discussed in Chap. 3.

## 2 Thermodynamics of Polymer Solutions

The thermodynamics of polymer solutions has been well described in the literature. For a polymer, there are good solvents that dissolve the polymer well and non-solvents that do not dissolve it. A solvent with an intermediate quality can dissolve the polymer to some extent.

While amorphous polymers (for example, polystyrene and polymethylmethacrylate) are readily dissolved in the good solvent, semi-crystalline polymers (for example, polyethylene, polypropylene, cellulose, chitin, and curdlan) are not easy to dissolve. Polymer chains within a crystallite are in a thermodynamically stable state. Heat treatment may help their dissolution. Notably, the dissolution of cellulose and chitin has long been a very difficult problem, and it has traditionally been mainly dissolved by organic solvents and high-temperature heating (Kim et al. 2013; Kaliannan et al. 2001). Lina Zhang's group broke through the traditional method of heating organic solvents to dissolve macromolecules, proposing a new method for dissolving poorly soluble natural polysaccharides such as cellulose, chitin, and chitosan in low-temperature alkali/urea aqueous solution system, and revealed its mechanism (Cai and Zhang 2010).

There are some concentration regimes in the polymer solution, i.e., dilute, semi-dilute, and concentrated solution. Here, the thermodynamics of dilute solutions is primarily focused. With the increase of the polymer concentration, the thermodynamics of the polymer solution will deviate from that of the ideal solution.

Thermodynamic properties of the polymer solution depend not only on the polymer itself but also on how good the solvent is for the polymer. The solvent/polymer interaction and the degree of polymerization dictate the properties. The Flory–Huggins mean-field theory describes well the features of polymer solutions, which has been well verified in literature.

## 2.1 Flory–Huggins Mean-Field Theory

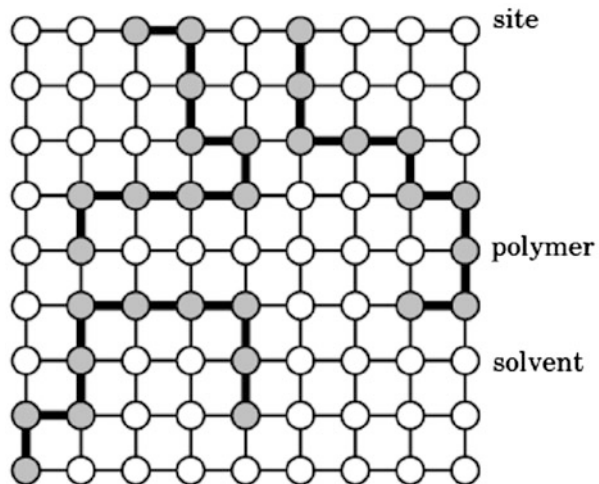
### 2.1.1 Lattice Chain Model

The miscibility of the polymer with a given solvent can be well explained in the mean-field theory. Flory applied this theory to polymer solutions. The simplest lattice chain theory is generally referred to as Flory–Huggins mean-field theory. For the polymer solution, the mean-field theory compares the free energy of the polymer/solvent system before and after mixing.

Figure 2.1 shows a two-dimensional version of the lattice model. The system consists of  $n_{\text{site}}$  sites. Each site can be occupied by either a solvent molecule or a monomer of the polymer. Double occupancy and vacancy are not allowed. A linear polymer chain occupies  $N$  sites on a string of  $N - 1$  bonds. Polymer chains, each consisting of  $N$  monomers, are laid onto empty sites one by one until there are a total of  $n_{\text{p}}$  chains. Then, the unoccupied sites are filled with solvent molecules. The polymer volume fraction  $\phi$  is related to  $n_{\text{p}}$  by  $n_{\text{p}} = n_{\text{site}}\phi/N$  and the number of the solvent molecules  $n_{\text{S}}$  is thus given by  $n_{\text{S}} = n_{\text{site}}(1 - \phi)$ .

Before mixing, the polymer molecule and the solvent occupy the volume of  $n_{\text{p}}N\nu_{\text{site}}$  and  $n_{\text{S}}\nu_{\text{site}}$ , respectively, where  $\nu_{\text{site}}$  is the volume per site. Upon mixing, the total volume  $n_{\text{site}}\nu_{\text{site}}$  does not change. The enthalpy of mixing  $\Delta H_{\text{mix}}$  and the

**Fig. 2.1** The Lattice model for polymer solution. Gray and white sites are occupied by polymer chains and solvent molecules, respectively. Reproduction with permission from Teraoka (2002), Copyright 2002 John Wiley and Sons



Gibbs free energy change  $\Delta G_{\text{mix}}$  thus are equal to the change in the internal energy  $\Delta U_{\text{mix}}$  and the Helmholtz free energy change  $\Delta A_{\text{mix}}$ , respectively.

### 2.1.2 Flory–Huggins Interaction Parameter $\chi$

The entropy of mixing, especially at low concentrations, is small for polymer–solvent systems. Therefore, upon mixing (i.e., enthalpy of mixing), the change in the interactions governs the miscibility. The interactions here are typically van der Waals interactions, dipole–dipole interactions, and hydrogen bonding.

The lattice fluid model only considers the interactions between nearest neighbors. The interactions reside in the contacts. Mixing the polymer and solvent changes the overall interaction energy through the rearrangement of contacts. The Flory–Huggins interaction parameter  $\chi$  is defined as the product of the lattice coordinate  $Z$  and the energy change reduced by  $k_B T$ :

$$\chi = Z \left[ \epsilon_{\text{PS}} - \frac{(\epsilon_{\text{PP}} + \epsilon_{\text{SS}})}{2} \right] / k_B T \quad (2.1)$$

where  $k_B$  is the Boltzmann constant,  $\epsilon_{\text{SS}}$ ,  $\epsilon_{\text{PP}}$ , and  $\epsilon_{\text{PS}}$  are used to denote the interactions for a solvent–solvent (S–S) contact, a polymer–polymer (P–P) contact, and a polymer–solvent (P–S) contact, respectively.

A positive  $\chi$  suggests that the P–S contacts are less favored compared with the P–P and S–S contacts. A negative  $\chi$  means that P–S contacts are preferred, promoting solvation of the polymer. Generally,  $\chi$  decreases with an increase of  $T$ . In a hydrogen bonding pair, for example,  $\chi$  usually changes from negative to positive with increasing  $T$ .

The importance of  $\chi$  parameter stems from being the only way to consider the specific chemical nature of polymer and solvent. For many systems,  $\chi$  has been reported to increase with increasing the polymer concentration and decrease with temperature (Fig. 2.2).  $\chi$  value can be obtained commonly by osmotic pressure measurements (Lei et al. 2016).

### 2.1.3 Gibbs Free Energy and Osmotic Pressure

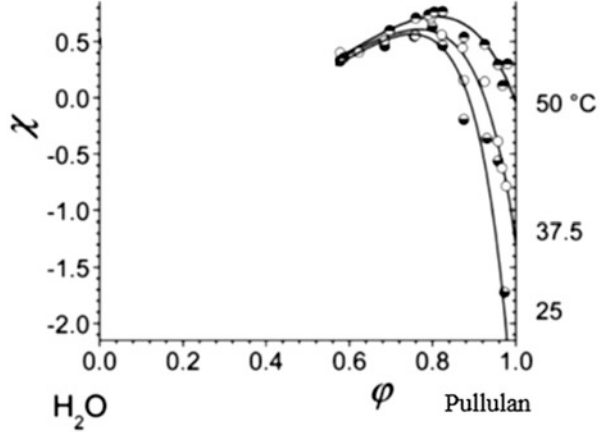
Flory obtained the entropy of mixing  $\Delta S_{\text{mix}}$  per site as

$$-\Delta S_{\text{mix}} / (k_B n_{\text{site}}) = \frac{\phi}{N} \ln \phi + (1 - \phi) \ln (1 - \phi) \quad (2.2)$$

$\Delta S_{\text{mix}}$  given by Eq. (2.2) is greater than the entropy of mixing for an ideal solution of  $n_P$  solute molecules and  $n_S$  solvent molecules.

The change  $\Delta U_{\text{mix}}$  in the internal energy per site is

**Fig. 2.2** Flory–Huggins interaction parameters measured at different temperatures (●: 50 °C; ○: 37.5 °C; and ◐: 25 °C) for the mixing systems of H<sub>2</sub>O and pullulan. Reproduction with permission from Eckelt et al. (2008), Copyright 2008 ACS



$$\Delta U_{\text{mix}}/(n_{\text{site}}k_B T) = \chi\phi(1 - \phi) \quad (2.3)$$

$\Delta U_{\text{mix}}$  maximizes at  $\phi = 1/2$ . The sign of  $\Delta U_{\text{mix}}$  is the same as that of  $\chi$  since  $\phi(1 - \phi) > 0$  for  $0 < \phi < 1$ .  $\Delta U_{\text{mix}}$  depends on the interaction through  $\chi$ . The system with the same  $\chi$  has the same  $\Delta U_{\text{mix}}$ . The solution with  $\chi = 0$  is called an athermal solution. In the athermal solution,  $\Delta U_{\text{mix}} = \Delta H_{\text{mix}} = 0$  regardless of  $\phi$ .

From Eqs. (2.2) and (2.3), the Helmholtz free energy of mixing,  $\Delta A_{\text{mix}} = \Delta U_{\text{mix}} - T\Delta S_{\text{mix}}$ , per site is given as

$$\frac{\Delta A_{\text{mix}}}{n_{\text{site}}k_B T} = \frac{\phi}{N} \ln \phi + (1 - \phi) \ln (1 - \phi) + \chi\phi(1 - \phi) \quad (2.4)$$

The osmotic pressure  $\Pi$  is given as

$$\frac{\Pi\nu_{\text{site}}}{k_B T} = \frac{\Pi V}{n_{\text{site}}k_B T} = \frac{\phi}{N} - \ln (1 - \phi) - \phi - \chi\phi^2 \quad (2.5)$$

where  $V = \nu_{\text{site}} n_{\text{site}}$  is the volume of the solution.

The chain connectivity, rigidity, and the shape of the monomer are neglected in the Flory–Huggins theory. Modifications to this theory are possible by taking these effects into account.

## 2.2 Flory–Krigbaum Dilute Theory

For dilute solutions, when  $\phi \ll 1$ , taking into account  $\ln (1 - \phi) = -\phi - \frac{1}{2}\phi^2 - \frac{1}{3}\phi^3 - \dots$ , then Eq. (2.5) is rewritten to



$$\frac{\Pi V}{n_{\text{site}} k_B T} = \frac{\phi}{N} + \left(\frac{1}{2} - \chi\right) \phi^2 + \frac{1}{3} \phi^3 \dots \quad (2.6)$$

In the low concentration limit, Eq. (2.6) gives the osmotic pressure  $\Pi_{\text{ideal}}$  of the ideal solution:

$$\Pi_{\text{ideal}} = \frac{n_{\text{site}} \phi}{NV} k_B T \quad (2.7)$$

Thus, the ratio of  $\Pi$  to  $\Pi_{\text{ideal}}$  compared at the same concentration is

$$\frac{\Pi}{\Pi_{\text{ideal}}} = 1 + N \left[ \left(\frac{1}{2} - \chi\right) \phi^2 + \frac{1}{3} \phi^3 \dots \right] \quad (2.8)$$

To compare the theory with experiments,  $\Pi$  is expressed in terms of mass concentration  $c$ . Using the identity  $c = \frac{M}{N_A N} \frac{\phi}{\nu_{\text{site}}}$ , where  $M/(N_A N)$  is the mass of the monomer, with  $N_A$  being the Avogadro's number (the number of molecules in a mole of a substance, ca.  $6.02 \times 10^{23}$ /mol).

$\Pi/(N_A k_B T)$  is generally expanded in a power series of  $c$ :

$$\frac{\Pi}{N_A k_B T} = \frac{c}{M} + A_2 c^2 + A_3 c^3 + \dots \quad (2.9)$$

In this virial expansion,  $A_2$  is the (osmotic) second virial coefficient. The meaning of  $A_2$  will become clearer when expressing it in the lattice model by comparing Eqs. (2.8) and (2.9):

$$A_2 = \left(\frac{1}{2} - \chi\right) N_A \nu_{\text{site}} \left(\frac{N}{M}\right)^2 \quad (2.10)$$

The above-mentioned Flory–Huggins interaction parameter  $\chi$  and the second virial coefficient  $A_2$  are important parameters representing the interaction between the polymer and the solvent molecules. A positive  $A_2$  (polymer in good solvent) deviates  $\chi$  upward compared to that of the ideal solution  $\left(\frac{\Pi_{\text{ideal}}}{(N_A k_B T)} = c/M\right)$ . When  $A_2 = 0$ , the solution in a wide range of concentrations is close to the ideal solution (the solvent is called as  $\theta$  solvent). When the solvent quality decreases,  $\chi$  increases. For  $\chi > 1/2$ ,  $A_2$  is negative. In poor solvent, the polymer chain becomes compacted, the solvent becomes unable to dissolve the polymer. According to Eq. (2.10), Table 2.1 summarizes the relationship between  $A_2$  and  $\chi$ .  $A_2$  is a measure of the nonideality of the polymer solution, also indicative of solvent–polymer interaction.  $A_2 = 0$  when the entropy of mixing compensates repulsive polymer–solvent interactions or attractive polymer–polymer interactions. For a given polymer–solvent system, the light scattering experiment at different concentrations of the polymer gives an estimate of  $A_2$ .

**Table 2.1** Relationship between  $A_2$  and  $\chi$  for polymer in solvent. Reproduction with permission from Teraoka (2002), Copyright 2002 John Wiley and Sons

$A_2$	$\chi$	Solvent quality	Chain conformation
+	$<1/2$	Good	Extended
0	$=1/2$	$\theta$	
-	$>1/2$	Poor	Compacted

**Table 2.2** Distinction of the freely jointed chain, freely rotating chain, and real chain. Reproduction with permission from Teraoka (2002), Copyright 2002 John Wiley and Sons

Model	Bond length	Bond angle	Torsion angle
Freely jointed chain	Fixed	Free	Free
Freely rotating chain	Fixed	Fixed	Free
Real chain	Fixed	Fixed	restricted

### 3 Chain Model (Teraoka 2002; Rubinstein and Colby 2003; Strobl 1997)

A chain with no interactions between monomers that are separated by a sufficient number of bonds along the chain is called an ideal chain. Real chains interact with both their solvent and themselves. In a real polymer chain, the effect that two monomers cannot occupy the same space is called an excluded volume effect, and the excluded volume plays a more important role in polymer solutions than it does in small molecule solutions. According to the lattice model, an ideal chain has no excluded volume allowing an overlap of the monomers. A real chain is a regular chain with an excluded volume. Although the ideal chain does not exist in reality, the model allows solving many polymer solution problems in a mathematically rigorous way extensively. In the ideal situation, the real chain behaves like an ideal chain, like in a dilute solution with a special kind of solvent called a theta solvent.

There are several classical models to describe ideal chains, such as freely jointed chain model, freely rotating chain model, restricted rotation chain model, equivalent freely jointed chain (Gaussian chain) model, and wormlike chain model. Each model makes different assumptions about the allowed values of torsion and bond angles. However, every model ignores interactions between monomers separated by a large distance along the chain. One of the simplest models of ideal chains is the freely jointed chain model with a constant bond length and no correlations between the directions of different bond vectors, while freely rotating chain model assumes all bond lengths and bond angles are fixed, and all torsion angles are equally likely and independent of each other. The distinction of freely jointed chain, freely rotating chain, and a real chain is described in Table 2.2. A simple unified description of all ideal polymers is provided by the equivalent freely jointed chain model (Kuhn model). The equivalent freely jointed chain has  $N_K$  freely jointed effective bonds of length  $L_K$ . The effective bonds constitute a Kuhn segment, and the length  $L_K$  is called the Kuhn segment length, characterizing the stiffness of a given polymer

**Fig. 2.3** Representation of a random coil (a) as a real chain; the circles represent the monomer units which are linked by the bonds (short thin lines); (b) in the Kuhn model (long thin lines), the long lines indicate the Kuhn segments; (c) as a wormlike chain (long smooth solid line).  
 Reproduction with permission from Denkinger and Burchard (1991), Copyright 1991 John Wiley and Sons



chain,  $N_K$  is the number of Kuhn segments per chain. The Kuhn model is shown in Fig. 2.3.

As far as the wormlike chain model is concerned, it is a freely rotating chain with a fixed bond angle but an unrestricted torsion angle, and the chain conformation is not zigzag but a smooth curve in a three-dimensional space, as shown in Fig. 2.3. A wormlike chain is specified by the persistence length  $L_p$  (in the wormlike chain model,  $L_p$  is equal to the average projection length along the initial direction of the polymer chain) and the contour length  $L_c$  (the length of the fully extended chain). When  $L_p \gg L_c$ , the chain is either sufficiently short or rigid; in the limit of  $L_c/L_p \rightarrow 0$ , the wormlike chain is a rod; for  $L_c \gg L_p$ , the chain is sufficiently long or flexible; in the limit of  $L_c \rightarrow \infty$ , the wormlike chain is the same as the ideal chain. In addition, the physical feature of the wormlike chain is that its Kuhn length  $L_K$  is twice the persistence length  $L_p$ .

## 4 Concentration Regimes: Dilute, Semi-dilute, and Concentrated

Polymer solutions are broadly classified into three regimes: dilute, semi-dilute, and concentrated (de Gennes 1980; Graessley 1980). Further, semi-dilute and concentrated solutions may be entangled or nonentangled. The polymer chains in the solution can be regarded as spherical coils. Figure 2.4 depicts three ranges of polymer concentration  $c$ :  $c \ll c^*$ ,  $c \cong c^*$ , and  $c \gg c^*$ , where  $c^*$  is the so-called overlap concentration of the polymer.

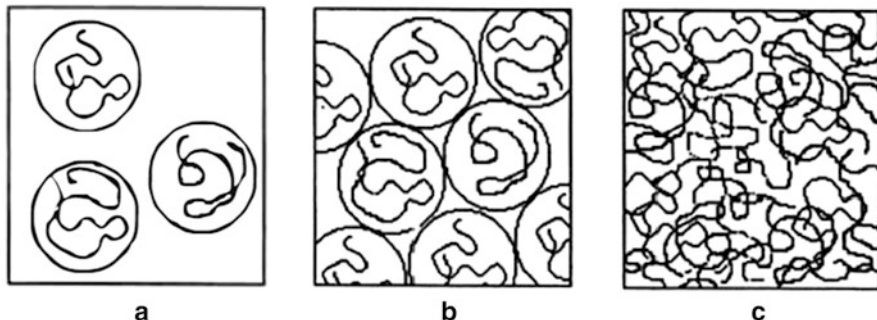


**Fig. 2.4** Concentration regimes for solutions of linear flexible polymers: dilute solution,  $c \ll c^*$ ; solution at the overlap concentration  $c \cong c^*$ ; semi-dilute solution,  $c \gg c^*$ . Reproduction with permission from de Gennes (1980), Copyright 1980 Cornell University Press

When  $c$  is below  $c^*$ , the solution is called dilute. At  $c \ll c^*$ , the coils are separated from each other, behaving more or less independently (Fig. 2.4a). The chains interact primarily with solvent molecules. Thus, the solution is close to an ideal solution.

As the concentration  $c$  increases, the coils become congested and eventually contact each other. At  $c^*$ , the whole volume of the solution is filled with these spheres (Fig. 2.4b). At  $c \gg c^*$ , chains are overlapped and entangled. In comparison with the chains in dilute solutions, their mobility is greatly reduced. The solution in this regime is called semi-dilute. The thermodynamic properties of the semi-dilute solutions are very different from those of an ideal solution extrapolated to the same concentration. In semi-dilute solutions, polymer chains have many other chains overlapping them though monomers are not congested. As a whole, the chains are congested, and the interactions between the chains are therefore strong. With a further increase in  $c$ , the overlaps become more serious.

The existence of the semi-dilute regime is characteristic of polymer solutions. The properties of semi-dilute solutions are different significantly from those of dilute solutions. With a tenfold increase in the concentration, the  $\Pi$  can easily increase by a factor of several hundred, whereas in the ideal solution, the osmotic pressure is proportional to  $c$ . Furthermore, in semi-dilute solutions, the overall chain motion is slow because of the entanglement of the chains. A semi-dilute solution of a high  $M_w$  polymer can barely flow due to its high viscosity. The  $\Pi$  and the time scale of motion depend heavily on concentration and  $M_w$  of the polymer.

The upper limit of the semi-dilute range is sometimes denoted by  $c^{**}$ . Above  $c^{**}$ , the monomers are congested, and sometimes the solution is called concentrated, in which each segment of the polymer chain does not have sufficient available space. Typically, the polymer volume fraction at  $c^{**}$  is between 0.2 and 0.3. For a polymer with a sufficiently high  $M_w$ , there is a broad range of concentrations between  $c^*$  and  $c^{**}$ . The semi-dilute regime is often specified by  $c^* \ll c < c^{**}$ .

### 4.1 Relationship Between Overlap Concentration $c^*$ and Chain Dimension

In a dilute solution where chains do not overlap, the whole single chain can be regarded as roughly being confined in a sphere of diameter  $R_F$ , the root-mean-square end-to-end distance ( $R_F$ ) of the chain, which follows

$$R_F \simeq L_K N_K^\nu \quad (2.11)$$

where  $\nu$  is an exponent that depends on solvent quality.  $\nu$  is 0.5 for neutral polymers in  $\theta$  solvent, 0.588 for neutral polymers in good solvent and polyelectrolytes with added salt, and 1 for polyelectrolytes in salt-free solutions (Lopez et al. 2017; Colby 2010).

The overlap concentration  $c^*$  is given by

$$c^* \simeq (M_w/M_0)/R_F^3 \sim (M_w/M_0)^{1-3\nu} \quad (2.12)$$

where  $M_0$  is the molar mass of a monomer. The exponent  $(1-3\nu)$  is  $-1/2$  (for  $\nu = 0.5$ ) for an ideal chain and  $-4/5$  (i.e.,  $-0.77$  for  $\nu = 0.59$ ) for a real chain.

Alternatively,  $c^*$  can be expressed as

$$c^* \simeq (M_w/N_A)/R_g^3 \quad (2.13)$$

where  $M_w/N_A$  is the mass of each chain, with  $N_A$  being the Avogadro's number,  $R_g$  is the chain dimension, i.e., the root-mean-square radius of gyration (the radius of the sphere in which the chain roughly occupies its space). For an ideal chain, the ratio of  $R_F$  to  $R_g$  is  $6^{0.5} \simeq 2.45$ .

Note that different from  $R_F$  that is defined for linear chains only,  $R_g$  is defined for any chain architecture, including nonlinear chains such as branched chains. Thus, Eq. (2.14) gives a universal measure for  $c^*$ .

For rigid-chain polymers in solution, the overlap concentration  $c^*$  is given by

$$c^* \simeq (M/N_A)/L_c^3 \quad (2.14)$$

where  $L_c$  is the contour length of a thin rod-like polymer chain.  $c^*$  of a rod chain is much lower as compared with a flexible linear chain.

Experimentally,  $c^*$  can also be determined as the reciprocal of another characteristic parameter of a polymer, the intrinsic viscosity  $[\eta]$  as will be discussed in the following.

## 4.2 Molecular Weight $M_w$ and Molecular Weight Distribution $M_w/M_n$

Compared with low molecular weight compounds, besides the difference of very high molecular weight of the polymer, another significant character of polymer is that nearly all of the polymer is a molecule mixture with a different degree of polymerization. This polydispersity is present, especially in plant polysaccharides. Polymers are usually polydisperse and have distribution in molecular weight. Some representative values are used as a typical molecular weight of the polymer, i.e., different average molecular weights (Lapasin et al. 1992).

Let the polymer consists of  $n_i$  chains of exact molecular weight  $M_i$ , in which the  $i$ th component has a degree of polymerization  $i$ . The difference between  $M_i$  and  $M_{i+1}$  is the mass of the repeating unit. The number-average molecular weight  $M_n$  is defined as

$$M_n = \frac{\sum_i n_i M_i}{\sum_i n_i} \quad (2.15)$$

The weight-average molecular weight  $M_w$  is defined as

$$M_w = \frac{\sum_i n_i M_i^2}{\sum_i n_i M_i} \quad (2.16)$$

Also used is the z-average molecular weight  $M_z$  further weighted with  $M_i$ :

$$M_z = \frac{\sum_i n_i M_i^3}{\sum_i n_i M_i^2} \quad (2.17)$$

The viscosity-average molecular weight  $M_\eta$  is defined as

$$M_\eta = \left( \frac{\sum_i n_i M_i^\alpha}{\sum_i n_i M_i} \right)^{\frac{1}{\alpha}} \quad (2.18)$$

where  $\alpha$  is the exponent of the Mark–Houwink equation. Generally,  $\alpha$  is in the range of 0.5–1.0, thus  $M_n < M_\eta < M_w$ , and  $M_\eta$  is closer to  $M_w$ .

For a perfectly monodisperse polymer,  $M_n = M_w = M_z$ . Otherwise,  $M_n < M_w < M_z$ . The ratio of  $M_w$  to  $M_n$  is used to express the polydisperse of the polymer. The ratio, often abbreviated as  $M_w/M_n$ , is called polydispersity index:

$$M_w/M_n = \frac{\sum_i n_i \sum_i n_i M_i^2}{\left( \sum_i n_i M_i \right)^2} \quad (2.19)$$

Unless the polymer is monodisperse,  $M_w/M_n > 1$ . A sample with a greater  $M_w/M_n$  has a broader molecular weight distribution.

One of the most important experimental techniques for determining the dilute solution behavior of polysaccharides is light scattering. Light scattering has been often used to characterize polymer chains in a solution, by which  $M_w$  and  $M_w/M_n$  as well as  $R_g$ , and  $A_2$  can be obtained, and furthermore, the information on the conformation of the polymer chain—whether it is spherical, random-coiled, or rod-like, can be recognized.

Size exclusion chromatography (SEC) coupled with multiangle laser light scattering (MALLS) has been widely used to characterize the molecular weight and molecular weight distribution of a polymer. Although SEC uses a flow system, the separation principle and the analysis are based on a static property of the polymer chains in solution. SEC sometimes is also called gel permeation chromatography (GPC) for organic solvent as mobile phase, or gel filtration chromatography (GFC) or aqueous GPC for aqueous mobile phase. GPC is, by now, one of the most routine and effective techniques for characterizing the polydispersity of polymeric materials. Some other techniques include the concentration gradient multiangle laser light scattering (CG-MALLS), asymmetric flow field flow fractionation-multiangle laser light scattering (AF4-MALLS), and horizontal agarose gel electrophoresis (AGE) (Zhang et al. 2015; Striegel and Timpa 1996).

### 4.3 Intrinsic Viscosity $[\eta]$

As it is known, one of the most salient features of macromolecules is the intense increment in viscosity that they produce when, even in minute amounts, they are dissolved in ordinary solvents. The viscosity intensifying effect, characterized by the intrinsic viscosity  $[\eta]$ , is extensively used for analysis or characterization of synthetic polymers, biomacromolecules, nanoparticles, and colloids. The  $[\eta]$  is a quantitative characteristic of a polymer, representing an increase in the solution viscosity when the polymer concentration is raised to some level. As expected, a polymer chain with a greater dimension has a larger  $[\eta]$ . In the Zimm model, it is assumed that as the polymer moves, it drags the solvent inside its pervaded volume with it (Rubinstein and Colby 2003). The Zimm model has the correct physics for  $[\eta]$ , which provides information about fundamental properties of the solute and its interaction with the solvent, and can be precisely related to the conformation of either linear or nonlinear flexible chains, wormlike macromolecules and micelles, and rigid particles of arbitrary shape.

The increment in the solution viscosity,  $\eta$ , with respect to that of the pure solvent,  $\eta_0$ , the relative viscosity, is the ratio  $\eta_r = \eta/\eta_0$ . The specific viscosity of a solution of concentration  $c$  is defined as  $\eta_{sp} = \frac{(\eta - \eta_0)}{\eta_0} = \eta_r - 1$ . The intrinsic viscosity  $[\eta]$  is defined as:

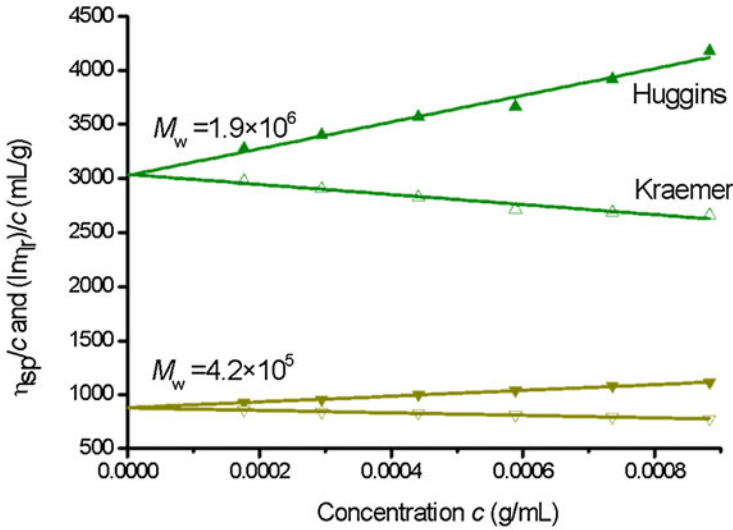


**Fig. 2.5** The specific viscosity  $\eta_{sp}$  (filled symbols) and the logarithm of relative viscosity  $\ln \eta_r$  over concentration  $c$  (open symbols) plotted and linearly fitted based on Huggins equation and Kraemer equation, respectively, vs. polymer concentration of hyaluronic acid in 0.1M NaCl at 25 °C

$$[\eta] = \frac{\eta_{sp}}{c} = \frac{\eta_r - 1}{c} \quad (2.20)$$

The  $[\eta]$  value can be obtained as the intercept in a linear least-squares fit of the reduced specific viscosity,  $\eta_{sp}/c$ , based on the Huggins equation. Alternatively, it can be obtained by linear extrapolation of the inherent viscosity,  $(\ln \eta_r)/c$  to zero concentration, according to the Kraemer equation (Goh et al. 2006a, b).

$$\frac{\eta_{sp}}{c} = [\eta] + K'[\eta]^2 c \quad \text{Huggins equation} \quad (2.21)$$

$$(\ln \eta_r)/c = [\eta] + K''[\eta]^2 c \quad \text{Kraemer equation} \quad (2.22)$$

where  $K'$  and  $K''$  are the Huggins and Kraemer constants, respectively. For a polymer in good solvents,  $K'$  value is within 0.3–0.4, and in  $\theta$  solvents its value is 0.5–0.8; and if aggregation of the polymers occurs,  $K'$  will be above 0.8. A relationship holds between the dimensionless constants  $K'$  and  $K''$ , for a random coil polymer,  $K' - K'' = 0.5$ .

A classical procedure for the determination of  $[\eta]$  consists of the measurement of solution viscosities at a series of concentrations, followed by extrapolation of  $\eta_{sp}/c$  to zero concentration. The measurements of  $[\eta]$  are usually made with Ubbelohde glass capillary viscometers that allow in situ dilution. It is often to display the  $[\eta]$  determination in a dual Huggins–Kraemer plot, as illustrated in Fig. 2.5.

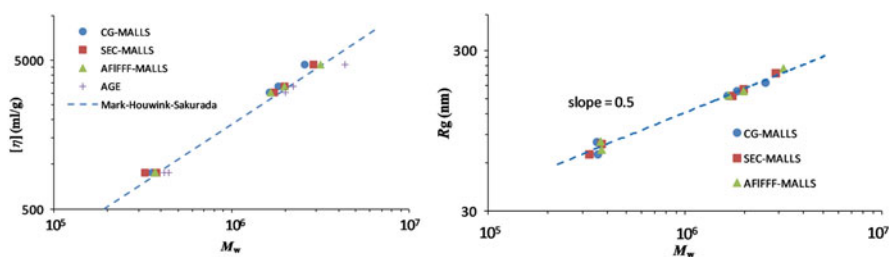


**Table 2.3** Molecular parameters of hyaluronic acid (HA) with different molecular weights and corn fiber gum (CFG)

Polysaccharide	$M_w \times 10^{-5}$	$[\eta]$ (dL/g)
CFG	3.33	1.48
HA-1	3.56	8.78
HA-2	12.9	12.89
HA-3	22.3	33.98

**Table 2.4** Molecular parameters of some branched polysaccharides

Polysaccharide	$M_w \times 10^{-5}$	$[\eta]$ (dL/g)
CFG	2.0	1.12
SSPS	8.5	0.34
GA	10.2	0.18
OSA-s	144	0.39

**Fig. 2.6** Comparison of  $[\eta]$  (left) and  $R_g$  (right) of HA measured by different characterization techniques as a function of molecular weight. Mark–Houwink relationship for  $M_w$  is included as a reference in dashed line using published  $K$  and  $\alpha$  parameters ( $K = 0.0336$  ml/g and  $\alpha = 0.79$ ) (Milas et al. 2001) (left figure). The dashed line (right figure) represents a linear fit of the data points. The solvent is 0.1 M NaCl solution. Reproduction with permission from Luan et al. (2011), Copyright 2011 Elsevier

The reciprocal of the intrinsic viscosity  $1/[\eta]$  can be used to represent the overlap concentration  $c^*$  of a given polymer.

The intrinsic viscosity  $[\eta]$  is a characteristic property of polysaccharide solutions. Table 2.3 compares the different molecular features of hyaluronic acid (HA) and corn fiber gum (CFG) with different  $M_w$ . Since HA macromolecules possess a linear chain structure, the  $[\eta]$  values of their solutions are high and increase significantly with  $M_w$ , for instance, from 8.78 dL/g for  $M_w = 3.56 \times 10^5$  (HA-1) to 33.98 dL/g for  $M_w = 2.23 \times 10^6$  (HA-3). Furthermore, when comparable  $M_w$  is considered, the  $[\eta]$  of HA-1 (8.78 dL/g) is much bigger than that of the highly branched CFG macromolecules (1.48 dL/g) (Zhang et al. 2015; Luan et al. 2011). In comparison with a linear chain of HA, like CFG, the  $[\eta]$  values of some other branched polysaccharides such as gum arabic (GA), octenyl succinate anhydride-modified starch (OSA-s), and soluble soybean polysaccharides (SSPS) that have densely branched structures are also very small, although their  $M_w$  can be quite high, e.g.,  $M_w = 1.02 \times 10^6$  for GA and even  $M_w = 1.44 \times 10^7$  for OSA-s (Table 2.4) (Jin et al. 2017).

**Table 2.5** Polydispersity index  $M_w/M_n$  of several hyaluronic acid (HA) samples measured by different techniques

Sample	SEC-MALLS	AFIFFF-MALLS	AGE
HA-1	1.2	1.2	1.2
HA-2	1.1	1.1	1.8
HA-3	1.5	1.5	1.4
HA-4	1.0	1.1	1.9

A scaling law of  $[\eta]$  with  $M_w$  known as the Mark–Houwink equation has been established for a number of polysaccharides, which will be discussed in the following.

Figure 2.6 and Table 2.5 display an example of measured results of hyaluronic acid by using different abovementioned characterization techniques (Goh et al. 2006a). This work compares the application of different techniques that provide consistent results on the conformational properties of HA in solutions (Luan et al. 2011).

The  $[\eta]$  is determined by dilute solution viscometry. When light scattering techniques and viscometry measurements are combined,  $M_w$  and  $M_w/M_n$ ,  $R_g$ ,  $A_2$ , and  $[\eta]$  can be determined, which provides a basis for understanding the solution properties of polysaccharides.

#### 4.4 Scaling of Viscosity

The scaling of various properties such as viscosity with polymer concentration as well as molecular weight governs much of the practical use of polymer in industry. A power-law type correlation between the zero-shear specific viscosity  $\eta_{sp,0}$  and the polysaccharide concentration  $c$  (Eq. 3.13) with different values of  $b$  in the two regimes can be applied (Lapasin et al. 1992). The use of zero-shear specific viscosity  $\eta_{sp,0}$  instead of zero-shear viscosity  $\eta_0$  removes the contribution of solvent viscosity.

$$\eta_{sp,0} = ac^b \quad (2.23)$$

For polymers with different primary structures but similar conformational characteristics, the range of  $b$  values in both regimes is relatively narrow. For the dilute regime, the exponent  $b$  is 1.0–1.5, and for the semi-dilute regime  $b$  is 3.5–4.5. Many polysaccharides such as hyaluronic acid, guar gum, carboxymethyl cellulose, carboxymethyl amylose, and  $\lambda$ -carrageenan can be fitted to this form of the master curve (Lapasin et al. 1992; Morris et al. 1981; Ren et al. 2003). Table 2.6 shows the exponent  $b$  values in the dilute and concentrated regimes. For most polysaccharides with the random coil conformation in concentrated solutions, typically,  $\eta_{sp,0} \sim c^{3.3}$ , similar to the theoretical prediction of  $\eta_{sp,0} \sim c^{3.75}$  by de Gennes (de Gennes 1980). This strong dependence of  $\eta_{sp,0}$  on  $c$  reflects the dominant role played by the intermolecular interactions.

**Table 2.6** Values of the exponent  $b$  in the dilute and concentrated regimes, and of  $c^*[\eta]$  for some polysaccharides in aqueous solution at 25 °C

Polymer	$b$ (dil.)	$b$ (conc.)	$c^*[\eta]$	Notes	Ref.
Hyaluronic acid	1.4	3.3	4	0.015 M NaCl, pH = 7	Morris et al. (1980, 1981)
	1.4	3.9	2.5	0.15 M NaCl, pH = 2.5	Morris et al. (1980, 1981)
	1.0	3.5	–	Salt-free	Yu et al. (2014)
	1.5	4.2	–	0.15 M NaCl	Yu et al. (2014)
Alginate	1.4	3.3	4	0.2 M NaCl, pH = 7	Morris et al. (1981)
	1.1	2.0	1.5	0.1 M NaCl	Krause et al. (2001)
	1.0	4.15	6	0.1 M NaCl	Milas (1996)
Xanthan	1.1	4.0	3.2	0.1 M NaCl	Gravanis et al. (1987)
			1	0.1 M NaCl	Esquenet and Buhler (2002), Brunchi et al. (2014)
	1.4	3.3	1.4	1 M KCl	Stokke et al. (1992)
Cellulose	0.7	2.2	1.4	[amim]Cl	Kuang et al. (2008)
Carboxymethyl cellulose	1.3	3.9	–	0.1 M NaCl, pH = 7	Ellis and Ring (1985)
	0.7– 1.3	3.5	1	Water ~ 2 M NaCl	Lopez et al. (2017)
Amylose	1.05	1.9	1	H <sub>2</sub> O (65 °C)	Ellis and Ring (1985)
Carboxymethyl amylose	1.4	3.3	4	0.5 M NaCl, pH = 7	Morris et al. (1981)
L-carrageenan	1.25	3.2	3.0	0.75 M NaCl	Pereira et al. (1982)
Guar gum	1.3	5.1	3.3	0.1 M urea	Robinson et al. (1982)
Pectin	1.2	3.3	–	0.1 M NaCl	Axelos et al. (1989)
Scleroglucan	1.4	3.3	1.4	1 M KCl	Stokke et al. (1992)
Schizophyllan	1.5	4.3	1.2	DMSO, $M_w = 8 \times 10^4$	Fang et al. (2010)
	1.6	2.8	4.3	DMSO, $M_w = 14.8 \times 10^4$	Fang et al. (2010)
Xyloglucan	1.3	4.0	1	H <sub>2</sub> O	Wang et al. (1997)
Colanic acid	1	3.6	–	0.2 M NaCl or 0.2 M CaCl <sub>2</sub>	Ren et al. (2003)

It is customary to refer to the generalized representation as suggested by Morris et al. (1981), consisting of a master curve of reference coordinates  $\eta_{sp,0}$  and  $c[\eta]$ , of which an example is shown in Fig. 2.7 for a series of polysaccharides. Moreover, the  $\eta_{sp,0} \sim c[\eta]$  plot associates the transition from a dilute to a concentrated regime to the coil overlap parameter  $c[\eta]$ . Thereby the approximate value of  $c^*$  can be obtained from  $[\eta]$  data. Experimental  $c^*[\eta]$  values for many polysaccharides such as hyaluronic acid, alginate, guar gum, carboxymethyl amylose,  $\lambda$ -carrageenan, and so on fall in the range 2.5–4, or even a wider range 1–6 (see Table 2.6), much higher

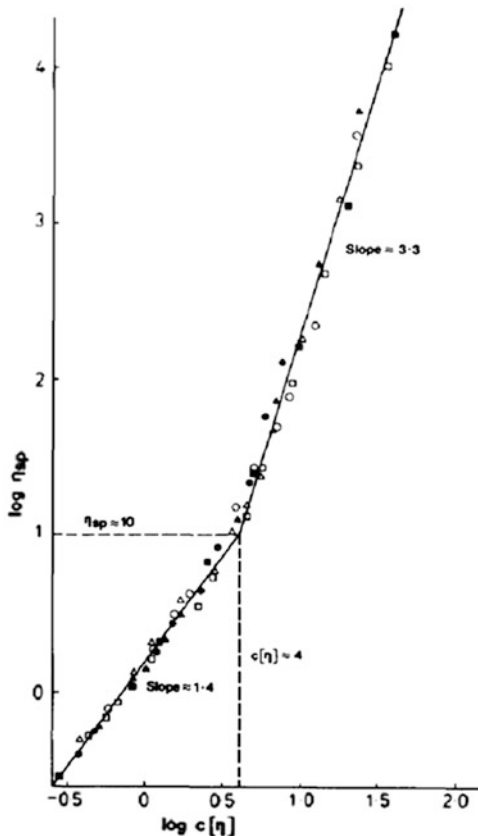


**Fig. 2.7** Zero-shear specific viscosity as a function of the coil overlap parameter,  $c[\eta]$ , for a range of random coil polysaccharides in salt solution at  $\text{pH} = 7$ . (open circle) dextran; (filled circle) carboxymethyl amylose (0.5M NaCl); (open triangle) high mannuronate alginate (0.2M NaCl); (filled triangle) high guluronate alginate (0.2M NaCl); (open square)  $\lambda$ -carrageenan (0.075M KCl); and (filled square) hyaluronic acid (0.015M NaCl). Reproduction with permission from Morris et al. (1981), Copyright 1981 Elsevier

than those calculated theoretically from the Simha critical condition of coil overlapping (Weissberg et al. 1951; Simha and Utracki 1975).

The addition of salt can strongly influence the correlation between  $\eta_{sp, 0}$  and the polyelectrolyte polysaccharide concentration  $c$ . Figure 2.8 shows the specific viscosity of semi-flexible polyelectrolytes of CMC ( $M_w = 3.2 \times 10^5$ ,  $\text{DS} \approx 1.2$ ) (Lopez et al. 2017) and hyaluronic acid ( $M_w = 1.8 \times 10^6$ ) (Yu et al. 2014) solutions as a function of polymer and added salt concentration, respectively. As seen in Fig. 2.8 (left), the solution viscosities of CMC decrease with increasing the salt concentration, the effect being more pronounced at lower CMC concentrations. In diluted regime, the scaling relationship between specific viscosity and CMC concentration changes from  $\eta_{sp} \sim c^{1.3}$  for  $c_{\text{salt}} = 2 \text{ M}$  to  $\eta_{sp} \sim c^{0.68}$  for the salt-free solution. However, a similar scaling relationship of  $\eta_{sp} \sim c^{3.5}$  is observed at high CMC concentration. In

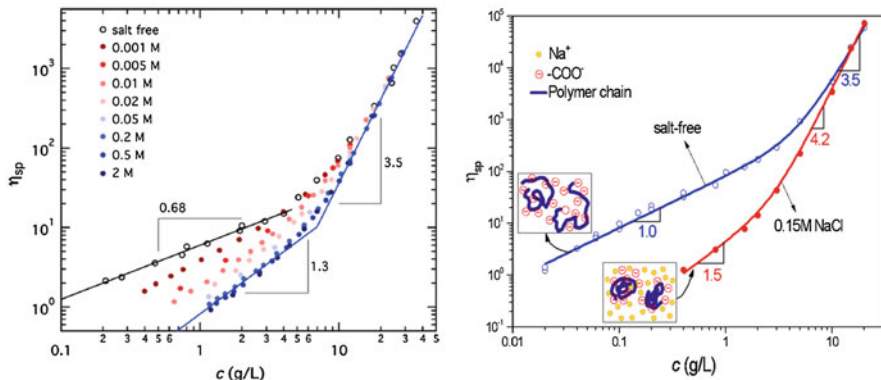


**Fig. 2.8** Double-logarithmic plot of specific zero-shear viscosity versus concentration of CMC (left). (Reproduction with permission from Lopez et al. (2017), Copyright 2017 ACS) and hyaluronic acid solution (right) (Reproduction with permission from Yu et al. (2014), Copyright 2014 Elsevier)

addition, the scaling of entanglement concentration in 0.01M and 0.1M NaCl shows a behavior of neutral polymer in good solvent, characteristic of highly screened polyelectrolyte solutions. For HA, salt-free HA solutions present a scaling relationship as  $\eta_{sp} \sim c^{1.0}$  (in dilute concentration region) and  $\eta_{sp} \sim c^{3.5}$  (in semi-dilute concentration region); for saline HA solutions (0.15M NaCl), the scaling exponents are 1.5 and 4.2, corresponding to dilute and semi-dilute concentration region, respectively (Fig. 2.8, right plot) (Yu et al. 2014).

## 5 Chain Conformational Analysis of Polysaccharides in Solution

### 5.1 Hydrodynamic Radius $R_h$ , Radius of Gyration $R_g$ , and Shape-Factor $\rho$

The size of polysaccharides in solution can be measured by a number of techniques, typically, the dynamic and static light scattering method. The root mean square radius of gyration  $R_g$ , obtained by static scattering experiments, serves as a practical overall parameter for coil dimensions. The effective hydrodynamic radius  $R_h$  of a macromolecule represents another useful quantity for polymer dimensions.

Based on the dynamic light scattering method,  $R_h$  can be calculated using the Einstein–Stokes equation:

$$R_h = \frac{k_B T}{6\pi\eta D} \quad (2.24)$$

where  $D$  is the diffusion coefficient,  $k_B$ ,  $T$ , and  $\eta$  are the Boltzmann constant, the absolute temperature, and the solvent viscosity, respectively.

Since the definitions of  $R_g$  and  $R_h$  are different, they do not normally coincide with a given polymer chain, although every single dimension can indicate the size of the coil. It has been recognized that chains cannot be properly described by just one of these radii. A combination of both quantities, the shape-factor or asymmetry-factor  $\rho$ , enables detailed insight into the chain architecture:

$$\rho = \frac{R_g}{R_h} \quad (2.25)$$

For rigid chains  $\rho \geq 2$ , for flexible random coils  $\rho$  is 1.5–1.8 (Kok and Rudin 1981; Harding et al. 1992) in a good solvent and 1.3 in a  $\theta$  solvent (Kok and Rudin 1981), and for compact spheres  $\rho$  is about 0.775 (Brant 1981). For instance, the  $\rho$  value of a  $\text{Na}^+$ -type deacetylated gellan gum in NaCl solution at 25 °C, existing as rigid double-stranded chains, is ca. 3, whereas it is ca. 2 at 40 °C at which gellan gum molecules take the conformation of single-stranded chains (Takahashi et al. 2004; Takahashi 1999). For high acyl gellan gum in DMSO solution,  $\rho$  value is 1.67, indicating a flexible structure of the chain (Kang et al. 2017).

Different from the hydrodynamic radius  $R_h$  defined from the diffusion coefficient  $D$ , another hydrodynamics-related radius, the viscometric radius  $R_\eta$  determined from the intrinsic viscosity (Flory 1953), is also an indicator of the coil size.

$$R_\eta = \left( \frac{3[\eta]M}{10\pi N} \right)^{1/3} \quad (2.26)$$

In comparison with  $R_h$ , theory predicts  $R_\eta/R_h$  values of ca. 1.2 (Lewis et al. 1991; Oono 1983; Pyun and Fixman 1964; Chong and Fixman 1965). For hyperbranched chains, experimentally  $R_\eta$  slightly smaller than  $R_h$  and their ratio  $R_\eta/R_h$  roughly remaining 0.95 have been reported (Li et al. 2013).

## 5.2 Scaling of $[\eta]$ , $R_g$ , and $A_2$ with $M_w$

### 5.2.1 Mark–Houwink Equation

Intrinsic viscosity  $[\eta]$  is a measure of the capacity of a polymer molecule to enhance the viscosity. It depends on the size and the shape of the polymer molecule. Experimentally, the intrinsic viscosity  $[\eta]$  of a polymer in solution is related to molecular weight  $M$  by the Mark–Houwink equation

$$[\eta] = KM^\alpha \quad (2.27)$$

where  $K$  is a constant of the unit of L/g, and  $\alpha$  is called a Mark–Houwink exponent. Figure 2.9 is an example of the molecular weight dependence of  $[\eta]$  for amylose in DMSO.

It is known that the value of parameters  $K$  and  $\alpha$  is different from polymer to polymer, related to the shape and chain structure of the macromolecule, and can

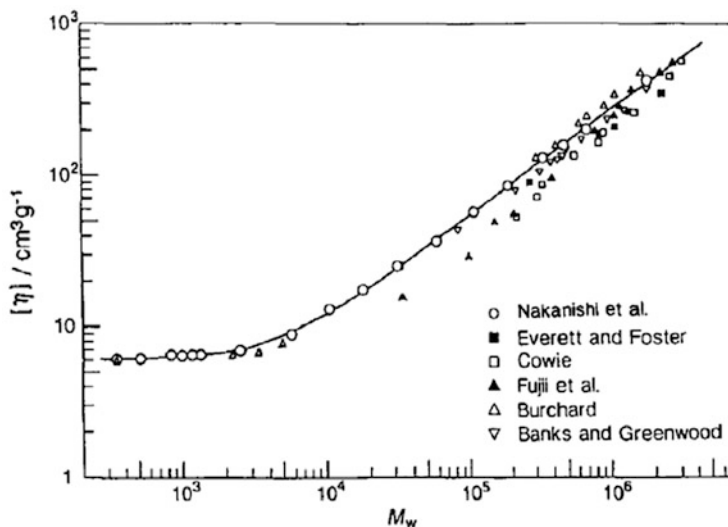


**Fig. 2.9** Molecular weight dependence of  $[\eta]$  for amylose in DMSO reported in the literature. Reproduction with permission from Norisuye (1996). Copyright 1996 Elsevier

**Table 2.7** Mark–Houwink exponents

Chain conformation	Solvent	$\alpha$
Linear flexible	$\theta$ solvent	0.5
Linear flexible	Good solvent	0.7–0.8
Rigid	–	>1

depend on the nature of solvent as well. In ordinary good solvents, the constants  $K$  and  $\alpha$  obtained are valid only within a rather limited range of  $M$ .

The polymer conformation parameter  $\alpha$  decreases with increasing molecular compactness. Apparently,  $\alpha$  is greater for a more extended conformation. The values of  $\alpha$  are 0–0.5, 0.5–0.8, and 0.8–1.8 for spherical, random coil, and rod conformations, respectively (Burchard 1996). Generally,  $\alpha$  is in the range of 0.5–0.8 for linear flexible polymer in good solvent (Miyaki et al. 1980; Lewis et al. 1991; Kniewske and Kulicke 1983). When the polymer chain is more extended, or presents as semi-stiff conformation, the  $\alpha$  value will be above 0.8 and even beyond. In the  $\theta$  solvent, the flexible chain has  $\alpha = 0.5$ . Note that the apparent  $\alpha$  exponent for hyperbranched polymers in a good solvent can be less than 0.5 (Lu et al. 2013). Values of  $\alpha$  are listed in Table 2.7 for some typical shapes and conformations of the polysaccharides.

The Mark–Houwink equation has been established as summarized in the following Table 2.8 for the given polysaccharide of hyaluronic acid and Table 2.9 for many other polysaccharides.

**Table 2.8** The reported  $K$  and  $\alpha$  of the Mark–Houwink equation for hyaluronic acid in literature

$M_w \times 10^4$	$K$ (mL/g)	$\alpha$	Solvent	$T$ (°C)	Ref.
>10	0.0279	0.763	0.1 M HCl	25	Cleland and Wang (1970)
	0.0228	0.816	0.2 M NaCl	25	
	0.0318	0.777	0.5 M NaCl	25	
7.70–170	0.036	0.78	0.2 M NaCl	25	Laurent et al. (1960)
80–220	0.033	0.79	0.1 M NaCl	25	Milas et al. (2001)
1–100	0.033	0.79	0.1 M NaCl	25	Luan et al. (2011)
10–100	0.057	0.75	0.15 M NaCl	25	Terbojevich et al. (1986)
<10	0.0013	1.056	0.15 M NaCl	37	Mendichi et al. (2003)
10–100	0.0339	0.778	0.15 M NaCl	37	
>100	0.395	0.604	0.15 M NaCl	37	
10–300	0.029	0.8	0.15 M NaCl	25	Li et al. (1997)
<100	0.00346	0.779	0.15 M NaCl	25	Bothner et al. (1988)
>100	0.0397	0.601	0.15 M NaCl	25	
–	0.029	0.8	0.15 M NaCl	25	Wedlock et al. (1983)
–	0.039	0.77	0.15 M NaCl	30	Ueno et al. (1988)
180–1250 (hylan form)	0.033	0.77	0.15 M NaCl	25	Al-assaf et al. (1995)
40–200	0.0508	0.716	0.2 M NaCl	20	Gura et al. (1998)
40–270	0.0199	0.829	0.2 M NaCl	25	Yanaki and Yamaguchi (1994)
42–140	0.0278	0.78	0.1 M NaNO <sub>3</sub>	25	Soltes et al. (2002)
1–7.2	0.0003	1.2	0.2 M PBS pH 7.3	37	Shimada and Matsumura (1975)
31–150	0.057	0.76	0.2 M PBS pH 7.3	37	

### 5.2.2 Scaling of $R_g$ with $M_w$

Table 2.10 shows the molecular weight dependence of  $R_g$  of hyaluronic acid in 0.1M NaCl and a comparison of the magnitude of  $R_g$  for this linear polymer and the branched polysaccharide of CFG with a similar  $M_w$ . Similar to the impact of  $M_w$  on the  $[\eta]$  (Table 2.4), the  $R_g$  values of the linear hyaluronic acid increase significantly with  $M_w$ , from 81 nm for  $M_w = 3.56 \times 10^5$  (HA-1) to 167 nm for  $M_w = 2.23 \times 10^6$  (HA-3), and for a comparable  $M_w$ , the  $R_g$  of HA-1 (81 nm) is much bigger than that of the high branched CFG macromolecules (24 nm) (Zhang et al. 2015).

$R_g$  can also be related to  $M_w$  by the relation:

$$R_g = kM_w^{\alpha'} \quad (2.28)$$

where  $k$  and  $\alpha'$  are constants for a given polymer at a given temperature in a given solvent. Usually,  $\alpha'$  of  $\sim 0.7$  indicates a relatively stiff rod-like conformation,  $\sim 0.6$  for



**Table 2.9** The parameters of the Mark–Houwink equation for various polysaccharides in different solutions at different temperatures

Polysaccharide	Solvent	$T$ (°C)	$M_w \times$ $10^{-4}$	$K \times$ $10^4$ (mL/ g)	$\alpha$	Ref.
Amylose	1 M KOH	25	22–310	118	0.89	Cowie (1960)
	DMSO	25	22–310	125	0.87	
	EDA	25	22–310	1550	0.70	
Cellulose	DMAc-LiCl	30	12.5–70	1.278	1.19	McCormick et al. (1985b)
	EMIMAc	0–100	3–100	–	0.4–0.6	Gericke et al. (2009)
Carboxymethyl cellulose	0.2 M NaCl	30	0.21–0.52	43.0	0.74	da Silva et al. (2018)
	0.01 M NaCl	25	21–229	87.76	0.93	Clasen and Kulicke (2001)
Methyl cellulose	0.1 M NaNO <sub>3</sub>	25	–	800	0.92	Schittenhelm and Kulicke (2000)
Sulfoethyl cellulose	0.1 M NaNO <sub>3</sub>	25	56	1.74	1.19	
Carboxymethylsulfoethyl cellulose	0.1 M NaNO <sub>3</sub>	25	135.5	65.8	0.91	
Hydroxyethylsulfoethyl cellulose	0.1 M NaNO <sub>3</sub>	25	29.4–30.3	230	0.80	
Hydroxyethyl cellulose	0.1 M NaNO <sub>3</sub>	25	–	410	0.73	
Hydroxypropyl cellulose	0.1 M NaNO <sub>3</sub>	25	–	420	0.68	
Hydroxyethylmethyl cellulose	0.1 M NaNO <sub>3</sub>	25	–	1700	0.60	
Hydroxypropylmethyl cellulose	0.1 M NaNO <sub>3</sub>	25	–	3600	0.53	
	H <sub>2</sub> O	25	49–380	850	0.51	
Cellulose acetate	DMAc	25	4.55–14.5	1900	0.60	Kamide et al. (1981)
	DMSO	25	4.55–14.5	1700	0.61	
	H <sub>2</sub> O	25	4.55–14.5	2000	0.60	
	Formamide	25	4.55–14.5	2000	0.60	
	0.01 M NaCl	25	21–229	87.76	0.93	
Pullulan	H <sub>2</sub> O	25	0.5–240	221	0.66	Kato et al. (1984)
	H <sub>2</sub> O	25	2.08–123.8	236	0.658	Kawahara et al. (1984)
	0.1 M NaCl	25	4.8–150	1.79	0.67	Kato et al. (1983)
	H <sub>2</sub> O	25	0.53–101.5	–	0.675	Nishinari et al. (1991)

(continued)

**Table 2.9** (continued)

Polysaccharide	Solvent	$T$ (°C)	$M_w \times$ $10^{-4}$	$K \times$ $10^4$ (mL/ g)	$\alpha$	Ref.
Chitosan	0.2 M CH <sub>3</sub> COOH/ 0.1 M CH <sub>3</sub> COONa	30	94–251	1.04– 168	0.81– 1.12	Wang et al. (1991)
	0.1 M AcOH/ 0.2 M NaCl	25	4.78– 63.01	18.1	0.93	Roberts and Domszy (1982)
	0.1 M AcOH/ 0.02 M NaCl	25	4.78– 63.01	30.4	1.26	
	0.2 M AcOH/ 0.1 M AcONa/4 M urea	25	–	893	0.71	Lee (1975)
	0.3 M AcOH/ 0.2 M AcONa (DA = 2%)	25	20	820	0.76	Rinaudo et al. (1993)
	0.3 M AcOH/ 0.2 M AcONa (DA = 0–3%)	25	6–28.5	790	0.79	Brugnerotto et al. (2001)
	0.3 M AcOH/ 0.2 M AcONa (DA = 12%)	25	6–28.5	740	0.80	
	0.3 M AcOH/ 0.2 M AcONa (DA = 22– 24%)	25	6–28.5	700	0.81	
	0.3 M AcOH/ 0.2 M AcONa (DA = 40%)	25	6–28.5	630	0.83	
	0.3 M AcOH/ 0.2 M AcONa (DA = 56– 61%)	25	6–28.5	570	0.825	
0.02 M ace- tate buffer/0.1 M NaCl	25	9.5–18	843	0.92	Berth and Dautzenberg (2002)	
Chitin	2.77 M NaOH	20	10–120	1000	0.68	Einbu et al. (2004)
	DMAc/5% LiCl	25	9–51	24	0.69	Terbojevich et al. (1988)
	DMAc/5% LiCl	30	8–71	76	0.95	Poirier and Charlet (2002)
Agarose	0.75 M NaSCN	35	8–14	700	0.72	Rochas and Lahaye (1989)

(continued)

**Table 2.9** (continued)

Polysaccharide	Solvent	$T$ (°C)	$M_w \times 10^{-4}$	$K \times 10^4$ (mL/g)	$\alpha$	Ref.
Alginate	0.01 M NaCl	20	10–270	0.048	1.15	Smidsrød (1970)
	0.1 M NaCl	20	10–270	0.20	1.0	
	1 M NaCl	20	10–270	0.91	0.87	
	$I \sim \infty$	20	10–270	1.20	0.84	
Lentinan	0.1 M NaOH	25	14.5–113	51	0.81	Zhang et al. (2005)
Curdlan	DMSO	25	5–100	1.60	0.74	Futatsuyama et al. (1999)
	DMSO	25	5.1–192	4.80	0.65	Zhang and Nishinari (2009)
	H <sub>2</sub> O:cadoxen (1:1)	25	7–68	2.50	0.65	Hirano et al. (1979)
	0.3 M NaOH	25	5.3–200	79.0	0.78	Nakata et al. (1998)
Konjac glucomannan	H <sub>2</sub> O	25	4.9–120	5.30	0.78	Prawitwong et al. (2007)
	Cadoxen	25	26–69	3.55	0.69	Kohyama (1993)
Methyl-konjac glucomann	H <sub>2</sub> O	30	16–120	6.37	0.74	Kishida et al. (1978)
Gellan gum	0.025 M TMACl	25	1.3–6.2	74.8	0.91	Drevetton et al. (1996)
	0.01 M NaCl	25	6.8	1660	0.89	Masuelli (2014)
Na <sup>+</sup> high acyl gellan gum	DMSO	25	42–101	11.6	0.67	Kang et al. (2017)
Xanthan gum	0.01 M NaCl	25	170	0.046	1.41	Masuelli (2014)
	0.1 M NaCl	25	30–1000	1.70	1.14	Milas et al. (1985)
Pectin	PBS	20–60	8.45–10.28	0.234	0.8224	Kar and Arslan (1999)
	0.0155 M NaCl	25	2.3–7.1	1.4	1.34	Owens et al. (1946)
$\kappa$ -carrageenan	0.028 NaCl	20	0.58–46	77.8	0.90	Vreeman et al. (1980)
	0.118 NaCl	20	0.58–46	88.4	0.86	
	0.218 NaCl	20	0.58–46	209	0.78	
	$I \sim \infty$	20	0.58–46	520	0.67	
	0.1 M NaCl	25	25–40	30	0.95	Kalitnik et al. (2013)
$\lambda$ -carrageenan	0.1 M NaCl	20	34–87	–	0.6	Almutairi et al. (2013)

(continued)

**Table 2.9** (continued)

Polysaccharide	Solvent	$T$ (°C)	$M_w \times 10^{-4}$	$K \times 10^4$ (mL/g)	$\alpha$	Ref.
Guar gum	0.1 M urea	25	44–165	3.8	0.72	Robinson et al. (1982)
	H <sub>2</sub> O	25	38–140	7.76	0.98	Doublier and Launay (1981)
Dextran	0.1 M NaCl	25	0.94–519.3	13.6	0.47	Kato et al. (1983)
Schizophyllan	0.01 M NaOH	25	10.7–568	–	1.1, 1.8	Kashiwagi et al. (1981b)
	DMSO	25	10.7–568	231.4	0.69	

**Table 2.10** The values of  $R_g$  of hyaluronic acid (HA) with different molecular weight and corn fiber gum (CFG)

Polysaccharide	$M_w \times 10^{-5}$	$R_g$ (nm)
CFG	3.33	24
HA-1	3.56	81
HA-2	12.9	120
HA-3	22.3	167

flexible random coils in a good solvent, and  $\sim 0.5$  for flexible random coils and  $\sim 0.33$  for compact coils in a  $\theta$  solvent. For instance, for pullulan in water,  $\alpha' = 0.568$  (De Nooy et al. 1996), and in the  $\theta$  solvent of ethylene glycol,  $\alpha' = 0.5$  (Nordmeier 1993).

Table 2.11 summarizes the parameters in the relationship between the radius of gyration and the molecular weight for a series of polysaccharides and their derivatives.

### 5.2.3 Scaling of $A_2$ with $M_w$

The  $A_2$  value directly reflects the degree of interactions between polymers and solvents. For polymers in a good solvent the value of  $A_2$  is positive; and  $A_2 \leq 0$  for polymers in a  $\theta$  solvent or aggregation. Usually,  $A_2$  decreases with increasing  $M_w$  as well as  $R_g$ , and obeys the following scaling rule:

$$A_2 = KM_w^{-n} \quad (2.29)$$

where  $K$  and  $n$  are constants for a given polymer at a given temperature in a given solvent. The  $n$  value is normally 0.2–0.3 at a good solvent limit (Takahashi et al.

**Table 2.11** The parameters of Eq. (3.4) for the selected list of polysaccharides

Polysaccharide	Solvent	$T$ (°C)	$M_w \times 10^{-4}$	$k \times 10^4$	$\alpha'$	Ref.
Hyaluronic acid	0.1 M NaCl	25	1–100	–	0.5	Luan et al. (2011)
	0.2 M NaCl	25	66.7–423	–	0.5	Takahashi et al. (2003)
	0.15 M NaCl	25	600–800	–	0.57–0.60	Cowman and Matsuoka (2005)
Amylose	1 M KOH	70	141–223	–	0.80	Ahmad et al. (1999)
	0.1 M KOH	25	1.2–120	–	0.62	Roger et al. (2000)
	H <sub>2</sub> O	25	24–120	–	0.52	
Amylopectin	1 M KOH	70	141–223	–	0.58	Ahmad et al. (1999)
Cellulose	DMAc-LiCl	30	12.5–70	–	–	McCormick et al. (1985b)
Cellulose diacetate	DMAc	25	19.4	680	0.53	Muroga et al. (1987)
	THF	25	19.4	299	0.56	
	Acetone	25	19.4	7390	0.31	
Cellulose triacetate	DMAc	25	8.0	463	0.55	Schittenhelm and Kulicke (2000)
Methyl cellulose	0.1 M NaNO <sub>3</sub>	25	–	440	0.55	
Sulfoethyl cellulose	0.1 M NaNO <sub>3</sub>	25	56	120	0.65	
Carboxymethyl cellulose	0.1 M NaNO <sub>3</sub>	25	–	66	0.70	
Hydroxyethylsulfoethyl cellulose	0.1 M NaNO <sub>3</sub>	25	29.4–30.3	380	0.58	
Hydroxyethyl cellulose	0.1 M NaNO <sub>3</sub>	25	–	260	0.59	
	0.1 M NaNO <sub>3</sub>	25	–	330	0.55	
Hydroxypropyl cellulose	0.1 M NaNO <sub>3</sub>	25	–	250	0.56	
	0.1 M NaNO <sub>3</sub>	25	–	660	0.51	
Hydroxyethylmethyl cellulose	0.1 M NaNO <sub>3</sub>	25	–	380	0.53	
	0.1 M NaNO <sub>3</sub>	25	–	260	0.59	
hydroxyethylethyl cellulose	0.1 M NaNO <sub>3</sub>	25	–	140	0.63	
Hydroxypropylmethyl cellulose	0.1 M NaNO <sub>3</sub>	25	–	470	0.51	
Pullulan	H <sub>2</sub> O	25	6.5	164	0.57	
	H <sub>2</sub> O	25	0.5–240	147	0.58	Kato et al. (1984)
	0.1 M KOH	25	0.62–130	–	0.62	Roger et al. (2000)
	H <sub>2</sub> O	25	0.6–130	–	0.58	
Chitin	2.77 M NaOH	20	10–120	1700	0.46	Einbu et al. (2004)
	DMAc-LiCl	25	9–51	240	0.69	Terbojevich et al. (1988)

(continued)

**Table 2.11** (continued)

Polysaccharide	Solvent	$T$ (°C)	$M_w \times 10^{-4}$	$k \times 10^4$	$\alpha'$	Ref.
Chitosan	0.2 M $\text{NH}_4\text{OAc}$	25	3.6–46	299	0.59	Christensen et al. (2008)
	0.02 M acetate buffer/0.1 M NaCl	25	9.5–18	750	0.55	Cowie (1960)
Lentinan	0.1 M NaOH	25	14.5–113	2300	0.58	Zhang et al. (2005)
Konjac glucomannan	$\text{H}_2\text{O}$	25	4.9–120	277	0.60	Prawitwong et al. (2007)
$\text{Na}^+$ high acyl gellan	DMSO	25	42–101	206	0.61	Kang et al. (2017)

*DMAc* dimethylacetamide, *THF* Tetrahydrofuran

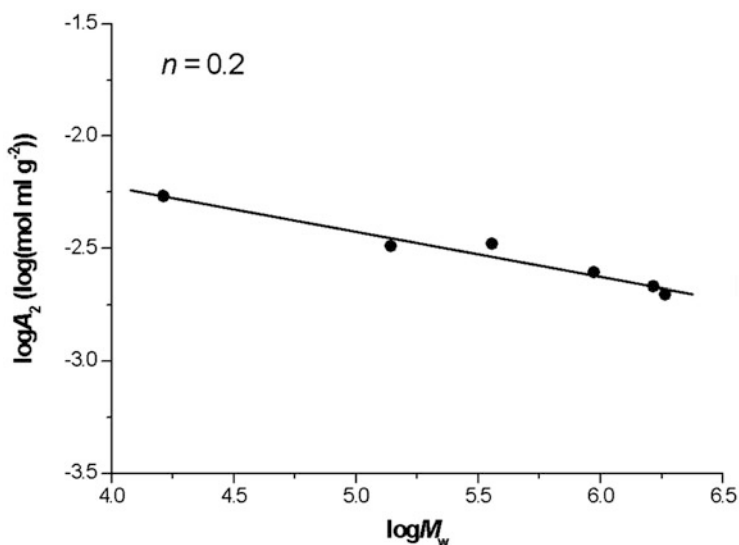


**Fig. 2.10** Relationship between  $A_2$  and  $M_w$  for hyaluronic acid in 0.1M NaCl. Reproduction with permission from Luan et al. (2011), Copyright 2011 Elsevier

2003; Cowman and Matsuoka 2005); and a higher value ( $>0.5$ ) is a characteristic of branched structures (Tao et al. 2007). For, example,  $n = 0.61$ ,  $0.80$ ,  $0.66$  for amylopectin, glycogen and dextran, respectively (Burchard 2001). The scaling rule holds only in the semi-dilute regime.

$A_2$  is in the range of  $1.0 \times 10^{-3}$  to  $3.5 \times 10^{-3}$  mol·ml  $\text{g}^{-2}$  for hyaluronic acid in 0.1M NaCl, depending on its  $M_w$  (Luan et al. 2011). Figure 2.10 shows the power-law relationship linking  $A_2$  and  $M_w$  for a series of hyaluronic acid samples. The obtained exponent of  $n = 0.2$  is in very good agreement with the predicted value of

0.2 (Cowman and Matsuoka 2005) as well as the experimental value of 0.19 (Takahashi et al. 2003).

A famous relation between intrinsic viscosity  $[\eta]$ , coil size  $R_g$ , and molar mass  $M$ , for linear chains, is known as the Fox–Flory equation (Rubinstein and Colby 2003)

$$[\eta] = \Phi \left( \frac{R_g^3}{M} \right) \quad (2.30)$$

where  $\Phi$  is the Flory hydrodynamic constant, which is roughly related to the chain draining in solution.  $\Phi = 2.5 \times 10^{23}/\text{mol}$  is a universal constant for all polymer-solvent systems, and in theta solvent  $\Phi = 2.84 \times 10^{23}/\text{mol}$ .

In the Zimm model, the following relationship among these physical parameters can be established (Lopez et al. 2017):

$$[\eta] \sim \frac{N_A R_g^2 R_h}{M_w} \quad (2.31)$$

The main property of the above relationship is that the ratio of  $([\eta]M_w)/(N_A R_h R_g^2)$  is a constant. For high acyl gellan gum chains in the good solvent of DMSO, a value of ca. 4 for the ratio of  $([\eta]M_w)/(N_A R_h R_g^2)$  is found (Kang et al. 2017).

#### 5.2.4 Persistence length ( $L_p$ )

Polysaccharides may exhibit different conformations in solutions. The wormlike chain model is famous for describing the chain flexibility in solutions.

The persistence length ( $L_p$ ) is a key parameter characterizing the flexibility of linear polymers and therefore their conformation. The value of  $L_p$  for a given polymer can be taken as a measure of the chain stiffness. It is notable that the values of  $L_p$  of various polysaccharides may greatly vary as a function of  $M_w$ , solvent conditions, and characterization techniques, also strongly depending on the calculation methods. There are various methods to determine  $L_p$ .  $L_p$  can be derived from the light scattering data by Benoit–Doty treatment of the wormlike chains (Benoit and Doty 1953).  $L_p$  may also be obtained by using the  $M_w$  dependence of the  $[\eta]$  from the slope in the Bushin–Bohdanecky plot based on the Yamakawa–Fujii–Yoshizaki (YFY) theory (Bohdanecky 1983).

A summary and comparison of  $L_p$  for various polysaccharides are given in Table 2.12. The well-known  $L_p$  values for DNA are also shown for comparison.

It is shown in Table 2.12 that the  $L_p$  values of the stiff-chains are much larger than those of the flexible random chains. Generally speaking, as the values of  $L_p$  increase, the macromolecules become stiffer, more extended, indicating a stretching semi-flexible chain. The quality of solvent undoubtedly has a significant effect on the polymer conformation. While an  $L_p$  value is 5.2 nm for  $K^+$  acetylated gellan in pure

**Table 2.12** Persistence length,  $L_p$ , for various polysaccharides

Sample	Solvent	$T$ (°C)	$M_w \times 10^{-4}$	$L_p$ (nm)	Ref.
Na <sup>+</sup> high acyl gellan	50 mM NaNO <sub>3</sub> /DMSO	25	42.0–100.7	8–10	Kang et al. (2017)
K <sup>+</sup> acetylated gellan	DMSO	25	220	5.2	Brownsey et al. (1984)
	90% DMSO	25	160	11.64	
K <sup>+</sup> deacetylated gellan	90% DMSO	25	88–96	13.14–15.54	
Na <sup>+</sup> deacetylated gellan	25 mM NaCl	40	3.47–11.5	9.4	Takahashi et al. (2004)
		–	9.47	17	Takahashi (1999)
	75 mM NaCl	25	23.8	98	Okamoto et al. (1993)
		–	43.4	102	Dentini et al. (1988)
Konjac glucomannan	Phosphate buffer	20	24–74	13	Kök et al. (2009)
Amylose	DMAC-3% LiCl	25	50–200	3.26	Cao et al. (2000)
	H <sub>2</sub> O	25	–	1.5	Roger et al. (2000)
	0.1 M KOH	25	–	1.6	
	D <sub>2</sub> O	25	30–80	1.9–3.2	
	KOD	25	–	4.2	
	DMSO	25	0.56–170	1.2	Nakanishi et al. (2002)
Cellulose	9%, 10% LiCl/DMAC	25, 30	1.65–70	11–25	Terbojevich et al. (1985); McCormick et al. (1985a)
Carboxymethyl cellulose	0.02 M, 0.1 M NaNO <sub>3</sub>	25	12–120	12–16	Hoogendam et al. (1998)
	High salt concentrations	–	–	5.0	
	water/cadoxen	–	–	8.5	
Cellulose diacetate	DMAC	25	19.4	139	Muroga et al. (1987)
Cellulose diacetate	THF	25	19.4	39	
Cellulose diacetate	Acetone	25	19.4	77	
Cellulose triacetate	DMAC	25	8.0	59	
Galactomannan	H <sub>2</sub> O	20	–	8–10	Patel et al. (2006), Morris et al. (2008a)
Pectin	0.1 M NaCl	20	15–18	10–13	Morris et al. (2008b)
Hyaluronic acid	0.15 M NaCl	37	4–550	6–8	Robinson et al. (1982)
Curdlan	DMSO	25	5.1–192	5.81	Zhang and Nishinari (2009)
Lentinan	0.2 M LiCl/DMSO	25	21.7–84.7	6.0	Wang et al. (2012)
		25	–	5.1	
	DMSO	25	19.1–53.8	4.8	Wang and Zhang (2009)

(continued)



**Table 2.12** (continued)

Sample	Solvent	$T$ (°C)	$M_w \times 10^{-4}$	$L_p$ (nm)	Ref.
Chitin	8% NaOH/4% urea	25	215.6	4	Li et al. (2010)
	2.77 M NaOH	20	10–120	11.5–13	Einbu et al. (2004)
	5% LiCl/DMAc	25	9–51	15–50	Terbojevich et al. (1988)
Chitosan	265 mM HAc/ 200 mM NH <sub>4</sub> Ac	25	3.27– 42.66	9.5	Kang et al. (2018)
Pullulan	H <sub>2</sub> O	25	6.5 ( $M_n$ )	1.2–1.9	Muroga et al. (1987)
	H <sub>2</sub> O	25	10–100	1.4–3.1	Adolphi and Kulicke (1997)
Alginate	H <sub>2</sub> O	25	–	9 ± 1	Stokke and Brant (1990)
	0.001–0.1 M NaNO <sub>3</sub>	22.5	95.9	4–6	Muroga et al. (1987)
	0.2 M NH <sub>4</sub> OAc	25	3.6–46	12	Christensen et al. (2008)
Single-stranded xanthan	0.02 mM NaCl	25	–	30 ± 4	Stokke and Brant (1990)
Double-stranded xanthan	0.02 mM NaCl	25	–	68 ± 7	
Double-helix xanthan	0.1 M NaCl	25	740– 7400	120	Sato et al. (1984)
<i>ι</i> -carrageenan (random coil)	0.1 M NaCl	25	–	22.6	Schefer et al. (2014)
<i>ι</i> -carrageenan (helix)	0.1 M NaCl	25	–	26.4	
Succinoglycan	0.01 M NaCl	25	35.4– 71.4	50	Nakanishi and Norisuye (2003)
Scleroglucan	H <sub>2</sub> O	25	–	80 ± 10	Stokke and Brant (1990)
Schizophyllan	0.01 M NaOH	25	10.7–568	180 ± 30	Kashiwagi et al. (1981a)
	H <sub>2</sub> O	25	50–570	100–200	Chun and Park (1994)
DNA: single-stranded	8 M urea	21	2800– 53860 bases	4	Tinland et al. (1997)
Double-stranded	0.1 M NaCl	20, 25	–	58–68	Norisuye (1993)

DMSO (Brownsey et al. 1984), it is 11.64 nm for this polysaccharide in 90% DMSO aqueous solution at 25 °C. Significantly different values of  $L_p$  are also reported for chitin in different solvents as 4 nm in 8% NaOH/4% urea (Li et al. 2010), 11.5–13 nm in 2.77M NaOH (Einbu et al. 2004), and 15–50 nm in 5% LiCl/DMAc (Terbojevich et al. 1988).

### 5.2.5 Chain Stiffness Parameter $B$

Smidsrød and Haug (1971) proposed an empirical method to determine the empirical chain stiffness parameter  $B$  for polyelectrolyte polysaccharides:

$$B = S/[\eta]_{0.1}^{\nu} \quad (2.32)$$

where  $S$  is a constant,  $[\eta]_{0.1}$  is the  $[\eta]$  at 0.1M NaCl ionic strength, and the exponent  $\nu$  usually ranges from 1.2 to 1.4.

A number of polysaccharides contain acidic groups (typically  $-\text{COOH}$ ), which are essentially polyelectrolytes. Their  $[\eta]$  value decreases with increasing ionic strengths of the solution according to the following relation:

$$[\eta] = [\eta]_{\infty} + SI^{-1/2} \quad (2.33)$$

where  $[\eta]_{\infty}$  is the  $[\eta]$  at infinite ionic strength, and  $I$  is the ionic strength of the solution. The  $[\eta]_{\infty}$  and  $S$  values can be derived from the intercept and the slope of the linear functions by the measurement of the  $[\eta]$  at different  $I$ , of which Figs. 2.11 and 2.12 are examples for hyaluronic acid (Luan et al. 2011) and chitosan (Gooday et al. 1986), respectively.

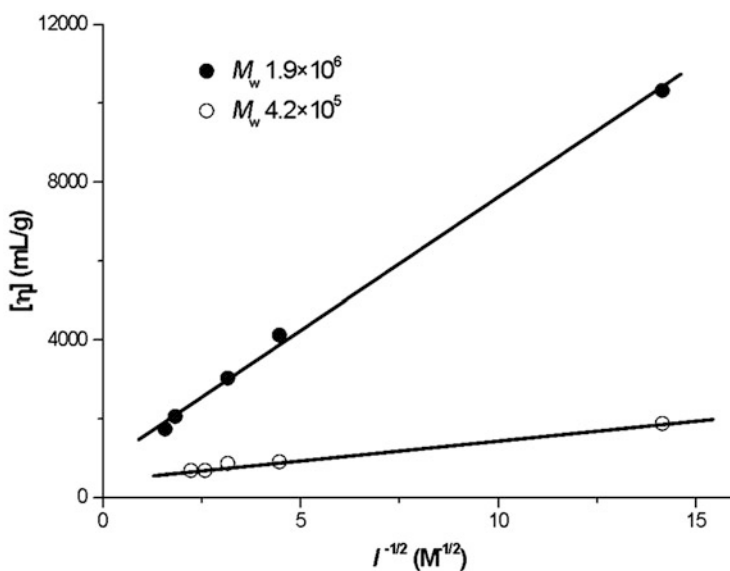
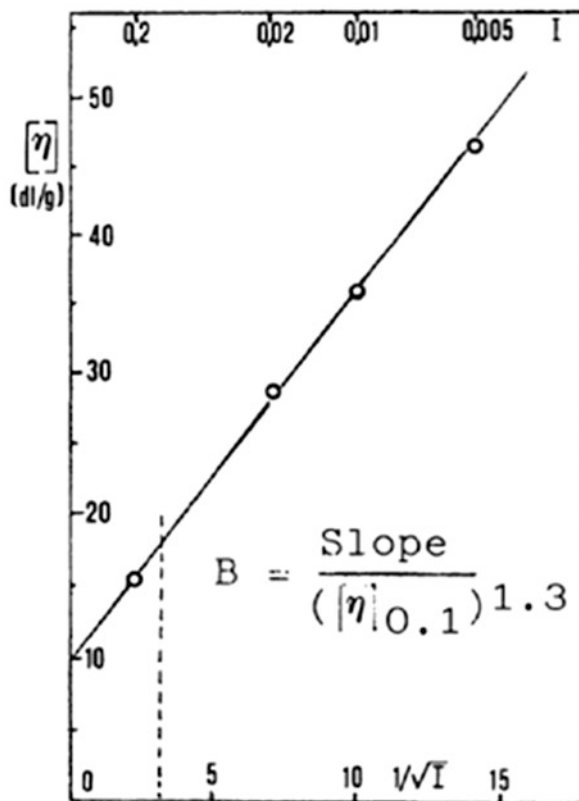


**Fig. 2.11** Plots of intrinsic viscosity  $[\eta]$  versus  $I^{-1/2}$  for hyaluronic acid in aqueous solution (NaCl as a supporting electrolyte). Reproduction with permission from Luan et al. (2011), Copyright 2011 Elsevier

**Fig. 2.12** Plot of intrinsic viscosity  $[\eta]$  versus  $I^{-1/2}$  for chitosan with the degree of acetylation of 0.42. Reproduction with permission from Gooday et al. (1986), Copyright 1986 Springer Nature



A list of stiffness  $B$  parameters of different polysaccharides has been compiled (Lapasin et al. 1992) (Table 2.13). A lower value of  $B$  is associated with stiffer chain conformation. For example, a small  $B$  value of 0.00525 for xanthan gum indicates that the polymer adopts a stiff conformation (Tinland and Rinaudo 1989), whereas the  $B$  value is 0.045–0.065 for flexible carboxymethyl cellulose (Smidsrød and Haug 1971), 0.10 for  $k$ -carrageenan (Vreeman et al. 1980), and is 0.0147–0.0201 for hyaluronic acid with intermediate stiffness (Luan et al. 2011). Variation in structure composition, type, DS, the molecular weight of the polysaccharide as well as chemical modification to the molecular structure can strongly influence the magnitude of  $B$  value, i.e., the stiffness of the polymer chain. Alginate with different ratios of guluronate/mannuronate and alternate block ranks shows different chain stiffness (Smidsrød et al. 1973). Similar situation can be observed for xanthan with different ratios of Ac/Pyr substitution (Shatwell et al. 1990). The flexibility of the chitosan chain increases with increasing the degree of deacetylation (Gooday et al. 1986). With the increase in DS, the CMC chain becomes more flexible (Smidsrød and Haug 1971). For pectin, high DS content makes the chain much stiffer (Smidsrød and Haug 1971). The high  $M_w$  hyaluronic acid chain is more flexible than low  $M_w$  one (Luan et al. 2011).  $\lambda$ -carrageenan chain has a smaller  $B$  than  $k$ -carrageenan chain, and

**Table 2.13** Stiffness parameter *B* for various polysaccharides (*B* value of DNA is also shown for comparison)

Polymer	B	Notes	Ref.
Alginate	0.031	High guluronate	Smidsrød et al. (1973)
	0.040	High mannuronate	
	0.065	Alternate block copolymer of guluronate and manuronate	
	0.02	High guluronate	Abodinar et al. (2014)
	0.022	Low guluronate	
Amylose xanthate	0.22	–	Smidsrød and Haug (1971)
Carboxymethyl amylose	0.20	DS = 0.80	Trivedi and Patel (1982)
Carboxymethyl cellulose	0.044	DS = 0.40	
	0.045	DS = 0.56	
	0.045	DS = 0.73	
	0.065	DS = 1.00	
	0.078	DS = 1.00	
	0.075	DS = 1.08	
	0.065	DS = 1.35	
$\lambda$ -carrageenan	0.053	–	Morris et al. (1978)
$\kappa$ -carrageenan	0.10	–	Vreeman et al. (1980)
Chitosan	0.043	DD = 0.48	Gooday et al. (1986)
	0.061	DD = 0.58	
	0.091	DD = 0.88	
	0.1	DD = 1.00	
	0.03	–	Abodinar et al. (2014)
	0.02–0.1	–	Anthonsen et al. (1993)
	0.08	–	Kienzle-Sterzer (1984)
	0.043	DA = 0.52	Muzzarelli et al. (1986)
	0.061	DA = 0.42	
	0.060	DA = 0.20	
0.091	DA = 0.12		
Hyaluronic acid	0.0147–0.0201	$M_w = 1 \times 10^4 - 1 \times 10^6$	Luan et al. (2011)
	0.065	–	Smidsrød and Haug (1971)
Pectin	0.034–0.044	DS = 0	Smidsrød and Haug (1971)
	0.044	DS = 0.27	
	0.052	DS = 0.58	
	0.026	DS = 0.78	

(continued)

**Table 2.13** (continued)

Polymer	B	Notes	Ref.
	0.005	DS = 0.89	
	0.015	HM + 60% sucrose	Michel et al. (1984)
	0.020	Without sucrose	
	0.03	LM	Abodinar et al. (2014)
	0.03	LM	
Xanthan	0.12	0.1 M NaCl Ac:Pyr = 1:1	Shatwell et al. (1990)
	0.00044	0.1 M NaCl Ac:Pyr = 9:2	
	0.00615	0.1 M NaCl Ac:Pyr = 48:1	
	0.00662	0.1 M NaCl Ac:Pyr = 1:4	
	0.00545	0.1 M NaCl	Brunchi et al. (2014)
DNA	0.0055	–	Sharp and Bloomfield (1968)

*DS* degree of substitution, *DD* degree of deacetylation, *DA* degree of acetylation, *HM* high-methoxyl, *LM* low-methoxyl, *Ac/Pyr* the ratio of degrees of acetyl (Ac) and pyruvic acid (Pyr) substitution

chemical modification can make it less stiff (Morris et al. 1978; Vreeman et al. 1980).

Note that in comparison with the method to deduce conformation parameters of the polymer chain in solution by using the well-known Mark–Houwink equation, the main advantage of this method is that the stiffness can be determined solely from the intrinsic viscosity data without any knowledge of  $M_w$ .

## 6 Polysaccharide Liquid Crystal

Liquid crystals (LCs)—alternatively named anisotropic fluids—are intermediate between ordinary fluids. LCs are endowed with only short-range order or structure, and crystalline solids.

As concerns the formation of polysaccharide liquid crystals, a lot of polysaccharides have been found to give mesomorphic phases in the aqueous environment and other solvents, e.g., cellulose and some cellulose derivatives (Gilbert 1990), schizophyllan (Van and Teramoto 1982), scleroglucan (Yanaki et al. 1984), xanthan gum (Salamone et al. 1982; Lim et al. 1984), curdlan (Dobashi et al. 2004, 2005), konjac glucomannan (Dave et al. 1998).

Cellulose and many cellulose derivatives can form lyotropic LCs in suitable solvents, whereas other cellulose derivatives give thermotropic LCs. For instance, cellulose acetate and cellulose triacetate form anisotropic solutions in different

solvents such as mixtures of trifluoroacetic acid and chlorinated liquids (Gilbert 1990). Hydroxypropyl cellulose (HPC) is reported to form stable and easy-to-handle mesophases in water and in dimethylacetamide (Werbowj and Gray 1976). HPC also forms thermotropic LCs (Suto et al. 1982). Cellulose tricarbonylate yields liquid crystalline solutions when dissolved in methyl ethyl ketone (Vogt and Zugenmaier 1983) and cellulose itself is found to form LCs in dimethylacetamide/LiCl solvent system. Nanocellulose suspensions can form a liquid crystalline structure at a critical concentration due to its inherent properties from the attractive van der Waals forces and repulsive electrostatic forces (Moon et al. 2011; Habibi et al. 2010). Aqueous suspensions of nanocrystalline cellulose colloidal rods can be used to establish a new anisotropic soft material—a liquid crystal “hydroglass” (Xu et al. 2019).

Aqueous xanthan gum solution presents excellent viscosity, also exhibits liquid crystalline behavior with high stability in a wide range of concentrations (Rwei and Nguyen 2014b). The viscosity of the xanthan gum solution in the liquid crystal region follows a power law with an index  $n$  of roughly 0.08, independent of the xanthan gum concentration (Rwei and Nguyen 2014a).

Liquid crystal behavior is also found in the biphasic systems of single-walled carbon nanotubes dispersed in hyaluronic acid solutions, which exhibits liquid crystalline nematic phases in equilibrium with the isotropic domains (Moulton et al. 2007).

## 7 Conclusions

In this chapter, we concisely introduced the thermodynamics of polymer solutions, which has been well described in the literature, especially the Flory–Huggins mean-field theory and the concept of two vital physical parameters of  $\chi$  and  $A_2$ . While the concentration regimes and the scaling law of polymer solutions are detailed, several key molecular and conformation parameters are summarized.

However, the determination of molecular parameters and conformation characteristics has been a particularly challenge because of some factors such as the extremely low water-solubility, high molecular weight and polydispersity, sensitivity to the side substituents, and especially the polyelectrolyte nature and the strong tendency of the polymer chain to aggregate even in a very dilute solution. These parameter values may significantly vary depending on the molecular weight, solvent conditions, and characterization techniques, as well as the calculation methods. The conformation parameters may also be sensitive to variations of the polydispersity of the polymer. To deduce a global conformation of the polymer chain, the theory of scaling functions presupposes homogeneous monodisperse fractions in molar mass and dimension of the polymers. However, in comparison with the relatively readily available synthetic polymers with narrow molecular weight distribution, natural biopolymer samples, especially plant polysaccharides and algal polysaccharides,

generally possess a broad molecular weight distribution. Therefore, it is necessary and essential to make conformation analysis by using samples with pertinent  $M_w$  and narrow polydispersity.

The full understanding of the molecular structures, chain conformation, functionalities, and solution properties of typical food hydrocolloids and their relationships are prerequisite for food researchers to efficiently utilize them on food product innovation due to the complexity of these diverse natural biopolymers with varied molecular structures and physicochemical properties, manufacturing processes, and consumption requirements. With the emergence of different characterization methods, recently, the determination of molecular chain conformation and the illumination of its importance on solution properties remain the pressing issues in the food hydrocolloids field. To design and develop more rational macromolecule structures and build functional food materials with good performance based on the relationship between chain conformation and solution properties will still be an acclaimed methodology to achieve deeper application value.

## References

- Abodinar A, Smith AM, Morris GA (2014) A novel method to estimate the stiffness of carbohydrate polyelectrolyte polymers based on the ionic strength dependence of zeta potential. *Carbohydr Polym* 112:6–9
- Adolph U, Kulicke WM (1997) Coil dimensions and conformation of macromolecules in aqueous media from flow field-flow fractionation/multi-angle laser light scattering illustrated by studies on pullulan. *Polymer* 38(7):1513–1519
- Ahmad FB, Williams PA, Doublier JL, Durand S, Buleon A (1999) Physico-chemical characterisation of sago starch. *Carbohydr Polym* 38(4):361–370
- Al-assaf S, Phillips GO, Deeb DJ, Parsons B, Starnes H, Vonsontag C (1995) The enhanced stability of the cross-linked hylan structure to hydroxyl (OH) radicals compared with the uncross-linked hyaluronan. *Radiat Phys Chem* 46(2):207–217
- Almutairi FM, Adams GG, Lawson CJ, Gahler R, Wood S, Foster TJ, Rowe AJ, Harding SE (2013) An analytical ultracentrifugation based study on the conformation of lambda carrageenan in aqueous solution. *Carbohydr Polym* 97(1):203–209
- Anthonsen MW, Vårum KM, Smidsrød O (1993) Solution properties of chitosans: conformation and chain stiffness of chitosans with different degrees of N-acetylation. *Carbohydr Polym* 22(3):193–201
- Axelos MAV, Thibault JF, Lefebvre J (1989) Structure of citrus pectins and viscometric study of their solution properties. *Int J Biol Macromol* 11(3):186–191
- Benoit H, Doty P (1953) Light scattering from non-Gaussian chains. *J Phys Chem* 57(9):958–963
- Berth G, Dautzenberg H (2002) The degree of acetylation of chitosans and its effect on the chain conformation in aqueous solution. *Carbohydr Polym* 47(1):39–51
- Bohdanecky M (1983) New method for estimating the parameters of the wormlike chain model from the intrinsic viscosity of stiff-chain polymers. *Macromolecules* 16(9):1483–1492
- Bothner H, Waaler T, Wik O (1988) Limiting viscosity number and weight average molecular weight of hyaluronate samples produced by heat degradation. *Int J Biol Macromol* 10(5):287–291

- Brant DA (1981) Solution properties of polysaccharides. American Chemical Society, Washington, DC
- Brownsey GJ, Chilvers GR, Anson KI, Morris VJ (1984) Some observations (or problems) on the characterization of gellan gum solutions. *Int J Biol Macromol* 6(4):211–214
- Brugnerotto J, Desbrières J, Roberts G, Rinaudo M (2001) Characterization of chitosan by steric exclusion chromatography. *Polymer* 42(25):9921–9927
- Brunchi CE, Morariu S, Bercea M (2014) Intrinsic viscosity and conformational parameters of xanthan in aqueous solutions: salt addition effect. *Colloids Surf B: Biointerfaces* 122:512–519
- Burchard W (1996) Combined static and dynamic light scattering. *Light scattering: principles and some applications*. Clarendon Press, Oxford, pp 439–476
- Burchard W (2001) Structure formation by polysaccharides in concentrated solution. *Biomacromolecules* 2(2):342
- Cai J, Zhang L (2010) Rapid dissolution of cellulose in LiOH/urea and NaOH/urea aqueous solutions. *Macromol Biosci* 5(6):539–548
- Cao X, Sessa DJ, Wolf WJ, Willett JL (2000) Static and dynamic solution properties of corn amylose in N,N-dimethylacetamide with 3 LiCl. *Macromolecules* 33(9):3314–3323
- Chong WP, Fixman M (1965) Intrinsic viscosity of polymer chains. *J Chem Phys* 42 (11):3838–3844
- Christensen BE, Vold IMN, Vårum KM (2008) Chain stiffness and extension of chitosans and periodate oxidised chitosans studied by size-exclusion chromatography combined with light scattering and viscosity detectors. *Carbohydr Polym* 74(3):559–565
- Chun MS, Park OO (1994) On the intrinsic viscosity of anionic and nonionic rodlike polysaccharide solutions. *Macromol Chem Phys* 195(2):701–711
- Clasen C, Kulicke WM (2001) Determination of viscoelastic and rheo-optical material functions of water-soluble cellulose derivatives. *Prog Polym Sci* 26(9):1839–1919
- Cleland RL, Wang JL (1970) Ionic polysaccharides. III. Dilute solution properties of hyaluronic acid fractions. *Biopolymers* 9(7):799–810
- Colby RH (2010) Structure and linear viscoelasticity of flexible polymer solutions: comparison of polyelectrolyte and neutral polymer solutions. *Rheol Acta* 49(5):425–442
- Cowie J (1960) Studies on amylose and its derivatives. Part I. Molecular size and configuration of amylose molecules in various solvents. *Macromol Chem Phys* 42(1):230–247
- Cowman MK, Matsuoka S (2005) Experimental approaches to hyaluronan structure. *Carbohydr Res* 340(5):791–809
- da Silva GM, da Rocha RFP, da Costa MPM, de Mello Ferreira IL, Delpech MC (2018) Evaluation of viscometric properties of carboxymethylcellulose and gellan. *J Mol Liq* 268:201–205
- Dave V, Sheth M, McCarthy SP, Ratto JA, Kaplan DL (1998) Liquid crystalline, rheological and thermal properties of konjac glucomannan. *Polymer* 39(5):1139–1148
- de Gennes PG (1980) Scaling concepts in polymer physics. *Phys Today* 33(6):51–54
- De Nooy A, Besemer AC, Van Bekkum H, Van Dijk J, Smit J (1996) TEMPO-mediated oxidation of pullulan and influence of ionic strength and linear charge density on the dimensions of the obtained polyelectrolyte chains. *Macromolecules* 29(20):6541–6547
- Denkinger P, Burchard W (1991) Determination of chain stiffness and polydispersity from static light-scattering. *J Polym Sci B Polym Phys* 29(5):589–600
- Dentini M, Coviello T, Burchard W, Crescenzi V (1988) Solution properties of exocellular microbial polysaccharides. 3. Light scattering from gellan and from the exocellular polysaccharide of *Rhizobium trifolii* (strain TA-1) in the ordered state. *Macromolecules* 21(11):3312–3320
- Dobashi T, Nobe M, Yoshihara H, Yamamoto T, Konno A (2004) Liquid crystalline gel with refractive index gradient of curdlan. *Langmuir* 20(16):6530–6534
- Dobashi T, Yoshihara H, Nobe M, Koike M, Yamamoto T, Konno A (2005) Liquid crystalline gel beads of curdlan. *Langmuir* 21(1):2–4



- Doublier J, Launay B (1981) Rheology of galactomannan solutions: comparative study of guar gum and locust bean gum. *J Texture Stud* 12(2):151–172
- Dreveton E, Monot F, Lecourtier J, Ballerini D, Choplin L (1996) Influence of fermentation hydrodynamics on gellan gum physico-chemical characteristics. *J Ferment Bioeng* 82(3):272–276
- Eckelt J, Sugaya R, Wolf BA (2008) Pullulan and dextran: uncommon composition dependent Flory-Huggins interaction parameters of their aqueous solutions. *Biomacromolecules* 9(6):1691–1697
- Einbu A, Naess SN, Elgsaeter A, Vårum KM (2004) Solution properties of chitin in alkali. *Biomacromolecules* 5(5):2048–2054
- Ellis HS, Ring SG (1985) A study of some factors influencing amylose gelation. *Carbohydr Polym* 5(3):201–213
- Esquenet C, Buhler E (2002) Aggregation behavior in semidilute rigid and semirigid polysaccharide solutions. *Macromolecules* 35(9):3708–3716
- Fang Y, Takahashi R, Nishinari K (2010) Rheological characterization of schizophyllan aqueous solutions after denaturation-renaturation treatment. *Biopolymers* 74(4):302–315
- Flory PJ (1953) Principles of polymer chemistry. Cornell University Press, Ithaca
- Futatsuyama H, Yui T, Ogawa K (1999) Viscometry of curdlan, a linear (1→3)- $\beta$ -D-glucan, in DMSO or alkaline solutions. *Biosci Biotechnol Biochem* 63(8):1481–1483
- Gericke M, Schlufter K, Liebert T, Heinze T, Budtova T (2009) Rheological properties of cellulose/ionic liquid solutions: from dilute to concentrated states. *Biomacromolecules* 10(5):1188–1194
- Gilbert RD (1990) Cellulose and cellulose derivatives as liquid crystals. In: *Agricultural and synthetic polymers*, vol 433. American Chemical Society, Washington, DC, pp 259–272
- Goh KKT, Haisman DR, Singh H (2006a) Characterisation of a high acyl gellan polysaccharide using light scattering and rheological techniques. *Food Hydrocoll* 20(2):176–183
- Goh KKT, Pinder DN, Hall CE, Hemar Y (2006b) Rheological and light scattering properties of flaxseed polysaccharide aqueous solutions. *Biomacromolecules* 7(11):3098–3103
- Gooday GW, Jeuniaux C, Muzzarelli R (1986) Chitin in nature and technology. Plenum Press, New York
- Graessley WW (1980) Polymer chain dimensions and the dependence of viscoelastic properties on concentration, molecular weight and solvent power. *Polymer* 21(3):258–262
- Gravanis G, Milas M, Rinaudo M, Tinland B (1987) Comparative behavior of the bacterial polysaccharides xanthan and succinoglycan. *Carbohydr Res* 160(87):259–265
- Gura E, Huckel M, Mullet PJ (1998) Specific degradation of hyaluronic acid and its rheological properties. *Polym Degrad Stab* 59(1-3):297–302
- Habibi Y, Lucia LA, Rojas OJ (2010) Cellulose nanocrystals: chemistry, self-assembly, and applications. *Chem Rev* 110(6):3479–3500
- Harding SE, Sattelle DB, Bloomfield VA (1992) Laser light scattering in biochemistry. Cambridge University Press, Cambridge
- Hirano I, Einaga Y, Fujita H (1979) Curdlan (bacterial  $\beta$ -1, 3-glucan) in a cadoxen-water mixture. *Polym J* 11(11):901
- Hoogendam CW, Keizer A, Cohen Stuart MA, Bijsterbosch BH, Smit JAM, Dijk JAPP, Horst PM, Batelaan JG (1998) Persistence length of carboxymethyl cellulose as evaluated from size exclusion chromatography and potentiometric titrations. *Macromolecules* 31:6297–6309
- Jin Q, Cai Z, Li X, Yadav MP, Zhang H (2017) Comparative viscoelasticity studies: corn fiber gum versus commercial polysaccharide emulsifiers in bulk and at air/liquid interfaces. *Food Hydrocoll* 64:85–98
- Kaliannan P, Gromiha MM, Elanthiraiyan M (2001) Solvent accessibility studies on polysaccharides. *Int J Biol Macromol* 28(2):135–141

- Kalitik AA, Byankina Barabanova AO, Nagorskaya VP, Reunov AV, Glazunov VP, Solov'eva TF, Yermak IM (2013) Low molecular weight derivatives of different carrageenan types and their antiviral activity. *J Appl Phycol* 25(1):65–72
- Kamide K, Saito M, Abe T (1981) Dilute solution properties of water-soluble incompletely substituted cellulose acetate. *Polym J* 13(5):421
- Kang D, Cai Z, Wei Y, Zhang H (2017) Structure and chain conformation characteristics of high acyl gellan gum polysaccharide in DMSO with sodium nitrate. *Polymer* 128:147–158
- Kang Y, Wu X, Ji X, Bo S, Liu Y (2018) Strategy to improve the characterization of chitosan by size exclusion chromatography coupled with multi angle laser light scattering. *Carbohydr Polym* 202:99–105
- Kar F, Arslan N (1999) Effect of temperature and concentration on viscosity of orange peel pectin solutions and intrinsic viscosity–molecular weight relationship. *Carbohydr Polym* 40(4):277–284
- Kashiwagi Y, Norisuye T, Fujita H (1981a) Triple helix of *Schizophyllum commune* polysaccharide in dilute solution. 4. Light scattering and viscosity in dilute aqueous sodium hydroxide. *Macromolecules* 14(5):1220–1225
- Kashiwagi Y, Norisuye T, Fujita H (1981b) Triple helix of *Schizophyllum commune* polysaccharide in dilute solution. 4. Light scattering and viscosity in dilute aqueous sodium hydroxide. *Macromolecules* 14(5):1231–1235
- Kato T, Tokuya T, Takahashi A (1983) Comparison of poly (ethylene oxide), pullulan and dextran as polymer standards in aqueous gel chromatography. *J Chromatogr A* 256:61–69
- Kato T, Katsuki T, Takahashi A (1984) Static and dynamic solution properties of pullulan in a dilute solution. *Macromolecules* 17(9):1726–1730
- Kawahara K, Ohta K, Miyamoto H, Nakamura S (1984) Preparation and solution properties of pullulan fractions as standard samples for water-soluble polymers. *Carbohydr Polym* 4(5):335–356
- Kienle-Sterzer C (1984) Transport properties of a cationic polyelectrolyte in dilute and concentrated solutions. Massachusetts Institute of Technology, Chitosan
- Kim J, Yang SY, Mahadeva SK (2013) Effects of solvent systems on its structure, properties and electromechanical behavior of cellulose electro-active paper. *Curr Org Chem* 17(1):83–88
- Kishida N, Okimasu S, Kamata T (1978) Molecular weight and intrinsic viscosity of konjac glucomannan. *J Agric Chem Soc Jpn* 42(9):1645–1650
- Kniewske R, Kulicke WM (1983) Study on the molecular weight dependence of dilute solution properties of narrowly distributed polystyrene in toluene and in the unperturbed state. *Die Makromol Chem* 184(10):2173–2186
- Kohyama K (1993) A mixed system composed of different molecular weights konjac glucomannan and kappa-carrageenan: large deformation and dynamic viscoelastic study. *Food Hydrocoll* 7(3):213–226
- Kok CM, Rudin A (1981) Relationship between the hydrodynamic radius and the radius of gyration of a polymer in solution. *Rapid Commun* 2(11):655–659
- Kök MS, Abdelhameed AS, Ang S, Morris GA, Harding SE (2009) A novel global hydrodynamic analysis of the molecular flexibility of the dietary fibre polysaccharide konjac glucomannan. *Food Hydrocoll* 23(7):1910–1917
- Krause WE, Bellomo EG, Colby RH (2001) Rheology of sodium hyaluronate under physiological conditions. *Biomacromolecules* 2(1):65–69
- Kuang QL, Jun Chai Z, Yan Hua N, Jun Z, Gang WZ (2008) Celluloses in an ionic liquid: the rheological properties of the solutions spanning the dilute and semidilute regimes. *J Phys Chem B* 112(33):10234–10240
- Lapasin R, Pricl S, Tracanelli P (1992) Carboxymethyl starch: a rheological study. *J Appl Polym Sci* 46(10):1713–1722

- Laurent TC, Ryan M, Pietruszkiewicz A (1960) Fractionation of hyaluronic acid. The polydispersity of hyaluronic acid from the bovine vitreous body. *Biochim Biophys Acta* 42(3):476–485
- Lei Q, Zhang M, Shen L, Li R, Liao B, Lin H (2016) A novel insight into membrane fouling mechanism regarding gel layer filtration: Flory-Huggins based filtration mechanism. *Sci Rep* 6:33343
- Lewis ME, Nan S, Mays JW (1991) Hydrodynamic properties of polystyrene in dilute n-butyl chloride solution. *Macromolecules* 24(1):197–200
- Li M, Rosenfeld L, Vilar RE, Cowman MK (1997) Degradation of hyaluronan by peroxydinitrite. *Arch Biochem Biophys* 341(2):245–250
- Li G, Du Y, Tao Y, Liu Y, Li S, Hu X, Yang J (2010) Dilute solution properties of four natural chitin in NaOH/urea aqueous system. *Carbohydr Polym* 80(3):970–976
- Li L, Lu Y, An L, Wu C (2013) Experimental and theoretical studies of scaling of sizes and intrinsic viscosity of hyperbranched chains in good solvents. *J Chem Phys* 138(11):114908
- Lim T, Uhl JT, Prud'homme RK (1984) Rheology of self-associating concentrated xanthan solutions. *J Rheol* 28(4):367–379
- Lopez CG, Colby RH, Graham P, Cabral JT (2017) Viscosity and scaling of semiflexible polyelectrolyte NaCMC in aqueous salt solutions. *Macromolecules* 50(1):332–338
- Lu Y, An L, Wang Z-G (2013) Intrinsic viscosity of polymers: general theory based on a partially permeable sphere model. *Macromolecules* 46(14):5731–5740
- Luan T, Fang Y, Al-Assaf S, Phillips GO, Zhang H (2011) Compared molecular characterization of hyaluronan using multiple-detection techniques. *Polymer* 52(24):5648–5658
- Masueli MA (2014) Mark-Houwink parameters for aqueous-soluble polymers and biopolymers at various temperatures. *J Polym Biopolym Phys Chem* 2(2):37–43
- McCormick CL, Callais PA, Hutchinson BH (1985a) Solution studies of cellulose in lithium chloride and N,N-dimethylacetamide. *Macromolecules* 27(2):91–92
- McCormick CL, Callais PA, Hutchinson BH Jr (1985b) Solution studies of cellulose in lithium chloride and N,N-dimethylacetamide. *Macromolecules* 18(12):2394–2401
- Mendichi R, Šoltés L, Schieron AG (2003) Evaluation of radius of gyration and intrinsic viscosity molar mass dependence and stiffness of hyaluronan. *Biomacromolecules* 4(6):1805–1810
- Michel F, Thibault J-F, Doublier J-L (1984) Viscometric and potentiometric study of high-methoxyl pectins in the presence of sucrose. *Carbohydr Polym* 4(4):283–297
- Milas M (1996) Crossover behavior in the viscosity of semiflexible polymers: solutions of sodium hyaluronate as a function of concentration, molecular weight, and temperature. *J Rheol* 40(6):1155–1166
- Milas M, Rinaudo M, Tinland B (1985) The viscosity dependence on concentration, molecular weight and shear rate of xanthan solutions. *Polym Bull* 14(2):157–164
- Milas M, Rinaudo M, Roue I, Al-Assaf S, Phillips GO, Williams PA (2001) Comparative rheological behavior of hyaluronan from bacterial and animal sources with cross-linked hyaluronan (hylan) in aqueous solution. *Biomolecules* 59(4):191–204
- Miyaki Y, Einaga Y, Fujita H, Fukuda M (1980) Flory's viscosity factor for the system polystyrene + cyclohexane at 34.5 °C. *Macromolecules* 13(3):588–592
- Moon RJ, Martini A, Nairn J, Simonsen J, Youngblood J (2011) Cellulose nanomaterials review: structure, properties and nanocomposites. *Chem Soc Rev* 40(7):3941–3994
- Morris ER, Rees DA, Welsh EJ, Dunfield LG, Whittington SG (1978) Relation between primary structure and chain flexibility of random coil polysaccharides: calculation and experiment for a range of model carrageenans. *J Chem Soc* 8:793–800
- Morris ER, Rees DA, Welsh EJ (1980) Conformation and dynamic interactions in hyaluronic solutions. *J Mol Biol* 138(2):383–400
- Morris ER, Cutler AN, Ross-Murphy SB, Rees DA, Price J (1981) Concentration and shear rate dependence of viscosity in random coil polysaccharide solutions. *Carbohydr Polym* 1(1):5–21

- Morris GA, Patel TR, Picout DR, Ross-Murphy SB, Ortega A, JGdl T, Harding SE (2008a) Global hydrodynamic analysis of the molecular flexibility of galactomannans. *Carbohydr Polym* 72 (2):356–360
- Morris GA, Torre JG, Ortega A, Castile J, Smith A, Harding SE (2008b) Molecular flexibility of citrus pectins by combined sedimentation and viscosity analysis. *Food Hydrocoll* 22 (8):1435–1442
- Moulton SE, Maugey M, Poulin P, Wallace GG (2007) Liquid crystal behavior of single-walled carbon nanotubes dispersed in biological hyaluronic acid solutions. *J Am Chem Soc* 129 (30):9452–9457
- Muroga Y, Yamada Y, Noda I, Nagasawa M (1987) Local conformation of polysaccharides in solution investigated by small-angle X-ray scattering. *Macromolecules* 20(12):3003–3006
- Muzzarelli R, Cosani A, Fornasa A, Kienzle Sterzer C, Rha C, Rodriguez Sanchez D, Scandola M, Terbojevich M, Vincendon M (1986) Chitin and chitosan solutions. In: *Chitin in nature and technology*. Springer, New York, pp 337–351
- Nakanishi T, Norisuye T (2003) Thermally induced conformation change of succinoglycan in aqueous sodium chloride. *Biomacromolecules* 4(3):736–742
- Nakanishi Y, Norisuye T, Teramoto A, Kitamura S (2002) Conformation of amylose in dimethyl sulfoxide. *Macromolecules* 26(16):4220–4225
- Nakata M, Kawaguchi T, Kodama Y, Konno A (1998) Characterization of curdlan in aqueous sodium hydroxide. *Polymer* 39(6):1475–1481
- Nishinari K, Kohyama K, Williams P, Phillips G, Burchard W, Ogino K (1991) Solution properties of pullulan. *Macromolecules* 24(20):5590–5593
- Nordmeier E (1993) Static and dynamic light-scattering solution behavior of pullulan and dextran in comparison. *J Phys Chem* 97(21):5770–5785
- Norisuye T (1993) Semiflexible polymers in dilute solution. *Prog Polym Sci* 18(3):543–584
- Norisuye T (1996) Conformation and properties of amylose in dilute solution. *Food Hydrocoll* 10 (1):109–115
- Okamoto T, Kubota K, Kuwahara N (1993) Light scattering study of gellan gum. *Food Hydrocoll* 7 (5):363–371
- Oono Y (1983) Crossover behavior of transport properties of dilute polymer solutions: Renormalization group approach. *J Chem Phys* 79(9):4629–4642
- Owens H, Lotzkar H, Schultz T, Maclay W (1946) Shape and size of pectinic acid molecules deduced from viscometric measurements. *J Am Chem Soc* 68(8):1628–1632
- Patel TR, Picout DR, Ross-Murphy SB, Harding SE (2006) Pressure cell assisted solution characterization of galactomannans. 3. Application of analytical ultracentrifugation techniques. *Biomacromolecules* 7(12):3513–3520
- Pereira MC, Wyn-Jones E, Morris ER, Ross-Murphy SB (1982) Characterisation of interchain association in polysaccharide solutions by ultrasonic relaxation and velocity. *Carbohydr Polym* 2(2):103–113
- Poirier M, Charlet G (2002) Chitin fractionation and characterization in N, N-dimethylacetamide/lithium chloride solvent system. *Carbohydr Polym* 50(4):363–370
- Prawitwong P, Takigami S, Phillips GO (2007) Effects of  $\gamma$ -irradiation on molar mass and properties of Konjac mannan. *Food Hydrocoll* 21(8):1362–1367
- Pyun CW, Fixman M (1964) Frictional coefficient of polymer molecules in solution. *J Chem Phys* 41(4):937–944
- Ren Y, Ellis PR, Sutherland IW, Ross-Murphy SB (2003) Dilute and semi-dilute solution properties of an exopolysaccharide from *Escherichia coli* strain S61. *Carbohydr Polym* 52(2):189–195
- Rinaudo M, Milas M, Le Dung P (1993) Characterization of chitosan. Influence of ionic strength and degree of acetylation on chain expansion. *Int J Biol Macromol* 15(5):281–285
- Roberts GA, Domszy JG (1982) Determination of the viscometric constants for chitosan. *Int J Biol Macromol* 4(6):374–377

- Robinson G, Ross-Murphy SB, Morris ER (1982) Viscosity-molecular weight relationships, intrinsic chain flexibility, and dynamic solution properties of guar galactomannan. *Carbohydr Res* 107(1):17–32
- Rochas C, Lahaye M (1989) Average molecular weight and molecular weight distribution of agarose and agarose-type polysaccharides. *Carbohydr Polym* 10(4):289–298
- Roger P, Axelos MA, Colonna P (2000) SEC-MALLS and SANS studies applied to solution behavior of linear  $\alpha$ -glucans. *Macromolecules* 33(7):2446–2455
- Rubinstein M, Colby RH (2003) *Polymer physics*. Oxford University Press, New York
- Rwei SP, Nguyen TA (2014a) Liquid crystalline phase in xanthan gum (XG)/H<sub>2</sub>O/H<sub>3</sub>PO<sub>3</sub> and XG/H<sub>2</sub>O/H<sub>3</sub>PO<sub>4</sub> tertiary systems: a thermal and rheological study. *Cellulose* 21(5):3231–3241
- Rwei SP, Nguyen TA (2014b) Phase formation and transition in a xanthan gum/H<sub>2</sub>O/H<sub>3</sub>PO<sub>4</sub> tertiary system. *Cellulose* 21(3):1277–1288
- Salamone J, Clough S, Salamone AB, Reid K, Jamison D (1982) Xanthan gum-A lyotropic, liquid crystalline polymer and its properties as a suspending agent. *Soc Pet Eng J* 22(04):555–556
- Sato T, Norisuye T, Fujita H (1984) Double-stranded helix of xanthan: dimensional and hydrodynamic properties in 0.1 M aqueous sodium chloride. *Macromolecules* 17(12):2696–2700
- Schefer L, Adamcik J, Mezzenga R (2014) Unravelling secondary structure changes on individual anionic polysaccharide chains by atomic force microscopy. *Angew Chem Int Ed* 53(21):5376–5379
- Schittenhelm N, Kulicke W (2000) Producing homologous series of molar masses for establishing structure-property relationships with the aid of ultrasonic degradation. *Macromol Chem Phys* 201(15):1976–1984
- Sharp P, Bloomfield VA (1968) Intrinsic viscosity of wormlike chains with excluded-volume effects. *J Chem Phys* 48(5):2149–2155
- Shatwell KP, Sutherland IW, Ross-Murphy SB (1990) Influence of acetyl and pyruvate substituents on the solution properties of xanthan polysaccharide. *Int J Biol Macromol* 12(2):71–78
- Shimada E, Matsumura G (1975) Viscosity and molecular weight of hyaluronic acids. *J Biochem* 78(3):513–517
- Simha R, Utracki L (1975) The viscosity of concentrated polymer solutions: corresponding states principles. In: *Rheological theories measuring techniques in rheology test methods in rheology fractures rheological properties of materials rheo-optics biorheology*. pp 371–380.
- Smidsrød O (1970) Solution Properties of Alginates. *Carbohydr Res* 13(3):359–372
- Smidsrød O, Haug A (1971) Estimation of the relative stiffness of the molecular chain in polyelectrolytes from measurements of viscosity at different ionic strengths. *Biopolymers* 10(7):1213–1227
- Smidsrød O, Glover R, Whittington SG (1973) The relative extension of alginates having different chemical composition. *Carbohydr Res* 27(1):107–118
- Soltes L, Mendichi R, Lath D, Mach M, Bakos D (2002) Molecular characteristics of some commercial high-molecular-weight hyaluronans. *Biomed Chromatogr* 16(7):459–462
- Stokke BT, Brant DA (1990) The reliability of wormlike polysaccharide chain dimensions estimated from electron micrographs. *Biopolymers* 30(13-14):1161–1181
- Stokke BT, Elgsaeter A, Bjørnstad EØ, Lund T (1992) Rheology of xanthan and scleroglucan in synthetic seawater. *Carbohydr Polym* 17(3):209–220
- Striegel AM, Timpa JD (1996) Gel permeation chromatography of polysaccharides using universal calibration. *Int J Polym Anal Charact* 2(3):213–220
- Strobl GR (1997) *The physics of polymers*. Springer, Berlin
- Suto S, White J, Fellers J (1982) A comparative study of the thermotropic mesomorphic tendencies and rheological characteristics of three cellulose derivatives: ethylene and propylene oxide ethers and an acetate butyrate ester. *Rheol Acta* 21(1):62–71
- Takahashi R (1999) Characterization of gellan gum in aqueous NaCl solution. *Progr Colloid Polym Sci* 114(5):1–7

- Takahashi R, Al-Assaf S, Williams PA, Kubota K, Okamoto A, Nishinari K (2003) Asymmetrical-flow field-flow fractionation with on-line multiangle light scattering detection. 1. Application to wormlike chain analysis of weakly stiff polymer chains. *Biomacromolecules* 4(2):404–409
- Takahashi R, Tokunou H, Kubota K, Ogawa E, Oida T, Kawase T, Nishinari K (2004) Solution properties of gellan gum: change in chain stiffness between single- and double-stranded chains. *Biomacromolecules* 5(2):516–523
- Tao Y, Zhang L, Yan F, Wu X (2007) Chain conformation of water-insoluble hyperbranched polysaccharide from fungus. *Biomacromolecules* 8(7):2321–2328
- Teraoka I (2002) *Polymer solutions: an introduction to physical properties*. Polytechnic University, Brooklyn
- Terbojevich M, Cosani A, Conio G, Ciferri A, Bianchi E (1985) Mesophase formation and chain rigidity in cellulose and derivatives. 3. Aggregation of cellulose in N,N-dimethylacetamide-lithium chloride. *Macromolecules* 18(4):640–646
- Terbojevich M, Cosani A, Palumbo M (1986) Structural properties of hyaluronic acid in moderately concentrated solutions. *Carbohydr Res* 149(2):363–377
- Terbojevich M, Carraro C, Cosani A, Marsano E (1988) Solution studies of the chitin-lithium chloride-N, N-di-methylacetamide system. *Carbohydr Res* 180(1):73–86
- Tinland B, Rinaudo M (1989) Dependence of the stiffness of the xanthan chain on the external salt concentration. *Macromolecules* 22(4):1863–1865
- Tinland B, Pluen A, Sturm J, Weill G (1997) Persistence length of single-stranded DNA. *Macromolecules* 30(19):5763–5765
- Trivedi HC, Patel RD (1982) Studies on carboxymethylcellulose: estimation of the relative stiffness of the polyions. *Macromol Rapid Commun* 3(5):317–321
- Ueno Y, Tanaka Y, Horie K, Tokuyasu K (1988) Low-angle laser light scattering measurements on highly purified sodium hyaluronate from rooster comb. *Chem Pharm Bull* 36(12):4971–4975
- Van K, Teramoto A (1982) Isotropic-liquid crystal phase equilibrium in aqueous solutions of a triple-helical polysaccharide schizophyllan. *Polym J* 14(12):999
- Vogt U, Zugenmaier P (1983) Investigations on the lyotropic mesophase system cellulose tricarbanilate/ethyl methyl ketone. *Communications* 4(12):759–765
- Vreeman H, Snoeren T, Payens T (1980) Physicochemical investigation of k-carrageenan in the random state. *Biopolymers* 19(7):1357–1374
- Wang X, Zhang L (2009) Physicochemical properties and antitumor activities for sulfated derivatives of lentinan. *Carbohydr Res* 344(16):2209–2216
- Wang W, Bo S, Li S, Qin W (1991) Determination of the Mark-Houwink equation for chitosans with different degrees of deacetylation. *Int J Biol Macromol* 13(5):281–285
- Wang Q, Ellis PR, Ross-Murphy SB, Burchard W (1997) Solution characteristics of the xyloglucan extracted from *Detarium senegalense* Gmelin. *Carbohydr Polym* 33(2):115–124
- Wang X, Zhang X, Xu X, Zhang L (2012) The LiCl effect on the conformation of lentinan in DMSO. *Biopolymers* 97(10):840–845
- Wedlock DJ, Phillips GO, Davies A, Gormally J, Wynjones E (1983) Depolymerization of sodium hyaluronate during freeze drying. *Int J Biol Macromol* 5(3):186–188
- Weissberg S, Simha R, Rothman S (1951) Viscosity of dilute and moderately concentrated polymer solutions. *J Res Natl Bur Stand* 47(4):298–314
- Werbowj RS, Gray DG (1976) Liquid crystalline structure in aqueous hydroxypropyl cellulose solutions. *Mol Cryst Liq Cryst* 34(4):97–103
- Xu Y, Atrons AD, Stokes JR (2019) Liquid crystal hydroglass formed via phase separation of nanocellulose colloidal rods. *Soft Matter* 15(8):1716–1720
- Yanaki T, Yamaguchi M (1994) Shear-rate dependence of the intrinsic viscosity of sodium hyaluronate in 0.2 M sodium chloride solution. *Chem Pharm Bull* 42(8):1651–1654
- Yanaki T, Norisuye T, Teramoto A (1984) Cholesteric mesophase in aqueous solutions of a triple helical polysaccharide scleroglucan. *Polym J* 16(2):165
- Yu F, Zhang F, Luan T, Zhang Z, Zhang H (2014) Rheological studies of hyaluronan solutions based on the scaling law and constitutive models. *Polymer* 55(1):295–301

- Zhang H, Nishinari K (2009) Characterization of the conformation and comparison of shear and extensional properties of curdlan in DMSO. *Food Hydrocoll* 23(6):1570–1578
- Zhang X, Xu J, Zhang L (2005) Effects of excluded volume and polydispersity on solution properties of lentinan in 0.1 M NaOH solution. *Biopolymers* 78(4):187–196
- Zhang F, Luan T, Kang D, Jin Q, Zhang H, Yadav MP (2015) Viscosifying properties of corn fiber gum with various polysaccharides. *Food Hydrocoll* 43:218–227

# Chapter 3

## Rheological and Thickening Properties



Katsuyoshi Nishinari

**Abstract** Rheology in food studies all the mechanical properties relating deformation and flow. Since the texture is known to be important to govern the palatability with taste and aroma, and also recognized as a key factor in designing foods for persons with difficulty in mastication and deglutition, hydrocolloids controlling rheological and thickening properties have been attracting more attention than before. This chapter describes the necessity and importance of rheology and then, fundamental concept of elasticity, viscosity, static and dynamic viscoelasticity, and the measuring methods in relation with the molecular structure. Although yield stress and thixotropy have been recognized and studied, they are both not so well understood, and recent developments are described in relation with thickening properties. Recent development of fractional calculus and microrheology is described. Application of thickening properties is also described.

**Keywords** Viscosity · Elasticity · Viscoelasticity · Yield stress · Thixotropy

### 1 Introduction

Rheology is a science on the deformation and flow of matters. The word rheology is the combination of “rheo”—flow and “logy”—science in Greek. In the early stage of rheology, British Rheologists Club (1942) proposed a classification of deformation which is divided into elastic deformation and flow. Between the two most simple extremities, Hookean elasticity and Newtonian viscosity, viscoelastic deformation has been most well studied in relation with plastic industry and food industry. Rheology has been proved to be useful to understand quantitatively the gelation process (treated in the next chapter), the transformation of a liquid to solid, dispersed systems, the mixture of different materials because most foods consist of many

---

K. Nishinari (✉)

Glyn O. Phillips Hydrocolloids Research Centre, School of Food and Biological Engineering,  
Hubei University of Technology, Wuhan, PR China  
e-mail: [katsuyoshi.nishinari@hbut.edu.cn](mailto:katsuyoshi.nishinari@hbut.edu.cn)



ingredients. Rheology is developing steadily influenced by the development of other related science. The new measurement techniques such as atomic force microscopy, optical tweezers in microrheology make possible to detect the nano/micro scale distance, and the length scale studied in rheology is widened to nano, micro, meso, and macroscale. Femtosecond spectroscopy and time-resolved X-ray diffraction photoelectron spectroscopy study the very fast change of rheological properties accompanying the structural changes, and the timescale is also widened. Rheology is also closely related with dielectric (e.g. broadband dielectric measurement) and related studies, and thus can be treated from the common background such as stimulus-response theory. Stimulus-response approach has been proved useful to understand systematically the transient phenomena in statistical physics, but now it seems to be used also in psychology. Remember the conditioned reflexes of Pavlov's dog. It is expected to be applied to sensory evaluation of texture and flavor of foods. Soft matters such as foods, biological tissues, polymers, colloids are now understood based on common background (de Gennes 1979; Doi 2013). Rheology in food has been studied extensively because the perceived texture is closely correlated with rheology (Bourne 2002; Chen and Engelen 2012; Nishinari and Fang 2018). As is widely recognized, texture and flavor are most important attributes governing the palatability of foods. With the advent of aged society, the number of persons who have the difficulty in the mastication and swallowing is increasing, which increases the number of cases of pneumonia and other symptoms. Rheology is not yet completed for food science, and more developments are expected to solve these problems and to create better foods, better storage, and distribution methods in collaboration with other disciplines. It is widely recognized that instrumental measurements give the objective evaluation and basis of the perceived texture of foods which are described by subjective terms. Interpretation of sensory terms such as firm, hard, stiff, rigid, etc. is often confusing and depends on individuals.

Although the elastic modulus obtained from the initial slope of force-deformation curves of the agar gel is larger than that of the gelatin gel (Fig. 3.1a), the breaking strength of the agar gel turns out to be smaller than that of the gelatin gel even after the calibration of the cross-sectional area. Therefore, it is impossible to answer to a question "which of the two gels, an agar gel or a gelatin gel, is 'firmer' or 'harder'?" if the definition of the hardness or the firmness is not given.

In Fig. 3.1b, how we could answer to the question "Which of the two liquids, sugar syrup or mayonnaise, is thicker?" Most people reply that sugar syrup is thicker than mayonnaise. This indicates that most people sense the viscosity at a higher shear rate than ca.  $1 \text{ s}^{-1}$  in the mouth. As shown in this example, daily language such as "thick" and "thin" is vague.

Scott Blair studied the relation between the instrumental measurement and sensory evaluation of texture using fractional calculus which has recently re-attracted more attention. Although the theory of viscoelasticity is well developed in the linear region where the stress and strain or strain rate are in the linear relation, the large deformation and fracture are not so well established. In this chapter, after describing the basic concepts in the linear viscoelasticity, large amplitude oscillatory shear (LAOS), yield stress, thixotropy, microrheology are described. Application of thickening agents in food production is also described. Then, recent application of

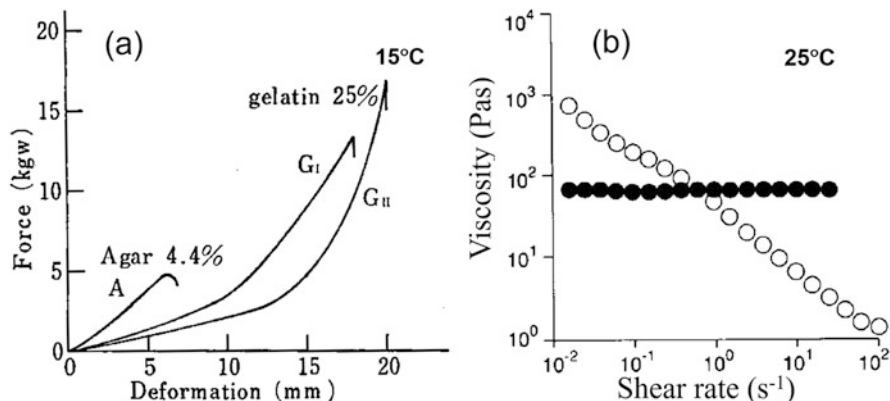


**Fig. 3.1** (a) Force-deformation curves of cylindrical (20 mm diameter and 30mm height) gels of 4% agar and 25% gelatin at a compression velocity of 10 mm/min. The curve  $G_I$  and  $G_{II}$  for gelatin gels were obtained with approximately equal probability (Nishinari et al. 1980). (b) The viscosity as a function of shear rate for sugar syrup (closed circle, flow behavior similar to honey) and mayonnaise (open circle). Reproduction with permission from Nishinari et al. (1980). Copyright 1980 JSFST

fractional calculus and also the relation between the molecular structure and viscosifying function are described.

## 2 Elasticity

Theory of elasticity treats the deformation of solids. Solids do not flow and maintain a certain shape. A solid which does not deform at all even under a force is called a “rigid body.” The distance between two points in a rigid body is regarded as constant. The concept of a rigid body is an ideal model. In reality, even a diamond or iron deforms when it is subjected to a large force.

The simplest model of a deformable solid is an elastic body. An elastic body shows a constant strain (ratio of deformation) instantaneously, that is without delay, when it is subjected to a constant stress (force per unit area). This solid is called a Hookean body. Imagine a rod of a radius  $r$  and a length  $l$  which is subjected to a force  $f$ . Hooke’s law for this rod is written as  $f/(\pi r^2) = E (\delta l/l)$ , where the left-hand side is the force per unit area, which is called (elongational or compressional) stress, while the right-hand side is the product of the elastic constant  $E$  and the (elongational or compressional) strain. Elongational strain indicates the ratio of the deformation  $\delta l$  to the initial length  $l$ , and it is often written as  $\varepsilon = \delta l/l$ . Elastic constant  $E$  defined for the elongational or compressional deformation is called Young’s modulus, which represents the stress required to produce the unit elongation or unit contraction. It indicates the resistance to the deformation. The unit of  $E$  is force over area, that is  $\text{Pa} = \text{N/m}^2$ , in SI.

When the force  $f$  is exerted on the upper surface of the parallelepiped body to the parallel direction of the surface, then it shows a uniform deformation which is

**Table 3.1** The relation between 4 elastic parameters

	$G, E$	$G, \kappa$	$E, \kappa$	$G, \mu$	$E, \mu$	$\kappa, \mu$
$G$	$G$	$G$	$\frac{3\kappa E}{9\kappa - E}$	$G$	$\frac{E}{2(1+\mu)}$	$\frac{3\kappa(1-2\mu)}{2(1+\mu)}$
$E$	$E$	$\frac{9G\kappa}{G+3\kappa}$	$E$	$2(1+\mu)G$	$E$	$3\kappa(1-2\mu)$
$\kappa$	$\frac{GE}{9G-3E}$	$\kappa$	$\kappa$	$\frac{2(1+\mu)G}{3(1-2\mu)}$	$\frac{E}{3(1-2\mu)}$	$\kappa$
$\mu$	$\frac{E-2G}{2G}$	$\frac{3\kappa-2G}{2(3\kappa+G)}$	$\frac{3\kappa-E}{6\kappa}$	$\mu$	$\mu$	$\mu$

characterized by a small angle  $\gamma$ . For a small angle,  $\tan \gamma$  can be approximated by  $\gamma$ , which is called the shear strain. Then, Hooke's law is written as  $f/A = G\gamma$ , where  $G$  is called shear modulus or rigidity.

Next, let us consider the volume change of a spherical elastic body (volume  $v$ ) which is surrounded by liquid. When the liquid pressure is raised from  $p$  to  $p+\Delta p$  by a pump, the volume of the sphere will decrease from  $v$  to  $v-\delta v$ . Then, Hooke's law is written as  $\delta p = -\kappa \delta v/v$ . Since it is the custom to represent the sign of the compressional pressure as positive, the negative sign in the right-hand side originates from the decrease of the volume under compression. Here,  $\kappa$  is called bulk modulus, and its inverse  $1/\kappa$  is called compressibility.

When a cylinder of length  $l$  and the radius  $r$  is extended to its axial direction without any force at side surface, the radius will be decreased from  $r$  to  $r-\delta r$ . The ratio of the transverse strain  $-\delta r/r$  to the longitudinal strain  $\delta l/l$  is called Poisson's ratio  $\mu$ :  $\mu = -(\delta r/r)/(\delta l/l)$ . The negative sign originates from the fact that when the length of cylinder is increased ( $\delta l > 0$ ), the radius is decreased ( $\delta r < 0$ ). Generally, the value of Poisson ratio ranges from 0.5 for incompressible material like rubber to 0 for porous material like cork.

### The Relation Among Four Elastic Parameters $E, G, \kappa$ , and $\mu$

Commonly used four elastic constants  $E, G, \kappa$ , and  $\mu$  are not independent, and are related with each other as shown in Table 3.1. Only two constants are independent, and therefore, when two constants are determined the other two can be calculated. On the other hand, the determination of only one constant is not complete to understand the whole elastic property of that material.

As mentioned above, the Poisson ratio  $\mu$  ranges from 0 to 0.5. In Table 3.1, the bulk modulus  $\kappa$  is given as a function of  $E$  and  $\mu$ . When  $\mu$  approaches 0.5, the denominator  $(1-2\mu)$  approaches to zero and thus the bulk modulus approaches to infinity, therefore, the bulk modulus is much larger than the other elastic parameter  $G$  and  $E$ . This is just the case for rubber. The fact that the bulk modulus is much larger than  $G$  and  $E$  means that this material needs a very high pressure to reduce the volume, hence this is called an incompressible material. In such a case, Young's modulus is about three times of the shear modulus:  $E = 3G$ .

Shear deformation appears in the torsion, and can be determined by the measurement of the moment. The deformation mode is the same as in rotational viscometer.

When a beam is bent by an applied couple, an upper part is stretched and the lower part is compressed. There is a part near the middle layer which retains the

original length, and is called a neutral layer. Then, Young's modulus is involved in the bending, and is obtained from the determination of the sag.

Since measurement of bending is easy, it is often used to study rheological properties of solids. To apply three point bending test to a soft matter such as agarose gels, the points were replaced by cylindrical rods (Bonn et al. 1998).

Strain energy of elastic materials is given by the elastic modulus  $\times$  (strain)<sup>2</sup>/2 for all deformation modes, elongation, shear, and expansion.

Poisson's ratio of most engineering solids, metals, plastics, and glasses is known to be about 0.3 while those of many soft foods such as cheese and jellies are reported as 0.5 just like a rubber. Cork and flexible foams show no lateral expansion when compressed thus their Poisson's ratio is very close to zero. Poisson's ratios of vegetables and fruits are reported higher than those of metals and plastics but lower than those for cheese and jellies, for example, 0.37 for an apple tissue (Powel 1994). It is also important to take into account the deformation rate (in most cases compression is selected), since the real food is not purely elastic but rather viscoelastic, and shows a time dependence. When a 1.33% gel of gellan was compressed slowly at 0.005 mm/min, no lateral expansion was observed (Nakamura et al. 2001).

### 3 Viscosity: Newtonian Fluid

There are many models for viscous fluids, and a Newtonian fluid is the simplest model. In this model, the tangential stress is written by a linear equation of the shear rate.

Imagine the fluid is filled between the lower and the upper plates (Fig. 3.2). When the upper plate is moved to the right direction parallel to the x-axis, the fluid in the neighborhood of the upper plate is dragged with the plate, and the fluid far from the upper plate is dragged with a slower velocity.

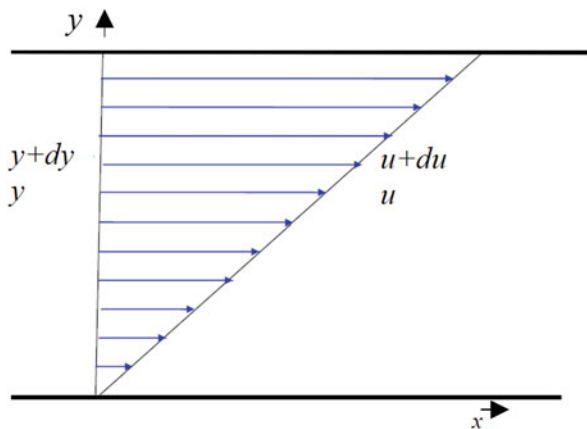


**Fig. 3.2** Fluid flow in a narrow gap  $\delta$  between two very large planes. Upper plate ( $y = \delta$ ) moves parallel to x-axis. Lower plate ( $x$ -axis) is fixed at  $y = 0$ . Velocity gradient  $\partial u/\partial y$  is given by shear rate  $\dot{\gamma}$  because the shear  $\dot{\gamma}$  is  $dx/dy$ , and the velocity  $u$  is  $dx/dt$

The velocity vector is written as  $u = [u(y), 0, 0]$ . In the Newtonian fluid, the tangential stress  $\tau$  is proportional to the velocity gradient,  $\partial u/\partial y$ , the change in the velocity of the fluid flow in the direction perpendicular to the direction of fluid flow,  $\tau = \eta \partial u/\partial y$ , where the proportional coefficient  $\eta$  is called viscosity. This is called a Newton's law of viscosity. When a constant shear stress is given, the velocity gradient  $\partial u/\partial y$  is small for a fluid of which the viscosity is large. The viscosity represents the tangential stress which is required to produce the unit velocity gradient, thus it is the resistance to the flow.

The viscosity of the fluid can be determined by various methods as described below.

### 3.1 Capillary Viscometer

Let us imagine a fluid flow in a capillary. Symmetrical considerations indicate that the velocity distribution in the liquid will be symmetrical around the axis of the capillary, and have its maximum value on this axis. Flow rate  $Q$  of a Newtonian fluid (viscosity  $\eta$ ) in a capillary (radius  $a$  and length  $l$ ) under a pressure difference  $\Delta p$  is given by

$$Q = \int_0^a 2\pi r u dr = \pi \Delta p a^4 / 8\eta l$$

taking into account that  $u$  is the flow velocity at  $r$  (the distance from the axis  $r = 0$ ), and  $2\pi r dr$  is the area of the circular ring from  $r$  to  $r+dr$ . The flow velocity  $u = (\Delta p / 4\eta l) (a^2 - r^2)$  takes maximum at the central line  $r = 0$ , and becomes slower with increasing distance from the central line. The viscosity of the liquid can be determined by measuring  $Q$ , volume  $V$  of liquid flowing through the capillary in time  $t$ , i.e.  $Q = V/t$ . This is called Hagen–Poiseuille equation.

### 3.2 Falling Ball Viscometer

This is the simplest evaluation of the sedimentation of food particles in the suspension and creaming in the emulsion. Imagine a solid sphere (radius  $a$  and density  $\rho$ ) is falling slowly at a velocity  $v$  in a surrounding infinite medium (viscosity  $\eta$ , density  $\rho_0$ ). The frictional force exerting on the falling sphere is given by Stokes law  $6\pi a \eta v$  when the velocity is slow. When the falling velocity is constant (acceleration is zero), the upward force and downward force should be balanced, and thus the falling velocity  $v$  is given by

$$v = \frac{2a^2}{9\eta} (\rho - \rho_0) g$$

where  $g$  is the gravitational acceleration. When the density of the sphere  $\rho$  is lower than that of the medium  $\rho_0$ , the sphere will float up, and the floating velocity can be calculated in the same way. If the spherical material is not a solid but immiscible liquid such as in the case of creaming up oil droplet in water, the coefficient in the Stokes formula is given by  $4\pi a\eta$  instead of  $6\pi a\eta$ . If the sphere is a gas bubble, this coefficient is known to be closer to the solid sphere  $6\pi a\eta$  rather than to that of the liquid sphere because the surface of the bubble is usually covered with a hard layer.

Various rotational viscometers are used: liquid samples are put between the cone and plate in cone plate viscometers, and samples are put between an inner cylinder and an outer cylinder in coaxial cylindrical viscometers (called also Couette viscometers).

### 3.3 Reynolds Number

In the above-mentioned viscometers, viscosity can be determined only for a laminar flow in which the fluid moves in parallel layers. In the laminar flow, the streamlines show regular shapes and do not intersect each other. In fluid flow of high velocity, the flow becomes turbulent where the fluid shows a non-regular motion and the velocity at any point varies in both direction and magnitude with time. Turbulent motion is accompanied by the formation of eddies and the rapid interchange of momentum in the fluid. The change from the laminar flow to turbulent flow occurs at a critical value of Reynolds number  $Re$ :  $Re = \rho vl/\eta$ , where  $\rho$  is the density of the fluid,  $\eta$  is the viscosity of the fluid,  $v$  is the velocity of the fluid in motion relative to some solid body characterized by a linear dimension  $l$  (called characteristic dimension).

$$Re = \frac{\rho vl}{\eta} = \frac{\rho l^3 (v^2/l)}{\eta (v/l) l^2} = \frac{\text{mass} \times \text{acceleration}}{\text{viscosity} \times \text{shear rate} \times \text{area}} = \frac{\text{inertial force}}{\text{viscous force}}$$

Thus, the physical meaning of Reynolds number is the ratio of the inertial force to the viscous force. Characteristic length represents the radius or the diameter for spheres, and is an equivalent diameter (or radius) for non-spherical objects. The equivalent radius is defined for non-spherical objects based on Stokes' law. The Reynolds number is used to predict the transition from laminar flow to turbulent flow.

## 4 Non-Newtonian Flow: Shear Thinning and Shear Thickening

Most liquid foods, except water, alcohol, oil, are not Newtonian fluids. Simple models frequently used to analyze the flow behavior of liquid foods are shown in Fig. 3.3.

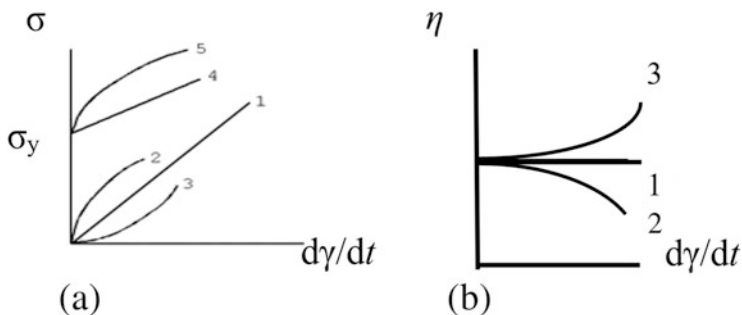


**Fig. 3.3** (a) Shear stress plotted against shear rate for commonly used simple models of fluids. (1) Newtonian fluid  $\sigma = \eta (d\gamma/dt)$ , (2) Power law fluid (shear thinning)  $\sigma = \eta (d\gamma/dt)^n$ ,  $n < 1$ , (3) Power law fluid (shear thickening)  $\sigma = \eta (d\gamma/dt)^n$ ,  $n > 1$ , (4) Bingham fluid  $\sigma = \eta (d\gamma/dt) + \sigma_y$ , (5) Herschel–Bulkley fluid  $\sigma = \eta (d\gamma/dt)^n + \sigma_y$ . (b) Viscosity as a function of shear rate for Newtonian (1), shear thinning (2) and shear thickening (3) fluids

Newtonian fluid shows a linear relation between shear stress and shear strain, and the straight line for shear stress vs shear strain passes through the origin. The viscosity defined by the shear stress divided by shear strain for a power law fluid  $\sigma = \eta (d\gamma/dt)^n$  with  $n < 1$  decreases with increasing shear rate, and the behavior is called shear thinning (Model 2 in Fig. 3.3b). Most common liquids show such a behavior. Shear thinning may be attributed to many reasons depending on the sample structure: alignment of rod-like particles or molecules in the flow direction, disintegration of aggregated particles. The viscosity for a power law fluid with  $n > 1$  increases with increasing shear rate, and the behavior is called shear thickening (Model 3 in Fig. 3.3b). There are not so many examples, but starch paste and some other examples are shown later.

Liquid foods filled in tubes such as mayonnaise or tomato ketchup or tooth paste do not begin to flow if it is not subjected to a certain stress. The minimum stress required to cause a flow is defined as yield stress. A fluid which has a yield stress and shows a linear stress–strain rate as in Newtonian flow above the yield stress is called a Bingham liquid (Model 4 in Fig. 3.3a). Herschel–Bulkley liquid is a fluid which has a yield stress and shows a non-linear stress–strain rate above the yield stress (Model 5 in Fig. 3.3a). Spreadability of butter, cream, jam, paste (legume, fish, meat, nuts, seed, spice, herb, etc.) is closely related with yield stress, and is discussed later.

In addition to these five models, the following Casson equation is also frequently used.

$$\sigma^{1/2} = \sigma_c^{1/2} + \eta_c^{1/2}(d\gamma/dt)^{1/2}$$

where  $\sigma_c$  and  $\eta_c$  are called the Casson yield stress and the Casson viscosity coefficient, respectively. The intercept of fitting line is square root of Casson yield stress. Casson yield stress is the minimum stress that is needed for the fluid to flow. Casson's equation has been widely used in the evaluation of chocolate.

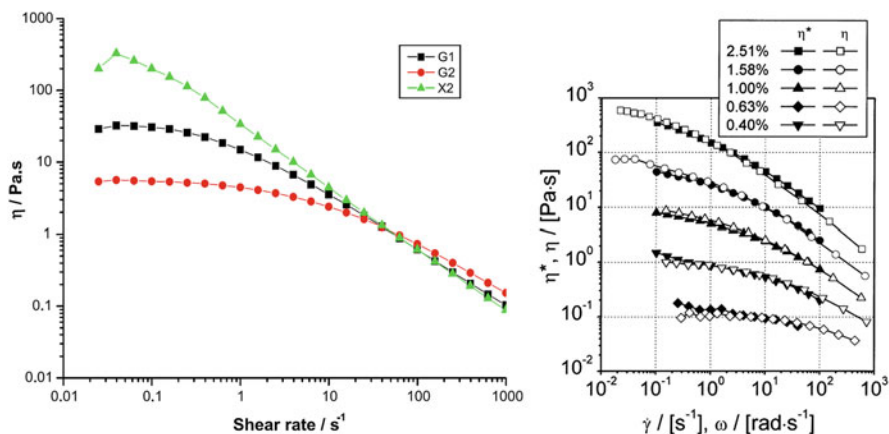


**Fig. 3.4** (a) Shear rate dependence of the viscosity of xanthan and guar solutions showing the crossover at  $50 \text{ s}^{-1}$ . The shear rate was changed stepwise from  $0.03$  to  $1000 \text{ s}^{-1}$  for  $10 \text{ min}$ . Closed square G1,  $2.0 \text{ wt\%}$  guar ( $M_w = 1.4 \times 10^6$ ) solution; closed circle G2,  $2.6 \text{ wt\%}$  guar ( $M_w = 6.3 \times 10^5$ ), closed triangle, X2,  $4.1 \text{ wt\%}$  xanthan ( $M_w = 3.4 \times 10^6$ ) solution. Reproduction with permission from Nishinari et al. (2011), Copyright 2011 Elsevier. (b) Cox–Merz plot for aqueous solution of hydroxypropylmethyl cellulose ( $M_w = 2.6 \times 10^6$ ) with different concentrations. Complex viscosity  $\eta^*$  is defined in Sect. 5. Reproduction with permission from Clasen and Kulicke (2001). Copyright 2001 Elsevier

### 4.1 Steady Shear Viscosity of Polymer Solutions

Polysaccharide thickening agents show shear thinning behavior. Xanthan is a microbial polysaccharide consisting of a linear (1–4) linked  $\beta$ -D-glucose backbone with a trisaccharide chain on every other glucose at C-3, containing a glucuronic acid residue linked (1–4) to a terminal mannose unit and (1–2) to a second mannose that connects the backbone, and has also been used widely in food industry as a thickener and texture modifier because its solution is stable over a wide pH and temperature range (Sworn 2021). The persistence length of xanthan was determined as  $120 \text{ nm}$  (Sato et al. 1984) and it explains well why this polysaccharide is an excellent thickener. Guar is one of galactomannans consisting of a mannan backbone and galactose side chains (Nishinari et al. 2007). The ratio of mannose to galactose is approximately 2:1. Rheological and related characteristics of guar have been extensively studied, and Mark–Houwink–Sakurada exponent and the persistence length are reported as  $0.7$  and  $4 \text{ nm}$ , respectively (Picout and Ross-Murphy 2007; Picout et al. 2001). In comparison with corresponding data  $0.65$  and  $2.5 \text{ nm}$  for a standard flexible polysaccharide, pullulan (Nishinari et al. 1991; Shingel 2004) it is evident that guar is slightly stiffer and its solution with the same molar mass and concentration shows higher viscosity than that of pullulan.

Steady shear viscosity of aqueous solutions of guar gum and xanthan gum solutions as a function of shear rate is shown in Fig. 3.4a. Xanthan solution shows pronounced shear thinning as reported by many previous workers. An apparent shear thickening behavior at lower shear rate is caused by structural formation after the



preparation of solution and it does not appear in the curve observed by lowering the shear rate. Wagner et al. (2016) recently reexamined this problem.

The lower molar mass guar shows less shear thinning and an apparent Newtonian plateau at lower shear rate as expected (Clasen and Kulicke 2001). This is consistent with previous data for guar gum fractions degraded enzymatically by  $\beta$ -mannanase for different times (Cheng and Prud'homme 2000).

When the complex viscosity  $\eta^* = G^*/i\omega$  (Sect. 5) as a function of angular frequency  $\omega$ , and the steady shear viscosity  $\eta$  as a function of shear rate  $dy/dt$  are plotted, the so-called Cox–Merz plot, both viscosities coincide as shown in Fig. 3.4b. When the complex viscosity and the steady shear viscosity do not coincide, it may mean that the microstructure at the relaxed state is destroyed by shear force. Then, the steady shear viscosity at higher shear rate may be smaller than the corresponding complex viscosity. However, it should be reminded that more fine local structure cannot be detected by this method. It is yet useful to see the validity of Cox–Merz rule for solutions of thickening agents.

Richardson and Ross-Murphy (1987a, b) reported that 3% guar gum solutions obeyed the Cox–Merz rule, but xanthan solutions deviated from it, and they ascribed it to some microstructure, “weak gel” (although senior author of this paper regretted to use this term 20 years later and prefers to use “structured liquid” because it is not a gel) formation in xanthan solutions. While guar gum solutions can be “thickeners,” xanthan solutions are “stabilizers” in which fine particles can be suspended without sedimentation. This suggests that some “structure” exists in xanthan solutions. Wientjes et al. (2000) did not find the validity of Cox–Merz rule for guar gum solutions. It is difficult to know the cause of the discrepancy between papers of these two groups.

Steady shear viscosity of xanthan solution has been studied extensively. Since xanthan chain is very stiff (persistence length 120 nm as mentioned above), the solution shows a shear thinning behavior. Yet, Einaga et al. (1977) show a Newtonian plateau at very low shear rates for a solution of much stiffer schizophyllan (persistence length 180 nm,  $M = 4.3 \times 10^6$ ) in water at 30 °C using a Zimm–Crothers type viscometer.

It was shown that globular protein solutions do not obey the Cox–Merz rule (Ikeda and Nishinari 2001a, b).

One important reason why xanthan is widely used as a thickener and stabilizer is that its remarkable shear thinning behavior in comparison to galactomannans such as guar and locust bean gum (LBG) in addition to its insensitivity to the change in temperature and pH. The high viscosity at low shear rates makes xanthan a good stabilizer which suspends fine particles of herbs at rest, and the low viscosity at higher shear rate confers it a flowability in motion. Recently, the steady shear viscosity of bacterial cellulose (BC) was compared with that of xanthan and LBG, and it was found the BC solution was more shear thinning than xanthan solution even at a lower concentration (Paximada et al. 2016). BC is also reported to be a good suspending agent for chocolate drink preventing the precipitation of cocoa particles, and in addition BC has a great heating stability after sterilization and thus the viscosity remains unchanged after heat treatment (Shi et al. 2014). This potential of BC was not exploited so much although it has attracted more attention as a unique jelly dessert known as *nata de coco* or stabilizer of ice cream (Azeredo et al. 2019).

The occurrence of shear thickening depends on the phase volume, particle size (distribution), particle shape, as well as those of the suspending phase (Barnes 1989, 2000). The increase of the viscosity above a critical shear rate is ascribed to the transition from a two- to a three-dimensional spatial arrangement of the particles. After this transition, the viscosity decreases again with increasing further shear rate.

Shear thickening behavior in food systems has been overviewed (Bagley and Dintzis 1999). Suchkov et al. (1997) reported a shear thickening behavior of 11S broad bean globulin (legumin) in 0.6 mol/dm<sup>3</sup> NaCl at pH 4.8 which was shown to have an upper critical temperature of 21 °C and a critical protein concentration of 18%. Dintzis et al. (1996) reported that waxy starches (corn (maize), rice, barley, and potato) showed shear thickening to a greater extent than did wheat, normal rice or normal corn starches when dissolved gently and dispersed at 3.0% concentration in 0.2N NaOH.

Shear thickening was observed for a 17.22% schizophyllan ( $M_w = 450$  kDa) solution around a shear rate of 0.01–0.1 s<sup>-1</sup> (Fang et al. 2004b). At the same shear rate range, a steep change in the birefringence was observed indicating an abrupt increase in molecular orientation. This is due to the extreme stiffness of schizophyllan chain as mentioned above.

Recently, the classical most well-known corn starch suspension was revisited, and shown that the so-called walking on water effect could be observed only above 52.5 wt% (42 vol%); a 2.1 kg rock laid on starch suspension with different concentrations fell, but a falling rock was bounced when it hit the surface of the starch slurry of 52.5 wt% (Crawford et al. 2013).

Solutions of mamaku polysaccharide extracted from black tree fern were shown to show the shear thickening behavior (Goh et al. 2007). Another example of shear thickening behavior was reported for sulfated polysaccharides from seaweeds (Shao et al. 2014).

## 4.2 Concentration Dependence of Viscosity

To understand the concentration dependence of the viscosity of polymer solutions, it is necessary to take into account the molar mass, molecular conformation, and shear rate dependence as is described in Chap. 2. The concentration dependence of viscosity of flexible polymers is usually represented by the relation between zero shear specific viscosity and the coil-overlap parameter defined by the product ( $C[\eta]$ ) of the concentration ( $C$ ) with the intrinsic viscosity  $[\eta]$ . Morris et al. 1981 Here, the intrinsic viscosity is determined by the extrapolation of the specific viscosity to zero concentration. The specific viscosity  $\eta_{sp}$  is defined as  $\eta_r - 1$ , where the relative viscosity  $\eta_r$  is defined as the ratio of the viscosity of the solution to that of the solvent  $\eta_s$ :  $\eta_r = \eta/\eta_s$ .

As shown above, most polymer solutions are non-Newtonian fluids and show a shear thinning behavior. At sufficiently low shear rate, the viscosity does not depend on the shear rate and shows a Newtonian plateau, so the viscosity observed at the

shear rate extrapolated to zero can be obtained, and it is called simply a zero shear viscosity ( $\eta_0$ ).

As described above, some models have been proposed to interpret the shear rate dependence of the viscosity of polymer solutions most of which are non-Newtonian liquids. Cross model is widely used to fit the observed shear rate dependence where both the zero shear viscosity  $\eta_0$  and the infinite shear viscosity  $\eta_\infty$  are observed:

$$\frac{\eta - \eta_\infty}{\eta_0 - \eta_\infty} = \frac{1}{1 + (K\dot{\gamma})^m},$$

where  $K$  has the dimension of time, and  $m$  is dimensionless. The value of  $m$  ranges from 0 to 1, and represents the degree of shear thinning. When  $m$  is closer to zero it tends to more Newtonian liquids, while the most shear thinning liquids have a value of  $m$  tending to unity.

Some other models Carreau model, Sisko model, etc. are also used (see more different models in Barnes (2000) and Lapasin and Pricl (1999)). Risica et al. (2010) used Cross eq to analyze the shear rate dependence of guar gum and hydroxypropylmethyl guar aqueous solutions.

The double logarithmic plot of the zero shear specific viscosity ( $\eta_{sp0}$ ) of polymer solutions and polymer concentration shows two straight lines. The slope of these straight lines is smaller at lower concentrations than at higher concentrations, and the crossover point  $C^*$  of these straight lines shifts to lower concentrations with increasing molar mass of a polymer.

Irrespective of chain flexibility, the slope at lower concentrations is reported as ca.1 and the slope at higher concentrations as 3.3 for many polysaccharides, but some other slopes are also reported and tabulated in Lapasin and Pricl 1999. When the zero shear specific viscosity is represented by a power law ( $\eta_{sp,0} \sim C^n$ ), the exponent ( $n$ ) takes different values below and above  $C^*$ . The exponent  $n$  for most polysaccharide solutions ranges from 1.1 to 1.6 below  $C^*$ , and from 1.9 to 5.6 above  $C^*$  (tabulated in Lapasin and Pricl 1999).

### 4.3 Salt Effect

The viscosity of polyelectrolyte solutions is influenced strongly by the presence of salt. In contrast to the common procedure to determine the intrinsic viscosity of non-electrolytic polymers, the reduced viscosity ( $\eta_{sp}/C$ ) of polyelectrolyte solutions shows a turn up in the extrapolation of polymer concentration. It is caused by the polymer coil expansion by electrostatic repulsion. By adding salt, the reduced viscosity decreases and the extrapolation to zero concentration becomes possible. See, for example, the zero shear rate reduced viscosity vs. equivalent monomer concentration of sodium pectate at various counterion concentrations (Lapasin and Pricl (1999)). Smidsrød and Haug (1971) proposed an empirical method to determine the stiffness parameter  $B$  by determining the intrinsic viscosity at 0.1M ionic strength (See Chap. 2). While the viscosity of flexible polyelectrolyte solutions is

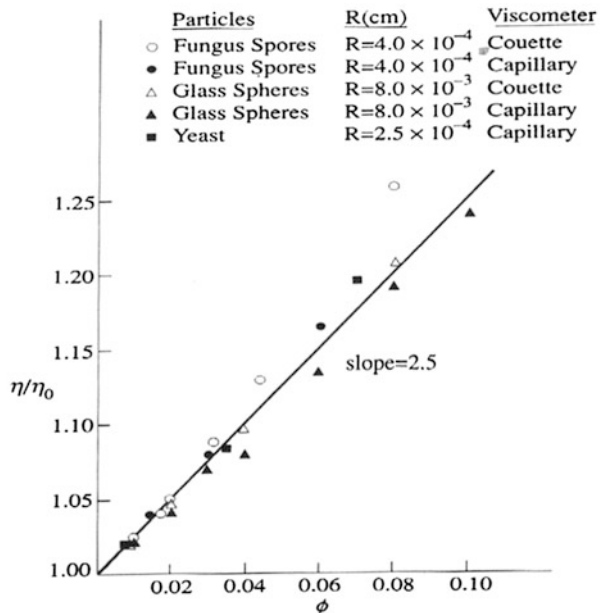
decreased by the addition of salt, that of stiff chains such as xanthan is comparatively insensitive to the addition of salt because the volume occupied by the stiff chain in the solution is not so much reduced as in the case of flexible chains. This comparative insensitivity/stability of the viscosity is one of the reasons why xanthan is used widely in food processing as mentioned before.

Wyatt et al. (2011) reported that the zero shear viscosity of xanthan showed different behaviors in the presence of salt depending on the polymer concentration. They observed that the zero shear viscosity of dilute xanthan solutions (500 ppm and 50 ppm) decreased while that of concentrated solution (4000 ppm) increased significantly by the addition of salt (50 mM NaCl). They also observed a similar behavior for anionic polysaccharides carrageenan and welan and also for a cationic polysaccharide chitosan. They stated that these results could be understood by scaling theories. Wyatt et al. (2011) found that Cox–Merz rule was valid for xanthan solutions, which is contradictory with previous reports by Lee and Brant (2002) and Richardson and Ross-Murphy (1987b), and they attributed this disagreement to the difference in the concentration.

### 4.4 Viscosity of Suspensions

The viscosity of dilute suspensions is well described by Einstein’s equation  $\eta = \eta_0 (1 + 2.5\phi)$ , where  $\eta_0$  is the viscosity of a suspending medium, and  $\phi$  represents the volume fraction of the dispersed phase. Figure 3.5 shows the normalized viscosity

**Fig. 3.5** Verification of Einstein’s equation. Reproduction with permission from Hunter (1998). Copyright 1998 Oxford University Press



(the ratio of the viscosity of the suspension to that of the solvent) vs. the volume fraction for various materials. It is striking that this equation holds well irrespective of the different nature of materials tested, spores, glass, and yeast. It is dependent only on the volume fraction.

This equation does not hold, however, for concentrated suspensions, and various modified equations have been proposed (Hunter 1998).

## 4.5 *Extensional Viscosity*

There have been many studies on the extensional viscosity but less than those on shear viscosity because of the difficulty in the measurements. Methods of measurements are stretching liquid between two flat plates, cylindrical viscoelastic filament uniaxially extended by rotating clamp, crossed slot devices, and opposed jets (Barnes 2000, p. 160; Larson 1999, p. 19). While the shear viscosity is defined by  $\eta_s = \tau/\dot{\gamma}$  where  $\tau$  is the shear stress and  $\dot{\gamma}$  is the shear strain rate, the extensional viscosity is defined by  $\eta_e = \sigma/\dot{\epsilon}$  where  $\dot{\epsilon}$  is the extensional strain rate. In Newtonian fluids, it is known that  $\eta_e = 3\eta_s$ . However, most food fluids are non-Newtonian, and the ratio of  $\eta_e/\eta_s$ , which is called Trouton ratio, is generally greater than 3. When a stick or a plate in a viscous liquid such as sugar syrup or honey is pulled up, the liquid flows downward and does not flow upward because they are Newtonian fluids. But, imagine the suspending of egg white just after cracking an eggshell or drooling from the mouth of a baby. Both of these liquids egg white/ saliva flow downward but then flow upward because of their elasticity. Egg white plays a role of cushion for an egg yolk and saliva and other mucins in humans have their own biological function which cannot be achieved if they are Newtonian liquids.

Chan et al. (2007) performed a comparative study of shear and extensional viscosity of casein, waxy maize, and their mixtures. They measured the extensional viscosity by observing the filament thinning when the liquid filament was extended. Chan et al. (2007) found that the maximum stretchable length of casein, waxy maize, and their mixtures were well described by a master curve using a capillary number (the product of the viscosity and the stretching speed divided by the surface tension) for viscous fluids, but the more concentrated samples showed a deviation from this master curve indicating the important effect of viscoelasticity.

Extensional viscosity of thickening agents has attracted much attention recently in relation with developing dysphagic treatments. Thickening agents are widely used in hospitals to prevent the aspiration. Thickening of a thin liquid such as tea, juice, or soup is effective (Cichero 2013). In addition to the increase of the viscosity, the cohesiveness of the liquid is believed to be necessary for safe swallowing, and the liquid extension test is suitable for this (Nishinari et al. 2019).

## 5 Viscoelasticity

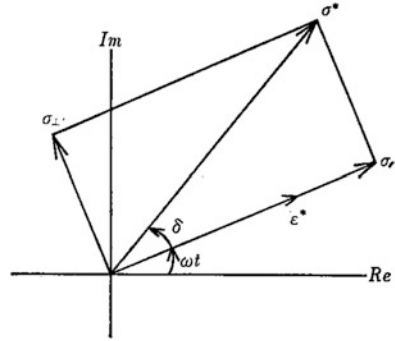
Simple mechanical models consisting of a spring which obeys the *Hooke's elasticity* law  $\sigma = G \varepsilon$  ( $\sigma$  stress;  $G$  elastic modulus;  $\varepsilon$  strain) and a dashpot which obeys the *Newtonian viscosity* law  $\sigma = \eta d\varepsilon/dt$  ( $\eta$  viscosity) are used widely. A spring represents an ideal elastic body which deforms instantaneously (without delay) and recovers to the initial state when the external force is removed. A dashpot is an ideal viscous material where the shear stress  $\sigma$  is proportional to the shear rate  $d\varepsilon/dt$ . In the shear deformation,  $\tau$  and  $\gamma$  are used for stress and strain in most textbooks.

Viscoelasticity is a relaxational phenomenon which depends on the time scale of the measurement. Typical viscoelastic phenomena are stress relaxation and creep. In the former, when the constant strain is given to a viscoelastic material, the induced stress decreases with the lapse of time, and it is called stress relaxation. In the latter, when a viscoelastic material is subjected to a constant stress, the induced strain increases with the lapse of time, and it is called creep. In these experiments, the stimulus causing the response is step-like and kept constant (does not depend on the time), and then, this is called static viscoelasticity.

A simple model consisting of a spring and a dashpot combined in series is called a *Maxwell element*. When a stress  $\sigma$  is applied to this model, the total strain  $\varepsilon$  is the sum of strains of each element, spring, and dashpot, and the total stress is equal to the stress of each element  $\sigma = \sigma_1 = \sigma_2$  because they are combined in series. Therefore,  $\sigma = G\varepsilon_1 = \eta d\varepsilon_2/dt$ , where the suffixes 1 and 2 refer to the spring and dashpot, respectively. Substituting these into  $\varepsilon = \varepsilon_1 + \varepsilon_2$ , the relation between stress and strain (called *constitutive equation*) for a Maxwell element is obtained:  $d\varepsilon/dt = (1/G)(d\sigma/dt) + (\sigma/\eta)$ . A Maxwell model represents a liquid-like viscoelasticity because it shows an infinite deformation because of the dashpot. When this viscoelastic material is subjected to a step strain at time  $t = 0$ , the stress is decreased with the lapse of time. This phenomenon is called *stress relaxation*. The above Maxwell eq gives the solution for this phenomenon,  $\sigma(t) = \varepsilon_0 G e^{-t/\tau}$ , where  $\tau = \eta/G$  is called the *relaxation time*, indicating that the stress decreases exponentially.

A simple model consisting of a spring and a dashpot combined in parallel is called a *Kelvin–Voigt element*. When a stress  $\sigma$  is applied to this model, the total stress  $\sigma$  is the sum of stresses of each element, and the total strain is equal to the strain of each element,  $\varepsilon = \varepsilon_1 = \varepsilon_2$  because they are combined in parallel. Therefore,  $\sigma_1 = G\varepsilon_1$  and  $\sigma_2 = \eta d\varepsilon_2/dt$ , respectively. Substituting these into  $\sigma = \sigma_1 + \sigma_2$ , the constitutive equation for a Kelvin–Voigt element is obtained:  $\sigma = G\varepsilon + \eta d\varepsilon/dt$ . A Kelvin–Voigt model represents a solid-like viscoelasticity in spite of the presence of a dashpot because it is combined in parallel with the spring which shows only a finite deformation. When a viscoelastic material is subjected to a step stress  $\sigma_0$  at time  $t = 0$ , the strain is increased with the lapse of time. This phenomenon is called *creep*. The above Kelvin–Voigt eq gives the solution,  $\gamma(t) = (\sigma_0/G) [1 - \exp(-t/\tau_r)]$ , where  $\tau_r = \eta/G$  is called *retardation time*. The retardation time is the time at which the strain reaches  $(1-1/e)$  times the final strain  $(\sigma_0/G)$  after an infinite time.

**Fig. 3.6** Strain vector  $\epsilon^*$  and stress vector  $\sigma^*$  on the complex plane.  $\epsilon^*$  rotates around the origin with constant angular velocity  $\omega$ , while  $\sigma^*$  also rotates with the same  $\omega$  with a leading phase  $\delta$ .  $\sigma_{\parallel}$  and  $\sigma_{\perp}$  show stress components with the same phase and the leading phase to  $\epsilon^*$



In real material, the two element model such as Maxwell element and Kelvin–Voigt element cannot describe well the rheological behavior. Assume that the strain  $\epsilon(t)$  of the material subjected to the constant stress  $\sigma_0$  at time  $t = 0$  is proportional to  $\sigma_0$ , then  $\epsilon(t) = \sigma_0 J(t)$  where  $J(t)$  is called *creep compliance*. When  $J(t)$  does not depend on  $\sigma_0$ , this material behavior is called linear. If  $\sigma_0$  is doubled,  $\epsilon(t)$  induced by the stress is also doubled in this case.

$J(t)$  consists of three parts:

$$J(t) = J_0 + J_d \varphi(t) + t/\eta \quad (*)$$

where  $J_0$  is the instantaneous compliance which obeys Hooke’s law,  $t/\eta$  is the viscous flow following the Newton’s law, and the  $J_d \varphi(t)$  is the retarded elasticity, and  $\varphi(t)$  is called creep function,  $\varphi(0) = 0$ ,  $\varphi(\infty) = 1$ . This is generally valid irrespective of the model. The creep function is given by  $\varphi(t) = 1 - \exp(-t/\tau_r)$ . These parameters can be determined graphically.

**Dynamic Viscoelasticity**

In the dynamic viscoelastic measurements, the viscoelastic material is subjected to the sinusoidal strain or stress, and the induced sinusoidal stress or strain is observed. The oscillational stress and strain can be represented in complex plane as vectors rotating at an angular velocity  $\omega$  as shown in Fig. 3.6, where  $\delta$  is the phase difference.

The shear strain is written as  $\gamma^* = \gamma_0 \exp(i\omega t) = \gamma_0 e^{i\omega t}$ , and the shear stress is  $\sigma^* = \sigma_0 e^{i(\omega t + \delta)}$ . The complex elastic modulus is defined by  $G^* = \sigma^*/\gamma^*$ . Therefore,  $G^* = (\sigma_0/\gamma_0)e^{i\delta} = (\sigma_0/\gamma_0) (\cos\delta + i \sin\delta)$ .

When  $G^*$  is written as  $G' + iG''$ , the real part  $G'$  is called storage modulus, and the imaginary part  $G''$  is called loss modulus.

$$G' = (\sigma_0/\gamma_0) \cos \delta, G'' = (\sigma_0/\gamma_0) \sin \delta$$

The ratio  $G''/G'$  is called mechanical loss tangent  $\tan \delta = G''/G'$ , which is related to the energy loss as shown below.

Complex viscosity is defined by

$$\eta^* = G^*/i\omega = \eta' - i\eta''$$

And its absolute value is  $|\eta^*| = [(G')^2 + (G'')^2]^{1/2}/\omega$

$$\eta' = G'/\omega, \eta'' = G''/\omega$$

For some polysaccharide solutions, the so-called Cox–Merz rule, which states that the complex viscosity plotted vs angular frequency agrees with the steady shear viscosity plotted vs shear rate, holds as is shown in Fig. 3.4b. But, this rule is an empirical rule with no sound theoretical validation, and many deviations are also reported.

### Dynamic Behavior of Maxwell Element and Kelvin–Voigt Element

When a sinusoidal strain  $\epsilon_0 e^{i\omega t}$  is given to a Maxwell element, the frequency dependence of complex modulus is given by

$$G_M^*(i\omega) = \frac{i\omega\tau G}{1 + i\omega\tau}$$

and the storage and loss moduli are

$$G_M'(\omega) = G \frac{\omega^2 \tau^2}{1 + \omega^2 \tau^2}$$

$$G_M''(\omega) = G \frac{\omega\tau}{1 + \omega^2 \tau^2}$$

When a sinusoidal stress  $\sigma_0 e^{i\omega t}$  is given to a Kelvin–Voigt element, the frequency dependence of complex compliance is given by

$$J_{KV}^*(i\omega) = \frac{1}{G} \frac{1}{1 + i\omega\tau}$$

### Loss Modulus is Related to the Energy Loss

**Question:** Calculate the energy dissipated in a viscoelastic material during one period of oscillation, and show that it is proportional to  $G''$

**Answer**

$$\int_0^{\frac{2\pi}{\omega}} \eta \dot{\gamma} \frac{d\gamma}{dt} dt = \int_0^{\frac{2\pi}{\omega}} \eta \dot{\gamma}^2 dt = \int_0^{\frac{2\pi}{\omega}} \eta (\gamma_0 \omega \cos \omega t)^2 dt = \eta \omega^2 \gamma_0^2 \frac{\pi}{\omega} = \pi \gamma_0^2 \omega \eta = \text{const} G''$$

### Mechanical Spectra: Frequency Dependence of Storage and Loss Moduli

Frequency dependence of storage and loss moduli for polymer solutions or colloid dispersions can be classified into four categories as shown in Fig. 3.7. In the dilute solutions where polymers dissolve with little or no overlap with each other,  $G' < G''$



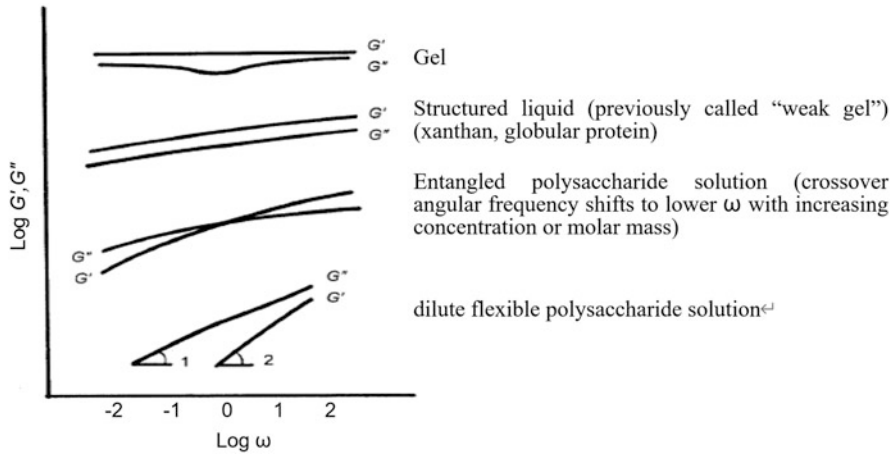


**Fig. 3.7** Typical angular frequency  $\omega$  dependence of  $G'$  and  $G''$  of commonly used thickening agents. It should be noted that values of  $G'$  and  $G''$  depend not only on the concentration but also on the molar mass and conformation of hydrocolloids or the coil-overlap parameter

and at very low frequencies it is seen that  $G' \sim \omega^2$ ,  $G'' \sim \omega$ . At higher concentrated solutions  $G' < G''$  at lower frequencies, but at higher frequencies  $G' > G''$  and thus at an intermediate frequency the crossover  $G' = G''$  is observed. This is interpreted as follows: at higher frequencies entangled polymer chains play a knot of temporary network and thus somewhat a solid-like behavior is observed, but at lower frequencies, the time of oscillational period is long enough for chains to disentangle, and thus it shows a liquid-like behavior  $G' < G''$ . The transition from the dilute region to entangled region is seen by the coil-overlap parameter = intrinsic viscosity  $\times$  polymer concentration as mentioned before. For networks or elastic gels,  $G' > G''$  at a wider frequency range and  $\tan \delta < 0.1$ . Between an elastic gel and concentrated (entangled) polymer solutions, another frequency dependence is observed, and it is called a structured liquid. This frequency dependence is also seen in globular protein solutions. Previously, it was called a weak gel. But, as will be discussed in detail in the next chapter, it is essentially a liquid and flows above a yield stress, which is discussed later in this chapter.

**Time–Temperature Superposition**

As is well known a material behaves like a liquid for a slow deformation, and shows a solid-like behavior for a fast deformation (see e.g. [https://en.wikipedia.org/wiki/Pitch\\_drop\\_experiment](https://en.wikipedia.org/wiki/Pitch_drop_experiment)). We also know that many solids become soft or firm when heated or cooled. For many synthetic polymers, the data obtained at low (high) temperatures are equivalent to those obtained at a high (low) frequency or a short (long) time scale, and then it was found that the data can be superposed by shifting horizontally (parallel to the time or temperature axis). When such a superposition between time and temperature is possible, it is called *thermorheologically simple*, and the resulted curve is called a *master curve*. The time–temperature superposition was successfully applied to many synthetic polymers, but great caution is needed to apply to food biopolymers.

### Lissajous–Bowditch Figure and LAOS (Large Amplitude Oscillatory Shear)

When the sinusoidal stress and strain,  $\sigma = \sigma_0 \sin \omega t$  and  $\gamma = \gamma_0 \sin \omega t$ , are taken as x-axis and y-axis in the orthogonal coordinate system, the Lissajous–Bowditch figure is obtained. In the elastic material, the stress and strain are in phase, and the Lissajous–Bowditch figure is a straight line. In the viscous material, the stress and strain are  $\pi/2$  out of phase, and the Lissajous–Bowditch figure is a circle. In the viscoelastic material, the stress and strain are  $\delta$  out of phase, and the Lissajous–Bowditch figure is an ellipse.

Generally, the linear viscoelastic range is wider for flexible linear polymer solutions than for structured liquids. Beyond the linear viscoelastic range, the resulted Lissajous–Bowditch figure is skewed. While the deviation from the elliptical shape is very small for a concentrated polysaccharide solution (hydroxyethyl guar gum), a pronounced distortion was recognized for a structured liquid (scIeroglucan) particularly at low frequency (Lapasin and Pricl 1999).

To understand quantitatively the non-linear viscoelastic behavior of food materials, large amplitude oscillatory shear (LAOS) has recently been attracting much attention. LAOS behaviors are often shown by the strain dependence of  $G'$  and  $G''$  at a constant angular frequency  $\omega$ , and are classified into four types: (1) strain thinning ( $G'$  and  $G''$  decreasing); (2) strain hardening ( $G'$  and  $G''$  increasing); (3) weak strain overshoot ( $G'$  decreasing,  $G''$  increasing followed by decreasing); (4) strong strain overshoot ( $G'$  and  $G''$  increasing followed by decreasing) (Hyun et al. 2011). However, this presentation cannot capture and clarify the whole characteristics of non-linear rheology. Chebyshev polynomial presentation has been proposed to get more physical meaning from LAOS data (Cho et al. 2005; Ewoldt et al. 2008).

The elastic ( $\sigma'$ ) and viscous ( $\sigma''$ ) stress are given by

$$\sigma' (x) = \gamma_0 \sum_{n: \text{odd}} e_n (\omega, \gamma_0) T_n (x)$$

$$\sigma'' (x) = \gamma_0 \sum_{n: \text{odd}} v_n (\omega, \gamma_0) T_n (y)$$

where  $T_n (x)$  is the  $n$ th order Chebyshev polynomial of the first kind,  $T_1(x) = x$ ,  $T_3(x) = 4x^3 - 3x$ ,  $T_5(x) = 16x^5 - 20x^3 + 5x$ ,  $\dots$

and  $x = \gamma/\gamma_0$ ,  $y = \dot{\gamma}/\dot{\gamma}_0$ , provide the appropriate domains of  $[-1, +1]$  for orthogonality,  $e_n (\omega, \gamma_0)$  and  $v_n (\omega, \gamma_0)$  are elastic and viscous Chebyshev coefficients.

In the Fourier representation of LAOS, the stress response  $\sigma (t; \omega, \gamma_0)$  to the strain stimulus  $\gamma (t) = \dot{\gamma}_0 \sin \omega t$  or strain rate stimulus  $\dot{\gamma} (t) = \dot{\gamma}_0 \sin \omega t$  is given by

$$\sigma (t; \omega, \gamma_0) = \gamma_0 \sum_{n \text{ odd}} \{G'_n (\omega, \gamma_0) \sin n\omega t + G''_n (\omega, \gamma_0) \cos n\omega t\},$$

$$\sigma (t; \omega, \gamma_0) = \dot{\gamma}_0 \sum_{n \text{ odd}} \{\eta''_n (\omega, \gamma_0) \sin n\omega t + \eta'_n (\omega, \gamma_0) \cos n\omega t\}.$$

The relationships between the Chebyshev coefficients in the strain or strain rate domain and the Fourier coefficients in the time domain are given by

$$e_n = G'_n (-1)^{(n-1)/2} \quad n : \text{odd},$$

$$v_n = G''_n / \omega = \eta'_n \quad n : \text{odd},$$

In the linear regime at small strains,  $e_3/e_1 \ll 1$  and  $v_3/v_1 \ll 1$ , and the linear viscoelastic relations

$$e_1 \rightarrow G' \text{ and } v_1 \rightarrow \eta' = G''/\omega.$$

are obtained. The strain-stiffening ratio  $S$  and the shear thinning ratio  $T$  are defined as follows:

$$S = (G'_L - G'_M)/G'_L = (4e_3 + \dots)/(e_1 + e_3 + \dots)$$

$$T = (\eta'_L - \eta'_M)/\eta'_L = (4v_3 + \dots)/(v_1 + v_3 + \dots)$$

where  $G'_L$  and  $G'_M$  are large strain modulus and minimum strain modulus respectively;

$$G'_M \equiv \left. \frac{d\sigma}{d\gamma} \right|_{\gamma=0} = \sum_{n \text{ odd}} n G'_n = e_1 - 3e_3 + \dots,$$

$$G'_L \equiv \left. \frac{\sigma}{\gamma} \right|_{\gamma=\pm\gamma_0} = \sum_{n \text{ odd}} G'_n (-1)^{(n-1)/2} = e_1 + e_3 + \dots,$$

For a linear elastic response,  $S = 0$  and  $S > 0$  means intracycle strain stiffening. For a linear elastic response,  $T = 0$  and  $T > 0$  means intracycle shear thickening.

LAOS studies on dough and gluten gels have been done using this method (Ng et al. 2011; Yazar et al. 2017a).

The characteristic shapes of Lissajous–Bowditch figures for a gluten gel over a range of strain amplitudes from  $\gamma_0 = 0.02$  to 6.0 at a fixed angular frequency at  $\omega = 1.0 \text{ rad s}^{-1}$  are plotted in Fig. 3.8 (Ng et al. 2011).

At smaller strain amplitudes, the relation between the stress and strain appears as an ellipse:

$$\sigma^2 - 2\sigma\gamma G' + \gamma^2 (G'^2 + G''^2) = G''^2 \gamma_0^2,$$

This quadratic form can be diagonalized, and the major and minor axes of the ellipse are centered at the origin. The enclosed area is given by  $\pi\gamma_0^2 G''$ , indicating the energy lost during one cycle of oscillation. As the strain amplitude is increased, the material response and shape of the Lissajous–Bowditch curves shown in Fig. 3.8 deviate significantly from this simple behavior. First a gradual “softening” of the

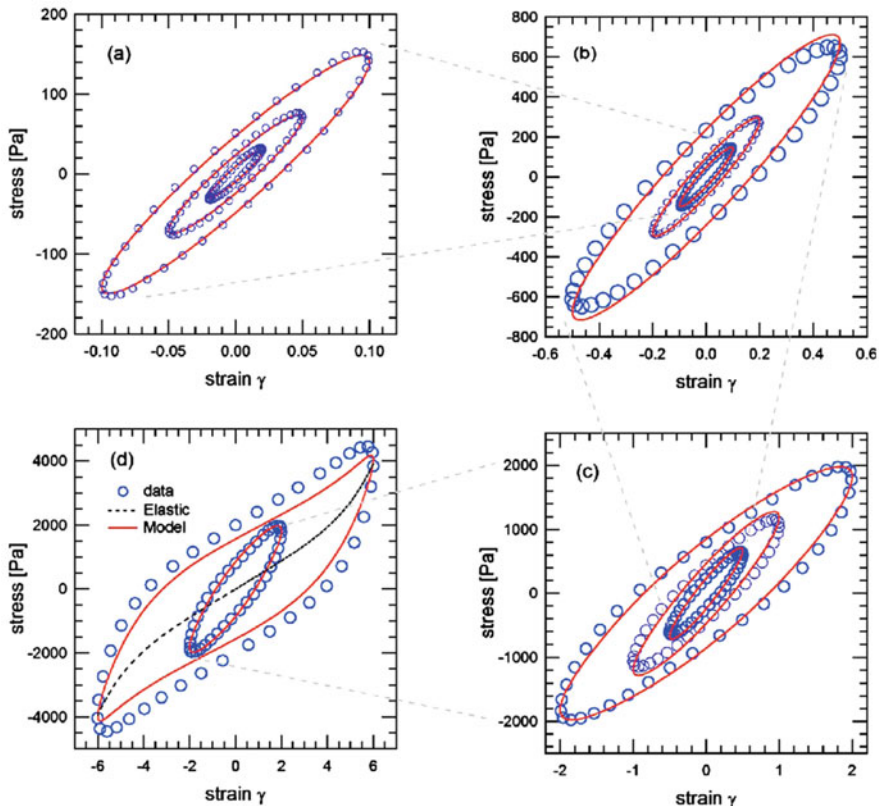


**Fig. 3.8** Lissajous–Bowditch curves after 12 oscillatory cycles for a gluten gel at a fixed angular frequency  $\omega = 1.0 \text{ rad s}^{-1}$  with (a)  $\gamma_0 = 0.02, 0.05, 0.10$ ; (b)  $\gamma_0 = 0.10, 0.20, 0.50$ ; the curve for  $\gamma_0 = 0.10$  from (a) is repeated. (c)  $\gamma_0 = 0.50, 1.00, 2.00$ ; (d)  $\gamma_0 = 2.0$  and  $6.00$ . As the imposed strain amplitude  $\gamma_0$  increases from (a) to (d), the magnitude of the maximum stress grows and the axes are rescaled. Experimental data are plotted as open symbols. The decomposed elastic stresses are shown in the lower panel as a dotted line for  $\gamma_0 = 6$ . Predictions from the nonlinear generalized gel model are plotted as a solid line for each strain amplitude. Reproduction with permission from Ng et al. (2011). Copyright 2011 AIP

material is indicated by the clockwise rotation of the major axis toward the strain-axis. Second, a distinct “stiffening,” indicated by the upturn of the shear stress, is observed at large strains (Fig. 3.8d). The magnitude of the enclosed area also increases with increasing amplitude, indicating an increasingly dissipative response. These non-linear features cannot be fully captured by simply reporting  $G'$  and  $G''$  as a function of strain amplitude, as is usually done in linear viscoelasticity analysis (Ng et al. 2011).

Duvarci et al. (2017) applied this method to suspensions, emulsions, and elastic networks (tomato juice, mayonnaise, soft and hard dough). In the strain dependence of  $G'$  and  $G''$  at a constant angular frequency, tomato paste showed the type (I), strain thinning ( $G'$  and  $G''$  decreasing) while mayonnaise showed the type (III), weak

strain overshoot ( $G'$  decreasing,  $G''$  increasing followed by decreasing). A slight strain softening ( $S < 0$ ,  $e_3/e_1 < 0$ ) at smaller strains and strain hardening at larger strains were observed for tomato paste and mayonnaise. Strain hardening ( $e_3/e_1 > 0$ ) and shear thinning ( $v_3/v_1 < 0$ ) were observed for soft dough and hard dough.

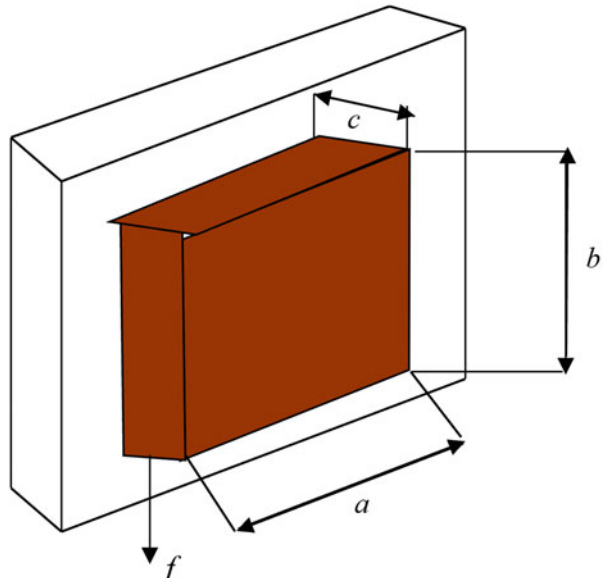
Biaxial deformation has been widely used in baking investigation, and gluten doughs showing high resistance to biaxial deformation and pronounced strain hardening behavior were found to be good for baking, i.e., larger bread volume (Kokelaar et al. 1996). Bread volume has been used as an index of the bread forming performance of dough. Recently, bread volume of gluten-free flour doughs were plotted as a function of large strain modulus  $G'_L$  or minimum strain modulus  $G'_M$ , and it was found that the bread volume increased with increasing  $G'_L$  and or  $G'_M$  (Yazar et al. 2017b).

## 6 Yield Stress

The concept of yield stress is intuitively evident: most fluid foods filled in tubes such as mayonnaise, mustard, ketchup, pastes, etc. begin to flow only when they are subjected to a certain value of stress. The minimum stress required to cause flow is the yield stress. The first simplest model is a Bingham fluid:  $\sigma = \eta_B (dy/dt) + \sigma_y$ , where  $\sigma_y$  is the yield stress,  $\eta_B$  is the Bingham plastic viscosity. Another simple model, Herschel–Bulkley fluid  $\sigma = \eta_{HB} (dy/dt)^n + \sigma_y$  has also been used for better describing the behavior.

Yield stress governs the thickness of coated chocolate on the biscuit as shown below (Fig. 3.9).

**Fig. 3.9** Chocolate coating on biscuit. The yield stress of chocolate dictates the thickness of chocolate



The gravitational force exerting on the melted chocolate  $f$  is given by  $f = mg = V\rho g$ , where  $m$  is the mass,  $V = a \times b \times c$  is the volume,  $\rho$  is the density of the chocolate. From the definition of the yield stress, this gravitational force should balance with the yield stress  $\times$  surface area  $= \tau_y \times a \times b$

Therefore,  $a \times b \times c \times \rho \times g = \tau_y \times a \times b$

The thickness  $c$  of the chocolate is  $c = \tau_y / \rho g$

For a chocolate with  $\tau_y = 5$  Pa,  $\rho = 1.06 \times 10^3$  kg/m<sup>3</sup>, the thickness of the chocolate is given by

$$c = 5 \text{ N m}^{-2} / (1.06 \times 10^3 \text{ kg/m}^3 \times 9.8 \text{ m s}^{-2}) = 0.00048 \text{ m} = 0.48 \text{ mm}.$$

Yield stress can in principle be determined by decreasing the shear rate in the plot of the shear stress vs shear rate. Then, the shear stress obtained at zero shear rate is the yield stress. Rigorously speaking, it is impossible to determine the absolute yield stress which is conceptually the *idealization*. In a very long time scale everything flows even at a very low stress (Barnes 1999).

Although it is not easy to measure, the concept of the yield stress is meaningful in food science and technology, and it should be reminded that the yield stress values obtained by different methods can be compared only over the same range of shear rates (Barnes 1999; Bonn et al. 2017).

Many papers have been published on the existence of the true yield stress. Using four model yield stress materials, 0.2% carbopol, a commercial hair gel (containing carbopol, water triethanolamine as a stabilizing agent), a commercial shaving foam, and a cosmetic water-in-oil emulsion (composed of 80% water with carbopol 940 (1%) in Vaseline oil (6%) and Polyethylene glycol 600 (6%) with several additives, so that it remains stable under shear when used), Mϕller et al. (2009) showed that the yield stress really exists and it marks a transition between the fluid which flows and the solid which does not flow. These four samples are called “simple” yield stress materials because the viscosity depends only on the shear rate, and the yield stress is a material property while for thixotropic yield stress materials the viscosity depends also on the shear history, which is discussed in the next Sect. 7. “Apparent” viscosity = stress/(instantaneous shear rate) which is time dependent and therefore not “true” viscosity, of all the four materials as a function of stress showed a steep rise with decreasing stress and then leveled off to show a plateau value below a certain stress. The plateau value of the apparent viscosity increased with the measurement time up to  $\sim 10^3$  s. Fig. 3.10a shows the apparent viscosity of 0.2% carbopol as a function of time for different stress values.

Above the stress 27 Pa, the apparent viscosity quickly reaches the steady value and then it stays constant up to  $\sim 10^3$  s, while below the stress 25 Pa, the apparent viscosity continues to increase even at  $10^4$  s. Therefore, above the stress 27 Pa, the material flows at a constant viscosity which is a decreasing function of the stress, while the apparent viscosity continues to increase with time as  $\eta \sim t^{0.6}$  as indicated by the dashed straight line, indicating that the system behaves almost as a solid having a very large viscosity within the experimentally accessible observation time. Thus, this stress 27 Pa can be defined as a yield stress. The same phenomenon was also observed for other three different materials. Below a critical stress, the viscosity

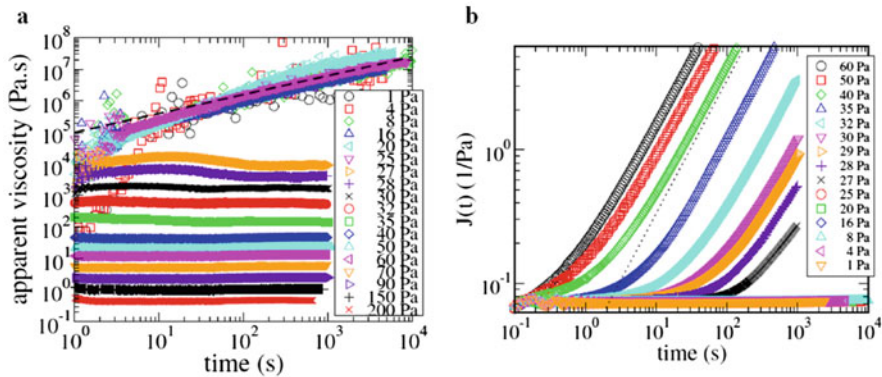


**Fig. 3.10** (a) Apparent viscosity of 0.2% carbopol as a function of time at different stresses. At and above the stress 27 Pa, the apparent viscosity  $\eta$  of the sample shows a constant value (time independent) while at and below the stress 25 Pa,  $\eta$  increases with increasing time  $\eta \sim t^{0.6}$  as indicated by the dashed straight line. (b) A creep compliance  $J(t)$  of the same data as in left figure. At large  $t$  a fluid state will have a slope of 1 (indicated by the dotted line), while a solid state will have a slope of 0. At stresses of 27 Pa and above, slopes are nearly 1, while they are nearly 0 at 25 Pa and below—data for six stresses are collapsed and hardly discernable. Reproduction with permission from Mϕller et al. (2009). Copyright 2009 IOP

increases in time; the material eventually stops flowing. Above the critical stress, the viscosity decreases continuously in time; the flow accelerates. Thus the viscosity jumps discontinuously to infinity at the critical stress. This phenomenon is thus called viscosity bifurcation (Coussot et al. 2002a, b)

As shown clearly in Fig. 3.10b, at and below the stress 25 Pa the deformation was zero indicating the solid behavior below this critical stress (yield stress), while the compliance increases with increasing time with the slope 1 indicating the fluid behavior at and above the stress 27 Pa. Both Fig. 3.10a, b show clearly the existence of the yield stress, and this is also recognized also in the other three different yield stress materials, a hair gel, a shaving foam, and a water-in-oil emulsion.

Many methods have been proposed to determine the yield stress. Dinkgreve et al. (2016) using the same four model simple yield stress materials compared the yield stress values, and concluded that the Herschel–Bulkley fit to the stress–shear rate gives the lowest and the most reliable value for the yield stress. Vane geometry is sometimes useful to determine the yield stress because it is free from slippage (Stokes and Telford 2004).

## 7 Thixotropy

The viscosity of many structured liquids at a constant shear rate decreases with the lapse of time, which is called thixotropy. It is different from shear thinning behavior which is defined as the decreasing of the viscosity when the shear rate is increased.



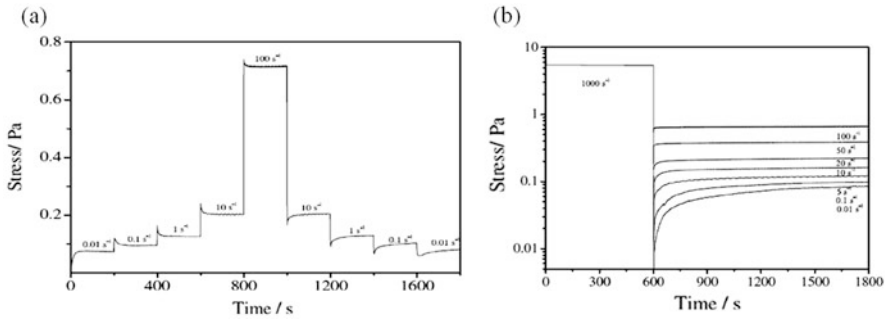


**Fig. 3.11** (a) Shear stress transients in step shear rate tests for 6 wt% gum arabic in water. The shear rates of different steps were shown in the panel (b) Time evolution of the transient shear stress in sudden reduction of shear rate from  $1000 \text{ s}^{-1}$  to different lower shear rates for 6 wt% gum arabic solution. The different lower shear rates were shown in the panel. Reproduction with permission from Li et al. (2011). Copyright 2011 Elsevier

All the shear thinning liquid show a thixotropic behavior since it takes a time to recover the initial microstructure even if it is short.

Thixotropy is a time dependent rheological phenomenon, and it is understood as the microstructural formation at rest and the breakdown of that structure during shearing. The thixotropy is explained by the competing two processes *aging* (structure formation) and *rejuvenation* (structure breakdown).

Delayed failure of fish myosin gels was studied, and the time to failure as a function of scaled applied stress showed two regimes (Brenner et al. 2013). This time depends on the bond reformation rate; the time is short when the stress is high and bond reformation is not sufficient while it is long when the stress is low and bond is reformed (Sprakel et al. 2011; Lindstrom et al. 2012).

A hysteresis loop test which records a stress–shear rate curve is a simple demonstration of the thixotropic behavior and has been used widely for many foodstuffs such as yogurt. Although a loop test, shear stress vs shear rate, has been frequently used to study thixotropic behavior because it is easy to do, Barnes (1997) depreciated this method. Though it gives some qualitative information, he recommends the stepwise experiments where the shear rate or stress is changed from one constant value to another with a carefully controlled prehistory. The advantages of the stepwise change of shear rate in comparison with the hysteresis loop method are that not only the initial condition can be well-defined and reproducible, but also the shear rate during the actual test remains constant. Hence, the effect on an established structure of shearing at a fixed shear rate can be measured as a function of time (Mewis and Wagner 2012).

Figure 3.11 shows an example of such an experiment for solutions of gum Arabic which is widely used as emulsifiers and stabilizers in food industry. When the shear rate is increased/decreased in a step-like manner, the induced stress shows an overshoot/undershoot, and then decreases/increases to a stationary value. The transient stress shown in Fig. 3.11 can be written



$$\sigma = \frac{1}{\left[ \frac{1}{\sqrt{\sigma_s}} + \left( \frac{1}{\sqrt{\sigma_i}} - \frac{1}{\sqrt{\sigma_s}} \right) \exp(-kt) \right]^2}$$

where  $\sigma_i$  and  $\sigma_s$  represent the initial and stationary values of the stress, respectively, and  $k$  is a kinetic constant with  $k = k_f + k_b$ . Here,  $k_f$  and  $k_b$  are rate constants, which modulate the kinetics of structural buildup and breakdown processes, respectively. The rate constant  $k_f$  depends on temperature, whereas  $k_b$  is a function of the applied shear rate, and  $t$  is the testing time. Although old textbooks describe a gum Arabic solution as a Newtonian solution, the recent improvement of the rheometry makes it possible the measurement at low shear rates. The deviation from the Newtonian behavior at low shear rates ( $<10 \text{ s}^{-1}$ ) suggests the existence of the molecular aggregation which is broken down by shear flow. The above equation was also used by Grassi et al. (1996) for scleroglucan and by Fang et al. (2004a) for schizophyllan. Oleogel consisting of rapeseed oil and shellac (a resin secreted by an insect) also showed a thixotropic behavior (Patel et al. 2013). This indicates that an oleo gel is a structured liquid and not a gel as defined in the next chapter. Actually, this oleo gel shows a flow behavior without fracturing when it is subjected to shear which is widely observed for structured liquids with yield stress such as xanthan, welan, rhamsan, schizophyllan, and scleroglucan.

The stepwise experiment to examine the thixotropic nature of low-fat mayonnaise-like emulsion gels, containing egg yolk, rapeseed oil (30% instead of 80% in full-fat mayonnaise), salt, sugar, vinegar, and 4.0% alginate solution and KGM powder, was performed (Yang et al. 2020). Structural recoverability was found for the low-fat mayonnaise-like emulsion gels in the stepwise experiment, and the stackability was enhanced by adding small amount of calcium ions. Stackability is required for mayonnaise, and is related with yield stress.

The opposite behavior of thixotropy is called *antithixotropy* where start-up flow or a sudden increase in shear rate causes an *increase* in viscosity over time (Mewis and Wagner 2012).

The dilute solution of globular protein shows another unique aspect, an antithixotropic rheological behavior; the viscosity of beta-lactoglobulin solutions at a fixed low shear rate increased with the lapse of time (Renard et al. 1996).

## 8 Microrheology

In the conventional or bulk rheology, the sample size is generally mm order and  $1 \text{ cm}^3$  in volume, and therefore it is difficult to get the information of local region of inhomogeneous sample. Microrheology is useful to examine the rheological properties of a local region in inhomogeneous materials such as cytoplasm, thick egg white, and emulsion gels. The idea to determine the elasticity and viscosity in inhomogeneous materials dates back to Freundlich and Seifriz, and Heilbronn in 1920s, and development of theories on Brownian motion and experimental

techniques, electronics, spectroscopy, light scattering, thereafter made the method more quantitative.

There are two types of measurements in microrheology: passive and active methods. The microrheological information obtained by these two methods are equivalent by virtue of the fluctuation–dissipation theorem (FDT) in the equilibrium state (Doi 2013; Waigh 2016; Yang et al. 2017).

In the passive microrheology, the mean square displacement (MSD) of the probe particle is detected and analyzed by video tracking, laser tracking, and diffusing wave spectroscopy.

Multi-particle tracking microrheology was performed to obtain local elasticity and heterogeneities of gellan microgels using fluorescent colloidal particles with diameter of 0.5  $\mu\text{m}$  (Caggioni et al. 2007).

## 9 Fractional Calculus Bridging the Instrumental Measurement and Sensory Evaluation

### 9.1 *Scott Blair's Approach to Understand the Firmness Judged by Humans*

Intermediate materials between elastic solid and viscous fluid such as cheese cannot be characterized only by modulus or by viscosity. In most food rheology, the intermediate state of the elasticity and viscosity has been studied as viscoelasticity where the rheological behavior of such materials is analyzed by static or dynamic viscoelastic measurement such as creep, stress relaxation or oscillation measurement, and large deformation and fracture mechanics have also been studied. Scott Blair proposed alternative method to analyze the rheological behavior of foods and other industrial materials by virtue of the “principle of intermediacy” (Scott Blair 1969). Instead of the complex plane representation of the storage modulus and loss modulus, he proposes a Cartesian coordinate consisting of the modulus  $G = \sigma/\epsilon$  and the viscosity  $\eta = \sigma/(d\epsilon/dt)$  to explain the “principle of intermediacy.” An intermediate material between the elastic solid and the viscous liquid can be represented in this plane as a vector  $\varphi = d^k\epsilon/dt^k$ , where  $k$  is a fraction and  $d^k\epsilon/dt^k$  is a fractional derivative which Scott Blair introduced into rheology to understand the relation between the sensory assessment and the instrumental measurement. The elastic material with  $k = 0$  is judged by the strain  $\epsilon$  and the viscous material with  $k = 1$  is judged by the strain rate, that is  $d^1\epsilon/dt^1$ , and therefore, it is reasonable to think that the fractional differentiation of the strain  $d^k\epsilon/dt^k$  should be used for the judgment of the firmness for the materials with  $0 < k < 1$  intermediate between the elastic material and the viscous material.

To represent the intermediate state of the elasticity and viscosity, the quasi-property  $\chi$  was defined as (Scott Blair 1947)

$$\chi = \sigma / (d^k \varepsilon / dt^k)$$

where  $d^n \varepsilon / dt^n = \psi^{-1} \sigma k(k-1)(k-2) \cdots (k-n+1) t^{(k-n)} = \psi^{-1} \sigma t^{(k-n)} \Gamma(k+1) / \Gamma(k-n+1)$ ,  
 where,  $\Gamma(k-n+1)$  is a gamma function

$$\Gamma(k+1) = \int_0^{\infty} e^{-z} z^k dz = k \Gamma(k) = k(k-1)(k-2) \cdots (k-n+1)$$

Although most physicists had not agreed to use “quasi-properties,” Reiner supported Scott Blair’s concept.

The fractional calculus has been used to discuss the rheological properties of various soft materials (Koeller 1984; Jaishankar and McKinley 2012; Rogosin and Mainardi 2014). The mechanical element having an intermediate behavior of the spring and dashpot is called Scott Blair element or springpot model having a constitutive equation

$$\sigma = G \frac{d^\beta \gamma}{dt^\beta} \quad (0 < \beta < 1)$$

Therefore, from the experimental observation of  $J(t)$ , or  $G(t)$ , or  $G'(\omega)$  and  $G''(\omega)$ , parameters  $G$  and  $\beta$  of springpot model can be determined.

## 9.2 Recent Development of the Application of Fractional Calculus to Liquid Foods

Wagner et al. (2017) based on fractional calculus studied the rheological properties of thickening agents used in dysphagia. Fractional Maxwell model (FMM) and Fractional Jeffereys model (FJM) were used. FMM is a series combination of two springpots with quasi-properties  $V$ ,  $\alpha$  and  $G$ ,  $\beta$ , and it is reduced to a spring or dashpot when  $\alpha = 0$  or  $\alpha = 1$ , respectively. FJM is a parallel combination of FMM and a dashpot with the viscosity  $\eta_s$ .

The steady shear viscosity can be also written using these parameters. Wagner et al. (2017) used the Cox–Merz rule to correlate the small amplitude oscillational data of  $G'$  and  $G''$  with the steady shear viscosity, and they found generally a good agreement although they needed some corrections taking into account the viscosity at higher shear rate. They fitted the experimental data of polysaccharide thickening solutions used for dysphagic treatment, a commercial thickener TUC and saliva, using the above equations, and obtained the parameters  $V$ ,  $\alpha$ ,  $G$ ,  $\beta$  and  $\eta_s$  of fractional models. They replaced  $G$  with  $K$ , and  $\beta$  with  $n$ , where  $K$  is the so-called consistency index of the fluid in the power law fluids (Curves 2 and 3 in Fig. 3.3a). Instead of  $\eta$  in power law models (2) and (3) in Fig. 3.3a,  $K$  is often used and called consistency index (with the unit of Pa  $s^n$ ), while  $n$  is called flow behavior index (dimensionless).

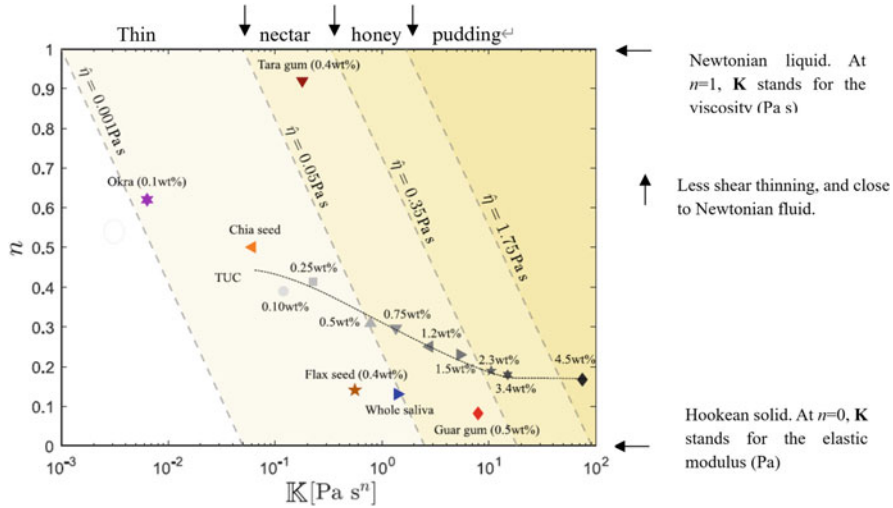


**Fig. 3.12** Fractional parameter phase space for food consistency. The markers correspond to the values of the quasi-property  $K$  and fractional exponent  $n$  best describing the shear thinning in the steady shear viscosity of the TUC solutions, polysaccharides, and whole saliva at  $\dot{\gamma}=50 \text{ s}^{-1}$ . The dashed diagonal lines bordering the shaded regions denote isoviscosity curves at  $\dot{\gamma}=50 \text{ s}^{-1}$  corresponding to the “thin” (0.001–0.05 Pa s) “nectar-like” (0.05–0.35 Pa s), “honey-like” (0.35–1.75 Pa s), and “pudding-like” ( $>1.75$  Pa s), preparations of starch solutions by the National Dysphagia Diet Task Force. Reproduction with permission from Wagner et al. (2017). Copyright 2017 Elsevier

They analyzed the thickening behavior of various polysaccharides and a commercially available thickening agent TUC using fractional calculus power law model using the Cox–Merz rule

$$n(\dot{\gamma})|_{\dot{\gamma}=\omega} = |\eta^*(\omega)| = K\omega^{n-1}$$

In the fractional calculus treatment of viscoelasticity,  $K$  is called quasi-property. They found an excellent fitting using this equation for thickeners and plotted the data in the  $K$ - $n$  plane (Fig. 3.12).  $K$  is taken as an abscissa and  $n$  is taken as an ordinate. The exponent  $n = 1$  corresponds to the purely Newtonian viscous liquid, and  $n = 0$  corresponds to a Hookean elastic solid. Each point in the interior of this parameter space in the range  $0 < n < 1$  represents viscoelastic power law fluids.

In this  $K$ - $n$  plane, equations of the dashed diagonal straight lines are

$$n = 1 + \frac{\log \bar{\eta}}{\log 50} - \frac{\log K}{\log 50}$$

where  $\bar{\eta} = 0.001, 0.05, 0.35,$  and  $1.75$  from the left to right, and the slope of the diagonal straight lines is  $-1/\log 50$ .

As is seen clearly from Fig. 3.12, it is evident that the characterization of the “thickness” of these fluids only by the viscosity is insufficient. Tara gum is close to

the  $n = 1$  Newtonian line, but the other fluids flax seed, whole saliva, guar gum, and TUC are all below  $n = 0.5$ , and elasto-plastic or yield stress like response is very important. The importance of the elastic contribution for the dysphagia treatment is in good agreement with the concept that cohesiveness of bolus is important for safe swallowing (Nishinari et al. 2019). The advantage of the analysis based on fractional analysis is that it contains only a few parameters which can be determined by the well-defined rheological measurements.

Faber et al. (2017a, b) studied the texture of cheese using the fractional calculus. They favored their approach based on the springpot model over the more undirected approach of statistically correlating large amounts of rheological data to the results from quantitative descriptive analysis (QDA) of multiple texture attributes. Their reservations to the latter approach are for two reasons. First the deformations and observations in QDA that lead to the texture judgment are ill-defined and may vary from subject to subject. This a priori weakens correlations with the measurements obtained from the carefully designed rheological experiment. Their second argument to favor the fractional calculus approach is that material properties are intrinsic properties whereas texture attributes are extrinsic in nature (Reiner 1971).

## 10 Further Developing of Thickening Properties

### 10.1 Viscosity of Mixed Hydrocolloids

The viscosity of the mixture of hydrocolloids has been studied from a long time ago. The so-called synergistic interaction between xanthan and guar, the viscosity of mixed solution as a function of mixing ratio showed a maximum, was reported (Sanderson 1981). The word synergism is used when the viscosity of the mixture is higher than the sum of the viscosities of the individual gum dispersions. However, in most cases, the viscosity of the mixture is lower than the sum, for example, the viscosity of mixtures of konjac glucomannan with xanthan, guar gum, carrageenan, sodium alginate, methyl cellulose, hydroxymethyl cellulose, sodium carboxymethyl cellulose, all the mixture except with xanthan showed the lower viscosity than the sum of the individual polysaccharide (Liang et al. 2011).

Recently, Zhang et al. (2015) examined the interaction of corn fiber gum (CFG) with various polysaccharides, hyaluronan (HA), guar gum (GG), carboxymethylcellulose (CMC), hydroxyethyl cellulose (HEC), konjac glucomannan (KGM), pectin, and chitosan using a shear stress synergy index  $I_s$ , which is defined by

$$I_s = \frac{\bar{\sigma}_{i+j}}{\bar{\sigma}_i + \bar{\sigma}_j},$$

where  $\bar{\sigma}_{i+j}$ ,  $\bar{\sigma}_i$  and  $\bar{\sigma}_j$  represent the shear stress for the mixture of  $i$  and  $j$ ,  $i$  alone and  $j$  alone in the flow curve  $\sigma \sim \dot{\gamma}$  written as follows:

$$\bar{\sigma} = \frac{1}{\dot{\gamma}_2 - \dot{\gamma}_1} \int_{\dot{\gamma}_1}^{\dot{\gamma}_2} \sigma d\dot{\gamma},$$

(Pellicer et al. 2000). This index  $I_s$  was used to judge whether the interaction is synergistic or antagonistic. When  $I_s > 1$  it is judged as synergistic while when  $I_s < 1$  it is judged as antagonistic or lack of synergism. Zhang et al. (2015) found the synergistic interaction, i.e.  $I_s > 1$  for CFG with HA, HEC, GG, KGM, pectin, chitosan and concluded that CFG has a great potential as a viscosifying polysaccharide. CFG itself shows a very low viscosity and almost a Newtonian behavior like gum Arabic, while the interaction with other polysaccharides induces a greater viscosity.

As for the temperature dependence of viscosity of thickening agents, xanthan shows low temperature dependence and so stable, but in heat processing the viscosity lowering is sometimes required so that the stirring force can be weak. Xyloglucan (XG) is suitable for such requirement. Viscosity of tapioca starch (TS) suspension is reported to be more heat resistant when xyloglucan was added (Pongsawatmanit et al. 2006). The influence of temperature on the apparent viscosity of TS paste was estimated by an Arrhenius plot  $\ln(\text{viscosity})$  vs  $1/T$ . The activation energy  $E_a$  determined from the slope of this plot for TS mixed with XG was found much smaller than for TS alone, indicating that the addition of XG improved the heat stability. It was also found that the water separation from freeze-thaw samples was much reduced by XG.

Exactly the same reasoning was used in the same year 2006, to show the thermal stability of the mixture of hydroxypropyl-substituted guar (HPG) and carboxymethyl hydroxypropyl-substituted guar (CMHPG) in comparison with each individual HPG and CMHPG (Zhang and Zhou 2006). Zhang and Zhou found that the activation energy was smaller for the mixed CMHPG/HPG solution indicating that the mixture showed the improved temperature tolerance with respect to the viscosity. They also found that the viscosity of the 1:1 mixed solution was higher than that of each individual solution.

## 10.2 Molecular Structure and Viscosifying Function

The beneficial effect of dietary fibers is recognized well, and this function is generally believed to be conferred by high viscosity. However, in the supplement utilization, too high viscosity hinders the sufficient intake of dietary fibers, and therefore enzymatically degraded guar gums, degraded sodium alginate, dietary fiber from psyllium seed husk, and other polysaccharides have been commercialized ([www.mhlw.go.jp/english/topics/foodsafety/fhc/02.html](http://www.mhlw.go.jp/english/topics/foodsafety/fhc/02.html)).

Cellulose chemists have modified the structure of cellulose by adding some residues at C2, C3, and C6 thus controlling the solubility and viscosifying properties.

Similar trials have been made for various polysaccharides using chemical and enzymatic modifications.

Recently, new variants of xanthan were created using genetic engineering (Wu et al. 2019). Since the shear rate dependence of these variants shows quite a different behavior, the further developments are expected.

Zhao et al. (2017) found that a new exopolysaccharide from a strain *Klebsiella* sp. is very resistant against the extreme pH. Although solutions of this new polysaccharide show a commonly observed shear thinning behavior at pH range from 2 to 12, this polysaccharide is degraded outside of this pH range. However, when the alkaline degraded polysaccharide is acidified into neutral pH, both moduli increased and the crossover was observed at pH 10.5. Below that pH, the solution showed a structured liquid behavior. It suggests that the backbone structure of this polysaccharide was not degraded, and some conformational change was reversible as observed in scleroglucan, which showed a rheological recovery induced by the partial recovery of triple helices from coil conformation after the degradation at high pH (Aasprong et al. 2003). The advantage of this new polysaccharide is that the viscosifying properties are stable and not so much changed by the addition of sodium, potassium, magnesium, and calcium ions as in xanthan.

## 11 Application of Hydrocolloids as a Thickener

### 11.1 Controlling the Viscosity and Stabilizing of Liquid Foods, Acidified Milk, Sauces

High methoxyl pectin (HMP) has been used widely to stabilize acidified milk drinks for over 60 years. Stabilization mechanism of HMP was attributed to the steric repulsion among HMP adsorbed casein aggregates and not by a weak gel network, and the adsorption of HMP to the surface of casein aggregates was by electrostatic attraction (Parker et al. 1994; Jensen et al. 2010). Kiani et al. (2010) studied the stabilization of a traditional Iranian yogurt drink by gellan/HMP, and suggested that gellan confers the additional stabilization effect. Recently, another pectic polysaccharide extracted from *Ulmus davidiana* was found effective to stabilize yogurt preventing syneresis and also promoting the growth of lactic acid bacteria (Yeung et al. 2019). Many other hydrocolloids with low viscosity such as soluble soybean polysaccharides (Maeda and Nakamura 2021), gum tragacanth, and Persian gum (Azarikia and Abbasi 2016) were also shown effective for the stabilization of acidified milk drinks. While low viscosity acidified yogurt drinks are liked by healthy young consumers, high viscosity ones are preferred by traditionalists and also believed to be safer for dysphagic patients in hospitals.

Since starch is the most widely used hydrocolloids, it is important to know the effect of seasonings on rheological properties. Hirashima et al. (2005, 2012) found

the great difference of the viscosities of 3 wt% maize starch suspensions/pastes to which sucrose, acids, and salt were added before and after the heating.

Xanthan is used frequently to thicken the starch paste. Caramel sauces made from potato starch containing glucose syrup were thickened by xanthan (Krystyjan et al. 2012). Xanthan was also added to tapioca starch paste to increase the viscosity and the stability against heating (Chantaro et al. 2013).

Low calorie mayonnaise using xanthan gum has been commercialized in Japan. A body mouthfeel should be maintained while reducing oil content in mayonnaise. The viscosifying function of xanthan surely plays an important role here, but its stability in acidic pH and the texture constancy in the presence of salt are also required. A good flavor release is also required and it is related with shear thinning behavior of xanthan. A mixture of xanthan, locust bean, guar and tamarind gums is used to make a tofu of higher water holding capacity and with a good mouthfeel. Xanthan is used to prevent retrogradation of rice-cake (*mochi*) and also to improve the texture. A thickener consisting of xanthan and low methoxyl pectin is proposed. Japanese noodles containing xanthan are reported to have an elastic texture. Xanthan is also used for glaze in order to protect frozen fish and vegetables preventing syneresis (Nishinari 1988).

*Hanpen* is a traditional fish product in Japan. It contains many air bubbles and has a sponge-like texture. Meat of sharks and cod are mashed with yams and then boiled in hot water. Sharks and yams are necessary for producing air bubbles. A traditional sponge cake containing many foams and with a moist mouthfeel, *Karukan*, also relies on yam polysaccharides. The foam producing and stabilizing capacity of yam polysaccharides is believed to originate from high viscosity but also from some elasticity.

Spinnability is related with the breakup length when the liquid is subjected to extension. When a glass rod is immersed into a liquid and then pulled up vertically, even sugar syrup which is very close to a Newtonian fluid shows a thread because a liquid adhering on the glass rod is flowing down, and when all the liquid flows down, the thread breaks. However, when the fluid has a certain elasticity, the fluid extends by rubber elasticity and when the fluid breaks, the suspending fluid jumps up because of the elastic recovery. Therefore, the maximum extendable length of the fluid depends on the ratio of the viscosity and elasticity, which is known as the relaxation time (See Sect. 5). This property of fluid is closely related with cohesiveness which plays an important role together with viscosity in the safe swallowing (Nishinari et al. 2019). Elongational measurement is important for evaluating the spinnability and thickened fluids used in dysphagic treatments (Turcanu et al. 2018) because it is related with not only viscosity but also with elasticity.

In some thickening application, the short texture is required rather than long texture. Here, the “short” means neat and tidy mouthfeel and the draining and dripping off in the processing, which can be quantified by the break up length when the liquid is subjected to extension. In the operation of spreading honey on the bread, long texture hampers it. Some patent proposes to mix agar to make the texture short. This short texture is also preferred in thick sauce for breaded cutlets, and xyloglucan is often used for such a requirement. This short texture is also



suitable in sauce for barbecued /grilled meat and for a round dumpling made from powdered rice.

Many polysaccharides such as arabinoxylans, cereal beta-glucans, chitin and chitosan, dextran, mesquite gum, pullulan as well as vegetable proteins and milk proteins are used as thickening as well as stabilizing and emulsifying agents in various foods (Nussinovitch and Hirashima 2019).

Although the detailed mechanism of aspiration in dysphagic patients is not yet understood, thickening of liquid foods has been found effective to reduce the risk of aspiration. Thickening slows the liquid flow so that the epiglottis may be able to close the airway to prevent the penetration of the food bolus, although this scenario was not demonstrated so well (Cichero 2013; Steele et al. 2015; Nishinari et al. 2016). Many kinds of thickening agents are commercially produced and used in hospitals and organizations for disadvantaged persons (IDDSI, International Dysphagia Diet Standardisation Initiative: <https://iddsi.org/>; Japan Care Food Conference: <https://www.udf.jp/>).

## ***11.2 Rheological Control of Texture by Polysaccharide Thickeners: Noodles/Pasta and Breads***

Noodles are popular foods especially in Asia, and pasta, spaghetti, and macaroni, etc. are also popular in Western countries. Rice noodles are popular in Vietnam, Thailand, and other Asian countries, and high amylose rice (long grain indica type) is suitable for noodles. Recently, to reduce the excessive inventory and promote the utilization of low amylose rice (short grain japonica type), hydrocolloids are added to powdered rice to improve the texture in Japan. Noodles from low amylose rice are evaluated too sticky and not enough firm. Nitta et al. (2018) compared the texture of rice noodles treated by  $\text{Ca}^{2+}$ -induced setting of alginate or LM pectin, and found that the stickiness was reduced and the firmness was increased by the addition of alginate or pectin. Kita et al. (2009) reported the similar improvement of the texture of japonica rice noodles by adding tamarind seed gum (TSG). They found that the decrease in hardness of noodles by frozen storage was reduced by the addition of TSG. Chitosan was also used for rice noodles (Klinmalai et al. 2017). Esterified tapioca starch was also used for salted noodles (Eguchi et al. 2014). Silva et al. (2013) examined the effect of adding various polysaccharides, guar gum, LBG, KGM, HPMC, and xanthan on the mechanical properties of sweet potato noodles containing broccoli powders. They found that shear modulus of noodles was lowest in noodles with hydroxypropyl methylcellulose (HPMC) and xanthan, which was attributed to the restriction of swelling of starch granules by these polysaccharides with high water binding capacity.

Dough rheology has been a very important applied rheology since the birth of rheology, and the relation between the bread making property and the rheological properties of dough has been extensively studied. Viscosifying hydrocolloids have

been widely used for this, but the relation between the viscosifying property and the final bread property is not so well understood. Gluten plays a crucial role in the baking to form and keep “cell” walls, and many hydrocolloids are expected to improve the baking performance, but it was only partially successful. Doughs showing a strain hardening behavior in extension test were affirmed to have a good bread making property (Kokelaar et al. 1996). Since glutenin was identified as a main gluten fraction which plays an important role in elastic and strain hardening properties of dough, instead of using gluten whey protein particles are mixed with wheat starch to make a dough showing a similar strain hardening behavior to a normal wheat dough (van Riemsdijk et al. 2011).

Application of hydrocolloids for rice bread has also been reported. It has attracted much attention to make the gluten-free bread since the celiac disease was recognized to be caused by gluten. Hydrocolloids at 1% and 2% w/w, pectin, carboxymethyl-cellulose (CMC), agarose, xanthan or oat  $\beta$ -glucan were added to rice flour for gluten-free bread (Lazaridou et al. 2007). The loaf volume is one of most important index for bread making quality and it was found that the incorporation of xanthan at 1% into the gluten-free breads did not change the loaf volume and at 2% supplementation level even decreased the volume; this formulation exhibited the lowest volume among all preparations. This was consistent with previous findings. Recently, however, in comparison of locust bean gum, guar gum, xanthan gum, tamarind seed gum, native gellan gum, dextrin, LM pectin, fermented cellulose CMC, konjac glucomannan, HM pectin,  $\kappa$ -carrageenan,  $\iota$ -carrageenan, and  $\lambda$ -carrageenan in baking, the highest loaf volume was found when xanthan was used (Morimoto et al. 2015). HPMC, guar gum, pectin, xanthan gum, TSG were added to rice flour to make a gluten-free bread (Jang et al. 2018), and the authors concluded TSG gave the best bread among these hydrocolloids. The inconsistency among reported results may be due to the difference in the hydrocolloids because most commercially available polysaccharides have many variations: molar mass may be different, degree of substitutions or branching if any, cation type if it is charged polymers, etc. Therefore, unfortunately, it is impossible to compare directly the papers without confirming that the hydrocolloids used are the same or not in addition to the other factors such as mixing ratios and mixing conditions. This situation led Japanese workers to form a collaborative research group using the common samples of gellan to study the gelling and viscosifying properties as described in the next chapter for gelling properties.

Because of the issue of celiac disease, gluten-free pasta and bread have been investigated by many research groups which tried to use various hydrocolloids to improve the quality and especially textural properties (Padalino et al. 2016; Pahwa et al. 2016; Rai et al. 2018). Lynch et al. (2018) reviewed potential application of exopolysaccharides for gluten-free bread, and showed that the added dextran increased the specific volume and reduced the crumb hardness and extend the shelf life of the bread better than HPMC, which was attributed mainly to water binding ability of this high molar mass and branched dextran (Rühmkorf et al. 2012).

## References

- Aasprong E, Smidsrød O, Stokke BT (2003) Scleroglucan gelation by in situ neutralization of the alkaline solution. *Biomacromolecules* 4:914–921. <https://doi.org/10.1021/bm025770c>
- Azarikia F, Abbasi S (2016) Mechanism of soluble complex formation of milk proteins with native gums (Tragacanth and Persian Gum). *Food Hydrocolloids* 59:35–44. <https://doi.org/10.1016/j.foodhyd.2015.10.018>
- Azeredo HMC, Barud H, Farinas CS, Vasconcellos VM, Claro AM (2019) Bacterial Cellulose as a raw material for food and food packaging applications. *Frontiers in Sustainable Food Systems*. <https://doi.org/10.3389/fsufs.2019.00007>
- Bagley EB, Dintzis FR (1999) Shear thickening and flow induced structures in foods and biopolymer systems. In: Siginer DA, De Kee D, Chhabra RP (eds) *Advances in flow and rheology of non-Newtonian fluids*. Elsevier, London, pp 63–86
- Barnes HA (1989) Shear-thickening (“Dilatancy”) in suspensions of nonaggregating solid particles dispersed in Newtonian liquids. *Journal of Rheology* 33:329–366. <https://doi.org/10.1122/1.550017>
- Barnes HA (1997) Thixotropy - a review. *Journal of Non-Newtonian Fluid Mechanics* 70:1–33. [https://doi.org/10.1016/S0377-0257\(97\)00004-9](https://doi.org/10.1016/S0377-0257(97)00004-9)
- Barnes HA (1999) The yield stress -a review or ‘*παντα ρει*’- everything flows? *Journal of Non-Newtonian Fluid Mechanics* 81:133–178
- Barnes HA (2000) *A handbook of elementary rheology*. University of Wales, Aberystwyth
- Bonn D, Kellay H, Prochnow M, Ben-Djemaa K, Meunier J (1998) Delayed fracture of an inhomogeneous soft solid. *Science* 280:265–267. <https://doi.org/10.1126/science.280.5361.265>.
- Bonn D, Denn MM, Berthier L, Divoux T, Manneville S (2017) Yield stress materials in soft condensed matter. *Reviews of Modern Physics* 89:035005. <https://doi.org/10.1103/RevModPhys.89.035005>
- Bourne MC (2002) *Food texture and viscosity*, 2nd edn. Academic Press, New York
- Brenner T, Matsukawa S, Nishinari K, Johannsson R (2013) Failure in a soft gel: delayed failure and the dynamic yield stress. *Journal of Non-Newtonian Fluid Mechanics* 196:1–7. <https://doi.org/10.1016/j.jnnfm.2012.12.011>
- British Rheologists Club (1942) Classification of rheological properties. *Nature* 149:702. <https://doi.org/10.1038/149702a0>
- Caggioni M, Spicer PT, Blair DL, Lindberget SE, Weitz DA (2007) Rheology and microrheology of a microstructured fluid: the gellan gum case. *Journal of Rheology* 51:851–865. <https://doi.org/10.1122/1.2751385>
- Cao Y, He J, Fang Y, Nishinari K, Phillips GO (2014) Interactions between Schizophyllan and Curdlan molecules in solutions. *Bioactive Carbohydrates Dietary Fibre* 3:89–95. <https://doi.org/10.1015/j.bcdf.2014.03.002>
- Chan PSK, Chen J, Ettelaie R, Law Z, Aleviopoulos S, Day E, Smith S (2007) Study of the shear and extensional rheology of casein, waxy maize starch and their mixtures. *Food Hydrocolloids* 21:716–725. <https://doi.org/10.1016/j.foodhyd.2007.02.001>
- Chantaro P, Pongsawatmanit R, Nishinari K (2013) Effect of heating-cooling on rheological properties of tapioca starch paste with and without Xanthan Gum. *Food Hydrocolloids* 13:183–194. <https://doi.org/10.1016/j.foodhyd.2012.10.026>
- Chen J, Engelen L (eds) (2012) *Food oral processing: fundamentals of eating and sensory perception*. Wiley-Blackwell, Chichester
- Cheng Y, Prud’homme RK (2000) Enzymatic degradation of guar and substituted guar galactomannans. *Biomacromolecules* 1:782–788. <https://doi.org/10.1021/bm005616v>
- Cho KS, Hyun K, Ahn KH, Lee SJ (2005) A geometrical interpretation of large amplitude oscillatory shear response. *Journal of Rheology* 49:747–758. <https://doi.org/10.1122/1.1895801>

- Cichero JAY (2013) Thickening agents used for dysphagia management: effect on bioavailability of water, medication and feelings of satiety. *Nutrition Journal* 12:54. <https://doi.org/10.1186/1475-2891-12-54>
- Clasen C, Kulicke W-M (2001) Determination of viscoelastic and rheo-optical material functions of water-soluble cellulose derivatives. *Progress in Polymer Science* 26:1839–1919. [https://doi.org/10.1016/S0079-6700\(01\)00024-7](https://doi.org/10.1016/S0079-6700(01)00024-7)
- Coussot P, Nguyen QD, Huynh HT, Bonn D (2002a) Viscosity bifurcation in thixotropic, yielding fluids. *Journal of Rheology* 46:573–589. <https://doi.org/10.1122/1.1459447>
- Coussot P, Nguyen QD, Huynh HT, Bonn D (2002b) Avalanche behavior in yield stress fluids. *Physical Review Letters* 88:175501. <https://doi.org/10.1103/PhysRevLett.88.175501>
- Cragg LH, Bigelow CC (1955) The viscosity slope constant  $k'$  of ternary systems: polymer–polymer–solvent. *Journal of Polymer Science* 16:177–191. <https://doi.org/10.1002/pol.1955.120168208>
- Crawford NC, Popp LB, Johns KE, Caire LM, Peterson BN, Liberatore MW (2013) Shear thickening of corn starch suspensions: does concentration matter? *Journal of Colloid and Interface Science* 396:83–89. <https://doi.org/10.1016/j.jcis.2013.01.024>
- Davies HS, Pudney PDA, Georgiades P, Waigh TA, Hodson NW, Ridley CE, Blanch EW, Thornton DJ (2014) Reorganisation of the salivary mucin network by dietary components: insights from green tea polyphenols. *PLoS ONE* 9:e108372. <https://doi.org/10.1371/journal.pone.0108372>
- de Gennes PG (1979) *Scaling concepts in polymer physics*. Cornell University Press, Ithaca
- Dealy J, Plazek D (2009) Time-temperature superposition - a users guide. *Rheology Bulletin* 78:16–31
- Dinkgreve M, Paredes J, Denn MM, Bonn D (2016) On different ways of measuring “the” yield stress. *Journal of Non-Newtonian Fluid Mechanics* 238:233–241. <https://doi.org/10.1016/j.jnnfm.2016.11.001>
- Dintzis FR, Berhow MA, Bagley EBWYV, Felker F (1996) Shear-thickening behavior and shear-induced structure in gently solubilized starches. *Cereal Chemistry* 73:638–643
- Doi M (2013) *Soft matter physics*. Oxford University Press, Oxford
- Duvarci OC, Yazar G, Kokini JL (2017) The comparison of LAOS behavior of structured food materials (suspensions, emulsions and elastic networks). *Trends in Food Science and Technology* 60:2–11. <https://doi.org/10.1016/j.tifs.2016.08.014>
- Eguchi S, Kitamoto N, Nishinari K, Yoshimura M (2014) Effects of esterified tapioca starch on the physical and thermal properties of Japanese white salted noodles prepared partly by residual heat. *Food Hydrocolloids* 35:198–208. <https://doi.org/10.1016/j.foodhyd.2013.05.012>
- Einaga Y, Miyaki Y, Fujita H (1977) A rotational viscometer permitting successive dilution. *Nihon Reorogi Gakkaishi* 5:188–193. [https://doi.org/10.1678/rheology1973.5.4\\_188](https://doi.org/10.1678/rheology1973.5.4_188)
- Ewoldt RH, Hosoi AE, McKinley GH (2008) New measures for characterizing nonlinear viscoelasticity in large amplitude oscillatory shear. *Journal of Rheology* 52:1427–1458. <https://doi.org/10.1122/1.2970095>
- Faber TJ, Jaishankar A, McKinley GH (2017a) Describing the firmness, springiness and rubberiness of food gels using fractional calculus. Part I: theoretical framework. *Food Hydrocolloids* 62:311–324. <https://doi.org/10.1016/j.foodhyd.2016.05.041>
- Faber TJ, Jaishankar A, McKinley GH (2017b) Describing the firmness, springiness and rubberiness of food gels using fractional calculus. Part II: measurements on semi-hard cheese. *Food Hydrocolloids* 62:325–339. <https://doi.org/10.1016/j.foodhyd.2016.06.038>
- Fang Y, Takahashi R, Nishinari K (2004a) Rheological characterization of schizophyllan aqueous solutions after denaturation–renaturation treatment. *Biopolymers* 74:302–315. <https://doi.org/10.1002/bip.20081>
- Fang Y, Takemasa M, Katsuta K, Nishinari K (2004b) Rheology of schizophyllan solutions in isotropic and anisotropic phase regions. *Journal of Rheology* 48:1147–1166. <https://doi.org/10.1122/1.1781170>

- Goh KKT, Matia-Merino L, Hall CE et al (2007) Complex rheological properties of a water-soluble extract from the fronds of the black tree fern, *Cyathea medullaris*. *Biomacromolecules* 8:3414–3421. <https://doi.org/10.1021/bm7005328>
- Grassi M, Lapasin R, Pricl S (1996) A study of the rheological behavior weak gel systems. *Carbohydrate Polymers* 29:169–181
- Hirashima M, Takahashi R, Nishinari K (2005) Changes in the viscoelasticity of maize starch pastes by adding sucrose at different stages. *Food Hydrocolloids* 19:777–784. <https://doi.org/10.1016/j.foodhyd.2004.09.009>
- Hirashima M, Takahashi R, Nishinari K (2012) The gelatinization and retrogradation of cornstarch gels in the presence of citric acid. *Food Hydrocolloids* 27:390–393. <https://doi.org/10.1016/j.foodhyd.2011.10.011>
- Hunter RJ (1998) Introduction to modern colloid science. Oxford University Press, Oxford, p 110
- Hyun K, Wilhelm M, Klein CO, Cho KS, Nam JG, Ahn KH, Lee SJ, Ewoldt RH, McKinley GH (2011) A review of nonlinear oscillatory shear tests: Analysis and application of large amplitude oscillatory shear (LAOS). <https://doi.org/10.1016/j.progpolymsci.2011.02.002>
- Ikeda S, Nishinari K (2001a) Solid-like mechanical behaviors of ovalbumin aqueous solutions. *International Journal of Biological Macromolecules* 28:315–320. [https://doi.org/10.1016/S0141-8130\(01\)00128-3](https://doi.org/10.1016/S0141-8130(01)00128-3)
- Ikeda S, Nishinari K (2001b) Structural changes during heat-induced gelation of globular protein dispersions. *Biopolymers* 59:87–102. [https://doi.org/10.1002/1097-0282\(200108\)59:2<87::AID-BIP1008>3.0.CO;2-H](https://doi.org/10.1002/1097-0282(200108)59:2<87::AID-BIP1008>3.0.CO;2-H)
- Jaishankar A (2014) The linear and nonlinear rheology of multiscale complex fluids. (PhD thesis). MIT, USA. <https://dspace.mit.edu/handle/1721.1/92159>
- Jaishankar A, McKinley GH (2012) Power-law rheology in the bulk and at the interface: quasi-properties and fractional constitutive equations. *Physical and Engineering Sciences* 469:1–21. <https://doi.org/10.1098/rspa.2012.0284>
- Jaishankar A, McKinley GH (2014) A fractional KBKZ constitutive formulation for describing the nonlinear rheology of multi-scale complex fluids. *Journal of Rheology* 58:1751–1788. <https://doi.org/10.1122/1.4892114>
- Jaishankar A, Wee M, Matia-Merino L, Goh KKT, McKinley GH (2015) Probing hydrogen bond interactions in a shear thickening polysaccharide using nonlinear shear and extensional rheology. *Carbohydrate Polymers* 123:136–145. <https://doi.org/10.1016/j.carbpol.2015.01.006>
- Jang KJ, Hong YE, Moon Y, Jeon S, Angalet S, Kweon M (2018) Exploring the applicability of tamarind gum for making gluten-free rice bread. *Food Science and Biotechnology* 27:1639–1648. <https://doi.org/10.1007/s10068-018-0416-z>
- Jensen S, Rolin C, Ipsen R (2010) Stabilisation of acidified skimmed milk with HM pectin. *Food Hydrocolloids* 24:291–299. <https://doi.org/10.1016/j.foodhyd.2009.10.004>
- Kiani H, Mousavi ME, Razavi H, Morris ER (2010) Effect of Gellan, alone and in combination with high-methoxy pectin, on the structure and stability of doogh, a yogurt-based Iranian drink. *Food Hydrocolloids* 24:744–754. <https://doi.org/10.1016/j.foodhyd.2010.03.016>
- Kita N, Senda M, Nagatsuka N, Nagao K (2009) Mechanical Properties and radical scavenging activity of unpolished rice noodles with added tamarind. *Journal of Cookery Science of Japan* 42:183–187. <https://doi.org/10.11402/cookeryscience.42.183>
- Klinmalai P, Hagiwara T, Sakiyama T, Ratanasumawong S (2017) Chitosan effects on physical properties, texture, and microstructure of flat rice noodles. *LWT - Food Science and Technology* 76:117–123. <https://doi.org/10.1016/j.lwt.2016.10.052>
- Kobayashi N, Kohyama K, Shiozawa K (2010) Fragmentation of a viscoelastic food by human mastication. *Journal of the Physical Society of Japan* 79:044801. <https://doi.org/10.1143/JPSJ.79.044801>
- Koeller RC (1984) Applications of fractional calculus to the theory of viscoelasticity. *Journal of Applied Mechanics* 51:299–307. <https://doi.org/10.1115/1.3167616>

- Kokelaar JJ, van Vliet T, Prins A (1996) Strain hardening properties and extensibility of flour and gluten doughs in relation to breadmaking performance. *Journal of Cereal Science* 24:199–214. <https://doi.org/10.1006/jcrs.1996.0053>
- Krystijan M, Sikora M, Adamczyk G, Tomasiak P (2012) Caramel sauces thickened with combinations of potato starch and Xanthan Gum. *Journal of Food Engineering* 112:22–28. <https://doi.org/10.1016/j.jfoodeng.2012.03.035>
- Lapasin R, Prici S (1999) *Rheology of industrial polysaccharides: theory and applications*. Springer, New York
- Larson RG (1999) *The Structure and rheology of complex fluids*. Oxford University Press, Oxford
- Lazaridou A, Duta D, Papageorgiou M, Belc N, Biliaderis CG (2007) Effects of hydrocolloids on dough rheology and bread quality parameters in gluten-free formulations. *Journal of Food Engineering* 79:1033–1047. <https://doi.org/10.1016/j.jfoodeng.2006.03.032>
- Lee HC, Brant DA (2002) Rheology of concentrated isotropic and anisotropic xanthan solutions. 2. A semiflexible wormlike intermediate molecular weight sample. *Macromolecules* 35:2223–2234. <https://doi.org/10.1021/ma011527e>
- Li X, Fang Y, Zhang H, Nishinari K, Al-Assaf S, Phillips GO (2011) Rheological properties of gum arabic solution: from Newtonianism to thixotropy. *Food Hydrocolloids* 25:293–298. <https://doi.org/10.1016/j.foodhyd.2010.06.006>
- Liang S, Li B, Ding Y, Xu BL, Chen J, Zhu B, Ma MH, Kennedy JF, Knill CJ (2011) Comparative investigation of the molecular interactions in konjac gum/hydrocolloid blends: concentration addition method (CAM) versus viscosity addition method (VAM). *Carbohydrate Polymers* 83:1062–1067. <https://doi.org/10.1016/j.carbpol.2010.08.026>
- Lindstrom SB, Kodger TE, Sprakel J, Weitz DA (2012) Structures, stresses, and fluctuations in the delayed failure of colloidal gels. *Soft Matter* 8:3657–3664. <https://doi.org/10.1039/C2SM06723D>
- Lynch KM, Coffey A, Arendt EK (2018) Exopolysaccharide producing lactic acid bacteria: their techno-functional role and potential application in gluten-free bread products. *Food Research International* 110:52–61. <https://doi.org/10.1016/j.foodres.2017.03.012>
- Maeda H, Nakamura A (2021) Soluble soybean polysaccharide. In: Phillips GO, Williams PA (eds) *Handbook of hydrocolloids*, 3rd edn. Woodhead Publishing, Cambridge, pp 463–480. <https://doi.org/10.1016/B978-0-12-820104-6.00025-5>
- Mewis J, Wagner NJ (2012) *Colloidal suspension rheology*. Cambridge University Press, Cambridge
- Morimoto N, Tabara A, Seguchi M (2015) Effect of Xanthan Gum on improvement of bread height and specific volume upon baking with frozen and thawed dough. *Food Science and Technology Research* 21:309–316. <https://doi.org/10.3136/fstr.21.309>
- Morris ER, Cutler AN, Ross-Murphy SB, Rees DA, Price J (1981) Concentration and shear rate dependence of viscosity in random coil polysaccharide solutions. *Carbohydrate Polymers* 1:5–21. [https://doi.org/10.1016/0144-8617\(81\)90011-4](https://doi.org/10.1016/0144-8617(81)90011-4)
- Møller PCF, Mewis J, Bonn D (2006) Yield stress and thixotropy: on the difficulty of measuring yield stresses in practice. *Soft Matter* 2:274–283. <https://doi.org/10.1039/b517840a>
- Møller PCF, Fall A, Bonn D (2009) Origin of apparent viscosity in yield stress fluids below yielding. *Europhysics Letters* 87:38004. <https://doi.org/10.1209/0295-5075/87/38004>
- Nakamura K, Shinoda E, Tokita M (2001) The influence of compression velocity on strength and structure for gellan gels. *Food Hydrocolloids* 15:247–252. [https://doi.org/10.1016/S0268-005X\(01\)00021-2](https://doi.org/10.1016/S0268-005X(01)00021-2)
- Ng TSK, McKinley GH, Ewoldt RH (2011) Large amplitude oscillatory shear flow of gluten dough: a model power-law gel. *Journal of Rheology* 55:627–654. <https://doi.org/10.1122/1.3570340>
- Nishinari K (1988) Food hydrocolloids in Japan. In: Phillips GO, Wedlock DJ, Williams PA (eds) *Gums and stabilisers for the food industry*, vol 4. IRL Press, Oxford, pp 373–390
- Nishinari K (2004) Rheology, food texture and mastication. *Journal of Texture Studies* 35:113–124. <https://doi.org/10.1111/j.1745-4603.2004.tb00828.x>



- Nishinari K, Fang Y (2018) Perception and measurement of food texture: solid foods. *Journal of Texture Studies* 49:160–201. <https://doi.org/10.1111/jtxs.12327>
- Nishinari K, Horiuchi H, Ishida K, Ikeda K, Date E, Fukada E (1980) A new apparatus for rapid and easy measurement of dynamic viscoelasticity for gel-like foods. *Nippon Shokuhin Kogyo Gakkaishi* 27:227–233. [https://doi.org/10.3136/nskkk1962.27.5\\_227](https://doi.org/10.3136/nskkk1962.27.5_227)
- Nishinari K, Kohyama K, Williams PA, Phillips GO, Burchard W, Ogino K (1991) Solution properties of pullulan. *Macromolecules* 24:5590–5593
- Nishinari K, Takemasa M, Zhang H, Takahashi R (2007) Storage plant polysaccharides: xyloglucans, galactomannans, glucomannan. In: Kamerling JP (ed) *Comprehensive glycoscience*, vol 2. Elsevier, London, pp 614–652
- Nishinari K, Takemasa M, Su L, Michiwaki Y, Mizunuma H, Ogoshi H (2011) Effect of shear thinning on aspiration - toward making solutions for judging the risk of aspiration. *Food Hydrocolloids* 25:1737–1743. <https://doi.org/10.1016/j.foodhyd.2011.03.016>
- Nishinari K, Takemasa M, Brenner T, Su L, Fang Y, Hirashima M, Yoshimura M, Nitta Y, Moritaka H, Tomczynska-Mleko M, Mleko S, Michiwaki Y (2016) The food colloid principle in the design of elderly food. *Journal of Texture Studies* 47:284–312. <https://doi.org/10.1111/jtxs.12201>
- Nishinari K, Turcanu M, Nakauma M, Fang Y (2019) Role of fluid cohesiveness in safe swallowing. *NPJ Science of Food* 3:5. <https://doi.org/10.1038/s41538-019-0038-8>
- Nitta Y, Yoshimura Y, Ganeko N, Ito H, Okushima N, Kitagawa M, Nishinari K (2018) Utilization of Ca<sup>2+</sup>-induced setting of alginate or low methoxyl pectin for noodle production from japonica rice. *LWT - Food Science and Technology* 97:362–369. <https://doi.org/10.1016/j.lwt.2018.07.027>
- Nussinovitch A, Hirashima M (2019) More cooking innovations –novel hydrocolloids for special dishes. CRC Press, Cleveland
- Padalino L, Conte A, Del Nobile MA (2016) Overview on the general approaches to improve gluten-free pasta and bread. *Foods* 5:87. <https://doi.org/10.3390/foods5040087>
- Pahwa A, Kaur A, Puri R (2016) Influence of hydrocolloids on the quality of major flat breads: a review. *Journal of Food Processing* 2016:8750258. <https://doi.org/10.1155/2016/8750258>
- Parker A, Boulenguer P, Kravtchenko TP (1994) Effect of the addition of high methoxy pectin on the rheology and colloidal stability of acid milk drinks. In: Nishinari K, Doi E (eds) *Food hydrocolloids: structures, properties, and functions*. Springer, Boston, pp 307–312. [https://doi.org/10.1007/978-1-4615-2486-1\\_48](https://doi.org/10.1007/978-1-4615-2486-1_48)
- Patel AR, Schatteman D, De Vos WH, Lesaffer A, Dewettinck K (2013) Preparation and rheological characterization of shellac oleogels and oleogel-based emulsions. *Journal of Colloid and Interface Science* 411:114–121. <https://doi.org/10.1016/j.jcis.2013.08.039>
- Paximada P, Koutinas A, Scholten E, Mandala IG (2016) Effect of bacterial cellulose addition on physical properties of WPI emulsions. comparison with common thickeners. *Food Hydrocolloids* 54:245–254. <https://doi.org/10.1016/j.foodhyd.2015.10.014>
- Pellicer J, Delegido J, Dolz J, Dolz M, Hernández MJ, Herráez MJ (2000) Influence of shear rate and concentration ratio on viscous synergism. application to xanthan-locust bean gum-NaCMC mixtures. *Food Science and Technology International* 6:415–423. <https://doi.org/10.1177/10820132000600508>
- Peyron MA, Woda A (2016) An update about artificial mastication. *Current Opinion in Food Science* 9:21–28. <https://doi.org/10.1016/j.cofs.2016.03.006>
- Picout DR, Ross-Murphy SB (2007) On the Mark–Houwink parameters for galactomannans. *Carbohydrate Polymers* 70:145–148
- Picout DR, Ross-Murphy SB, Errington N, Harding SE (2001) Pressure cell assisted solution characterization of polysaccharides I: guar gum. *Biomacromolecules* 2:1301–1309
- Pongsawatmanit R, Temsiripong T, Ikeda S, Nishinari K (2006) Influence of tamarind seed xyloglucan on rheological properties and thermal stability of tapioca starch. *Journal of Food Engineering* 77:41–50. <https://doi.org/10.1016/j.jfoodeng.2005.06.017>
- Powel PC (1994) *Engineering with fibre-polymer laminates*. Springer, New York, p 68

- Rai S, Kaur A, Chopra CS (2018) Gluten-free products for celiac susceptible people. *Frontiers in Nutrition* 5:116. <https://doi.org/10.3389/fnut.2018.00116>
- Renard D, Axelos MAV, Boue F, Lefebvre J (1996) Small Angle neutron scattering and viscoelasticity study of the colloidal structure of aqueous solutions and gels of a globular protein. *Journal de Chimie Physique et de Physico-Chimie Biologique* 93:998–1015. <https://doi.org/10.1051/jcp/1996930998>
- Reiner M (1971) *Advanced rheology*. Lewis, London
- Richardson RK, Ross-Murphy SB (1987a) Non-linear viscoelasticity of polysaccharide solutions. 1: guar galactomannan solutions. *International Journal of Biological Macromolecules* 9:250–256. [https://doi.org/10.1016/0141-8130\(87\)90062-6](https://doi.org/10.1016/0141-8130(87)90062-6)
- Richardson RK, Ross-Murphy SB (1987b) Non-linear viscoelasticity of polysaccharide solutions. 2: Xanthan polysaccharide solutions. *International Journal of Biological Macromolecules* 9:257–264. [https://doi.org/10.1016/0141-8130\(87\)90063-8](https://doi.org/10.1016/0141-8130(87)90063-8)
- Risica D, Barbetta A, Vischetti L, Cametti C, Dentini M (2010) Rheological properties of guar and its methyl, hydroxypropyl and hydroxylpropyl-methyl derivatives in semidilute and concentrated aqueous solutions. *Polymer* 51:1972–1982. <https://doi.org/10.1016/j.polymer.2010.02.041>
- Rogosin S, Mainardi F (2014) George William Scott Blair -- The Pioneer of Fractional Calculus in Rheology. arXiv:1404.3295. <https://doi.org/10.1685/journal.caim.481>
- Rühmkorf C, Rübsam H, Becker T, Bork C, Voiges K, Mischnick P, Brandt MJ, Vogel RF (2012) Effect of structurally different microbial homoexopolysaccharides on the quality of gluten-free bread. *European Food Research and Technology* 235:139–146. <https://doi.org/10.1007/s00217-012-1746-3>
- Sanderson GR (1981) Applications of Xanthan Gum. *The British Polymer Journal* 13:71–75. <https://doi.org/10.1002/pi.4980130207>
- Sato T, Norisuye T, Fujita H (1984) Double-stranded helix of xanthan: dimensional and hydrodynamic properties in 0.1 M aqueous sodium chloride. *Macromolecules* 17:2696–2700
- Scott Blair GW (1947) The role of psychophysics in rheology. *Journal of Colloid Science* 2:21–31. [https://doi.org/10.1016/0095-8522\(47\)90007-X](https://doi.org/10.1016/0095-8522(47)90007-X)
- Scott Blair GW (1969) *Elementary rheology*. Academic, London
- Shao P, Qin M, Han L, Peilong Sun P (2014) Rheology and characteristics of sulfated polysaccharides from chlorophytan seaweeds *ulva fasciata*. *Carbohydrate Polymers* 113:365–372. <https://doi.org/10.1016/j.carbpol.2014.07.008>
- Shi Z, Zhang Y, Phillips GO, Yang G (2014) Utilization of bacterial cellulose in food. *Food Hydrocolloids* 35:539–545. <https://doi.org/10.1016/j.foodhyd.2013.07.012>
- Shingel KI (2004) Current knowledge on biosynthesis, biological activity, and chemical modification of the exopolysaccharide pullulan. *Carbohydrate Research* 339:447–460
- Silva E, Birkenhake M, Scholten E, Sagis LMC, van der Linden E (2013) Controlling rheology and structure of sweet potato starch noodles with high broccoli powder content by hydrocolloids. *Food Hydrocolloids* 30:42–52. <https://doi.org/10.1016/j.foodhyd.2012.05.002>
- Smidsrød O, Haug A (1971) Estimation of the relative stiffness of the molecular chain in polyelectrolytes from measurements of viscosity at different ionic strengths. *Biopolymers* 10:1213–1227. <https://doi.org/10.1002/bip.360100711>
- Sprakel J, Lindstrom SB, Kodger TE, Weitz DA (2011) Stress enhancement in the delayed yielding of colloidal gels. *Physical Review Letters* 106:248303. <https://doi.org/10.1103/PhysRevLett.106.248303>
- Steele CM, Alsanei WA, Ayanikalath S, Barbon CE, Chen J, Cichero JA, Coutts K, Dantas RO, Duivestijn J, Giosa L, Hanson B, Lam P, Lecko C, Leigh C, Nagy A, Namasivayam AM, Nascimento WV, Odendaal I, Smith CH, Wang H (2015) The influence of food texture and liquid consistency modification on swallowing physiology and function: a systematic review. *Dysphagia* 30:2–26. <https://doi.org/10.1007/s00455-014-9578-x>
- Stokes JR, Telford JH (2004) Measuring the yield behaviour of structured fluids. *Journal of Non-Newtonian Fluid Mechanics* 124:137–146. <https://doi.org/10.1016/j.jnnfm.2004.09.001>



- Suchkov VV, Popello IA, Grinberg VY, Tolstoguzov VB (1997) Shear effects on phase behaviour of the legumin-salt-water system. Modelling protein recovery. *Food Hydrocolloids* 11:135–144. [https://doi.org/10.1016/S0268-005X\(97\)80021-5](https://doi.org/10.1016/S0268-005X(97)80021-5)
- Sun ZH, Wang W, Feng ZL (1992) Criterion of polymer– polymer miscibility determined by viscometry. *European Polymer Journal* 28:1259–1261. [https://doi.org/10.1016/0014-3057\(92\)90215-N](https://doi.org/10.1016/0014-3057(92)90215-N)
- Sworn G (2021) Xanthan gum. Woodhead Publishing pp, Cambridge, pp 833–853. <https://doi.org/10.1016/B978-0-12-820104-6.00004-8>
- Turcanu M, Siegert N, Secouard S, Brito-de la Fuente E, Balan C, Gallegos C (2018) An alternative elongational method to study the effect of saliva on thickened fluids for dysphagia nutritional support. *Journal of Food Engineering* 228:79–83. <https://doi.org/10.1016/j.jfoodeng.2018.02.015>
- van Riemsdijk LE, van der Goot AJ, Hamer RJ (2011) The use of whey protein particles in gluten-free bread production, the effect of particle stability. *Food Hydrocolloids* 25:1744–1750. <https://doi.org/10.1016/j.foodhyd.2011.03.017>
- Wagner CE, Barbati AC, Engmann J, Burbidge AS, McKinley GH (2016) Apparent shear thickening at low shear rates in polymer solutions can be an artifact of non-equilibration. *Applied Rheology* 26:54091. <https://doi.org/10.3933/AppRheol-26-54091>
- Wagner CE, Barbati AC, Engman J, Burbidge AS, McKinley GH (2017) Quantifying the consistency and rheology of liquid foods using fractional calculus. *Food Hydrocolloids* 69:242–254. <https://doi.org/10.1016/j.foodhyd.2017.01.036>
- Waigh TA (2016) Advances in the microrheology of complex fluids. *Reports on Progress in Physics* 79:074601. <https://doi.org/10.1088/0034-4885/79/7/074601>
- Wientjes RHW, Duits MHG, Jongschaap RJJ, Mellema J (2000) Linear rheology of guar gum solutions. *Macromolecules* 33:9594–9605. <https://doi.org/10.1021/ma001065p>
- Wu M, Qu J, Tian X, Zhao X, Shen Y, Shi Z, Chen P, Li G, Ma T (2019) Tailor-made polysaccharides containing uniformly distributed repeating units based on the xanthan gum skeleton. *International Journal of Biological Macromolecules* 131:646–653. <https://doi.org/10.1016/j.ijbiomac.2019.03.130>
- Wyatt NB, Gunther CM, Liberatore MW (2011) Increasing viscosity in entangled polyelectrolyte solutions by the addition of salt. *Polymer* 52:2437–2444. <https://doi.org/10.1016/j.polymer.2011.03.053>
- Yalpani M, Hall LD, Tung MA, Brooks DE (1983) Unusual rheology of a branched, water-soluble chitosan derivative. *Nature* 302:812–814. <https://doi.org/10.1038/302812a0>
- Yang N, Lv R, Jia J, Nishinari K, Fang Y (2017) Application of microrheology in food science. *Annual Review of Food Science and Technology* 8:23.1–23.29. <https://doi.org/10.1146/annurev-food-030216-025859>
- Yang X, Gong T, Lu YH, Li A, Sun L, Guo Y (2020) Compatibility of sodium alginate and konjac glucomannan and their applications in fabricating low-fat mayonnaise-like emulsion gels. *Carbohydrate Polymers* 229:115468. <https://doi.org/10.1016/j.carbpol.2019.115468>
- Yazar G, Duvarci O, Tavman S, Kokini JL (2017a) LAOS behavior of the two main gluten fractions: gliadin and glutenin. *Journal of Cereal Science* 77:201–210. <https://doi.org/10.1016/j.jcs.2017.08.014>
- Yazar G, Duvarci O, Tavman S, Kokini JL (2017b) Non-linear rheological behavior of gluten-free flour doughs and correlations of laos parameters with gluten-free bread properties. *Journal of Cereal Science* 74:28–36. <https://doi.org/10.1016/j.jcs.2017.01.008>
- Yeung YK, Lee YK, Chang YH (2019) Physicochemical, microbial, and rheological properties of yogurt substituted with pectic polysaccharide extracted from *Ulmus davidiana*. *Journal of Food Process and Preservation* 43:e13907. <https://doi.org/10.1111/jfpp.13907>
- Zhang L, Zhou F (2006) Synergistic viscosity characteristics of aqueous mixed solutions of hydroxypropyl- and carboxymethyl hydroxypropyl-substituted guar gums. *Colloids and Surfaces A* 279:34–39. <https://doi.org/10.1016/j.colsurfa.2005.12.030>

- Zhang F, Luan T, Kang D, Jin Q, Zhang H, Yadav MP (2015) Viscosifying properties of corn fiber gum with various polysaccharides. *Food Hydrocolloids* 43:218–227. <https://doi.org/10.1016/j.foodhyd.2014.05.018>
- Zhao M, Cui N, Qu F, Huang X, Yang H, Nie S, Zha X, Cui SW, Nishinari K, Phillips GO, Fang Y (2017) Novel nano-particulated exopolysaccharide produced by *Klebsiella* sp. PHRC1.001. *Carbohydrate Polymers* 171:252–258. <https://doi.org/10.1016/j.carbpol.2017.05.015>

# Chapter 4

## Gelling Properties



Katsuyoshi Nishinari

**Abstract** Except beverages, soups, and dried foods, most foods are eaten in gel state, and thus it is important to understand the mechanisms of gel formation to improve the food quality. Starting from the definition and classification of gels, this chapter describes the molecular forces responsible for gel formation, how the network structure is formed, rheological determination of gel point, critical molar mass and concentration below which no gelation occurs. Then, characterization methods, gelation kinetics, mechanical spectra, and thermal scanning rheology are described based on studies performed for gelation of polysaccharides and proteins. Various factors influencing structure and properties of polysaccharide and protein gels, in particular, gelation rate, temperature, molar mass, concentration, interaction between long chains and short chains, small molecules such as sugars, acids, salts, and polyphenols are described. Release of molecular chains followed by erosion of gels induced by immersion in solvents is also described. Special categories of gels, microgels, mixed gels, cryogels, and oleogels are also described.

**Keywords** Definition · Classification · Transition · Polysaccharides · Proteins

### 1 Introduction

Gels are everywhere around us. In the breakfast, boiled or fried eggs are served. Tofu, yogurt or cheese is also served. They all are gels. Jams on the toast are also gels. There are many food gels, dessert jellies, pudding, marshmallow, etc. When water used to boil fish or meat is concentrated and cooled, a gel is formed. Though raw rice grains are not gels, cooked rice grains, and cooked pasta and noodles might be family members of gels. When dried foods with very low water content are masticated and crushed into small fragments, they are mixed with saliva forming a

---

K. Nishinari (✉)

Glyn O. Phillips Hydrocolloids Research Centre, School of Food and Biological Engineering,  
Hubei University of Technology, Wuhan, People's Republic of China  
e-mail: [katsuyoshi.nishinari@hbut.edu.cn](mailto:katsuyoshi.nishinari@hbut.edu.cn)

bolus and then swallowed. Before swallowing, the solid foods are transformed to gels before forming a swallowable bolus. Our gastric juice is in acidic pH ca. 1–1.5. Why the stomach wall is not injured? It is protected by mucin gels. Acid-induced gelling property of alginate has been used for treating gastroesophageal reflux disorder. When some part of our body is injured, blood comes out and it clots (gels). When we catch a cold, sputum is formed. It is also a gel. They all are formed from a liquid which is solidified or a solid becomes a gel by absorbing liquid. Therefore, apart from two extremes, very dried foods and liquids, most semi-solid foods can be called gels although mainly polysaccharide and protein gels are discussed in this chapter. Some shampoos are called gels although they are not gels in a scientific word. It is necessary to define a gel.

## 2 What Is a Gel?

The definition of gels has been a problem discussed for a long time. Jordan Lloyd said “The colloidal condition, the ‘gel’, is one which it is easier to recognize than to define”. In the review on structure of gels, she classified gels into (1) heat-reversible gels such as gelatin or agar in water, cellulose acetate in benzoyl alcohol and (2) heat-irreversible gels such as silica in water, colloid in chloroform and alcohol, many metallic sulfides and oxides in water. Since then, many definitions have been done for polymer gels (Djabourov et al. 2013). Recently, low molar mass gelator has been attracting attention in relation to pharmaceutical and cosmetic industry but not so much applications are found in food industry except oleogel. Gels formed from synthetic and biological polymers have many things in common and it is useful to discuss together comparing each other (Djabourov et al. 2013; Nishinari et al. 2016a; Tokita and Nishinari 2009) although the present chapter focuses mainly on polysaccharide and protein gels. Gels can be defined both from a rheological behavior and from a structural feature.

*Rheological definition* of a gel is that the system does not flow, and it can be characterized by the presence of a plateau region of storage modulus and the low  $\tan\delta$  ( $<0.1$ ) at an angular frequency range from  $10^{-3}$  to  $10^2$  rad/s, which is accessible by many commercially available rheometers. This should be called an operational definition and it cannot exclude the possibility to find the violation of this definition if a material obeying this definition shows a liquid-like rheological behavior at further lower frequencies. We should remember a famous saying of a prophetess Deborah “Even the mountains flow before the Lord” or everything flows. We could enjoy to visit the Website of a pitch drop experiment. A drop of the pitch flows (falls) every 9 years or 10 years or 11 years. It shows clearly that the distinction of a liquid and a solid is not simple, and depends on the “patience” of the observer. Since it is difficult to set the reasonable time-scale for both patient and impatient persons, it is more practical to clarify the fluidity by the *yield stress* concept (discussed in the previous Chap. 3) and the large deformation behavior above the yield stress. In this sense, a commonly used tube tilting method is not a good method because of its

dependence on the patience of the observer. Impatient observers will not see whether it flows after a long time under the gravity which does not induce flow during a short time (see the discussion on delayed failure in Chap. 3). If it flows above the yield stress, it is a structured liquid and should not be called a gel as mentioned below. If it is a gel, it will be broken down into separate parts and will not flow. If divided parts recover the initial continuity immediately on contact, such materials could be used in various areas in adhesive, coating, electric conductivity, and tissue engineering. These are called *self-healing gels* (Cordier et al. 2008; Halake and Lee 2017), and it is expected that the principle may be also applied in encapsulation of bioactives and durable packaging materials in the future.

*Structural definition* of a gel is based on the connectivity of the system. Gel is a system consisting of molecules, particles, chains, or other structural elements which are partially connected to each other in a fluid medium by crosslinks to the macroscopic dimensions. According to this structural definition, the loss of fluidity is the result of connectivity. Entanglement of long object may be regarded as connected by delocalized crosslinks. The sol-gel transition can be treated by a percolation theory (Tokita 1989). This is also another operational definition, and it cannot exclude the possibility of finding gels whose constituents are not directly connected.

There are two material groups having a name “gel,” but it can cause a confusion. These two are a weak gel and a fluid gel. Weak gel was named for structured liquids which show a weak frequency dependence for storage and loss modulus at a commonly accessible angular frequency range from  $10^{-3}$  to  $10^2$  rad/s, and the mechanical loss tangent is higher than 0.1. These materials are essentially liquid but it does not flow below its yield stress, thus it is apparently different from other liquids with no yield stress. Since yield stress has attracted further attention recently, it was discussed in the previous chapter for rheology. It may be better to mention here that it is not a good question to ask “which is more viscous, mayonnaise or whip cream and sugar syrup or honey?” The former has a yield stress and the latter not. In the present chapter, this is not called a weak gel but called structured liquid because it is essentially a liquid with non-zero yield stress.

The second class material, fluid gel is against the definition of gels mentioned above in the sense that it flows; fluid includes the meaning of flow. In this case, we should define the length scale of the “phase.” Strictly speaking, the so-called fluid gels should be called microgels. Everybody knows that sands “flow.” And there is an expression “flowing sands.” Everybody also knows that a grain of sand is a solid although a mass of sands “flows.” These granular materials like sands, powders, and other solid particles flow, but this flow is different from the liquid flow which has been studied in fluid dynamics. The flow of granular materials stops at the angle of repose of these granular solids when put on the horizontal plane while liquids with no yield stress (described in the previous chapter) flatten showing no angle of repose. Dried sands and powders don’t stick each other, and therefore contradict with the connectivity in the above definition, but this situation can be modified by increasing moisture content or adding liquids. Such a material has, however, been called a paste rather than a gel. They are similar to slurries. But, it is difficult to make a clear

distinction between a gel and a paste. It may be impossible to define the highest and the lowest liquid content for gels. This is related to the following problem.

Emulsion gel and oleogel are different from food polymer gels consisting of polysaccharides and proteins. In fats such as butter or margarine, the solid fat content is an index to characterize the state of the material. This index decreases with increasing the temperature. The difference between the gel-sol transition and the melting of fat is that the latter is more crystalline than the former. What is the border of the crystallinity or the orderliness of the structure when we define the gel? There may be gels very close to crystalline state and also other gels very close to amorphous state. It may be impossible to define a borderline which depends on many factors, which is discussed later.

It is therefore difficult to propose the simple definitive definition of gels, and the present author has a similar feeling with his good friend, Nijenhuis who says *A gel is a gel, as long as one cannot prove that it is not a gel*. The difficulty arises when we define a border between a gel and non-gel as pointed above such as liquid content, and the degree of the order, and glass. If the border can be found as a discontinuous transition, it can be clearly defined, but if the border is not discontinuous and vague, it might be difficult to distinguish the materials on both sides, gel and non-gel. The above tentatively proposed definition of gels could be operationally practical, but the author will be happy if more persuasive definition is proposed because the science is the never-ending endeavor of human beings.

### 3 Classification of Food Gels

Gels can be classified from various points of views based on mechanical properties, molecular forces, constituting ingredients, temperature dependence of elastic modulus, transparency, electric charges, etc.

#### 3.1 *Classification of Food Gels Based on Mechanical Properties*

When we hear that it is easier to recognize than to define a gel, we expect that a gel may wobble which is easy to recognize. The amplitude we observe is related to the elastic modulus (Nishinari 1976) or simply we can push a gel with a finger. Gels may not have the elastic modulus of common solids such as metals, stones, glass, or plastics which have the moduli  $>10^9\text{--}11$  Pa. Moduli of most rubbers are of the order of  $10^6$  Pa. What is the maximum and the minimum moduli for gels? There is no consensus about this because there may be a very firm gel which is very close to solids, and a very tenuous or sloppy gel very close to liquids. The minimum modulus

necessary for a gel to be self-standing is  $\text{ca}10^3$  Pa, and this and yield stress are recognized important in 3D printing (Nan et al. 2020).

Beyond the small deformation range, gels show a failure or fracture. Gels close to liquids show failure but not clear fracture. The strain at failure or fracture is an important property in the application of gels. Generally, gels consisting of long chains show a deformable behavior while gels consisting of short chains or small molecules show a failure at small strain and are brittle. Obviously, textures of deformable gels and brittle gels are very different (Nishinari 2000a).

Soft gels are not chewed by teeth but compressed/squeezed between the tongue and the hard palate. The transition of the mastication mode from the tongue-palate squeezing to the chewing by teeth could be well predicted by a simulating compression experiment of a gel between an artificial tongue and the base plate of the uniaxial compression machine, and depended on the deformability of gels (Ishihara et al. 2013, 2014).

### 3.2 Classification of Food Gels Based on Molecular Forces

Molecular forces which form gel network are covalent and non-covalent bonds such as hydrogen bonds, hydrophobic interactions, ionic bonds. Gels formed by non-covalent weak secondary forces such as hydrogen bonds, hydrophobic interactions, van der Waals forces are called *physical gels*, while gels formed by covalent bonds are called *chemical gels*. In many food protein gels, physical and chemical bonds coexist (Djabourov et al. 2013).

It seems that it is still not possible to understand the structure-property relation of all different gels in common language which is aimed in this chapter. Researchers studying polysaccharide gels consisting of linear chain molecules use the network theory derived from rubber elasticity and the ordering process is related with coil-helix transition and aggregation processes while globular protein gels are studied from the viewpoint of molecular rearrangement (Nishinari and Takahashi 2003; Nishinari et al. 2000). Gelatin is a fibrous molecule and its gelation has been studied extensively, but in food area, particle gels formed from globular proteins are another important material. Helix-coil transition is also a molecular rearrangement, but this term is not so much used among researchers interested in polysaccharide gels or gelatin gels which are jokingly called an honorary polysaccharide. Both of these gels are common in a sense that structural elements are connected or in modern parlance, after de Gennes' introduction, "percolated" to span the space. The term percolation originates from a coffee percolator (Djabourov et al. 2013).

### ***3.3 Classification of Food Gels Based on Molar Mass of Network Elements***

Most food gels are made from polysaccharides or proteins. When they are degraded into lower mass compounds, they cease to form a gel. Everybody knows that sucrose solutions don't form a gel even if they are concentrated. They precipitate above a certain concentration at each temperature. An important difference between lower molar mass compounds such as sugar or salt and higher molar mass compounds (polymer) is that the former solutions precipitate when the temperature or pressure or concentration is changed so that the extrinsic condition is outside of the condition of saturated solution while the latter materials have plural conformations such as helix and coil and their aggregates which lead to network structure called commonly gels. Precipitated lower molar mass materials such as butter or margarine are usually not called gels. However, lower molar mass gelators (Weiss and Terech 2006) have been attracting much attention and especially oleogels in food area (Singh et al. 2017). Pullulan is one of most soluble polysaccharides and its films are used in food packaging, but its gels are not studied in gel technology so much, because materials called gelling agents form a gel at lower concentrations.

### ***3.4 Classification of Food Gels Based on Ingredients***

In foods, many polysaccharide gels and protein gels have been known, and gels consisting of mixed polysaccharides and proteins have also been studied. Emulsion gels which consist of polysaccharide or protein gels containing oil droplet have been attracting much attention in the past two decades. Aerated gels have been also studied recently because it can reduce the calorie inducing satiety thus can be a convenient tool to prevent the obesity. Recently, gelation of oils has attracted much attention, and is described later.

### ***3.5 Classification of Food Gels Based on Origin***

Gels can be also classified by the origin of materials, plant or animals, sea weed, seed, bean, legume, fish, meat, egg, milk, and microbial origin such as curdlan, gellan, and so on. This viewpoint is important in designing food products (Phillips and Williams 2020).



### ***3.6 Classification of Food Gels Based on Temperature Dependence of Elastic Modulus***

Some biopolymer solutions of agar, carrageenan, gellan, and gelatin form a gel on cooling, but egg white, milk proteins, solutions of methylcellulose and other cellulose derivatives, and curdlan form a gel on heating (Nishinari 2000b; Nishinari and Zhang 2004). They are often called cold-set gels and heat-set gels, respectively. Some of them are thermoreversible and the others are thermo-irreversible; gels of agar, carrageenan, gellan, gelatin are formed on cooling, return to sol state on heating, thus called thermoreversible gels, while boiled egg white or tofu or konjac is a typical thermo-irreversible gel because they do not show gel-sol transition after gel formation. However, some thermoreversible gelation of ovalbumin (OVA), one of the main proteins in egg white, is well-known and studied extensively (Doi 1993).

### ***3.7 Classification of Food Gels Based on Optical Properties***

Gels of gellan and gelatin are transparent while egg white gels, starch gels, and many other gels are opaque. But it is well established to make a transparent egg white protein gel (Doi 1993). Most pigments are added artificially but some gels have a color in gels where naturally binding pigments exist.

### ***3.8 Classification of Food Gels Based on Shape of Network Elements or Crystallinity***

Fibrous gel, particle gels, or mixture of these may exist, since rearrangements or ageing always occurs and these may be related to syneresis. Partially ordered structured gels or liquid crystalline gels also exist. Even in apparently homogeneous gels, an internal structure consists of ordered domains and amorphous domains. It may be impossible to define the upper and lower limit of the degree of order.

### ***3.9 Classification of Food Gels Based on Electric Charges***

Most gelling polysaccharides have anionic groups such as carboxyl group (gellan (Morris et al. 2012)) or sulfate group (carrageenan) while chitosan molecule has a positive charge. Gels of agarose, curdlan, and starch are electrically neutral without electric charges although most commercially available samples contain some ions. Since amino acids are positively or negatively charged, gelling behavior of proteins is strongly influenced by pH and ionic strength.

### 3.10 Classification Based on Other Criteria

It is also possible to classify gels based on size (microgels and bulk gel), pH dependence, water holding capacity, thermal conductivity, liquid (water, oil, alcohol), or gas content. This viewpoint is useful in food processing and preservation. Macroscopic shape such as spherical, rod, tetrahedron, rectangular can be controlled if it is moldable, but these geometrically regular shaped gels may not be naturally occurring gels. It is an important problem to keep a shape in food processing and flavor release.

## 4 Gel-Sol Transition

### 4.1 Molecular Forces

Suzuki et al. (1972) examined whether the pressure would prompt the gel formation in which hydrogen bonds play a main role, while the pressure would retard it in which hydrophobic interactions play a main role. Investigating the dependence of equilibrium constant  $K$  in the gel-sol phase transition on the temperature and pressure ( $\partial \ln K / \partial T$ )<sub>p</sub> =  $\Delta H / RT^2$  and ( $\partial \ln K / \partial P$ )<sub>T</sub> =  $-\Delta V / RT$ , respectively, they studied the effect of pressure and temperature on the gelation of gelatin and methylcellulose (MC). They found that the pressure prompted the gel formation of gelatin, while the pressure retarded that of MC, and therefore, it is concluded that hydrogen bonds and hydrophobic interactions are dominating molecular forces for gelatin and MC, respectively. However, they noticed that  $\Delta V$  changes the sign above 6000 atm, and stated that both hydrophobic interaction and hydrogen bonds concern in the gelation of MC.

Kometani et al. (2015) studied the pressure effect on the gelation of agarose and MC (Fig. 4.1). The cloud-point temperature,  $T_{\text{cloud}}$ , was determined from cooling curves by the temperature of 75% transmittance because it corresponds to the steepest point of decreasing transmittance in all curves. In the same way, the “transparency temperature,”  $T_{\text{trans}}$ , at which the solution returns to a transparent sol state was determined from heating curves by the temperature of 75% transmittance. From the Clapeyron-Clausius relation  $dT/dP = T\Delta V/\Delta H$  together with the enthalpy change determined by thermal measurements, the volume change for agarose was determined as  $\Delta V = -4.57 \times 10^{-6} \text{ m}^3/\text{kg}$  which is an order of magnitude larger than that for gelatin (Fig. 4.1a). This suggests that the gels of agarose and gelatin are stabilized under high pressure, but their stabilization mechanism may be different. In addition, it should be mentioned that both  $\kappa$ - and  $\iota$ -carrageenan gels formed also by hydrogen bonds are destabilized by pressure (Gekko and Kasuya 1985).

The slope  $dT/dP = 2.97 \times 10^{-2} \text{ K/MPa}$  determined from Fig. 4.1b for MC is consistent with the reported values  $\Delta V = 0.80 \times 10^{-6} \text{ m}^3/\text{kg}$  and  $\Delta H = 11.8 \text{ kJ/kg}$

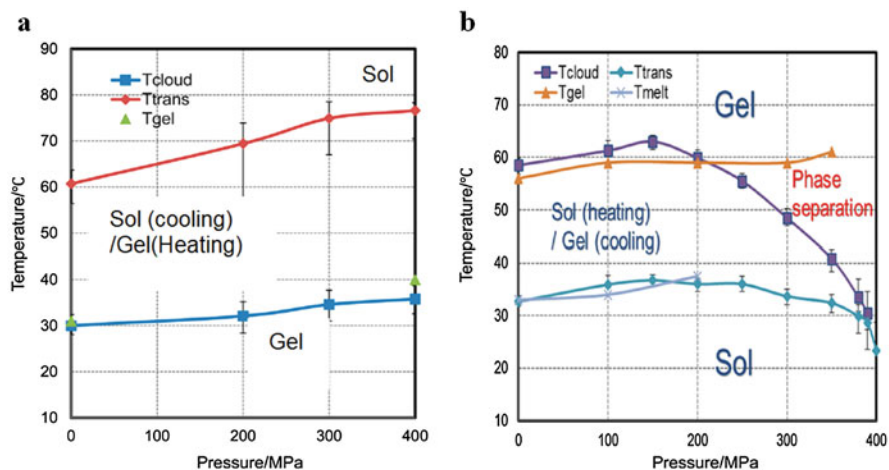


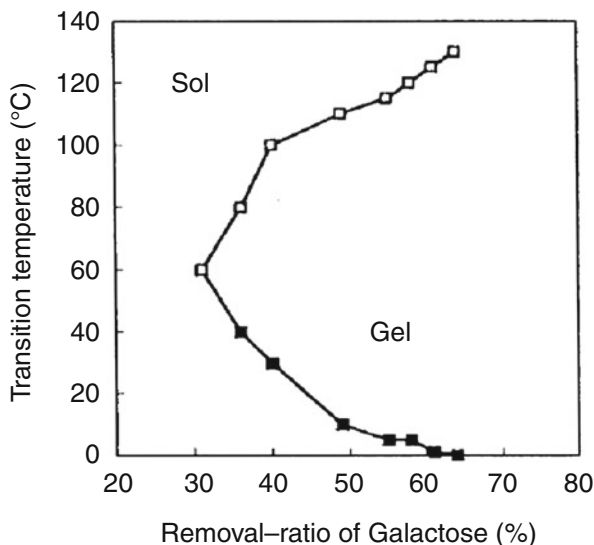
**Fig. 4.1** Plots of  $T_{cloud}$  (square) and  $T_{trans}$  (diamond) as a function of pressure for 1 wt % solutions of agarose (Fig. 4.1a) and methylcellulose (Fig. 4.1b). Triangles and cross show the gelling temperature  $T_{gel}$  and melting temperature  $T_{melt}$ , respectively, measured by the falling-ball method. Reproduced with permission from Kometani et al. (2015), Copyright 2015ACS

taken from literatures, and indicates that MC gel is destabilized by compression as contrasted with agarose (Kometani et al. 2015).

The main molecular forces responsible for gel formation in agarose and MC are hydrogen bonds and hydrophobic interaction, respectively, and both appear as an endothermic peak on heating in DSC. In the former, gel-to-sol transition occurs, while in the latter sol-to-gel transition occurs. However, in the latter, at some intermediate concentration range, an exothermic peak appears on heating which is attributed to the appearance of anisotropic phase (Yin et al. 2006). This anisotropic phase formation at higher concentration for stiff molecules is also known for xanthan (Lee and Brant 2002), gellan (Nitta et al. 2010), schizophyllan (Fang et al. 2004), and other biopolymers (Djabourov et al. 2013).

Shirakawa et al. (1998a, b) found that xyloglucan from which galactose residues were removed formed a gel on heating and returned into sol state on further heating and that this transition was thermally reversible (Fig. 4.2). Enthalpy change  $\Delta H$  accompanying gel to sol transition on heating was reported 24.2 J/g for gelatin (Gekko et al. 1992), 33.2 J/g for  $\kappa$ -carrageenan (Watase and Nishinari 1987a), 40 J/g for agarose (Watase and Nishinari 1987b) while  $\Delta H$  accompanying sol to gel transition on heating is 16.0 J/g (Haque and Morris 1993) or 10–17 J/g (Funami et al. 2007) for methylcellulose, 6.9 J/g for methylhydroxypropylcellulose (Yuguchi et al. 1995).  $\Delta H$  found for the degalactosylated xyloglucan was 4.4 J/g, which is the same order of magnitude to the latter group where hydrophobic interaction plays a main role. The gelation of xyloglucan by galactose removal is still studied recently (Sakakibara et al. 2017).

**Fig. 4.2** Sol-gel transition temperature for xyloglucan as a function of galactose removal ratio. ■ lower temperature transition point; □ higher temperature transition point. Reproduced with permission from Shirakawa et al. (1998a), Copyright 1998 Elsevier



As is seen in the gelation of MC and xyloglucan, the chemical modification changes the solubility or gel forming ability. Gel forming ability is the intermediate between the insolubility and solubility. Carboxymethylation of curdlan confers curdlan water solubility but makes lose its gelling ability (Jin et al. 2006; Nishinari and Zhang 2004).

On the other hand, molecular forces in the gelation of globular protein gels are more complicated (Djabourov et al. 2013; Walstra 2003).

## 4.2 Rheological Determination of Sol-Gel Transition

One of the most widely used methods for the determination of sol-gel transition is that proposed by Winter and Chambon (1986). These authors examined the gelation process of polydimethylsiloxane (PDMS) to determine the gel point. PDMS was chosen for its well-defined chemical nature, the need of catalysis, the availability of prepolymers with different molecular weights, and the elastomeric nature of the samples after crosslinking. The advantage of this method was to stop the catalyst action instantaneously to prevent the further crosslinking reaction. Since the measurement of the frequency dependence of  $G'$  and  $G''$  takes a time, it was examined before and after the crossover of  $G'$  and  $G''$ , which was possible by stopping the crosslinking reaction by stopping the catalytic action by stopping agent (sulfur). By this method, they could observe the storage modulus  $G'$  and loss modulus  $G''$  as a function of frequency near the crossover point of  $G'$  and  $G''$  observed as a function of time at a constant frequency. Before the gelation point GP,  $G' < G''$  and after GP,  $G' > G''$ . The frequency dependence of  $G'$  and  $G''$  was observed from 6 min before

the time of crossover of  $G'$  and  $G''$ ,  $t_0$ , to the time after 6 min of  $t_0$ . At an earlier stage of the crosslinking reaction, both  $G'$  and  $G''$  are strongly frequency dependent and  $G' < G''$ , and at time  $t_0$ , both  $G'$  and  $G''$  show a similar frequency dependence, and after the time  $t_0$ ,  $G'$  tends to show a plateau which is a characteristic mechanical behavior for rubbers. They proposed the following criterion for the critical gelation point.

$$G' \sim G'' \sim \omega^n \quad (1)$$

$$\tan\delta = G''/G' = \tan(n\pi/2) \quad (2)$$

which is now called Winter-Chambon criterion. At the critical point, both of these two equations should be satisfied simultaneously. The exponent  $n$  in the two equations should be the same. These equations are valid at times longer than a certain characteristic time  $t_0$  or at lower frequencies than  $1/t_0$ . First, this criterion was proposed for such a chemical gel, but later, Nijenhuis and Winter (1989) found that this criterion is valid also for physical gels of polyvinyl chloride (PVC). Since then many papers have been published to study the critical gelation point, and although initially the exponent was proposed as 0.5, other values between 0.3 and 0.7 have been reported for various gelation processes (Winter 2016). Figure 4.3a shows the mechanical spectra, i.e., the frequency dependence of  $G'$  and  $G''$  of a 2.5 wt %

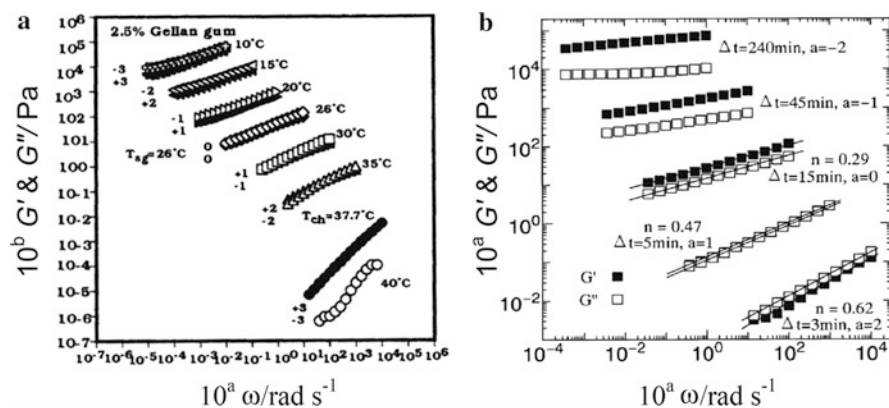


**Fig. 4.3** (a) Angular frequency dependence of  $G'$  (open symbols) and  $G''$  (filled) for a 2.5% gellan gum solution at various temperatures shown on the right side of each curve. The data are shifted along both the horizontal and the vertical axes by shift factors "a" and "b," respectively, to avoid overlapping. Numbers on the left side of each curves represent "a" and "b," respectively. Reproduced with permission from Miyoshi and Nishinari (1999), Copyright 1999 Springer. (b) Angular frequency dependence of  $G'$  (filled symbols) and  $G''$  (open) for a 50 mg cm<sup>-3</sup> OVA solutions heated at 80 °C for 60 min and then reheated after addition of 60 mM NaCl for various times  $\Delta t = 3, 5, 15, 45,$  and 240 min. The data are shifted along both the horizontal and the vertical axes by shift factor "a" to avoid overlapping. Reproduced with permission from Koike et al. (1998), Copyright 1998 Elsevier

sodium type gellan solution at temperatures from 40 °C to 10 °C (Miyoshi and Nishinari 1999). At higher temperatures,  $G'$  and  $G''$  of the solution shows strong frequency dependence and  $G' < G''$  while at low temperatures  $G' > G''$  and both moduli tend to show a plateau. At 26 °C, the solution satisfies the above equations, and is in the critical state.

Figure 4.3b shows the mechanical spectra of  $G'$  and  $G''$  of a 50 mg cm<sup>-3</sup> OVA solution prepared by a two-step heating method; first heating at 80 °C for 60 min and then cooled, and then reheated at the same temperature for various heating time periods  $\Delta t$  (Koike et al. 1998). Critical gels satisfying the eqs. (1) and (2) were observed for  $\Delta t$  from 3 to 30 min indicating the fractal structure persisted in this range of the heating time. Koike et al. (1998) had reported that OVA formed linear aggregates, worm-like cylinder, diameter 12 nm, persistence length 23 nm, and the molar mass per contour length 16,000 nm<sup>-1</sup> after heating the solution at 80 °C by dynamic laser scattering (Nemoto et al. 1993) (See Fig. 4.13). Transparent gels were formed by both one-step and two-step heating in a certain condition of the salt concentration and heating time, and these gels were found to satisfy the critical condition eqs. (1) and (2). However, such a critical gel behavior was not observed for translucent gels. Although these authors ascribed the main molecular forces for the gel formation are hydrophobic interaction, they found the necessity of further structural study based on neutron scattering and SEM, and this is discussed again in Sect. 7.

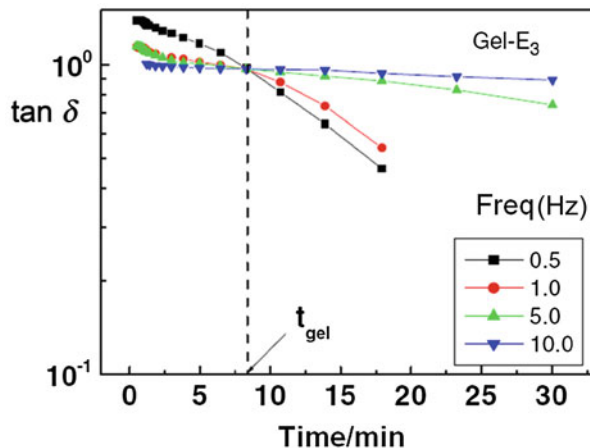
Hossain et al. (1997) studied the gelation of iota-carrageenan solutions, and found that  $G' = G''$  at 57°C and  $n = 0.42$ . The value of  $n$  was found to decrease with increasing concentration of iota- carrageenan. The crossover of  $G'$  and  $G''$  as a function of time or temperature has often been taken as an indication for the gelation point, but this is only right for a critical gel with the relaxation exponent  $n = 0.5$ . Very small values 0.1 for the relaxation exponent were reported for bacterial polyester, poly( $\beta$ -hydroxyoctanoate), and gelatin. The critical gelation point at which  $G'$  and  $G''$  show the same frequency dependence may lie in between the entangled solution behavior and a weak gel behavior described before. To determine the gelation point by Winter-Chambon criterion, it is convenient to plot the  $\tan \delta$  observed at different frequencies as a function of time.

Figure 4.4 shows gelation process of carboxymethyl cellulose crosslinked with polyfunctional glycidyl ether.

However, this method of determination of gel point was found not applicable in some systems. In the gelation of pluronic (called also poloxamer, PEO-PPO-PEO triblock copolymer, where PEO = poly(ethylene oxide), PPO = poly(propylene oxide)) used in drug delivery, it was found that at lower temperatures (33 °C) a liquid-like behavior  $G' < G''$  was found, on further heating gel is formed at >34 °C, however, at higher temperatures it was found that  $G' > G''$  at high frequencies and  $G' < G''$  at low frequencies, which is characteristic for entangled polymer solutions (Nyström and Walderhaug 1996).

Globular protein solutions show mechanical spectra similar to those of structured liquids such as xanthan solutions, that is,  $G' > G''$  at the angular frequency range from 10<sup>-1</sup> to 10<sup>2</sup> rad s<sup>-1</sup> and  $\tan \delta \geq 0.1$  (Ikeda and Nishinari 2000; Ikeda and Nishinari

**Fig. 4.4** Loss tangent  $\tan \delta$  as a function of time for the hydrogels at various fixed frequencies (0.5, 1, 5, 10 Hz) measured at constant temperature 60 °C.  $t_{\text{gel}}$  is the gel point. Reproduced with permission from Lawal et al. (2011), Copyright 2011 Springer



2001a, b; Matsumoto and Inoue 1993). During isothermal heating at 70°C, 5% w/w  $\beta$ -lactoglobulin in a 0.1 mol/dm<sup>3</sup> NaCl aqueous solution shows a gelation behavior (Ikeda and Nishinari 2001a). It was observed that  $G' > G''$  all the time, and the gelation occurred at around 3000 s, which was also confirmed by tilting tube. Thus, the Winter-Chambon criterion cannot be used. For such a case, the temperature or the time at which  $G'$  begins to increase steeply is generally taken as the gelation point (Tobitani and Ross-Murphy 1997).

### 4.3 Spinodal Decomposition or Nucleation and Growth?

Gelation of agarose was thought to progress through spinodal transition based on Cahn's theory (Feke and Prins 1974). San Biagio et al. (1996a) recognized the characteristic or "signature" behavior of spinodal decomposition in the gelation of agarose (concentration < 1%); the occurrence of a low-angle scattering ring, the exponential increase of scattered light, its typical dependence upon the scattering vector represented by linear Cahn's plot, the occurrence of a transient viscosity peak. Summarizing their data, they constructed a  $C$ - $T$  phase diagram according to which at higher concentrations (> 1.5%), only direct gelation occurs at  $60 \pm 10$  °C, and below this temperature range both demixing mediated and direct gelation are thought to be possible. They conclude that this approach is useful to understand the gelation beginning from the break of symmetry, the formation of inhomogeneous structure from a homogeneous sol state through the spinodal decomposition, and the possibility to control the final gel structure. San Biagio et al. (1996b) studied the gelation of bovine serum albumin (BSA) by the same approach and found the occurrence of spinodal demixing of sol after the unfolding of the native BSA.

Morita et al. (2013) constructed a  $C$ - $T$  phase diagram of agarose, and found that an agarose solution formed a gel on cooling and then the phase separation occurred, which was detected as a cloud point. The spinodal points are found below these

temperatures. They also recognize characteristic features of spinodal decomposition mentioned above. They attributed the opacity of agarose gels to the frozen concentration fluctuation within the gel already formed. They pointed out that the sol-gel transition and the phase separation are independent phenomena, and showed a porous structure of a quenched gel. They finally emphasize the importance to take into account this porous structure induced by spinodal decomposition in addition to the formation of the crosslinking points (junction zones) to understand the macroscopic properties of gels.

MC gelation has been studied by many research groups. Group of Lodge (Arvidson et al. 2013) studied gelation and phase separation of MC with three different Mw using Winter-Chambon criteria and light transmittance. The gelation point was determined by frequency independent  $\tan \delta$  for concentrated solutions ( $C \geq 10C^*$ , where  $C^*$  is the coil-overlap concentration). They found a high correlation between the  $T_{\text{gel}}$  and the cloud point which is different from previous papers reporting the phase separation and the gelation are distinct events. In addition, they showed that gelation of MC has strong dependence on heating rate while the melting of the gel has little dependence on cooling rate, and thus suggested that thermogelation of MC proceeded by a nucleation and growth mechanism (McAllister et al. 2015) rather than spinodal decomposition although they cited several papers which propose the different mechanism that the gelation of MC is induced by spinodal decomposition.

#### ***4.4 Jamming Transition: Another Molecular Rearrangement Induced by Shear***

In relation to shear thickening of suspensions, shear induced close packing formation has been attracting much attention. Jamming transition is functionally defined to occur when, with increasing packing fraction or decreasing applied shear stress, a yield stress is first observed (Liu and Nagel 1998). Tanaka (2011) classifies jamming gels with delocalized crosslinks as viscoelastic fluids with long relaxation times.

The minimum packing fraction where a yield stress is observed depends on a number of suspension properties, including shape, polydispersity, friction coefficient, roughness, density matching, temperature, and attractive forces (Brown and Jaeger 2014).

#### ***4.5 Zippering and the Size of Junction Zone***

To correlate the microscopic states of a macroscopic system with thermodynamic state variables such as the temperature, volume, and pressure, it is necessary to determine the partition function in the statistical mechanics. A simple **zipper model**



for thermoreversible gels consists of aggregated ordered structures such as helices and stiff chains which can be opened from both ends (Nishinari et al. 1990). From the partition function including the number of parallel links  $N$ , the number of zippers  $\mathbf{N}$ , binding energy  $\epsilon$  and the degeneracy (rotational freedom)  $g$ , the heat capacity  $C$  can be calculated.

In the heating DSC measurements,  $dT/dt$  is positive, then the endothermic peak is equivalent to the maximum of the heat capacity  $C$ . In the cooling DSC measurements,  $dT/dt$  is negative, then the exothermic peak is again equivalent to the maximum of  $C$ . When the concentration of gels increases, the mobility of chain molecules decreases, and then the degeneracy  $g$  will decrease. As a result, the peak of the heat capacity shifts to higher temperatures. This is in accordance with Eldridge-Ferry's empirical formula. This zipper model approach can also explain that the transition is sharper in cooling than in heating as has been observed for many polysaccharide gels such as agarose,  $\kappa$ -carrageenan, and gellan (Watase and Nishinari 1987b; Miyoshi and Nishinari 1999).

A single DSC endothermic peak for a  $\kappa$ -carrageenan gel on heating was successfully fitted by choosing appropriate structural parameters. This treatment was extended to multi-component systems in which junction zones consist of associations with different kinds of zippers. A broader DSC endothermic peak for 0.42%  $\kappa$ -carrageenan /0.186% konjac glucomannan gel was thus fitted (Nishinari et al. 1990).

Using van't Hoff's law, Eldridge and Ferry (1954) proposed a method to determine the heat  $\Delta H_m$  absorbed on forming a mole of crosslinks— $d \ln C / dT_m = \Delta H_m / RT_m^2$ , where  $R$  is the gas constant,  $T_m$  (gel melting/K) is the transition temperature, and  $C$  is the gel concentration. Integration of this equation leads to  $\ln C = \Delta H_m / RT_m + \text{const}$ . This EF equation is based on the following chemical equilibrium: 2 moles crosslinking loci  $\rightarrow$  1 mole crosslinks.

Tanaka and Nishinari (1996) modified the EF equation taking into account the molar mass dependence and proposed a method to estimate the bonding energy  $\epsilon$  (i.e., the enthalpy change for binding a single repeat unit into the network junction), the number  $\zeta$  of repeating unit in the molecular chain constituting a crosslink, and the junction multiplicity  $s$  (the number of polymer chains combined in a single junction) (Nishinari et al. 1996). It is expected that this method is applied for food polymers although it is not so easy to get food polymers with different molar masses (Nishinari and Fang 2021).

#### 4.6 Critical Molar Mass and Concentration for Gelation

For thermoreversible gels, the term "junction zone" has been frequently used to describe the crosslink because each crosslink involves aggregates of ordered molecular chains like helices or extended stiff chains. It is required to know the lower limit of the molar mass below which a helix is not formed for each polymers. The minimum concentration necessary for gelation might be related to a persistent length of the chain. It has never been found that gels are formed in a dilute solution of flexible polymers such as polyethylene oxide or pullulan which only entangle each

other but don't form junction zones. Such a system cannot retain water solvent, and the system flows if the concentration is not high enough. Koga and Tanaka reported that the critical concentration for gelation shifted to lower concentrations with increasing persistence length of linear chain molecules by Monte Carlo simulation. Solutions of flexible chains, like pullulan, polyethylene oxide, don't form a gel even at quite a high concentration. However, since it is known that these polymer solutions produce a film when the solvent water is evaporated they should form a gel before becoming a solid film. It is evident that solutions of monomers of these polymers, glucose, or ethylene glycol do not form a gel even if solvents are evaporated. These substances with low molar mass are known to form a crystal when the solution is concentrated. Therefore, there should be a critical molar mass of polymers below which no gelation occurs.

Ogawa et al. (2006) prepared 6 gellan gum samples with different molar masses converted to sodium form and examined the helix-coil transition. The weight average molar mass for higher molar mass samples at 25 °C ( $M_{w,25}$ ) determined by DLS was two times higher than that determined at 40 °C ( $M_{w,40}$ ), indicating the double helix formation while the ratio  $M_{w,25}/M_{w,40}$  is becoming smaller with decreasing molar mass, and was 1 for the lowest molar mass sample ( $M_w = 17,000$ ) indicating that the lowest molar mass sample does not form a double helix. This is consistent with results obtained by circular dichroism and DSC. The minimum molar mass for gelation of pectin,  $\kappa$ -carrageenan, and alginate has been discussed recently (Nishinari and Fang 2021).

The critical gelation concentration has been determined by scaling in which the shear modulus  $G'$  near the gelation threshold is plotted against the distance of the concentration from the critical concentration:  $G' \sim (C - C_{cr})^t$ . The critical exponent  $t \approx 2$  has been reported by many workers (Djabourov et al. 2013). Joly-Duhamel et al. (2002) reported that the  $G'$  of gelatin gels could be represented well by the helix concentration for all the gelatin extracted from various fish although gelatin extracted from warm water fish begins to form a gel at a higher temperature than that from cold water fish.

Concentration dependence of the elastic modulus of gels has been studied for a long time, and it has been known empirically that the modulus is represented by a power law. The exponent for agarose has been known larger  $\sim 4$  at lower concentrations and smaller  $\sim 2$  at higher concentrations. A cascade treatment and a modified rubber elasticity theory were applied to fit the concentration dependence of moduli for agarose, amylose, pectin,  $\kappa$ -carrageenan, etc. Both these theories predict that the exponent is larger at lower concentration region and smaller at higher concentration region. However, an opposite tendency was found in heated ovalbumin gels: the exponent is about 4 at lower concentration region and about 10 at higher concentration region (Koike et al. 1996).

Generally, the minimum concentration required for gelation is found lower for linear polymers but gelatin needs higher concentration than agarose or gellan (Fig. 4.5). This is not a rigorous statement because it may be possible to make the opposite situation by preparing gels with short chain gellan samples which need

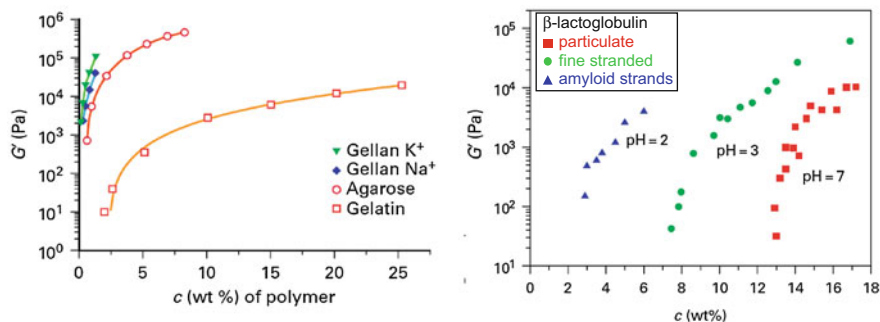


**Fig. 4.5** Storage modulus of linear chain polymers and globular protein gels as a function of concentration. This comparison is not strict because the molar masses and other molecular parameters are not the same. Taken from Djabourov et al. (2013) collecting the data from Clark et al. (1983); Milas, Rinaudo (1996); Kavanagh et al. (2000); Veerman et al. (2002). Reproduced with permission from Djabourov et al. (2013), Copyright 2013 Cambridge University Press

higher concentration than agarose. Djabourov et al. (1988, 2013) plotted  $G'$  of gelatin gels as a function of helix content  $\chi$  and found  $G' = 0$  at  $\chi < 8\%$ .

## 4.7 Rigid Network Chains

Common characteristics in physical gels are that network chains are very stiff. Stiff chains tend to align to form a liquid crystal. Structure formation has been discussed in relation to Flory's phase diagram (1956) for rod-like polymers; agarose (Hayashi et al. 1978), MC (McAllister et al. 2015), xanthan (Lee and Brant 2002). Since stiff chains are expected to form a gel at a low concentration, it has been attracting much attention.

Fibrils have been attracting much attention in relation to amyloidosis diseases such as Alzheimer's, Creutzfeldt-Jakob disease (CJD), and type II diabetes (van der Linden 2012). Recently,  $\beta$ -lactoglobulin ( $\beta$ -lg) fibrils formed after heating at 80 °C and pH 2 for 10 h were observed by atomic force microscopy (AFM) and it was reported that the fibrils have a multi-stranded helical shape with twisted ribbon-like structures having persistence length from 1000 to 3000 nm (Adamcik et al. 2010). Since the fibrils of globular proteins have a similar structure to those causing amyloidosis diseases, it is necessary to confirm the safety of these materials. Bateman et al. (2010) reported that  $\beta$ -lg fibrils could be digested in simulated gastric fluid. They found that the fibrils were digested completely by pepsin within 2 min. Fibrils of  $\beta$ -lg are known to form a gel above a certain concentration depending on pH, ionic strength ( $I$ ), and temperature. A phase diagram of solutions of  $\beta$ -lg fibrils at pH 2 was constructed as a function of concentration (0–2 wt%) and ionic strength (0–800 mM NaCl) at 20 °C (Bolisetty et al. 2012). Gel phase is found in the region  $C = 0.3$ –2.0 wt% and  $I = \text{ca } 40$ –100 mM. Recently, Cao et al. (2018) found that the

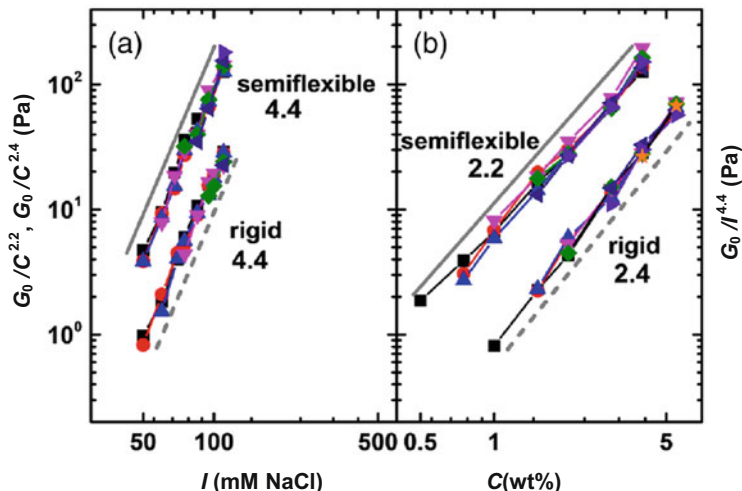


**Fig. 4.6** Normalized  $G_0$  of BLG fibril networks as a function of (a) ionic strength  $I$  (mM NaCl) and (b) polymer concentration  $C$  (wt%). Reproduced with permission from Cao et al. (2018), Copyright 2018 APS

dependence of plateau modulus  $G_0$  on the polymer concentration  $C$  scales as  $G_0 \sim C^{2.2}$  for semiflexible fibrils or  $G_0 \sim C^{2.4}$  for rigid fibrils (Fig. 4.6b).

Based on the recent theoretical treatment on the stiff chain networks by groups of MacKintosh, Janmey, Weitz, Cao et al. deduced  $G_0 \sim C^{11/5}$  for semiflexible fibrils network and  $G_0 \sim C^{5/2}$  for rigid fibrils network, which coincided well with their experimental observation (Fig. 4.6b). As for the dependence of plateau modulus  $G_0$  on the ionic strength  $I$ , Cao et al. (2018) found  $G_0 \sim I^{4.4}$  for both semiflexible fibrils and rigid fibrils (Fig. 4.6a). They explained this high exponent taking into account the DLVO theory which led to the exponent 4.1.

It was shown recently that  $\beta$ -lg fibrils in the presence of transglutaminase (TGase) form a gel at a much lower  $\beta$ -lg concentration (Wu et al. 2016) because TGase has a crosslinking ability to form isopeptide bonds between glutamine and lysine residues in proteins, thus introducing both inter- and intramolecular covalent crosslinks.

#### 4.8 Interaction of Short Chains and Long Chains

Fang et al. (2007) re-examined the so-called egg-box model which has been proposed for the gelation of alginates and pectins, where two or more chains are involved in cooperative binding, forming the egg-box structure, by isothermal titration calorimetry (ITC). Three distinct and successive steps in the binding of calcium to alginate were identified with increasing concentration of Ca ions. They were assigned to (1) interaction of  $\text{Ca}^{2+}$  with a single guluronate unit forming monocomplexes; (2) propagation and formation of egg-box dimers via pairing of

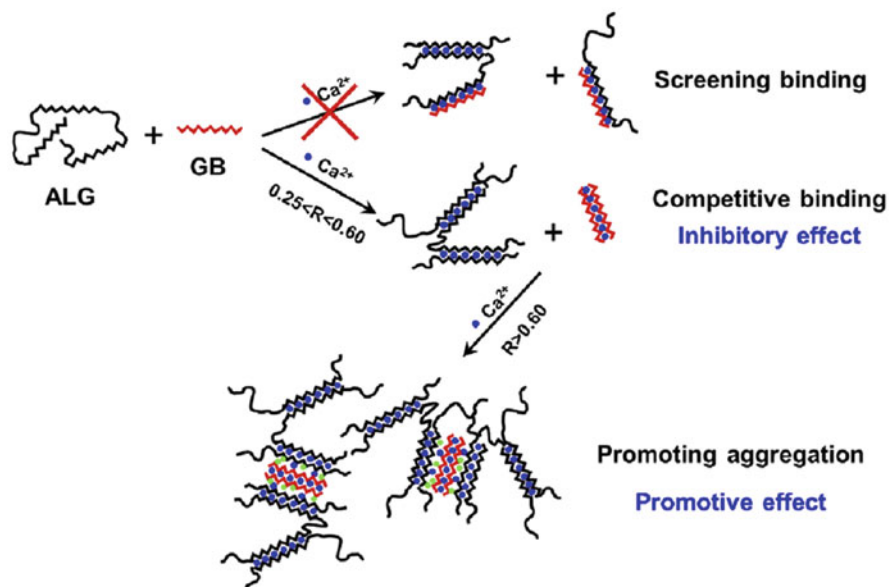


**Fig. 4.7** Coexistence of oligogulonate (GB), short chain guluronate, with alginates promotes the aggregation and strengthens the gel in the presence of sufficient calcium while at low  $\text{Ca}^{2+}$  it inhibits the network growth by binding with calcium. The blue dots represent  $\text{Ca}^{2+}$  and the green dots represent  $\text{Na}^+$  and  $\text{H}_2\text{O}$  etc. Reproduced with permission from Liao et al. (2015), Copyright 2015 Elsevier

these monocomplexes; and (3) lateral association of the egg-box dimers, generating multimers.

Since alginates and pectins both are known to have a similar structure and form gels in the presence of calcium, it is expected to see the similar multiple step gelation process also in pectin. The different behaviors in alginates and pectin gelation were attributed to the structural difference; alginates are block-copolymer while arrangement of copolymer units in pectins is more random (Fang et al. 2008).

Recently, effects of the addition of oligogulonate, guluronate block (GB) to alginates with and without salt on rheological properties were studied, and the ratio of Ca to guluronate G,  $R(\text{Ca}/\text{G})$  was found to play an important role (Liao et al. 2015). The addition of GB was inhibitive in the range of  $0.25 < R(\text{Ca}/\text{G}) < 0.60$  and promotive in the range of  $R > 0.60$ . These two effects were shown to be associated with the different molecular events that dominate the gelation of alginate, namely, egg-box dimerization and lateral aggregation. Quantitative analysis indicates a competitive binding rather than a screening binding during egg-box dimerization, which led to the inhibitory effect in the lower Ca concentration regime. On the other hand, in the higher Ca concentration regime where alginate gelation is predominated by chain lateral aggregation, the dimers formed by GB could act as a binder to enhance the aggregation of alginate dimers, resulting in a promotive effect on alginate gelation (Fig. 4.7). The results are consistent with the microstructures observed by AFM.

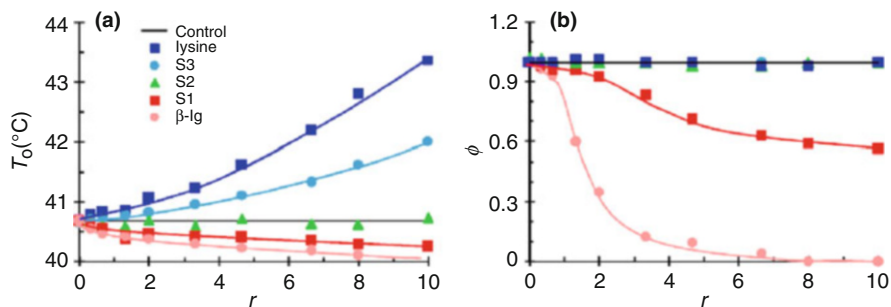


**Fig. 4.8** The effect of  $\beta$ -Ig or its hydrolysates on the onset DSC temperature ( $T_0$ ) of helix formation of  $\kappa$ -car (a) and relative extent ( $\phi$ ) of the conformational transition of  $\kappa$ -car (b) as a function of the mixing ratio  $r = \beta$ -Ig/ $\kappa$ -car. The concentration of  $\kappa$ -car 0.15%; pH = 4.7. Reproduced with permission from Cao et al. (2016b), Copyright 2016 ACS

Cao et al. (2016a) studied the mixture of  $\kappa$ -carrageenan ( $\kappa$ -car) and  $\beta$ -Ig with different mixing ratios  $r = \beta$ -Ig/ $\kappa$ -car, and found that the exothermic peak enthalpy of  $\kappa$ -car accompanying coil to helix transition detected by DSC decreased with increasing  $r$ . It was analyzed quantitatively based on a theory of McGhee and von Hippel (1974) which was used to explain the binding of protein to DNA. The relative extent of conformational transition  $\phi$  ( $r$ ) could be experimentally measured as the ratio of the enthalpy change of conformational transition of protein/polyelectrolyte mixture ( $\Delta H(r)$ ) to that of pure polyelectrolyte ( $\Delta H(r = 0)$ ). The inhibiting degree  $\phi$  of  $\kappa$ -car helix formation by  $\beta$ -Ig was quantified by the enthalpy change as a function of  $r$ . Electrostatic complexation in soluble state had subtle effect on the coil-to-helix transition of  $\kappa$ -car, which is due to the relatively high freedom of  $\kappa$ -car at the initial stage of protein binding. Electrostatic complexation in insoluble state however greatly suppressed the conformational transition, which is due to the high physical hindrance imposed by  $\beta$ -Ig upon extensive protein binding. The effect of protein/polyelectrolyte electrostatic complexation on the conformation transition of polyelectrolyte was described quantitatively. The effect was closely associated with the molar mass of  $\beta$ -Ig or its hydrolysates: Larger hydrolysates S1 (>2000 Da) had an inhibitory effect on the conformational transition of  $\kappa$ -car, smaller hydrolysates S3 (<1000 Da) tended to promote it (Fig. 4.8).

#### 4.9 Cation- or Acid-Induced Gelation

Gelation of globular proteins can be induced either by heating (heat induced gelation) or by cold gelation. In the cold gelation, a low concentration solution of native proteins is heated or subjected to high pressure and soluble aggregates are formed. The aggregates remain soluble on cooling. Then, gelation is induced either by adding salt or by changing the pH toward the isoelectric point of the proteins in order to reduce the electrostatic repulsion. Cold-set gels have been used as a vehicle

to deliver thermally labile and water insoluble functional ingredients (Chen et al. 2006), and recently cold-set emulsion gels are also attracting much attention (McClements 2017; Khalesi et al. 2019).

Ion-induced gelation of alginate has been used to produce an imitation *ikra* (salmon roe). When a droplet of non-gelling sodium alginate falls into calcium lactate solution, a thin film is formed on the surface of droplet. This process was patented by a Japanese chemical industry (Nishinari 1988). This very fast gelation can be used to produce artificial berries and onion rings (Draget 2021). Since this gelation of sodium alginate is too fast and leads to inhomogeneous gel formation, slow release of calcium ions from insoluble calcium salts is used by chelating agents (EDTA, citrate) or glucono-delta-lactone to control the gelation rate and to form homogeneous gels (Draget 2021). Alginate is also used to treat heart burn (acid reflux) since alginate solution forms a gel raft on the top surface in the stomach because of its low pH (ca 1.5) (Gaviscon has been used).

## 5 Characterization Methods

### 5.1 *Gelation Kinetics: Time Dependence of Storage and Loss Moduli $G'$ and $G''$ of a Solution at a Constant Temperature and a Frequency*

When a solution prepared at a non-gelling temperature is kept at a certain gelling temperature,  $G^*$  begins to increase with lapse of time. Generally employed condition of the measurements are as follows: the frequency and the amplitude should be as low as possible so that the structure being formed might not be broken, however, the frequency ca 1 Hz has been chosen in most cases. The geometry of the apparatus for viscoelastic measurements should be chosen so that the injected sample solution can be quenched (cooled rapidly) or can be heated rapidly. This can be satisfied generally if the required volume of sample solution is small.

Generally, the gelation proceeds faster at higher temperatures for a heat-setting system whilst it proceeds faster at lower temperatures for a cold-setting system. It is easier to carry out the rheological measurement at the temperature where the gelation proceeds slowly for the analysis of kinetics. In the first order kinetics, the storage modulus is written as follows:

$$G'(t) = G'_{\text{sat}} [1 - \exp(-k(t - t_0))],$$

where  $t_0$  is the latent time (gelation time),  $k$  is the rate constant,  $G'_{\text{sat}}$  is the saturated value of the storage modulus after a long time. Solutions of some biopolymers such as methyl cellulose, degalactosylated xyloglucan, curdlan, glycinin, and  $\beta$ -conglycinin form a gel on heating, while solutions of other biopolymers such as agarose, carrageenan, gelatin, and gellan form a gel on cooling (All these were cited



in Nishinari 1997). When the gelling polymer is composed of fast gelling and slow gelling components, the above kinetic equation can be modified using two rate constants and two latent times for each components. More kinetic models have been proposed, see p. 386 in Lapasin and Prici (1999). Recently, the gelation of  $\beta$ -lactoglobulin was analyzed by a simple eq.  $G'(t) = G'_{\text{sat}} \exp(-\beta/t)$  proposed by Scott Blair in 1963.

Lapasin et al. (1990) reported that both moduli increased first and then decreased during gelation of calcium pectate. The decrease of the moduli was attributed to the structure breakdown into smaller flow units.

Rennet-induced gels have been studied extensively by many groups as a basis for cheese production. The dependence of casein micelle size on the gelation has been studied using micelles with different sizes prepared by differential centrifugation, and it was found that smaller casein micelles form a stronger gel faster (Niki et al. 1994). It was interpreted on the basis that the  $\kappa$ -casein, which plays a main role in rennet-induced casein gelation, is abundant on the surface of casein micelles.

As in the enzymatic modification of casein, partial hydrolysis has a great potential to control the structure and property of proteins. Doi et al. (1987) performed a limited proteolysis of ovalbumin (OVA) ( $M_w = 45,000$ ) using a pepsin, and obtained an intermediate OVA ( $M_w = 42,500$ ), called p-OVA having a similar physicochemical properties with native OVA, and compared the gelation. This will be described later in Sect. 7.

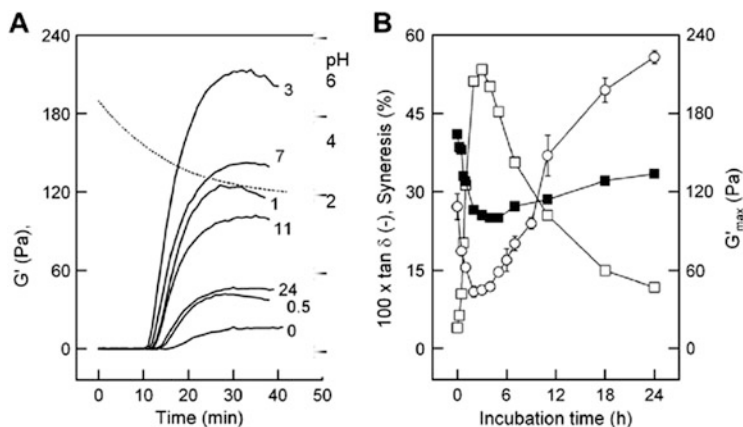
To control the rheological and structural properties of proteins, transglutaminase (TGase) was used by several research groups. Jaros et al. (2010) reported  $G'_{\text{max}}$  in GDL-induced gelation process of TGase-treated casein solution at 30 min after the GDL addition, and  $G'_{\text{max}}$  depended strongly on the incubation time by TGase.  $G'_{\text{max}}$  increased and then decreased with the incubation time, and was attributed to rearrangement and not due to the slippage frequently observed in gelation experiments. Syneresis and  $\tan\delta$  showed the minimum at 30 min after the GDL addition when  $G'$  showed the maximum (Fig. 4.9). In the processing of yogurt, various polysaccharides or microparticulated whey proteins are added to increase  $G'$ , which reduces the syneresis and increases the creaminess (Jørgensen et al. 2019).

Soy protein gels are used not only for tofu but also attracted attention as raw materials for cheese and yogurt to replace animal milk, and the optimization condition has been studied by many research groups (Nishinari et al. 2018).

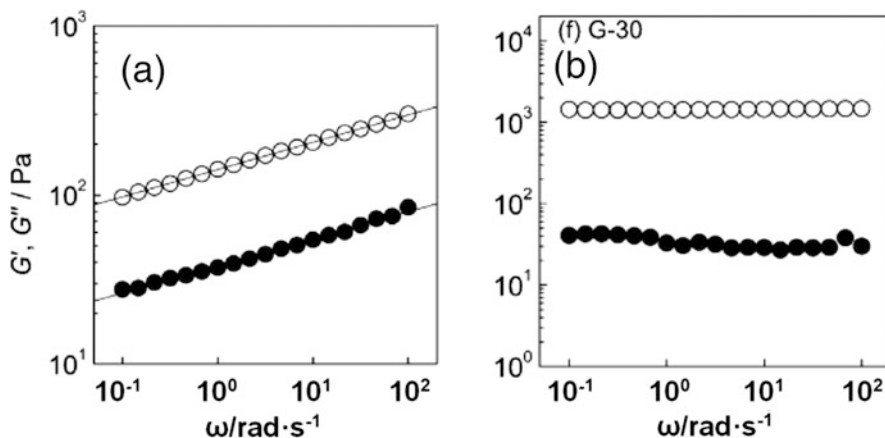
## 5.2 Mechanical Spectra: Frequency Dependence of $G'$ and $G''$ at a Constant Temperature

Figure 4.10 shows the frequency dependence of gellan solutions with a small and large amount of NaCl. Most commonly available commercial gellan samples contain salts to enhance the gelling ability. This figure shows the behavior of gellan which is converted into pure sodium type to see the effect of salts on the gelation behavior.





**Fig. 4.9** (a) Averaged gelation curves of three enzyme treated casein solutions ( $27 \text{ g kg}^{-1}$ ). TGase treatment was with  $3 \text{ U TGase g}^{-1}$  protein at  $40^\circ \text{C}$ , the numbers refer to incubation times in hours. Inactivation was with  $1 \text{ g L}^{-1}$  N-Ethylmaleimide, and gelation was induced by  $40 \text{ g L}^{-1}$  GDL at  $30^\circ \text{C}$ . Dotted line shows the corresponding pH decay. (b)  $G'_{\text{max}}$  ( $\square$ ) with the corresponding  $\tan \delta$  ( $\blacksquare$ ) and syneresis ( $\circ$ ) of cross-linked casein gels as affected by enzyme incubation time. Data are mean values  $\pm$  standard deviations of three individual experiments. Reproduced with permission from Jaros et al. (2010), Copyright 2010 Elsevier



**Fig. 4.10** Frequency dependence of  $G'$  (open) and  $G''$  (closed) of 2 wt% sodium type gellan with 30 mM NaCl at  $5^\circ \text{C}$  (a) and 0.3 wt% sodium type gellan with 100 mM NaCl at  $35^\circ \text{C}$  (b) Reproduced with permission from Nitta et al. (2010), Copyright 2010 ACS

Both storage modulus  $G'$  and loss modulus  $G''$  show a weak frequency dependence in Fig. 4.10a, while both  $G'$  and  $G''$  show a plateau in Fig. 4.10b although the polymer concentration is much lower in the latter.

The behavior in Fig. 4.10a is seen in a structured liquid (often called a “weak gel,” but this term was not to be used because it is essentially a liquid), and is different

from a “true gel” or “elastic gel” behavior shown in Fig. 4.10b. The difference between a structured liquid and an elastic gel appears in a larger value of tangent delta for the former because of its liquid nature. The large deformation behavior shows a more clear difference between a structured fluid and an elastic gel; the former flows while the latter fractures above the yield stress. For example, see the strain dependence of  $G'$  and  $G''$  in Fig. 4.4 and the frequency dependence  $G'$  and  $G''$  in Fig. 4.3 for  $\kappa$ -carrageenan in a paper by Ikeda and Nishinari (2001d).

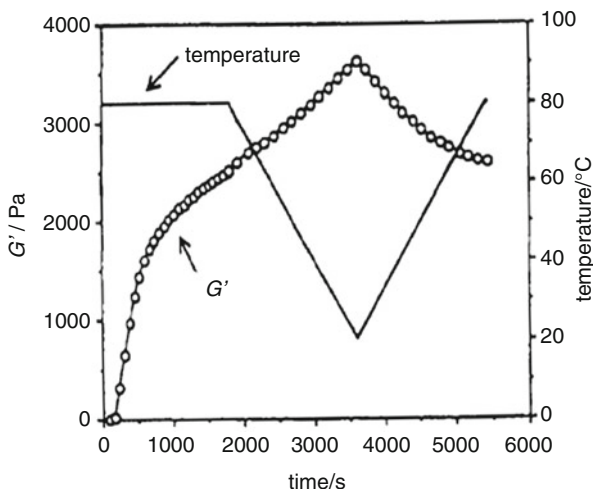
In the globular protein such as soybean  $\beta$ -conglycinin, the gelation commences only at higher temperatures than the denaturation temperature. The frequency dependence for  $G'$  and  $G''$  of  $\beta$ -conglycinin or glycinin solution begins to show a plateau at 68 °C or 80 °C, respectively (Nagano et al. 1994a; Nishinari et al. 2014).

### 5.3 Thermal Scanning Rheology

Temperature dependence of storage and loss moduli  $G'$  and  $G''$  of a solution at a constant frequency.

Figure 4.11 shows the gelation process of a 15% soybean  $\beta$ -conglycinin solution. At a constant temperature of 80 °C,  $G'$  increased, and continued to increase when the temperature was lowered from 80 °C to 20 °C at the rate of 2 °C/min.  $G'$  decreased with increasing temperature from 20 °C to 80 °C at the same rate. Values of  $G'$  are symmetrical about the vertical line at  $t = 3600$  s. The increase in  $G'$  after 1800 s when heating is stopped and the temperature is lowered is attributed to the further formation of network structure by hydrogen bonding which may be broken by subsequent heating from 20 °C to 80 °C. Although it is almost impossible to evaluate the contribution of hydrophobic interactions, hydrogen bonding, ionic interactions, and covalent bonding quantitatively because these interactions operate

**Fig. 4.11** Gelation process of 15% soybean  $\beta$ -conglycinin solution at pH 7.6. The solution was heated at 80 °C for 30 min (=1800 s), and then cooled to 20 °C at 2 °C/min, and heated again to 80 °C at the same rate. Reproduced with permission from Nagano et al. (1994b), Copyright 1994 ACS



simultaneously, Fig. 4.11 clearly shows the important contribution of hydrogen bonding to the gel formation of  $\beta$ -conglycinin.

At higher temperatures for a 2 wt% solution of sodium type gellan,  $G' < G''$  while on cooling moduli show a steep increase at ca 35 °C ( $T_{ch}$ ) which is attributed to coil-to-helix transition, which coincides with the temperature at which the molecular ellipticity shows a transition. On further cooling,  $G'$  and  $G''$  show a crossover at 8 °C ( $T_{sg}$ ) which is ascribed to sol-gel transition (Miyoshi and Nishinari 1999). This sol-gel transition was found not the formation of a true gel but a structured liquid. Strictly speaking, this procedure to determine the gelation point is not precise because the crossover point depends on the frequency of measurement in addition to scan rate.

For gelling polysaccharides, it is necessary to pay attention to the slippage which sometimes leads to a serious misinterpretation. The cooling curve of  $G'$  and  $G''$  using a normal cone and plate geometry showed a peak for both  $G'$  and  $G''$  in the cooling process of carrageenan solutions, while that using perforated cylinders which prevent the slippage, no peak of  $G'$  and  $G''$  was observed (Richardson and Goycoolea 1994). Zhang et al. (2001) also found the peak of  $G'$  and  $G''$  as a function of time for 2% dispersions of KGM at higher temperatures at  $\omega = 1\text{rad/s}$ . It is known that gelation of KGM is faster at higher temperatures. Zhang et al. (2001) measured the compressive force during gelation of KGM which is free from slippage, and then they did not observe the peak even at higher temperatures confirming that the peak of  $G'$  and  $G''$  observed was caused by the slippage.

## 6 Physical Properties of Gels

### 6.1 Effect of Gelling Rate on Gel Properties

The elastic modulus of gelatin gels increased with time at lower temperatures not reaching an equilibrium value even after 100 h (Nijenhuis 1981, 1997). The thermal stability of gelatin gels increased with increasing storage time at the temperature which is a little higher than gelation temperature (Michon et al. 1997). For agarose gels, which are other helix-forming thermoreversible gels, the effect of the storage temperature near the gelation temperature on rheological and structural properties has been studied and it was found to differ from the behavior of gelatin gels. Aymard et al. (2001) found that holding solutions of agarose for long times at high temperatures decreased the strength of the gels formed on cooling. They interpreted this by structural observation that during the holding period the un-gelled solutions resolved progressively into regions of high and low polymer concentration, and that the resulting heterogeneity gave weaker networks when the solutions were gelled by cooling. On the other hand, Mohammed et al. (1998) reported that agarose gels showed larger elastic modulus and were more thermally stabilized by cooling more slowly. Recently, it was shown that storage Young's modulus and the fracture stress and strain of gellan gels increased with decreasing cooling rate (Nitta et al. 2014).

As mentioned before, a gel may be formed before a solid film is formed when the solvent is evaporated from, for example, solutions of pullulan which is usually not called a gelling polysaccharide because it forms a gel only at higher concentrations. The evaporation speed influences the length scale of the structure being formed, but this problem has only been tackled recently (Schaefer et al. 2015) mainly in relation to spin coating. This may be called a kind of concentration quench, as temperature quench influenced the formation of gel structure.

## 6.2 *Temperature Dependence of Elasticity of Gels*

Sol-gel transition in polysaccharides can be classified into four groups: (1) cold-set gels like agarose, kappa- and iota-carrageenans, and gellans which form a gel on cooling the solution; (2) heat-set gels like some cellulose derivatives such as methyl cellulose (MC), curdlan, konjac glucomannan (KGM) which form a gel on heating the solution; (3) inverse reentrant gels like a mixed solution of methyl cellulose and gelatin, which forms a gel at higher and lower temperatures and stays a sol state at an intermediate temperature range. Gelatin may be replaced by some polysaccharides which form a gel on cooling; and (4) reentrant gels like xyloglucan from which some galactose residues are removed. It forms a gel at an intermediate specific temperature range and remains in the sol state at higher and lower temperatures outside of this specific temperature range. Some copolymer gels show a complex temperature dependence: Sol-gel transition is observed at two or three different temperatures, i.e. they show reentrant transition (Nishinari 2000a, b, 2001, 2009).

There have been many investigations and debate on the temperature dependence of the elastic modulus of gels relating with the entropic and energetic contribution. Since it was difficult to observe the elastic modulus of thermoreversible gels as a function of temperature from a low temperature, the increase in modulus with increasing temperature was not observed. It was concluded that the gel elasticity is energetic elasticity in previous studies while the opposite was also asserted. To understand this problem it is effective by dividing the elastic modulus into entropic and energetic contribution from the temperature dependence of the elastic modulus of gels of agarose with different molar masses (Nishinari et al. 1984).

*Reel-chain model* was proposed to explain the temperature dependence of thermoreversible gels (Nishinari et al. 1985). In this model, network consists of Langevin chains which allow to treat large deformation. On heating, some segments are released from junction zones consisting of aggregated helices. There should be a limit for number of segments released before gel-to-sol transition occurs. Some statistical calculations gave the elastic modulus as a function of the binding energy, upper limit number of segments released from the junction zone, average distance between junction zones. It predicts the monotonic increase of the modulus for a high binding energy as expected from rubber elasticity theory, and the monotonic decrease for a low binding energy, and an intermediate behavior showing the

maximum of the modulus as a function of temperature. This theory was applied to many thermoreversible gels to explain the temperature dependence of the modulus.

### 6.3 Molar Mass Dependence of Elastic Modulus

Since it is difficult to prepare samples with different molar masses with a narrow molar mass distribution, there have not been so many studies on the molar mass dependence of elastic modulus of gels. Saunders and Ward (1955) studied rheological properties of gelatin gels with different molar masses and showed that the elastic modulus increased with increasing molar mass up to a certain value and then leveled off whilst the breaking stress continued to increase with increasing molar mass. Similar tendency was observed for gels of alginate (Smidsrød 1974) and  $\kappa$ -carrageenan (Rochas et al. 1990). The gelation kinetics of dispersions of konjac glucomannan with different molar masses has been studied by measurements of storage shear modulus and it was shown that the storage modulus of the dispersion of the same concentration increased with increasing molar mass (Yoshimura and Nishinari 1999).

Effects of molar mass on the stress-strain curve and on the temperature dependence of the modulus of agarose gels are shown in Fig. 4.12. Both the stress and strain at break increased (Fig. 4.12a), and the entropic behavior of elastic moduli was enhanced (Fig. 4.12b) with increasing molar mass of agarose.

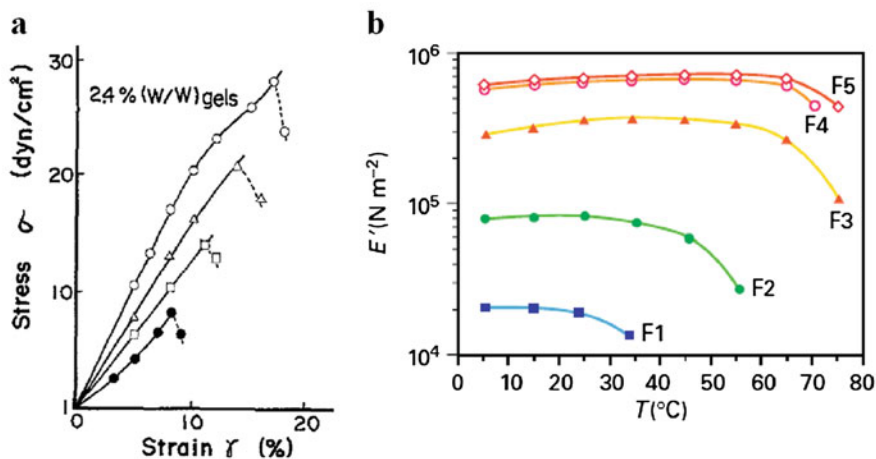


**Fig. 4.12** (a) Stress-strain relation of 2.4% (w/w) gels of agarose with different molar masses ( $\bullet < \square < \triangle < \circ$ ) at 25 °C. Reproduced with permission from Watase and Nishinari (1983), Copyright 1983 Springer. (b) Temperature dependence of storage modulus  $E'$  for five agarose fractions with  $M_w$  from  $3.4 \times 10^4 \text{ g mol}^{-1}$  (F1) to  $48.5 \times 10^4 \text{ g mol}^{-1}$  (F5) (Nishinari and Watase 1993)

Molar mass dependence of the moduli was found sometimes contradictory (Nishinari and Fang 2021). While from a figure of  $G'$  as a function of concentration in amylose gels showed a greater  $G'$  for a higher molar mass amylose (Clark et al. 1989), a similar plot for oat  $\beta$ -glucan showed a greater  $G'$  for a lower molar mass (Lazaridou et al. 2003). This apparent inconsistency is originated from the non-equilibrium nature of these physical gels. In both amylose and oat  $\beta$ -glucan, the gelation proceeded faster for lower molar mass because of the higher mobility. This slower pace of gelation is different in amylose and  $\beta$ -glucan, and therefore, great care is required to compare the molar mass dependence of the modulus. Gel formation of higher molar mass fractions is so slow that the modulus at a time not long enough is smaller than that for lower mass fractions. Gelation of gelatin is also known to take a long time as mentioned before (Nijenhuis 1981, 1997).

#### 6.4 Molecular Motion (Rearrangement) in Gels

Agarose forms a gel at a very low concentration  $< 0.1$  wt% depending on the molar mass, sulfate content (purified agarose or idealized agarose contains no sulfate groups but most commercially available agarose contains a small amount of sulfate groups). Even after gelation it is not in the equilibrium state. Syneresis, which is an exudation process of water from the network, is also observed in globular protein gels such as cheese (syneresis is necessary) and yogurt (syneresis is not preferable). This process is not so fast, and therefore gel engineers study small and large deformation rheological behavior of these gels in pseudo-equilibrium state. Agarose gels as well as other polysaccharide gels are believed to be formed by aggregated double helices connected by flexible chains. Since the concentration is low, there are free spaces where molecular motion is occurring.

A step-like decrease of  $\tan \delta$  was observed while the endothermic peak in DSC and the steep change in the specific ellipticity in CD were observed at 25 °C on heating a 1.6% gellan gel, and these changes are attributed to helix-coil transition (Nitta et al. 2001; Nishinari et al. 2001). A molecular motion or molecular rearrangement such as the helix-coil transition occurs in an apparently solid material with the elastic modulus of ca  $10^5$  Pa. This was a surprise for authors because of the appearance of a solid of the gellan gels. From the viewpoint of the solid content, most part of the gel consists of water and thus there must be much enough space where large-scale molecular motion or rearrangement can occur.

Helix-coil transition can occur in different ways. Segments can be released from junction zones on heating as was discussed in reel-chain model approach (See Sect. 6.2). On cooling, these released segments are reeled into junction zones so that junction zones become longer and/or thicker. If the elastic modulus is mainly determined by the number of elastically active chains which connect junction zones as in the theory of rubber elasticity, the increase in elastic modulus should be attributed to the increase in the number of elastically active chains rather than to the thickening or lengthening of junction zones. It is quite possible that long

segments released from junction zones form a new junction by helix formation. Helix-coil transition does not necessarily occur only at the chain ends, but it also may occur at the intermediate point of long chains.

There may be different junction zones with different thermal stabilities. Weak junction zones with low thermal stabilities may disintegrate at lower temperatures which are directly related to helix-coil transitions, and these chains produced from the disintegration of helices may form helices on cooling only at lower temperatures. The distribution of thermal stability may cause a broad endo- and exo-thermic peak in DSC heating and cooling curves as well as gradual increase and decrease of the specific ellipticity in heating and cooling CD measurements. According to a fibrous model (Morris et al. 2000), the elasticity of gels arises mainly from stretching and bending of fibers that consist of aggregated helices. When some ends of these fibers are converted into flexible chains by helix-coil transition, these ends will cease to contribute to the elasticity and then the elastic modulus will decrease. Even if one of these conformational changes occurs, it does not necessarily lead to the gel-to-sol transition. When these changes are only local, only less ordered helices are converted into coils, and the whole network structure is not broken down, and keeps the size and shape of the self-supporting gel.

## 6.5 Chain Release and Erosion of Gels

Most gel technologists using chemical gels formed by covalent bonds believe that a polymer gel consists of a three-dimensional crosslinked network and swells in a solvent to a certain finite extent, but does not dissolve even in a good solvent. It was found that some molecular chains in a gellan gel release out from the gel when it is immersed in a solvent such as water or salt solutions (Tanaka and Nishinari 2007; Hossain and Nishinari 2009). After a long time, the gel swells infinitely, and disperses completely in a great amount of water. On immersion of gels in water, cations and non-crosslinked chains diffuse out from the gel into the surrounding medium, and the gel structure is weakened. Salt diffusion from the gels into the surrounding medium is faster than chain release; chains which lose condensed or bound ions cannot retain a helical conformation, and so they then diffuse out. Analysis of the released chains revealed that the shorter chains are released predominantly. The modulus increase by immersion was observed at first, and it was suggested by stiffening of elastically active chains. Potassium ions in the external solvent were found to strengthen the gel structure of gellan, yet tetramethylammonium (TMA) ions in the external solvent, which are known to inhibit the gelation though not inhibiting helix formation, were also found to increase the modulus.

A mass loss in gellan gels prepared by calcium ions were also found, and after 28 days these gels maintained constant composition without further mass loss during the remainder of the test period between 28 and 164 days (De Silva et al. 2013). This shows the difference between monovalent cations and divalent cations as will be discussed in Sect. 6.7.

## 6.6 Syneresis/Water Holding Capacity (WHC)

Syneresis is a phenomenon in which water oozes out from the gel network, and is known from long time ago but its mechanism is not so well understood although the importance has been recognized because of its close relation with flavor release and juiciness perception. Many methods of measurements have been proposed: centrifugation, compression, wiping the surface, measuring water on the top of a test tube containing the gel, etc. As Mizrahi described (Mizrahi 2010), the syneresis may be governed by the swelling pressure which is the difference between the osmotic pressure and the network pressure  $\Pi_{sw} = \Pi_{os} - \Pi_{net}$ , where the osmotic pressure is produced by polymer chains in the gel and it drives water into the gel, thus causing the swelling and stretching of polymer network. Stretched chains tend to contract to compensate the decrease of the entropy caused by the chain stretching, thus giving rise to an internal pressure which is called a network pressure. Mizrahi (2010) suggested several methods to prevent the syneresis by increasing the osmotic pressure, controlling network pressure and crosslinking.

Miwa et al. (1994) compared the syneresis of 3–4 wt % gels of curdlan, carrageenan, agar, konjac after kept at 4 °C for 20 h, and the syneresis of both curdlan and konjac was 10.3% which was much larger than that of carrageenan (1.4%) and agar (0.6%). However, after freezing and thawing, syneresis of both curdlan and konjac increased to ca 21% while it was much more than that for carrageenan and agar because these gels became sponge-like and water ran out through larger pores. This encouraged food industry to use curdlan and konjac in frozen foods such as surimi to improve the texture. Syneresis of agar gels was reported to decrease with increasing agar concentration/added sucrose/sulfate residue. It should be reminded that the order of the addition of sucrose to make polysaccharide gels, before or after gelation, changes the structure/mechanical properties and syneresis. For example, the addition of a higher sucrose content (>55 wt%) in 1 wt% agar gelation before heating was found to make the gel inhomogeneous and led to a weaker gel with more syneresis (Yang et al. 2015). It was found that the elastic modulus decreased after syneresis although the concentration was increased by syneresis, and it was attributed to the loosening of the network structure caused by syneresis (Nagasaka and Taneya 2000; Nishinari and Fang 2016, 2017). It was also shown that syneresis was reduced by adding sucrose or starch to curdlan though it also reduced the gel strength. While this practical manipulation may be sometimes useful, the basic understanding of syneresis in polysaccharide gels is not yet reached (Ako 2017; Divoux et al. 2015).

Syneresis in globular protein gels may be understood in the first approximation by permeability  $B$  which is proportional to the area and the fraction of pores in a cross section of the gel (Walstra 2003). Walstra explains the great difference in the syneresis in ground coffee ( $B \sim 10^{-8} \text{ m}^2$ ), rennet milk gel ( $B \sim 10^{-12} \text{ m}^2$ ), and polysaccharide gel ( $B \sim 10^{-17} \text{ m}^2$ ) by the approximate value of the permeability. The difference of  $B$  values roughly explains that some polysaccharide gels retain water while globular protein gels show a much more syneresis. While syneresis is undesirable in most gels, it is an essential process in cheese making, where most of the liquid (whey) in the rennet gel has to be removed (Walstra 2003). In these protein



gels, rearrangements of strands consisting of globular protein aggregates lead to loose ends which in turn form junctions thus becoming more compact expelling liquids. When junctions are broken, a pressure is built up, which is called “endogenous syneresis pressure,” that is causing syneresis even without external pressure such as gravity. However, the experimental determination of the endogenous syneresis pressure seems to be difficult, and thus the complete understanding of the syneresis of protein gels is still a challenge.

Nieuwland et al. (2016) found a good correlation between the structure, mechanical properties, and WHC for ovalbumin (OVA) gels at a pH range from 5.8 to 6.8: the microstructure of OVA gels became less dense based on SEM and CLSM, and the Young’s modulus decreased, in parallel with the decrease in WHC with decreasing pH.

Urbonaite et al. (2016) prepared 14 w/w% WPI gels at pH 7.2 with different pore sizes ranging from  $10^{-2}$  to  $10^0$   $\mu\text{m}$  by changing NaCl content from 0 to 300 mM to examine the effect of coarseness (pore size) and the mechanical properties, Young’s modulus on WHC. They found that, depending on the lower or higher than 100 mM NaCl, fine stranded gels (length scale  $<0.1\mu\text{m}$ ) or coarse stranded gels ( $>0.1\mu\text{m}$ ) were formed. They found the Young’s modulus showed the maximum at 100 mM NaCl, while the WHC decreased with increasing concentration of added NaCl, and concluded that coarseness was more dominant than stiffness (Young’s modulus) for water holding.

Dai et al. (2016) examined the effects of the addition of 0.5% KGM on the physicochemical properties of yogurt, and found that the syneresis was decreased while retaining the structural stability and the firmness of full-fat yogurt. They found the suppression of syneresis was equivalent to previous reports in which inulin or orange fiber was added to skimmed yogurt and noticed that total solid content was also responsible for the reduction of syneresis.

To improve the texture and water holding capacity of myofibrillar protein gels, dietary fibers are widely used. Effects of the addition of insoluble fibers (microcrystalline cellulose, oat fiber, walnut shell flour) and native and modified starches (potato, tapioca) on liquid loss, hardness and resilience (recoverable deformation) of chicken breast myofibrillar proteins were measured (Gravelle et al. 2017). Since fat and connective tissues were removed, the samples were myofibrillar protein gels, and liquid loss was mainly from water. Among the fillers tested, native potato starch was most effective to reduce the liquid loss, which was attributed to the difference in hydration estimated by  $T_2$  relaxation time of water.

### ***6.7 Effect of Sugars, Salt, Acid, and Polyphenols on Rheological Behavior of Gels***

It has been empirically known that the addition of sucrose to polysaccharide gels make them transparent, less brittle and reduce the syneresis. The Young’s modulus,

fracture stress, and melting enthalpy increased and then decreased with increasing sucrose or glucose in agarose or  $\kappa$ -carrageenan gels (Nishinari and Fang 2016). The different strengthening effect of sugars has been correlated with a number of equatorial hydroxyl residues in sugars. Kawai et al. (2007, 2008) extended the reel-chain model in which flexible chains are released from junction zones constituting aggregated helices to explain the observed strain hardening and then softening in uniaxial compression. As the end-to-end distance increases due to the deformation, more and more segments are reeled out from the junction zone. Finally, one end of the chain is liberated from the junction and the chain becomes dangling. The appearance of dangling chains causes the strain softening because they cease to contribute to the elasticity.

Drying of gels has been studied from various viewpoints, and recently the effect of sugars on drying kinetics of agarose gels was studied (Mao et al. 2017).

Epigallocatechin gallate (EGCG), a polyphenol abundant in tea leaves was found to induce gelation of non-gelling xyloglucan (Nitta et al. 2004). Yan et al. (2016) further reported that other gallate analogs also induce gelation of xyloglucan.

Generally, salt does not influence so much the gelation of neutral polysaccharides such as agarose but sometimes enhances the gelation of KGM or xyloglucan. Effects of salts on gelation of charged polysaccharides have been extensively studied. While the monovalent cations shield the electrostatic repulsion of carboxyl groups in gellan, divalent cations bind different molecular chains of gellan, and therefore once the gel is formed it does not return to the sol state on heating up to 90 °C (Miyoshi et al. 1994; Djabourov et al. 2013).

## 7 Particulate Disordered Structure: Globular Protein Gels

When globular proteins are denatured by heating, high pressure or denaturants such as urea or guanidine hydrochloride, hydrophobic portion folded and buried inside were exposed outside, which is called unfolding, and then unfolded polypeptide chains form a three-dimensional network (Doi 1993). In comparison with network structure formed from long chain molecules which are predominantly entropic and have been successfully elucidated to some extent by developing rubber elasticity theory, particulate disordered gels are less well understood. Rheology and structure of rennet-induced or acid-induced casein or whey protein gels (Nicolai et al. 2011), ovalbumin gels (Nemoto 2000; Nieuwland et al. 2016) as well as soybean proteins (Nishinari et al. 2014), and other plant proteins have been extensively studied.

A great difference from thermoreversible polysaccharide gels such as agarose, kappa-carrageenan, gellan is that the minimum concentration required is much higher for globular protein gels, but recently, gelation of fibrils made from globular protein changed this common knowledge. This was described in “4.7 Rigid network chains.” Most polysaccharide gels except cellulose derivatives such as methyl cellulose form a gel by hydrogen bonds and thus form a gel on cooling while globular protein gels are formed on heating and it is thought that the denaturation

of the native protein structure is prerequisite for gel formation. The main force responsible for gelation is thought to be hydrophobic interaction, but other secondary forces are also contributing.

Dutch school employed a fractal model and measured the permeability and rheology to correlate the structure and property of milk protein gels. Bremer et al. (1989) concluded that acid casein gels can be described very well by a fractal model with a fractal dimension 2.3, while it was not applicable for rennet-induced casein gels because of microsineresis. The modulus decreased with increasing temperature which contradicts some earlier publications affirming that the casein gels are entropic like rubber elasticity (van Vliet and Walstra 1985). The increase of the aging temperature to 50 °C and extending the aging time to 157 h changed the gel to a more solid like material; the storage modulus tends to show a rubber like plateau and the loss tangent decreased. Storage modulus  $G'$  as a function of measuring temperature  $T_m$  for acid sodium caseinate gels aged at different temperatures increased with increasing aging temperature, but decreased with the temperature of measurement (Roefs and van Vliet 1990). It is generally accepted that in casein gels, an ultimate effect of structural rearrangement is syneresis: expulsion of liquid. Syneresis is desired for manufacturing of cheese but not for yogurt.

Doi (1993) classified the gelation of globular protein into random aggregates and string beads network. His group studied the gelation of ovalbumin (OVA) by rheology, dynamic light scattering (DLS), CD, TEM, SEM, CLSM based on the conformational studies reporting that OVA molecules are worm-like chains, linear aggregates, with cylindrical diameter 12 nm and the persistence length 23 nm (Doi et al. 1987; Nemoto 2000). As a result of heat denaturation, hydrophobic regions are exposed on the surface, and linear polymer or aggregate is formed depending on the balance of hydrophobic interaction and electrostatic repulsion (Fig. 4.13).

They found that the heat induced gelation of 39–59% OVA solution showed a critical structure obeying the Winter-Chambon criteria (Koike et al. 1996), and found a very low exponent 0.09–0.14. Gels formed with concentrations lower than 25% and higher than 59% did not show critical structure. The exponent of concentration dependence was found to change from 4 below 59% to 10 above the concentration range from 59% to 89%, where the modulus an order of  $10^9$  Pa close to the glass modulus was found. This is totally different from common concentration dependence of modulus for polysaccharide gels where the exponent is ca 4 at lower concentration range, but ca 2 at a higher concentration range as described in “4.6 Critical molar mass and concentration for gelation.”

A two-step heating was employed in addition to one-step heating; the OVA solution was first heated without NaCl for 60 min, and quickly quenched to room temperature where linear aggregates molar mass higher than several millions were formed. After addition of NaCl (20, 60, and 100 mM) to the viscous solutions, they were reheated for various time periods from 2 to 240 min and then immediately cooled (Koike et al. 1998). Transparent gels were obtained by both the one-step and the two-step heating. Doi (1993) described methods to obtain transparent egg white or milk whey protein gels controlling the pH and ionic strength by two-step heating.

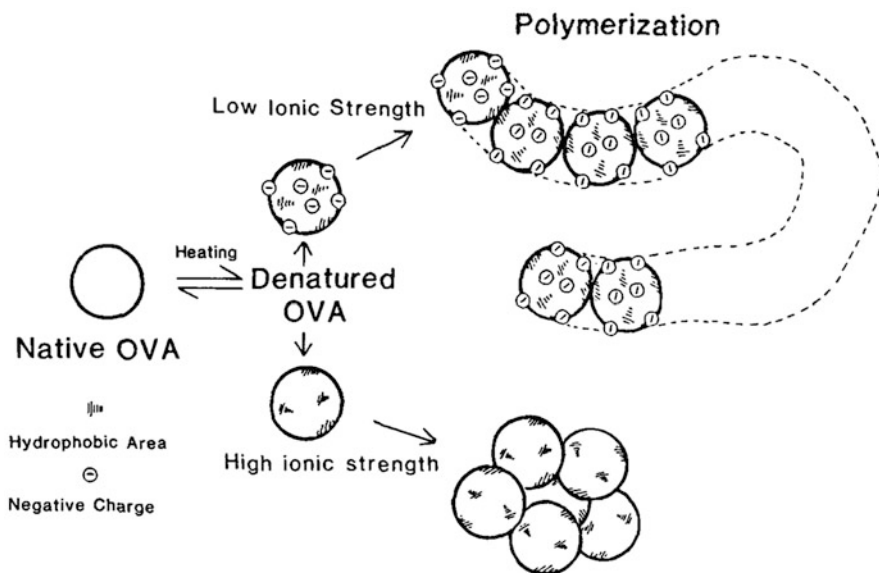


**Fig. 4.13** Schematic representation of the heat denaturation of OVA, leading to the formation of linear polymer or aggregate (Doi et al. 1987). Reproduced with permission from Doi et al. (1987), Copyright 1987 John Wiley & Sons

More recently, gelling behavior of OVA and p-OVA (formed by a limited hydrolysis with pepsin) was analyzed based on SANS (small angle neutron scattering) in addition to DLS (Hiroi et al. 2016). In spite of the similarity of physico-chemical properties, intrinsic viscosity, secondary structure, denaturation temperature, OVA and p-OVA showed significantly different gelling behaviors on heating. Heating 6 wt% solutions at neutral pH without salt led to a transparent gel for OVA while a turbid gel was formed for p-OVA. On heating OVA solution, the resulted aggregate size was found proportional to the protein concentration judging from the independence of the peak position in the SANS intensity as a function of scattering angle. On the contrary, an increase in the amount of large clusters formed on heating was thought to disturb the correlation of p-OVA dimers resulting in wide distribution of the distance between each solute and thus a two-phase separated structure was formed. The fact that the cleavage of only 22 N-terminal residues from OVA led to a very different gelling behavior is expected to be a hint to develop further utilization of OVA.

Globular protein solutions show a “solid-like” mechanical spectra (shown in Chap. 3) even before gelation probably because they form a colloidal crystalline structure (Matsumoto and Inoue 1993; Ikeda and Nishinari 2001a, b, c). Tobitani and Ross-Murphy (1997) made a temperature-concentration diagram constructed by the gelation temperature for each concentration of globular protein which is determined

by interpolation and extrapolation of the data set, a locus of nominally infinite gelation time.

## 8 Mixed Gels

Just as in alloys of metals and plastics, many mixed gels have been prepared to respond to the demand of various functionalities (Morris 1986). Many papers have been published on the mixed gels of xanthan, locust bean gum, konjac mannan, etc., and some common features are recognized for synergistic interaction, which means that the only one polysaccharide does not form a gel at that concentration, but forms a gel by mixing with other polysaccharide. 1) One polysaccharide undergoes coil-helix conformational transition, such as agarose, carrageenan, furcellaran, gellan, and xanthan gum. 2) The backbone linkage of the other polysaccharide in the mixture is  $\beta(1,4)$  linkage, such as in konjac glucomannan or galactomannan, or xyloglucan (Morris 1994).

Polysaccharide mixture gels have been extensively studied, and Unilever model and Norwich model have been proposed and examined. Gels of the mixture of xanthan and galactomannan or konjac glucomannan have been studied, and it was proposed that helical xanthan associates with the smooth region of galactomannan devoid of galactose side chains (Unilever model, Dea et al. 1977) while Norwich model proposed that the mixed gel was formed between coiled xanthan and galactomannan or KGM because gels were formed only after the helical xanthan was denatured into coil state (Brownsey et al. 1988). The latter statement was affirmed by adding helix enhancing cations to raise the helix-coil transition and in such a condition the mixture did not form a gel on cooling. However, the gelation in the mixture of pyruvate free xanthan (PFX) and KGM was observed to start about 40 °C more than 60 °C lower than coil-to-helix transition temperature of xanthan at acidic pH (3.5 and 4) higher than 100 °C, and that the synergistic gelation of KGM with PFX and commercial xanthan was not so different. Thus, the above-mentioned prerequisite of Norwich group for the gel formation of the mixture, the conformation of xanthan should be in coil state, was refuted (Agoub et al. 2007).

The effect of salt is important to study the mixtures. Annable et al. (1994) studied the mixture of xanthan and KGM in the presence of different salts using dynamic viscoelasticity, DSC, and ESR. They showed that the gelation temperature shifted to lower temperatures when electrolyte is present, with divalent cations having a greater effect than monovalent cations. These observations are explained by the fact that electrolyte promotes xanthan self-association at the expense of xanthan/KGM interaction, and thus the temperature for gelation on cooling shifted to lower temperatures with increasing xanthan self-association. The effect of salt follows the Hofmeister series. The strength of the cationic effect was as follows:  $K^+ \sim Cs^+ < Na^+ \sim NH_4^{4+} \sim Ba^{2+} < Mg^{2+} \sim Ca^{2+}$  (Annable et al. 1994).

Recently, Takemasa and Nishinari (2016) found the nuclear Overhauser effect (NOE) between low molar mass galactomannan and xanthan, which is a direct

evidence for the synergistic interaction because NOE is seen only for nuclei closer than about 0.5 nm.

Although synergistic interaction leading to an industrially interesting phenomenon such as enhancement of thickening and gelling ability has been attracting great interest, the most common phenomenon occurring in the mixing of different biopolymers is phase separation. Fang et al. (2006) constructed a state diagram of gelatin/ $\kappa$ -carrageenan aqueous mixtures based on turbidity measurement, confocal scanning laser microscopy (CSLM), DSC, and zeta potential measurements. They found a coexistence of associative and segregative (associative-*co*-segregative) phase separations at low temperature and low NaCl concentration in addition to compatible, associative, and segregative phase separation behaviors. A coexistence of associative and segregative phase separations was observed and it was attributed to a kinetically trapped state by gelation.

The effect of the addition of insoluble fibers and starches (discussed in Sect. 6.6 Syneresis) on mechanical properties of myofibrillar protein gels (Gravelle et al. 2017) is discussed here. When the addition of fiber was low (mass fraction  $m_f$  of filler  $<0.1$ – $0.15$ ), the hardness increased with increasing  $m_f$ . While the resilience, estimated from the immediately recovered deformation, was decreased with increasing  $m_f$  in myofibrillar protein gels with insoluble fibers, that of starch-filled protein gels was almost independent of  $m_f$ . This was interpreted that swelling of starch granules made the filler more flexible and diminished the stress concentration at the interface. The stress concentration  $S_c$  as a function of  $m_f$  estimated for completely bonded interface was shown to decrease, and thus the relative strength  $R_s$  which is an inverse of the stress concentration,  $R_s = 1/S_c$ , increased with increasing  $m_f$  (Gao and Lelievre 1994).

The fundamental problems and many examples of mixed gels are discussed in Chap. 10 of Djabourov et al. (2013) Cao et al. (2016a, b) and in Nicolai (2019).

## 9 Fracture of Food Gels

Fracture of gels can be divided into brittle fracture and ductile fracture. Fracture occurs at the structural defects. To avoid the uncertain distribution of structural defects, the fracture test is sometimes done for notched samples (van Vliet and Walstra 1995). While Young's modulus obtained at the small deformation is not so influenced by the depth of the notch  $l$ , the fracture stress decreased with increasing  $l$ .

In the extension test, the gel tends to fracture at the clamps or slips if the gel is not clamped tightly or too loosely, therefore it is not easy to obtain reproducible results. A memorable record in food gels was reported by van Kleef (1986) who could use 224 experiments which were successfully performed free from slippage or fracture of the gels at the clamps among more than several hundreds of experiments for OVA gels. He got the relation between the fracture stress and the protein concentration  $C$ :  $\sigma_b = 102C^{2.6}$  for the pH 10 gels and  $\sigma_b = 5.89C^{3.2}$  for the pH 5 gels.

Fragment size distribution of masticated fish sausages was analyzed, and it was found that the distribution was fitted well by combination of the lognormal

distribution with exponential tail indicating that the fragmentation process has a size-segregation-structure between large and small parts. For large fragments population, incorporation of exponential distribution  $N(s) = Ae^{-s/B}$  in addition to lognormal distribution was effective. In the mastication, the segregation of fragments into larger and smaller fragments occurs, but the number of large fragments decreases with the progress of mastication and the value of B decreases with the increasing number of mastication (Kobayashi et al. 2010). Recently, the fragmentation process in the mastication was studied using agarose gels with different sizes and with different molar masses. The effects of gel size and molar mass were recognized in the early stage of mastication. The average particle size showed a high correlation with the hardness (Moritaka et al. 2019).

Soft gels are known to be crushed between the tongue and the hard palate (Nishinari et al. 2020). Many such food gels have recently been produced for disadvantaged persons. Ishihara et al. (2013, 2014) studied the compression of agar gels and gellan gels using an artificial tongue made from silicone gel, and the transition from the tongue only breaking to chewing by teeth was found to be predicted from the instrumental uniaxial compression.

## 10 Microgels (Fluid Gels)

Microgels can be produced by shearing the gelling polymer solutions undergoing sol-gel transitions (Norton et al. 1999) or other method using emulsion in which gelling polysaccharides are dispersed. These microgels have been used as texture modifiers, stabilizers and especially for reduced fat foods. With a finite yield stress, microgels behave as a solid at rest but flow when subjected to a stress above the yield stress. In addition to many kind of polysaccharides from agar (Farres and Norton 2015), carrageenan (Garrec et al. 2013), and other origins, whey protein isolate (Moakes et al. 2015) was also used to make microgels.

Microgels of alginates were studied to encapsulate probiotics such as lactobacillus which are labile in severe gastrointestinal environments. In comparison with external gelation where alginate solution is dripping into calcium chloride solution, internal gelation of alginate is performed in alginate emulsion containing insoluble calcium carbonate particles by slowly lowering pH using GDL, which can produce small alginate beads ca 1 $\mu$ m or even smaller than 200 nm (Paques et al. 2013). Smaller gel beads are advantageous because larger particles than 25 $\mu$ m (this value depends on the shape of particles, hard and irregular particles are perceived as gritty than soft and round particles of similar size; Engelen et al. 2005) are detected on the palate, and thus can extend the application. Cai et al. (2014) compared alginate beads prepared using calcium carbonate and calcium disodium ethylenediamine-tetraacetate and found that encapsulation using the former protected *L. acidophilus* more effectively in the survival test, which was related to the mechanical strength of the microcapsules.

Protein microgels can be also produced by ultrasonication of heated  $\beta$ -Ig at low pH (Murphy et al. 2017, 2018). Produced microgels of  $\beta$ -Ig with a diameter ca



230 nm were shown to be stable without coalescence over 6 weeks storage; however, emulsions containing limonen stabilized by the microgels were susceptible to creaming, flocculation, and limonen was lost during storage, which remain as future problems.

## 11 Cryogels

A cryogel is formed by the cryogenic treatment, freezing–frozen storage–thawing of the precursor system. Scientific research became active since the discovery of cryogels of poly(vinyl alcohol) (Lozinsky and Okay 2014). According to this definition, traditional Japanese foods such as *koori-tofu* (dried tofu after freezing), *bo kanten* (agar-stick, resulting from freezing–thawing) are cryogels but since they are xerogels and are eaten after absorbing solvent (water) by cooking, the characteristics of these xerogels are quite different from those of swollen food gels. Most gels lose their elastic characteristics once they are frozen and thawed. Most of them lose their solvents and only dried framework remains like agar-stick and *koori-tofu*. Cryogels keeping the rubber-like texture and water even after freeze–thaw cycles have been studied extensively including PVA and hyaluronan (Djabourov et al. 2013; Zhang et al. 2013). Other cryogels of amylopectin, gelatin, maltodextrin, potato starch, oat  $\beta$ -glucan have also been studied, but most of them are sponge-like cryogels (Lozinsky and Okay 2014). LBG solution was found to form a gel after the repeating cycles of freezing and thawing (Tanaka et al. 1998). It was found that LBG does gel from solutions containing in excess of 1% solids at room temperature on a time-scale of several months. The gelation mechanism of LBG in concentrated sucrose solutions was shown to be governed by frustrated crystallization process with nucleation and growth stages rather than reversible pairwise crosslinking and the gelation rate became maximum at  $-5\text{ }^{\circ}\text{C}$  (Richardson and Norton 1998). This experimental finding may give a clue to explain the well-known fact that LBG forms a gel via a freeze–thaw cycle.

Giannouli and Morris (2003) reported that ca. 0.5% xanthan solution forms a cryogel when subjected to a freeze–thaw cycle. As has been known, xanthan solution is a structured liquid and can suspend solid particles. This network is known to be strengthened by calcium ions. Giannouli and Morris reported that the cryogelation was abolished by adding sucrose higher than 30% and also by adding 0.4 mM calcium ions. The inhibiting role of sucrose was attributed to the freezing point depression, and thus ice crystallization was inhibited leading to the insufficient alignment and association of xanthan chains. The weakening of cryogelation of xanthan by calcium ions was suggested that the strengthening the structure of xanthan by calcium restricts the alignment during freezing, thus hampering the cryogel formation.

Doyle et al. (2006) studied the effect of sugars (sucrose, glucose and fructose) and sorbitol on the cryogelation of galactomannans. They prepared galactomannans with different M/G ratios from 2.65 to 4.16 by enzymatic modification of guar gum



( $M/G \sim 1.6$ ), and in addition they used LBG with much higher molar mass. They found that Young's modulus determined from the initial slope of the compression curve, the stress at break, increased up to ca 50% sugar and then decreased with increasing concentration of sugars. On the other hand, the strain at break was found to decrease monotonically with increasing sugar concentration. In addition, they found that Young's modulus, stress at break as a function of  $M/G$  increased steeply around  $M/G = 4$ , and the chain length did not affect so much for these behaviors. They raise again the freezing point depression as one of the reasons. Since the concentration of sugars used in this study was 40–60% and was lower to make the system glassy state where conformational ordering of polysaccharide chains was inhibited. Then, the inhibition of polymer–polymer association by binding of sugar molecules to polysaccharide chains was thought to be the main reason for the decrease in Young's modulus, and stress at break after reaching the maximum.

It was found that cereal  $\beta$ -glucans from oat, barley, and wheat (molar mass ca.  $200 \times 10^3$ ) form cryogels, and both elastic modulus and the fracture stress increased with increasing freeze–thaw cycles (Lazaridou and Biliaderis 2004). They further examined the effects of sugars and polyols (fructose, glucose, sorbitol, sucrose, and xylose) on rheological and thermal properties of cryogels of barley  $\beta$ -glucans (Lazaridou et al. 2008). While both  $G'$  and  $G''$  decreased by adding fructose, glucose, sucrose, and xylose, both modulus increased by adding sorbitol. On heating,  $G'$  of cryogels slightly decreased up to 50–60 °C, then decreased steeply indicating the melting. The melting temperature shifted to lower temperatures except cryogels with sorbitol. Heating DSC curves also showed the endothermic peak accompanying the melting, and the melting peak temperature shifted to lower temperatures in the presence of polyols. However, the endothermic enthalpy was increased by the addition of polyols. They interpreted these experimental results by the freezing point depression of the  $\beta$ -glucan solutions by adding of sugars that may decrease the ice crystallization leading to the weaker structural formation of cryogels. They attributed the difference between rheological behavior and thermal behavior to the difference in the global structure and local structure.

Though some trial cryogel production of food hydrocolloids such as hydroxyethyl cellulose irradiated with UV-visible light at room temperature and in the frozen state or chitosan cryogels formed in moderately frozen aqueous solutions using glutaraldehyde as a crosslinker (Okay 2014), they are not still acceptable in food use. It is expected that other polysaccharide or protein cryogels are developed.

## 12 Oleogels

Since the findings of adverse effect of trans fatty acids on blood lipids and coronary heart disease risk in the early 1990s, food industry tries to find a better way to modify the texture-property of oil/fat products without using a large amount of crystalline triacylglycerol molecules which are rich in saturated and or trans fatty acids. Solid fat foods such as butter and margarine keep a shape but are spreadable when

subjected to shear stress higher than their yield stress. One of the most important differences between polysaccharide and protein gels and solid fat is that the linear elastic range is very narrow in the latter in comparison with the former because of the crystalline nature in the latter. The most widely employed method of producing oleogels is dispersing a gelator into liquid oil. The well-known gelators include waxes such as rice bran waxes, beeswax, shellac, and ethylcellulose (Singh et al. 2017; Patel and Dewettinck 2016). All the edible oleogels reported show a structured liquid behavior as described earlier, that is, both  $G'$  and  $G''$  are almost independent of frequency and  $G' > G''$ ,  $\tan \delta > 0.1$  (de Vries et al. 2017; Moschakis et al. 2016; Zetzl et al. 2014; Patel et al. 2013).

The finding that the slowly formed gels have a stronger structure is widely observed for polymer gels but the different behavior is reported for **oleogels** made by dispersing gelator in edible oil. Oleogels of shellac, a natural resin secreted by lac insect, were prepared in the following way: the dispersion of shellac in the rapeseed oil was heated above melting temperature of shellac ( $>85$  °C), and then cooled to room temperature resulting in oleogels. The onset of nucleation and crystal formation was delayed on slower cooling resulting in larger and less dense crystals. The storage modulus was found to decrease with lowering the cooling rate (Patel et al. 2013). This was explained by the increase in total effective area for smaller crystals which leads to the stronger network formation due to the higher crystal–crystal interactions.

### 13 Applications of Gelling Agents in Food Industry

*Nata de coco*, a kind of bacterial cellulose produced from coconut water, has been a favorite dessert jelly, and boomed in the 1990s especially in Japan, and still continued to be consumed all over the world, may be because of its health benefits, lowering cholesterol, and effective for diabetes and obesity in addition to its peculiar textural characteristics (Fontana et al. 2017). It has an anisotropic fibrous texture and thus expected to be a suitable matrix as vegetarian “meat,” since it can have various colors and meat-like flavors (Fontana et al. 2017). The addition of small amount of bacterial cellulose increased the gel strength of tofu and *kamaboko* and thus improved the sensory evaluation (Okiyama et al. 1992, 1993; Shi et al. 2014).

In the preparation of mixed gels of  $\kappa$ -carrageenan, KGM, and LBG, the small deformation rheology was governed by  $\kappa$ -carrageenan, and Young’s modulus decreased with decreasing  $\kappa$ -carrageenan concentration. The large deformation behavior examined by gel ring extension test, however, was dominated by KGM, and the rupture strain increased with increasing KGM concentration (Brenner et al. 2013). These two opposing trends led to a maximum in rupture stress. It should be noted that only  $\kappa$ -carrageenan has a gelling ability in this combination at neutral or lower pH, and KGM gels only at higher pH. This result may be generalized to design texture of food gels consisting of a deformable component and a brittle component.

The instantaneous gelation ability of alginate is applied to make an imitation *ikura* (salmon roe). A drop of salad oil is introduced into a sol of carrageenan or

xanthan which does not form a gel. This sol is wrapped by a film of alginate or pectin. The appearance resembles a natural salmon roe so even a fisherman cannot distinguish between them (Ueda 1985; Kishi 1977). This is quite often used for *sushi* and some other snacks. This became a popular demonstration in open campus event in universities.

Fish paste gels (*surimi* or *kamaboko*) show rubber-like behavior and frequently added starch plays a role of filler reducing the entropic nature of elasticity (Nishinari 1988). Many trials to improve the texture of *surimi* or meat products have been done by adding cellulose, KGM, curdlan, and other polysaccharides (Kaur and Sharma 2019; Zhuang et al. 2020). Anisotropy is an important factor controlling the fibrous texture, and has been successfully introduced in softened meat and string cheese (Nishinari 2020). A Japanese invention, crab stick (*kani-kama*) is consumed internationally, and the fibrousness is conferred by making the structure anisotropic sometimes adding alginates or other polysaccharides.

Frozen tofu containing curdlan keeps the smooth texture after thawing (Nakao et al. 1994) whilst when usual tofu is frozen, the texture becomes rough, which has been used as *koori-tofu* in Japanese and Chinese dishes.

Agar has been used widely in Japanese cuisine, and higher molar mass agar ( $M_w \sim 5 \cdot 10^5$ ) is used for *tokoroten* (noodle-shaped agar gel served with vinegar and soy sauce or brown sugar syrup), while medium molar mass agar ( $M_w \sim 3 \cdot 10^5$ ) is used for sweets and yogurt, and lower molar mass agar ( $M_w < 10^5$ ) gels with low gel strength break down into microgels by a weak force, and thus suitable for mixing with honey to make it less sticky and easy to spread on toasted bread (Nishinari and Shiba 2007). Strictly speaking, agar is not a molecule but a mixture of agarose and agaropectin, and thus the molar mass is a kind of the average. This concept of the average molar mass has also been used for alginate, starch, and other biopolymers.

Melt-in-the-mouth sensation of foods are liked in chocolate, ice cream and jellies. This means that most humans like the sensation or feeling when chocolate, ice cream and jellies are melted. Fish gelatin exploitation was pursued by many hydrocolloids research groups to overcome the BSE issue or religious issues. Xanthan cryogel (0.5%) (Giannouli and Morris 2003) and mixed gels of xanthan and KGM at acidic pH (3.5 and 4) (Agoub et al. 2007) were found to melt in the mouth temperature range, which might be useful for fruit jellies.

Aerogels have attracted much attention because of the light mouth feel and low calorie. Marshmallow, soufflé, and *hanpen* are typical examples and have been enjoyed before a short note with colloids science view appeared in *Nature* (Kistler 1931). Endeavor to develop aerogels more systematically to apply them in delivery carrier of active compounds using starch-based aerogels containing agar or microcrystalline cellulose (Dogenski et al. 2020) or in food packaging as absorber matrix (da Silva et al. 2020) is in progress.

Gelling polysaccharides agar, alginate, KGM, curdlan, carrageenan, gellan, pectin, starch are used in controlling the texture, water holding capacity of meat and fish products, and are also used to make dessert jellies (Nussinovitch and Hirashima 2014; Nishinari 2020).

## References

- Adamcik J, Jung JM, Flakowski J, De Los RP, Dietler G, Mezzenga R (2010) Understanding amyloid aggregation by statistical analysis of atomic force microscopy images. *Nat Nanotechnol* 5:423–428. <https://doi.org/10.1038/nnano.2010.59>
- Agoub AA, Smith AM, Giannouli P, Richardson RK, Morris ER (2007) “Melt-in-the-mouth” gels from mixtures of xanthan and konjac glucomannan under acidic conditions: a rheological and calorimetric study of the mechanism of synergistic gelation. *Carbohydr Polym* 69:713–724. <https://doi.org/10.1016/j.carbpol.2007.02.014>
- Ako K (2017) Yield study with the release property of polysaccharide-based physical hydrogels. *Int J Biol Macromol* 101:660–667. <https://doi.org/10.1016/j.ijbiomac.2017.03.145>
- Annable P, Williams PA, Nishinari K (1994) Interaction in xanthan-glucomannan mixtures and the influence of electrolyte. *Macromolecules* 27:4204–4211. <https://doi.org/10.1021/ma00093a023>
- Arvidson SA, Lott JR, McAllister JW, Zhang J, Bates FS, Lodge TP, Sammler RL, Li Y, Brackhagen M (2013) Interplay of phase separation and thermoreversible gelation in aqueous methylcellulose solutions. *Macromolecules* 46:300–309. <https://doi.org/10.1021/ma3019359>
- Aymard P, Martin DR, Plucknett K, Foster TJ, Clark AH, Norton IT (2001) Influence of thermal history on the structural and mechanical properties of agarose gels. *Biopolymers* 59:131–144. [https://doi.org/10.1002/1097-0282\(200109\)59:3<131::AID-BIP1013>3.0.CO;2-8](https://doi.org/10.1002/1097-0282(200109)59:3<131::AID-BIP1013>3.0.CO;2-8)
- Bateman L, Ye A, Singh H (2010) In vitro digestion of  $\beta$ -lactoglobulin fibrils formed by heat treatment at low pH. *J Agric Food Chem* 58:9800–9808. <https://doi.org/10.1021/jf101722t>
- Bolisetty S, Harnau L, Jung JM, Mezzenga R (2012) Gelation, phase behavior, and dynamics of  $\beta$ -lactoglobulin amyloid fibrils at varying concentrations and ionic strengths. *Biomacromolecules* 13:3241–3252. <https://doi.org/10.1021/bm301005w>
- Bremer LGB, van Vliet W, Walstra (1989) Theoretical and experimental study of the fractal nature of the structure of casein gels. *J Chem Soc Faraday Trans 1 Phys Chem Condensed Phases* 85:3359–3372. <https://doi.org/10.1039/F19898503359>
- Brenner T, Achayuthakan P, Nishinari K (2013) Linear and nonlinear rheology of mixed polysaccharide gels. Pt. I. Young’s modulus, ring extension and uniaxial compression tests. *J Texture Stud* 44:66–74. <https://doi.org/10.1111/j.1745-4603.2012.00366.x>
- Brown E, Jaeger HM (2014) Shear thickening in concentrated suspensions: phenomenology, mechanisms and relations to jamming. *Rep Prog Phys* 77:046602. <https://doi.org/10.1088/0034-4885/77/4/046602>
- Brownsey G, Cairns P, Miles MJ, Morris VJ (1988) Evidence for intermolecular binding between xanthan and the glucomannan konjac mannan. *Carbohydr Res* 176:329–334. [https://doi.org/10.1016/0008-6215\(88\)80146-0](https://doi.org/10.1016/0008-6215(88)80146-0)
- Cai S, Zhao M, Fang Y, Nishinari K, Phillips GO, Jiang F et al (2014) Microencapsulation of lactobacillus acidophilus CGMCC1.2686 via emulsification/internal gelation of alginate using Ca-EDTA and CaCO<sub>3</sub> as calcium sources. *Food Hydrocoll* 39:295–300. <https://doi.org/10.1016/j.foodhyd.2014.01.021>
- Cao Y, Fang Y, Nishinari K, Phillips GO (2016a) Effects of conformational ordering on protein/polyelectrolyte electrostatic Complexation: ionic binding and chain stiffening. *Sci Rep* 6:23739. <https://doi.org/10.1038/srep23739>
- Cao Y, Li S, Fang Y, Nishinari K, Phillips GO (2016b) Conformational transition of polyelectrolyte as influenced by electrostatic complexation with protein. *Biomacromolecules* 17:3949–3956. <https://doi.org/10.1021/acs.biomac.6b01335>
- Cao Y, Bolisetty S, Adamcik J, Mezzenga R (2018) Elasticity in physically cross-linked amyloid fibril networks. *Phys Rev Lett* 120:158103. <https://doi.org/10.1103/PhysRevLett.120.158103>
- Chen LY, Remondetto GE, Subirade M (2006) Food protein-based materials as nutraceutical delivery systems. *Trends Food Sci Technol* 17:272–283. <https://doi.org/10.1016/j.tifs.2005.12.011>

- Clark AH, Gidley MJ, Richardson RK, Ross-Murphy SB (1989) Rheological studies of aqueous amylose gels: the effect of chain length and concentration on gel modulus. *Macromolecules* 22:346–351. <https://doi.org/10.1021/ma00191a063>
- Clark AH, Richardson RK, Ross-Murphy SB, Stubbs JM (1983) Structural and mechanical properties of agar/gelatin co-gels. Small-deformation studies. *Macromolecules* 16:1367–1374. <https://doi.org/10.1021/ma00242a019>
- Cordier P, Tournilhac F, Soulié-Ziakovic C, Leibler L (2008) Self-healing and thermoreversible rubber from supramolecular assembly. *Nature* 451:977–980. <https://doi.org/10.1038/nature06669>
- da Silva FT, de Oliveira JP, Fonseca LM, Bruni GP, da Rosa Zavareze E, Dias ARG (2020) Physically cross-linked aerogels based on germinated and nongerminated wheat starch and PEO for application as water absorbers for food packaging. *Int J Biol Macromol* 155:6–13. <https://doi.org/10.1016/j.jbiomac.2020.03.123>
- Dai S, Corke H, Shah NP (2016) Utilization of konjac glucomannan as a fat replacer in low-fat and skimmed yogurt. *J Dairy Sci* 99:7063–7074. <https://doi.org/10.3168/jds.2016-11131>
- De Silva DA, Poole-Warren LA, Martens PJ, Panhuis M (2013) Mechanical characteristics of swollen gellan gum hydrogels. *J Appl Polym Sci* 130:3374–3383. <https://doi.org/10.1002/app.39583>
- Dea ICM, Morris ER, Rees DA, Welsh EJ, Barnes HA, Price J (1977) Associations of like and unlike polysaccharides: mechanism and specificity in galactomannans, interacting bacterial polysaccharides, and related systems. *Carbohydr Res* 57:249–272. [https://doi.org/10.1016/S0008-6215\(00\)81935-7](https://doi.org/10.1016/S0008-6215(00)81935-7)
- de Vries A, Wesseling A, van der Linden E, Scholten E (2017) Protein oleogels from heat-set whey protein aggregates. *J Colloid Interface Sci* 486:75–83. <https://doi.org/10.1016/j.jcis.2016.09.043>
- Divoux T, Mao B, Snabre P (2015) Syneresis and delayed detachment in agar plates. *Soft Matter* 11:3677–3685. <https://doi.org/10.1039/C5SM00433K>
- Djabourov M, Leblond J, Papon P (1988) Gelation of aqueous gelatin solutions. II. Rheology of the sol-gel transition. *J de Phys* 49:333–343. <https://doi.org/10.1051/jphys:01988004902033300>
- Djabourov M, Nishinari K, Ross-Murphy SB (2013) Physical gels from biological and synthetic polymers. Cambridge University Press, Cambridge. <https://doi.org/10.1017/CBO9781139024136>
- Dogenski M, Navarro-Díaz HJ, de Oliveira JV, Ferreira SRS (2020) Properties of starch-based aerogels incorporated with agar or microcrystalline cellulose. *Food Hydrocoll* 108:106033. <https://doi.org/10.1016/j.foodhyd.2020.106033>
- Doi E (1993) Gels and gelling of globular proteins. *Trends Food Sci Technol* 4:1–5. [https://doi.org/10.1016/S0924-2244\(05\)80003-2](https://doi.org/10.1016/S0924-2244(05)80003-2)
- Doi E, Koseki T, Kitabatake N (1987) Effects of limited proteolysis on functional properties of ovalbumin. *J Am Oil Chem Soc* 64:1697–1703. <https://doi.org/10.1007/BF02542506>
- Doyle JP, Giannouli P, Martin EJ, Brooks M, Morris ER (2006) Effects of sugars, Galactose content and chain length on freeze–thaw gelation of galactomannans. *Carbohydr Polym* 64:391–401. <https://doi.org/10.1016/j.carbpol.2005.12.019>
- Dragnet K (2021) Alginate. In: Phillips GO, Williams PA (eds) *Handbook of hydrocolloids*, 3rd edn. Woodhead Publishing, pp 805–829. <https://doi.org/10.1016/B978-0-12-820104-6.00007-3>
- Eldridge JE, Ferry JD (1954) Studies of the cross-linking process in gelatin gels. III. Dependence of melting point on concentration and molecular weight. *J Phys Chem* 58:992–995. <https://doi.org/10.1021/j150521a013>
- Engelen L, van der Bilt A, Schipper M, Bosman F (2005) Oral size perception of particles; effect of size, type, viscosity and method. *J Texture Stud* 39:83–113. <https://doi.org/10.1111/j.1745-4603.2005.00022.x>
- Fang Y, Al-Assaf S, Phillips GO, Nishinari K, Funami T, Williams PA (2008) Binding behavior of calcium to polyuronates: comparison of pectin with alginate. *Carbohydr Polym* 72:334–341. <https://doi.org/10.1016/j.carbpol.2007.08.021>

- Fang Y, Al-Assaf S, Phillips GO, Nishinari K, Funami T, Williams PA, Li L (2007) Multiple steps and critical behaviors of the binding of calcium to alginate. *J Phys Chem B* 111:2456–2462. <https://doi.org/10.1021/jp0689870>
- Fang Y, Li L, Inoue C, Leif Lundin L, Appelqvist I (2006) Associative and segregative phase separations of gelatin/k-carrageenan aqueous mixtures. *Langmuir* 22:9532–9537. <https://doi.org/10.1021/la061865e>
- Fang Y, Takemasa M, Katsuta K, Nishinari K (2004) Rheology of Schizophyllan solutions in isotropic and anisotropic phase regions. *J Rheol* 48:1147–1166. <https://doi.org/10.1122/1.1781170>
- Fares IF, Norton IT (2015) The influence of co-solutes on tribology of agar fluid gels. *Food Hydrocoll* 45:186–195. <https://doi.org/10.1016/j.foodhyd.2014.11.014>
- Feke GT, Prins W (1974) Spinodal phase separation in a macromolecular sol-gel transition. *Macromolecules* 7:527–530. <https://doi.org/10.1021/ma60040a022>
- Fontana JD, Koop HS, Tiboni M, Grzybowski A, Pereira A, Kruger CD, da Silva MGR, Wielewski LP (2017) Chapter 7 New insights on bacterial cellulose. In: Grumezescu AM, Hilban AM (eds) *Food biosynthesis, handbook of food bioengineering*, vol 1. Academic Press, Elsevier, Amsterdam. <https://doi.org/10.1016/B978-0-12-811372-1.00007-5>
- Funami T, Kataoka Y, Hiroe M, Asai I, Takahashi R, Nishinari K (2007) Thermal aggregation of methylcellulose with different molecular weights. *Food Hydrocoll* 21:46–58. <https://doi.org/10.1016/j.foodhyd.2006.01.008>
- Gao YC, Lelievre J (1994) A theoretical analysis of the strength of composite gels with rigid filler particles. *Polym Eng Sci* 34:1369–1376. <https://doi.org/10.1002/pen.760341802>
- Garrec DA, Guthrie B, Norton IT (2013) Kappa carrageenan fluid gel material properties. Part 1: rheology. *Food Hydrocoll* 33:151–159. <https://doi.org/10.1016/j.foodhyd.2013.02.014>
- Gekko K, Kasuya K (1985) Effect of pressure on the sol-gel transition of carrageenans. *Int J Biol Macromol* 7:299–306. [https://doi.org/10.1016/0141-8130\(85\)90028-5](https://doi.org/10.1016/0141-8130(85)90028-5)
- Gekko K, Li X, Makino S (1992) Effects of polyols and sugars on the sol-gel transition of gelatin. *Biosci Biotechnol Biochem* 56:1279–1284. <https://doi.org/10.1271/bbb.56.1279>
- Giannouli P, Morris ER (2003) Cryogelation of xanthan. *Food Hydrocoll* 17:495–501. [https://doi.org/10.1016/S0268-005X\(03\)00019-5](https://doi.org/10.1016/S0268-005X(03)00019-5)
- Gravelle AJ, Barbut S, Marangoni AG (2017) Food-grade filler particles as an alternative method to modify the texture and stability of myofibrillar gels. *Sci Rep* 7:11544. <https://doi.org/10.1038/s41598-017-11711-1>
- Halake K, Lee J (2017) Functional hyaluronic acid conjugates based on natural polyphenols exhibit antioxidant, adhesive, gelation, and self-healing properties. *J Ind Eng Chem* 54:44–51. <https://doi.org/10.1016/j.jiec.2017.04.018>
- Haque A, Morris ER (1993) Thermogelation of methylcellulose. Part I: molecular structures and processes. *Carbohydr Polym* 22:161–173. [https://doi.org/10.1016/0144-8617\(93\)90137-S](https://doi.org/10.1016/0144-8617(93)90137-S)
- Hayashi A, Kinoshita K, Kuwano M, Nose A (1978) Studies on the agarose gelling system by the fluorescence polarization method II. *Polym J* 10:485–494. <https://doi.org/10.1295/polymj.10.485>
- Hiroi T, Okazumi Y, Littrell KC, Narita Y, Tanaka N, Shibayama M (2016) Mechanism of heat-induced gelation for ovalbumin and its N-terminus cleaved form. *Polymer* 93:152–158. <https://doi.org/10.1016/j.polymer.2016.04.036>
- Hossain KS, Nemoto N, Nishinari K (1997) Dynamic viscoelasticity of iota carrageenan gelling system near sol-gel transition. *Nihon Reorji Gakkaishi* 25:135–142. [https://doi.org/10.1678/rheology1973.25.3\\_135](https://doi.org/10.1678/rheology1973.25.3_135)
- Hossain KS, Nishinari K (2009) Chain release behavior of gellan gels. *Progr Colloid Polym Sci* 136:177–186. [https://doi.org/10.1007/978-3-642-00865-8\\_25](https://doi.org/10.1007/978-3-642-00865-8_25)
- Ikedo S, Nishinari K (2000) Intermolecular forces in bovine serum albumin solutions exhibiting solidlike mechanical behaviors. *Biomacromolecules* 1:757–63. <https://doi.org/10.1021/bm005587o>



- Ikeda S, Nishinari K (2001a) On solid-like rheological behaviors of globular protein solutions. *Food Hydrocoll* 15:401–406. [https://doi.org/10.1016/S0268-005X\(01\)00052-2](https://doi.org/10.1016/S0268-005X(01)00052-2)
- Ikeda S, Nishinari K (2001b) Solid-like mechanical behaviors of ovalbumin aqueous solutions. *Int J Biol Macromol* 28:315–320. [https://doi.org/10.1016/S0141-8130\(01\)00128-3](https://doi.org/10.1016/S0141-8130(01)00128-3)
- Ikeda S, Nishinari K (2001c) Structural changes during heat-induced gelation of globular protein dispersions. *Biopolymers* 59:87–102. [https://doi.org/10.1002/1097-0282\(200108\)59:2<87::AID-BIP1008>3.0.CO;2-H](https://doi.org/10.1002/1097-0282(200108)59:2<87::AID-BIP1008>3.0.CO;2-H)
- Ikeda S, Nishinari K (2001d) “Weak gel”-type rheological properties of aqueous dispersions of nonaggregated  $\kappa$ -carrageenan helices. *J Agric Food Chem* 49:4436–4441. <https://doi.org/10.1021/jf0103065>
- Ishihara S, Isono M, Nakao S, Nakauma M, Funami T, Hori K, Ono T, Kohyama K, Nishinari K (2014) Instrumental uniaxial compression test of Gellan gels of various mechanical properties using artificial tongue and its comparison with human Oral strategy for the first size reduction. *J Texture Stud* 45:354–366. <https://doi.org/10.1111/jtxs.12080>
- Ishihara S, Nakao S, Nakauma M, Funami T, Hori K, Ono T, Kohyama K, Nishinari K (2013) Compression test of food gels on artificial tongue and its comparison with human test. *J Texture Stud* 44:104–114. <https://doi.org/10.1111/jtxs.12002>
- Jaros D, Jacob M, Otto C, Rohm H (2010) Excessive cross-linking of caseins by microbial transglutaminase and its impact on physical properties of acidified milk gels. *Int Dairy J* 20:321–327. <https://doi.org/10.1016/j.idairyj.2009.11.021>
- Jin Y, Zhang H, Yin Y, Nishinari K (2006) Comparison of curdlan and its carboxymethylated derivative by means of rheology, DSC, and AFM. *Carbohydr Res* 341:90–99. <https://doi.org/10.1016/j.carres.2005.11.003>
- Joly-Duhamel C, Hellio D, Ajdari A, Djabourov M (2002) All gelatin networks: 2. The master curve for elasticity. *Langmuir* 18:7158–7166. <https://doi.org/10.1021/la020190m>
- Jørgensen CE, Abrahamsen RK, Rukke E-O, Hoffmann TK, Johansen A-G, Skeie SB (2019) Processing of high-protein yoghurt - a review. *Int Dairy J* 88:42–59. <https://doi.org/10.1016/j.idairyj.2018.08.002>
- Kaur R, Sharma M (2019) Cereal polysaccharides as sources of functional ingredient for reformulation of meat products: a review. *J Funct Foods* 62:103527. <https://doi.org/10.1016/j.jff.2019.103527>
- Kavanagh GM, Clark AH, Ross-Murphy SB (2000) Heat-induced gelation of globular proteins: 4. Gelation kinetics of low pH b-lactoglobulin gels. *Langmuir* 16:9584–9594. <https://doi.org/10.1021/la0004698>
- Kawai S, Nitta Y, Nishinari K (2007) Large deformation analysis of gellan gels. *J Appl Phys* 102:043507. <https://doi.org/10.1063/1.2769143>
- Kawai S, Nitta Y, Nishinari K (2008) Model study for large deformation of physical polymeric gels. *J Chem Phys* 128:134903. <https://doi.org/10.1063/1.2894845>
- Khalesi H, Emadzadeh B, Kadhodaee R, Fang Y (2019) Effect of Persian gum on whey protein concentrate cold-set emulsion gel: Structure and rheology study. *Int J Biol Macromol* 125:17–26. <https://doi.org/10.1016/j.ijbiomac.2018.12.051>
- Kishi S (1977) Nippon Carbide Kogyo Co. Ltd., Jap. Pat. 52-59079
- Kistler SS (1931) Coherent expanded aerogels and jellies. *Nature* 127:741. <https://doi.org/10.1038/127741a0>
- Kobayashi N, Kohyama K, Shiozawa K (2010) Fragmentation of a viscoelastic food by human mastication. *J Phys Soc Jpn* 79:044801. <https://doi.org/10.1143/JPSJ.79.044801>
- Koike A, Nemoto N, Doi E (1996) Structure and dynamics of ovalbumin gels. I. Gel induced by high temperature heat treatment. *Polymer* 37:587–593. [https://doi.org/10.1016/0032-3861\(96\)83145-4](https://doi.org/10.1016/0032-3861(96)83145-4)
- Koike A, Takada A, Nemoto N (1998) Structure and dynamics of ovalbumin gels: II. Gels induced by heat treatment at 80°C. *Polym Gels Networks* 6:257–271. [https://doi.org/10.1016/S0966-7822\(98\)00018-5](https://doi.org/10.1016/S0966-7822(98)00018-5)

- Kometani K, Tanabe M, Su L, Yang K, Nishinari K (2015) In situ observations of Thermoreversible gelation and phase separation of agarose and methylcellulose solutions under high pressure. *J Phys Chem B* 119(22):6878–6883. <https://doi.org/10.1021/acs.jpcc.5b03632>
- Lapasin R, Prici S (1999) Rheology of industrial polysaccharides: theory and applications. Springer, Berlin
- Lapasin R, Prici S, Paoletti S, Zanetti F (1990) Novel rheological model for the gelatin kinetics of ionic polysaccharides. *J Appl Polym Sci* 41:1395–1410. <https://doi.org/10.1002/app.1990.070410704>
- Lawal OS, Yoshimura M, Fukae R, Nishinari K (2011) Microporous hydrogels of cellulose ether cross-linked with di- or polyfunctional glycidyl ether made for the delivery of bioactive substances. *Colloid Polym Sci* 289:1261–1272. <https://doi.org/10.1007/s00396-011-2458-0>
- Lazaridou A, Biliaderis CG (2004) Cryogelation of cereal  $\beta$ -glucans: structure and molecular size effects. *Food Hydrocoll* 18:933–947. <https://doi.org/10.1016/j.foodhyd.2004.03.003>
- Lazaridou A, Biliaderis CG, Izydorczyk MS (2003) Molecular size effects on rheological properties of oat  $\beta$ -glucans in solutions and gels. *Food Hydrocoll* 17:693–712. [https://doi.org/10.1016/S0268-005X\(03\)00036-5](https://doi.org/10.1016/S0268-005X(03)00036-5)
- Lazaridou A, Vaikousi H, Biliaderis CG (2008) Effects of polyols on cryostructuring of barley  $\beta$ -glucans. *Food Hydrocoll* 22:263–277. <https://doi.org/10.1016/j.foodhyd.2006.11.012>
- Lee HC, Brant DA (2002) Rheology of concentrated isotropic and anisotropic xanthan solutions. I. A rodlike low molecular weight sample. *Macromolecules* 35:2212–2222. <https://doi.org/10.1021/ma011526m>
- Liao H, Ai W, Zhang K, Nakauma M, Funami T, Fang Y, Nishinari K, Draget KI, Phillips GO (2015) Mechanisms of oligogulonate modulating the calcium-induced gelation of alginate. *Polymer* 74:166–175. <https://doi.org/10.1016/j.polymer.2015.08.007>
- Liu AJ, Nagel SR (1998) Jamming is not just cool any more. *Nature* 396:21–22. <https://doi.org/10.1038/23819>
- Lozinsky VI, Okay O (2014) Basic principles of cryotropic gelation. In: Okay O (ed) Polymeric cryogels-macroporous gels with remarkable properties. Springer International Publishing, Heidelberg, pp 49–101. [https://doi.org/10.1007/978-3-319-05846-7\\_2](https://doi.org/10.1007/978-3-319-05846-7_2)
- Mao B, Divoux T, Snares P (2017) Impact of saccharides on the drying kinetics of agarose gels measured by *In-situ* interferometry. *Sci Rep* 7:41185. <https://doi.org/10.1038/srep41185>
- Matsumoto T, Inoue H (1993) Analysis of a novel phenomenon in a solidlike structure in ovalbumin aqueous colloids using the Yukawa potential. *J Appl Phys* 74:2415–2419. <https://doi.org/10.1063/1.355323>
- McAllister JW, Schmidt PW, Dorfman KD, Lodge TP, Bates FS (2015) Thermodynamics of aqueous methylcellulose solutions. *Macromolecules* 48:7205–7215. <https://doi.org/10.1021/acs.macromol.5b01544>
- McClements DJ (2017) Designing biopolymer microgels to encapsulate, protect and deliver bioactive components: physicochem aspects. *Adv Colloid Interf Sci* 240:31–59. <https://doi.org/10.1016/j.cis.2016.12.005>
- McGhee JD, von Hippel PH (1974) Theoretical aspects of DNA-protein interactions: co-operative and non-co-operative binding of large ligands to a one-dimensional homogeneous lattice. *J Mol Biol* 86:469–489. [https://doi.org/10.1016/0022-2836\(74\)90031-X](https://doi.org/10.1016/0022-2836(74)90031-X)
- Michon C, Cuvelier G, Relkin P, Launay B (1997) Influence of thermal history on the stability of gelatin gels. *Int J Biol Macromol* 20: 259–264. doi: 10.1016/S0141-8130(97)00024-X
- Milas M, Rinaudo M (1996) The gellan sol-gel transition. *Carbohydr Polym* 30:177–184. [https://doi.org/10.1016/S0144-8617\(96\)00090-2](https://doi.org/10.1016/S0144-8617(96)00090-2)
- Miwa M, Nakao Y, Nara K (1994) Food applications of curdlan. In: Nishinari K, Doi E (eds) Food hydrocolloids: structures, properties, and functions. Plenum Press, New York, pp 307–312
- Miyoshi E, Nishinari K (1999) Rheological and thermal properties near the sol-gel transition of gellan gum aqueous solutions. *Progress Colloid Polym Sci* 114:68–82. [https://doi.org/10.1007/3-540-48349-7\\_11](https://doi.org/10.1007/3-540-48349-7_11)



- Miyoshi E, Takaya T, Nishinari K (1994) Gel-sol transition in gellan gum solutions. I. Rheological studies on the effects of salts. *Food Hydrocolloids* 8:505–527. [https://doi.org/10.1016/S0268-005X\(09\)80062-3](https://doi.org/10.1016/S0268-005X(09)80062-3)
- Mizrahi S (2010) 11. Syneresis in food gels and its implications for food quality. In: Skibsted LH, Risbo J, Andersen ML (eds) *Chemical deterioration and physical instability of food and beverages*. Woodhead Publication, Oxford, pp 324–348
- Moakes RJA, Sullo A, Norton IT (2015) Preparation and characterisation of whey protein fluid gels: the effects of shear and thermal history. *Food Hydrocoll* 45:227–235. <https://doi.org/10.1016/j.foodhyd.2014.11.024>
- Mohammed ZH, Hember MWN, Richardson RK, Morris ER (1998) Kinetic and equilibrium processes in the formation and melting of agarose gels. *Carbohydr Polym* 36:15–26. [https://doi.org/10.1016/S0144-8617\(98\)00011-3](https://doi.org/10.1016/S0144-8617(98)00011-3)
- Morita T, Narita T, Mukai S, Tanagisawa M, Tokita M (2013) Phase behaviors of agarose gel. *AIP Adv* 3:042128. <https://doi.org/10.1063/1.4802968>
- Moritaka H, Yamanaka K, Kobayashi N, Ishihara M, Nishinari K (2019) Effects of the gel size before ingestion and Agarose molecular weight on the textural properties of a gel bolus. *Food Hydrocoll* 89:892–900. <https://doi.org/10.1016/j.foodhyd.2018.11.043>
- Morris ER (1994) Polysaccharide synergism - more questions than answers? In: Harding SE, Hill SE, Mitchell JR (eds) *Biopolymer mixtures*. Nottingham University Press, Nottingham, pp 247–288
- Morris ER, Nishinari K, Rinaudo M (2012) Gelation of gellan - a review. *Food Hydrocoll* 28:373–411. <https://doi.org/10.1016/j.foodhyd.2012.01.004>
- Morris VJ (1986) Multicomponent gels. In: Philips GO, Wedlock DJ, Williams PA (eds) *Gums and stabilisers for the food industry*, 3. Elsevier, London, pp 87–99
- Morris VJ, Gurning AP, Kirby AR, Mackie AR, Wilde PJ (2000) Viewing biopolymer networks, their formation and breakdown by AFM. In: Nishinari K (ed) *Hydrocolloids, part I: physical chemistry and industrial application of gels, polysaccharides, and proteins*. Elsevier, Amsterdam, pp 99–109. <https://doi.org/10.1016/B978-044450178-3/50012-3>
- Moschakis T, Panagiotopoulou E, Katsanidis E (2016) Sunflower oil organogels and organogel-in-water emulsions (part I): microstructure and mechanical properties. *LWT Food Sci Technol* 73:153–161. <https://doi.org/10.1016/j.lwt.2016.03.004>
- Murphy R, Farkas B, Jones O (2017) Effect of crosslinking on the physical and chemical properties of  $\beta$ -lactoglobulin (BLG) microgels. *J Colloid Interface Sci* 505:736–744. <https://doi.org/10.1016/j.jcis.2017.06.061>
- Murphy R, Zhu L, Narsimhan G, Jones OG (2018) Impacts of size and deformability of  $\beta$ -lactoglobulin microgels on the colloidal stability and volatile flavor release of microgel-stabilized emulsions. *Gels* 4:79. <https://doi.org/10.3390/gels4030079>
- Nagano T, Akasaka T, Nishinari K (1994a) Dynamic viscoelastic properties of glycinin and  $\beta$ -conglycinin gels from soybeans. *Biopolymers* 34:1303–1309. <https://doi.org/10.1002/bip.360341003>
- Nagano T, Mori H, Nishinari K (1994b) Effect of heating and cooling on the gelation kinetics of 7S globulin from soybeans. *J Agric Food Chem* 42:1415–1419. <https://doi.org/10.1021/jf00043a005>
- Nagasaka K, Taneya S (2000) Effects of sugars on syneresis of agarose gel. *Nippon Shokuhin Kagaku Kogaku Kaishi* 47:670–678. <https://doi.org/10.3136/nshkk.47.670>
- Nakao Y, Yamaguchi T, Taguchi T (1994) Preparations of freezable processed tofu and freeze-dried tofu by using curdlan. *Nippon Shokuhin Kogyo Gakkaishi* 41:141–147. <https://doi.org/10.3136/nshkk1962.41.141>
- Nan B, Galindo-Rosales FJ, Ferreira JMF (2020) 3D printing vertically: direct ink writing free-standing pillar arrays. *Mater Today* 35:16–24. <https://doi.org/10.1016/j.mattod.2020.01.003>
- Nemoto N (2000) Structure and dynamics of ovalbumin gels. In: Nishinari K (ed) *Hydrocolloids - Part 1 physical chemistry and industrial application of gels, polysaccharides, and proteins*.

- Elsevier Science B.V, Amsterdam, pp 45–52. <https://doi.org/10.1016/b978-0-444-50178-3.x5000-8>
- Nemoto N, Koike A, Osaki K, Koski T, Doi E (1993) Dynamic light scattering of aqueous solutions of linear aggregates induced by thermal denaturation of ovalbumin. *Biopolymers* 33:551–559. <https://doi.org/10.1002/bip.360330405>
- Nicolai T (2019) Gelation of food protein-protein mixtures. *Adv Colloid Interf Sci* 270:147–164. <https://doi.org/10.1016/j.cis.2019.06.006>
- Nicolai T, Britten M, Schmitt C (2011)  $\beta$ -lactoglobulin and WPI aggregates: formation, structure and applications. *Food Hydrocoll* 25: 1945–1962. doi: <https://doi.org/10.1016/j.foodhyd.2011.02.006>
- Nieuwland M, Bouwman WG, Pouvreau L, Martin AH, de Jongh HHJ (2016) Relating water holding of ovalbumin gels to aggregate structure. *Food Hydrocoll* 52:87–94. <https://doi.org/10.1016/j.foodhyd.2015.06.018>
- Nijenhuis KT (1981) Investigation into the ageing process in gels of gelatin/water systems by the measurement of their dynamic moduli part I – phenomenology. *Colloid Polym Sci* 259:522–535. <https://doi.org/10.1007/BF01397890>
- Nijenhuis KT (1997) Thermoreversible networks. Viscoelastic properties and structure of gels. *Adv Polym Sci* 130:160–193. <https://doi.org/10.1007/BFb0008699>
- Nijenhuis KT, Winter HH (1989) Mechanical properties at the gel point of a crystallizing poly (vinyl chloride) solution. *Macromolecules* 22:411–414. <https://doi.org/10.1021/ma00191a074>
- Niki R, Kohyama K, Sano Y, Nishinari K (1994) Rheological study on the rennet-induced gelation of casein micelles with different sizes. *Polym Gels Networks* 2:105–118. [https://doi.org/10.1016/0966-7822\(94\)90030-2](https://doi.org/10.1016/0966-7822(94)90030-2)
- Nishinari K (1976) Longitudinal vibrations of high-elastic gels as a method for determining viscoelastic constants. *Jpn J Appl Phys* 15:1263–1270. <https://doi.org/10.1143/JJAP.15.1263>
- Nishinari K (1988) Food hydrocolloids in Japan. In: Phillips GO, Wedlock DJ, Williams PA (eds) *Gums and stabilisers for the food industry* 4. IRL Press, Oxford, pp 373–390
- Nishinari K (1997) Rheological and DSC study of sol-gel transition in aqueous dispersions of industrially important polymers and colloids. *Colloid Polym Sci* 275:1093–1107. <https://doi.org/10.1007/s003960050189>
- Nishinari K (2000a) Rheology of physical gels and gelling processes. *Rep Progress Polym Phys Jpn* 43:163–192
- Nishinari K (2000b) Sol-gel transition of biopolymer dispersions. *Macromol Symp* 159:205–214. [https://doi.org/10.1002/1521-3900\(200010\)159:1<205::AID-MASY205>3.0.CO;2-B](https://doi.org/10.1002/1521-3900(200010)159:1<205::AID-MASY205>3.0.CO;2-B)
- Nishinari K (2001) Gel-sol transition in biopolymers. *Trans Mater Res Soc Jpn* 26:541–544
- Nishinari K (2009) Some thoughts on the definition of a gel. *Progr Colloid Polym Sci* 136:87–94. [https://doi.org/10.1007/978-3-642-00865-8\\_12](https://doi.org/10.1007/978-3-642-00865-8_12)
- Nishinari K (2020) *Textural characteristics of world foods*. Wiley
- Nishinari K, Fang Y (2016) Sucrose release from polysaccharide gels - a review. *Food Funct* 7:2130–2146. <https://doi.org/10.1039/C5FO01400J>
- Nishinari K, Fang Y (2017) Relation between structure and rheological and thermal properties of agar. A mini-review on the effect of alkali treatment and the role of Agarpectin. *Food Struct* 13:24–34. <https://doi.org/10.1016/j.foostr.2016.10.003>
- Nishinari K, Fang Y (2021) Molar mass effect in food and health. *Food Hydrocolloids* 112:106110. <https://doi.org/10.1016/j.foodhyd.2020.106110>
- Nishinari K, Fang Y, Guo S, Phillips GO (2014) Soy proteins: a review on composition, aggregation and emulsification. *Food Hydrocoll* 39:301–318. <https://doi.org/10.1016/j.foodhyd.2014.01.013>
- Nishinari K, Fang Y, Nagano T, Guo S, Wang R (2018) Soy as a food ingredient. In: Yada RY (ed) *Proteins in food processing*, 2nd edn. Woodhead Publishing, Elsevier. <https://doi.org/10.1016/B978-0-08-100722-8.00007-3>
- Nishinari K, Ishihara S, Hori K, Fang Y (2020) Tongue-palate squeezing of soft gels in food oral processing. *Trends Food Sci Technol* 99:117–132. <https://doi.org/10.1016/j.tifs.2020.02.023>

- Nishinari K, Kajiwaru K, Nagasaki Y, Kaneda I (2016a) Utilization of gels in food, cosmetics and medicine (popular Ed., in Japanese), 245 p, CMC Publ, Tokyo
- Nishinari K, Koide S, Ogino K (1985) On the temperature dependence of elasticity of thermoreversible gels. *J de Phys* 46:793–797. <https://doi.org/10.1051/jphys:01985004605079300>
- Nishinari K, Koide S, Williams PA, Phillips GO (1990) A zipper model approach to the Thermoreversible gel-sol transition. *J de Phys (France)* 51:1759–1768. <https://doi.org/10.1051/jphys:0199000510160175900>
- Nishinari K, Nitta Y, Miyoshi E, Ikeda S, Takaya T (2001) Helix-coil transition in the thermoreversible gels. In: Williams PA, Phillips GO (eds) *Gums & stabilisers for the food industry* 11. Royal Society of Chemistry, pp 85–94
- Nishinari K, Shiba K (2007) Polysaccharides from red seaweeds. In: Nishinari K (ed) *Food hydrocolloids: development and applications*. CMC Publ, Tokyo, pp 196–211. (In Japanese)
- Nishinari K, Takahashi R (2003) Interaction in polysaccharide solutions and gels. *Curr Opin Colloid Interface Sci* 8:396–400. [https://doi.org/10.1016/S1359-0294\(03\)00099-2](https://doi.org/10.1016/S1359-0294(03)00099-2)
- Nishinari K, Watase M (1993) Temperature dependence of elastic modulus of agarose gels with different molecular weights. *Rep Progress Polym Phys Jpn* 36:661–664
- Nishinari K, Watase M, Tanaka F (1996) Structure of junction zones in poly(vinyl alcohol) gels by rheological and thermal studies. *J Chim Phys Physicochim Biol* 93:880–886. <https://doi.org/10.1051/jcp/1996930880>
- Nishinari K, Watase M, Ogino K (1984) On the temperature dependence of elasticity of agarose gels. *Die Makromolekulare Chem* 185:2663–2668. <https://doi.org/10.1002/macp.1984.021851216>
- Nishinari K, Zhang H (2004) Recent advances in the understanding of heat set gelling polysaccharides. *Trends Food Sci Technol* 15:305–312. <https://doi.org/10.1016/j.tifs.2003.05.001>
- Nishinari K, Zhang H, Ikeda S (2000) Hydrocolloid gels of polysaccharides and proteins. *Curr Opin Colloid Interface Sci* 5:195–201. [https://doi.org/10.1016/S1359-0294\(00\)00053-4](https://doi.org/10.1016/S1359-0294(00)00053-4)
- Nitta Y, Fang Y, Takemasa M, Nishinari K (2004) Gelation of Xyloglucan by addition of epigallocatechin gallate as studied by rheology and differential scanning Calorimetry. *Biomacromolecules* 5:1206–1213. <https://doi.org/10.1021/bm034526y>
- Nitta Y, Ikeda S, Takaya T, Nishinari K (2001) Helix-coil transition in gellan gum gels. *Trans MRS-J* 26(2):621–624
- Nitta Y, Takahashi R, Nishinari K (2010) Viscoelasticity and phase separation of aqueous Na-type Gellan solution. *Biomacromolecules* 11:187–191. <https://doi.org/10.1021/bm901063k>
- Nitta Y, Yoshimura M, Nishinari K (2014) The effect of thermal history on the elasticity of K-type Gellan gels. *Carbohydrate Polym* 113:189–193. <https://doi.org/10.1016/j.carbpol.2014.06.084>
- Norton IT, Jarvis DA, Foster TJ (1999) A molecular model for the formation and properties of fluid gels. *Int J Biol Macromol* 26:255–261. [https://doi.org/10.1016/S0141-8130\(99\)00091-4](https://doi.org/10.1016/S0141-8130(99)00091-4)
- Nussinovitch A, Hirashima M (2014) *Cooking innovations –using hydrocolloids for thickening, gelling and emulsification*. CRC Press
- Nyström B, Walderhaug H (1996) Dynamic viscoelasticity of an aqueous system of a poly(ethylene oxide)–poly(propylene oxide)–poly(ethylene oxide) triblock copolymer during gelation. *J Phys Chem* 100:5433–5439. <https://doi.org/10.1021/jp952486p>
- Ogawa E, Takahashi R, Yajima H, Nishinari K (2006) Effects of molar mass on the coil to Helix transition of sodium-type gellan gums in aqueous solutions. *Food Hydrocoll* 20:378–385. <https://doi.org/10.1016/j.foodhyd.2005.03.016>
- Okay O (2014) *Polymeric Cryogels-macroporous gels with remarkable properties*. Springer, Berlin
- Okiyama A, Motoki M, Yamanaka S (1992) Bacterial cellulose II. Processing of the gelatinous cellulose for food materials. *Food Hydrocoll* 6:479–487. [https://doi.org/10.1016/S0268-005X\(09\)80033-7](https://doi.org/10.1016/S0268-005X(09)80033-7)
- Okiyama A, Motoki M, Yamanaka S (1993) Bacterial cellulose IV. Application to processed foods. *Food Hydrocoll* 6:503–511. [https://doi.org/10.1016/S0268-005X\(09\)80074-X](https://doi.org/10.1016/S0268-005X(09)80074-X)

- Paques JP, van der Linden E, van Rijn CJM, Sagis LMC (2013) Alginate submicron beads prepared through w/o emulsification and gelation with  $\text{CaCl}_2$  nanoparticles. *Food Hydrocoll* 31:428–434. <https://doi.org/10.1016/j.foodhyd.2012.11.012>
- Patel AR, Dewettinck K (2016) Edible oil structuring: an overview and recent updates. *Food Funct* 7:20–29. <https://doi.org/10.1039/C5FO01006C>
- Patel AR, Schatteman D, Vos D, Lesaffer A, Dewettinck K (2013) Preparation and rheological characterization of shellac oleogels and oleogel-based emulsions. *J Colloid Interface Sci* 411:114–121. <https://doi.org/10.1016/j.jcis.2013.08.039>
- Phillips GO, Williams PA (eds) (2020) *Handbook of hydrocolloids*, 3rd edn. Woodhead Publ, Cambridge
- Richardson RK, Goycoolea FM (1994) Rheological measurement of  $\kappa$ -carrageenan during gelation. *Carbohydr Polym* 24:223–225. [https://doi.org/10.1016/0144-8617\(94\)90134-1](https://doi.org/10.1016/0144-8617(94)90134-1)
- Richardson RK, Norton IT (1998) Gelation behavior of concentrated locust bean gum solutions. *Macromolecules* 31:1575–1583. <https://doi.org/10.1021/ma970550q>
- Rochas C, Rinaudo M, Landry S (1990) Role of the molecular weight on the mechanical properties of kappa carrageenan gels. *Carbohydrate Polym* 12:255–266. [https://doi.org/10.1016/0144-8617\(90\)90067-3](https://doi.org/10.1016/0144-8617(90)90067-3)
- Roefs SPFM, van Vliet T (1990) Structure of acid casein gels 2. Dynamic measurements and type of interaction forces. *Colloids Surf* 50:161–175. [https://doi.org/10.1016/0166-6622\(90\)80260-B](https://doi.org/10.1016/0166-6622(90)80260-B)
- Sakakibara CN, Sierakowski MR, Chassenieux C, Nicolai T, de Freitas RA (2017) Xyloglucan gelation induced by enzymatic degalactosylation; kinetics and the effect of the molar mass. *Carbohydr Polym* 174:517–523. <https://doi.org/10.1016/j.carbpol.2017.06.118>
- San Biagio PL, Bulone D, Emanuele A, Palma-Vittorelli MB, Palma MU (1996a) Spontaneous symmetry-breaking pathways: time-resolved study of agarose gelation. *Food Hydrocoll* 10:91–97. [https://doi.org/10.1016/S0268-005X\(96\)80059-2](https://doi.org/10.1016/S0268-005X(96)80059-2)
- San Biagio PL, Bulone D, Emanuele A, Palma MU (1996b) Self-assembly of biopolymeric structures below the threshold of random cross-link percolation. *Biophys J* 70:494–499. [https://doi.org/10.1016/S0006-3495\(96\)79595-4](https://doi.org/10.1016/S0006-3495(96)79595-4)
- Saunders PR, Ward AG (1955) Mechanical properties of degraded gelatins. *Nature* 176:26–27. <https://doi.org/10.1038/176026a0>
- Schaefer C, van der Shoot P, Michels JJ (2015) Structuring of polymer solutions upon solvent evaporation. *Phys Rev E* 91:022602. <https://doi.org/10.1103/PhysRevE.91.022602>
- Shi Z, Zhang Y, Phillips GO, Yang G (2014) Utilization of bacterial cellulose in food. *Food Hydrocoll* 35:539–545. <https://doi.org/10.1016/j.foodhyd.2013.07.012>
- Shirakawa M, Yamatoya K, Nishinari K (1998a) Tailoring of xyloglucan properties using an enzyme. *Food Hydrocoll* 12:25–28. [https://doi.org/10.1016/S0268-005X\(98\)00052-6](https://doi.org/10.1016/S0268-005X(98)00052-6)
- Shirakawa M, Uno Y, Yamatoya K, Nishinari K (1998b) Rheological and thermal studies on the sol-gel transition of aqueous solutions of enzymatically modified xyloglucan. In: Williams PA, Phillips GO (eds) *Gums and stabilisers for the food industry 9*. The Royal Society of Chemistry, pp 94–103
- Singh A, Auzanneaub F-I, Rogers MA (2017) Advances in edible oleogel technologies – a decade in review. *Food Res Int* 97:307–317. <https://doi.org/10.1016/j.foodres.2017.04.022>
- Smidsrød O (1974) Molecular basis for some physical properties of alginates in the gel state. *Faraday Dis Chem Soc* pp 263–274. <https://doi.org/10.1039/DC9745700263>
- Suzuki K, Taniguchi Y, Enomoto T (1972) The effect of pressure on the sol-gel transformation of macromolecules. *Bull Chem Soc Jpn* 45:336–338. <https://doi.org/10.1246/bcsj.45.336>
- Takemasa M, Nishinari K (2016) Solution structure of molecular associations investigated using NMR for polysaccharides: xanthan/Galactomannan mixtures. *J Phys Chem B* 120:3027–3037. <https://doi.org/10.1021/acs.jpcc.5b11665>
- Tanaka F (2011) *Polymer physics: applications to molecular association and Thermoreversible gelation*. Cambridge University Press, Cambridge. <https://doi.org/10.1017/CBO9780511975691>

- Tanaka F, Nishinari K (1996) Junction multiplicity in thermoreversible gelation. *Macromolecules* 29:3625–3628. <https://doi.org/10.1021/ma951577h>
- Tanaka R, Hatakeyama T, Hatakeyama H (1998) Formation of locust bean gum hydrogel by freezing-thawing. *Polym Int* 45:118–126. [https://doi.org/10.1002/\(SICI\)1097-0126\(199801\)45:1<118::AID-PI908>3.0.CO;2-T](https://doi.org/10.1002/(SICI)1097-0126(199801)45:1<118::AID-PI908>3.0.CO;2-T)
- Tanaka S, Nishinari K (2007) Unassociated molecular chains in physically crosslinked gellan gels. *Polym J* 39:397403. <https://doi.org/10.1295/polymj.PJ2006149>
- Tobitani A, Ross-Murphy SB (1997) Heat-induced gelation of globular proteins. 1. Model for the effects of time and temperature on the gelation time of BSA gels. *Macromolecules* 30:4845–4854. <https://doi.org/10.1021/ma970112j>
- Tokita M (1989) Gelation mechanism and percolation. *Food Hydrocoll* 3:263–274. [https://doi.org/10.1016/S0268-005X\(89\)80038-4](https://doi.org/10.1016/S0268-005X(89)80038-4)
- Tokita M, Nishinari K (2009) Gels: structures, properties and functions: fundamentals and applications. In: *Progress in colloid and polymer science*, vol 136. Springer, Berlin
- Ueda T (1985) (QP Co. Ltd.) Jap Pat. 60-83570
- Urbonaite V, van der Kaaij S, de Jongh HHJ, Scholten E, Ako K, van der Linden E, Pouvreau L (2016) Relation between gel stiffness and water holding for coarse and fine-stranded protein gels. *Food Hydrocoll* 56:334–343. <https://doi.org/10.1016/j.foodhyd.2015.12.011>
- van der Linden E (2012) From peptides and proteins to micro-structure mechanics and rheological properties of fibril systems. *Food Hydrocoll* 26:421–426. <https://doi.org/10.1016/j.foodhyd.2010.11.019>
- van Kleef FSM (1986) Thermally induced protein gelation: gelation and rheological characterization of highly concentrated ovalbumin and soybean protein gels. *Biopolymers* 25:31–59. <https://doi.org/10.1002/bip.360250105>
- van Vliet T, Walstra P (1985) Note on the shear modulus of rennet-induced milk gels. *Neth Milk Dairy J* 39:115–118
- van Vliet T, Walstra P (1995) Large deformation and fracture behaviour of gels. *Faraday Dis Chem Soc Gels* 101:359–370. <https://doi.org/10.1039/FD9950100359>
- Veerman C, Ruis H, Sagis LMC, van der Linden E (2002) Effect of electrostatic interactions on the percolation concentration of fibrillar  $\beta$ -lactoglobulin gels. *Biomacromolecules* 3:869–873. <https://doi.org/10.1021/bm025533+>
- Walstra P (2003) *Physical chemistry of foods*. Marcel Dekker, New York
- Watase M, Nishinari K (1983) Rheological properties of agarose gels with different molecular weights. *Rheol Acta* 22:580–587. <https://doi.org/10.1007/BF01351404>
- Watase M, Nishinari K (1987a) Rheological and thermal properties of carrageenan gels. *Die Makromolekulare Chem* 188:2213–2221. <https://doi.org/10.1002/macp.1987.021880918>
- Watase M, Nishinari K (1987b) Dynamic viscoelasticity and anomalous thermal behaviour of concentrated agarose gels. *Die Makromolekulare Chem* 188:1177–1186. <https://doi.org/10.1002/macp.1987.021880520>
- Weiss RG, Terech P (2006) *Molecular gels. Materials with self-assembled fibrillar networks*. Springer, Dordrecht
- Winter HH (2016) Gel point. In: Peterca M (ed) *Encyclopedia of polymer science and technology*. Wiley
- Winter H, Chambon F (1986) Analysis of linear viscoelasticity of a crosslinking polymer at the gel point. *J Rheol* 30:367–382. <https://doi.org/10.1122/1.549853>
- Wu X, Nishinari K, Gao Z, Zhao M, Zhang K, Fang Y, Phillips GO, Jiang F (2016) Gelation of  $\beta$ -lactoglobulin and its fibrils in the presence of transglutaminase. *Food Hydrocoll* 52:942–951. <https://doi.org/10.1016/j.foodhyd.2015.09.012>
- Yan Y, Takemasa M, Zhao C, Yu L, Nishinari K (2016) Structure-gelation research on gallate analogs and xyloglucan by rheology, thermal analysis and NMR. *Food Hydrocoll* 52:447–459. <https://doi.org/10.1016/j.foodhyd.2015.07.012>

- Yang K, Wang Z, Brenner T, Kikuzaki H, Fang Y, Nishinari K (2015) Sucrose release from agar gels: effects of dissolution order and the network inhomogeneity. *Food Hydrocoll* 43:100–106. <https://doi.org/10.1016/j.foodhyd.2014.05.005>
- Yin Y, Nishinari K, Zhang H, Funami T (2006) A novel liquid crystalline phase in dilute aqueous solutions of methyl cellulose. *Macromol Rapid Commun* 27:971–975. <https://doi.org/10.1002/marc.200600099>
- Yoshimura M, Nishinari K (1999) Dynamic viscoelastic study on the gelation of konjac glucomannan with different molecular weights. *Food Hydrocoll* 13:227–233. [https://doi.org/10.1016/S0268-005X\(99\)00003-X](https://doi.org/10.1016/S0268-005X(99)00003-X)
- Yuguchi Y, Urakawa H, Kitamura S, Ohno S, Kajiwaru K (1995) Gelation mechanism of methylhydroxypropylcellulose in aqueous solution. *Food Hydrocoll* 9:173–179. [https://doi.org/10.1016/S0268-005X\(09\)80213-0](https://doi.org/10.1016/S0268-005X(09)80213-0)
- Zetzl AK, Gravelle AJ, Kurylowicz M, Dutcher J, Barbut S, Marangoni A (2014) Microstructure of ethylcellulose oleogels and its relationship to mechanical properties. *Food Struct* 2(1–2):27–40. <https://doi.org/10.1016/j.foostr.2014.07.002>
- Zhang H, Yoshimura M, Nishinari K, Williams MAK, Foster TJ, Norton IT (2001) Gelation behaviour of konjac glucomannan with different molecular weights. *Biopolymers* 59:38–50. [https://doi.org/10.1002/1097-0282\(200107\)59:1<38::AID-BIP1004>3.0.CO;2-A](https://doi.org/10.1002/1097-0282(200107)59:1<38::AID-BIP1004>3.0.CO;2-A)
- Zhang H, Zhang F, Wu J (2013) Physically crosslinked hydrogels from polysaccharides prepared by freeze–thaw technique. *React Funct Polym* 73:923–928. <https://doi.org/10.1016/j.reactfunctpolym.2012.12.014>
- Zhuang X, Jiang X, Zhou H, Chen Y, Zhao Y, Yang H, Zhou G (2020) Insight into the mechanism of physicochemical influence by three polysaccharides on myofibrillar protein gelation. *Carbohydr Polym* 229:115449. <https://doi.org/10.1016/j.carbpol.2019.115449>

# Chapter 5

## Emulsifying Properties



Hui Zhang and Lingli Deng

**Abstract** To date, food hydrocolloids have been extensively studied as a surface-active ingredient adsorbing at the oil–water interface to stabilize emulsions through the interfacial properties. This chapter is aimed to review the formation, preparation methods, colloidal properties, and stability mechanisms of food emulsions. The effects of the absorbing and non-absorbing food hydrocolloids on the flocculation, coalescence, creaming/sedimentation, and Ostwald ripening of emulsions are discussed. Three classes of food hydrocolloids as emulsifiers are categorized: proteins (e.g., gelatin, zein, whey protein, casein, and  $\beta$ -lactoglobulin), polysaccharides (e.g., gum arabic, pectin, galactomannan, microcrystalline cellulose, and starch), and protein-polysaccharide conjugates, which can be covalently or electrostatically formed to provide the improved emulsifying and stabilizing properties. Due to the unique emulsifying properties, these food hydrocolloids have found a number of applications in beverages, dairy and meat products in the food industry. The future prospects of food hydrocolloids with emulsifying properties are proposed at the end of this chapter.

**Keywords** Emulsion stability · Emulsifier · Protein · Polysaccharide · Conjugates

### 1 Introduction

An emulsion is a colloid of two or more immiscible liquids where one liquid acts as a continuous phase and other liquids discontinuously disperse in it. During emulsion preparation, an emulsifying agent actively adsorbs at the newly formed oil–water interface to protect the newly formed droplets from immediate coalescence. Except

---

H. Zhang (✉)

College of Biosystems Engineering and Food Science, Zhejiang University, Hangzhou, China  
e-mail: [hubert0513@zju.edu.cn](mailto:hubert0513@zju.edu.cn)

L. Deng

College of Biological Science and Technology, Hubei Minzu University, Enshi, China



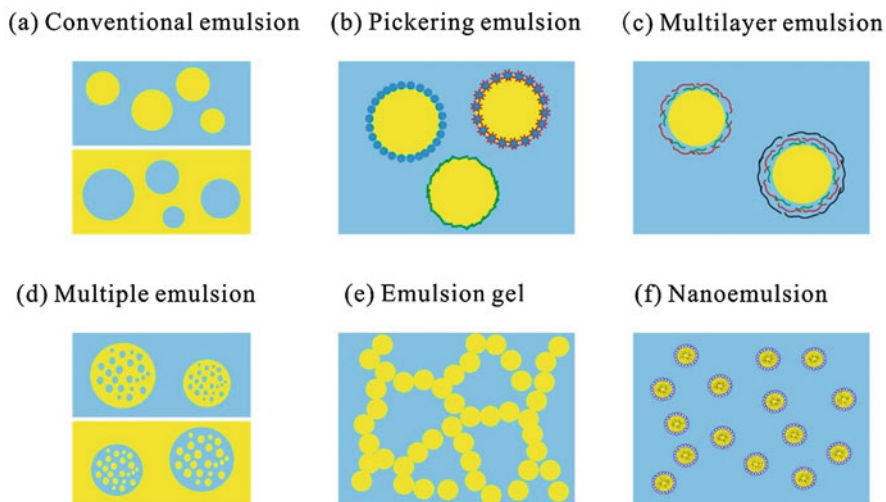


**Fig. 5.1** Structures of conventional emulsion (a), Pickering emulsion (b), multilayer emulsion (c), multiple emulsion (d), emulsion gel (e), and nanoemulsion (f)

for small molecular surfactants, food hydrocolloids are traditionally associated with thickening and gelling behaviors, which result in enhanced emulsion viscosity and retard the movement of oil droplets. On the other hand, there are some hydrocolloids which can influence the emulsion stability through the interfacial properties. Hence, a food hydrocolloid may serve as an emulsifier, as a stabilizer, or in both of these roles.

Based on the dispersed and continuous phase, food emulsions are commonly divided into two conventional emulsions, which are water-in-oil (W/O) and oil-in-water (W/O) emulsions. Additionally, the preparation of several sophisticated emulsions has been of wide interest to the food scientists (Fig. 5.1). Examples are Pickering emulsions, multilayer emulsions, multiple emulsions, emulsion gels, nanoemulsions, etc. (Sivapratha and Sarkar 2018). Nanoemulsions are dispersions of nanoscale droplets with a mean droplet diameter between 20 and 100 nm (Solans et al. 2005). The mean droplet diameter of nanoemulsions sometimes is the same as microemulsions, but the two systems are quite different, as nanoemulsions are thermodynamically unstable while microemulsions are thermodynamically stable (McClements 2012). In Pickering emulsions, solid particles are partly wetted by oil and water, and act as a physical stabilizer based on a steric mechanism (Chevalier and Bolzinger 2013). A densely packed layer composed of particles at the oil–water interface contributes to the formation of Pickering emulsions. Multilayer emulsions are usually fabricated by layer-by-layer electrostatic attraction. Water-in-oil-in-water (W/O/W) and oil-in-water-in-oil (O/W/O) emulsions are referred to as “emulsions of emulsions,” where the droplets of one dispersed liquid are further dispersed in another liquid (Benichou et al. 2007). Emulsions containing hydrogels have recently emerged as a new class of functional materials, which offer the advantage of



improved mechanical resistance for easier handling, and the opportunity for hydrophilic bioactive delivery (Dickinson 2012) as well as healthier fat replacers (Freire et al. 2018).

## 2 Methods for Creating Emulsion Systems

The homogenization process usually contains a single step or some consecutive steps, which is of great necessity to create an emulsion system from two immiscible liquids. During homogenization, a variety of methods for preparing emulsions greatly affect the flow conditions (i.e., laminar, turbulent, or cavitational) of emulsions, which determine the nature of the forces for disrupting a droplet. The methods such as high-speed mixers, colloid mills, high-pressure valve homogenization, ultrasonication, microfluidization, and membrane and microchannel homogenization are high-energy ones, while phase inversion and spontaneous emulsification techniques belong to low-energy methods (Fig. 5.2). Comparatively, low-energy methods are more applicable in the preparation of nanoemulsions, in which fine oil droplets are inclined to the spontaneous formation under specific environmental conditions (e.g., composition, stirring, temperature) (Rao and McClements 2010). Owing to less equipment requirement and energy costs, low-energy methods are attractive in the food and beverage industries. However, in low-energy methods, only a few types of oils and emulsifiers are suitable for preparing stable ultrafine droplets, and relatively high emulsifier-to-oil ratios are required. High-energy

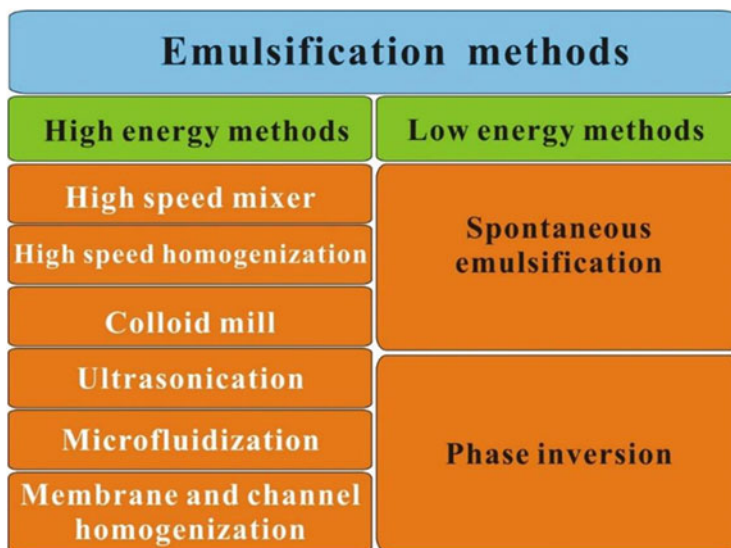


**Fig. 5.2** Illustration of the commonly used emulsification methods

methods are often effective for creating other emulsion systems. High-speed mixers and colloid mills are only available to form coarse emulsions, in which emulsion droplets have relatively large droplet sizes ( $r > 1\mu\text{m}$ ), but the other methods can be employed to form submicron droplets. In addition, different types of homogenizers are recommended according to the rheological characteristics of the materials. For example, the homogenization of highly viscous fluids needs the use of some high-speed mixers and colloid mills, while low or intermediate viscous materials can be handled by most other types of homogenizers. Moreover, the different size distribution of droplets can be accomplished by different methods. For the preparation of emulsions with narrow droplet size distributions, membrane and microchannel homogenizers are more effective than other methods. Consequently, a variety of factors (e.g., the rheological characteristics of materials, the desired droplet size distribution) should be considered for selecting an appropriate emulsification method, with a purpose of a particular application (Zhang et al. 2018).

### 3 Colloidal Properties

The appearance, texture, and shelf life of emulsion products are associated with the droplet size in emulsion systems. In general, the size of the droplets in a monodisperse emulsion is expressed as the droplet diameter or radius, while a particle size distribution is used to denote the fraction of droplets within a range of discrete size classes in a polydisperse emulsion. For low-energy methods, the dominant factors affecting the size distribution of droplets are emulsifier type, emulsifier-oil-water ratio, ionic strength, etc. The size distribution generated by high-energy methods mainly depends on emulsifier type and concentration, oil-water interfacial tension, viscosities of oil and water phases, and the intensity and duration of energy input (Jafari and McClements 2018). A static light scattering instrument is mainly used as a particle size analyzer on condition that the emulsion droplets can scatter incident light in a well-defined manner. But for concentrated emulsions, the extensive dilution and ultrasonic treatment are of necessity before the light scattering measurements to avoid inaccuracy of results. Alternatively, a light microscope is available to achieve the assessment of the microstructure and droplet size distribution of concentrated emulsions.

The interface of each emulsion droplet is a narrow region formed by accumulation of surface-active substances. The type and concentration of surface-active species determine the composition and structure of the interfacial region, which may influence the intermolecular distance and local concentration of reactive molecules, and then accelerate certain types of chemical reactions (e.g., oxidation) (McClements and Decker 2000). Typically, for monolayer emulsions stabilized by food-grade emulsifiers (e.g. proteins, polysaccharides, surfactants), the thickness of the interfacial layer is in the range of 1–10 nm, which is considered as a vital factor for emulsion stability.

**Table 5.1** The major colloidal interactions between oil droplets in emulsions (Piorkowski and McClements 2014)

Interactions	Sign	Magnitude	Range
Electrostatic	Repulsive	Strong to weak	Long to short
Steric	Repulsive	Strong	Short
Depletion	Attractive	Weak to medium	Short
Bridging	Attractive	Strong	Short
Van der Waals	Attractive	Intermediate	Intermediate
Hydrophobic	Attractive	Strong	Long

The electric properties of emulsion droplets, usually characterized in terms of zeta-potential ( $\zeta$ ), mainly depend on the solution conditions and the adsorbed emulsifier molecules that are ionized or ionizable (McClements 2010). For example, ionic surfactants in emulsion systems can be neutral, positively charged, or negatively charged. The electrical charge of proteins is associated with the isoelectric point and solution pH. Depending on the type of functional groups along the backbone, surface-active polysaccharides may also have an electrical charge. In general, the emulsion droplets are covered by the same type of emulsifier. Then, the electrostatic repulsion caused by the same electrical charge protects the droplets from aggregation, and significantly affects the interactions between emulsion droplets and other charged species (e.g., surfactants, hydrocolloids, flavors, antioxidants). For instance, the catalyst electrostatically absorbed on the droplet surface may promote the lipid oxidation of oil droplets, in comparison to free one (Mei et al. 1998).

In addition to electrostatic interactions, colloidal interactions such as van der Waals, steric, hydrophobic interactions, depletion, and salt-induced attraction can also play a significant role in emulsion systems (Table 5.1). Their magnitude (strong to weak), sign (attractive to repulsive), and range (long to short) determine the nature of interdroplet interactions, which strongly affect the overall characteristics (e.g., stability, rheology, and appearance) of a particular emulsion system. When attractive forces dominate the interactions, the droplets are inclined to associate with each other. While the dominant forces are repulsive, the droplets tend to retain their individual integrity (Zhang et al. 2018).

## 4 Emulsion Stability

When considering the stability of an emulsion, the distinguishment between its thermodynamic and kinetic stability is significant. From a thermodynamic point of view, an emulsion tends to separate due to the reduced interfacial energy. Therefore, all food emulsions are thermodynamic instability and will eventually break down as long as they are left long enough (McClements 2015).

The comparison of the free energy of a liquid–liquid system before and after homogenization can be used to explain the origin of such thermodynamically unstable systems. The free energies of an oil phase and a water phase keep constant before and after emulsification, so the difference in the free energy between the non-emulsified and emulsified states is analyzed as follow:

$$\Delta G_{\text{formation}} = G^f - G^i = G_I^f - G_I^i - \left( TS_{\text{config}}^f - TS_{\text{config}}^i \right) = \Delta G_I - T\Delta S_{\text{config}}$$

By definition, the difference in interfacial free energy ( $\Delta G_I$ ) between the initial and final states is equal to the increase in contact area ( $\Delta A$ ) between the oil and water phases, which is multiplied by the interfacial tension ( $\gamma$ ):  $\Delta G_I = \gamma\Delta A$ . Hence,

$$\Delta G_{\text{formation}} = \gamma\Delta A - T\Delta S_{\text{config}}$$

The increased contact area after emulsification always results in the positive change in interfacial free energy, which thus opposes emulsion formation. Additionally, due to the greater number of arrangements accessible to the droplets in the initial state than the final state, the configurational entropy term ( $-T\Delta S_{\text{config}}$ ) is always negative, which therefore contributes to emulsion formation. The overall free energy change concerned with the formation of a food emulsion can thus be expressed by

$$\Delta G_{\text{formation}} = \gamma\Delta A$$

Therefore, the creation of a food emulsion should be always thermodynamically unfavorable, because of the increased interfacial area after emulsification.

Compared with the thermodynamic stability, the kinetic stability of food emulsions is more attractive and interesting for food scientists and engineers, because of the particular importance to create food products with desirable properties. Between the two different free energy states ( $G_{\text{low}}$  and  $G_{\text{high}}$ ) probably occupied by plenty of molecules in a system, the molecules are most likely to occupy the state with the lowest free energy. At thermodynamic equilibrium, the two states are populated according to the Boltzmann distribution:

$$\frac{n_{\text{high}}}{n_{\text{low}}} = \exp\left(-\frac{(G_{\text{high}} - G_{\text{low}})}{kT}\right)$$

where  $n_{\text{low}}$  and  $n_{\text{high}}$  are the number of molecules that occupy the energy levels  $G_{\text{low}}$  and  $G_{\text{high}}$ ,  $k$  is Boltzmann's constant ( $k = 1.38 \times 10^{-23} \text{ J K}^{-1}$ ), and  $T$  is the absolute temperature.

Compared with the thermal energy of the system ( $kT$ ), the fraction of molecules in the lower free energy state becomes greater as the difference between the two free energy levels is larger. In practice, due to the presence of a free energy barrier,  $\Delta G^*$ , between the two states (Fig. 5.3), a free energy needs to be acquired to cross the

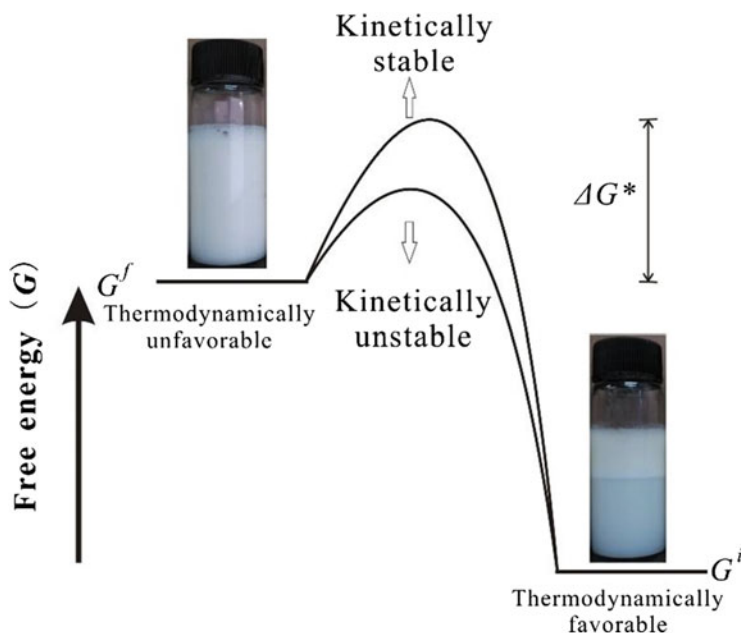


**Fig. 5.3** Emulsions are a thermodynamically unstable system, but may exist in a metastable state, therefore being kinetically stable

barrier if a high free energy state of a system moves into a low one, and the transformation rate decreases with the increasing barrier height. In general, the long-term stability of most emulsions needs an activation energy of about  $20kT$ . Actually, an emulsion system is in different metastable states, probably because of the sufficiently large barrier associated with a thermodynamically unstable state for a long time. Nevertheless, a single free energy barrier concerned with a particular physicochemical process is considered as a most important factor to determine the overall kinetic stability of an emulsion.

## 5 Stability Mechanisms

The most important phenomena affecting the long-term stability of an emulsion are gravitational separation, coalescence, flocculation, phase inversion, and Ostwald ripening (Fig. 5.4). Creaming, as one type of gravitational separation, describes that droplets in a system move upward owing to their lower density than the surrounding liquid, while sedimentation is the other type of gravitational separation, which describes that droplets move downward because of their higher density than the surrounding liquid. Flocculation and coalescence are both types of droplet aggregation. Flocculation describes the process that two or more droplets come

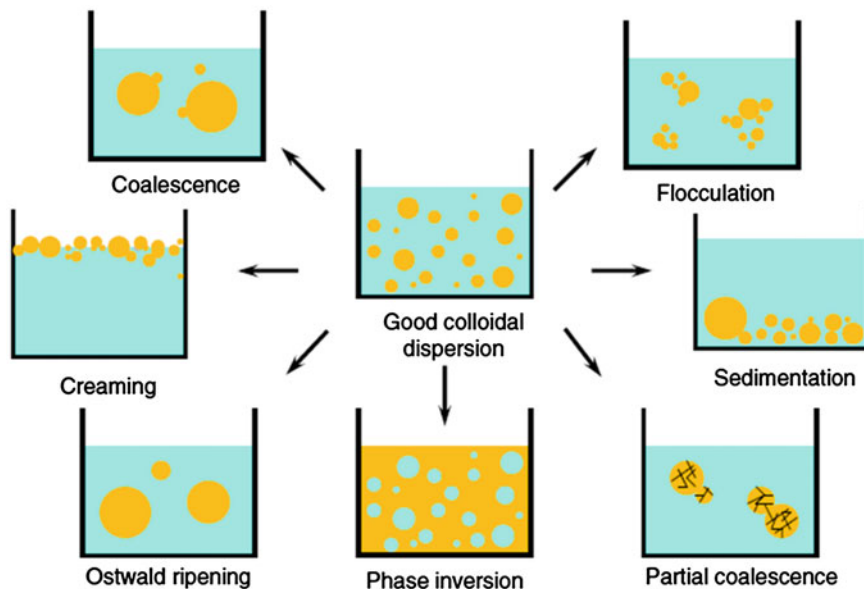


**Fig. 5.4** Mechanism of destabilization in a colloidal system. Reproduction with permission from (Kuroiwa et al. 2015), Copyright 2015 Elsevier

together but remain as individual entities, while coalescence occurs when two or more droplets merge together, resulting in the formation of a single larger droplet and eventually a separate layer of oil on the top of a system, namely, “oiling-off.” Phase inversion describes the conversion from an O/W emulsion to a W/O emulsion or vice versa. Ostwald ripening is the growth of one emulsion droplet at the expense of a smaller one as a result of the difference in chemical potential of the material within droplets. Small-sized unstable particles are being dissolved and re-attached on the surface of big particles, reaching a more stable thermodynamic state.

## 5.1 Flocculation

Flocculation is a reversible process of the sticking together of droplets upon collision, leading to an apparent increase in the droplet size and then an acceleration of creaming or sedimentation. As droplet collisions reduce or electrostatic and steric repulsion increase, flocculation can be decreased between droplets. Once droplets collide, the interface separating two droplets has a naturally thinner tendency and eventually ruptures. Then, coalescence occurs in a form of one larger droplet. Emulsions stabilized with ionic hydrocolloids are more likely sensitive to pH and ionic strength, which would induce flocculation by pH changes or specific types of ions. The conformation of the hydrocolloids is also affected by pH and ionic

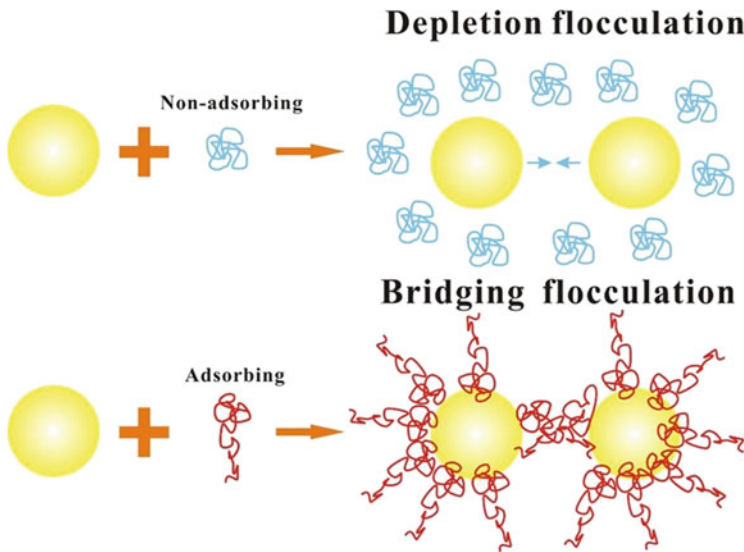


**Fig. 5.5** Schematic illustration of depletion and bridging flocculation

strength, especially the protein part. The addition of simple salts into the aqueous phase reduces the thickness of the electrical double-layer, and so diminishes the range of the electrostatic repulsion.

When a polymer is introduced into a colloidal system, flocculation is often observed, due to one of two distinct mechanisms—bridging or depletion flocculation (Fig. 5.5). Bridging flocculation is a process that the insufficient emulsifier cannot achieve the saturation of freshly formed surfaces and share the adsorbed layer among neighboring droplets. When the emulsifier adsorbs too slowly or is present at a very low concentration, most of the individual droplets tend to form an aggregate and cannot remain as their individual integrity as a result of coalescence or bridging flocculation.

If the amount of non-adsorbing hydrocolloids in an emulsion is not enough to immediately cover all the interface, depletion flocculation may occur. McClements (2000) defined four regions concerned with the instability of an emulsion system containing polysaccharides, and determined a critical flocculation concentration (CFC), which is the polysaccharide concentration producing depletion flocculation. When the polysaccharide concentration ( $c$ ) in an emulsion exceeds a particular value, termed as the critical viscosity concentration (CVC), creaming would be assumed to completely retard: (I) Unstable. No-flocculation ( $c < \text{CFC}$ ) and relatively low viscosity ( $c < \text{CVC}$ ). The droplets move upward at a rate that is proportional to the square of their diameter and the reciprocal of the aqueous phase viscosity. (II) Highly unstable. Flocculation ( $c > \text{CFC}$ ) and relatively low viscosity ( $c < \text{CVC}$ ). The effective size of the particles in the emulsion increases because of flocculation, but the viscosity is not high enough to prevent the flocculation. (III) Stable. No-flocculation ( $c < \text{CFC}$ ) and high viscosity ( $c > \text{CVC}$ ). The droplets are

not flocculated, but the viscosity of the aqueous phase is so large that they cannot move. (IV) Stable. Flocculation ( $c > CFC$ ) and high viscosity ( $c > CVC$ ). The droplets are flocculated, but the viscosity of the aqueous phase is so large that they cannot move.

## 5.2 Coalescence

Coalescence describes the merging of two or more emulsion droplets to form a larger single droplet. For an emulsion product, coalescence is perceived as highly unfavorable during storage. The shifting of the overall distribution towards larger droplet sizes may result in the enhanced creaming. However, partial coalescence for the development of structures is of great significance for some food products, such as whipped cream and ice cream, because of the conversion of a viscous liquid to a viscoelastic solid. For many of food triglyceride emulsions, particularly dairy emulsions, fat crystallization occurs in such emulsion droplets at storage temperature. Crystals are both radial and tangential to the surface, and actually growing or protruding through the membrane. The incomplete coalescence caused by crystals present in the oil phase results in the formation of irregularly aggregated droplets with the original identity (Fig. 5.6). Two important additional factors influencing partial coalescence are: (i) the temperature cycling of cream layers, which causes growth and melting of fat crystals, and (ii) agitation or stirring, which greatly increases the likelihood of collision-induced crystal penetration between droplets (Dickinson 2009).

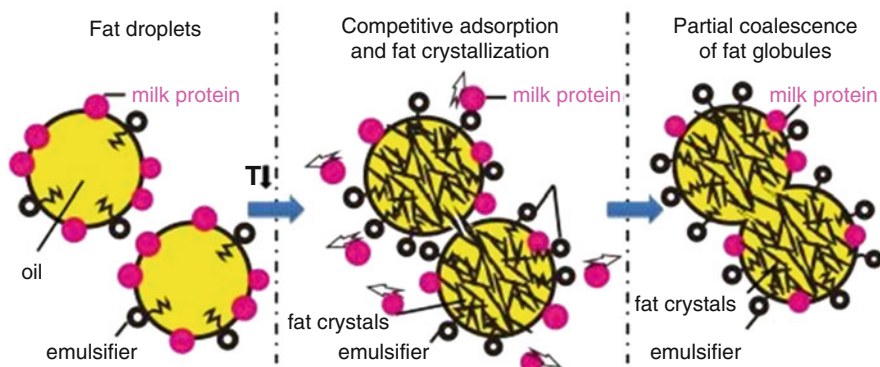


**Fig. 5.6** Schematic illustration of fat crystallization and partial coalescence. Reproduction with permission from Cheng et al. (2020) Copyright 2020 Elsevier



### **5.3 *Creaming/Sedimentation***

Creaming is a process that oil droplets driven by gravity move upward to form a concentrated cream layer at the top of an emulsion. The decreased droplet size of colloidal particles can retard creaming, which can be modified by the hydrocolloid concentration, emulsifying conditions (pH, ionic strength), and emulsification method. Beverage emulsions are sensitive to creaming due to the fact that the dilute emulsions are typically made up of a flavor oil blend containing a weighting agent, and a polymeric emulsifier or stabilizer (Given Jr 2009). Sedimentation also happens when the weighting agent is overused or supersaturated in the oil phase. Various hydrocolloids have been applied for manufacture of beverage flavor emulsions, such as octenyl succinylation starch, whey protein, arabinogalactan, etc. (Klein et al. 2010; Mora-Gutierrez et al. 2018). Electrostatic interactions between proteins and polysaccharides are used to fabricate sequential multilayers to build droplet shell integrity and stability against various environmental stresses (ionic strength, pH, presence of oxidation catalysts, heat, sunlight, etc.), because of the formation of a more robust interfacial complexes.

### **5.4 *Ostward Ripening***

The difference in the radius of droplet curvature results in the chemical potential of the materials within droplets and then Ostwald ripening, i.e., one emulsion droplet grows at the expense of a smaller one. Alternatively, the process may be purely viewed from a perspective of the reduced free energy in the system by means of the destructed interfacial area. Overall, the effect is an increase in the average radius of the emulsion droplets with time, as the smaller droplets dissolve and redeposit their materials onto the larger droplets (Taylor 1998). In theory, Ostward ripening can be decreased as the monodispersity of an emulsion increases, due to the fact that the thermodynamic driving force is associated with the size difference of droplets. In practice, the coarsening tendency can be reduced by mixing of another insoluble component into the dispersed phase, due to a large counteracting thermodynamic driving force provided in direct opposition to the Ostwald ripening effect (Kabal'Nov et al. 1987; Davis et al. 1981).

## **6 Proteins**

### **6.1 *Gelatin***

Gelatin is a natural protein hydrolyzed from animal collagen. It is widely used for foaming, emulsifying, and wetting purposes in food industry. Previous studies have

shown that gelatin acts as an emulsifier with surface activity in O/W emulsions (Table 5.2) (Lobo 2002). Its emulsification and foamability derive from the hydrophobic area of peptide chains on gelatin. Compared with other surface-active substances, such as globular proteins and gum arabic, gelatin is a weaker emulsifier, which often produces larger droplet sizes during homogenization when used alone. Hence, its effectiveness can be improved by either hydrophobically modification with the attachment of non-polar side-groups or used in combination with other emulsifiers as complex emulsifiers.

Gelatin from marine sources (warm- and cold-water fish skins, bones, and fins) is a possible alternative to bovine gelatin, with an advantage of being not associated with the risk of bovine spongiform encephalopathy. Moreover, fish gelatin is acceptable in Islam and can be used with minimal restrictions in Judaism and Hinduism. Surh et al. (2006) studied the emulsifying property of fish gelatin with various molecular weights, and the effects of pH, salt, and thermal processing on the stability of the gelatin-stabilized emulsions. It was observed that a higher ratio of large droplets led to an easier destabilization of the emulsions stabilized by low molecular weight fish gelatin than high molecular weight ones. Dickinson and Lopez (2001) compared the emulsifying property of fish gelatin with that of commercial milk proteins, and found that an optimization of the protein/oil ratio was expected to prevent coalescence caused by large droplets, especially at high ionic strength.

Due to the limited emulsifying property of gelatin, its complexes with other emulsifiers have been studied. In a reported study (Surh et al. 2005), the multilayer emulsions with SDS as the first layer and SDS-fish gelatin complex as the second layer were fabricated, the droplets in the secondary emulsions exhibited good stability against droplet aggregation in a water bath for 30 min at different temperatures ranging from 30 to 90 °C. It was also observed that the emulsions prepared with a complex of whey protein with fish gelatin using layer-by-layer interfacial deposition technique were more physiochemically stable than those with individual proteins (Taherian et al. 2011). Zeeb et al. (2011) studied the stabilizing effect of enzymatic crosslinking on the beet pectin-fish gelatin double coated emulsions, and found that the freeze-thaw stability and creaming behavior of the secondary emulsions treated by laccase were significantly improved, compared to the individual emulsions. Lately, the fish gelatin-gum arabic complexes were used to fabricate concentrated emulsions, and greater intermolecular connectivity between the adsorbed layers of adjacent oil droplets for a gel network extension was observed at lower pH (Anvari and Joyner 2017).

## 6.2 Zein

Zein, as a food-grade abundant material extracted from corn, has been attempted to accomplish extensive applications in various industries. The hydrophobic property of zein depends on its high proportion of hydrophobic amino acids, while the degree of ionization of basic and acid amino acid groups affects the degree of

**Table 5.2** Typical hydrocolloid emulsifiers and the related emulsions

Emulsifier	Emulsion type	References
Fish gelatin	Oil-in-water emulsion	Surh et al. (2006)
Fish gelatin/SDS	Oil-in-water emulsion	Surh et al. (2005)
Fish gelatin/whey protein isolate	Oil-in-water emulsion	Taherian et al. (2011)
Fish gelatin/sugar beet pectin	Multilayer emulsion	Zeeb et al. (2011)
Fish gelatin/gum arabic	Oil-in-water emulsion	Anvari and Joyner (2017)
Zein	Pickering emulsion	de Folter et al. (2012)
Zein/tannic acid complex particles	Pickering emulsion	Zou et al. (2015)
Zein/chitosan complex particles	Pickering emulsion	Wang et al. (2015)
Zein/propylene glycol alginate particles	Pickering emulsion	Dai et al. (2018)
Zein/gum arabic nanoparticles	Pickering emulsion	Li et al. (2018)
Zein/corn fiber gum	Pickering emulsion	Zhu et al. (2019)
Zein/propylene glycol alginate/rhamnolipid complex particles	Pickering emulsion (high internal phase)	Dai et al. (2019)
Zein/sodium caseinate/propylene glycol alginate	Pickering emulsion (high internal phase)	Sun et al. (2018)
Zein/tannic acid complex particles	High internal phase emulsion gel	Zou et al. (2019)
Whey protein/polysaccharides (locust bean gum, guar gum, xanthan gum, konjac gum)	Water-in-oil-in-water emulsion	Benichou et al. (2007)
Whey protein microgels/casein	Pickering emulsion	Chevallier et al. (2019)
Whey protein nanoparticles	Pickering emulsion	Wu et al. (2015)
Whey protein	Emulsion gel	Mantovani et al. (2016)
Whey protein microgel particles	Pickering emulsion	Sarkar et al. (2016)
Whey protein	Emulsion gel	Luo et al. (2019)
Sodium caseinate, whey protein isolate or isolated soy protein	Emulsion gel	Freire et al. (2018)
Casein	Emulsion gel	McIntyre et al. (2017)
Casein gel particles	Pickering emulsion	Wang et al. (2018a)
Casein/soy protein or casein/pea protein	Emulsion gel	Silva et al. (2019)
Casein/whey protein isolate	Emulsion gel	Balakrishnan et al. (2017)
$\beta$ -lactoglobulin	Oil-in-water emulsion	Purwanti et al. (2016)
$\beta$ -lactoglobulin	Nanoemulsion	Ali et al. (2016)
OSA modified quinoa starch granules	Water-in-oil-in-water Pickering emulsion	Marefati et al. (2015)
Guar gum	Water-in-oil-in-water emulsion	de Almeida Paula et al. (2018)

(continued)

**Table 5.2** (continued)

Emulsifier	Emulsion type	References
Microcrystalline cellulose/soybean protein hydrolysate	Oil-in-water emulsion	Xu et al. (2016)
Nanofibrillated cellulose/guar gum/carboxy methyl cellulose	Oil-in-water emulsion	Golchoobi et al. (2016)
Locust bean gum/sodium caseinate	Water-in-water emulsion	Moschakis et al. (2018)
Ball-milling and OSA modified areca taro starch	Pickering emulsion	Liu et al. (2018)
Gelatinized native rice starch, waxy maize starch	Pickering emulsion	Kasprzak et al. (2018)
Pectin/zein complex	Oil-in-water emulsion	Piriyaprasarth et al. (2016)
Waxy corn starch/locust bean gum	Water-in-water emulsion	Murray and Phisarnchananan (2016)
Octenylsuccinate quinoa starch	Pickering emulsion gel	Li et al. (2019)
Quinoa starch waxy maize starch oat starch	Pickering emulsion	Saari et al. (2019)
Native corn (NCS), rice (NRS), wheat (NWS), and waxy corn (WCS) starch	Oil-in-water emulsion	Gómez-Luría et al. (2019)
Rice, wheat, potato, OSA potato starch	Pickering emulsion	Chen et al. (2019)
Wheat native starch and OSA waxy maize starch	Emulsion gel	Torres et al. (2017)

hydrophobicity. It is classified into four classes with different solubility behaviors, which are known as  $\alpha$ -,  $\beta$ -,  $\gamma$ -, and  $\delta$ -zein (Anderson and Lamsal 2011). Zein cannot be easily dissolved in either water or oil, but it is expected to fabricate colloidal particles by anti-solvent precipitation.

Zein colloidal particles have been extensively studied for preparation of Pickering emulsions. de Folter et al. (2012) found that the Pickering emulsions stabilized by unmodified zein colloidal particles were unstable to creaming. However, the improved stability of emulsions may be obtained by the stabilization of complex particles of zein and other biopolymers (e.g., proteins and polysaccharides) against coalescence and creaming through the modified wettability (Wang et al. 2015; Piriyaprasarth et al. 2016; Li et al. 2018). Zou et al. (2015) fabricated the zein/tannic acid complex colloidal particles based on hydrogen bonding to stabilize emulsions, which were extensively crosslinked to form a continuous network among and around the oil droplets and protein particles, leading to the formation of stable Pickering emulsion gels. Recently, the zein-propylene glycol alginate complex particles with a neutral wettability were fabricated to stabilize emulsions with a higher stability against coalescence (Dai et al. 2018). Zhu et al. (2019) fabricated the zein/corn fiber gum complex colloidal particle-stabilized Pickering emulsions, which were observed to have a gel-like network behavior. A neutral wettability was obtained

when the mass ratio of zein to corn fiber gum was 2:1, and the prepared Pickering emulsions exhibited better physical stability.

Zein-based complex particles have been also applied for stabilization of high internal phase emulsions or emulsion gels. Zou et al. (2019) fabricated the high internal phase emulsion gels with an oil content ranging between 72 and 87% (w/w) stabilized with the zein/tannic acid complexes at a particle concentration range of 0.7–1.4%. Lately, the zein-propylene glycol alginate-rhamnolipid complex particles were prepared with suitable three-phase contact angles to stabilize O/W Pickering high internal phase emulsions with an oil phase ratio of 75% (Dai et al. 2019). Similarly, Sun et al. (2018) fabricated the high internal phase Pickering emulsions stabilized by the ternary zein/sodium caseinate/propylene glycol alginate complexes at a volume concentration of as much as 80% oil. In a recent report, the Pickering emulsions at a high oil volume ratio (60%) were fabricated, which were effectively stabilized by the zein/gum arabic nanoparticles through the formation of a stable and thick oil–water interfacial layer to hinder agglomeration and Ostwald ripening (Li et al. 2018).

### 6.3 Casein

As a heterogeneous phosphorylated protein, casein comprises the major proteinaceous component of mammalian milk. Owing to the self-assembly and surface-active characteristics, casein is expected to stabilize O/W emulsions as an emulsifying agent based on electrostatic and steric stabilization mechanisms. The emulsifying capacity of casein products differs from their form: acid casein > micellar casein > rennet casein (Roman and Sgarbieri 2006). Tan and McGrath (2012) studied the emulsion morphology diagrams of the sodium caseinate/oil/water system. For the lowest emulsifier concentration, bridging flocculation was evident and the emulsions were very unstable. Increasing the sodium caseinate concentration enhanced the emulsion stability and promoted the existence of distinct individual oil droplets. The further increase in the sodium caseinate concentration caused a reduced stability, which was ascribed to depletion flocculation. Then the sodium caseinate self-assembly was initiated. The emulsion stability was again enhanced due to the formation of a three-dimensional protein network at sufficiently high sodium caseinate and/or oil concentrations.

In addition, the thermo-reversible gelation behavior was observed in the sodium caseinate-stabilized emulsions (Dickinson and Casanova 1999). Once heated to 30–40 °C, a concentrated liquid-like emulsion is converted into a flocculated emulsion gel that supports its own weight. The emulsion gel “melts” again slowly upon cooling, and the return to the original low-viscosity state is accelerated by stirring. Aggregated casein networks are commonly encountered in making yogurt and other fermented dairy products. The addition of lactic acid bacteria lowers the pH from 6.7 to lower than 4.5, resulting in a liquid-like dispersion of casein particles into a soft solid-like aggregated network. When the pH of sodium caseinate-

stabilized emulsions is lowered towards the protein's isoelectric point, a transition from the net repulsion to net attraction occurs, leading to droplet flocculation and then soft solid-like emulsions. Normally, the stiffness of the casein stabilized emulsion gels increases with the increasing oil content, as the oil droplets act as active fillers (i.e. the oil droplets are covered with proteins which are bound to the surrounding protein network) in the emulsion gels (Silva et al. 2019; Balakrishnan et al. 2017). It was reported that the sodium caseinate-stabilized emulsions showed a shear-thinning behavior as a result of a more structured system at pH 7.0, while at pH 3.0 the addition of laccase improved the emulsion stability by narrowing the size distribution and increasing the viscosity (Sato et al. 2015). Radford et al. (2004) studied the effects of alcohol and calcium on the sodium caseinate-stabilized emulsions, and found that the addition of calcium ions and/or ethanol resulted in a pronounced reduction in viscosity and the onset of Newtonian flow. Balakrishnan et al. (2017) fabricated the emulsion gels by heating the homogenized suspensions of micellar casein mixed with sunflower oil at various pH (5.8, 6.0, and 6.3) and oil weight fractions (5, 10, and 15%). The gel stiffness increased with the decreasing pH and the increasing oil ratio. The gel stiffness did not change significantly after replacing up to 40% casein by whey protein at pH 5.8 or 6.0, but decreased significantly at pH 6.3. However, the addition of a small amount of casein into whey protein microgel stabilized Pickering emulsions effectively improved the heat stability of the emulsions by competitive adsorption at the interface (Chevallier et al. 2019). McIntyre et al. (2017) prepared the casein-based emulsion gels with milk fat or rapeseed oil at high (774 mg/100 g) or low (357 mg/100 g) calcium levels. Compared with the low-calcium emulsion gels, the high-calcium gels were significantly softer and showed the highest disintegrated rate during the simulated gastric digestion. The fatty acid releases were similar for all the emulsion gels made from milk fat, while a higher lipolysis was found in the high-calcium emulsion gels made from rapeseed oil. Silva et al. (2019) reported that micellar casein could be replaced by plant proteins (e.g. soy protein and pea protein) while maintaining the same emulsion gel stiffness.

Sodium caseinate has been found to facilitate the formation of the high internal phase Pickering emulsions stabilized by the zein/sodium caseinate/propylene glycol alginate complexes (Sun et al. 2018). The casein gel particles were also fabricated by covalently genipin crosslinking of a protein network with the self-associated sub-micelles or calcium induced casein micelles to stabilize Pickering emulsions (Wang et al. 2018a). The oil droplets stabilized by these particles exhibited higher stability against flocculation and creaming, compared to those stabilized only by sodium caseinate.

## 6.4 *Whey Protein*

Whey protein has been widely used in food industry as an emulsifier, which consists of  $\beta$ -lactoglobulin (~65%),  $\alpha$ -lactalbumin (~25%), bovine serum albumin (~8%),

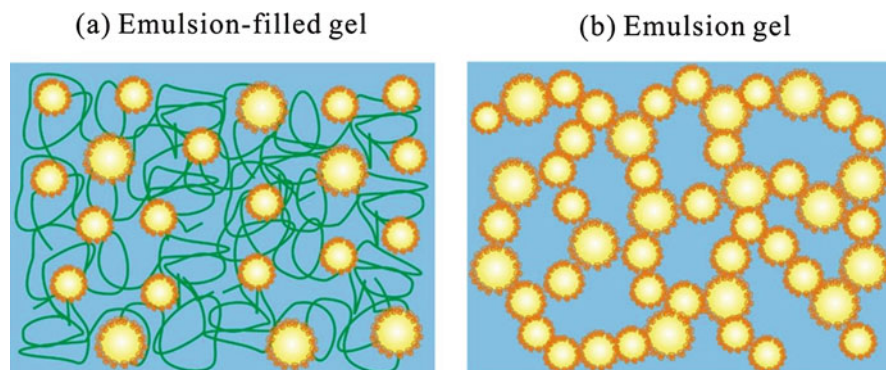


**Fig. 5.7** Schematic presentation of (a) an emulsion-filled protein gel and (b) a protein-stabilized emulsion gel. Yellow circle, oil; small red circle, protein; light blue, water; green curve, protein network

and immunoglobulins (Morr and Ha 1993). Compared to casein, whey protein can be used over a wider pH range since its solubility goes through a minimum at the isoelectric point at pH close to 5. This makes whey protein applicable to acidic environments where caseins cannot be used, especially at pH below 4.5. However, heat treatment has a significant effect on the properties of the whey protein-stabilized emulsions, since the non-covalent interactions maintaining the secondary and tertiary structures of the globular protein would be broken by thermal energy. It has been extensively investigated about the stability of the whey protein-stabilized emulsions in terms of the effect of heating. Euston et al. (2000) found that the interactions between the adsorbed protein at the emulsion droplet surface and the non-adsorbed heat denatured protein in the continuous phase were the main cause of aggregation, and the non-adsorbed protein acted as a “glue” holding the aggregated emulsion droplets together.

Whey protein has been used for preparation of emulsion gels as well, due to its characteristic heat-induced gelling property (Dickinson 2012). The major whey protein in cow’s milk is  $\beta$ -lactoglobulin, which denatures and aggregates upon heating to a temperature of 70 °C, like many other globular proteins. At the molecular level, this aggregation and subsequent gelation are a result of the developed hydrophobic interactions between the exposed non-polar regions of the unfolded  $\beta$ -lactoglobulin molecules. The sulfhydryl-disulfide interchange leading to covalent crosslinking may also improve the evolving network structure. Therefore, this complex colloidal system may exist as both an emulsion and a gel, which can be expressed as “emulsion gel” for understanding. To specify more precisely the properties of such protein-based systems, two structural arrangements can be distinguished: (a) the emulsion-filled protein gel and (b) the protein-stabilized emulsion gel. As shown in Fig. 5.7a, the emulsion-filled protein gel is a protein gel matrix within which emulsion droplets are embedded. It is a kind of particle-filled solid due to the network properties of the spatially continuous matrix in charge of its solid-like rheological properties. The protein-stabilized emulsion gel is shown schematically in



Fig. 5.7b. It is a type of particulate gel, and its rheological properties are mainly determined by the properties of the network of aggregated emulsion droplets.

Above a critical concentration, whey protein can be crosslinked to form a three-dimensional gel network by heating, acidification or enzymatic treatment. The whey protein emulsion gel structure can be modified by varying pH, droplet size, ionic strength, and temperature. Mantovani et al. (2016) studied the effect of pH on cold-set gel formation by acidification of emulsion gel (30% oil and 5% non-heated whey protein isolate (WPI)) and emulsion-filled gel (emulsion dispersed in heat-treated whey protein solution), and found that stronger gel strength was obtained at a pH near the isoelectric point of whey protein because of protein aggregation promoted by lower acidification rate and electrostatic repulsion. Guo et al. (2017) investigated the effect of gel structure and rheology on the intestinal digestion of canola oil dispersed within O/W emulsions gelled with WPI. The softer and microstructurally homogeneous gels were obtained at lower salt concentrations. The rate of lipid digestion increased due to the looser, less spatially heterogeneous protein matrix, in comparison to the firmer gels. Overall, the extent and rate of lipid digestion were modified by the strength and microstructure of the WPI-stabilized emulsion gels, which may be used to produce emulsion-based food products. For example, the emulsion gels containing  $\omega$ -3 fatty acids and condensed tannins were fabricated with WPI for potential use of healthier fat replacers (Freire et al. 2018). Luo et al. (2019) encapsulated capsaicinoids in whey protein emulsion gels, and studied the structural relationship with the in-mouth breakdown behavior. A greater hardness led to a smaller bolus particle size, but a higher degree of fragmentation caused greater surface exposure during mastication.

Besides, soft whey protein microgel particles used as an emulsion stabilizer can show the combined advantages of biocompatibility and an increased stability against coalescence. Wu et al. (2015) prepared the Pickering O/W emulsions stabilized by WPI nanoparticles in the size range of 200–500 nm, which exhibited good stability against coalescence. Sarkar et al. (2016) designed the Pickering O/W emulsions using whey protein microgels by a facile route of heat-set gel formation followed by mechanical shear, and studied the influence of heat treatment on the emulsions stabilized by these particles. In addition, the whey protein microgel particles could also act as a stabilizer for waxy corn starch/locust bean gum water-in-water emulsions (Murray and Phisarnchananan 2016).

## 6.5 $\beta$ -Lactoglobulin

$\beta$ -Lactoglobulin, a dominant globular protein found in whey fraction, possesses a remarkable emulsifying property, which is commonly used in the formulation of food emulsions.  $\beta$ -lactoglobulin has showed great potentials as a transport vehicle for hydrophobic compounds, since it can bind hydrophobic vitamins and fatty acids in inner cavities (Kimpel and Schmitt 2015). Moro et al. (2013) studied the effects of heat treatment on the emulsifying properties of  $\beta$ -lactoglobulin. For a shorter time



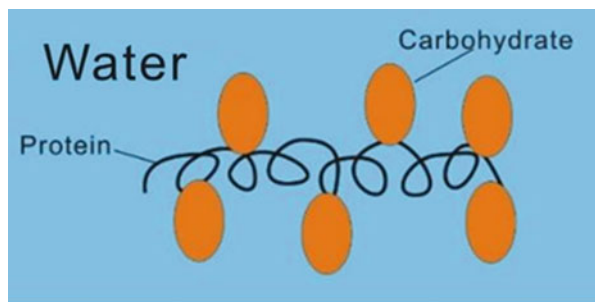
period of heating, both the foamability and foam stability were improved, but the emulsifying property diminished. However, after 10 min of heating at 85 °C, both the foaming and emulsifying properties were impaired. Purwanti et al. (2016) studied the unheated and heat-aggregated  $\beta$ -lactoglobulin stabilized clove oil-in-water emulsions and limonene-in-water emulsions by microchannel emulsification. The monodisperse emulsion droplets were consistently produced using unheated or heat-aggregated  $\beta$ -lactoglobulin with concentrations from 0.5 to 3% (w/w) at pH 7. Ali et al. (2016) fabricated the  $\beta$ -lactoglobulin stabilized biocompatible nanoemulsions prepared by high-pressure homogenization. The nanoemulsions with 1 wt%  $\beta$ -lactoglobulin and with 5 wt% Miglyol 812 (a mixture of medium chain triglycerides) had a relatively small particle size ( $\sim$ 200 nm) and a low polydispersity, when a homogenization pressure of 100 MPa was applied for 4 cycles. These nanoemulsions were made stable for at least 30 days. However, the emulsification capacity of  $\beta$ -lactoglobulin was reduced at higher homogenization pressures (200 MPa and 300 MPa).

## 7 Polysaccharides

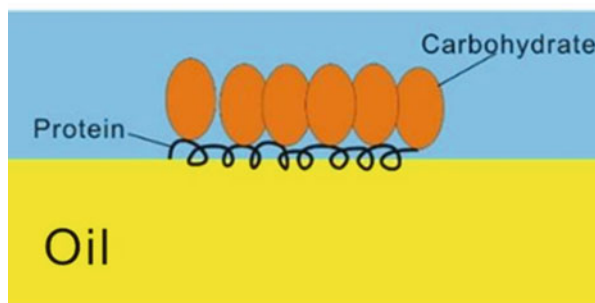
### 7.1 Gum Arabic

Gum arabic was once a kind of hydrocolloids widely used in food industry, and now there is still 40–50 thousand tons per year consumed in the worldwide market. It helps to stabilize the flavor and essential oils in production of soft drinks or concentrated juices. Gum arabic (*A. senegal*) is a complex branched heteropolyelectrolyte with a backbone of 1,3-linked  $\beta$ -galactopyranose units and side-chains of 1,6-linked galactopyranose units terminating in glucuronic acid or 4-O-methylglucuronic acid residues. There are three different fractions separated from gum arabic, namely, arabinogalactan ( $\sim$ 90% of total mass), arabinogalactan protein ( $\sim$ 10%), and glycoprotein ( $\sim$ 1%) (Randall et al. 1989). Gum arabic is a polysaccharide emulsifier naturally conjugated with protein. The structure of this protein-polysaccharide complex is known as the “wattle blossom” model (Fig. 5.8), in which the hydrophobic protein moieties adsorb onto the oil droplet surface, and the covalently attached hydrophilic carbohydrate blocks protrude into the aqueous phase against droplet flocculation and coalescence (Dickinson 2008). Though it serves as a stabilizer to form a thick steric stabilizing layer and protect the flavor and essential oils in emulsion products at intermediate pH values, high ionic strengths or high temperatures, gum arabic shows a lower affinity for the oil-water interface than most other surface-active biopolymers. The  $\alpha$ -tocopherol encapsulated nanoemulsions with gum arabic as an emulsifying and stabilizing agent were fabricated through solvent-displacement technique (Moradi and Anarjan 2018). The monomodal size distribution was successfully obtained with a mean particle size of 10.01 nm, 49.46 nm, and 171.2 nm for the emulsions prepared with 0.05%, 0.1%, and 0.15% gum arabic, respectively. Hu et al. (2019) reported that gum arabic

**Fig. 5.8** Schematic representation of the wattle blossom model of gum arabic (a) in solution and (b) at the oil-water interface. Hydrophilic carbohydrate blocks and the backbone chain of hydrophobic protein were illustrated



(a)



(b)

enriched with trace elements ( $Zn^{2+}$ ,  $Fe^{3+}$ ,  $Fe^{2+}$ ) had good emulsion stability as the molecular weight and arabinogalactan protein content increased, in comparison to the control gum arabic. Atgié et al. (2018) found that the protein-rich species of gum arabic irreversibly adsorbed as monolayers at the oil–water interface, and the absorbed amount drastically increased with both the decreasing ionic repulsions and the increasing gum concentration. However, those changes corresponded to only minor composition changes in the adsorbed layer, suggesting a significant role of controlling the interfacial density in a rational design of gum arabic-based formulations.

## 7.2 Pectin

Pectin is another class of hydrocolloid with a fascinating emulsifying character, while its emulsifying property differs depending on the varieties of plant sources. For example, citrus and apple pectin can form gels at low pH and serve as thickening agents but not effective emulsifying agents, while sugar beet pectin is normally used

as an excellent emulsifying agent owing to the protein moiety, acetyl groups, and highly branched polysaccharide structures, and it can form a thick hydrated layer that may prevent droplets from flocculation and coalescence through electrostatic and steric repulsive forces. Williams et al. (2005) found that the emulsifying property of sugar beet pectin was affected by the proportion of ester groups, the accessibility of the protein and ferulic acid groups to oil droplet surface, and the molecular mass distribution of the fractions. However, no simple relationship existed between the emulsifying property and the protein or ferulic acid content. Funami et al. (2011) reported that the emulsifying property of the deproteinized sugar beet pectin with a protein content ranging from 5 to 0.5% became worse than that of the untreated pectin. Siew et al. (2008) reported that an increase in the protein content (12% higher than the average) of sugar beet pectin would help adsorb onto the oil droplets. Chen et al. (2016a) observed a significant decrease in the droplet size of the sugar beet pectin stabilized emulsions, as the protein content of sugar beet pectin increased from 0.5 to 3%.

### 7.3 Galactomannan

As the most commonly used plant polysaccharides, galactomannans belong to the legume family consisting of  $\beta$ -(1-4-) linked D-mannan backbone by substitution of  $\alpha$ -(1-6-) linked D-galactose stubs for certain mannose residues. Locust bean gum and guar gum are high molecular weight galactomannans used as food additives, since no significant proportion of hydrophobic groups presents in the carbohydrate structure. This type of hydrocolloid can be assumed to be used for modifying the rheological properties of the continuous aqueous phase between dispersed particles or droplets. To date, the surface and interfacial properties of guar gum and locust bean gum have been extensively studied (Reichman and Garti 1991).

It was reported that the emulsions with similar droplet size distributions showed similar stability when crude, purified and bipurified guar gums were used to prepare emulsions under similar conditions (Garti and Reichman 1993). However, the emulsions made from the guar gum with a proteinaceous-rich fraction had larger droplets and relatively low stability with the fastest coalescence rate upon dilution. Later, Garti and Reichman (1994) found a similar degree of surface activity and emulsification ability when the guar gum was purified down to 0.8% protein. Thus, it is conceivable that the slight hydrophobicity of the polymannose backbone may contribute to some emulsion stabilizing properties.

In a recent study, guar gum was used to fabricate W/O/W double emulsions for improving the heat stability of anthocyanins at pH 4.0 (de Almeida Paula et al. 2018). In addition, various levels of guar gum (0.5, 1.0, and 1.5%) were used as a fat substitute to prepare low-fat meat emulsions. The reduction of fat by incorporation of guar gum was found to increase the emulsion stability and cooking yield but decrease the penetration force (Rather et al. 2017). To develop a new low-fat mayonnaise formulation, nine mayonnaise samples containing different

compositions of nanofibrillated cellulose, guar gum, and carboxymethyl cellulose were compared to the commercial low-fat mayonnaise with 30% fat (Golchoobi et al. 2016). In addition, the water-in-water emulsions containing sodium caseinate and locust bean gum have been also fabricated as potential functional ingredients to mimic fats (Moschakis et al. 2018).

#### 7.4 *Microcrystalline Cellulose*

Microcrystalline cellulose (MCC) is among the most common cellulose derivatives in food industry (Nsor-Atindana et al. 2017). It is a hydrocolloid without solubility in water but adsorbs mechanically at the oil–water interface (Garti and Reichman 1993). The cellulose crystallites are claimed to build a network made from the majority of the particles being less than 0.2 $\mu$ m. The formed colloidal network of the free MCC thickens the water phase between oil globules and provides effective stabilization against their subsequent coalescence (Milani and Maleki 2012).

When colloidal MCC is dispersed in water, it can be expected to simulate the fat-induced rheology owing to the inherent properties in food applications such as baked products, frozen desserts, mayonnaise, gravies, and sauces. For example, an emulsion with 60% soybean oil showed similar stability and rheology characteristics, compared to the emulsion containing 1–1.5% colloidal MCC and 20% soybean oil (Imeson 2011). The use of MCC as a fat substitute gives a rich creamy texture in low-fat sauces and dressings, because of the insoluble material to mimic fat. MCC may be used alone or in combination with other polysaccharides in ice cream, which is expected to increase the solid content and improve the stability and ice rheology (Nsor-Atindana et al. 2017).

In general, crystals of cellulose within micro/nanoscale dimension (MCC/NCC) have been commonly applied for preparation of Pickering emulsions. Kalashnikova et al. (2011) confirmed that Pickering O/W emulsions could be effectively stabilized by bacterial cellulose nanocrystals for several months if the particles were properly dispersed. The colloidal MCC particles (11% colloidal MCC combined with 1% sodium carboxymethylcellulose) could also form a network around the emulsified oils and then act as a stabilizer of O/W emulsions and W/O/W multiple emulsions (Jia et al. 2014), in which MCC not only thickened the continuous phase between the droplets, but also provided a mechanical barrier to prevent oil droplet coalescence (Dickinson 2013). In another study, the microrheological property of curcumin emulsions was changed by the addition of MCC, as evidenced by a transition from the viscous to viscoelastic behavior of the emulsions. The freeze-thaw stability of the emulsions was significantly improved by MCC, which was attributed to the enhanced repulsive steric forces between the curcumin droplets. In addition, stearylated microcrystalline cellulose was recently reported to fabricate high internal phase Pickering emulsions with the highest internal phase ratio of 89% (Pang et al. 2018).

## 7.5 Starch

Starch (including hydrophobically modified starch) is an abundant, inexpensive, and natural food ingredient, while the natural variation regarding the size, shape, and composition of starch granules normally occurs among its numerous botanical sources. For native starch, it cannot achieve adsorption to the oil–water interface as an emulsifying agent. Therefore, starch has been modified to become more suitable for emulsion stabilization. Physical modifications, including milling, non-solvent precipitation, ultrasonication, high-pressure treatment may be applied to reduce the size of starch. Decreasing the particle size of starch often relates to the increased storage stability of its Pickering emulsions. Octenyl succinic anhydride (OSA) modification is the most commonly used chemical modification method, which improves the hydrophobicity of starch. OSA modified starch with a degree of modification <3%, E1450, is a well-established food ingredient with no specific limitations on its use (Timgren et al. 2011). The Pickering emulsion gels were formed by stabilization of octenylsuccinate quinoa starch granules at an oil fraction ranging from 50 to 70% (Li et al. 2019). Liu et al. (2018) compared the stability of soybean oil-in-water Pickering emulsions stabilized by different areca taro starches (native starch, OSA esterified starch, ball-milled starch, and compound modified starch with ball-milling and OSA), and found that the compound modified starch showed strong surface activity and high emulsion viscosity, leading to the best emulsifying capacity and stability. Nevertheless, it should be noted that the amylose/amylopectin ratio also affects the emulsion properties. Lu et al. (2018) reported that the milled high-amylose maize starch particles had the best stabilization ability, followed by milled normal maize starch particles. Kasprzak et al. (2018) screened a series of commercially available food starches, and found that a waxy rice starch showed the O/W emulsifying ability following gelatinization. In addition, the OSA modified quinoa starch granules were also reported to be used to make W/O/W double emulsions with solid or liquid shea oil (Marefati et al. 2015). The double emulsions were freeze-dried and then rehydrated for emulsion reformation, which had a similar droplet size to that of the initial emulsion, suggesting a high process stability.

## 8 Protein-Polysaccharide Conjugates

Numerous studies on the emulsifying properties of protein-polysaccharide conjugates have been published in the last few years. A conjugate is the material made from a protein covalently linked by a polysaccharide via Maillard reaction, in which temperature, humidity, and concentration of ingredients need to be carefully controlled. Maillard reaction is a series of non-enzymatic browning reactions that occur naturally between the reducing end of a sugar and amino acids. The functional properties of protein and polysaccharide can be combined through Maillard reaction

from the production of a novel protein-polysaccharide conjugate, which may be expected to result in an enhanced protein functionality both as an emulsifier and a stabilizer.

Several methods including wet heating, dry heating, and molecular crowding are often used to induce Maillard reaction between proteins and polysaccharides. For dry heating, to ensure sufficient contact, the powders of the protein and polysaccharide are obtained by freeze-drying the mixture firstly dispersed in water, and then heated in an apparatus at the controlled time, temperature, and relative humidity. Wet heating can also be used to prepare protein-polysaccharide conjugates by heating the ingredients present in a buffer solution for hours. It is considered as a more efficient method with the improved control over the reaction advancement, in comparison to the dry heating technique. However, the concentration of reactants needs to be increased for a higher glycation level, as molecular crowding is of necessity for Maillard reaction under less adverse treatments in aqueous solutions (Perusko et al. 2015; Weng et al. 2016). In the presence of high concentrations of biological macromolecules, the reaction follows the excluded volume theory, and the crowded environment promotes the conjugation between protein and polysaccharide. In addition, the extent of protein aggregation can potentially be minimized in the macromolecular crowding environment. Recently, ultrasound has been applied to facilitate the Maillard reaction. It was reported that the conjugates obtained by the ultrasound treatment had better emulsifying properties, compared to those prepared by classical heating (Xue et al. 2017; Chen et al. 2016b; Liu et al. 2016). Stanic-Vucinic et al. (2013) found that high-intensity ultrasound efficiently promoted the glycation of  $\beta$ -lactoglobulin by Maillard reaction, and the obtained conjugates possessed the improved antioxidant capacity, with a minor influence on protein's secondary and tertiary structures.

Table 5.3 illustrates some studies involving the conjugates from proteins (e.g., whey protein, casein,  $\beta$ -lactoglobulin, and soy protein), and polysaccharides (e.g., guar gum, pectin, and dextran). High molecular weight conjugates possess the properties of protein, strongly adsorbing at the surface of oil droplets, as well as the hydrophilic properties of polysaccharide, being highly solvated by the aqueous medium. The conjugation between proteins and polysaccharides may provide much more improved steric stabilization for emulsion droplets, as illustrated in Fig. 5.9. As the molecular weight of the polysaccharide moiety sufficiently increases, a thicker stabilizing layer can be formed by the conjugate in an emulsion. Therefore, the well-prepared protein-polysaccharide conjugates may show the substantially improved emulsifying and stabilizing properties compared to native proteins (Sivapratha and Sarkar 2018).

Great concerns have been also raised by the presence of a protein and polysaccharide as naturally occurring substances with the emulsifying capacity produced by Maillard reaction. Cirre et al. (2014) conducted a heat-induced maturation treatment for corn fiber gum in the solid state, which induced a reduction in the solubility and incensement in the aggregation of the proteinaceous component. The emulsification performance and stability of the matured samples were greatly improved, in comparison with the control gum. A 3-fold increase in the proportion of the adsorbed

**Table 5.3** Formation, characterization, and functionality of protein-polysaccharide conjugates obtained via Maillard reaction

Protein	Polysaccharide	Reaction condition	Characterization methods	Main results	References
Whey protein	Guar gum	Wet heating, 50 or 70 °C, 15 min	SDS-PAGE (sodium dodecyl sulfate polyacrylamide gel electrophoresis)	Cumin seed oil (CSO) nanoemulsions were prepared using preheated 10% WPI and 0.2% guar gum in aqueous phase, and the mixture of CSO and corn oil (30:70) as oil phase.	Farshi et al. (2019)
Deamidated wheat gluten	Citrus pectin or maltodextrin	Dry heating, 80 °C, RH (relative humidity) 79%, 24 h	OPA (o-phthalaldehyde), SDS-PAGE, FTIR (Fourier transform infrared), CD (circular dichroism)	Conjugates prepared by dry heating deamidated wheat gluten/maltodextrin (1/1) for 9 h showed the best emulsifying properties.	Wang et al. (2019)
Whey protein	Pectin	Dry heating, 80 °C, RH 79%, 6–168 h	SDS-PAGE, HPSEC (high-pressure size exclusion chromatography)	Solubility and emulsion stability were improved.	Wefers et al. (2018)
Casein	Carrageenan	Dry heating, 60–80 °C, RH 79%, 6–72 h	OPA, Color, FTIR, fluorescence measurements	Conjugates obtained at 60 °C for 24 h showed the best emulsifying activity and stability.	Qiu et al. (2018)
Bovine serum albumin	Sugar beet pectin	Dry heating, 85 °C, RH 79%, 5 h	SDS-PAGE, Color, GPC (gel permeation chromatography)	Covalent conjugates exhibited good emulsion stability under the extreme environmental conditions.	Chen et al. (2018)
Rice protein	Dextran	Wet heating, pH 12, 80–100 °C, 10–30 min	TNBS (2,4,6-trinitrobenzene sulfonic acid), HPSEC, SDS-PAGE, FTIR	Emulsifying activity and stability were increased by factors of 1.79 and 2.2, respectively.	Cheng et al. (2018)
Egg-white lysozyme	Guar gum	Dry heating, 60 °C, RH 80%, 10 days	SDS-PAGE, Color, GPC, FTIR	Emulsion capacity and stability were significantly improved.	Hamdami et al. (2018)
Sodium caseinate	Locust bean gum	Dry heating, 80 °C, RH 79%, 4 days	SDS-PAGE, Color, FTIR	Conjugates produced at 80 °C after 24 h showed good emulsifying properties.	Barbosa et al. (2018)

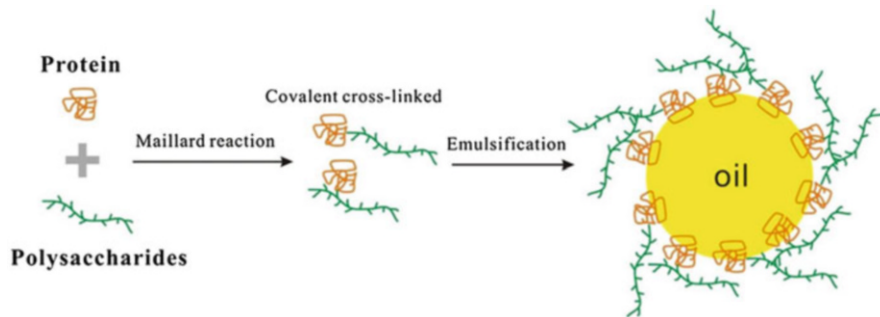
(continued)

Table 5.3 (continued)

Protein	Poly saccharide	Reaction condition	Characterization methods	Main results	References
Whey protein isolate (WPI)	Citrus pectin	Closed-cavity rheometer, 80–140 °C, 0.75–10 min	HPSEC, fluorescence measurements	A novel Maillard reaction method was applied to highly concentrated WPI-highly methylated citrus pectin blends at elevated temperatures.	Koch et al. (2017)
Soy protein isolate	Dextran	Dry heating, 60 °C, RH 79%, 8 days	SDS-PAGE, OPA, FTIR	Oil droplet size was decreased, and emulsion stability was improved.	Boostani et al. (2017)
Casein hydrophobic peptide (CHP)	<i>Acacia seyal</i> polysaccharide	Dry heating, 60 °C, RH 75%, 3 days	TNBS, HPSEC	Conjugates prepared from <i>A. seyal</i> polysaccharide and CHP with a degree of hydrolysis of 1.5% presented the best emulsifying properties.	Hou et al. (2017)
Soy protein isolate (SPI)	Soy hull hemi-cellulose (SHH)	Dry heating, 60 °C, RH 75%, 7 days	Color, FTIR, free amino acids	Optimized SHH-SPI conjugates exhibited the substantially improved emulsification capacity.	Wang et al. (2017)
WPI	Maltodextrin	Dry heating, 80 °C, RH 79%, 3 h	OPA	Emulsifying and colloid stabilizing properties were improved.	Ding et al. (2017)
Canola protein isolate	Gum arabic	Wet heating, pH 7.0, 90 °C, 15 min	SDS-PAGE, HPSEC	Conjugate-stabilized emulsions showed smaller droplet size, lower creaming index, and higher resistance to pH and heat.	Pirestani et al. (2017)
$\beta$ -lactoglobulin	Gum <i>Acacia Seyal</i>	Dry heating, 60 °C, RH 79%, 0–48 h	TNBS, SDS-PAGE	Emulsion stabilities against storage, pH, temperature, and salt were improved.	Bi et al. (2017)
$\beta$ -lactoglobulin	Chitosan	Wet heating, pH 6.0, 40 °C, 0–7 days	SDS-PAGE, fluorescence measurements	Emulsifying properties were improved.	Mengfbar et al. (2017)



Soy $\beta$ -conglycinin	Dextran	Macromolecular crowding, pH 7.0, 95 °C, 6 h; Dry heating, 65 °C, RH 75%, 96 h	SDS-PAGE, TNBS	Degree of conjugation grafting carried out in macromolecular crowding environment was generally higher than that produced by dry heating method.	Weng et al. (2016)
Buckwheat protein isolate	Dextran	Ultrasound-assisted wet heating, 70 °C, 80 min; Wet heating 70 °C, 40 h	FTIR, CD, fluorescence measurements	Emulsifying properties of the conjugates obtained by the ultrasound treatment were improved, compared to those obtained by classical heating.	Xue et al. (2017)
Peanut protein isolate (PPI)	Maltodextrin	Ultrasound-assisted wet heating, pH 7.0, 70 °C, 10–100 min	OPA, SDS-PAGE	High-intensity ultrasound promoted the production of glycosylated PPI.	Chen et al. (2016b)



**Fig. 5.9** Schematic representation of Maillard reaction between proteins and polysaccharides. The formed conjugates are used to improve stabilization of emulsions

fraction onto the oil–water interface accounted for the improved emulsification. As for okra hydrocolloid mucilage, it has both proteins and characteristic slimy polysaccharides. Heating at 100 °C for 6 h resulted in the conjugates that showed better emulsifying property than the ones formed between okra polysaccharides and bovine serum albumin (Temenouga et al. 2016). Lately, brea gum, which is an exudate from *Cercidium praecox* tree, was purified and subjected to thermal treatment at 110 °C for 24, 48, 72, and 96 h, respectively. The thermally treated brea gum presented changes in the molecular mass of its protein fractions and in its color parameters as a result of non-enzymatic browning reactions. The modifications in the gum structure produced an increase in its surface activity and improved its emulsifying/stabilizing capacity, leading to corn oil-in-water emulsions stable for several months (Castel et al. 2018).

## 9 Applications in Food Industry

The hydrocolloid stabilized emulsions have showed a number of applications in the food industry, such as dairy products, meat products, beverages, etc. (Fig. 5.10). Beverage emulsions are a unique class of emulsions, which are consumed in a highly dilute form. The emulsions in both the concentrate and diluted forms must be stable at least for 6 months. Gum arabic is the most widely used emulsifier as well as a stabilizer in beverage emulsions. The most accepted alternative to gum arabic for beverage emulsions is modified starches, whose lipophilic and hydrophilic groups can be balanced by modifications (Tan 2004). There are other hydrocolloids with good emulsifying properties to be used in beverage emulsions, for example, locust bean gum. In ice cream, hydrocolloids have been applied for various functions, especially as a stabilizer, fat replacer, and cryoprotectant (Javidi and Razavi 2019). Structurally, it consists of a complex matrix of fat globules, ice crystals, air bubbles, and a continuous phase of unfrozen water with dissolved sugars, proteins, and salts (Daw and Hartel 2015). Gelatin almost exclusively serves as a stabilizer in the ice



**Fig. 5.10** Major applications for hydrocolloid emulsifiers in food industry

cream industry, but has gradually been replaced by the polysaccharides of plant origin due to their increased effectiveness and reduced cost. Blends containing locust bean gum, guar, and carrageenan are excellent stabilizing systems for ice cream. Sausages are made of a fine homogenate by adding water and salt into chopping meat, in which the dispersion and emulsification of pork fat is further achieved. Solubilization of muscle protein is associated with the interactions with salt solutions during blending of meat. Then, a stable emulsion is formed due to the formation of a surrounding layer of the salt soluble proteins at the surface of the released fat. In sausage products, more myofibrillar proteins are extracted, thus heat treatment can contribute to the formation of a stronger gel. Sodium caseinate, soy protein isolate, guar gum, xanthan, gellan gum are commonly used in meat products as emulsifiers.

Due to the high calorific value and/or the fat-related health problems caused by high-fat diets, the demand for reduced-fat counterparts in food products has been developed in recent years (Azeredo et al. 2019). Some studies of fat replacement have been performed using different hydrocolloids in various products, such as ice cream, mayonnaise (Golchoobi et al. 2016), sausages (Pintado et al. 2018). Several structuring approaches have been reported to mimic the fat texture. Emulsion gels have been fabricated by casein, whey protein isolate, soy protein isolate as emulsifiers (Freire et al. 2018). Double emulsions (W/O/W) have been fabricated to maintain the contact area between fat and the oral surface in the mouth. Pickering emulsions have been successfully stabilized by zein, starch granules, cellulose crystals, whey protein microgels, crosslinked casein gel particles as potential fat replacers (Javidi et al. 2019; Wang et al. 2018b). Nanoemulsions are more stable against creaming, sedimentation, coalescence, and flocculation, and have higher surface area and more free energy, so they are suitable carrier systems. Recent researches have shown that the nanoemulsions stabilized with proteins were more stable than those stabilized by low molecular weight surfactants due to the formation

of an elastic film by proteins, which can inhibit coalescence of droplets in the dispersed phase. In addition, the bioactive encapsulated nanoemulsions have been prepared by stabilization of hydrocolloids, such as  $\beta$ -lactoglobulin (Ali et al. 2016), pectin/whey protein complexes (Esfanjani et al. 2015; Gharehbeblou et al. 2019).

## 10 Future Prospects

Over the last decade, a growing number of studies have focused on the characterization of the emulsifying properties of food hydrocolloids, leading to a fundamental understanding of the mechanisms of their interfacial functionalities. Apart from the known hydrocolloid emulsifiers, more and more naturally extracted biopolymers will be explored as a novel candidate for applications in foods, inspired by the consumer preference for clean label ingredients. Many studies have also shown that the protein-polysaccharide conjugates induced by Maillard reaction may present the improved emulsifying property compared to the single components, indicating the potentials to be used in beverages and dairy products. However, the main challenge for developing such novel emulsifiers is to select a conjugated fraction with high functionality in emulsions under a certain environmental condition for the desirable formulated products. Therefore, in future more studies are needed to understand the relationship between the conjugate structures and functional properties before use in practical applications.

## References

- Ali A, Mekhloufi G, Huang N, Agnely F (2016)  $\beta$ -lactoglobulin stabilized nanemulsions—formulation and process factors affecting droplet size and nanoemulsion stability. *Int J Pharm* 500 (1–2):291–304
- Anderson TJ, Lamsal BP (2011) Zein extraction from corn, corn products, and coproducts and modifications for various applications: a review. *Cereal Chem* 88(2):159–173
- Anvari M, Joyner HS (2017) Effect of fish gelatin-gum arabic interactions on structural and functional properties of concentrated emulsions. *Food Res Int* 102:1–7
- Atgié M, Masbernat O, Roger K (2018) Emulsions stabilized by gum Arabic: composition and packing within interfacial films. *Langmuir* 35(4):962–972
- Azeredo H, Barud HS, Farinas CS, Vasconcellos VM, Claro AM (2019) Bacterial cellulose as a raw material for food and food materials packaging applications. *Front Sustain Food Syst* 3:7
- Balakrishnan G, Nguyen BT, Schmitt C, Nicolai T, Chassenieux C (2017) Heat-set emulsion gels of casein micelles in mixtures with whey protein isolate. *Food Hydrocoll* 73:213–221
- Barbosa JM, Ushikubo FY, de Figueiredo Furtado G, Cunha RL (2018) Oil in water emulsions stabilized by maillard conjugates of sodium caseinate-locust bean gum. *J Dispers Sci Technol* 809:1–12
- Benichou A, Aserin A, Garti N (2007) W/O/W double emulsions stabilized with WPI-polysaccharide complexes. *Colloids Surf A* 294(1):20–32

- Bi B, Yang H, Fang Y, Nishinari K, Phillips GO (2017) Characterization and emulsifying properties of  $\beta$ -lactoglobulin-gum Acacia Seyal conjugates prepared via the Maillard reaction. *Food Chem* 214:614–621
- Boostani S, Aminlari M, Moosavi-Nasab M, Niakosari M, Mesbahi G (2017) Fabrication and characterisation of soy protein isolate-grafted dextran biopolymer: a novel ingredient in spray-dried soy beverage formulation. *Int J Biol Macromol* 102:297–307
- Castel V, Rubiolo AC, Carrara CR (2018) Improvement of emulsifying properties of Brea gum by controlled thermal treatment. *Food Hydrocoll* 85:93–101
- Chen H, Qiu S, Gan J, Liu Y, Zhu Q, Yin L (2016a) New insights into the functionality of protein to the emulsifying properties of sugar beet pectin. *Food Hydrocoll* 57:262–270
- Chen L, Chen J, Wu K, Yu L (2016b) Improved low pH emulsification properties of glycosylated peanut protein isolate by ultrasound Maillard reaction. *J Agric Food Chem* 64(27):5531–5538
- Chen H, Ji A, Qiu S, Liu Y, Zhu Q, Yin L (2018) Covalent conjugation of bovine serum albumin and sugar beet pectin through Maillard reaction/laccase catalysis to improve the emulsifying properties. *Food Hydrocoll* 76:173–183
- Chen B, Hu Z, Li H, Li Z, Li Q, Chen Y (2019) Intact starch granules for pickering emulsion: exploring mechanism of cleaning with washing rice water and floury soup. *Colloids Surf A* 561:155–164
- Cheng YH, Tang WJ, Xu Z, Wen L, Chen ML (2018) Structure and functional properties of rice protein–dextran conjugates prepared by the Maillard reaction. *Int J Food Sci Technol* 53(2):372–380
- Cheng J, Dudu OE, Li X, Yan T (2020) Effect of emulsifier-fat interactions and interfacial competitive adsorption of emulsifiers with proteins on fat crystallization and stability of whipped-frozen emulsions. *Food Hydrocoll* 101:105491
- Chevalier Y, Bolzinger M-A (2013) Emulsions stabilized with solid nanoparticles: Pickering emulsions. *Colloids Surf A* 439:23–34
- Chevallier M, Riaublanc A, Cauty C, Hamon P, Rousseau F, Thevenot J, Lopez C, Croguennec T (2019) The repartition of whey protein microgels and caseins between fat droplet surface and the continuous phase governs the heat stability of emulsions. *Colloids Surf A* 563:217–225
- Cirre J, Al-Assaf S, Phillips GO, Yadav MP, Hicks KB (2014) Improved emulsification performance of corn fibre gum following maturation treatment. *Food Hydrocoll* 35:122–128
- Dai L, Zhan X, Wei Y, Sun C, Mao L, McClements DJ, Gao Y (2018) Composite zein - propylene glycol alginate particles prepared using solvent evaporation: characterization and application as Pickering emulsion stabilizers. *Food Hydrocoll* 85:281–290
- Dai L, Yang S, Wei Y, Sun C, McClements DJ, Mao L, Gao Y (2019) Development of stable high internal phase emulsions by pickering stabilization: utilization of zein-propylene glycol alginate-rhamnolipid complex particles as colloidal emulsifiers. *Food Chem* 275:246–254
- Davis S, Round H, Purewal T (1981) Ostwald ripening and the stability of emulsion systems: an explanation for the effect of an added third component. *J Colloid Interface Sci* 80(2):508–511
- Daw E, Hartel R (2015) Fat destabilization and melt-down of ice creams with increased protein content. *Int Dairy J* 43:33–41
- de Almeida Paula D, Mota Ramos A, Basílio de Oliveira E, Maurício Furtado Martins E, Augusto Ribeiro de Barros F, Cristina Teixeira Ribeiro Vidigal M, de Almeida Costa N, Tatagiba da Rocha C (2018) Increased thermal stability of anthocyanins at pH 4.0 by guar gum in aqueous dispersions and in double emulsions W/O/W. *Int J Biol Macromol* 117:665–672
- de Folter JW, van Ruijven MW, Velikov KP (2012) Oil-in-water Pickering emulsions stabilized by colloidal particles from the water-insoluble protein zein. *Soft Matter* 8(25):6807–6815
- Dickinson E (2008) Interfacial structure and stability of food emulsions as affected by protein–polysaccharide interactions. *Soft Matter* 4(5):932–942
- Dickinson E (2009) Hydrocolloids and emulsion stability. In: *Handbook of hydrocolloids*. Elsevier, Cambridge, pp 23–49
- Dickinson E (2012) Emulsion gels: the structuring of soft solids with protein-stabilized oil droplets. *Food Hydrocoll* 28(1):224–241

- Dickinson E (2013) Stabilising emulsion-based colloidal structures with mixed food ingredients. *J Sci Food Agric* 93(4):710–721
- Dickinson E, Casanova H (1999) A thermoreversible emulsion gel based on sodium caseinate. *Food Hydrocoll* 13(4):285–289
- Dickinson E, Lopez G (2001) Comparison of the emulsifying properties of fish gelatin and commercial milk proteins. *J Food Sci* 66(1):118–123
- Ding R, Valicka E, Akhtar M, Ettelaie R (2017) Insignificant impact of the presence of lactose impurity on formation and colloid stabilising properties of whey protein–maltodextrin conjugates prepared via Maillard reactions. *Food Struct* 12:43–53
- Esfanjani AF, Jafari SM, Assadpoor E, Mohammadi A (2015) Nano-encapsulation of saffron extract through double-layered multiple emulsions of pectin and whey protein concentrate. *J Food Eng* 165:149–155
- Euston S, Finnigan S, Hirst R (2000) Aggregation kinetics of heated whey protein-stabilized emulsions. *Food Hydrocoll* 14(2):155–161
- Farshi P, Tabibiazar M, Ghorbani M, Mohammadifar M, Amirkhiz MB, Hamishehkar H (2019) Whey protein isolate-guar gum stabilized cumin seed oil nanoemulsion. *Food Biosci* 28:49–56
- Freire M, Cofrades S, Pérez-Jiménez J, Gómez-Estaca J, Jiménez-Colmenero F, Bou R (2018) Emulsion gels containing n-3 fatty acids and condensed tannins designed as functional fat replacers. *Food Res Int* 113:465–473
- Funami T, Nakauma M, Ishihara S, Tanaka R, Inoue T, Phillips GO (2011) Structural modifications of sugar beet pectin and the relationship of structure to functionality. *Food Hydrocoll* 25(2):221–229
- Garti N, Reichman D (1993) Hydrocolloids as food emulsifiers and stabilizers. *Food Struct* 12(4):3
- Garti N, Reichman D (1994) Surface properties and emulsification activity of galactomannans. *Food Hydrocoll* 8(2):155–173
- Gharehbeiglou P, Jafari SM, Hamishekar H, Homayouni A, Mirzaei H (2019) Pectin-whey protein complexes vs. small molecule surfactants for stabilization of double nano-emulsions as novel bioactive delivery systems. *J Food Eng* 245:139–148
- Given PS Jr (2009) Encapsulation of flavors in emulsions for beverages. *Curr Opin Colloid Interface Sci* 14(1):43–47
- Golchoobi L, Alimi M, Shokoobi S, Yousefi H (2016) Interaction between nanofibrillated cellulose with guar gum and carboxy methyl cellulose in low-fat mayonnaise. *J Texture Stud* 47(5):403–412
- Gómez-Luría D, Vernon-Carter EJ, Alvarez-Ramirez J, Cruz-Sosa F (2019) Insights of the ability of gelatinized fractions from non-chemical modified corn, rice, wheat, and waxy corn starches to stabilize O/W emulsions. *Food Hydrocoll* 89:726–734
- Guo Q, Bellissimo N, Rousseau D (2017) Role of gel structure in controlling in vitro intestinal lipid digestion in whey protein emulsion gels. *Food Hydrocoll* 69:264–272
- Hamdani AM, Wani IA, Bhat NA, Siddiqi RA (2018) Effect of guar gum conjugation on functional, antioxidant and antimicrobial activity of egg white lysozyme. *Food Chem* 240:1201–1209
- Hou C, Wu S, Xia Y, Phillips GO, Cui SW (2017) A novel emulsifier prepared from Acacia seyal polysaccharide through Maillard reaction with casein peptides. *Food Hydrocoll* 69:236–241
- Hu B, Han L, Kong H, Nishinari K, Phillips GO, Yang J, Fang Y (2019) Preparation and emulsifying properties of trace elements fortified gum arabic. *Food Hydrocoll* 88:43–49
- Imeson A (2011) Microcrystalline cellulose. In: *Food stabilisers, thickeners and gelling agents*. Wiley, New York, p 23
- Jafari SM, McClements DJ (2018) *Nanoemulsions: formulation, applications, and characterization*. Academic Press, Cambridge
- Javidi F, Razavi SM (2019) New hydrocolloids in ice cream. *Emerging natural hydrocolloids: rheology and functions*, pp 525–547
- Javidi F, Razavi SM, Amini AM (2019) Cornstarch nanocrystals as a potential fat replacer in reduced fat O/W emulsions: a rheological and physical study. *Food Hydrocoll* 90:172–181

- Jia X, Chen Y, Shi C, Ye Y, Abid M, Jabbar S, Wang P, Zeng X, Wu T (2014) Rheological properties of an amorphous cellulose suspension. *Food Hydrocoll* 39:27–33
- Kabal'Nov A, Pertzov A, Shechukin E (1987) Ostwald ripening in two-component disperse phase systems: application to emulsion stability. *Colloids Surf* 24(1):19–32
- Kalashnikova I, Bizot H, Cathala B, Capron I (2011) New Pickering emulsions stabilized by bacterial cellulose nanocrystals. *Langmuir* 27(12):7471–7479
- Kasprzak MM, Macnaughtan W, Harding S, Wilde P, Wolf B (2018) Stabilisation of oil-in-water emulsions with non-chemical modified gelatinised starch. *Food Hydrocoll* 81:409–418
- Kimpel F, Schmitt JJ (2015) Review: milk proteins as nanocarrier systems for hydrophobic nutraceuticals. *J Food Sci* 80(11):R2361–R2366
- Klein M, Aserin A, Svitov I, Garti N (2010) Enhanced stabilization of cloudy emulsions with gum Arabic and whey protein isolate. *Colloids Surf B* 77(1):75–81
- Koch L, Hummel L, Schuchmann H, Emin M (2017) Structural changes and functional properties of highly concentrated whey protein isolate-citrus pectin blends after defined, high temperature treatments. *LWT-Food Sci Technol* 84:634–642
- Kuroiwa T, Kobayashi I, Chuah AM, Nakajima M, Ichikawa S (2015) Formulation and stabilization of nano-/microdispersion systems using naturally occurring edible polyelectrolytes by electrostatic deposition and complexation. *Adv Colloid Interface Sci* 226:86–100
- Li J, Xu X, Chen Z, Wang T, Lu Z, Hu W, Wang L (2018) Zein/gum Arabic nanoparticle-stabilized pickering emulsion with thymol as an antibacterial delivery system. *Carbohydr Polym* 200:416–426
- Li S, Zhang B, Tan CP, Li C, Fu X, Huang Q (2019) Octenylsuccinate quinoa starch granule-stabilized pickering emulsion gels: preparation, microstructure and gelling mechanism. *Food Hydrocoll* 91:40–47
- Liu F, Ma C, McClements DJ, Gao Y (2016) Development of polyphenol-protein-polysaccharide ternary complexes as emulsifiers for nutraceutical emulsions: impact on formation, stability, and bioaccessibility of  $\beta$ -carotene emulsions. *Food Hydrocoll* 61:578–588
- Liu C, An F, He H, He D, Wang Y, Song H (2018) Pickering emulsions stabilized by compound modified areca taro (*Colocasia esculenta* (L.) Schott) starch with ball-milling and OSA. *Colloids Surf A* 556:185–194
- Lobo L (2002) Coalescence during emulsification: 3. Effect of gelatin on rupture and coalescence. *J Colloid Interface Sci* 254(1):165–174
- Lu X, Wang Y, Li Y, Huang Q (2018) Assembly of pickering emulsions using milled starch particles with different amylose/amylopectin ratios. *Food Hydrocoll* 84:47–57
- Luo N, Ye A, Wolber FM, Singh H (2019) Structure of whey protein emulsion gels containing capsaicinoids: impact on in-mouth breakdown behaviour and sensory perception. *Food Hydrocoll* 92:19–29
- Mantovani RA, Cavallieri ÂLF, Cunha RL (2016) Gelation of oil-in-water emulsions stabilized by whey protein. *J Food Eng* 175:108–116
- Marefati A, Sjöö M, Timgren A, Dejmek P, Rayner M (2015) Fabrication of encapsulated oil powders from starch granule stabilized W/O/W Pickering emulsions by freeze-drying. *Food Hydrocoll* 51:261–271
- McClements D (2000) Comments on viscosity enhancement and depletion flocculation by polysaccharides. *Food Hydrocoll* 14(2):173–177
- McClements DJ (2010) Emulsion design to improve the delivery of functional lipophilic components. *Annu Rev Food Sci Technol* 1:241–269
- McClements DJ (2012) Nanoemulsions versus microemulsions: terminology, differences, and similarities. *Soft Matter* 8(6):1719–1729
- McClements DJ (2015) *Food emulsions: principles, practices, and techniques*. CRC Press, Boca Raton
- McClements D, Decker E (2000) Lipid oxidation in oil-in-water emulsions: impact of molecular environment on chemical reactions in heterogeneous food systems. *J Food Sci* 65(8):1270–1282

- McIntyre I, Osullivan M, Oriordan D (2017) Altering the level of calcium changes the physical properties and digestibility of casein-based emulsion gels. *Food Funct* 8(4):1641–1651
- Mei L, Decker EA, McClements DJ (1998) Evidence of iron association with emulsion droplets and its impact on lipid oxidation. *J Agric Food Chem* 46(12):5072–5077
- Mengfābar M, Miralles B, Heras Á (2017) Use of soluble chitosans in Maillard reaction products with  $\beta$ -lactoglobulin. Emulsifying and antioxidant properties. *LWT-Food Sci Technol* 75:440–446
- Milani J, Maleki G (2012) Hydrocolloids in food industry. In: *Food industrial processes-methods and equipment*. IntechOpen, London
- Moradi S, Anarjan N (2018) Preparation and characterization of  $\alpha$ -tocopherol nanocapsules based on gum Arabic-stabilized nanoemulsions. *Food Sci Biotechnol* 28(2):413–421
- Mora-Gutierrez A, Attaie R, de González MN, Jung Y, Woldesenbet S, Marquez S (2018) Complexes of lutein with bovine and caprine caseins and their impact on lutein chemical stability in emulsion systems: effect of arabinogalactan. *J Dairy Sci* 101(1):18–27
- Moro A, Báez GD, Ballerini GA, Busti PA, Delorenzi NJ (2013) Emulsifying and foaming properties of  $\beta$ -lactoglobulin modified by heat treatment. *Food Res Int* 51(1):1–7
- Morr C, Ha E (1993) Whey protein concentrates and isolates: processing and functional properties. *Crit Rev Food Sci Nutr* 33(6):431–476
- Moschakis T, Chantzos N, Biliaderis CG, Dickinson E (2018) Microrheology and microstructure of water-in-water emulsions containing sodium caseinate and locust bean gum. *Food Funct* 9(5):2840–2852
- Murray BS, Phisarnchananan N (2016) Whey protein microgel particles as stabilizers of waxy corn starch + locust bean gum water-in-water emulsions. *Food Hydrocoll* 56:161–169
- Nsor-Atindana J, Chen M, Goff HD, Zhong F, Sharif HR, Li Y (2017) Functionality and nutritional aspects of microcrystalline cellulose in food. *Carbohydr Polym* 172:159–174
- Pang B, Liu H, Liu P, Peng X, Zhang K (2018) Water-in-oil pickering emulsions stabilized by stearoylated microcrystalline cellulose. *J Colloid Interface Sci* 513:629–637
- Perusko M, Al-Hanish A, Velickovic TC, Stanic-Vucinic D (2015) Macromolecular crowding conditions enhance glycation and oxidation of whey proteins in ultrasound-induced Maillard reaction. *Food Chem* 177:248–257
- Pintado T, Herrero AM, Jiménez-Colmenero F, Cavalheiro CP, Ruiz-Capillas C (2018) Chia and oat emulsion gels as new animal fat replacers and healthy bioactive sources in fresh sausage formulation. *Meat Sci* 135:6–13
- Piorkowski DT, McClements DJ (2014) Beverage emulsions: recent developments in formulation, production, and applications. *Food Hydrocoll* 42:5–41
- Pirestani S, Nasirpour A, Keramat J, Desobry S, Jasniewski J (2017) Effect of glycosylation with gum Arabic by Maillard reaction in a liquid system on the emulsifying properties of canola protein isolate. *Carbohydr Polym* 157:1620–1627
- Piriyaprasarth S, Juttulapa M, Sriamornsak P (2016) Stability of rice bran oil-in-water emulsions stabilized by pectin-zein complexes: effect of composition and order of mixing. *Food Hydrocoll* 61:589–598
- Purwanti N, Ichikawa S, Neves MA, Uemura K, Nakajima M, Kobayashi I (2016)  $\beta$ -lactoglobulin as food grade surfactant for clove oil-in-water and limonene-in-water emulsion droplets produced by microchannel emulsification. *Food Hydrocoll* 60:98–108
- Qiu J, Zheng Q, Fang L, Wang Y, Min M, Shen C, Tong Z, Xiong C (2018) Preparation and characterization of casein-carrageenan conjugates and self-assembled microcapsules for encapsulation of red pigment from paprika. *Carbohydr Polym* 196:322–331
- Radford SJ, Dickinson E, Golding M (2004) Stability and rheology of emulsions containing sodium caseinate: combined effects of ionic calcium and alcohol. *J Colloid Interface Sci* 274(2):673–686
- Randall R, Phillips G, Williams P (1989) Fractionation and characterization of gum from Acacia senegal. *Food Hydrocoll* 3(1):65–75



- Rao J, McClements DJ (2010) Stabilization of phase inversion temperature nanoemulsions by surfactant displacement. *J Agric Food Chem* 58(11):7059–7066
- Rather SA, Masoodi FA, Akhter R, Rather JA, Amin F (2017) Effects of guar gum as a fat substitute in low fat meat emulsions. *J Food Process Preserv* 41(6):e13249
- Reichman D, Garti N (1991) Galactomannans as emulsifiers. In: *Food polymers, gels and colloids*. Elsevier, Cambridge, pp 549–556
- Roman JA, Sgarbieri VC (2006) The hydrophilic, foaming and emulsifying properties of casein concentrates produced by various methods. *Int J Food Sci Technol* 41(6):609–617
- Saari H, Rayner M, Wahlgren M (2019) Effects of starch granules differing in size and morphology from different botanical sources and their mixtures on the characteristics of pickering emulsions. *Food Hydrocoll* 89:844–855
- Sarkar A, Murray B, Holmes M, Ettelaie R, Abdalla A, Yang X (2016) In vitro digestion of Pickering emulsions stabilized by soft whey protein microgel particles: influence of thermal treatment. *Soft Matter* 12(15):3558–3569
- Sato ACK, Perrechil FA, Costa AAS, Santana RC, Cunha RL (2015) Cross-linking proteins by laccase: effects on the droplet size and rheology of emulsions stabilized by sodium caseinate. *Food Res Int* 75:244–251
- Siew CK, Williams PA, Cui SW, Wang Q (2008) Characterization of the surface-active components of sugar beet pectin and the hydrodynamic thickness of the adsorbed pectin layer. *J Agric Food Chem* 56(17):8111–8120
- Silva JVC, Jacqueline B, Amagliani L, Schmitt C, Nicolai T, Chassenieux C (2019) Heat-induced gelation of micellar casein/plant protein oil-in-water emulsions. *Colloids Surf A* 569:85–92
- Sivapratha S, Sarkar P (2018) Multiple layers and conjugate materials for food emulsion stabilization. *Crit Rev Food Sci Nutr* 58(6):877–892
- Solans C, Izquierdo P, Nolla J, Azemar N, Garcia-Celma M (2005) Nano-emulsions. *Curr Opin Colloid Interface Sci* 10(3–4):102–110
- Stanic-Vucinic D, Prodic I, Apostolovic D, Nikolic M, Velickovic TC (2013) Structure and antioxidant activity of  $\beta$ -lactoglobulin-glycoconjugates obtained by high-intensity-ultrasound-induced Maillard reaction in aqueous model systems under neutral conditions. *Food Chem* 138(1):590–599
- Sun C, Gao Y, Zhong Q (2018) Properties of ternary biopolymer nanocomplexes of zein, sodium caseinate, and propylene glycol alginate and their functions of stabilizing high internal phase Pickering emulsions. *Langmuir* 34(31):9215–9227
- Surh J, Gu YS, Decker EA, McClements DJ (2005) Influence of environmental stresses on stability of O/W emulsions containing cationic droplets stabilized by SDS– fish gelatin membranes. *J Agric Food Chem* 53(10):4236–4244
- Surh J, Decker EA, McClements DJ (2006) Properties and stability of oil-in-water emulsions stabilized by fish gelatin. *Food Hydrocoll* 20(5):596–606
- Taherian AR, Britten M, Sabik H, Fustier P (2011) Ability of whey protein isolate and/or fish gelatin to inhibit physical separation and lipid oxidation in fish oil-in-water beverage emulsion. *Food Hydrocoll* 25(5):868–878
- Tan C-T (2004) Beverage emulsions. In: *Food emulsions*, 4th edn. CRC Press, Boca Raton, pp 485–524
- Tan HL, McGrath KM (2012) Na-caseinate/oil/water systems: emulsion morphology diagrams. *J Colloid Interface Sci* 381(1):48–58
- Taylor P (1998) Ostwald ripening in emulsions. *Adv Colloid Interface Sci* 75(2):107–163
- Temenouga V, Charitidis T, Avgidou M, Karayannakidis P, Dimopoulou M, Kalogianni E, Panayiotou C, Ritzoulis C (2016) Novel emulsifiers as products from internal Maillard reactions in okra hydrocolloid mucilage. *Food Hydrocoll* 52:972–981
- Timngren A, Rayner M, Sjöö M, Dejmeck P (2011) Starch particles for food based Pickering emulsions. *Procedia Food Sci* 1:95–103
- Torres O, Tena NM, Murray B, Sarkar A (2017) Novel starch based emulsion gels and emulsion microgel particles: design, structure and rheology. *Carbohydr Polym* 178:86–94

- Wang LJ, Hu YQ, Yin SW, Yang XQ, Lai FR, Wang SQ (2015) Fabrication and characterization of antioxidant pickering emulsions stabilized by zein/chitosan complex particles (ZCPs). *J Agric Food Chem* 63(9):2514–2524
- Wang L, Wu M, Liu H-M (2017) Emulsifying and physicochemical properties of soy hull hemicelluloses-soy protein isolate conjugates. *Carbohydr Polym* 163:181–190
- Wang P, Chen C, Guo H, Zhang H, Yang Z, Ren F (2018a) Casein gel particles as novel soft pickering stabilizers: the emulsifying property and packing behaviour at the oil-water interface. *Food Hydrocoll* 77:689–698
- Wang Y, Wang W, Jia H, Gao G, Wang X, Zhang X, Wang Y (2018b) Using cellulose nanofibers and its palm oil pickering emulsion as fat substitutes in emulsified sausage. *J Food Sci* 83(6):1740–1747
- Wang Y, Gan J, Li Y, Nirasawa S, Cheng Y (2019) Conformation and emulsifying properties of deamidated wheat gluten-maltodextrin/citrus pectin conjugates and their abilities to stabilize  $\beta$ -carotene emulsions. *Food Hydrocoll* 87:129–141
- Wefers D, Bindereif B, Karbstein H, van der Schaaf U (2018) Whey protein-pectin conjugates: linking the improved emulsifying properties to molecular and physico-chemical characteristics. *Food Hydrocoll* 85:257–266
- Weng J, Qi J, Yin S, Wang J, Guo J, Feng J, Liu Q, Zhu J, Yang X (2016) Fractionation and characterization of soy  $\beta$ -conglycinin–dextran conjugates via macromolecular crowding environment and dry heating. *Food Chem* 196:1264–1271
- Williams PA, Sayers C, Viebke C, Senan C, Mazoyer J, Boulenguer P (2005) Elucidation of the emulsification properties of sugar beet pectin. *J Agric Food Chem* 53(9):3592–3597
- Wu J, Shi M, Li W, Zhao L, Wang Z, Yan X, Norde W, Li Y (2015) Pickering emulsions stabilized by whey protein nanoparticles prepared by thermal cross-linking. *Colloids Surf B* 127:96–104
- Xu D, Zhang J, Cao Y, Wang J, Xiao J (2016) Influence of microcrystalline cellulose on the microrheological property and freeze-thaw stability of soybean protein hydrolysate stabilized curcumin emulsion. *LWT – Food Sci Technol* 66:590–597
- Xue F, Wu Z, Tong J, Zheng J, Li C (2017) Effect of combination of high-intensity ultrasound treatment and dextran glycosylation on structural and interfacial properties of buckwheat protein isolates. *Biosci Biotechnol Biochem* 81(10):1891–1898
- Zeeb B, Fischer L, Weiss J (2011) Cross-linking of interfacial layers affects the salt and temperature stability of multilayered emulsions consisting of fish gelatin and sugar beet pectin. *J Agric Food Chem* 59(19):10546–10555
- Zhang C, Feng F, Zhang H (2018) Emulsion electrospinning: fundamentals, food applications and prospects. *Trends Food Sci Technol* 80:175–186
- Zhu Q, Lu H, Zhu J, Zhang M, Yin L (2019) Development and characterization of pickering emulsion stabilized by zein/corn fiber gum (CFG) complex colloidal particles. *Food Hydrocoll* 91:204–213
- Zou Y, Guo J, Yin S-W, Wang J-M, Yang X-Q (2015) Pickering emulsion gels prepared by hydrogen-bonded zein/tannic acid complex colloidal particles. *J Agric Food Chem* 63(33):7405–7414
- Zou Y, Yang X, Scholten E (2019) Tuning particle properties to control rheological behavior of high internal phase emulsion gels stabilized by zein/tannic acid complex particles. *Food Hydrocoll* 89:163–170

# Chapter 6

## Liquid Foaming Properties



Yongguang Guan

**Abstract** Liquid foams are thermodynamically unstable colloidal systems with a vapor phase incorporated in a continuous phase, which can be considered as a composition of gas, foaming agents, and liquid. In this chapter, the foam formation and microstructure were firstly introduced to understand foaming processes and basic structural components in a foam system. Then, the foam instability mechanisms comprising drainage, coalescence, and disproportionation were introduced with an insight into the factors of floatation, coalescence, and Ostwald ripening for foam destabilization. Afterwards, the foam colloidal and functional properties including foam ability, foam stability, and stabilization strategies focusing on improving foam overrun and mean life by employing various foaming agents such as proteins, polysaccharides, and Pickering fine particles were discussed. Finally, potential applications of stable liquid foams in food industry manufactures of ice cream, beer, bread, food-grade packages, and foam-mats were illustrated. We expect this chapter may provide fundamental knowledge for readers to better understand food-grade liquid foams.

**Keywords** Liquid foam · Interface · Thin film · Foaming agents · Foam stability

### 1 Formation and Microstructure

Liquid foam is a multiscale system composed of gas, foaming agents, and liquid. Its formation is governed by transportation, penetration, and reorganization of the molecules at the gas–liquid interface, depending on surfactant size, surface viscoelasticity, and conformational flexibility (Wilde and Clark 1993). In foaming

---

Y. Guan (✉)

Department of Food Science and Engineering, School of Agriculture and Biology, Shanghai Jiao Tong University, Shanghai, China  
e-mail: [yguan@sjtu.edu.cn](mailto:yguan@sjtu.edu.cn)

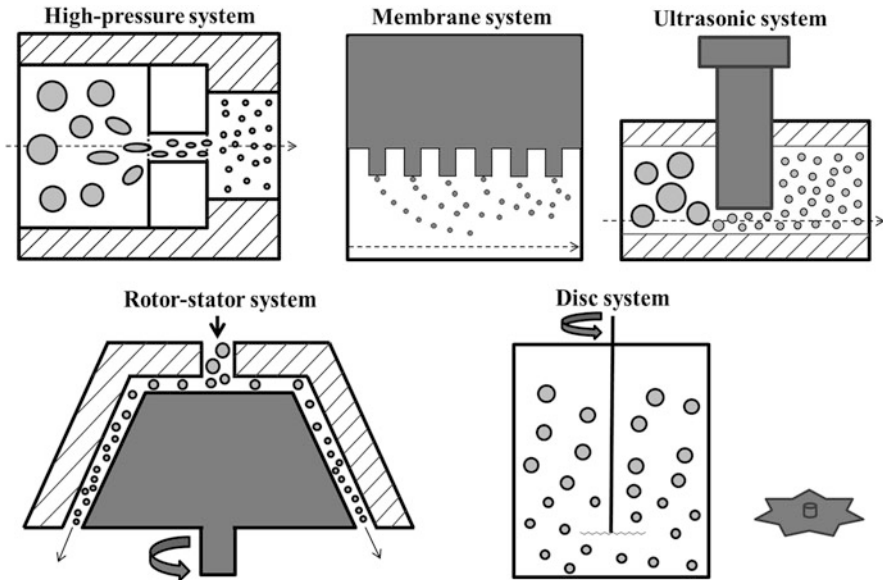


**Fig. 6.1** High-energy emulsifiers and homogenizers used for foam preparation. Gray circles and ovals denote gas in bubbles. This figure is plotted referring the work from Urban and co-workers (Urban et al. 2006)

processes such as employing high pressure, membrane, ultrasound, rotor-stator homogenizer, and disc whipper (introduced by Urban and co-workers (Urban et al. 2006) and shown in Fig. 6.1), energy is supplied from mixer into liquid to incorporate gas and, therefore, forms a cohesive gas–liquid interfacial layer (Djelveh and Gros 1995), which tears large bubbles to smaller ones primarily through simple shear flow and elongational flow (Fig. 6.2). After these foaming processes, two major foams, i.e., bubbly and polyhedral foams are fabricated (Fig. 6.3). The liquid bubbly foam is determined to be stable only in a high viscosity system such as syrup at high concentrations. Meanwhile, the polyhedral foam is considered to be generated through the bubble floatation originated from the initial bubbly foam (Fig. 6.4). A whole polyhedral foam structure can be denoted in Fig. 6.5, the separated gas–liquid system by surfactants supports foam with disperse phase of gas in bubbles and continuous phase of liquid in thin film. Moreover, the two adjacent interfacial layers and intermediate thin film (or thin liquid film) constitute a lamella (Wasan and Nikolov 2008). Although most of the surfactants, i.e., the surface active agents such as proteins and polysaccharides, are always adsorbed at the gas–liquid interface to decrease the interfacial tension, a portion of them can be presented in thin film (Wasan and Nikolov 2008), which is likely to form gel-like network. Thus, from a colloidal viewpoint, the stable liquid foam can be seen as a complex soft condensed matter rather than a simple solid, liquid, or gas. In this case, the interaction forces among bubbles are primary normal stresses without tangential forces (Labiausse

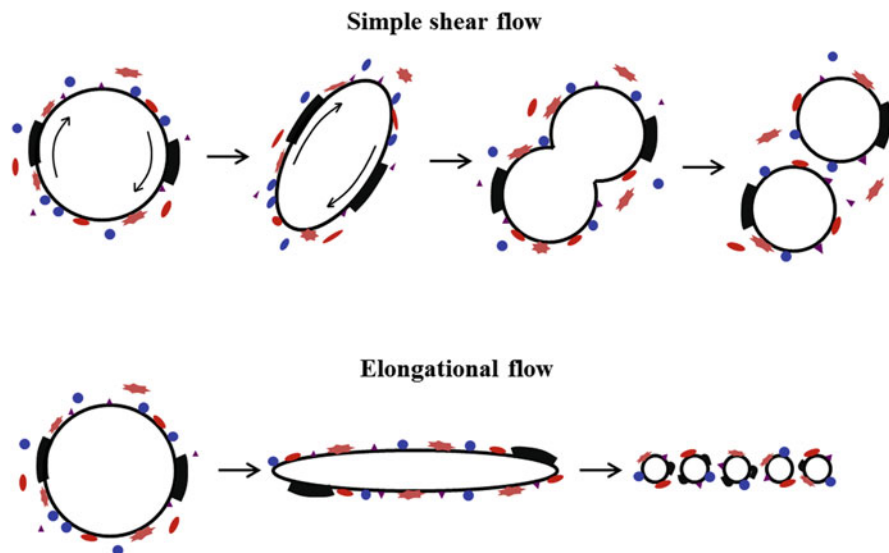


**Fig. 6.2** Two types of foam breakup through simple shear flow and elongational flow. Circles and ovals denote gas in bubbles. Particles with different shapes and colors were shown at the interfaces of bubbles

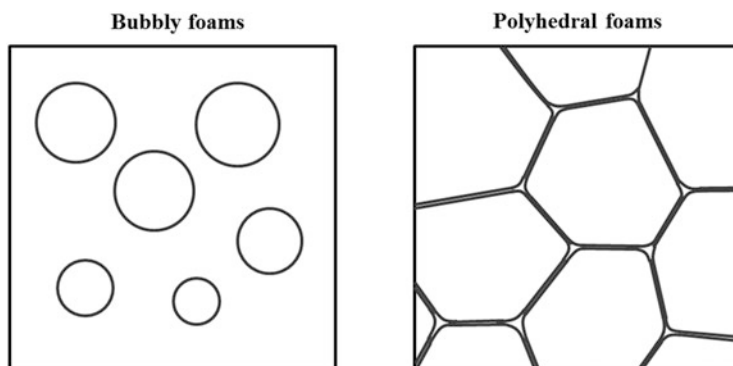


**Fig. 6.3** Two foam types, i.e., bubbly and polyhedral foams. Circles and polygons denote gas in bubbles

et al. 2007). The whole structure of foam follows the Plateau's equilibrium law, that is, four bubbles form a basic unit with one intersection, and each three bubbles constitute a Plateau border (Weaire and Fortes 1994). The curvature radius of a Plateau border is 10 nm to 1 mm depending on the synergetic interaction of liquid fraction, surface tension, and interfacial forces. The length of a Plateau border is approximately one-third of bubble diameter. The thin liquid film exists in two adjacent bubbles with the thickness of 0.01 nm to 1000 nm, which is the minimum distance among bubbles. The dihedral angles of two adjacent lamellae and Plateau

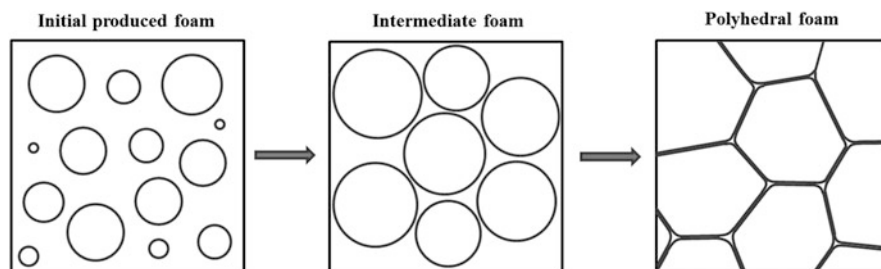


**Fig. 6.4** The formation pathway of polyhedral foam from the initial stage of bubbly foam generating an intermediate foam after floatation, coalescence, and even the Ostwald ripening (will be discussed below), and finally generating polyhedral foam. Circles and polygons denote gas in bubbles

borders are  $120^\circ$  and  $109.47^\circ$ , respectively (Stamenović 1991), which was elaborated by Weaire and Phelan (Weaire and Phelan 1996).

The morphologies of bubble interface membrane are formed attributing to the Laplace pressure primarily including compression driven force, phase separation, and buckling evolution, which generate various microstructures such as polygonal, bean, snowflake dendritic, and mesh structures. Electron microscopies can be used to observe bubble interfacial layer microstructures. For instance, a polygonal microstructure of the liquid foam membrane surface generated by gas in 1,2-distearoyl-sn-glycero-3-phosphatidylcholine monolayer was observed by the transmission electron microscopy (TEM). The evolutionary process of this polygonal microstructure was demonstrated by the transfer from a smooth microstructure in the initial stage of bubble formation to a wrinkling one during bubble storage attributing to the Laplace pressure (Kim et al. 2003). A regular hexagonal microstructure of elastic liquid foam membrane with equivalent diameter of 50–100 nm was also observed in a sucrose stearate-syrup homogeneous system. The formation of this hexagonal foam membrane microstructure is driven by the Laplace compression because of the mismatched curvature between the bubble core and the self-assembled surfactant membrane (Dressaire et al. 2008). Additionally, in a multi-agent foam system, phase separation is a main factor to generate diverse bubble interface membrane microstructures. The phase separation is mainly caused by the changes in temperature, shear rate, and liquid film viscosity (Borden et al. 2006, 2004), that is, the bubble interface diversity is attributed to the classical interface compression mechanism. For example, the L- $\alpha$ -1,2-dipalmitoyl-sn-glycero-3-phosphocholine (DPPC) can be isolated from the liquid foam system with multiple mixed surfactants during membrane melting and cooling, generating bean microstructure after the compression of the Langmuir film (Nandi and Vollhardt 2003; McConlogue and Vanderlick 1997). In addition, unstable growth of crystal nucleus with limited diffusion behavior also appears in the process of viscous film quenching, forming snowflake dendritic microstructure of the bubble interface membrane (McKiernan et al. 2000). Repeated compression and expansion of the foam monolayer can promote the formation of reticular microstructure at the liquid foam membrane interface. For instance, with a

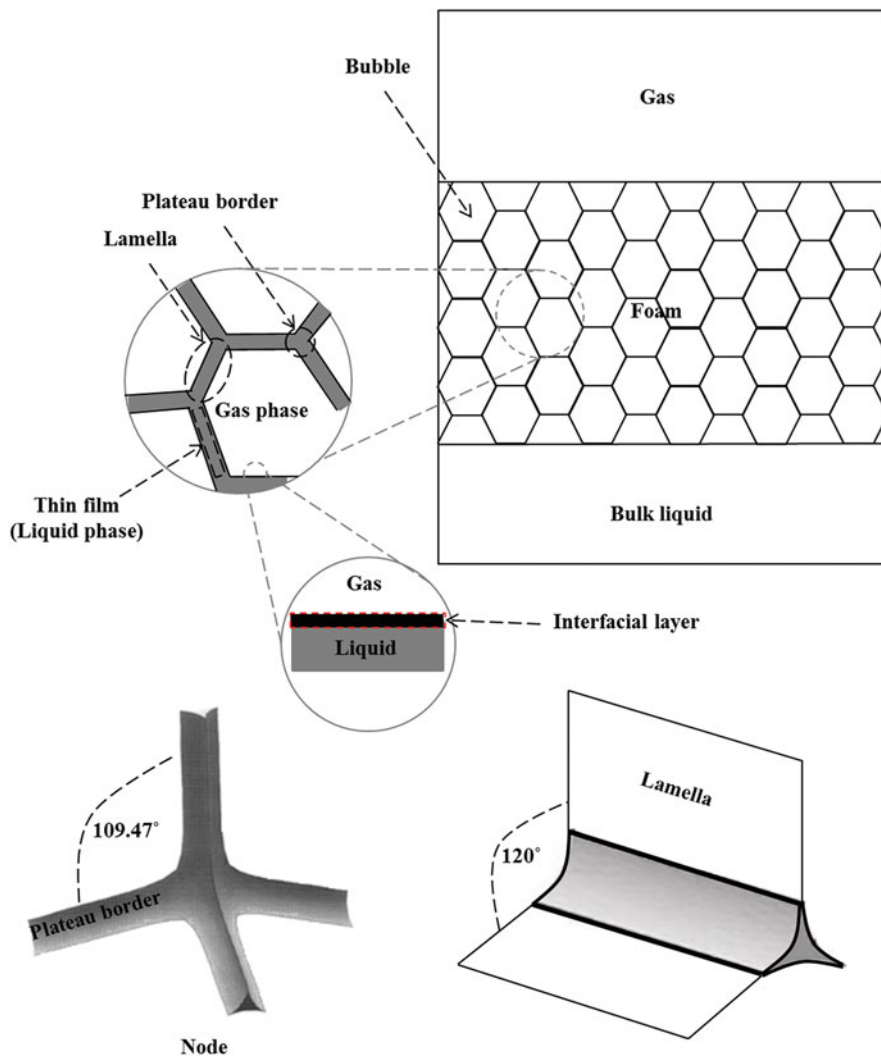


**Fig. 6.5** The simulated microstructure of bubble in liquid foam system is plotted referring the work of Weaire and Phelan (Weaire and Phelan 1996). Polygons denote gas in bubbles

rapid cooling under the ultrasonic treatment, the phospholipid cluster can interact with water molecules through hydrogen bonds, which further increases the foam membrane interface branch and therefore generates net membrane microstructure (Borden et al. 2004).

## 2 Instability of Foams

Liquid foams are thermodynamically unstable colloidal systems through floatation, coalescence, and Ostwald ripening to destabilize foams (Fig. 6.6) (Green et al. 2013), which is also denoted as three fundamental mechanisms, i.e., drainage, coalescence, and disproportionation (Horozov 2008).

### 2.1 Drainage

The drainage is a process that the lamella thickness becomes thin and consequently ruptures, attributing to the separated fluid between the thin film and bubble under the gravity due to the lighter density of bubble than liquid (Dickinson 1992). Once the liquid in the lamellae enters the Plateau borders, it will flow rapidly and be separated from thin liquid film caused by the drainage (Verbist et al. 1996; Rio et al. 2014). In a complete foam system, the drainage continues until the static pressure gradient in the gravity direction balances the gravitational acceleration. At this moment, the static pressure gradient is maintained by the disjoining pressure because of a very thin liquid film and therefore cannot further reduce the interfacial potential energy. The thickness of the thin liquid film is decreased following the height increase of the foam system (Verbist et al. 1996). The primary factor affecting discharge is thin liquid film characteristics, suggesting substances in the thin film with strong liquid holding capacity can slow down the drainage and increase the liquid foam stability (Verbist et al. 1996). A simulated diagram of drainage is plotted referring to published works (Weaire and Phelan 1996; Saint-Jalmes 2006) and shown in Fig. 6.7.

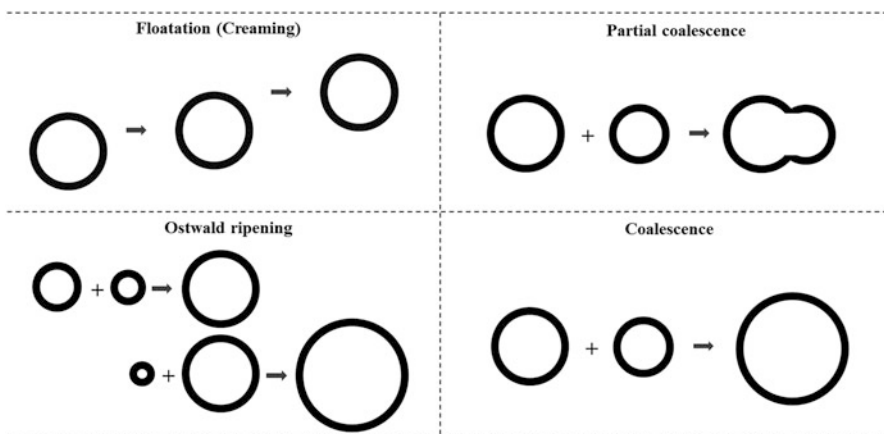


**Fig. 6.6** Schematic diagrams of unstable factors of floatation, coalescence, and Ostwald ripening for destabilizing foams. Circles denote gas in bubbles



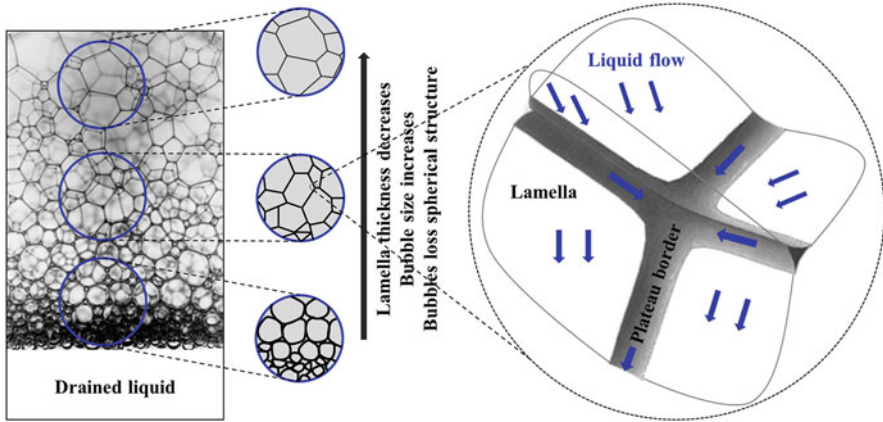


**Fig. 6.7** The simulated diagram of drainage is plotted referring published work (Weaire and Phelan 1996; Saint-Jalmes 2006), showing decreased lamella thickness, increased size, and losing spherical structure of bubbles with the increase in foam height, caused by the downward flow of liquid under the gravity, which suggests an accelerated rate of drainage when the liquid from the thin film of lamellae enters the Plateau borders

## 2.2 Coalescence

The coalescence is a process of bubble merging that a lamella between adjacent bubbles ruptures, causing the two bubbles combination, subsequent collapse, and loss of desirable structure and texture (Rio et al. 2014; Murray and Ettelaie 2004; Disalvo 1988; Marrucci 1969). A simulated bubble coalescence process is shown in Fig. 6.8. The coalescence is determined by the balance between capillary and disjoining pressures. That is, the disjoining pressure arises from forces between the two interfaces of the liquid lamella (Damodaran 2005; Oboroceanu et al. 2014), while the capillary pressure occurs because of the force between the gas and liquid phase, which is calculated by the Young–Laplace equation (Eq. 6.1, 6.2, and 6.3, Eq. 6.1, 6.2, and 6.3) (Lian et al. 1998; Thitakamol and Veawab 2009).

$$\Delta P = \gamma \left( \frac{1}{R} + \frac{1}{R'} \right) \quad (6.1)$$

$$2\pi x \gamma \sin\theta = V \Delta \rho g + \pi x^2 \Delta P \quad (6.2)$$

$$\Delta P = \frac{2\gamma}{R} \quad (6.3)$$

where  $\Delta P$  is the pressure difference between the inside and outside of a bubble at any point on the interface,  $\gamma$  is the surface tension,  $R$  and  $R'$  are the radii of curvature at the bubble apex,  $x$  is the Cartesian coordinate at any point of the bubble profile,  $\theta$  is the angle of the tangent to the bubble profile,  $V$  is the volume below a point plane,  $\Delta \rho$  is the difference of density between the two phases, and  $g$  is the gravitational

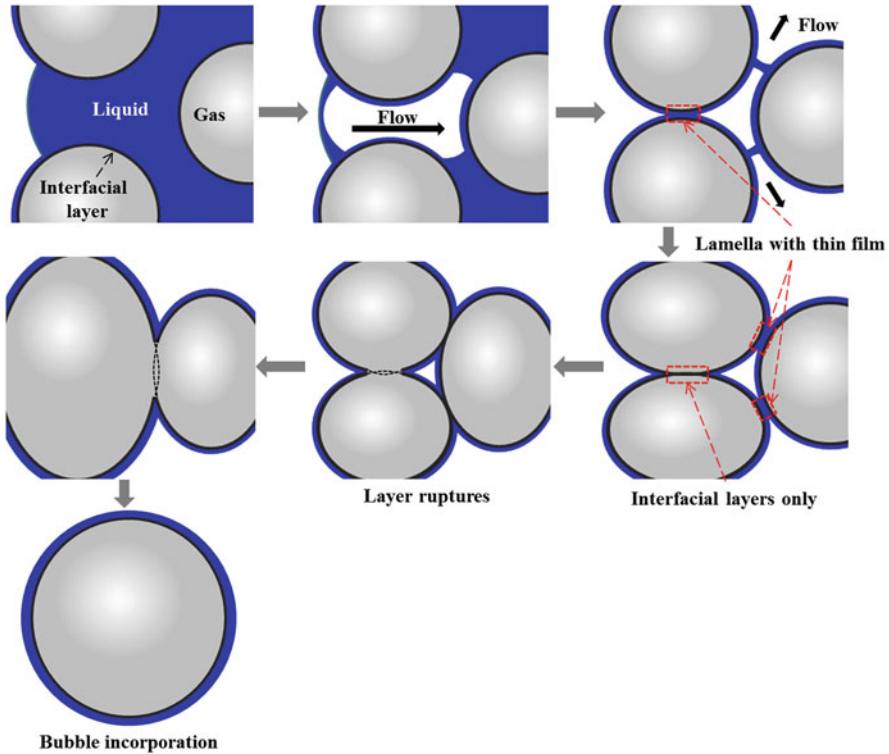


**Fig. 6.8** The simulated process of bubble coalescence suggests the thin film between two adjacent bubbles is dying out along with the loss of the liquid, a subsequent combination of interfacial layers, and a final rupture of the combined layer. This bubble coalescence process finally results in the incorporation of small bubbles to form big bubbles and collapses the foam structure. The dark blue ovals denote liquid. The grey circles and ovals denote gas in bubbles

acceleration. When the surface is a sphere,  $R$  is equal to  $R'$ , then Eq. 6.1 can be transferred to Eq. 6.3 (Thitakamol and Veawab 2009; Benjamins et al. 1996).

Furthermore, the main factors of the generated imbalance between capillary and disjoining pressures are the weaker surfactant molecular attraction against repulsive force and the lack of liquid fluidity in thin liquid film since the Marangoni effect (Marrucci 1969). An intact surfactant layer is capable of reducing the gas–liquid phase interfacial tension. However, when the intermolecular attraction among surfactants is weaker than the repulsive force, the originally compact surfactant layer is ruptured, leading to bubble coalescence. Additionally, as the lamellae of the adjacent bubbles are disturbed by external factors (e.g., temperature) to produce locally thinner liquid film, the flow of liquid in lamellae produced by the Marangoni effect will form the Marangoni flow under the surface tension gradient, restoring the thinner liquid film timely (Christenson and Yaminsky 1995). That is, the liquid rapidly moves from a lower bubble surface tension film along the tension gradient to

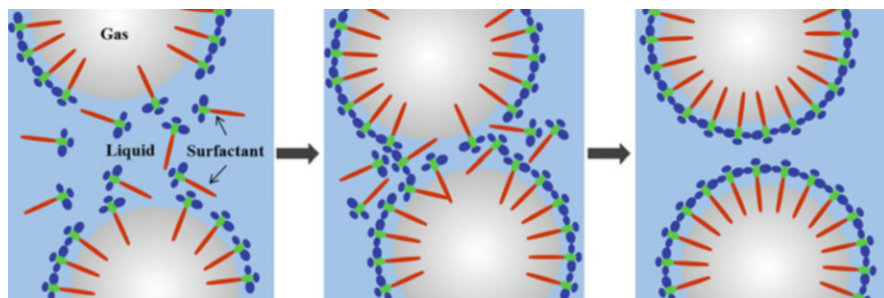


**Fig. 6.9** The simulated Marangoni effect denotes a protective effect of bubbles against coalescence through generating the Marangoni flow under the surface tension gradient and restoring the thinner liquid film timely. The light blue background denotes liquid, and gray circles denote gas in bubbles. The surfactants are denoted and composed of hydrophilic heads with dark blue and green ovals and hydrophobic chains with orange needles

a higher one (Fig. 6.9). However, when the fluid mobility of the liquid in thin film is decreased, the efficiency of restoring the thinner liquid film is therefore reduced, leading to the rupture of lamellae and bubble coalescence (Marrucci 1969).

### 2.3 Disproportionation

The disproportionation, driven by the difference of Laplace pressure between smaller and larger bubbles, is another important destabilization mechanism causing foam destabilization (Ettelaie et al. 2003). In foam disproportionation, gas molecules in high-energy smaller bubbles have higher solubility in liquid, and thereby are released in a single molecular form from original smaller bubbles (Fig. 6.10). The released gas molecules coalesce into larger bubbles until the foam reaches the minimum specific surface area and energy (Rio et al. 2014; Murray and Ettelaie 2004; Disalvo 1988). In an unstable foam system, the disproportionation becomes drastic as the dilatational modulus is larger than one-half of the surface tension (Rio et al. 2014; Murray and Ettelaie 2004). In addition, smaller bubbles have shorter curvature radius compared to bigger ones, which means the inner Laplace pressure of a smaller bubble is greater than that of a bigger one, although the Laplace pressure within bubbles also depends on the interfacial elasticity of the surfactant layers around the bubbles and their shrinkage extents. The Laplace pressure difference between smaller and bigger bubbles facilitates gas molecule diffusion from smaller to bigger bubbles driven by layer surface tension and finally reduces the specific surface area of gas–liquid interface. The disproportionation in foams is analogous to the Oswald ripening in emulsions but more dramatically caused by the smaller size of gas molecules with better liquid film permeability (Murray and Ettelaie 2004; Disalvo 1988).

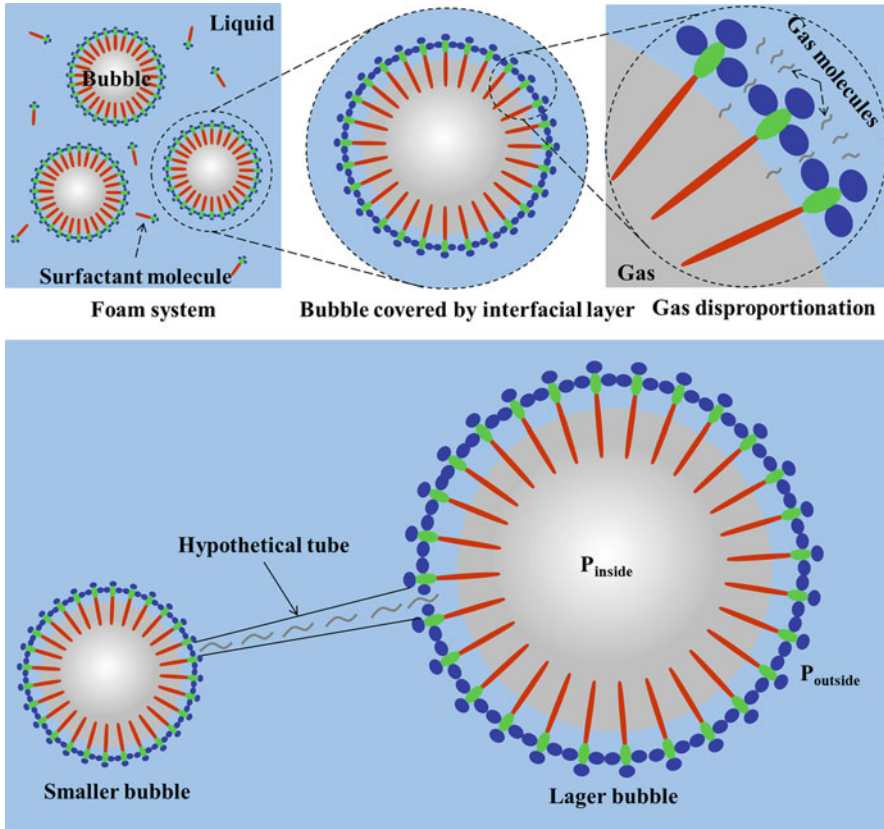


**Fig. 6.10** The simulated disproportionation suggests gas molecules can diffuse from bubble through the gap between surfactants of interfacial layer, leading to a decrease in original bubbles and therefore foam destabilization. The light blue background denotes liquid. The gray circles and curves denote gas in bubbles and gas molecules, respectively. The surfactants are denoted and composed of hydrophilic heads with dark blue and green ovals and hydrophobic chains with orange needles

Generally, the liquid foam drainage caused by gravity can be prevented when the static pressure gradient in the gravity direction is equal to the gravitational acceleration. Increasing the liquid holding capacity in thin film can significantly slow down the drainage (Bisperink et al. 1992; Narsimhan and Xiang 2018). The bubble coalescence caused by lamella rupture can be effectively inhibited by choosing appropriate interfacial stabilizer with stronger intermolecular attractions and surface activity (Lian et al. 1998; Christenson and Yaminsky 1995; Bisperink et al. 1992). The disproportionation is a very slow process and can be inhibited by building dense interfacial layer and stable thin liquid film (Ettelaie et al. 2003; Bisperink et al. 1992). However, a liquid foam system is always in thermodynamic non-equilibrium state, resulting in an unfulfillable complete prevention of gas molecule disproportionation (Kornev et al. 1999). That means the disproportionation is very difficult to

be prevented since even the well-packed interfacial layers at gas–liquid interface can only provide limited barriers against the gas diffusion through the transient gaps among surfactant molecules. The drainage, coalescence, and disproportionation synergistically disturb foam stability, showing time-dependent non-equilibrium characteristics. When drainage occurs, gas molecule diffusion from bubbles is facilitated by fluid flow in thin liquid film. While the disproportionation facilitates the coarsening of the bubble size, accelerating the drainage and coalescence.

### 3 Improvement of Foam Ability and Stability

#### 3.1 Physicochemical Characteristics

The foam ability and stability are two important parameters to evaluate the foaming properties. The foam ability is denoted as the percentage of overrun based on the volumes of fresh foam and totally whipped liquid, which can be expressed by Eq. 4 (Mitchell 1986).

$$\text{Overrun}(\%) = \frac{V_0 - V_1}{V_1} \times 100 \quad (6.4)$$

where  $V_0$  is the foam volume right after whipping, and  $V_1$  is the volume of liquid used for foaming. Higher overrun indicates a higher foam ability of the whipped materials.

The foam stability is calculated by an exponential decay law that the foam height is expressed in Eq. 6.5 and can be further expressed as an index of foam stability by the “mean life”  $\tau$  value that is used to evaluate the foam stand time and shown in Eq. 6 (Leike 2002).

$$H_t = H_0 \times e^{-\lambda t} \quad (6.5)$$

$$\tau = \frac{t}{\ln(H_t) - \ln(H_0)} \quad (6.6)$$

where  $H_t$  is the foam height after a storage time  $t$ , and  $H_0$  is the initial height of foam. The  $\lambda$  here is the foam decay constant. A larger  $\tau$  value means a more stable foam system.

The thermodynamics of foaming agent adsorbed layers at the gas–liquid interface can be expressed by the surface pressure isotherm, which is a relationship between the surface pressure and the foaming agent concentration (Patino et al. 2008). When using low molecular weight foaming agents, different supramolecular structures with covered gas are formed at a higher surfactant concentration than the critical micelle concentration (CMC). These bubbles built by low molecular weight agents show little repercussions on the surface pressure, and therefore, their surface

pressure isotherms are sensitive to temperature and pH (Patino et al. 2008; Niño and Patino 1998). The dependency between surface pressure and adsorption isotherms of foams prepared by biopolymers suggests a sigmoidal behavior, implying an increase in the surface pressure with biopolymer concentrations until tending to a plateau where the surface pressure reaches its maximum value over the range of biopolymer concentrations, which forms an irreversibly adsorbed monolayer or multilayer beneath the primary monolayer at the gas–liquid interface (Patino et al. 2008). These biopolymer-built foams are generally more stable compared to those using low molecular weight surfactants. The biopolymer adsorption at the gas–liquid interface is a complex process including (1) diffusion from the solution to the subsurface, (2) adsorption and unfolding at the interface, and (3) reorganization or rearrangement of segments previously adsorbed at the interface (Patino et al. 2008), which critically depends on the chemical constitutions of biopolymers and foaming systems.

The interfacial dilatational capacity, reflected by the interfacial dilatational modulus, provides the fundamental insight into the foam ability and stability from the interfacial perspective. The interfacial dilatational modulus ( $\varepsilon_d$ ) can be expressed as a linear response of film to sinusoidal deformation at a certain frequency and suggested by Eq. 6.7 (Maldonado-Valderrama et al. 2008).

$$\varepsilon_d = \varepsilon + i\omega\eta \quad (6.7)$$

where  $\varepsilon$  is the interfacial elasticity modulus (i.e., storage modulus) reflecting the ability of the layer restoring its interfacial tension after stress, which measures the resistance to deformation of the layer. While  $\eta$  is the interfacial viscosity, measuring the speed of the relaxation processes that restore the equilibrium after the disturbance. And the  $\omega\eta$  is the viscosity modulus (i.e., loss modulus), reflecting the energy loss of the layer after a stress induced deformation and, therefore, measures the capacity of the layer adapting a deformation (Maldonado-Valderrama et al. 2008). The interfacial viscosity of the protein adsorbed layer appears to be a key factor in the formation of foams (i.e., foam ability), whereas the interfacial elasticity is more concerned with the foam stability.

Based on the above mechanism, the increase in foam ability is expected to utilize low molecular weight surfactants with higher interfacial viscosity and surface activity. Nevertheless, the improvement in foam stability is expected to use high molecular weight biopolymers to prevent or delay gas–liquid phase separation and to reduce the gas–liquid interfacial energy. That is to prevent drainage in thin liquid film, coalescence of bubbles, and disproportionation of gas molecules. Smaller amphipathic surfactants have a higher interfacial viscosity and surface activity with faster diffusion rate to form interface layers to pack gas when the foam are formed in liquid. Larger biopolymers and their aggregates with different supramolecular configurations such as fibrils, micelles, and crystals have lower interfacial viscosity and cannot quickly diffuse to the gas–liquid interface because of larger size compared to the smaller ones, but they are capable of irreversible adsorption at the interfacial layer and/or dispersing in lamellae and Plateau borders, which can



effectively increase the interfacial elasticity and thin film viscosity in lamellae and Plateau borders for improving foam stability.

Wettability and spreading of particles at the interface can stabilize or destabilize foams, depending on their properties (Narsimhan and Xiang 2018). Similar to the Pickering emulsion that was first reported in the early 1900s by Pickering (Pickering 1907), the particle-stabilized strategy is important in foam stabilization. At present, these particles constituted by larger biopolymers or their aggregates can prevent bubble coalescence or rupture via steric hindrance in lamellae and inhibition of drainage in both lamellae and Plateau borders. In addition, these particulate-stabilized foam systems with an appropriate particle size require a higher energy to remove particles off from the interface for the destabilization when particles have a three phase contact angle close to  $90^\circ$  (Tzoumaki et al. 2015) and sizes ranging from 10 nm to  $30\mu\text{m}$  (Hunter et al. 2008). In this case, the interfacial area occupied by the particles allows the adsorption energy per particle to reach several thousands of  $kT$  and therefore is capable of preventing the symmetrical shrinkage of bubbles. The kinetic shrinkage of a single bubble suggests the existence of a critical bubble size, above which the bubble surface is covered rapidly by particles for the inhibition of bubble dissolution, while, below this critical size, the bubbles shrank too fast to be stabilized. The critical bubble size, commonly with the diameter of 60 to  $80\mu\text{m}$  (Dickinson et al. 2004), depends on the size of the particles or their aggregate forms in dispersions (Dickinson et al. 2004; Aveyard et al. 1994). Oversize dimension of particle, probably higher than  $30\mu\text{m}$ , reduces the diffusion coefficient and therefore foaming properties or form a possible sublayer assisting to stabilize lamella structure. While, too smaller particles with size less than 10 nm may lose their mechanical properties and further destabilize the foam stability (Lavoine and Bergström 2017; Lam et al. 2014). Moreover, particles with higher aspect ratio can better stabilize foams compared to the particles with spherical shape, which is speculated that the anisotropic particles promote greater capillary deformations at the interface (Campbell et al. 2009), generating stronger capillary attractive forces between adjacent particles at the interface and therefore leading to higher interfacial packing and higher mechanical rigid (Madivala et al. 2009). When such particles with irregular shape and appropriately large size are adsorbed at the interface, they can create a very close-packed structure at the gas–liquid interface to generate a colloidal barrier. This compactly covered interfacial layer can prevent or even completely inhibit the foam destabilization caused by coalescence and disproportionation (Tzoumaki et al. 2015; Dickinson 2010). Therefore, the surface free energy for particle adsorption at the interface can be calculated by Eq. 6.8.

$$G = \gamma_{1S}A_{1S} + \gamma_{2S}A_{2S} + \gamma_{12}A_{12} \quad (6.8)$$

where  $G$  is the surface free energy for a particle adsorption at interface, the  $\gamma_{1S}$ ,  $\gamma_{2S}$ , and  $\gamma_{12}$  are the interfacial tensions between phase 1 and the particle, phase 2 and the particle, and immiscible phases 1 and 2, respectively. The  $A_{1S}$ ,  $A_{2S}$ , and  $A_{12}$  are the contact area of phase 1 with adsorbed particle, phase 2 with the adsorbed particle,

and the contact area between the immiscible phases 1 and 2 eliminated by the adsorbed particle at the interface (Lam et al. 2014; Kralchevsky et al. 2005, 1992).

Equation 6.8 can be transferred to Eq. 6.9 when the particle is a spherical shape.

$$G = -\Delta E = \pi r^2 \gamma_{12} (1 - |\cos \theta_{12}|)^2 \quad (6.9)$$

where  $r$  is the particle radius,  $\gamma_{12}$  the interfacial tension of the immiscible phases, and  $\theta_{12}$  the three phase contact angle (Lam et al. 2014).

Based on Eqs. 6.8 and 6.9, the particle cannot be removed from the interface until the extrinsic energy is higher than the surface free energy ( $G$ ). When spherical particles adsorbed at the gas–liquid interface have larger interfacial tension and contact angle closer to  $90^\circ$ , more energetic adsorption of these particles at the biphasic interface is determined. That means such particles cannot be easily displaced from the interface by random fluctuations. However, if the particles are too hydrophobic with contact angle observably higher than  $90^\circ$ , they can bridge the surfaces of more than one bubbles resulting in bubble coalescence (Aveyard et al. 1994), which is similar to the antifoaming mechanism of surfactants with very low hydrophile–lipophile balance (HLB) values (always lower than 3.0). Besides the above mechanism focusing on the improvement of foam stabilization based on the adsorption of particles at the interface, the non-adsorbed particles still play an important role in improving foam stabilization through building stable thin film. In general, the non-adsorbed particles can be firmly trapped in lamellae and Plateau border when these particles have reasonable size, shape, as well as liquid holding capacity, which can provide additional repulsive interaction force based on steric hindrance of these non-adsorbed particles between gas–liquid interfacial layers (Murray and Ettelaie 2004). The greater repulsive interaction force can be determined when the non-adsorbed particles are better in-film packed with highly ordered structures. Additionally, these non-adsorbed particles can block Plateau border and therefore sufficiently slow down or completely inhibit drainage (Murray and Ettelaie 2004). All these adsorbed or non-adsorbed particles with the function to build interface and thin film (in lamellae and Plateau border) stabilization have been investigated in multiple literature researches. Here, focusing on the food-grade particles, they are classified as proteins, polysaccharides, and inorganic particles with the anisotropic shapes of fibers, rods, and sheets, and are comprehensively discussed in this chapter with a simulated diagram shown in Fig. 6.11.

## 3.2 Foaming Agents

### 3.2.1 Protein

Most protein molecules have hydrophilic–hydrophobic amphipathic chemical structure, considered as surface active macromolecules to stabilize liquid foams (Szilvay et al. 2007). Generally, the hydrophobic groups of proteins are capable of bonding



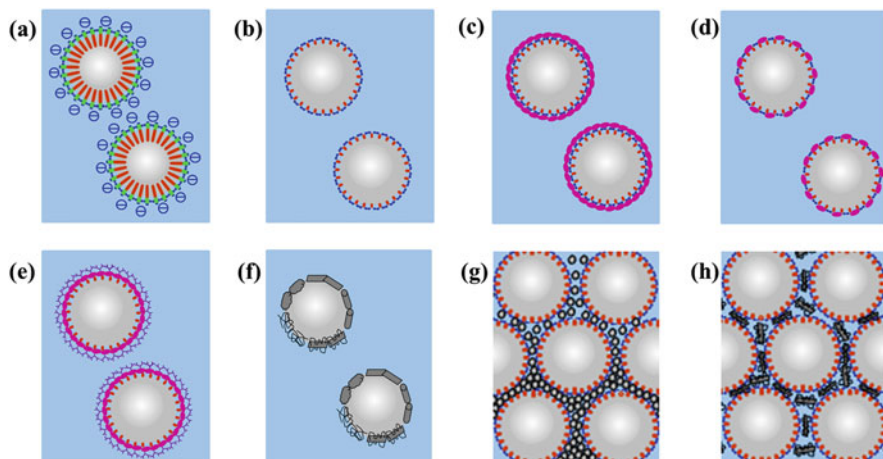


**Fig. 6.11** The foam stabilization by using biopolymers at interface or in liquid continuous phase with different mechanisms suggests through the electrostatic repulsion of interface (a), the low molecular weight polymers such as hydrolysates adsorbed at the gas–liquid interface (b), the large molecular weight polymers or aggregates attached with the interfacial layer (low molecular weight polymers) as a sublayer (c), the co-adsorption of low and large molecular weight polymers at the interface (d), the covalent linking (e.g., Maillard-type conjugation) of hydrophilic–hydrophobic biopolymers adsorbed at the interface (e), the biopolymer particle such as clay, fiber, rod, and amorphous nanoparticles adsorption at the interface based on the Pickering mechanism of stabilization (f), the formation of gel-like network in lamellae and Plateau border with a strong liquid holding capacity and increased steric hindrance among bubbles (g), and the particle adsorption at the interface and in lamellae and Plateau border to increase the mechanical strength (h). The light blue background denotes liquid, and gray circles denote gas in bubbles

with gas molecules by hydrophobic forces, while their hydrophilic groups with water molecules by hydrogen bonds. The amphipathic protein generates adsorbed layer at interface or sublayer that attaching interface to improve the interfacial rheological viscoelasticity and to form cohesive three-dimensional gels for packing gas (Szilvay et al. 2007). Higher interfacial activity and thicker interfacial layer are expected for foam stability, which strongly depends on the conformational aggregation and flexibility of protein. In principle, a reasonable protein layer can provide an energy barrier to decrease the rate and extent of bubble shrinkage that results from higher bubble–interfacial elasticity and viscosity, which suggests to be crucial for stabilizing foam by slowing down the gas disproportionation according to the interfacial elastic mechanism (Murray and Ettelaie 2004). In addition, macromolecular proteins are always composed of covalently bonded amino acid residues, meaning an infrequent thermodynamical rupture of bubble membrane compared to that by small molecular surfactants. Also, electrostatic repulsion between protein hydrophilic groups at adjacent bubble layers can enhance the foam stability by preventing bubble coalescence. Meanwhile, dispersed protein molecules in liquid film lamellae are also likely to provide dramatical steric hindrance against dynamic collision of adjacent bubbles,

which is much more possible to prevent bubble coalescence. Another important foam stability mechanism is that protein aggregates in thin film, i.e., continuous phase, can undergo a percolation process due to confinement, leading to a gel-like network formation, which is possibly to slow down the drainage in thin film. In brief, proteins influence both bulk foaming properties (e.g., overrun and stability) and interfacial properties (e.g., adsorption rates and interfacial rheology), and therefore are desirable foaming candidates. The commonly used food proteins to form stronger protein films for stabilizing foams are ovomucin, soy protein, whey protein, casein, and their aggregates or hydrolysates.

### Ovomucin

The ovomucin, accounting for ~3.5% of total egg white protein, being responsible for the thick gel characteristics of liquid egg white, has a long linear molecular chain with many coiled regions at its side chains, appears a randomly coiled structure, and hence shows a highly polymerized steric configuration (Omana et al. 2010). Early studies suggested that the ovomucin was an excellent foaming agent with a higher foam overrun and  $\tau$  value (Hammershoj et al. 2008; Hammershoj and Qvist 2001), because of its larger molecular size and intrinsic viscosity (Kato et al. 1985). Hydrolyzing ovomucin at a hydrolysis degree of 15 to 40% was found to further improve foaming ability (i.e., overrun), but little enhanced effect on foam stability (Hammershoj et al. 2008). Recent studies proposed that the increased foam ability mainly depended on the ovomucin network degradation to form small-sized fragments and protein unfolding, suggesting a break of S-S bonds by extra energy input to generate -SH groups, which is associated with the decrease in fibril size. Further inputting energy led to the re-aggregation of the new-generated fragments with the transformation of -SH groups to SS bonds, associating with partial recovery of ovomucin network (Fig. 6.12a) (Brand and Kulozik 2016). Therefore, this degradation of ovomucin by inputting energy such as under high hydrostatic pressure or high intensity ultrasound was promising to generate small particles with higher solubility and flexibility, resulting in a rapid adsorption at the gas-liquid interfacial layer to encapsulate gas (Gharbi and Labbafi 2019). For example, ultrasonically assisted foaming ovomucin was found to generate 4.9-fold higher foam overrun with clear foam microstructures observed by SEM (Fig. 6.12b) compared to that without the ultrasound radiation (Fig. 6.12c), which is caused by ovomucin molecular rearrangement to improve protein solubility and therefore to decrease gas-liquid interface tension (Gharbi and Labbafi 2018). A very interesting finding suggested that aggregates and fragments of ovomucin degradation products could be formed under a lower ultraviolet irradiation, which adsorbed at the interfacial layer and increased the interfacial viscoelasticity to improve the foam overrun. Nevertheless, larger aggregates of ovomucin hydrolysate were produced under ultraviolet irradiation at higher dose. These larger aggregates could not be adsorbed at the interfacial layer but effectively block the Plateau borders and slow down the drainage of liquid in lamellae to improve the foam stability (Gharbi and Labbafi

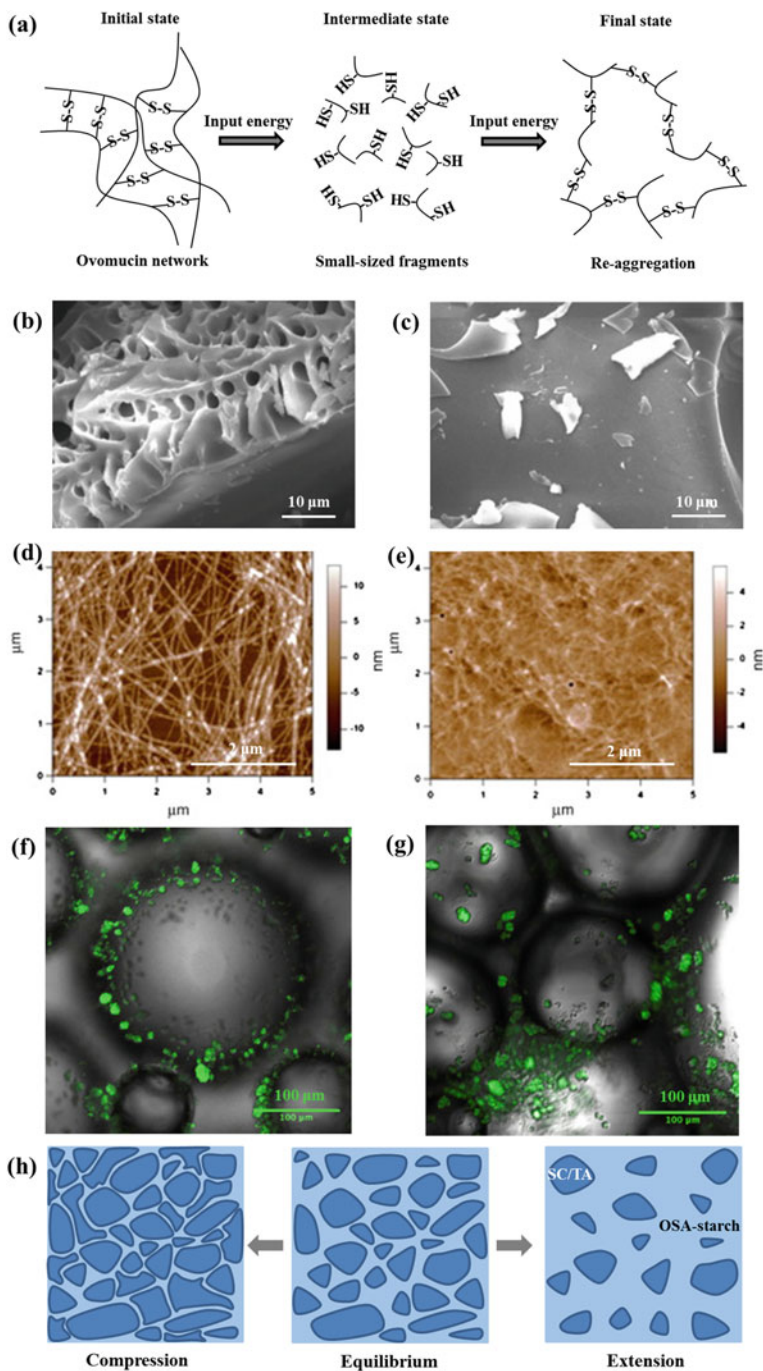


**Fig. 6.12** The schematic diagram proposing the degradation of the ovomucin network to form small-sized fragments and protein unfolding with the break of S-S bonds to form -SH groups at the initial stage of the extra energy input and a subsequent re-aggregation of the new-generated

2019). All these findings demonstrated that the well-known foam ability and stability of ovomucin make it an ideal candidate for foaming agent.

## Soy Protein

The soy protein and its hydrolysates are commonly used as food-grade foaming agents. Native soy protein is mainly composed of 7S and 11S globulins and shows high solubility (>90%) at alkaline but lower solubility as the pH is decreased and close to the isoelectric point ( $pI = 4.5$ ) (Wolf 1970). The relatively weaker hydration of soy protein is always deemed as limited foaming ability because of its compact tertiary structure at environmental pH values lower than 7. Utilizing modified soy proteins with improved conformational flexibility as foaming agents is an inchoate means to improve foam ability and stability. Early researchers fabricated cross-linked soy protein-glutaraldehyde biopolymers with a significant decrease in surface hydrophobicity compared to that by native soy protein, which allowed greater tensile strength with both improved foaming ability and stability (Park et al. 2000). A recent study reported that the hydrolyzing soy protein at a low hydrolysis degree of 0.4% was capable of increasing the surface activity with improved foam overrun. Further increasing soy protein hydrolysis degree contributed little in improving foam ability compared to the native soy protein, which was likely due to the formation of a stable surface film by the hydrophobic hydrolysates. In addition, the foam stability was also improved by the hydrolyzed soy protein at a lower hydrolysis degree of 0.4% because of the maintained considerable viscoelasticity of the surface films and water-holding capacity that could prevent liquid drainage in thin film. However, further increasing soy protein hydrolysis degree led to a decreased viscoelasticity of

---

**Fig. 6.12** (continued) fragments through the transformation of -SH groups to SS bonds at a further extra energy input with partial recovery of ovomucin network (a) (Gharbi and Labbafi 2019), the SEM images of ovomucin foams prepared with (b) and without (c) a 360-W ultrasound treatment (Gharbi and Labbafi 2018), the AFM images of the whey protein fibers for foaming after 20 h of heating at 80 °C and concentration of 2% w/w at pH 2 before (d) and after whipping (e) (Oboroceanu et al. 2014), the confocal images of whey protein fluid gels made at pH 5 (f) and 8 (g) with a green fluorescent probe suggesting the aggregated fluid gels at the gas-liquid interface at pH 5, and partially dispersed in liquid continuous phase with an increase in bulk and interfacial viscoelasticity (Lazidis et al. 2016), and a proposed interfacial structure of the SC/TA/OSA-starch complex at pH 6.0, suggesting a resistant capability of mechanical compression and extension to improve foam stability (h) (Zhan et al. 2019). The light blue background denotes liquid, and dark blue irregular shapes denote particles. The schematic diagrams of (a) and (h) were plotted by referring the corresponding literature. The images of (b)–(g) were reproduced from the corresponding references (Lian et al. 1998; Wolf 1970; Chen et al. 2018) with permission

foam liquid films, causing the promoted drainage with possible foam collapse (Martínez et al. 2009). Recently, applying physical means to rearrange soy protein molecular configuration to improve the foam ability and stability aroused an interest of researchers. Rearranging soy glycinin hydrolysates to form long semi-flexible 11S fibrils and peptides was found to provide much better foam stability at pH of 5 to 7 even at a very low concentration of 0.1% w/w. The mechanism was suggested that the adsorption kinetics of soy protein at gas–liquid interface was dramatically enhanced by the hydrolytic aggregates of fibril clusters and peptides and the formation of highly elastic surface layer by the peptides. The improved gas–liquid interface activity provided a potential to decrease the bubble layer rupture, which was capable of preventing coalescence (Wan et al. 2016). A novel and fairytale study reported that soy protein treated by subcritical water at 120 °C generated larger soluble aggregates with a lower aggregation degree and flexible conformation because of the intermolecular hydrophobic interactions, resulting in a higher surface activity at the gas–liquid interface and a significantly improved foam ability and stability (Wang et al. 2019). Therefore, it can be seen that the soy protein and its hydrolysates are promising foaming agents in food industry.

### Whey Protein

Dairy proteins are always used to fabricate foam with distinguished foam ability and stability. The whey protein is one of the main dairy proteins constituted by  $\beta$ -lactoglobulin,  $\alpha$ -lactalbumin, bovine serum albumin (BSA), and the immunoglobulins (Bryant and McClements 1998). Environmental factors such as pH and temperature play important roles in whey protein conformational aggregation and flexibility, managing whey protein surface activity, rheological viscoelasticity, and surfactant layer morphologies, which dramatically affects its foam ability and stability. Early study reported that heating 5-% w/w whey protein in aqueous at 70 °C for 1 min promoted whey protein conformational change and partial molecular aggregation, forming a mix system of monomers and soluble aggregates. Such soluble whey protein aggregates after heating at this condition were primarily formed by physical intermolecular attractions rather than covalent bond (e.g., sulfhydryl-disulfide interchange), which generates an increased interfacial area and foaming activity index with flexible conformation for desirable interfacial layer materials. In this case, denser foam with smaller average bubble size was measured with the maximum foam ability at the monomer to polymer mass ratio of 6:4 and the maximum foam stability at 4:6 (Zhu and Damodaran 1994). Whey protein long fibrils prepared in long-time of thermal treatment (80 °C and 20 hrs) at pH 2 showed much more significant improvement in foam ability and stability than native non-fibrillar whey protein, which was caused by the formation of thick layer with increased viscoelasticity adsorbed onto the gas–liquid interface and the generation of gel-like network in continuous phase. In addition, long fibrils of whey protein can adsorb at gas–liquid interface to increase the thickness of the liquid film and therefore to form polymeric structures, which was observed by atomic force

microscope (AFM) and shown in Fig. 6.12d and e (Oboroceanu et al. 2014). These stabilizing preconditions are capable of preventing liquid drainage or bubble coalescence. Another interesting finding applying whey protein fluid gels fabricated at heat induced gelation within the turbulent flow field at pH of 5 and 8 was demonstrated to produce very stable foams (Fig. 6.12f and g). The proposed mechanism to stabilize foams suggested that the smaller and free proteins (monomers or soluble oligomeric whey proteins) could diffuse quickly to the gas–liquid interface and reduce interfacial tension to promote foam generation. Subsequently, the larger protein aggregates (whey protein fluid gels) filled the free space by both adsorbing at the interfacial layers and existing as a network in continuous phase, thereby increased the flexibility of the interfacial layer and the local bulk viscosity, which improved foam stability primarily through inhibiting drainage and secondary through increasing interfacial elasticity. Therefore, employing whey protein fluid gels can prominently increase foam stability without significantly changing foam ability compared to using native whey protein (Lazidis et al. 2016). It is noteworthy that besides the thickness, viscosity, and flexibility of the interfacial layer, the lateral electrostatic repulsive interaction is still an important factor affecting bubble interfacial layer stability. A recent study reported that although transglutaminase repolymerized whey protein isolate thermolysin hydrolysates (TR-WPITHs) represent a larger size than 100 nm comparing to transglutaminase repolymerized whey protein isolate (TR-WPI) with size less than 100 nm, the strong electrostatic repulsive interactions between adsorbed TR-WPITHs highly ruptured and destabilized the interfacial layer, which led to a faster bubble coalescence (Chen et al. 2018). Thus, it can be seen that not only the size or surface activities (viscosity and flexibility), but also the electrostatic properties play a role in foam stability (Bhat and Karim 2011). Another research reported that binding polyphenols with whey protein improved the foam ability but decreased the foam stability. The mechanism of improving foam ability was generating a more effective protein crosslinking with polyphenols to form soluble composites adsorbed at interface, which increased the interfacial viscosity (Cao et al. 2018). However, phenolic compounds suppressed the dilatational elasticity of protein film via weakening protein interactions at the interface, which led to weakening foam stability.

## Casein

Casein is an alternative important protein in dairy, composed of four major fractions, i.e.,  $\alpha_{s1}$ -,  $\alpha_{s2}$ -,  $\beta$ -, and  $\kappa$ -casein in the mass proportion of 3:0.8:3:1 (Aoki et al. 1996), differing in many respects including charge ( $\alpha_{s1}$ - >  $\alpha_{s2}$ - >  $\beta$ - >  $\kappa$ -casein), sensitivity to ion-induced precipitation ( $\alpha_{s2}$ - >  $\alpha_{s1}$ - >  $\beta$ - >  $\kappa$ -casein), and foaming and emulsifying properties (Kruif et al. 2002). The  $\alpha_{s1}$ -,  $\alpha_{s2}$ -, and  $\beta$ -casein fractions



show a stronger gas–liquid interfacial adsorption than  $\kappa$ -casein, and among them,  $\beta$ -casein shows the highest surface activity (Fang and Dalgleish 1993). Sodium caseinate (SC), a primary sodium salt of casein, is prepared by reacting casein with sodium hydroxide and subsequently neutralizing the system pH to neutral. Casein and SC are distinguished by their good foaming properties such as forming strong gas–liquid interfacial layers, which is extremely able to diminish external disturbances that can prevent liquid film rupture, reflected by the interfacial dilatational modulus shown in Eq. 6.9 (Langevin 2000; Wilde 2000). Based on the principle of foam properties with the interfacial dilatational modulus, small and flexible  $\beta$ -casein has higher foaming ability due to its more rapid diffusion onto the surface. The interfacial viscosity of interface layers produced by individual  $\beta$ -casein showed a positive correlation with interfacial thickness (Martinez-Pedrero et al. 2018), suggesting that the individual  $\beta$ -casein at pH of 8.7 showed the highest foam ability, attributed to the dramatically amphipathic structure at this pH condition and the fastest diffusion rate for the adsorption onto gas–liquid interface (Barackov et al. 2012). In addition, the foam stability strongly depended on casein aggregate size. Casein micelle aggregates prepared at 4 °C (average particle size of ~500 nm) suggested a remarkably stable property compared to that prepared at 20 °C without aggregate formation (average particle size of ~200 nm) or SC (Chen et al. 2017). The mechanisms based on the interfacial elasticity and thin film properties were elucidated that the peptides, individual caseins, and small micelles could be quickly adsorbed onto gas–liquid interface to form a primary interfacial layer. Subsequently, the larger sized casein micelle aggregates were randomly incorporated and attached as sublayers with a simultaneously reversible adsorption of peptides and individual caseins pushing out of the interface and therefore form a heterogeneous thin film. This interfacial layer consisting of patches of peptides, individual caseins, and casein micelles and attached sublayers consisting of casein micelle aggregates showed a significantly increased elasticity modulus at a frequency of 0.005 Hz than that without casein micelle aggregates, which increased the interfacial dilatational modulus and was demonstrated an improved stability against film rupture (Chen et al. 2017). However, many researchers found that the increase in thin film viscosity was a more dominant factor prompting foam stability compared to increasing interfacial elasticity (Georgieva et al. 2009; Wierenga and Gruppen 2010). The thin film constituted by casein micelle aggregates was more heterogeneous with large aggregates stuck in the lamellae and Plateau borders, which dramatically increased the thin film viscosity and effectively slowed down or even stopped the liquid drainage (Chen et al. 2017). Further homogenizing large casein micelle aggregates to form smaller-sized micelles or individual caseins however could not maintain the film viscosity, which led to an instability of foam system (Chen et al. 2017). Same viewpoint suggested that aggregates did not inset into the gas–liquid interface but might be attached to interface as sublayers and dispersed in the thin film to stabilize liquid foam (Fameau and Salonen 2014). In recent studies, the complexes constituted by SC (1.0% w/w), tannin acid (TA, 0.3% w/w), and octenyl succinate starch (OSA-starch, 1.0% w/w) showed a significantly improved foam stability compared to that prepared by SC only at an equal concentration and pH 6.0. This investigation

suggested that although the polyphenols (such as TA) decreased the surface pressure leading to an inhibition of foam ability, the interfacial elasticity was significantly increased, generating a higher dilatational modulus of gas–liquid interface especially at a higher polyphenol concentration, which improved the foam stability. Furthermore, the addition of octenyl succinate starch increased the strain softening in expansion and the strain hardening in compression, which generated a possible segregated interfacial structure of SC/TA patches and OSA-starch patches (Fig. 6.12h) with a resistant capability of mechanical compression and extension (Zhan et al. 2019, 2018).

## Gelatin

Gelatin is a combination of denatured fibrous proteins mainly produced from porcine and bovine skin and bone and is composed of heterogeneous protein/polypeptide mixture of  $\alpha$ -chain (single chain),  $\beta$ -chain (two covalently cross-linked  $\alpha$ -chains), and  $\gamma$ -chain (three covalently cross-linked  $\alpha$ -chains) (Benjakul and Kittiphattanabawon 2019; Ramos et al. 2016). Gelatin can be classified into type A and type B gelatins prepared through acid and alkaline hydrolysis of collagen, respectively (Benjakul and Kittiphattanabawon 2019). The alkaline hydrolysis of collagen generally transforms glutamine and asparagine to glutamic acid and aspartic acid and therefore results in higher contents of aspartic acid and glutamic acid proportions in type B gelatin than those in type A (Duconseille et al. 2015). The most abundant sources of gelatin are pig skin (46%), bovine hides (29.4%), pig and cattle bones (23.1%), and fish (1.5%) (Duconseille et al. 2015), having molecular weight ranging from 15 to 400 kDa (Benjakul and Kittiphattanabawon 2019). The difference in amino acid compositions, molecular weight distributions, and sources significantly affects the foaming property of gelatin. Amino acid compositions of gelatin primarily depended on the sources of animal species and processing means. Generally, gelatin has a number of glycine (~33%), proline (~12%), alanine (~11%), and hydroxyproline (10%) residues but contains limited amino acid residues of histidine, methionine, and tyrosine (Karayannakidis and Zotos 2016). Among them, the proline and hydroxyproline residues, denoted as imino acid residues, play a critical role in rheological properties such as foaming property because of their hydrophobic structures. Gelatins with higher imino acid residue content are mainly from the sources of tropical animals with 194–225 imino acid residues per 1000 amino acid residues compared to those from temperate animals with 150–173 imino acid residues per 1000 residues (Benjakul and Kittiphattanabawon 2019; Abedinia et al. 2017; Kittiphattanabawon et al. 2016). Furthermore, the molecular weight of gelatin primarily depends on the temperature of collagen hydrolysis. Higher hydrolysis temperature facilitates rupture of intra- and intermolecular bonds of collagen protein chains, resulting in a more adequate degradation of collagen and generating lower molecular weight gelatin (Benjakul and Kittiphattanabawon 2019; Gomez-Guillen et al. 2002; Alfaro et al. 2015). Thus, it can be seen that gelatin obtained at a higher temperature with shorter chain length



and/or  $\alpha$ -component ( $\alpha$ -chain) is more likely to be employed for improving foam ability, while gelatin prepared at a milder process with longer chain length and more  $\beta$ - and  $\gamma$ -chains is appropriate for improving foam stability.

A conventional application of gelatin is development of marshmallow, a typical foam colloid, because of its acceptable viscosity, hardness, bloom strength, and foaming stability (Tan and Lim 2008). Broad application of gelatin as foaming agent was introduced in recent literature (Poursamar et al. 2015; Huang et al. 2017; Phawaphuthanon et al. 2019). Poursamar and co-workers applied gelatin as a base material to crosslink each other via glutaraldehyde and to fabricate porous scaffolds by a gas foaming method, which is promising to manufacture artificial tissue engineering scaffolds (Poursamar et al. 2015). However, a lower mechanical strength of the gelatin-built scaffolds, as a weakness, may be a concern in practical application. Gelatin–sodium alginate composites at a mass ratio of 5:1 and pH of 3.5 dramatically improved foam stability compared to gelatin only because of the electrostatic attraction induced intermolecular aggregation between gelatin and sodium alginate to generate charge-neutralized complexes, although a decreased foam ability was determined caused by the liquid viscosity (Phawaphuthanon et al. 2019). Huang and co-workers found that the addition of fish gelatin into egg white protein in subcritical water was capable of improving both foam ability and stability (Huang et al. 2017). The increased foam ability by the addition of fish gelatin was caused by a reduction in the gas–liquid interfacial tension, while the improved foam stability was demonstrated via building an interfacial viscoelastic network at gas–liquid interface with the increased surface dilational rheological behavior, inhibiting drainage in lamellae and bubble coalescence. These investigations above proved that the addition of gelatin in foaming agents is potential to improve foam properties especially stability.

Based on the discussions above, we can speculate that the ovomucin aggregates, soy protein fibrils, whey protein long fibrils, and casein micelle aggregates with larger sizes are very suitable to improve foam stability. The protein hydrolysates or individual protein with lower molecular weights such as ovomucin hydrolysates at a hydrolysis degree of 15–40%, soy protein hydrolysates at hydrolysis degree of 0.4%, and individual casein or casein hydrolysis are in favor of improving foam ability. Therefore, referring recent literature, proteins at various forms such as aggregates, fibrils, and hydrolysates are promising foaming agents in food and relevant fields.

### 3.2.2 Polysaccharides

The irregularly shaped polysaccharides with poly-dispersion in size and morphology are known as effective stabilizers against foam destabilization. The stabilization mechanism of these polysaccharides as foaming candidates is same as proteins. That is, increasing the elasticity of interfacial layers and sublayers and improving the viscosity and steric hindrance of lamellae and Plateau border. Three primary polysaccharides, i.e., cellulose, chitosan, and starch have been demonstrated as excellent foam agents (Dickinson 2017) and will be discussed in the following parts.

## Cellulose

Cellulose is a kind of linear polysaccharide consisting of  $\beta$ -(1,4)-linked glucopyranose units, which can be extracted from natural biomass such as the walls of plant cells, and obtained after further isolation as macroscopic fibers, microfibrillated cellulose, and nanofibrillated cellulose (Tingaut et al. 2012), which constitutes the largest portion (~50%) of the total biomass in nature (Mathur and Narang 1990). Cellulose has a semi-crystalline structure with various crystallinity degrees in nature, caused by its constitution of both crystalline and amorphous substructures (Tingaut et al. 2012). The amorphous portion of cellulose is capable of partial degradation via the acid treatment to form smaller-sized microcrystalline and nanocrystalline celluloses that contain abundant hydroxyl groups at the surface. These fiber-like native, microfibrillated, nanofibrillated celluloses, and their hydrolysates always have higher aspect ratio and liquid holding capacity, which is a potential to enhance the elasticity of interfacial layers or sublayers and the viscosity of liquid film and therefore makes them as ideal candidates for foaming agents. The larger dimensional cellulose fibers, with an average length of 2.3 mm and a spherical-shaped diameter of 35 to 40  $\mu\text{m}$ , from wood pulp were reported to generate stable foams after mixing with sodium dodecyl sulfate. Fundamental investigation on the viscoelasticity of film demonstrated that a mass of cellulose fibers was dispersed in the continuous phase resulting in the increase in thin film viscosity and the formation of gel-like network in both lamellae and Plateau borders, which could slow down the drainage. However, scarcely bound cellulose fibers at the interface were determined, speculating that the diffusion rate of larger sized cellulose fibers to the interface of gas–liquid interface was enormously slower than that of sodium dodecyl sulfate when the bubbles were formed during whipping (Al-Qararah et al. 2013). In addition, foams prepared by the mixture of cellulose fibers and sodium dodecyl sulfate were found to have a reduced bubble size compared to those prepared by the sodium dodecyl sulfate only. The magnitude of the size reduction was greater along with the increase in the cellulose fiber percentage. The decrease in bubble size along with the addition of cellulose fibers was likely due to the locally enhanced shear forces because of the increase in the breaking tendency of the larger bubbles by cellulose fiber inertia. The decrease in bubble size was always observed in stable region of foam instead of in an unstable one (Al-Qararah et al. 2013). The addition of smaller dimensional nanofibrillated cellulose fibers in the presence of octylamine was also reported to improve the foam stability, which was attributed to the reduction of the surface tension at gas–liquid interface as well as the charge density of nanofibrillated cellulose fibers and more hydrophobic properties (Cervin et al. 2013). In this case, smaller nanofibrillated cellulose fibers were able to diffuse to the interfacial layer accompanied by the octylamine during the foam formation (Cervin et al. 2013), enhancing the elasticity of interfacial layer and further the foam stability. Comparing to both researches above, it is not difficult to find that the factors for foam stabilization utilizing different cellulose fiber types are primarily the size and surface hydrophobicity. Smaller cellulose nanofibrils (approximately 4 nm in width and 500–1000 nm in length, mixing with octylamine and filtrated through a

200 nm filter) show faster diffusion rate and stronger hydrophobic forces with surfactants than larger cellulose fibers (an average length of 2.3 mm and diameter of 35 to 40  $\mu\text{m}$ ), while the larger cellulose fibers cannot be adsorbed at the interface and more likely to attach to the interface as sublayers or to disperse in thin film of lamellae and in Plateau border. Similar theory can explain that casein micelle aggregates with average particle size of  $\sim 500$  nm form a sublayer attaching to the gas–liquid interface rather than forming only a simple gas–liquid interface discussed above in this chapter. Furthermore, hydrophobic-modified celluloses were also utilized to improve the foam stability (Wege et al. 2008; Jin et al. 2012; Wang et al. 2017; Hu et al. 2016). Zhong and Velev reported an effective means using physically modified hydrophobic cellulose derivative, i.e., hypromellose phthalate to develop super stable liquid foam. The hypromellose phthalate particles were determined to be more easily adsorbed onto the gas–liquid interface created during shear blending, resulting in highly stable foams for insisting 1 month when the concentration of hypromellose phthalate in stock solution was ca. 1% w/w and was shown in Fig. 6.13a with a schematics of the forming mechanism in Fig. 6.13b (Wege et al. 2008). Another study demonstrated that the ethylcellulose particles were capable of adsorption at the gas surface to stabilize foam based on the Pickering mechanism observed through a cryo-SEM investigation and shown in Fig. 6.13c (Jin et al. 2012). A recent study found that cellulose nanocrystal particles twined by methylcellulose coils was liable to prepare thermostable foams. The prepared liquid foams showed the lowest density when the concentrations of cellulose nanocrystal particles and methylcellulose were 2.5% w/w and 0.5% w/w, respectively, implying the highest gas loading capacity. In this case, these foams were determined to sufficiently robust against defoaming at temperature of 70 °C for 6 hrs, which was likely due to that the reinforced methylcellulose fibrillar gel by cellulose nanocrystal particles could increase the gas–liquid interfacial elasticity and film viscosity (Hu et al. 2016). So far, sufficient evidences based on scientific researches have demonstrated that the foam stability could be remarkably strengthened ascribing the enhanced viscosity of thin film by the appropriate large dimension of celluloses with various types and also the increased elasticity of interfacial layer or sublayer, although the addition of celluloses decreases the diameter of bubble size (Wege et al. 2008; Hu et al. 2016). Thus, it follows that celluloses with various structures are promising to be desired foam stabilizers.

### Chitin/Chitosan

The chitin is another linear polysaccharide as a foam stabilizer and mainly obtained from the shells of crustaceans, insects, and microorganisms, which is the second most common portion of biomass in nature (Mathur and Narang 1990). The chemical structure of chitin contains  $\beta$ -(1,4)-2-acetamido-2-deoxy-D-glucopyranose units, which can be transferred to chitosan by the deacetylation using hot concentrated alkali, although the commercial chitosan still contains 20–25% of N-acetyl groups (Mathur and Narang 1990). The chitosan is similar to cellulose in chemical

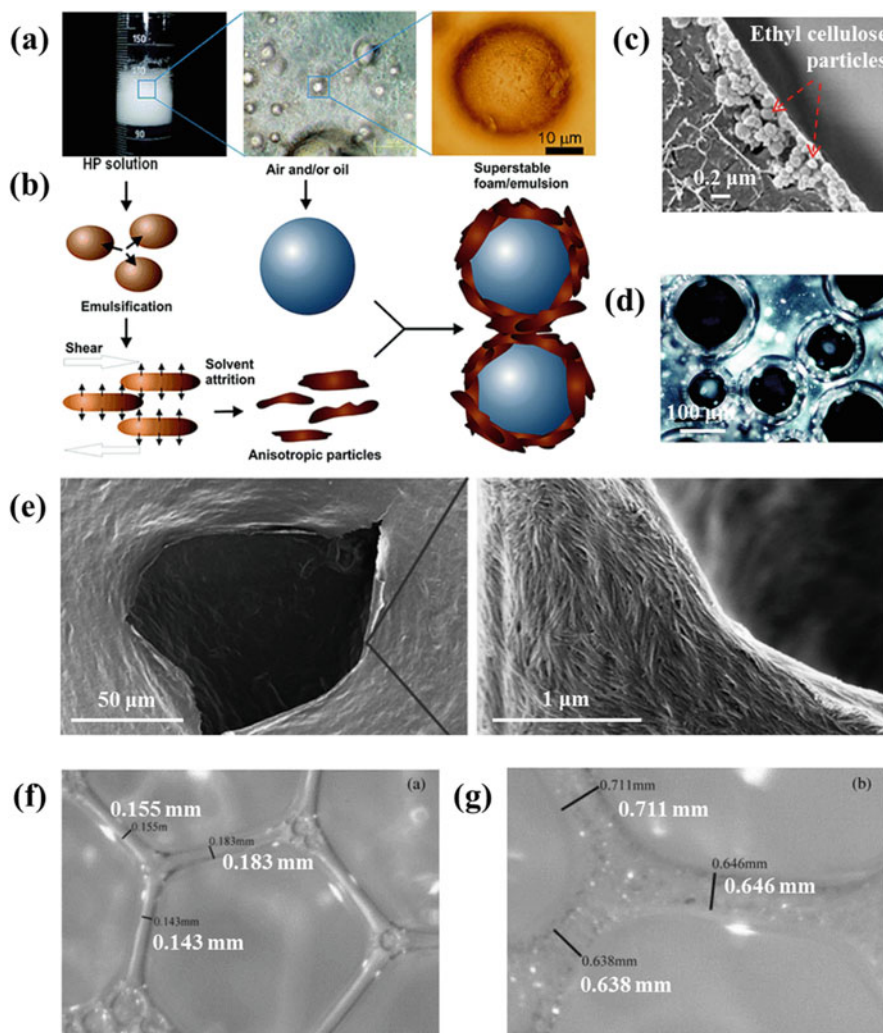


**Fig. 6.13** The foam system prepared by shearing 10% w/v hydrophobic cellulose particles in 1 mol/L acetate buffer at pH 4.2 and the images taken by a camera and an optical microscope (a) (Wege et al. 2008), the schematics of the forming mechanism of this hydrophobic cellulose particle foam (b) (Wege et al. 2008), the cryo-SEM image of the ethyl cellulose particle-stabilized foam in a 0.25% w/w xanthan solution at pH 3.0 shown with a cross-sectional view of the bubble surface (c) (Jin et al. 2012), the typical crossed-polarized optical micrograph of the chitin nanocrystal stabilized foam at chitin nanocrystal concentration of 1% w/w and pH of 7.0 (d), the microstructure observed by a SEM with low- and high-resolution microscopic images (e) (Tzoumaki et al. 2015), and the optical microscope images of foam film prepared by stirring a mixture of 4% w/w sodium dodecyl sulfate and 0.5% w/w KYPAM-2 (a kind of polyacrylamide) without (f) and with (g) 20% w/w starch particles in aqueous (Zhang et al. 2015). The images were reproduced from the corresponding references (Hunter et al. 2008; Jin et al. 2012; Wang et al. 2017; Asghari et al. 2016) with permission

construction and contains hydroxyl groups along its backbone with a molecular weight ranging from 50,000 to 2,000,000 Daltons (Poole 1989). However, because of the introduction of amine groups in side chains, the variation of the zeta-potential at different pH is opposite against celluloses, exhibiting a pH-dependent water-solubility at pH lower than 6 (Lam et al. 2014), causing by protonation with positive charges at the zeta-layer. The chitosan polymers, however, form uncharged self-aggregated particles with different types when increasing the pH higher than pKa in solution, resulting from the deprotonation of the  $-\text{NH}_3^+$  groups (Liu et al. 2012). In general, chitosan alone represents weak foaming properties such as producing very lower foaming overrun (Poole 1989). After covalently or non-covalently binding with other polymers, chitin and chitosan showed enhanced foaming properties via improving the rheological characteristics of interface and thin film. For instance, carbon nanotubes-chitosan composites were utilized to develop foams with ordered lamellar structure and enhanced mechanical strength, which presented excellent thermal stability (Yan et al. 2016). Crosslinking chitosan with cellulose or hemicellulose as foaming agents is another desirable method that is capable of improving the foam stability (Guibal et al. 2013; Salam et al. 2011). The composite of cellulose fibers with chitosan allowed changing the mechanical and microstructural properties of foams, suggesting a restriction of bubble size reduction during drying, resulting from a reinforcing structure against the collapse of the chitosan network and a possible prevention of chitosan chain aggregates (Guibal et al. 2013). Chemically modified chitosan by covalently linking hemicellulose citrate as foaming agent was found to form elastic, highly porous, and stable foams, which was likely due to the increase in viscoelasticity of interfacial layer ascribing the covalent hemicellulose citrate-chitosan complexes (Salam et al. 2011). The use of chitin nanocrystals, as colloidal rod-like particles with average dimensions around 240 nm in length and 18 nm in diameter (Tzoumaki et al. 2010), to stabilize aqueous foams has been reported in a recent study (Tzoumaki et al. 2015). The chitin nanocrystal stabilized foams without the presence of surfactants were prepared by acid hydrolysis of the original chitin in hydrochloric acid at temperature of 95 °C and pH of 3.0 for 90 min and a subsequent neutralization to a final pH of 7.0 by using sonication as a high-energy input technique that can produce better dispersed chitin nanocrystals with a higher surface coverage on bubbles and shown as a crossed-polarized optical micrograph in Fig. 6.13d. These chitin nanocrystal stabilized foams presented a stable volume life time of several days when the concentration of chitin nanocrystals was 1% w/w, which was much longer than those prepared by proteins or low molecular weight surfactants with generally stable time of several minutes (Tzoumaki et al. 2015). As shown in Fig. 6.13e, chitin nanocrystals are uniformly covered at a whole bubble surface and filled in thin film to build a stable foam structure. The Pickering mechanism on foam stability by such chitin nanocrystals here was elaborated as that no existing of larger electrostatic repulsion between the chitin particles at pH 7.0 resulted in an irreversibly packing of the chitin nanocrystals at the interface, especially with a greater amount of particles to form a colloidal armor at a higher nanocrystal concentration and thereby provided additional interfacial stability against coalescence and disproportionation (Tzoumaki et al. 2015).

Besides the interfacial stabilization, another primary factor improving the foam stability by chitin nanocrystals was the network formation in thin film between bubble interfacial layers. The anisotropic rod-like particles were liable to form gel-like network because they could more easily entangle, overlap, or form orientated domains than spherical-shaped particles and therefore provided an extra barrier against drainage or collapse of the foams. This gel-like network could even form solid-like lamellae along with the increase in the chitin nanocrystal concentration, which further prevented drainage and collapse for improving foam stabilization (Tzoumaki et al. 2015).

## Starch

Starch, obtained from grains, is the most abundant carbohydrate in the human diet. Similar to cellulose, starch is a semi-crystalline polymer that can produce nanosized crystalline or amorphous particles after hydrolysis, regeneration, and mechanical treatment (BelHaaj et al. 2013; Corre et al. 2010). Acidic and enzymatic hydrolysis of starch can fabricate starch nanocrystals with the average sizes of 15–40 nm and 500 nm, respectively (Corre et al. 2010; Buléon et al. 1998). While regenerating starch with subsequent co-crystallization and crosslinking forms crystalline nanocrystals with average size of 28–51 nm and amorphous nanoparticles of 50–100 nm, respectively (Angellier et al. 2004; Bondeson et al. 2006). Mechanical treatment of starch such as microfluidizer is a high-energy means that can form smaller-sized amorphous nanocolloids with average size of only 5–20 nm (Siqueira et al. 2008). These crystalline and amorphous particles are promising to reinforce and improve the barrier properties of thin film (Corre et al. 2010) such as in foam systems based on the Pickering mechanism. For instance, the addition of starch particles in a mixture of sodium dodecyl sulfate (4% w/w) and KYPAM-2 (a kind of polyacrylamide) (0.5% w/w) for having an insight into the foam stabilization based on the film dilational rheological behavior was revealed in recent literature, suggesting that the dilational viscoelasticity modulus, dilational elasticity modulus, dilational viscosity modulus, and foam strength were enhanced by the addition of starch particles. A thicker film could be clearly observed in the presence of starch particles with concentration of 20% w/w than a thinner film without starch particles and shown in Fig. 6.13f and g. These particles effectively gathered in Plateau border and slowed down the drainage leading to the formation of dilatant fluid with an increased viscosity of lamellae (Zhang et al. 2015). Further in-depth investigation suggested that the addition of hydrophobic ocentyl succinic anhydride modified rice starch particles with an average particle size of 150 nm and a contact angle with water drop of  $\sim 90^\circ$  enhanced foam stability 12 folds without compromising overrun compared to that by native starch particles. The improvement of foam stability attributed to the interaction of the ocentyl succinic anhydride modified starch particles and protein was first through the increase in the interfacial dilatation elasticity and viscosity, which resulted in a dramatic inhibition of initial drainage rate. Secondly, the ocentyl succinic anhydride modified starch particles provided a



robust energy barrier by forming a more concentrated film at gas–liquid interface to prevent the disproportionation. That is the crowding of modified starch particles at the interface increased the effective interfacial concentration of protein and thus improved the foam stability (Asghari et al. 2016). Less hydrophobic and smaller ocentyl succinic anhydride modified rice starch particles with an average size of 90 nm and a contact angle with water drop of  $\sim 65^\circ$  was also employed to stabilize foams, although the degree of stability was significantly lower than that utilizing hydrophobic and bigger ocentyl succinic anhydride modified starch particles (enhancement of  $\sim 2$  folds) (Asghari et al. 2016). This is caused by the thermodynamic exclusion of starch particles from the gas–liquid interface because a smaller particle needs less surface free energy for desorption than a larger particle. The excluded particles, however, can be dispersed in thin film with a relatively stronger liquid holding capacity due to smaller contact angle and thus increase foam stability through retardation of drainage rate. Thermal-treated rice starch particles with a much larger particle size of  $10.8\mu\text{m}$  and a small contact angle with water drop of  $\sim 38^\circ$  also showed effective synergy with protein to improve foam stability. The dominant stabilization mechanism was very different compared to that using ocentyl succinic anhydride modified starch particles, suggesting no enhancement of the interfacial dilational moduli because of their larger size and more hydrophilic nature. However, the thermal-treated starch particles trapped by the hydrodynamic pressure increased the viscosity of thin film, which formed a barrier to drainage and finally contributed to the overall structural stability of foam (Asghari et al. 2016). Therefore, it can be seen that these starch particles with different sizes and rheological properties can synergistically maintain the foam structure with proteins, obeying the mechanisms of increasing interface viscoelasticity and thin film viscosity.

Other polysaccharides that are also important in foam formulation and stabilization include but not limit alginate, carrageenan, and xanthan gum. These polysaccharides are expected to increase foam stability via improving rheological properties of the interfacial layers, lamellae, and Plateau border and still need further investigation as a potentially interesting research topic on foaming properties.

### 3.2.3 Inorganic Particles

The inorganic particles such as carbon particles, silicates, and clays have micro- or nano-dimensional irregular structures and large surface area so that they can be employed to stabilize colloidal systems, e.g., emulsions and foams (Lam et al. 2014; Gonzenbach et al. 2006). Incorporation of inorganic particles into biopolymers to form composites can improve foam stability. Three fundamental mechanisms elaborating the foam stability in detail by the inorganic particles are summarized here (Murray and Ettelaie 2004; Dickinson 2010). Firstly, the inorganic particles are dispersed in the thin film, which increases the viscosity and liquid holding capacity of the continuous phase via forming gel-like network and therefore slows down the drainage in lamellae. From the perspective of the microstructure of bubbles, the inorganic particles are also gathered in the Plateau borders, causing the increase of

regional area and curvature radius and a corresponding decrease of the Laplace pressure. While enhanced surface pressure generated by the enrichment of inorganic particles in the Plateau border dramatically strengthens the Gibbs–Marangoni effect, finally improves the foam stability. Secondly, the addition of inorganic particles is capable of increasing mechanical strength of lamellae and elasticity of interfacial layer or sublayer. The inorganic particles dispersed in thin film and adsorbed at interfacial layer or sublayer can resist external thermal and mechanical interference and therefore prevent the liquid film rupture and further bubble coalescence. At last, the inorganic particles always have highly ordered structure forming compact gas–liquid interface layer with a higher density than conventional liquid, and hence, can reduce the gas molecule diffusion from bubbles and prevent the disproportionation. In brief, the addition of inorganic particles in foams is a promising strategy to improve the mechanical features of liquid film, which can be used to prepare super stable foams.

## 4 Application in Food Industry

Stable foam system plays a critical role in food structural design, contributing to preparing ice cream (Pei and Schmidt 2010), beer (Imure et al. 2012), bread (Glenn et al. 2001; Shogren et al. 2002), food package (Andersen et al. 1999), foam-mat drying (Karim and Wai 1999), etc. Ice cream is a multiphase foam-type colloid matrix generally consisting of air, fat, proteins, polysaccharides, sugars, water, etc. The development of stable bubbles in ice cream has been suggested as the process that the emulsion with partially coalesced fat globules is first formed. During the aging step, the fat crystals are formed with a simultaneous rearrangement of the fat globule membrane leading to the lowest free energy state. In subsequent whipping and dynamic freezing, the fat globules with proteins adsorbed onto the air surface, together with ice crystals are dispersed by the shear forces in continuous phase. In a whole ice cream system, the air bubbles usually in the range of 20 to 50 $\mu\text{m}$  are partially coated by fat globules with and without fat globule membrane protein and further coated by whey protein and casein. That is, the fat globules with membrane protein, whey protein, and casein consist of the air–water interfacial layer. Additionally, sugars and polysaccharides are primarily dispersed in thin film forming a freeze-concentrated aqueous solution. Therefore, the ice cream can be seen as a constitution of discontinuous bubbles, a network of biopolymers (including fat, proteins, and polysaccharides) surrounding the air bubbles, ice crystals, and a continuous unfrozen aqueous solution (Goff 1997; Eisner et al. 2005).

Beer is one of the most widely consumed alcoholic drinks and the third most popular drink after water and tea in the world. An important evaluation standard of beer trait is its foam quality, which is characterized by stability, quantity, lacing, whiteness, creaminess, density, viscosity, and strength (Imure et al. 2012; Bamforth 1985). Among these characteristics, foam stability is the most important, which is promising to be improved by the addition of food-grade biopolymers such as



proteins and non-starch polysaccharides (Evans et al. 1999). The high molecular weight protein Z (35,000 to 40,000 Da) and low molecular weight lipid transfer protein (5000 to 15,000 Da) obtained from malts are positively correlated with foam stability (Evans and Sheehan 2002), mainly attributed to the interfacial hydrophobicity and viscometric activity. While the  $\beta$ -glucan and arabinoxylan, i.e., non-starch polysaccharides, play a part role in increasing the viscosity of the continuous phase (Evans et al. 1999). Additionally, filling beer with nitrogen has been applied to improve foam stability in beer industry because of the decreased gas (nitrogen) solubility in liquid and therefore to inhibit the disproportionation.

Bread is prepared from dough consisting of flour and water and is a prominent staple food in large parts of the world. An important factor affecting the texture and sensory of bread is embedded bubbles comprising up to 70% of the whole bread volume. Therefore, controlling the bubble size and number, especially retaining their stability within the bread baking process, becomes necessary to improve the bread quality with overall desirable structure and texture. Generally, the bubbles undergo instability processes primarily including drainage, coalescence, and disproportionation. However, much higher viscoelastic modulus of the dough prevents the floating of bubbles against gravity, and therefore reduces bread foam drainage. Whilst, disproportionation and coalescence are likely to be the main factors leading to bread foam instability (Mills et al. 2003; Gan et al. 1995). The starch-gluten matrix involving in building the structure of foams suggests that the low molecular weight lipids and surface active gluten proteins are the primary components adsorbed at the liquid films lining the bubbles. The soluble arabinoxylan in continuous phase ulteriorly increases the viscosity of thin liquid film and thereby further improves the stability of foam structure (Mills et al. 2003).

The application of food-grade foams in packaging is a possible alternative in food industry. Important properties of the food packaging materials include safety, biodegradability (Brant et al. 2018), resistance to heat transfer (Ahmadzadeh et al. 2015), low moisture susceptibility (Ahmadzadeh et al. 2015), high mechanical strength (Ahmadzadeh et al. 2015), and low cost of production (Singh et al. 2008). The cellulose-modified montmorillonite nanocomposite is one of such materials with potential in developing food-grade foams (Ahmadzadeh et al. 2015). The nanofoams prepared by high speed shearing the cellulose matrix incorporated with exfoliated surface-modified montmorillonite clay platelets suggest excellent mechanical and barrier properties and thermal insulation performance even though at a low concentration of exfoliated surface-modified montmorillonite clay platelets (Ahmadzadeh et al. 2015). This cellulose-modified montmorillonite nanocomposite constructed foam agent is promising to be used for chilled and cooked chains in food transportation. Moreover, starch and protein are also two available materials that are potential in foam development because of their thermoplasticity and biodegradability (Mensitieri et al. 2011).

Foam-mat drying is a promising food drying technology to obtain desirable food structure and inactivate microorganism. Polysaccharides and proteins and their composites including cellulose (Rajkumar et al. 2007; Hardy and Jideani 2017), ovalbumin (Rajkumar et al. 2007; Hardy and Jideani 2017; Franco et al. 2015),

maltodextrin (Hardy and Jideani 2017; Febrianto et al. 2012), and gum Arabic (Hardy and Jideani 2017; Febrianto et al. 2012) are commonly utilized additives for the foam-mat drying process. During a typical foam-mat drying process, the liquid foods are whipped into stable foams and then dried in air or heating conditions. At this moment, the foams are required to be stable and retain an open structure, which is capable of being dried rapidly. In theory, the degree of drying in the foam-mat drying process is very high resulting from the rapid massive increase in the gas–liquid interface, which occurs in more than one constant rate periods due to the periodic bursting of bubble successive layer and therefore exposing new surface for thermohydrodynamic mass transfer. This foam-mat drying process is suitable for heat sensitive, viscous, and sticky food materials that is unable to be dried through common drying means such as spray drying (Hardy and Jideani 2017).

## 5 Conclusions and Future Prospects

In conclusion, foam formation, microstructure, stabilization mechanisms, common food foaming agents, and their applications are introduced and discussed in this chapter. Drainage, coalescence, and disproportionation are the primary mechanisms destabilizing liquid foams, which can be prevented through three potential strategies including the enhancement of liquid holding capacity in both lamellae and Plateau borders, increase of space steric hindrance against the contact between adjacent gas–liquid interfaces, and improvement of the interface elasticity to resist interfacial tension. Pickering stabilization employing amphiphilic biopolymers is critical for the development of stable foams and therefore is worth in-depth study. Improving foam stability is likely to be achieved at the expense of foaming ability when utilizing a strategy to increase the interfacial elasticity. How to improve both foam stability and ability by using a simple and routine operation needs a deep thinking. For instance, the development of foams based on a viscoelastic variable medium such as syrup mixed medium having phase transition capacity between liquid and solid. In brief, although foam as one of the essential elements in modern food systems has been applied with a long history, there is much work still needs to be done to further improve their properties especially stability. We expect this chapter may provide fundamental knowledge for readers to better understand food-grade liquid foams.

**Acknowledgements** Yongguang Guan sincerely thanks Prof. Qixin Zhong at the University of Tennessee Knoxville for his kindly guidance in professional knowledge of liquid foams during post-doctoral training.

## References

- Abedinia A, Ariffin F, Huda N et al (2017a) Extraction and characterization of gelatin from the feet of Pekin duck (*Anas platyrhynchos domestica*) as affected by acid, alkaline, and enzyme pretreatment. *Int J Biol Macromol* 98:586–594
- Ahmadzadeh S, Nasirpour A, Keramat J et al (2015) Nanoporous cellulose nanocomposite foams as high insulated food packaging materials. *Colloid Surf A* 468:201–210
- Alfaro AT, Balbinot E, Weber CI et al (2015) Fish gelatin: characteristics, functional properties, applications and future potentials. *Food Eng Rev* 7:33–44
- Al-Qararah AM, Hjelt T, Koponen A et al (2013) Bubble size and air content of wet fibre foams in axial mixing with macro-instabilities. *Colloid Surf A* 436:1130–1139
- Andersen PJ, Kumar A, Hodson SK (1999) Inorganically filled starch based fiber reinforced composite foam materials for food packaging. *Mater Res Innov* 3:2–8
- Angellier H, Choinsard L, Molina-Boisseau S et al (2004) Optimization of the preparation of aqueous suspensions of waxy maize starch nanocrystals using a response surface methodology. *Biomacromolecules* 5:1545–1551
- Aoki T, Uehara T, Yonemasu A et al (1996) Response surface analyses of the effects of calcium and phosphate on the formation and properties of casein micelles in artificial micelles system. *J Agric Food Chem* 44:1230–1235
- Asghari AK, Norton I, Mills T et al (2016) Interfacial and foaming characterisation of mixed protein-starch particle systems for food-foam applications. *Food Hydrocolloid* 53:311–319
- Aveyard R, Binks BP, Fjetcher PDI et al (1994) Contact angles in relation to the effects of solids on film and foam stability. *J Disper Sci Technol* 15:251–271
- Bamforth CW (1985) The foaming properties of beer. *J I Brewing* 91:370–383
- Barackov I, Mause A, Kapoor S et al (2012) Investigation of structural changes of  $\beta$ -casein and lysozyme at the gas-liquid interface during foam fractionation. *J Biotechnol* 161:138–146
- BelHaaj S, Mabrouk AB, Thielemans W et al (2013) A one-step miniemulsion polymerization route towards the synthesis of nanocrystal reinforced acrylic nanocomposites. *Soft Matter* 9:1975–1984
- Benjakul S, Kittiphattanabawon P (2019) Gelatin. In: Melton L, Shahidi F, Varelis P (eds) *Encyclopedia of food chemistry*, 1st edn. Elsevier, London, pp 121–127
- Benjamins J, Cagna A, Lucassen-Reynders EH (1996) Viscoelastic properties of triacylglycerol/water interfaces covered by proteins. *Colloid Surf A* 114:245–254
- Bhat YHKR, Karim AA (2011) Emulsifying and foaming properties of ultraviolet-irradiated egg white protein and sodium caseinate. *J Agric Food Chem* 59:4111–4118
- Bisperink CGJ, Ronteltap AD, Prins A (1992) Bubble-size distributions in foams. *Adv Colloid Interf Sci* 38:13–32
- Bondeson D, Aji M, Kristiina O (2006) Optimization of the isolation of nanocrystals from microcrystalline cellulose by acid hydrolysis. *Cellulose* 13:171–180
- Borden MA, Pu G, Runner GJ et al (2004) Surface phase behavior and microstructure of lipid/PEG-emulsifier monolayer-coated microbubbles. *Colloid Surface B* 35:209–223
- Borden MA, Martinez GV, Ricker J et al (2006) Lateral phase separation in lipid-coated microbubbles. *Langmuir* 22:4291–4297
- Brand J, Kulozik U (2016) Comparison of different mechanical methods for the modification of the egg white protein ovomucin, part B: molecular aspects. *Food Bioprocess Technol* 9:1210–1218
- Brant AJC, Naime N, Lugaõ AB et al (2018) Influence of ionizing radiation on biodegradable foam trays for food packaging obtained from irradiated cassava starch. *Braz Arch Biol Technol* 61: e18160520
- Bryant CM, McClements DJ (1998) Molecular basis of protein functionality with special consideration of cold-set gels derived from heat-denatured whey. *Trends Food Sci Technol* 9:143–151
- Buléon A, Colonna P, Planchot V et al (1998) Starch granules: structure and biosynthesis. *Int J Biol Macromol* 23:85–112

- Campbell AL, Stoyanov SD, Paunov VN (2009) Fabrication of functional anisotropic food-grade micro-rods with micro-particle inclusions with potential application for enhanced stability of food foams. *Soft Matter* 5:1019–1023
- Cao Y, Xiong YL, Cao Y et al (2018) Interfacial properties of whey protein foams as influenced by preheating and phenolic binding at neutral pH. *Food Hydrocolloid* 82:379–387
- Cervin NT, Andersson L, Ng JBS et al (2013) Lightweight and strong cellulose materials made from aqueous foams stabilized by Nanofibrillated cellulose. *Biomacromolecules* 14:503–511
- Chen M, Sala G, Meinders MJB et al (2017) Interfacial properties, thin film stability and foam stability of casein micelle dispersions. *Colloid Surf B* 149:56–63
- Chen A, Tanidjaja I, Damodaran S (2018) Nanostructure and functionality of enzymatically repolymerized whey protein hydrolysate. *Food Chem* 256:405–412
- Christenson HK, Yaminsky VV (1995) Solute effects on bubble coalescence. *J Phys Chem* 99:10420–10420
- Corre DL, Bras J, Dufresne A (2010) Starch nanoparticles: a review. *Biomacromolecules* 11:1139–1153
- Damodaran S (2005) Protein stabilization of emulsions and foams. *J Food Sci* 70:R54–R66
- Dickinson E (1992) *An introduction to food colloids*. Oxford University Press, Oxford
- Dickinson E (2010) Food emulsions and foams: stabilization by particles. *Curr Opin Colloid Interf Sci* 15:40–49
- Dickinson E (2017) Biopolymer-based particles as stabilizing agents for emulsions and foams. *Food Hydrocolloid* 68:219–231
- Dickinson E, Ettelaie R, Kostakis T et al (2004) Factors controlling the formation and stability of air bubbles stabilized by partially hydrophobic silica nanoparticles. *Langmuir* 20:8517–8525
- Disalvo EA (1988) Permeability of water and polar solutes in lipid bilayers. *Adv Colloid Interf Sci* 29:141–170
- Djelveh G, Gros JB (1995) Estimation of physical properties of foamed foods using energy dissipation in scraped-surface heat exchangers. *J Food Eng* 26:45–56
- Dressaire E, Bee R, Bell DC et al (2008) Interfacial polygonal nanopatterning of stable microbubbles. *Science* 320:1198–1201
- Duconseille A, Astruc T, Quintana N et al (2015) Gelatin structure and composition linked to hard capsule dissolution: a review. *Food Hydrocolloid* 43:360–376
- Eisner MD, Wildmoser H, Windhab EJ (2005) Air cell microstructuring in a high viscous ice cream matrix. *Colloid Surf A* 263:390–399
- Ettelaie R, Dickinson E, Du Z et al (2003) Disproportionation of clustered protein-stabilized bubbles at planar air-water interfaces. *J Colloid Interf Sci* 263:47–58
- Evans DE, Sheehan MC, Stewart DC (1999) The impact of malt derived proteins on beer foam quality. Part II: the influence of malt foam-positive proteins and non-starch polysaccharides on beer foam quality. *J I Brewing* 105:171–178
- Evans DE, Sheehan MC (2002) Don't be fobbed off: the substance of beer foam—a review. *J Am Soc Brew Chem* 60:47–57
- Fameau AL, Salonen A (2014) Effect of particles and aggregated structures on the foam stability and aging. *CR Phys* 15:748–760
- Fang Y, Dalglish DG (1993) Dimensions of the adsorbed layers in oil-in-water emulsions stabilized by caseins. *J Colloid Interf Sci* 156:329–334
- Febrianto A, Kumalaningsih S, Aswari AW (2012) Process engineering of drying milk powder with foam-mat drying method. A study on the effect of the concentration and types of filler. *JBASR* 2:3588–3592
- Franco TS, Perussello CA, Ellenderson LSN et al (2015) Foam mat drying of yacon juice: experimental analysis and computer simulation. *J Food Eng* 158:48–57
- Gan Z, Ellis PR, Schofield JD (1995) Gas cell stabilisation and gas retention in wheat bread dough. *J Cereal Sci* 21:215–230
- Georgieva D, Cagna A, Langevin D (2009) Link between surface elasticity and foam stability. *Soft Matter* 5:2063–2071

- Gharbi N, Labbafi M (2018) Influence of high-intensity ultrasound on foaming and structural properties of egg white. *Food Res Int* 108:604–610
- Gharbi N, Labbafi M (2019) Influence of treatment-induced modification of egg white proteins on foaming properties. *Food Hydrocolloid* 90:72–81
- Glenn GM, Orts WJ, Nobes GAR (2001) Effect of starch, fiber and CaCO<sub>3</sub> on the properties of foams made by a baking process. *Ind Crop Prod* 14:201–212
- Goff HD (1997) Colloidal aspects of ice cream—a review. *Int Dairy J* 7:363–373
- Gomez-Guillen MC, Turnay J, Fernandez-Diaz MD et al (2002) Structural and physical properties of gelatin extracted from different marine species: a comparative study. *Food Hydrocolloid* 16:25–34
- Gonzenbach UT, Studart AR, Tervoort E et al (2006) Ultrastable particle-stabilized foams. *Angew Chem Int Edit* 45:3526–3530
- Green AJ, Littlejohn KA, Hooley P et al (2013) Formation and stability of food foams and aerated emulsions: hydrophobins as novel functional ingredients. *Curr Opin Colloid Interf Sci* 18:292–301
- Guibal E, Cambe S, Bayle S et al (2013) Silver/chitosan/cellulose fibers foam composites: from synthesis to antibacterial properties. *J Colloid Interf Sci* 393:411–420
- Hammershoj M, Qvist KB (2001) Importance of hen age and egg storage time for egg albumen foaming. *LWT-Food Sci Technol* 34:118–120
- Hammershoj M, Nebel CC, Carstens JH (2008) Enzymatic hydrolysis of ovomucin and effect on foaming properties. *Food Res Int* 41:522–531
- Hardy Z, Jideani VA (2017) Foam-mat drying technology: a review. *Crit Rev Food Sci Nutr* 57:2560–2572
- Horozov TS (2008) Foams and foam films stabilised by solid particles. *Curr Opin Colloid Interf Sci* 13:134–140
- Hu Z, Xu R, Cranston ED et al (2016) Stable aqueous foams from cellulose nanocrystals and methyl cellulose. *Biomacromolecules* 17:4095–4099
- Huang T, Tu ZC, Wang H et al (2017) Promotion of foam properties of egg white protein by subcritical water pre-treatment and fish scales gelatin. *Colloid Surf A* 512:171–177
- Hunter TN, Pugh RJ, Franks GV et al (2008) The role of particles in stabilising foams and emulsions. *Adv Colloid Interf Sci* 137:57–81
- Iimure T, Kimura T, Araki S et al (2012) Mutation analysis of barley malt protein Z4 and protein Z7 on beer foam stability. *J Agric Food Chem* 60:1548–1554
- Jin H, Zhou W, Cao J et al (2012) Super stable foams stabilized by colloidal ethyl cellulose particles. *Soft Matter* 8:2194–2205
- Karayannakidis PD, Zotos A (2016) Fish processing by-products as a potential source of gelatin: a review. *J Aquat Food Prod T* 25:65–92
- Karim AA, Wai CC (1999) Foam-mat drying of starfruit (*Averrhoa carambola* L.) purée. Stability and air drying characteristics. *Food Chem* 64:337–343
- Kato A, Oda S, Yamanaka Y (1985) Functional and structural properties of ovomucin. *Agric Biol Chem* 49:3501–3504
- Kim DH, Costello MJ, Duncan PB et al (2003) Mechanical properties and microstructure of polycrystalline phospholipid monolayer shells: novel solid microparticles. *Langmuir* 19:8455–8466
- Kittiphattanabawon P, Benjakul S, Sinthusamran S et al (2016) Gelatin from clown featherback skin: extraction conditions. *LWT-Food Sci Technol* 66:186–192
- Kornev KG, Neimark AV, Rozhkov AN (1999) Foam in porous media: thermodynamic and hydrodynamic peculiarities. *Adv Colloid Interf Sci* 82:127–187
- Kralchevsky PA, Ivanov IB, Ananthapadmanabhan KP et al (1992) A possible mechanism of stabilization of emulsions by solid particles. *J Colloid Interf Sci* 150:589–593
- Kralchevsky PA, Ivanov IB, Ananthapadmanabhan KP et al (2005) On the thermodynamics of particle-stabilized emulsions: curvature effects and catastrophic phase inversion. *Langmuir* 21:50–63

- Kruif CG, Tuinier R, Holt C et al (2002) Physicochemical study of  $\kappa$ - and  $\beta$ -casein dispersions and the effect of cross-linking by transglutaminase. *Langmuir* 18:4885–4891
- Labiausse V, Höhler R, Cohen-Adda S (2007) Shear induced normal stress differences in aqueous foams. *J Rheol* 51:479–492
- Lam S, Velikov KP, Velev OD (2014) Pickering stabilization of foams and emulsions with particles of biological origin. *Curr Opin Colloid Interf Sci* 19:490–500
- Langevin D (2000) Influence of interfacial rheology on foam and emulsion properties. *Adv Colloid Interf Sci* 88:209–222
- Lavoine N, Bergström L (2017) Nanocellulose-based foams and aerogels: processing, properties, and applications. *J Mater Chem A* 5:16105–16117
- Lazidis A, Hancocks RD, Spyropoulos F et al (2016) Whey protein fluid gels for the stabilisation of foams. *Food Hydrocolloid* 53:209–217
- Leike A (2002) Demonstration of the exponential decay law using beer froth. *Eur J Phys* 23:21–26
- Lian G, Thornton C, Adams MJ (1998) Discrete particle simulation of agglomerate impact coalescence. *Chem Eng Sci* 53:3381–3391
- Liu H, Wang C, Zou S et al (2012) Simple, reversible emulsion system switched by pH on the basis of chitosan without any hydrophobic modification. *Langmuir* 28:11017–11024
- Madivala B, Vandebriel S, Fransær J et al (2009) Exploiting particle shape in solid stabilized emulsions. *Soft Matter* 5:1717–1727
- Maldonado-Valderrama J, Martín-Rodríguez A, Gálvez-Ruiz MJ et al (2008) Foams and emulsions of  $\beta$ -casein examined by interfacial rheology. *Colloid Surf A* 323:116–122
- Marrucci G (1969) A theory of coalescence. *Chem Eng Technol* 24:975–985
- Mathur NK, Narang CK (1990) Chitin and chitosan, versatile polysaccharides from marine animals. *J Chem Educ* 67:938–942
- Martínez KD, Sánchez C, Patino JMR et al (2009) Interfacial and foaming properties of soy protein and their hydrolysates. *Food Hydrocolloid* 23:2149–2157
- Martínez-Pedrero F, Tajuelo J, Sánchez-Puga P et al (2018) Linear shear rheology of aging  $\beta$ -casein films adsorbing at the air/water interface. *J Colloid Interf Sci* 551:12–20
- McConlogue CW, Vanderlick TK (1997) A close look at domain formation in DPPC monolayers. *Langmuir* 13:7158–7164
- McKiernan AE, Ratto TV, Longo ML (2000) Domain growth, shapes, and topology in cationic lipid bilayers on mica by fluorescence and atomic force microscopy. *Biophys J* 79:2605–2615
- Mensitieri G, Di Maio E, Buonocore GG et al (2011) Processing and shelf life issues of selected food packaging materials and structures from renewable resources. *Trends Food Sci Technol* 22:72–80
- Mills ENC, Wilde PJ, Salt LJ et al (2003) Bubble formation and stabilization in bread dough. *Food Bioprod Process* 81:189–193
- Mitchell J (1986) Foaming and emulsifying properties of proteins. In: Hudson B (ed) *Developments in food proteins-4*. Elsevier, London, pp 291–338
- Murray BS, Ettelaie R (2004) Foam stability: proteins and nanoparticles. *Curr Opin Colloid Interf Sci* 95:314–320
- Nandi N, Vollhardt D (2003) Effect of molecular chirality on the morphology of biomimetic Langmuir monolayers. *Chem Rev* 103:4033–4076
- Narsimhan G, Xiang N (2018) Role of proteins on formation, drainage, and stability of liquid food foams. *Annu Rev Food Sci T* 9:45–63
- Niño MRR, Patino JMR (1998) Surface tension of bovine serum albumin and tween 20 at the air-aqueous interface. *J Am Oil Chem Soc* 75:1241–1248
- Oborocanu D, Wang L, Magner E et al (2014) Fibrillation of whey proteins improves foaming capacity and foam stability at low protein concentrations. *J Food Eng* 121:102–111
- Omana DA, Wang J, Wu J (2010) Ovomucin-a glycoprotein with promising potential. *Trends Food Sci Technol* 21:455–463
- Park SK, Bae DH, Rhee KC (2000) Soy protein biopolymers cross-linked with glutaraldehyde. *J Am Oil Chem Soc* 77:879–884

- Patino JMR, Sánchez CC, Niño MRR (2008) Implications of interfacial characteristics of food foaming agents in foam formulations. *Adv Colloid Interf Sci* 140:95–113
- Pei ZJ, Schmidt KA (2010) Ice cream: foam formation and stabilization—a review. *Food Rev Int* 26:122–137
- Phawaphuthanon N, Yu D, Ngamnikom P et al (2019) Effect of fish gelatine-sodium alginate interactions on foam formation and stability. *Food Hydrocolloid* 88:119–126
- Pickering SU (1907) Cxvii.-emulsions. *J Chem Soc Trans* 91:2001–2021
- Poole S (1989) The foam-enhancing properties of basic biopolymers. *Int J Food Sci Technol* 24:121–137
- Poursamar SA, Hatami J, Lehner AN et al (2015) Gelatin porous scaffolds fabricated using a modified gas foaming technique: characterisation and cytotoxicity assessment. *Mater Sci Eng C Mater* 48:63–70
- Rajkumar P, Kailappan R, Viswanathan R et al (2007) Drying characteristics of foamed alphonso mango pulp in a continuous type foam mat dryer. *J Food Eng* 79:1452–1459
- Ramos M, Valdés A, Beltrán A et al (2016) Gelatin-based films and coatings for food packaging applications. *Coatings* 6:41
- Rio E, Drenckhan W, Salonen A et al (2014) Unusually stable liquid foams. *Adv Colloid Interf Sci* 205:74–86
- Saint-Jalmes A (2006) Physical chemistry in foam drainage and coarsening. *Soft Matter* 2:836–849
- Salam A, Venditti RA, Pawlak JJ et al (2011) Crosslinked hemicellulose citrate-chitosan aerogel foams. *Carbohydr Polym* 84:1221–1229
- Shogren RL, Lawton JW, Tiefenbacher KF (2002) Baked starch foams: starch modifications and additives improve process parameters, structure and properties. *Ind Crop Prod* 16:69–79
- Singh SP, Burgess G, Singh J (2008) Performance comparison of thermal insulated packaging boxes, bags and refrigerants for single-parcel shipments. *Packag Technol Sci* 21:25–35
- Siqueira G, Bras J, Dufresne A (2008) Cellulose whiskers versus microfibrils: influence of the nature of the nanoparticle and its surface functionalization on the thermal and mechanical properties of nanocomposites. *Biomacromolecules* 10:425–432
- Stamenović D (1991) A model of foam elasticity based upon the laws of plateau. *J Colloid Interf Sci* 145:255–259
- Szilvay GR, Paananen A, Laurikainen K et al (2007) Self-assembled hydrophobin protein films at the air-water interface: structural analysis and molecular engineering. *Biochemistry* 46:2345–2354
- Tan JM, Lim MH (2008) Effects of gelatine type and concentration on the shelf-life stability and quality of marshmallows. *Int J Food Sci Technol* 43:1699–1704
- Thitakamol B, Veawab A (2009) Foaming model for CO<sub>2</sub> absorption process using aqueous monoethanolamine solutions. *Colloid Surf A* 349:125–136
- Tingaut P, Zimmermann T, Sèbe G (2012) Cellulose nanocrystals and microfibrillated cellulose as building blocks for the design of hierarchical functional materials. *J Mater Chem* 22:20105–20111
- Tzoumaki MV, Moschakis T, Biliaderis CG (2010) Metastability of Nematic gels made of aqueous chitin Nanocrystal dispersions. *Biomacromolecules* 11:175–181
- Tzoumaki MV, Karefyllakis D, Moschakis T et al (2015) Aqueous foams stabilized by chitin nanocrystals. *Soft Matter* 11:6245–6253
- Urban K, Wagner G, Schaffner D et al (2006) Rotor-stator and disc systems for emulsification processes. *Chem Eng Technol* 29:24–31
- Verbist G, Weaire D, Kraynik AM (1996) The foam drainage equation. *J Phys Condense Mater* 8:3715–3731
- Wan Z, Yang X, Sagis LMC (2016) Contribution of long fibrils and peptides to surface and foaming behavior of soy protein fibril system. *Langmuir* 32:8092–8101
- Wang L, Ishihara S, Hikima Y et al (2017) Unprecedented development of ultrahigh expansion injection-molded polypropylene foams by introducing hydrophobic-modified cellulose nanofibers. *ACS Appl Mater Interf* 9:9250–9254

- Wang MP, Chen XW, Guo J et al (2019) Stabilization of foam and emulsion by subcritical water-treated soy protein: effect of aggregation state. *Food Hydrocolloid* 87:619–628
- Wasan D, Nikolov A (2008) Thin liquid films containing micelles or nanoparticles. *Curr Opin Colloid* 13:128–133
- Weaire D, Fortes MA (1994) Stress and strain in liquid and solid foams. *Adv Phys* 43:685–738
- Weaire D, Phelan R (1996) The physics of foam. *J Phys-Condens Mater* 8:9519–9524
- Wege HA, Kim S, Paunov VN et al (2008) Long-term stabilization of foams and emulsions with in-situ formed microparticles from hydrophobic cellulose. *Langmuir* 24:9245–9253
- Wierenga P, Gruppen H (2010) New views on foams from protein solutions. *Curr Opin Colloid Interf Sci* 15:365–373
- Wilde PJ, Clark DC (1993) The competitive displacement of  $\beta$ -lactoglobulin by tween 20 from oil-water and air-water interfaces. *J Colloid Interf Sci* 155:48–54
- Wilde PJ (2000) Interfaces: their role in foam and emulsion behaviour. *Curr Opin Colloid Interf Sci* 5:176–181
- Wolf WJ (1970) Soybean proteins: their functional, chemical, and physical properties. *J Agric Food Chem* 18:969–976
- Yan J, Wu T, Ding Z et al (2016) Preparation and characterization of carbon nanotubes/chitosan composite foam with enhanced elastic property. *Carbohydr Polym* 136:1288–1296
- Zhan F, Li J, Wang Y et al (2018) Bulk, foam, and interfacial properties of tannic acid/sodium Caseinate Nanocomplexes. *J Agric Food Chem* 66:6832–6839
- Zhan F, Li J, Shi M (2019) Foaming properties and linear and nonlinear surface dilatational rheology of sodium Caseinate, tannin acid, and Octenyl succinate starch ternary complex. *J Agric Food Chem* 68:2340–2349
- Zhang Y, Chang Z, Luo W et al (2015) Effect of starch particles on foam stability and dilatational viscoelasticity of aqueous-foam. *Chinese J Chem Eng* 23:276–280
- Zhu H, Damodaran S (1994) Heat-induced conformational changes in whey protein isolate and its relation to foaming properties. *J Agric Food Chem* 42:846–855



# Chapter 7

## Tribological and Sensory Properties



Sandip Panda and Jianshe Chen

**Abstract** Eating, functionalized by mouth physiology, is performed through a series of processes which collectively helps in food ingestion, preparing the food for swallowing, ab-initio digestion, and food sensory perceptions. Sensory properties of food are typically defined by its texture, flavor, and color. Unlike flavor and color, characterizing texture perceptions remain a daunting task because of varied in-mouth breakdown mechanisms of food depending on several influencing factors. Therefore, it always remains a persisting challenge to correlate instrumental outputs with texture perception. Over the recent decade, principles of tribology—the subject of friction, wear, and lubrication—have been recognized in food sensory research in order to adopt novel instrumental approaches for texture perceptions. This idea of incorporating tribological principles stems from the availability of friction that arises while the tongue manipulates food over the palate during oral processing. Eventually, the terminology such as oral tribology has been introduced, and the subject is rapidly gaining maturity for food sensory applications especially to demonstrate some highly specific sensory descriptions and to define a quantifiable metric for those sensory descriptions. This chapter will revisit the various principles and applications of tribology in pertinence to texture characteristics of food in general and edible hydrocolloids in particular while attempting to identify potential research gaps and future research scopes.

**Keywords** Food oral processing · Soft tribology · Oral lubrication · Sensory perception · Saliva

---

S. Panda · J. Chen (✉)

Laboratory of Food Oral Processing, School of Food Science and Biotechnology, Zhejiang Gongshang University, Hangzhou, Zhejiang, China  
e-mail: [jschen@zjgsu.edu.cn](mailto:jschen@zjgsu.edu.cn)

## 1 Introduction

While our grandmothers, mothers, and great chefs work hard to formulate great recipes of all times to fill our plate with delectable dishes, scientists and researchers are also relentless to find the mystery behind senses of eating. How do we sense food while eating? This is a valid question worthy of scientific interrogations. Food oral processing involves complex and dynamical physico-chemical processes which occur over a shorter time scale (from few seconds to a few minutes at most) inside mouth; and our sensory perceptions during the oral processing depend on a number of factors. The evolution and synchronization of these oral processes and various influencing factors are critical to the success behind the perception and pleasure of eating. Food components vary widely in terms of its structure, texture, and chemistry. However, our perceptions may vary based on the oral physiology and health, condition of saliva, and psychophysical factors such as culture, the geographical location, and of course the availability of food resources, and many hitherto unknown factors. All these factors lead this subject of food oral processing and sensory perception towards many folds of complexity. Influence of many of these factors on food texture perception and mouthfeel are still not well known.

Majority of food sensory research until a decade back was limited to bulk mechanics and rheological experiments and expert panels' assessment despite the realization on the importance of tribology by as early as 1980 (Chen 2009). However, in recent time, there has been a strong inclination towards understanding and enabling methods and principles of tribology in food oral processing. Tribology, being primarily an engineering subject, covers the topics of contact mechanics, friction, wear, and lubrication studies. In the early stage of developments, the subject was growing around mechanical, industrial, and orthopedic applications. However, bringing this subject in to food oral perception research is relatively nascent and opening a new era in food sensory research especially in the direction to adopt more of an instrumental approach in food texture characterization. Laguna and Sarkar (2017) reported sub-quadratic growth in research publication data based on the search with the key word, "oral tribology," over the preceding decade up to May, 2017.

Concerning the thematic limitations, this chapter will primarily focus on applications of tribological principles in food oral processing emphasizing the case studies on food hydrocolloids. In general, food hydrocolloids refer to wide spectrum of edible components; nevertheless, a handful of model hydrocolloids will be referred here in pertaining to various case studies. In the following sections, beginning with an introduction to engineering tribology, this chapter will briefly introduce various concepts and methods of tribology being applied in food oral processing research. Inside oral cavity, tongue and palate constitute a soft tribological system; so, discussions on soft tribology section will be given little more elaboration in this context. Following on, various experimental and analytical techniques will be briefly covered. Few case studies on tribological assessment of food hydrocolloids are also discussed. Finally, the positive hindsight on the prospects of quantitative framework

of food sensory perception based on tribological assessment along with associated challenges and future research scopes will be discussed before the chapter concludes.

## 2 Tribology Basics

Tribology is the subject to study the mechanics and chemistry of interfaces between two surfaces which are moving relative to each other. Beyond the applications in engineering and design of industrial machinery, tribology in recent years has enabled us to understand and explain seemingly diverse phenomenon ranging from macro to cellular scale events such as movement of tectonic plates and glacial ice blocks, animal locomotion and physiology (Stachowiak 2017), and even in cancer growth (Pitenis et al. 2017). Therefore, concepts of tribology, at this stage, draw attention from many disciplines of science and engineering. It is nevertheless important to discuss some of the founding concepts of this subject as part of the present chapter. Figure 7.1 depicts a phenomenological schema of various independent and interdependent events which are likely to occur when two relatively moving surfaces come in contact to form a sliding interface. In a usual sliding process that involves two or three bodies in relative motion, the sliding interface experiences a series of physico-chemical interactions and phenomenological consequences such as friction, wear, and corrosion.

Phenomenological complexity and multi-physical interactions at the interface throw enormous challenges to engineers attempting to design and optimize machine elements such as bearings, gear teeth, piston ring-liner, artificial orthopedic joints,

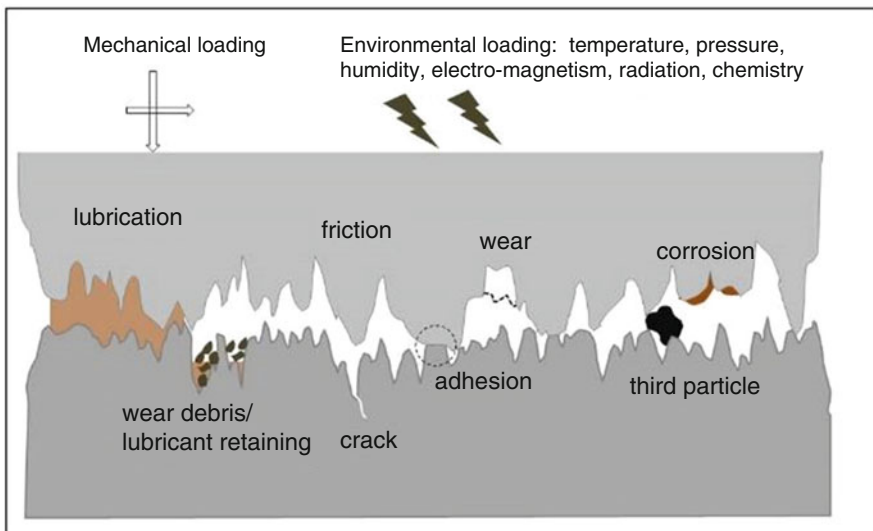
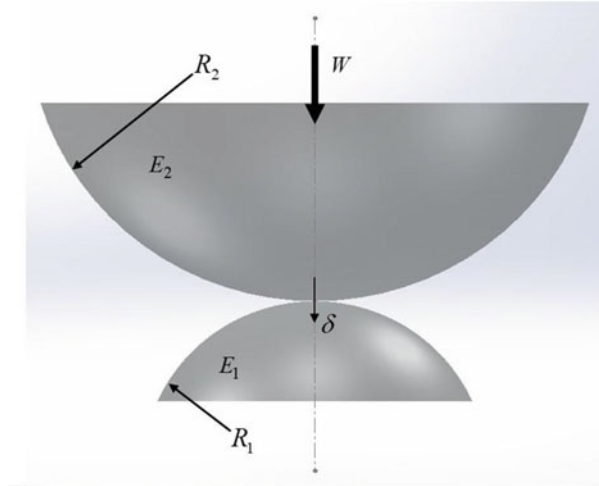


**Fig. 7.1** Schema of contact phenomenology of two interacting surfaces

**Fig. 7.2** Contact between two spherical bodies (the deformation,  $\delta$ , shown here is the cumulative deformation of the surface/point of contact and the down ward direction is assumed for representation)



and more. In the context of food oral processing, tribology of soft oral surfaces, saliva, and food ingredients in pertinence to assess food sensory properties has offered novel set of complex problems in the field and has gathered inter-disciplinary experts to collaborate in this new knowledge development process.

Contact mechanics, macroscopically, in between the nominal boundaries of the physical dimensions of the contacting surfaces, or, microscopically, in between two individual asperities often dominantly impact on the magnitude of friction. Based on classical continuum mechanics, Hertz has derived the first predictive theory for the force-displacement relationship between two spherical bodies building up a circular contact under an ideal hemi-spherical pressure distribution (Timoshenko and Goodier 1951).

Based on the Hertz theory, the mathematical relationships such as contact load-deformation and contact area-deformation can be derived in consistent with Fig. 7.2, where  $W$  is the load,  $a$  is the radius of circular contact area, and  $\delta$  is the deformation and the units of the quantities are as per SI system.

$$\text{Contact load : } W = KR^{1/2}\delta^{3/2} \tag{1a}$$

$$\text{Contact radius : } a = (R\delta)^{1/2} \tag{1b}$$

Maximum pressure at the geometric center of contact area,

$$p_{\max} = 1.5W/\pi a^2 \tag{1c}$$

where  $K$  = Hertzian modulus,  $K = (4/3) \left[ \sum_{i=1}^2 (1 - \nu_i^2)/E_i \right]^{-1}$  and  $R = \left[ \sum_{i=1}^2 1/2R_i \right]^{-1}$ , ( $\nu$  = Poisson's ratio)

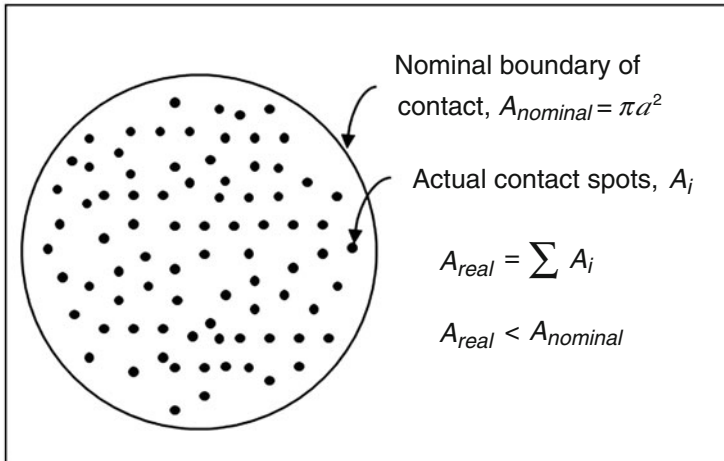


**Fig. 7.3** Contact area hypothesis: circular boundary is representing the nominal contact area and black dots are representing actual contact spots over asperities introduced by randomness, hierarchy, and scale of surface roughness

However, the Hertz theory encountered limitations in some practical instances. For example, contact between highly smooth and clean elastic solids under small external load unlikely to follow Hertz theory. In such cases, surface energy associated with the contacting surfaces actively influences the local contact condition, and hence the concept of adhesive contact theory was developed at later stage (Johnson et al. 1971; Fuller and Tabor 1975). Furthermore, every solid surface has small scale geometric features which are called *asperities*. Distribution of these asperities of varying shapes and sizes over the surface space forms the random and hierarchical micro-geometric structure on the surface popularly known as *surface roughness* (Panda et al. 2017). The shape, size, and distribution of asperities are naturally built for biological surfaces and inherited through the controlled production processes for engineering surfaces. Surface roughness is albeit another important consideration in tribology studies. This inherently introduces the randomness, hierarchy, and the scales at which the surfaces come in to contact. Some of these effects in asperity interactions are largely off-limits to observations. In short, the surface roughness introduces the difference between the nominal contact and the real contact area, where nominal contact area is defined by macro-geometric boundary and the real contact area is the summed-up area of all tiny contact spots (Fig. 7.3).

Surface roughness or asperities have been found to have much greater impact on the contact condition and the resulting friction and wear (Greenwood and Williamson 1966; Whitehouse and Archard 1970). It is eventually understood that the contact pressure experienced at the tiny contact spots of individual asperities is much higher than the nominal pressure over macro-contact area since  $A_{real} < A_{nominal}$ . Pressure over asperities often exceeds the strength of materials at interfacial junctions and results in microscopic material failures known as *wear*.

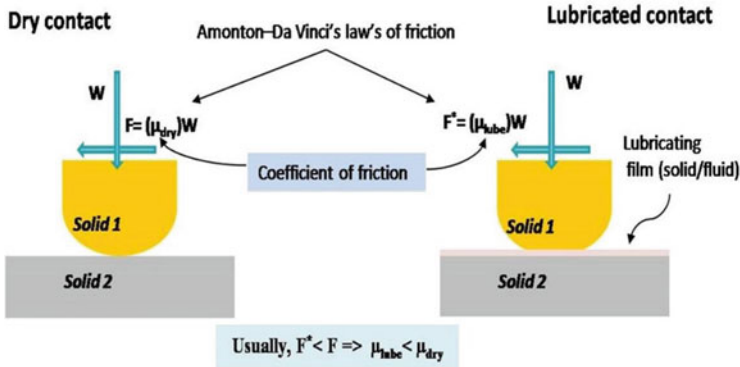
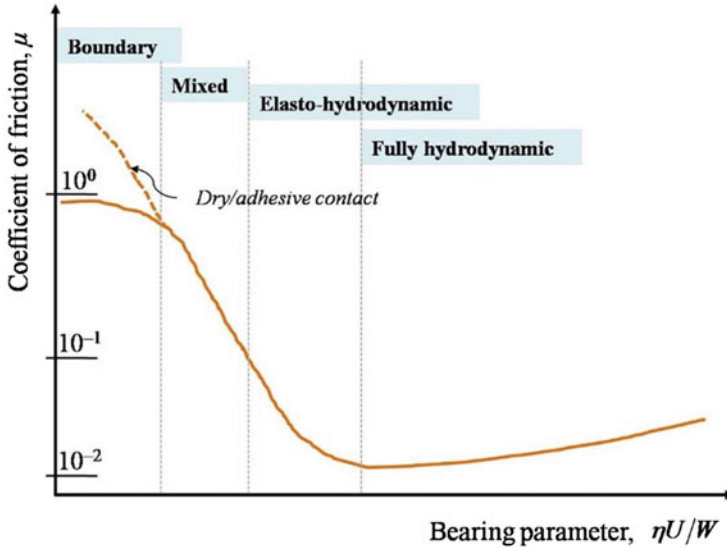


Fig. 7.4 Dry and lubricated contact scenarios

Wear of materials at the sliding/rolling interfaces resulting from the micro-mechanical failures, adhesion, and/or chemical actions are almost inevitable. A preventive action is therefore crucially important to avert excessive wear as well as to alleviate friction at the interface. Thereby, the idea of enabling a sustainable and protective film at the tribo-interface has been developed. Functions of such films are usually engineered to prevent the asperities and surfaces from coming to direct contact during sliding operation, and thereby preventing wear and reducing friction. The mechanism of interfacial film formation and its functions are commonly termed as *lubrication*. The subject of lubrication in industrial context has been well developed and optimized over the entire latter half of the previous century (Stachowiak 2017). However, in the last few decades, the knowledge of lubrication has been extended to several fields such as bio-medical, personal and beauty care product development, food oral processing, and in many other fields. In all these contexts, the use of a lubricating media such as a fluid is vital. In natural systems, the lubricant is naturally present such as synovial fluid in orthopedic joints and saliva in tongue-palate system; whereas in engineering systems, the lubricant is synthetically developed and applied depending on applications. In food oral processing context, saliva and some food compounds such as fat act as lubricating media. It is important to reiterate here that the usual understanding of lubrication is to enable easy in sliding by reducing friction. Figure 7.4 schematically demonstrates the difference between dry and lubricated contacts along with the description of Amontons–Da Vinci’s laws of friction (Hutchings 2016).

Engineering insights of lubrication is usually manifested by the *Stribeck* framework. This framework describes the variation of coefficient of friction with respect to the product of sliding velocity, lubricants’ viscosity, and inverse of normal load. Figure 7.5 shows a typical schematic of the *Stribeck* curve. This is often referred to distinguish between different regimes of lubrications termed as boundary, mixed, elasto-hydrodynamic, and purely hydrodynamic lubrication. For simplicity, the product representing the abscissa of Stribeck curve is termed as bearing parameter.



**Fig. 7.5** Schematic of the Stribeck framework ( $\eta$  = dynamic viscosity,  $U$  = sliding velocity;  $W$  = normal load)

From this graph, it can be apparently understood that with the increase in the bearing parameter,  $\eta U/W$ , the coefficient of friction drops and reaches to minima before starts rising slowly again. This gradual rise in COF occurs in full film condition at high speed and attributes to the fluid viscous friction and turbulence.

Understanding and utilization of Stribeck curve has been increasingly important in oral lubrication context. Firstly, because it is hard to generalize the governing regime of lubrication concerning one typical kind of food–saliva mixture, so presenting the friction response over a range of parametric inputs might give better clarification on friction–sensory relationship. Secondly, it is also naive to claim an absolute value of friction coefficient for a system or material; so, it is more invigorating to produce a map of friction coefficient as a function of parametric inputs. In some attempts to simplify, friction coefficient is often shown as function of speed instead of the product,  $\eta U/W$ , in the Stribeck curve. Nevertheless, use of only sliding speed in the abscissa of Stribeck curve is actually a compromise since the precise load variation in between the oral surfaces and the real viscosity of the non-Newtonian food–saliva mixture is yet to be known.

Applications of tribology for sensory studies are rapidly emerging. While the model of tongue–food/saliva–palate sliding system can be easily recognized, the challenges persist in establishing an appropriate tribological set-up to replicate this tribo-system. This is critically important to note here that the performance of lubrication is collectively dependent on the whole system and surroundings. Therefore, lubrication and/or friction are not intrinsic properties of any specific material such as food articles in the present context. Some of the most influencing parameters are load, speed, lubricant’s viscosity, temperature, interfacial chemistry, surface

roughness, and materials' properties. Moreover, oral surface materials are soft biological tissues which exhibit typical visco-elastic behavior. Therefore, mechanics and tribology of soft materials ought to be understood in some details.

### 3 Soft Tribology in Oral Processing

Soft tribology basically deals with the studies on governing principles behind tribological performances of soft materials such as elastomers, biological tissues, and bio-polymers (Pitenis et al. 2017). From an engineering point of view, solid or semi-solid material systems below elastic moduli of 100 MPa are usually considered as soft materials; however, in biological structures, materials below 100 kPa are commonly found and possess an even ultra-soft characteristic. The low elastic modulus governs the load-deformation behavior of these material systems, the system encounters large deformations even under extremely low load, which makes these systems vulnerable to inaccurate measurements and linear theories of mechanics often become inadequate to describe some of these behaviors. It is likely that soft material behaviors are somewhere in between the solid and fluid constitutive characteristics, so a combined constitutive behavior termed as visco-elasticity needs to be properly evaluated for the soft material systems. From the tribological perspectives of soft materials, large deformation leads to a larger area of contact under small load which drastically reduces the contact pressure, and thereby, exhibits a unique frictional response which is different from most engineering materials such as metals, alloys, and hard polymers.

Any tribological pair can be categorized as hard-hard, hard-soft, and soft-soft systems based on the contacting materials' constitutive behaviors in relative to each other. Measurements and theories have been optimized over the years to bring in our present day understanding on the behaviors of the engineering systems to deal with hard-hard and, to some extent, hard-soft contacts. These developments for conventional systems are nevertheless limited to capture the behavior of soft-soft systems; where each material has non-linear, time dependent, visco-elastic characteristics which often limit the use of linear theories of mechanics. Both in nature and engineering applications, numerous examples of soft-soft systems can be found. Understanding and capturing the behavior of soft-soft tribo-systems therefore have burgeoning research scopes to bring in novel applications and to optimize the existing applications for societal needs. In particulate to oral systems, both tongue and palate are made up of biological tissues and constitutively soft on their surfaces as well as bulk. Noteworthy, the palate is comparatively harder than the tongue. Thereby, tongue-palate system is an excellent example of soft tribology applications in nature which is crucial to food oral processing and sensory perceptions. Figure 7.6 shows a schematic depiction of tongue-palate system.

In the process of eating, at certain stage the tongue manipulates food by sweeping it on the surface of the upper palate. At this stage the friction that arises at the interfaces between food and tongue contributes to certain amount of sensory



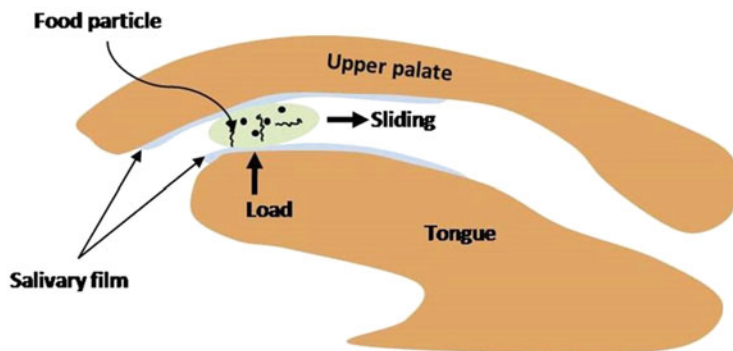


Fig. 7.6 Schematic of tongue–palate tribo-system

perceptions such as smoothness, creaminess, and slipperiness (Kokini et al. 1977; Kokini 1987).

Saliva keeps the oral surfaces protected from bacterial colonization and irritated rubbing. One can perform simple voluntary experiments to check the saliva starved situation on oral surfaces: for example, dry up the tongue and palate by wiping the surfaces with a piece of cotton and then allow tongue to slide on the palate; the irritation can be easily felt. This kind of oral irritation results from the rise in friction by the absence of saliva. In tongue-palate systems, presently it has been well recognized that salivary film works as a lubricant. Friction coefficients of mechanically stimulated saliva roughly fall in between 0.02 and 0.45 when tested in a PDMS (poly-di-methyl-siloxane) ball-on-disc tribo-system; and interestingly, friction coefficient of saliva remained always lower while compared to fresh water under various tribological testing conditions (Bongaerts et al. 2007b). Typically, saliva consists of nearly 99% water and around 1% of other components which include mostly proteins, enzymes, and some inorganic elements. Therefore, the low friction coefficient of saliva as compared to water may be attributed to certain other major components such as mucin proteins. Overall, the viscosity, the coating ability, and the lubricating behavior of saliva are governed by the intertwining actions of various mucins. More detailed information about saliva and the functions of mucin can be drawn from a recent review on age-saliva relationships (Xu et al. 2019), a special issue on food-saliva interactions (Mosca et al. 2019), and a model demonstrating the anchoring of MUC5B mucin on the oral epithelial cells (Ployon et al. 2016).

In pertinence to the lubricating characteristics of saliva, tribological experimentation can be an important instrumental approach for assessing typical sensory attributes such as *astringency*. Astringency is thought out to be due to high friction out of saliva starved situation or saliva breakdown during oral processing of a variety of foods and beverages such as fruits, tea, and wine (Upadhyay et al. 2016; Laguna and Sarkar 2017).

It has been practically important to analyze the soft tongue-palate tribo-system in presence of salivary fluid and food article in order to establish friction-sensory relationships. This is a complex natural system; nevertheless, the theory of soft

elasto-hydrodynamic (soft-EHL) lubrication received much appreciation in this context (de Vicente et al. 2006; Bongaerts et al. 2007a). In usual engineering lubrication studies, Stribeck curve accommodates elasto-hydrodynamic lubrication regime as a threshold frictional response before the full film hydrodynamic lubrication. This regime is special because of its dependency on two apparently important factors: (1) the elastic response of contacting materials; and (2) lubricant's piezo-viscous characteristics. Several empirical correlations manifest dramatic increase in the viscosity of lubricants with respect to pressure (Sargent 1983); and this phenomenon is known as piezo-viscous. Thereby, under piezo-viscous situation, an increase in contact pressure results in thickening of the lubricating fluid.

In much opposed to the hypothesis of classical EHL theory, in soft contacts—where elastic moduli are in the order of few MPa or few kPa—an increase in contact load is easily accommodated by more deformation of the soft materials. More contact deformation in turn alleviates contact pressure. This can be simply checked by deploying Hertz contact equations (Eqs. 1a, b, and c) for equal  $W$  and  $R$ , and varying  $K$  for a hard–hard, hard–soft, and soft–soft contacts. The dramatic reduction in contact pressure for soft–soft contacts results in trivial piezo-viscous influences. Also, more deformation at the contact allows lubricant to easily spread out and might result in further alleviation of the piezo-viscous impact. Recently, Masjedi and Khonsari (2017) estimated trivial differences (<0.5% error for central film thickness) between piezo-viscous and iso-viscous solutions for mixed-EHL contacts of soft materials having elastic moduli of 100 MPa. It is therefore fair to consider an iso-viscous condition for the soft-EHL contacts. Overall, the visco-elastic behavior of soft materials and lubricating characteristic of salivary fluid jointly define the frictional response of tongue–food/saliva–palate tribo-system.

In the theory of lubrication, Reynolds' equation governs the flow and pressure development in the mixed, EHL, and hydrodynamic regimes. The equation is fundamentally a reduced form of the well-known Navier-Stokes' equation which governs the fluid mechanics. A detailed discussion on the derivation and solution of the Reynolds' equation is beyond the scope of the present chapter. However, it is important to include some contextual solutions of the Reynolds' equation: de Vicente et al. (2006) solved the Reynolds' equation for soft-EHL problems concerning food colloids (e.g. xanthan gum, guar gum, etc.) as lubricating media and estimated an empirical formulation of friction coefficient in EHL regime as given below:

$$\mu_{\text{EHL}} = \frac{0.75(\text{SRR})(\eta U)^{0.34}}{R^{0.09} W^{0.12} K^{0.22}} \quad (2)$$

In the above expression, SRR is the slide to roll ratio. SRR can be defined for any given tribo-pair mechanisms (e.g. gear teeth, ball/roller bearings, ball-on-disc, etc.). Mathematically, it is the ratio of *relative* sliding velocity to the *mean* sliding velocity at the center of contact. For instance, in case of a ball-on-disc tribometer, if  $U_{\text{ball}} \neq U_{\text{disc}}$ , then:

**Table 7.1** Tribological case studies on food hydrocolloids

Reference	Experimental details	Coefficients and indices to fit “master” Stribeck curve
(Bongaerts et al. 2007a)	<ul style="list-style-type: none"> <li>• Ball-on-disc (PDMS-PDMS)</li> <li>• Ball dia. = 19 mm</li> <li>• Composite RMS roughness ~ 27.4 nm</li> <li>• SRR = 0.5; <math>W = 1.3</math> N; <math>U = 1</math>–2400 mm/s</li> <li>• Samples: Water; Corn syrup (95%)</li> </ul>	$h = 4.75$ ; $k = 0.11$ ; $l = 0.07$ ; $m = 2.7$ ; $n = 0.5$ ; $B = 3.8e-5$ $(10^{-7} < \eta U < 2)$
(Krop et al. 2019)	<ul style="list-style-type: none"> <li>• Ball-on-disc (PDMS-PDMS)</li> <li>• Ball dia. = 19 mm</li> <li>• Composite cla roughness ~50 nm</li> <li>• SRR = 0.5; <math>W = 2</math> N; <math>U = 1</math>–1000 mm/s</li> <li>• Samples: hydrogels (<math>\kappa</math>-Carrageenan; <math>\kappa</math>-C + locust bean gum; <math>\kappa</math>-C+ calcium/sodium alginate)</li> </ul>	$h = 11$ ; $k = 0.0065$ ; $l = 0.075$ ; $m = 1$ ; $n = 0.55$ ; $B = 3.3e-5$ $(10^{-6} < \eta U < 10)$

RMS Root mean square, CLA Center line average, SRR Slide to roll ratio

$$SRR = |U_{\text{ball}} - U_{\text{disc}}|/U, \quad \text{where } U = (U_{\text{ball}} + U_{\text{disc}})/2 \quad (3)$$

Physically, the value of SRR determines whether the contact is sliding or rolling motion dominated. SRR can be 0 for a *pure rolling* condition and 2 for a *pure sliding* condition. Moreover, a value of SRR below 1 means that the contact is mostly rolling and above 1 means it is mostly sliding. Notably, SRR of the tongue–palate system is hitherto unknown; nevertheless, a value of 0.5 is usually taken in oral tribology experiments. This is albeit counter intuitive. In consistent with the expression of SRR, if either disc or ball is static, then SRR = 2. This means, if one element in the tribo-pair is fixed or quasi-static, then the contact predominantly slides. In tongue-palate system, the palate is almost quasi-static with respect to the tongue. Therefore, an SRR of more than 1 seems more appropriate choice for oral tribology experiments.

Bongaerts et al. (2007a) attempted to fit a “master” Stribeck curve by covering entire regimes of lubrication and proposed an empirical expression of friction coefficient assuming power law characteristics:

$$\begin{aligned} \mu &= \mu_{\text{EHL}} + \left( \frac{|\mu_{\text{Boundary}} - \mu_{\text{EHL}}|}{1 + (\eta U/B)^m} \right) \quad \text{where, } \mu_{\text{EHL}} \\ &= k(\eta U)^n \quad \text{and} \quad \mu_{\text{boundary}} = h(\eta U)^l \end{aligned} \quad (4)$$

Further, the coefficients  $h$ ,  $k$ , and indices  $l$ ,  $m$ , and  $n$  can be estimated by fitting experimental data with the above equation. Moreover, the value of  $B$  is the upper limit of  $\eta^U$  for boundary lubrication regime for any given case. It is important to note here that not all but many experimental data may be fitted with the above equation to plot a “master” Stribeck curve. Table 7.1 shows data from two cases on tribological testing of food hydrocolloids, where the above equation has been used to obtain the “master” Stribeck curve.

Significant differences in these two experimental cases are in food samples, tribo-pair roughness, load, and range of speeds. Substantial changes in the fitting parameters are in the values of  $h$  and  $k$ ; notably,  $h$  and  $k$  are power law coefficients in boundary and EHL lubrication regimes (Eq. 4), respectively. In logarithmic scales, these coefficients determine the intercept on friction coefficient axis. Physically, an increase in  $h$  means the boundary friction value rises towards the lower limit of  $\eta U$ , and a drop in the value of  $k$  means, the limiting friction for starting-up EHL regime is reduced. This means, in the case of (Krop et al. 2019), the boundary and mixed regime are elongated as compared to the EHL regime. Therefore, two different studies on different hydrocolloid samples produced two different Stribeck curves. This is a caveat; and the idea of producing generic “master” Stribeck curve for hydrocolloid samples need more data for further optimizations. In fact, some important effects such as surface roughness, hydrophobicity, and presence of surface active elements are hitherto not included. These effects significantly influence the performance of biological surfaces such as the tongue.

Tongue surface is biologically textured with two main types of papillae (Sarkar et al. 2019) covering nearly 70% of the frontal surface area: (1) filly form, without any taste buds and with hair like appearance on top; (2) fungi form, containing taste buds, and has mushroom like appearance. The filly form hairs high around 250  $\mu\text{m}$  are most protruding and taking part in active sliding friction while tongue swipes over the palate. These altogether constitute an intricate micro-geometric structure on the surface of tongue. Saliva introduces further complexity. Mucin in saliva forms a *salivary pellicle* of thickness up to 100 nm by getting adsorbed on the base surface of tongue, and this *salivary pellicle* holds the fluidic structure of the saliva. The salivary pellicle thickness varies and at some point may be nearly vanishing during oral processing. This leads to a saliva starved situation. Sarkar et al. (2019) postulated three types of adsorbed film formation: (1) saliva-rich/deficient film; (2) saliva–food mixture dominated film; and (3) food dominated film. One or more of these adsorption films implicate the food–saliva chemistry which in turn impact on the friction and mechano-sensation during oral processing and generates a series of sensory perceptions such as astringency, creaminess, smoothness, etc.

Furthermore, the soft and protruded papillae textures constitute a spongy structure on the tongue surface. In the presence of salivary papillae and other surface active agents, the microscopic spongy maze on the tongue surface may store certain amount of salivary fluid and mechanically squeeze it out under pressure. This mechanism may possibly develop a salivary fluid film whenever the tongue applies pressure on food/palate. This may resemble the tongue surface structure as *poroelastic* material system. Poroelasticity is usually exhibited by a bi-phasic material system, where a spongy solid structure retains a fluid; and the load-deformation behavior is governed by the solid–fluid interaction. Mammalian cartilage is a striking example of *poroelastic* structure made up of collagen, water, and synovial fluid (Neville et al. 2007). In fact, tongue surface as a poroelastic structure is still a conjecture; and it is clearly naive at present to accept mechanistic behavior of tongue as closely similar to that of cartilage. Future research on the mechanistic aspects of tongue–food–palate contact is likely to bring in more insights in these aspects.

## 4 Experimental Techniques in Oral Tribology Characterization

In pertaining to tribology–sensory studies, an appropriate *in vitro* experimental methodology is vital in order to ascertain the situations inside oral cavity as closely as possible. Rheology and bulk mechanical experiments have dominated the food oral processing and sensory relationships over many years. The seminal work of Kokini et al. (1977) has produced ab-initio empirical models to establish the role of \*friction\* in addition to \*flow\* to provide texture perceptions such as *smoothness*, *slipperiness*, and *creaminess*:

$$\begin{aligned} \text{creaminess} &\propto (\text{thickness})^{0.54} \times (\text{smoothness})^{0.84}, \quad \text{where smoothness} \\ &\propto 1/\text{friction} \end{aligned}$$

It can be naively understood from the above correlation that certain texture perceptions depend more on the tribological behavior of the food articles during oral processing.

After a decade, Hutchings and Lillford (1988) have drawn philosophical perspectives on how eating and sensation, both of which are dynamical in nature, could best be correlated with the instrumental methods. The observations hypothesized a three-dimensional “mouth process model” to demonstrate the criterion of swallowing of food following a “breakdown path” which is unique to food, individual eater, and eating occasions. In their model, one typical criterion plane defines the “*degree of lubrication*,” where the other two planes are on the basis of “*degree of structure*,” and “*time*.” The model emphasized the importance of “*degree of lubrication*” and appended difficulties to define it. According to this model, the normal trajectory of food breakdown with respect to *time* in most cases follows a downward direction in the *degree of structure* and in the increasing direction in the *degree of lubrication*; nevertheless, in some exceptional cases such as for peanut butter or sesame paste, the trajectory may move opposite to the normal path at the initial stage of oral process by quickly absorbing saliva before taking the normal direction (i.e. decreasing the *degree of structure* and increasing the *degree of lubrication*) (Nishinari et al. 2019).

Overall, it is understood that a single instrumental approach can be very inadequate to bring in comprehensive correlation between instrumental findings and sensory perceptions, and possibly, a combination of instrumental methods ought to be designed. Surprisingly, this model did not correspond to the earlier findings of Kokini et al. (1977) in regard to the in-mouth lubrication and friction–sensory relationships. Further, despite its comprehensiveness, the Hutchings and Lillford model remained almost unrecognizable until the end of previous decade due mainly to dearth of sophisticated instrumental techniques (Chen 2009).

The importance of in-mouth lubrication during food oral processing for both swallowing and sensory perception has been eventually realized. These developments led towards a paradigm shift in the food sensory research which is turning towards the regimes of tribology and rheology instead of mere rheology and bulk

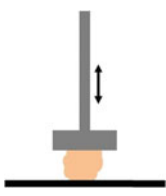
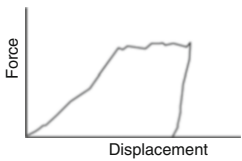
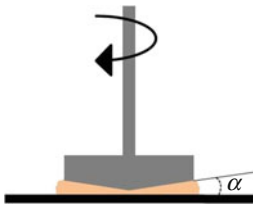
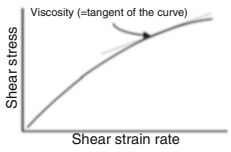
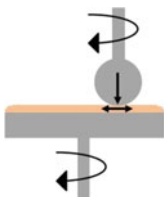
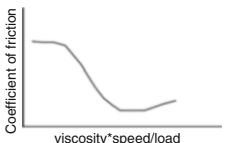
mechanics. Chen and Stokes (2012) have illustrated the changes in the governing mechanisms of eating as a function of oral processing time. They highlighted the change in length scale of food articles which undergo changes from centimeter during ingestion to micron/sub-micron scale during swallowing. This change in length scale is governed initially by mechanical breaking, fracture, and bulk deformation and gradually by saliva mixing, moistening, and shearing. Overall, it was understood that eating or food oral processing is a complex dynamical process and so is the sensory perception. Therefore, the sensory attributes also evolve, which means the mouthfeel at an early stage of oral processing may be different than at later stage for the same food component, where the early stage mouthfeel depends largely on bulk mechanical properties and rheology and the later stage, feelings are more linked to thin film shearing resulting in friction and lubrication.

Tribological experiments on food articles have since been recognized as much important as rheology measurements and quality descriptive sensory statistics. Also, in the intermediate stage of oral processing, rheology and tribology jointly contribute to mouthfeel factors in an implicit manner. This framework is particularly useful to classify the growing vocabulary of sensory descriptions based on driving mechanisms of oral processing: mechanics; rheology; tribology; and rheo-tribology. These typical mechanisms can be adopted in instrumental techniques, and further the instrumental outputs can be linked to typical sensory descriptions. Overall, three mechanical instruments, namely, texture analyzer, rheometer, and tribometer, have been adopted and being continuously optimized for analyzing foods and colloids. A comprehensive assessment of food articles for sensory attributes can be largely possible by one or more of these instruments. The instrumental outputs can eventually be calibrated to a metric for instrumental sensory descriptions. Table 7.2 is furnished with some details about these experimental techniques and attached sensory descriptions.

It must be noted here that tribology measurements of food articles depend heavily on the systems and surroundings and thereby tribological parameters (friction/lubrication) are not intrinsic properties of food compounds. With these caveats, it is vital to have better understanding of the systems being used for *in vitro* tribological assessment which include: the instrument, model tribological pairs, model food items, application of saliva, and system operating variables and surrounding environments.

In early stages of oral tribology studies, varieties of tribo-contact configurations and contacting materials were tested. Pradal and Stokes (2016) have reviewed different types of tribo-configurations. Due to available variations on the choice of instruments, material pairs, and model food systems, it is hard to argue over, advantage of one specific system over others. However, there should be clear understanding of the system and surroundings being used. Amongst all, a specialized commercial tribometer, namely, mini traction machine (MTM) has been most frequently used and eventually popularized. The machine is a modified ball-on-disc system; where a combined sliding-rolling motion of the contact is given by rotating both ball and disc and maintaining a constant slide to roll ratio. A schematic of this system can be seen in the last row of Table 7.2, the geometric figure is a

**Table 7.2** Instrumental methods in food oral processing in correspondence to sensory studies

Test type	Geometric configuration	Representative test outputs	Textural attributes
Texture property analysis (Mechanical compression)		 (To characterize bulk mechanical strengths)	Hardness, Springiness, Crispness
Rheology (Flow, squeezing, and bulk shearing)		 (To characterize constitutive behavior and viscosity)	Thickness, Pasty, Smoothness, Slipperiness, Creaminess
Tribology (Thin film shearing, sliding, and rolling)		 (To characterize friction at different lubricating regimes)	Astringency, Smoothness, Slipperiness, Creaminess

Note: Textural attributes as noted in the last column are not the direct outcome of the test outputs obtained from any of the tests. In fact, the relationships between test results and sensory attributes are often complex and depend on additional parameters. For example, to use the *force-displacement* curve as an assessment of *hardness*, one needs to know the size and shape of the sample

representative tribometer; however, in the actual MTM machine the ball holder is usually tilted with respect to the disc plane in order to avoid the spinning of the ball with respect to holder axis.

Recent advances in instrumentation and material science have greatly augmented the applications of tribological experiments in food sensory research. Currently, PDMS rubber ( $E \sim 1\text{--}100$  MPa) is the most popular material being used as model tribo-pairs. Soft and visco-elastic behavior, tunable mechanical properties, and excellent formability, which enables advanced manufacturing technology such as 3D printing to process PDMS in desired shapes, sizes and properties, are the reasons behind the popularity of PDMS. However, properties of PDMS are still more than ten times higher than the maximum pressure experienced in oral conditions (Sarkar et al. 2019). This means the effect of contact deformation on lubrication in PDMS–PDMS contact cannot be extrapolated to draw the similar effects in biological contacts. In fact, the challenge persists to address two main aspects here: first, the

elastic response of the model components which should be equivalent to biological components; and second, the model surface microstructure and chemistry should mimic the biological surfaces.

Other important aspects of oral tribological experiments are proper and adequate application of saliva to model food samples and to the system. In fact, it is challenging to address the complex salivating process in *in vitro* experiments. Currently, either simulated saliva or artificial saliva is being used to apply on the model surfaces and samples before or during experiments. Presence of saliva on tribo-surfaces is critical to the frictional response of the system; and maintaining the situation in a tribometer set-up needs challenging arrangement such as submerging the PDMS ball/disc in to saliva and/or establishing a supply system to keep applying saliva while the tribometer is running.

## 5 Case Studies on Tribological Evaluation of Food Hydrocolloids

In particulate to food hydrocolloids, Chojnicka-Paszun et al. (2014) examined the tribology–sensory relationships for model solutions of polysaccharides with protein particle dispersions. Three selected polysaccharide stocks are locust bean gum, pectin, and xanthan; spherical protein particles were mainly abstract from whey protein isolate/locust bean gum gel. Tribological evaluations were correlated with quantitative descriptive analysis (QDA). An attempt has been made in this chapter to summarize some of these findings in Table 7.3 below.

Looking in to these case studies on polysaccharides, it appears that tribological evaluation correlates weakly with the sensory attributes as characterized by QDA scores. In the absence of particle, lubricating ability of xanthan solution is most superior followed by pectin and LBG, respectively. This order is likely to change with the add-on protein particles. Except for pectin, the presence of particles caused dramatic changes in the lubricating ability of xanthan. In the presence of larger particle size, friction coefficient of xanthan solution increases. On the other hand, the change in “powdery” sensation is more prominent in case of xanthan. In fact, LBG without particle has poorest lubrication and paltry powdery sensation; whereas xanthan with large protein particles has superior powdery sensation despite diminishing lubricating ability. These observations are highly counterintuitive, and, therefore, the “powdery” attribute could not be directly linked to friction. Thereby, this attribute can possibly be linked to other mechanical characteristics such as *hardness* or *elasticity* of the tiny protein spheres.

It is intriguingly intuitive to link “slippery” and “stickiness” with respect to lubricating ability of the samples. Nevertheless, “slippery” and “stickiness” loosely relates to tribological evaluations of the polysaccharide solutions. These weak correlations are likely to be influenced by other factors, and may vary sample to sample as well as individual to individual. Overall, the poor reflection of tribological



**Table 7.3** Relationships between lubricating ability, protein particle size, and sensory attributes for polysaccharide solutions (data from Chojnicka-Paszun et al. 2014)

Parameters	Ordering of the samples		
	Without any particles	With small protein beads of size 15 $\mu\text{m}$	With large protein beads of size 56 $\mu\text{m}$
Lubricating ability <sup>a</sup> ( $W = 2\text{N}$ ; $U = 5\text{--}100\text{ mm/s}$ )	<b>Xanthan &gt; Pectin &gt; LBG</b>	<b>Pectin &gt; Xanthan &gt; LBG</b>	<b>Pectin ~ LBG &gt; Xanthan</b>
Sensory attributes <sup>b</sup>	Powdery	<b>Pectin &gt; Xanthan &gt; LBG</b>	<b>Pectin &gt; LBG &gt; Xanthan</b>
	Slippery	<b>Xanthan &gt; LBG &gt; Pectin</b>	
	Stickiness	<b>Pectin &gt; LBG &gt; Xanthan</b>	
	Filminess		
Sliminess			

<sup>a</sup>The ordering of lubricating ability of samples, xanthan (2%), pectin (2.25%), and LBG (1%) are based on **significant differences** in the values of friction coefficient plotted in the Stribeck curve

<sup>b</sup>The ordering of the sensory attributes of samples is based on **marginal differences** in the respective QDA scores

evaluation on sensory attributes indicates that despite tribology has become a vital instrumental approach, nevertheless, additional measurements like fracture properties, hardness, etc. should supplement the tribological evaluation in order to achieve more conclusive correlations.

Polysaccharides are quite common as thickeners in food articles; thereby, tribology–sensory relationships for these compounds are of specific interest. Zinoviadou et al. (2008) studied the role of saliva in tribology, rheology, and spreadability of cross-linked starch and LBG. The addition of saliva dramatically reduces the apparent viscosity, moderately increases friction and slightly enhances spreadability (lower contact angle) for starch samples. Overall, these comparisons attempted to capture the significance of saliva–polysaccharide interactions in oral processing and sensory implications. Furthermore, starch microstructure is more like “spherical” granules, and these shapes can be responsible for low friction; however, after being exposed to saliva, these granules breakdown. Therefore, sustenance of low friction for starch–saliva mixture as compared with pure starch sample was identified as a function of the rate at which the starch granules get affected by saliva induced digestion. The impact of oral processing time on shape and size breakdown of food compounds is therefore critical to its tribological properties and subsequent sensory perceptions. In fact, this study was not conclusive on sensory properties linked to the findings.

In another interesting study, Nguyen et al. (2017) made an appreciable attempt to mix some of the hydrocolloids (gelatin, xanthan, Carrageenan, and modified starch) with low fat skimmed yogurt (<0.1% fat) in order to arrive at a full fat yogurt experience. The study employs texture, rheology, tribology, and QDA assessment with the selected samples and total of eight different sensory attributes: thickness, smoothness, creaminess, powdery, stickiness, lumpiness, oily coating, and residue coating. From QDA statistics, the gelatin was found to be most influencing hydrocolloids to push the sensory attributes of skim yogurt for enhanced thickness, smoothness, and creaminess. The QDA assessment was in agreement with the instrumental assessments. This study implicates the utilization of hydrocolloids as fat replacements and the establishment of tribology–sensory relationship for their successful characterization.

Recently, Krop et al. (2019) have presented an extensive study on the relationships between tribology, rheology, and sensory attributes for  $\kappa$ -Carrageenan and some inhomogeneous gels prepared by mixing  $\kappa$ -Carrageenan with locust bean gum, sodium/calcium alginate, etc. In particular to “slippery,” the Pearson’s correlation coefficients for QDA scores of “slippery” with respect to fracture stress, fracture strain, and COF at 50 mm/s appear to be 0.80, 0.80, and 0.82, respectively. These correlations are strikingly consistent and good indicators that slippery is linked to COF and fracture properties; nevertheless, the authors pointed out that “slippery” is indeed a difficult perception and panelists ought to be properly trained to score this attribute. Additionally, on the contrary with the empirical model of Kokini (1987), the “smoothness” perception was not found to be correlated with any of the instrumental outputs; and this situation was attributed to the composite nature of the samples used in the study. Based on the assessments of comprehensive

experimental observations (fracture properties; viscosity; and tribology), descriptive sensory analysis, and statistical correlations among the various quantities, the study established certain relationships between mechanical (fracture) and flow properties (viscosity), and texture attributes (smoothness, slippery, pasty, etc.) of hydrocolloids especially at early stages of oral processing.

At the later stages of oral processing, surface properties become more dominant to produce thin film on the oral surfaces, so lubrication/friction characteristics are vital to establish tribology–sensory or rheo–tribology–sensory relationships (Chen and Stokes 2012). In fact, at the early stages of oral processing of hydrocolloids, simultaneous actions of fracture, flow, and friction are crucial to determine sensory perception. It is important to mention here that food hydrocolloids structures may vary widely and ample number of inhomogeneous gel structure may be produced, there by the behavior of food structures under oral processing might vary accordingly. Follow-up studies on hydrocolloids are therefore needed to further consolidate the fracture–flow–friction–sensory relationships.

## 6 Challenges and Future Prospects

Challenges associated with tribology-sensory research basically originate from the fact that tribological parameters are system dependent and not intrinsic properties of the food itself. The friction/lubrication parameters are highly sensitive to the tribo-pair material system, model food colloids, operating variables, and environmental influences. Thereby, it requires a number of variables to be controlled in order to mimic the system as nearly as possible to the actual oral processing system. Further, replication of actual oral surfaces is yet to be achieved. Hierarchical surface texture and bulk properties of biological tongue enhances this complexity by manifolds. There have been recent advancements towards a better understanding of tongue surface texture and the mechanics (Funami 2016). Human variation of tongue topography in relation to oral tribology has also been recently investigated in some details (Wang et al. 2019). It can be easily realized that the friction/lubrication characteristics in actual oral processing has strong dependence on the “filly” and “fungi” form structures of the tongue surface. At this stage, it is important to incorporate more of the tongue surface features, material property variations, and surface characteristics such as hydrophobic effects. The motion and dynamics of oral processing are important especially when friction is to be evaluated. Thereby, implementation of actual oral motion (the ratio of rolling/sliding and impact, etc.) and the degrees of freedom that the tongue enjoys can be taken up in follow-up researches.

Saliva–food interaction is another important influencing factor to the sensory perceptions and eating experience as it was aptly put in words, “*what is perceived in-mouth is a food–saliva mixture rather than the food on the plate*” (Mosca and Chen 2017). Thereby, the food–saliva interactions in many cases may result in new compounds as well as very different microstructures, which may eventually impact

on the friction and lubrication scenarios. These important effects in oral tribology experiments are yet to be captured.

Sensory perceptions are dynamical functions of food breakdown length scale and oral processing time. It is therefore vital to estimate the duration that a model food samples needs to be exposed in the tribometer in order to synchronize with the “breakdown path.” These factors must be duly incorporated and optimized to corroborate the friction–sensory relationships.

## 7 Summary

The idea of enabling tribological principles in food sensory property assessment basically stem from three basic understanding: (1) saliva is a lubricant; (2) tongue–food/saliva–palate is a natural sliding system; (3) the friction that arises in this natural sliding system relates to a handful of sensory perceptions. The fundamental aim behind this idea is to use friction coefficient in order to arrive at some standard quantitative metric that will determine a particular sensory attribute attached to a particular food component. The impact that these ideas can bring are multifaceted: for example, to devise fat replacements having equal pleasure of fat in order to challenge obesity, to reduce the cost of employing expert sensory panel, to design food for orally impaired patients, and more.

However, tribological experiments depend largely on the systems and surroundings and the system output, usually, the friction coefficient can be variable for same food articles being tested at different set-ups in two different laboratories. Therefore, research community in the field may agree on some standards or protocols for tribological testing with food samples which can avoid redundancies and anomalies. The “master” Stribeck curve is another interesting idea; after proper optimization, a standard “master” curve representing a specific group of fundamental and integrated food articles (e.g. hydrocolloids, dairy colloids, etc.) can be very useful in the field. Further, the tribological characterization is bringing in more comprehensiveness in sensory analysis; and correlation between instrumental outputs with typical sensory descriptions with the help of quantitative metrics can be a striking breakthrough in food sensory studies.

**Acknowledgements** Authors acknowledge financial support for this work by the Natural Science Funding Council of China (grant number 31871885).

## References

- Bongaerts JHH, Fourtouni K, Stokes JR (2007a) Soft-tribology: lubrication in a compliant PDMS–PDMS contact. *Tribol Int* 40(10–12):1531–1542. <https://doi.org/10.1016/J.TRIBOINT.2007.01.007>

- Bongaerts JHH, Rossetti D, Stokes JR (2007b) The lubricating properties of human whole saliva. *Tribol Lett* 27(3):277–287. <https://doi.org/10.1007/s11249-007-9232-y>
- Chen J (2009) Food oral processing—a review. *Food Hydrocolloids* 23(1):1–25. <https://doi.org/10.1016/J.FOODHYD.2007.11.013>
- Chen J, Stokes JR (2012) Rheology and tribology: two distinctive regimes of food texture sensation. *Trends Food Sci Technol* 25(1):4–12. <https://doi.org/10.1016/J.TIFS.2011.11.006>
- Chojnicka-Paszun A, Doussinault S, de Jongh HHJ (2014) Sensorial analysis of polysaccharide-gelled protein particle dispersions in relation to lubrication and viscosity properties. *Food Res Int* 56:199–210. <https://doi.org/10.1016/J.FOODRES.2013.12.035>
- de Vicente J, Stokes JR, Spikes HA (2006) Soft lubrication of model hydrocolloids. *Food Hydrocolloids* 20(4):483–491. <https://doi.org/10.1016/j.foodhyd.2005.04.005>
- Fuller KNG, Tabor D (1975) The effect of surface roughness on the adhesion of elastic solids. *Proc Royal Soc Math Phys Eng Sci* 345(1642):327–342. <https://doi.org/10.1098/rspa.1975.0138>
- Funami T (2016) Tongue pressure measurement in food science. *Curr Opin Food Sci* 9:29–33. <https://doi.org/10.1016/J.COFS.2016.04.003>
- Greenwood JA, Williamson JBP (1966) Contact of nominally flat surfaces. *Proc Royal Soc Lond Ser A Math Phys Sci* 295(1442):300–319. <https://doi.org/10.1098/rspa.1966.0242>
- Hutchings IM (2016) Leonardo da Vinci's studies of friction. *Wear* 360–361:51–66. <https://doi.org/10.1016/J.WEAR.2016.04.019>
- Hutchings JB, Lillford PJ (1988) The perception of food texture - the philosophy of the breakdown path. *J Text Stud* 19(2):103–115. <https://doi.org/10.1111/j.1745-4603.1988.tb00928.x>
- Johnson KL, Kendall K, Roberts AD (1971) Surface energy and the contact of elastic solids. *Proc Royal Soc A Math Phys Eng Sci* 324(1558):301–313. <https://doi.org/10.1098/rspa.1971.0141>
- Kokini JL (1987) The physical basis of liquid food texture and texture-taste interactions. *J Food Eng* 6(1):51–81. [https://doi.org/10.1016/0260-8774\(87\)90021-5](https://doi.org/10.1016/0260-8774(87)90021-5)
- Kokini JL, Kadane JB, Cussler EL (1977) Liquid texture perceived in the mouth. *J Text Stud* 8(2):195–218. <https://doi.org/10.1111/j.1745-4603.1977.tb01175.x>
- Krop EM et al (2019) On relating rheology and oral tribology to sensory properties in hydrogels. *Food Hydrocolloids* 88:101–113. <https://doi.org/10.1016/j.foodhyd.2018.09.040>
- Laguna L, Sarkar A (2017) Oral tribology: update on the relevance to study astringency in wines. *Tribol Mater Surf Interf* 11(2):116–123. <https://doi.org/10.1080/17515831.2017.1347736>
- Masjedi M, Khonsari MM (2017) Mixed lubrication of soft contacts: an engineering look. *Proc Inst Mech Eng Part J J Eng Tribol* 231(2):263–273. <https://doi.org/10.1177/1350650116652286>
- Mosca AC, Chen J (2017) Food-saliva interactions: mechanisms and implications. *Trends Food Sci Technol*. <https://doi.org/10.1016/j.tifs.2017.06.005>
- Mosca AC, Feron G, Chen J (2019) Saliva and food oral processing. *J Text Stud* 50(1):4–5. <https://doi.org/10.1111/jtxs.12389>
- Neville A et al (2007) Synovial joint lubrication — does nature teach more effective engineering lubrication strategies? *Proc Inst Mech Eng Part C J Mech Eng Sci* 221(10):1223–1230. <https://doi.org/10.1243/09544062JMES724>
- Nguyen PTM et al (2017) Effect of different hydrocolloids on texture, rheology, tribology and sensory perception of texture and mouthfeel of low-fat pot-set yoghurt. *Food Hydrocolloids* 72:90–104. <https://doi.org/10.1016/J.FOODHYD.2017.05.035>
- Nishinari K, Fang Y, Rosenthal A (2019) Human oral processing and texture profile analysis parameters: bridging the gap between the sensory evaluation and the instrumental measurements. *J Text Stud* 50:369–380. <https://doi.org/10.1111/jtxs.12404>
- Panda S et al (2017) Spectral approach on multiscale roughness characterization of nominally rough surfaces. *J Tribol* 139(3). <https://doi.org/10.1115/1.4034215>
- Pitenis AA et al (2017) Challenges and opportunities in soft tribology. *Tribol Mater Surf Interf* 11(4):180–186. <https://doi.org/10.1080/17515831.2017.1400779>
- Ployon S et al (2016) The membrane-associated MUC1 improves adhesion of salivary MUC5B on buccal cells. Application to development of an in vitro cellular model of oral epithelium. *Arch Oral Biol* 61:149–155. <https://doi.org/10.1016/j.archoralbio.2015.11.002>

- Pradal C, Stokes JR (2016) Oral tribology: bridging the gap between physical measurements and sensory experience. *Curr Opin Food Sci* 9:34–41. <https://doi.org/10.1016/J.COFS.2016.04.008>
- Sargent LB (1983) Pressure–viscosity coefficients of liquid lubricants. *A S L E Transact* 26(1):1–10. <https://doi.org/10.1080/05698198308981471>
- Sarkar A et al (2019) Lubrication of soft oral surfaces. *Curr Opin Colloid Interf Sci* 39:61–75. <https://doi.org/10.1016/J.COCIS.2019.01.008>
- Stachowiak GW (2017) How tribology has been helping us to advance and to survive. *Friction* 5(3):233–247. <https://doi.org/10.1007/s40544-017-0173-7>
- Timoshenko S, Goodier N (1951) *Theory of elasticity*. McGraw Hill
- Upadhyay R, Brossard N, Chen J (2016) Mechanisms underlying astringency: introduction to an oral tribology approach. *J Phys D Appl Phys* 49(10):104003. <https://doi.org/10.1088/0022-3727/49/10/104003>
- Wang X, Wang X, Upadhyay R, Chen J (2019) Topographic study of human tongue in relation to oral tribology. *Food Hydrocolloids* 95:116–121. <https://doi.org/10.1016/j.foodhyd.2019.04.022>
- Whitehouse DJ, Archard JF (1970) The properties of random surfaces of significance in their contact. *Proc Royal Soc A Math Phys Eng Sci* 316(1524):97–121. <https://doi.org/10.1098/rspa.1970.0068>.
- Xu F, Laguna L, Sarkar A (2019) Aging-related changes in quantity and quality of saliva: where do we stand in our understanding? *J Text Stud* 50(1):27–35. <https://doi.org/10.1111/jtxs.12356>
- Zinoviadou KG, Janssen AM, de Jongh HHJ (2008) Tribological properties of neutral polysaccharide solutions under simulated oral conditions. *J Food Sci* 73(2):E88–E94. <https://doi.org/10.1111/j.1750-3841.2007.00649.x>

# Chapter 8

## Coating and Film-Forming Properties



Qian Xiao

**Abstract** Hydrocolloid-based coatings and films, produced from polysaccharides, proteins, and their blends, have emerged as alternatives to synthetic polymers for food and packaging applications, because they are edible, versatile, renewable, and biodegradable. Coatings are formed as a thin layer directly onto food surfaces by dipping, spraying, brushing, fluidized bed, or panning method. By contrast, films are standalone pre-formed materials either placed between food components or sealed into pouches, and they are manufactured by wet- or dry-casting method. Overall, hydrocolloid-based coatings and films possess excellent barrier properties to CO<sub>2</sub>, O<sub>2</sub>, and oil under certain conditions, but moderate water vapor barrier properties. Their formation mechanisms are closely correlated with conformation of biopolymers, their aggregation and crystalline state, as well as their interactions with additives and water. This chapter discusses the existing and potential applications of coatings and films, focusing on the developments and trends of hydrocolloid-based coatings and films for the food industry.

**Keywords** Hydrocolloids · Coatings · Films · Physicochemical properties · Applications

### 1 Introduction

Petrochemical-based plastics, such as polyethylene (PE), poly(ethylene terephthalate) (PET), polypropylene (PP), polyvinylchloride (PVC), have dominated the food packaging market for their functionality, lightweight, ease of processing, and low cost (Siracusa et al. 2008). Despite these advantages, increased use of plastic packaging materials has led to serious ecological problems, since they are neither fully recyclable nor biodegradable. While the materials can be incinerated to reclaim

---

Q. Xiao (✉)

School of Food Science and Technology, Hunan Agricultural University, Changsha, Hunan, China

e-mail: [qianxiao@hunau.edu.cn](mailto:qianxiao@hunau.edu.cn)

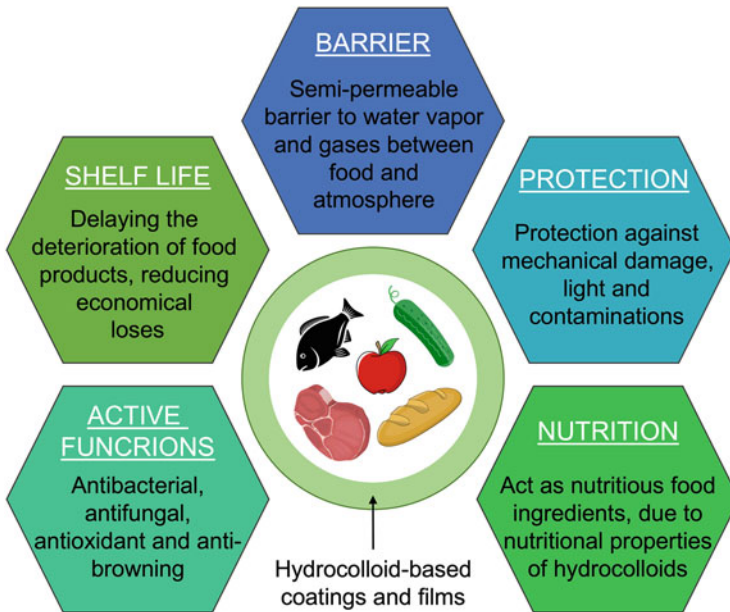


**Fig. 8.1** Summary of characteristics and advantages of hydrocolloid-based coatings and films

the energy, this end-of-life approach can produce toxic compounds, including furans and dioxins, such as those produced from burning PVC (Marsh and Bugusu 2007). To address these issues, edible coatings and films have emerged as an alternative to synthetic petroleum-based polymers for food packaging because they are versatile, renewable, and biodegradable (Siew et al. 1999). They have the potential to delay the deterioration of food products and to prolong their shelf life due to their selective barrier properties against oxygen, carbon dioxide, water vapor, and flavor compounds (Giancone et al. 2008). Global edible packaging market is expected to reach USD 1097 million by 2023, from USD 697 million in 2016, growing at a compound average growth rate (CAGR) of 6.81% (Edible packaging-global market outlook from 2017 to 2023 2017).

Polysaccharides, proteins, lipids, and composites derived from these materials, can be used as base materials to prepare edible coatings and films (Gennadios et al. 1996). Hydrocolloids based on polysaccharides and proteins are used extensively for the formation of coatings and films for food preservation, because of their desirable mechanical and gas barrier properties. Besides providing protective function, coatings and films can act as nutritious food ingredients due to the unique nutritional and functional properties of hydrocolloids (Viebke et al. 2014). A scheme illustrating the main characteristics of hydrocolloid-based coatings and films is shown in Fig. 8.1. Generally, there are no fundamental differences in material composition between coatings and films, other than their method of manufacture. Coatings are formed as a thin layer directly onto food surfaces by dipping, spraying, brushing, fluidized bed,



or panning method (Andrade et al. 2012). By contrast, films are standalone pre-formed material either placed between food components or sealed into pouches, and they are manufactured by wet- or dry-casting method (Janjarasskul and Krochta 2010). The performance and functionality of hydrocolloid-based coatings and films are evaluated by their mechanical properties, barrier effects against oxygen (O<sub>2</sub>), carbon dioxide (CO<sub>2</sub>) and water vapor, and thermal stability. These characteristics are strongly correlated with material compositions, manufacture methods, and the end-use conditions (e.g., relative humidity, temperature, and pH) (Rojas-Graü et al. 2009).

This chapter provides an overview on different categories of hydrocolloids for coating and film formation. Methods of preparation, forming mechanisms, and the physicochemical properties for coatings and films are also discussed. Finally, recent developments and trends for packaging applications involving hydrocolloids are summarized.

## 2 Components of Coatings and Films

Hydrocolloid-based coatings and films are produced from polysaccharides, proteins, their blends, and/or food-grade additives. Their functional, organoleptic, nutritional, and mechanical properties are modified by addition of food-grade additives, including plasticizers, antimicrobials, antioxidants, anti-browning and crosslinking agents, nanofillers, colorants, and flavors (Otoni et al. 2017). The main components for formulation of hydrocolloid-based coatings and films are summarized in Fig. 8.2.

### 2.1 Polysaccharides

Polysaccharides are nontoxic and naturally occurring biopolymers. The polysaccharide film-forming materials include starch and starch derivatives, cellulose derivatives, alginate, carrageenan, chitosan, various plant gums (pectin, konjac, locust bean gum, and guar gum) and microbial gums (pullulan, xanthan) (Cazón et al. 2017). Although polysaccharide-based coatings and films have superlative barrier properties to CO<sub>2</sub>, O<sub>2</sub>, and oil under certain conditions, and high strength and structural integrity, they tend to present a poor barrier to water vapor due to their hydrophilic properties (Yang and Paulson 2000).

#### 2.1.1 Starch and Starch Derivatives

Starch, an agricultural biopolymer found in a variety of plants, is a mixture of amylose and amylopectin whose content varies depending on its botanic origin (LeCorre et al. 2011). Amylose, a nearly linear biopolymer of  $\alpha$ -1,4 anhydroglucose

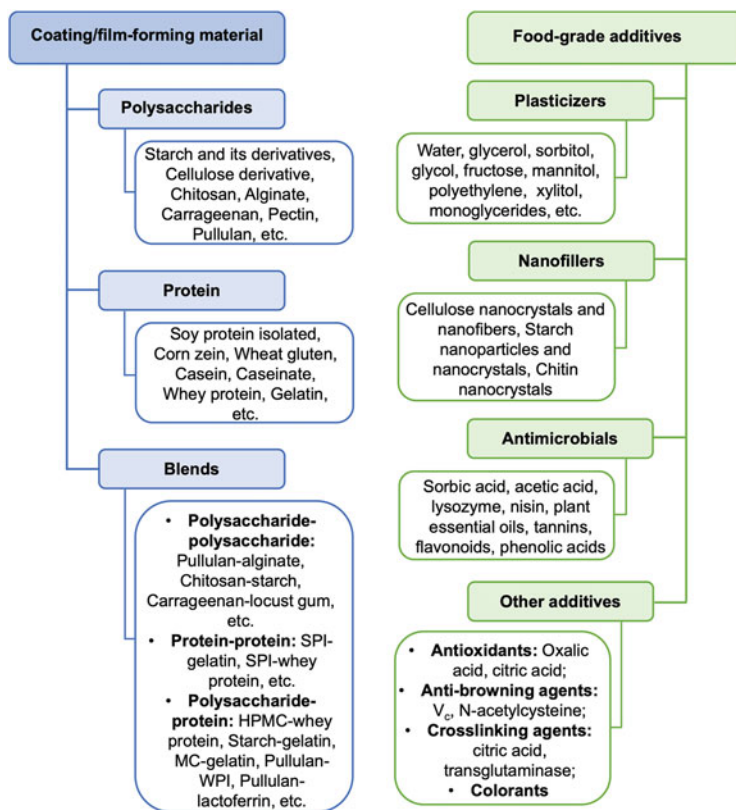


Fig. 8.2 Main components for formulation of hydrocolloid-based coatings and films

units, is known to form a coherent and relatively strong films (Campos et al. 2011). In contrast, amylopectin is a highly branched biopolymer of short  $\alpha$ -1,4 chains linked by  $\alpha$ -1,6 glucosidic branching points occurring every 25–30 glucose units (Durrani and Donald 1995). Its branched structure leads to form brittle and non-continuous films (De Azeredo et al. 2014). In comparison with native starch, modified starches, like acetylated starch, hydroxypropyl starch, and oxidized-starch, have been reported to form stronger and more flexible films (López et al. 2008, 2010; Hu et al. 2009).

### 2.1.2 Cellulose Derivatives

Cellulose, the main component of plant fibers, is essentially a linear high-molecular weight biopolymer of D-glucose units linked through  $\beta$ -1,4 glycosidic bonds. The close packing of cellulose chains makes it highly crystalline, fibrous, and insoluble in water (Wang et al. 2016). Water-soluble cellulose derivatives, such as methylcellulose (MC), hydroxypropyl methylcellulose (HPMC), carboxymethylcellulose

(CMC), and hydroxypropyl cellulose (HPC), possess good film-forming characteristics (Dhall 2013). Among them, MC films show the lowest hydrophilic properties, whereas the water vapor permeability of HPMC and CMC films is relatively high (Sánchez-González et al. 2009; Kester and Fennema 1989). In addition, the substitution type and degree in cellulose derivatives are critical factors determining the performance of cellulose-based films (Espinoza-Herrera et al. 2011).

### 2.1.3 Chitosan

Chitosan is a functional biopolymer derived from chitin by deacetylation in alkaline media. It consists of randomly distributed  $\beta$ -(1,4)-2-acetamido-D-glucose and  $\beta$ -(1,4)-2-amino-D-glucose units, with the latter usually exceeding 60% (Kim et al. 2006). Chitosan has a wide spectrum of activity and high killing rate against Gram-positive and Gram-negative bacteria (Chung and Chen 2008). The antimicrobial activity and film-forming ability of chitosan are correlated to its degree of acetylation or deacetylation, and molecular weight (Hosseinnejad and Jafari 2016). Owing to its outstanding characteristics, chitosan could be potentially utilized as the antimicrobial packaging materials to improve food quality and shelf life.

### 2.1.4 Polysaccharides Extracted from Seaweed

Alginate, a linear polysaccharide extracted from brown seaweed, is composed of variable proportions of  $\beta$ -D-mannuronic acid (M block) and  $\alpha$ -L-guluronic acid (G block) linked by 1,4 glycosidic bonds. The block copolymer consists of homopolymeric regions of M- and G-blocks, separated by regions that contain M and G units (Fu et al. 2011). The proportion and distribution of these blocks determine the physicochemical properties of the biopolymer (Lacroix and Le Tien 2005). Alginate dissolves readily in water to form homogeneous film-forming solutions, which upon drying can yield coherent, and transparent films that have a wide range of food applications (Xiao et al. 2012).

Carrageenan is an anionic linear polysaccharide, extracted from edible red seaweeds of *Rhodophyceae* class. It is formed by alternate units of D-galactose and 3,6-anhydrogalactose linked by  $\alpha$ -1,3 and  $\beta$ -1,4 glycosidic linkage (Cosenza et al. 2014). There are three types ( $\kappa$ ,  $\iota$ , and  $\lambda$ ) of carrageenan with varying number and position of sulfate groups on the galactose dimer (Liu et al. 2015). In comparison with  $\iota$ -carrageenan films,  $\kappa$ -carrageenan films showed the higher moisture barrier and mechanical properties, except for its flexibility (Paula et al. 2015).

### 2.1.5 Pectin

Pectin consists of linear homo-galacturonan ( $\alpha$ -1,4-galacturonic acids) chains interspersed with branched rhamnogalacturonan ( $\alpha$ -1,4-galacturonic acid to

$\alpha$ -1,2-rhamnose) chains (Jolie et al. 2010). According to its degree of esterification (DE), pectin can be classified as high-methoxyl pectin (HMP, DE > 50%) and low-methoxyl pectin (LMP, DE < 50%) (Espitia et al. 2014). The mechanical, water barrier properties and thermal stability of HMP films are better than that of LMP films (Lorevice et al. 2016).

### 2.1.6 Pullulan

Pullulan is an extracellular and water-soluble microbial polysaccharide produced by *Aureobasidium pullulans*. The linear polymer mainly consists of maltotriose units interconnected to each other by  $\alpha$ -(1,6) glycosidic bonds, which are responsible for the flexible conformation and the ensued amorphous character of this polysaccharide in the solid state (Sutherland 1998). This unique linkage pattern endows pullulan with distinctive physical properties to form film that is strong, transparent, and with low permeability to oil and oxygen (Xiao et al. 2012, 2015).

## 2.2 Proteins

Proteins used for film-forming materials can be categorized into two groups based on their origin of sources: plant-derived proteins, such as corn zein, soy protein, and wheat gluten, or animal-derived proteins like casein, whey protein, gelatin, and collagen proteins (Han 2014). Depending on amino acid composition and sequence, the structure of protein can be random coil, fibrous, or globular. For globular proteins (i.e., soy protein, wheat gluten), they must be denatured by heat, acid, and/or solvent to shape extra extended structures that are required for film formation (Dhall 2013). Overall, protein-based coatings and films display considerably lower O<sub>2</sub> and CO<sub>2</sub> permeability and CO<sub>2</sub>/O<sub>2</sub> permeability ratio, and moderate mechanical and water vapor barrier properties (Song and Zheng 2014).

### 2.2.1 Corn Zein

Corn zein, a prolamin protein, has a molecular weight ranging from 18 to 45 kDa. As a relatively hydrophobic protein, the hydrophobicity of zein is related to its high content of non-polar amino acids residues including leucine, alanine, and proline (Shukla and Cheryan 2001). Corn zein dissolves in aqueous ethanol solution to form the glossy, greaseproof, and brittle films through the hydrophobic, hydrogen, and limited disulfide (SS) bonds between zein chains (Ghanbarzadeh et al. 2007).

### 2.2.2 Wheat Gluten

Wheat gluten, an ethanol-soluble protein in wheat flour, is composed of gliadin and glutenin. Gliadin is monomeric protein with molecular weight of 28–55 kDa, while glutenin is aggregated protein linked by interchain SS bonds with molecular weight of about 500 to 10,000 kDa (Wieser 2007). Glutenin films presented higher mechanical strength and lower water vapor permeability than gliadin films (Hernández-Muñoz et al. 2003). Moreover, the purity of wheat gluten has positive effect on the appearance and mechanical attributes of wheat gluten films (Gennadios et al. 1993).

### 2.2.3 Soy Protein

Soy protein is comprised of two major components, 7S ( $\beta$ -conglycinin) and 11S (glycinin), representing 37% and 31% of soy protein, respectively. 7S is rich in asparagine, glutamine, leucine, and arginine residues with a molecular weight of 180 kDa. 11S has a molecular weight of 320–360 kDa and contains 20 intramolecular SS bonds (Kumar et al. 2002). Films made from 11S fraction are smooth and opaque, whereas 7S films exhibit transparent and creased appearance (Kunte et al. 1997). At low relative humidity (RH),  $O_2$  permeability of soy protein isolate (SPI) films was lower than that of films based on low-density polyethylene (LDPE), methylcellulose, starch and pectin, respectively (Song et al. 2011a).

### 2.2.4 Casein and Caseinate

Casein mainly consists of five fractions including  $\alpha_{s1}$ ,  $\alpha_{s2}$ ,  $\beta$ ,  $\kappa$ , and  $\delta$ -casein, and their sizes vary from 11.5 to 25 kDa. Among them,  $\beta$ -casein is the most interesting one, as it produces films with lower permeability to water vapor than other milk protein (Mauer et al. 2000). Caseinate is a mixture of casein monomers and small aggregates formed after removing of colloidal calcium phosphate from casein micelles. Compared to casein, caseinate, particularly for sodium caseinate, is more soluble and has better film-forming capacity. Films produced from sodium caseinate possess excellent barriers to  $O_2$ ,  $CO_2$ , and aromas, and thermal resistance (Khwaldia et al. 2004a).

### 2.2.5 Whey Protein

Whey protein includes  $\beta$ -lactoglobulin,  $\alpha$ -lactalbumin, bovine serum albumin, immunoglobulins, lactoferrin, and proteose-peptones (Mulvihill and Ennis 2003). Films prepared from whey protein isolates (WPI) exhibited promising mechanical features, as well as moderate moisture permeability and good oxygen barrier properties, compared to the synthetic polymer films, e.g., low-density polyethylene

(LDPE), high density polyethylene (HDPE), PVDC, cellophane, and polyester (Khwaldia et al. 2004b).

### 2.2.6 Gelatin

Gelatin is an animal protein obtained by hydrolysis of collagen. It is a combination of many fractions varying in size, including the whole  $\alpha$ -chain of tropocollagen molecule (a trimer of around 330 kDa that aggregates to form the larger collagen structures) and hydrolytic fragments of parts of the  $\alpha$ -chains (Boran and Regenstein 2010). Gelatin films display effective barriers against O<sub>2</sub> and aromas at low or intermediate RH, but weak water resistance due to its hydrophilic nature. Furthermore, their mechanical properties are closely related to the renaturation level of gelatin (Bigi et al. 2004).

## 2.3 Food-Grade Additives

### 2.3.1 Plasticizers

Plasticizers are low molecular weight compounds with non-volatile compounds. Their primary role is to enhance the flexibility and processability of hydrocolloid-based coatings and films. However, their barrier properties are impaired as result of the increased free volume and molecular mobility after plasticizers addition (Sothornvit and Krochta 2005; Vieira et al. 2011). Food-grade plasticizers mainly include glycerol, sorbitol, polyethylene glycol, sucrose, glucose, fructose, mannitol, xylitol, fatty acids, and monoglycerides (Vieira et al. 2011).

### 2.3.2 Polysaccharide Nanofillers

Nanofillers (at least one dimension smaller than 100 nm) provide reinforcement effects due to their high aspect ratio and surface-to-volume ratios (Crosby and Lee 2007). Considering the application and safety for hydrocolloid-based coatings and films in food packaging, the polysaccharide nanofillers, e.g., cellulose nanoparticles, cellulose nanocrystals, starch nanoparticles, starch nanocrystals, chitin nanowhiskers, and chitin nanofibers, have been used as excellent candidates for improvement of their mechanical, barrier, and thermal properties (Otoni et al. 2017).

### 2.3.3 Antimicrobial Additives

Incorporation of antimicrobial compounds into packaging materials provides inhibitory effects against spoilage and pathogenic bacteria by maintaining active

compounds on food surface (Gennadios et al. 1997). There are several categories of antimicrobial compounds that have been employed in hydrocolloid-based coatings and films, including organic acids (sorbic and its potassium salt, acetic acid, and malic acid), polypeptides and bacteriocins (lysozyme and nisin), plant essential oils (cinnamon, oregano, rosemary, and lemongrass), and polyphenols (flavonoids and phenolic derivatives) (Franssen and Krochta 2003).

### **3 Preparation Methods**

#### ***3.1 Preparation of Hydrocolloid-Based Coatings***

##### **3.1.1 Spray Coating**

Spray coating is a commonly used technique for food coatings, especially for fruits and vegetables. In this process, food products are placed on a rotating platform, then the coating-forming solution forms droplets and distributes them over the food surface by means of a set of spraying nozzles (Debeaufort and Voilley 2009). The main advantages of this technique offer uniform coating, thickness control, and the possibility of multilayer applications, such as using alternating sodium alginate and chitosan solutions (Ustunol 2009).

##### **3.1.2 Dip Coating**

Dip coating involves submerging food products into a vat containing coating solution. After dipping the products and draining away excess coating, it is dried either at room temperature or with the aid of a dryer (Andrade et al. 2012). The advantage of this method is to obtain good uniformity around the irregularly-shaped and rough food surface. Several problems may occur by using this method, such as coating dilution, build-up of trash or dirt, and microorganism growth in the dipping tank (Andrade et al. 2012).

##### **3.1.3 Fluidized-Bed Coating**

Fluidized beds are categorized by three different configurations: top spray, bottom spray, and rotating-fluidized bed. The conventional top-spray method has a greater possibility of success in the food industry compared to other methods (Andrade et al. 2012). As presented in Fig. 8.3, the coating solution is sprayed through a set of nozzles onto the surface of fluidized particles to form a shell-type structure. Its application focuses on the functional ingredients and food additives, i.e., leavening agents, enzymes, vitamins, minerals, and spices (Chen et al. 2009).

**Fig. 8.3** Schematic of top-spray fluidized-bed coating process, adapted from (Dewettinck and Huyghebaert 1999) with permission

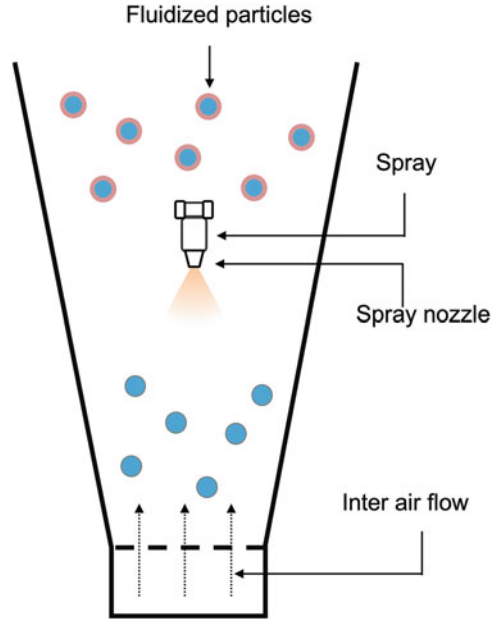
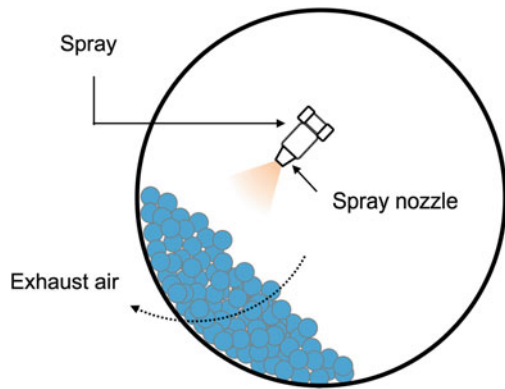


**Fig. 8.4** Schematic of pan coating process, adapted from (Agrawal and Pandey 2015) with permission



### 3.1.4 Pan Coating

The schematic of pan coating process is displayed in Fig. 8.4. As shown, the coating solution is sprayed into a rotating bowl (referred to as pan), and the food particles are tumbled within the pan to distribute the coating solution over their surface. Forced air, either ambient or elevated temperature, is utilized to dry the coating (Agrawal and Pandey 2015). Pan coating is mainly used for the confectionery and chocolate industries or particularly small food items like nuts and raisins (Andrade et al. 2012).



## 3.2 Preparation of Hydrocolloid-Based Films

### 3.2.1 Wet Method

The wet method, also known as solvent casting, can be sub-classified to bench casting and continuous casting, respectively. The bench casting is commonly utilized to fabricate films at laboratory scale as it is simple and cost effective. In this method, the film-forming solution is deposited over a rimmed plate, and then followed by drying to produce a cohesive and free-standing film.

Continuous casting is more suitable for industrial applications, because it requires less space and labor. As shown in Fig. 8.5, film-forming solution is uniformly spread on a continuous steel belt that passes through a drying chamber. The dried film is then stripped from the steel belt and wound into film roller. The advantage of this method is optimizing uniformity, heat transfer, and drying efficiency, while avoiding expense of a separate substrate (Rossman 2009).

### 3.2.2 Dry Method

Dry method, i.e., compression molding and extrusion processing, is based on the thermoplastic properties of polysaccharides and proteins. In the presence of plasticizers, at low moisture levels and high temperatures and with pressure, biopolymers acquire a viscoelastic behavior that allows them to be shaped for the production of films (Gómez-Estaca et al. 2016). In general, compression molding is studied at laboratory scale as a precursor to extrusion with the aim of determining the suitable processing conditions (Hernandez-Izquierdo and Krochta 2008).

Extrusion processing is a highly efficient manufacturing method with commercial potential for large-scale production of biopolymer films (Fishman et al. 2000). The

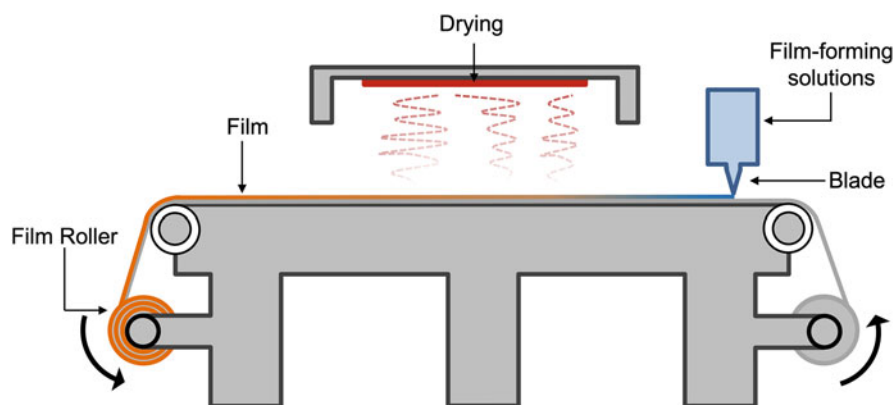


**Fig. 8.5** Schematic of continuous casting technique to prepare hydrocolloid-based films, adapted from (Borges et al. 2015) with permission

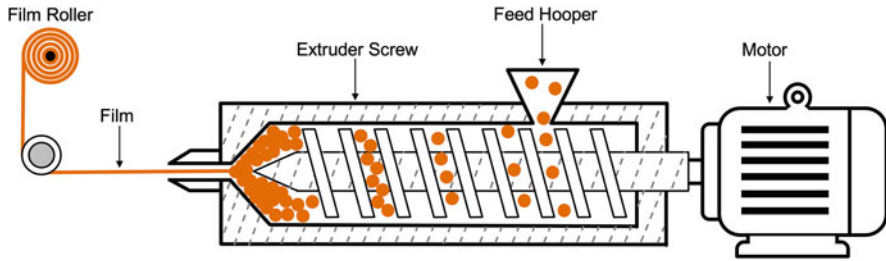


**Fig. 8.6** The configuration of one-screw extruder, adapted from (Borges et al. 2015) with permission

configuration of one-screw extruder is presented in Fig. 8.6. The extruder basically consists of an endless screw inside a barrel with a double casing that permits control of temperature. The biopolymer is fed from a hopper and pushed by the screw towards a die (Nur Hanani et al. 2012). To date, dry method has been successfully used in preparation of starch, alginate, wheat gluten, soy protein, and whey protein films (Mendes et al. 2016; Hernandez-Izquierdo and Krochta 2008; Azevedo et al. 2017; Ciannamea et al. 2014).

## 4 Microstructural and Physicochemical Characterization

The microstructural characteristics (such as chemical, crystalline structure, and morphology) of hydrocolloid-based coatings and films are closely correlated with their packaging performance (e.g., mechanical, barrier, and thermal properties).

### 4.1 Structural Analysis

Microscopy and spectroscopic techniques have been utilized to study the architecture and structure of hydrocolloid-based films at micro and nanometric scales. Ultrastructural and internal structure in films have been characterized by confocal laser scanning microscopy (CSLM), while scanning electron microscopy (SEM) and atomic force microscopy (AFM) are more used to study their surface and cross-section morphology (Arzate-Vázquez et al. 2012; Andreuccetti et al. 2009). Fourier transform infrared spectroscopy (FTIR) analyzes the possible functional chemical groups, conformational transitions, and molecular interactions (Yadav et al. 2014). Nuclear magnetic resonance (NMR) spectroscopy provides information about the chemical and physical properties of atoms or their related molecules, as well as reaction state, dynamics, structure and chemical environment (Karbowiak et al. 2008). For instance, for hsian-tsoo gum (HG)-casein films, the hydrogen bonding interactions and Maillard reactions between HG and casein were revealed by FTIR

data. Meanwhile, NMR analysis indicated that HG addition significantly changed the mobility of water molecule in casein films (Yang et al. 2015). Other complementary techniques are also utilized for structural analysis of hydrocolloid-based coatings and films, such as X-ray diffraction (XRD) to identify the information about crystalline/amorphous structures, and small-angle X-ray scattering (SAXS) to monitor crystalline and aggregate structures of membrane materials (Bodnár et al. 2007).

## 4.2 Mechanical Properties

Favorable mechanical properties are essential for packaging materials to perform their protective functions efficiently. Mechanical properties of selected hydrocolloid-based films are listed in Table 8.1. A standard method, ASTM-D882–91, originally developed to evaluate mechanical properties such as tensile strength (TS), elongation at break (EAB), elastic modulus (EM), and toughness of commercial plastic, is also applied to hydrocolloid-based films (ASTM-D882-91 1991). As shown in Fig. 8.7, the mechanical parameters are calculated by determining the relationship between stress and strain, when film is stretched at a set rate (distance/time). EM, a measure of intrinsic film stiffness, is the slope of the linear range of the stress–strain curve (Mauer et al. 2000). Toughness refers to the ability of a material to absorb energy during deformation up to fracture, determined as the area under the stress–strain curves (Fig. 8.7b). TS is the maximum strength measuring the resistance of the film, whereas the percentage of EAB is a measure of the stretching capacity of flexibility of the film prior to breaking. They are calculated by using Eqs. 8.1 and 8.2:

$$TS = F/A \quad (8.1)$$

where TS is the tensile strength (MPa),  $F$  is the force (N) at maximum load, and  $A$  is the initial cross-sectional area ( $\text{m}^2$ ) of the film specimen.

$$EAB = 100 \times (l - l_1)/l_1 \quad (8.2)$$

where EAB is the elongation at break (%),  $l_1$  is the initial length, and  $l$  is the length of the film at breaking point.

## 4.3 Barrier Properties

The basic function of packaging materials is to control mass transfer between food and the ambient atmosphere. Water vapor in environment transferring to packaged food results in problematic microbial growth, and undesirable textural changes. Oxygen can cause deterioration of food due to oxidation of lipids and other

**Table 8.1** Mechanical properties and water vapor, oxygen, and carbon dioxide permeability values of selected hydrocolloid-based films

Composites <sup>a</sup>	Mechanical properties			WVP		Gas permeability			Reference
	TS (MPa)	EAB (%)	EM (MPa)	Test conditions	(g.m.Pa <sup>-1</sup> .h <sup>-1</sup> .m <sup>-2</sup> )	Test conditions	O <sub>2</sub> P (cm <sup>3</sup> .mm.m <sup>-2</sup> .d <sup>-1</sup> .Pa <sup>-1</sup> )	CO <sub>2</sub> P (cm <sup>3</sup> .mm.m <sup>-2</sup> .d <sup>-1</sup> .Pa <sup>-1</sup> )	
HMw chitosan	61.82	4.59	–	38 °C, 90% RH	$1.34 \times 10^{-10}$	23 °C, 50% RH	6.65	–	(Leceta et al. 2013)
LMw chitosan	55.83	4.58	–	38 °C, 90% RH	$1.53 \times 10^{-10}$	23 °C, 50% RH	7.70	–	(Leceta et al. 2013)
Pullulan	73.89	1.67	4938	23 °C, 100% RH	$7.05 \times 10^{-6}$	23 °C, 23% RH	0.48	–	(Xiao et al. 2012, 2015)
Alginate	74.04	4.60	3047	23 °C, 100% RH	$25.75 \times 10^{-6}$	23 °C, 23% RH	8.94	–	(Xiao et al. 2012, 2015)
Sweet potato starch-chitosan	33.8	2.02	–	25 °C, 75% RH	$7.09 \times 10^{-6}$	23 °C, 50% RH	4.09	–	(Shen et al. 2010)
WPC-GLY (40% w/w)	0.72	50	78	20 °C, 50% RH	$4.50 \times 10^{-6}$	20 °C, 50% RH	0.2	1.02	(Ramos et al. 2013)
WPI-GLY (40% w/w)	0.9	55	95	20 °C, 50% RH	$3.43 \times 10^{-6}$	20 °C, 50% RH	0.41	1.58	(Ramos et al. 2013)
Vetch seed protein	1.59	32.08	78.14	–	–	25 °C, 55% RH	20.16	24.84	(Porta et al. 2015)
Papaya puree-gelatin (8:1)	6.7	18.09	–	38 °C, 90% RH	$6.62 \times 10^{-5}$	23 °C, 50% RH	8.24	10.25	(Tulamandi et al. 2016)
Papaya puree-defatted soy protein (8:4)	5.13	28.11	–	38 °C, 90% RH	$7.52 \times 10^{-5}$	23 °C, 50% RH	8.92	10.89	(Tulamandi et al. 2016)
WPI-okra polysaccharide (1:1)	2.3	31.4	68.2	23 °C, 100% RH	$3.23 \times 10^{-5}$	20 °C, 50% RH	5.67	–	(Prommakool et al. 2011)
WPI-LBG (0.025% w/w)	2.66	11.4	–	20 °C, 100% RH	$4.97 \times 10^{-7}$	20 °C, 50% RH	0.78	4.71	(Silva et al. 2016)

<sup>a</sup>HMw high molecular weight, LMw low molecular weight, WPC whey protein concentrate, GLY glycerol, LBG locust bean gum

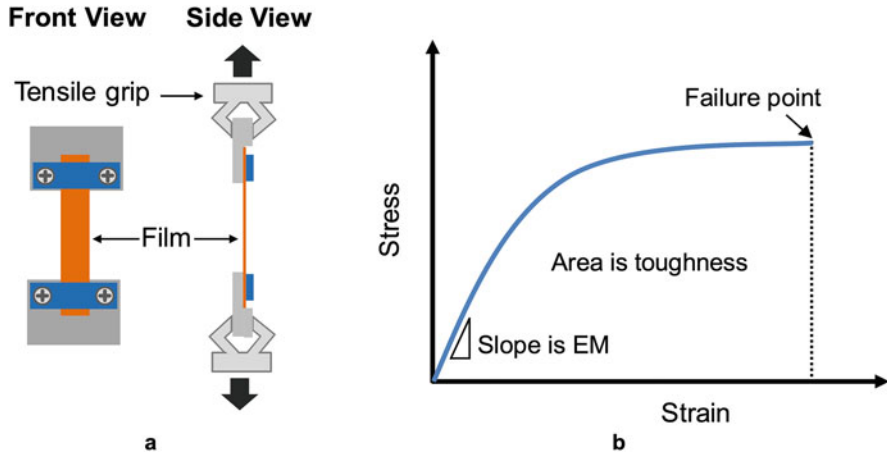


**Fig. 8.7** (a) Schematic of tension test setup, adapted from (Pham et al. 2008) with permission, (b) mechanical properties determined from the typical stress-strain curve

oxygen-sensitive components. Thus, water vapor and gas permeability is a vital property for selecting or tailoring the hydrocolloid-based films.

### 4.3.1 Water Vapor Permeability (WVP)

Table 8.1 shows WVP values of selected hydrocolloid-based films. These data are obtained gravimetrically following the ASTM Standard Test Method E96, known as the “cup method” (ASTM-E96-92 1990). According to this method, a cup with an open mouth is filled with distilled water or desiccant. The film is sealed on the open mouth of the cup, the assembly is weighed, and placed under controlled temperature and RH conditions (Cazón et al. 2017). WVP is calculated according to the combined Fick–Henry laws for gas diffusion through films (Eq. 8.3).

$$\text{WVP} = \frac{\Delta w}{\Delta t \times A} \times \frac{L}{\Delta p} \quad (8.3)$$

where  $\Delta w/\Delta t$  is the rate of water gain (g/h),  $A$  is the exposed area of the film ( $\text{m}^2$ ),  $L$  is the mean thickness of film specimens (m), and  $\Delta p$  is the difference in partial water vapor pressure between the two sides of film specimens.

### 4.3.2 Gas Permeability

Oxygen permeability ( $\text{O}_2\text{P}$ ) and carbon dioxide permeability ( $\text{CO}_2\text{P}$ ) are evaluated on the basis of the ASTM D 3985–02 method (ASTM-D3985-02 2002). The films are sealed between two chambers with each having two channels to the exterior. In

the lower chamber, O<sub>2</sub> or CO<sub>2</sub> is supplied at a controlled flow rate to maintain the pressure constant in that compartment. The other chamber is purged by a stream of nitrogen, also at a controlled flow. In the case of O<sub>2</sub>P measurement, the nitrogen flow leaving this chamber is connected to an O<sub>2</sub> sensor installed on-line which measures the O<sub>2</sub> concentration. For CO<sub>2</sub>P measurement, the nitrogen flow leaving this chamber is collected in a syringe for CO<sub>2</sub> quantification by a gas chromatograph (Cerqueira et al. 2009). The O<sub>2</sub>P and CO<sub>2</sub>P of selected hydrocolloid-based films are listed in Table 8.1.

#### 4.4 Thermal Properties

One key factor that influences the processing and operating temperatures of hydrocolloid-based coatings and films is their thermal properties. The properties are investigated by differential scanning calorimetry (DSC), thermogravimetric analysis (TGA), and dynamic mechanical analysis (DMTA). DSC technique is used to determine the glass transition temperature ( $T_g$ ), melting temperature ( $T_m$ ), crystallization temperature, heat capacity difference at  $T_g$  of hydrocolloid-based coatings and films (Cheng 2002). TGA is widely employed to examine their decomposition temperature, weight loss, and activation energy of decomposition (Cheng 2002). Furthermore, the structural and viscoelastic properties of films are investigated by DMTA. Dynamic modulus, dynamic loss modulus, temperature of main chain relaxation, and temperature of local mode relaxation are measured as functions of temperature and frequency by forced oscillation method (Brown and Gallagher 2011).

### 5 Film-Forming Mechanism

Understanding the film-forming mechanism is important to predict material properties of hydrocolloid-based films, which is essential for the optimization of drying and processing condition. As previously mentioned, both processing methods (wet and dry) have been widely used to prepare the films. The wet method requires solubilizing the hydrocolloids in a solvent, spreading the solution onto a flat surface, and then followed by drying to produce a film. The film-forming mechanism involves conformational change of the biopolymer, as well as solvent-biopolymer and biopolymer-biopolymer interactions that continue to evolve as the solvent evaporates under different drying conditions (Watanabe et al. 2006; Xiao et al. 2014b). However, a number of polysaccharides and proteins have capacity to form gel during film-forming process, and their film-forming mechanism is related to the gelation mechanism. Although a few researchers proposed that the transition from wet gel (biopolymer-in-water) to dry film (water-in-biopolymer) is a critical stage during

film-forming process, the complete transition mechanism after gelation have not yet been fully explained (Szabó et al. 2012).

By contrast, dry method involves heating and mixing biopolymers and plasticizers by extrusion and/or compression molding techniques. Over the course of extrusion, biopolymer chains denature, dissociate, unravel and align, and then recombine, crosslink, and aggregate via specific linkages with heat and pressure, which result in film formation through complete restructuring of biopolymer molecules. Thus, the film-forming mechanism is correlated with conformation changes of biopolymers, their aggregation and crystalline state, as well as the interactions among biopolymer, plasticizer, and water.

## 5.1 Polysaccharide-Based Films

Polysaccharides (with the exception of glycogen, etc.) are long-chain biopolymers formed from mono- or disaccharide repeating units joined together by glycosidic bonds. Owing to the presence of a large number of hydroxyl and other polar groups in their structure, hydrogen bonds and/or electrostatic interactions have a crucial function in film formation (Han 2014). Polysaccharide films are fabricated by disrupting interactions among polysaccharide segments and forming new intermolecular hydrophilic interactions and hydrogen bonding (Rhim and Ng 2007).

### 5.1.1 Formation Mechanism of Solvent Casting Films

For starch films, their formation mechanism depends on the starch concentration and amylose content. At relatively high concentration, aggregation and packing of swollen granules dominated the film formation, whereas both coil-to-helix transition and aggregation of double helices were operative during the film formation from dilute starch solutions (Liu 2005). Xiao et al. (2014a, b) elaborated the formation mechanism of pullulan and alginate films by monitoring the conformational change of polysaccharides, water-polysaccharide, and polysaccharide-polysaccharide interactions during drying. As pullulan drying process progressed, the oxygen atoms at the C<sub>5</sub> and C<sub>6</sub> carbons of the D-glucopyranose ring might preferentially form hydrogen bond with water or pullulan molecules, resulting in more-ordered structure with increased interchain interactions in pullulan films. Moreover, the less-ordered structure domain of the pullulan was first affected during drying, followed by pullulan skeleton segments. Finally, conformational changes in pullulan chains occurred as the drying process completion (Xiao et al. 2014b). In the course of the formation of alginate film, the oxygen atoms at the C<sub>2</sub> and C<sub>3</sub> carbons of the pyranose ring preferentially formed hydrogen bond with water or alginate molecules, while the skeletal vibrations of pyranose ring (e.g., C-C and C-O-C groups) were less perturbed than the stretching vibrations of COO<sup>-</sup> group and O-H bending vibration of alginate with drying (Xiao et al. 2014a). The film-forming mechanism of

*Flammulina velutipes* polysaccharide might be associated with the intermolecular and intramolecular hydrogen bonds between polysaccharide chains and the formation of  $\beta$ -glycosidic bonds upon drying (Du et al. 2016). Li et al. (2019) proved that the electrostatic interactions and hydrogen bonds are crucial in fabricating the multilayer films based on chitosan and alginate by layer-by-layer (LbL) technique. Strong intermolecular interactions occurred among the amino, carboxyl, and hydroxyl groups of the chitosan and alginate.

### 5.1.2 Formation Mechanism of Extruded and Compression-Molded Films

Pushpadass et al. (2009) reported that glycerol and/or water destroyed the crystallinity of native starch, then the starch fragmentation converted into thermoplastic starch with heat and shear. During extrusion process, the inter- and intra-hydrogen bonds of starch would be unraveled when the glycerol was added into starch, and the new hydrogen bonds between starch and glycerol were formed simultaneously (Pushpadass et al. 2009). Afterwards, the starch recrystallization induction process among the helical amylose molecule occurred during cooling, which led to the Vh-type crystalline arrangement (Azevedo et al. 2017). According to Gao et al. (2017), neat alginate granules were largely de-structured by glycerol and water, and glycerol increased the mobility of alginate chains while promoting the crystallization of alginate chains with structural reorganization during compression molding.

## 5.2 Protein-Based Films

The main formation mechanism of protein films involves denaturation of the protein initiated by heat, solvent, or change in pH, followed by association of extended peptide chains through new intermolecular interactions, such as covalent (SS bond or crosslinking) and electrostatic, hydrophobic, or ionic interactions between protein chains (Janjarasskul and Krochta 2010).

### 5.2.1 Formation Mechanism of Solvent Casting Films

The formation of intact and water-insoluble WPI films was realized by heat denaturation of aqueous protein solution (Pérez-Gago and Krochta 2002). Heat denaturation unfolded whey protein and promoted the exposure of SH and hydrophobic groups. The unfolded protein might then undergo intermolecular interactions (hydrogen bonds, hydrophobic, covalent and electrostatic interactions). It is noteworthy that the cohesion of WPI films relied principally on the intermolecular SS bonds via sulphhydryl/disulphide (SH/SS) exchange reactions (Guckian et al. 2006).



On the other hand, WPI had the ability to form water-soluble films without heat denaturation. Since most of the hydrophobic and SH groups are buried in the interior of WPI molecule, their film-forming mechanism involves the intermolecular hydrogen bonding between protein molecules, rather than the hydrophobic and covalent interactions (Guckian et al. 2006; Pérez-Gago et al. 1999). Ciannamea et al. (2014) also proved that hydrogen bonds and hydrophobic interactions played a more important role in the formation of soy protein films. During the film formation of 11S, along with disappearance of its  $\alpha$ -helices and disordered structures, the intermolecular hydrogen bonds between  $\beta$ -sheet segments predominated the aggregation of 11S (Robert et al. 2001; Subirade et al. 1998). Similar to the 11S films, the high density of intermolecular hydrogen-bonded  $\beta$ -sheets were conducive to the formation of gliadin network during drying (Mangavel et al. 2001). According to Pankaj et al. (2014), the film-forming mechanism of caseinate was attributed to their random coil structure which allowed them to form extensive intermolecular hydrogen, electrostatic, and hydrophobic bonds, resulting in increased interchain cohesion.

In comparison, the formation mechanism of gelatin films is related to the temperature during drying due to thermo-reversible gelation behavior of gelatin. When the gelatin films were prepared below the helix-coil transition temperature, partial renaturation of collagen in gelatin took place, which resulted in the formation of a collagen-like triple-helix structure. Moreover, the partial renaturation only took place during the advanced stage of drying (Ghoshal et al. 2014). On the contrary, a helix structure was rarely formed in gelatin films when they were dried above the helix-coil transition temperature.

### 5.2.2 Formation Mechanism of Extruded and Compression-Molded Films

For compression-molded soybean protein films, the high temperature promoted the crosslinking between soybean proteins through intermolecular SS bonds, either from free sulfhydryl (SH) groups or through SH/SS exchange reactions, which predominated the formation of film matrix (Ciannamea et al. 2014). During extrusion process, the aggregation and reorganization of wheat gluten molecules were principally related to the formation of intermolecular SS crosslinking bonds via oxidation of SH groups and SH/SS exchange reactions between glutenin and gliadin (Lagrain et al. 2010). The formation schematic of intermolecular SS bonds between glutenin and gliadin during heat processing is illustrated in Fig. 8.8.

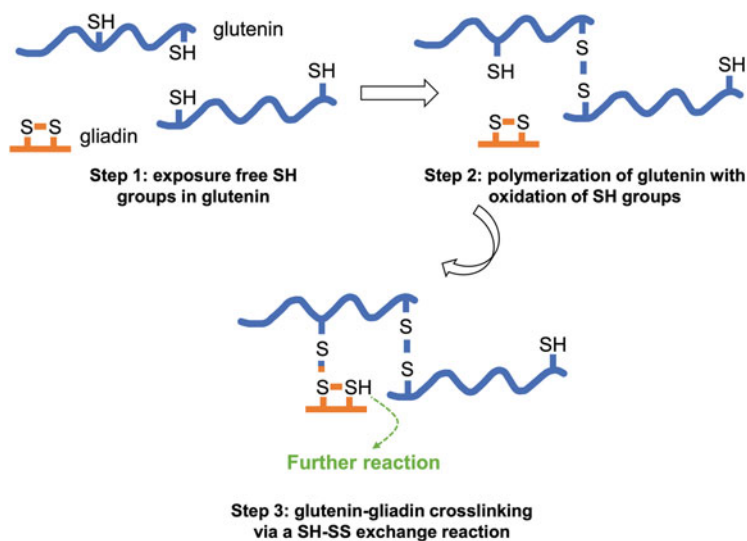


**Fig. 8.8** Schematic of the formation of intermolecular SS crosslinking bonds between glutenin and gliadin during heat processing. Adopted and modified from (Lagrain et al. 2010) with permission

## 6 Applications and Recent Developments

Oxidation, microbial spoilage, and metabolism are the main causes of deterioration of food products. Thus, the primary function of packaging materials based on hydrocolloids is to maintain the quality and safety of food products during storage and conveyance. Normally, fruits and vegetables have short shelf life due to its perishable nature. Hydrocolloid-based coatings and films may act as a semipermeable barrier to selectively control the exchange of  $\text{CO}_2$ ,  $\text{O}_2$ , and ethylene, resulting in the reduction in ethylene levels, ripening, respiration rate, and water loss on fruits and vegetables (Valencia-Chamorro et al. 2011). Several studies shown in Table 8.2. have demonstrated the ability of hydrocolloid-based coatings and films carrying bioactive compounds to retard browning reactions and microbial growth in fruits and vegetables, especially the minimally processed (MP) fruits and vegetables. Ramos-García et al. (2012) reported that lime essential oil incorporated into chitosan-beeswax blend coatings on tomato showed strong inhibitory effect against *Rhizopus stolonifer* and *Escherichia coli* DH<sub>5</sub> $\alpha$  during storage at 12 and 23 °C. Sarengaowa et al. (2018) coated the fresh-cut “Red Fuji” apples with alginate coatings containing thyme oil, cinnamon oil, and/or oregano oil, and observed that reduction of total coliform, yeast and mold counts in comparison with control and alginate-coated samples. Meanwhile, the respiration rate, weight loss, firmness, and browning reactions in fresh-cut apples stored at 4 °C were significantly decreased.

Recently, the development of multilayer and nanomultilayer coatings based on hydrocolloids, formed by LbL deposition technique, gained much attention for the preservation of fruits and vegetables. For instance, the multilayer coatings based on gelatin and chitosan predominantly enhanced physiological quality and reduced the

**Table 8.2** Recent applications of hydrocolloid-based coatings and films in fruits and vegetables

Coating/film composites	Form	Food products	Main benefits	References
		Fruits and vegetables		
Pectin-pullulan-chitosan with sodium benzoate and potassium sorbate	Coatings	Strawberry ( <i>Fragaria ananassa</i> )	Reduced weight loss, fruit softening and microbial growth (total aerobic counts, molds, and yeasts), delayed alteration of color and total soluble solids content	(Treviño-Garza et al. 2015)
Alginate with carvacrol and methyl cinnamate	Coatings	Strawberry	Inhibited the <i>Escherichia coli</i> O157:H7 and <i>Botrytis cinerea</i>	(Peretto et al. 2014)
Alginate-pectin	Coatings	Blueberry	Improved the firmness, significantly reduced growth kinetics of yeasts and mesophilic aerobic bacteria	(Mannozi et al. 2017)
Gum arabic- <i>Aloe vera</i> -chitosan combined with thyme oil	Coatings	Avocado ( <i>Persea americana</i> Mill.)	Reduced the anthracnose incidence during the postharvest supply chain, inhibited mycelial growth of <i>Colletotrichum gloeosporioides</i>	(Bill et al. 2014)
Chitosan-carrageenan	Coatings	Longan ( <i>Dimocarpus longan</i> )	Reduced weight loss, respiration rate and color changes	(Lin et al. 2018)
Chitosan-cassava starch with essential oil extract from <i>Lippia gracilis</i>	Coatings	Guavas ( <i>Psidium guajava</i> L.)	Reduced total aerobic mesophilic bacteria, mold and yeast counts, exhibition lower titratable acidity value	(de Aquino et al. 2015)
Pea starch-guar gum with shellac and oleic acid	Coatings	'Valencia' oranges	Reduced fruit respiration rate, ethylene production, weight and firmness loss, and peel pitting	(Saber et al. 2018)
CMC-chitosan	Bilayer coatings	Citrus fruit	Increased fruit firmness, and enhanced fruit gloss	(Arnon et al. 2014)
Gum arabic with cinnamon oil	Coatings	Banana and papaya	Delayed ripening, weight loss, fruit firmness, and titratable acidity, fungicidal effects against	(Maqbool et al. 2011)

(continued)

**Table 8.2** (continued)

Coating/film composites	Form	Food products	Main benefits	References
			<i>Colletotrichum musae</i> and <i>Colletotrichum gloeosporioides</i>	
HPMC-beeswax	Coatings	Plums (Cv. <i>Angeleno</i> )	Reduced water loss, flesh softening and internal breakdown	(Navarro-Tarazaga et al. 2011)
HPMC with oregano essential oil	Coatings	'Formosa' plum	Reduced the respiration rate, ethylene production, total weight loss	(Choi et al. 2016)
Chitosan with <i>Artemisia annua</i> oil	Coatings	Cherry tomato	Decreased <i>Escherichia coli</i> O157:H7	(Cui et al. 2017)
Chitosan-beeswax with lime essential oil	Coatings	Tomato	No growth of <i>Rhizopus stolonifer</i> and <i>Escherichia coli</i> DH <sub>5α</sub>	(Ramos-García et al. 2012)
Pectin-chitosan	Nanomultilayer coatings	'Tommy Atkins' mangoes	Presented a lower mass loss, lower total soluble solids and higher titratable acidity	(Medeiros et al. 2012a, b)
Starch-gelatin	Coatings	Refrigerated red crimson grapes	Enhanced appearance and decreased weight loss	(Fakhouri et al. 2015)
<i>Aloe vera</i> -gum tragacanth	Coatings	Button mushroom	Reduced weight loss, color changes and softening	(Mohebbi et al. 2012)
Chitosan-banana flour	Films	Asparagus and corn	Inhibited growth of <i>Staphylococcus aureus</i>	(Pitak and Rakshit 2011)
		MP fruits and vegetables		
Cassava starch-potassium sorbate	Coatings	Minimally processed strawberry	Reduced respiration rate, increased water vapor resistance	(Garcia et al. 2010)
Gellan with geraniol	Coatings	Fresh-cut strawberry	Significantly reduced microbial counts	(Tomadoni et al. 2018)
Alginate-chitosan	Nanomultilayer coatings	Fresh-cut mangoes	Lower values of mass loss, pH, malondialdehyde content, browning rate, soluble solids	(Souza et al. 2015)
κ-Carrageenan-lysozyme	Nanomultilayer coatings	Whole and fresh-cut 'Rocha' pear	Presented lower mass loss, and total soluble solids and higher titratable acidity	(Medeiros et al. 2012a, b)
SPI with ferulic acid	Coatings	Fresh-cut apples	Effective in controlling their weight loss and firmness	(Alves et al. 2017)

(continued)

**Table 8.2** (continued)

Coating/film composites	Form	Food products	Main benefits	References
Alginate with thyme/ cinnamon/oregano oil	Coatings	Fresh-cut 'Red Fuji' apples	Significantly inhibited the microbial growth, respiration, weight loss, firmness and browning	(Sarengaowa et al. 2018)
Gelatin-chitosan	Multilayer coatings	Fresh-cut melon	Effective inhibition of the total microbial growth	(Poverenov et al. 2014)
Sodium alginate with lemongrass essential oil	Nanoemulsion coatings	Fresh-cut Fuji apples	A greater inactivation of <i>Escherichia coli</i> during storage time	(Salvia-Trujillo et al. 2015)
Whey protein-pectin	Crosslinked coatings	Fresh-cut apples	Reduced the weight loss, prevented microbial growth	(Rossi Marquez et al. 2017)
Chitosan	Coatings	Fresh-cut broccoli	Decreased in total mesophilic and psychrotrophic bacteria counts, inhibited opening florets	(Moreira et al. 2011b)
Starch with carvacrol	Coatings	Minimally processed pumpkin	Decreased counts of <i>Escherichia coli</i> O157:H7, and <i>Staphylococcus aureus</i>	(Santos et al. 2016)
Whey protein-pectin	Crosslinked coatings	Fresh-cut potatoes and carrots	Reduced the weight loss, prevented microbial growth	(Rossi Marquez et al. 2017)

bacteria, yeast, and fungi counts of fresh-cut melons (Poverenov et al. 2014). Souza et al. (2015) reported that the nanomultilayer coatings, made of alginate and chitosan, considerably inhibited putrefaction of fresh-cut mangoes during 14 days at 8 °C. At the end of the storage period, the lower values of mass loss, pH, malondialdehyde content, and browning rate were observed in the coated mangoes. Furthermore, nanoemulsion-based sodium alginate coatings with lemongrass essential oil at 0.5% or 1% (v/v) were created to completely inhibit the natural microflora of fresh-cut Fuji apples during 2 weeks at 23 °C. The application of this coating on fresh-cut apples exhibited a faster and greater inactivation of *Escherichia coli* during storage time compared with conventional emulsions (Salvia-Trujillo et al. 2015). Rossi Marquez et al. (2017) reported that transglutaminase crosslinked coatings prepared from whey protein and pectin were able to totally prevent the weight loss of fresh-cut potato and carrot at least until the sixth day of storage, which also maintained the phenolic and carotenoid content of fresh-cut carrot during storage.

Meat, poultry, and seafood products are common sources of proteins, yet susceptible to the spoilage microorganisms and food-borne pathogens. Thus, the hydrocolloid-based coatings and films with antimicrobial and/or antioxidant

**Table 8.3** Recent applications of hydrocolloid-based coatings and films in meat, poultry, and seafood

Coating/film composites	Form	Food products	Main benefits	References
Chitosan with <i>Satureja</i> plant essential oil	Nanoencapsulation coatings	Lamb meat	Retention of the good quality characteristics, improvement of microbiological safety, and extension of shelf life	(Pabast et al. 2018)
Chitosan–nanocelullose	Nanocomposite films	Ground meat	Decreased lactic acid bacteria population	(Dehnad et al. 2014)
Sodium caseinate with pomegranate peel extract	Films	Ground beef	More pronounced against gram-positive bacteria compared with gram-negative bacteria	(Emam-Djomeh et al. 2015)
Distiller dried grains-soluble protein with tea extract	Films	Pork meat	Decreased lipid oxidation	(Yang et al. 2016)
Perilla seed meal protein with clove oil	Films	Pork sausages	Reduced the microbial growth, and decreased peroxide value and thiobarbituric acid value	(Song et al. 2015)
Chitosan with thymus moroderi and piperella essential oil	Films	Cooked cured ham	Decreased the counts of aerobic mesophilic bacteria and lactic acid bacteria, and lipid oxidation	(Ruiz-Navajas et al. 2015)
WPI with oregano/clove essential oils	Coatings	Chicken breast fillets	Decreased counts of total mesophilic aerobic, enterobacteriaceae, <i>Pseudomonas spp.</i> , and lactic acid bacteria	(Fernández-Pan et al. 2014)
Sodium caseinate with ginger essential oil	Nanoemulsion coatings	Chicken breast fillets	Significantly decreased the total aerobic psychrophilic bacteria, maintained food color	(Noori et al. 2018)

(continued)

**Table 8.3** (continued)

Coating/film composites	Form	Food products	Main benefits	References
Chitosan-cyclo-dextrin with carvacrol	Films	Chicken breast fillet	A bactericidal effect against <i>Staphylococcus aureus</i> and <i>Escherichia coli</i> O157:H7	(Higuera et al. 2014)
Skate skin gelatin with thyme essential oil	Films	Chicken tenderloin	Inhibited the growth of <i>Listeria monocytogenes</i> and <i>Escherichia coli</i> O157:H7	(Lee et al. 2016b)
Chitosan with lauric alginate ester	Coatings	Ready-to-eat deli Turkey meat	Reduced the growth of <i>Listeria innocua</i>	(Guo et al. 2014)
Sunflower seed protein-red algae with grapefruit seed extract	Films	Smoked duck meat	Decreased population of <i>Listeria monocytogenes</i>	(Song et al. 2013)
Chitosan with citric acid/licorice extract	Coatings	Japanese sea bass ( <i>Lateolabrax japonicus</i> )	Reduced the TVB-N levels, showed antioxidant and antimicrobial effects	(Qiu et al. 2014)
Alginate with V <sub>c</sub> /tea polyphenols	Coatings	Refrigerated bream ( <i>Megalobrama amblycephala</i> )	Efficiently inhibited the growth of total viable counts, chemical spoilage, and water loss	(Song et al. 2011b)
Chitosan with grape seed extract and tea polyphenols	Coatings	Refrigerated red drum ( <i>Sciaenops ocellatus</i> ) fillets	Maintained lower pH values, inhibited the degradation of ATP and lipid oxidation	(Li et al. 2013)
Chitosan	Coatings	Frozen Atlantic salmon	Maintained the color, controlled microbial activity	(Soares et al. 2015)
Chicken feather protein-gelatin with clove oil	Films	Smoked salmon	Decreased the populations of <i>Escherichia coli</i> O157:H7 and <i>Listeria monocytogenes</i> , decreased peroxide and thiobarbituric acid value	(Song et al. 2014)

(continued)

**Table 8.3** (continued)

Coating/film composites	Form	Food products	Main benefits	References
Gelatin with lemongrass essential oil	Films	Sea bass slices	Retarded growth of lactic acid bacteria, psychrophilic bacteria and spoilage microorganisms, lowered changes of color, K value, and total volatile base nitrogen	(Ahmad et al. 2012)
Quince seed mucilage with thyme/oregano essential oil	Films	Rainbow trout fillets	Decreased peroxidation values, reduced the changes of color, texture, and lipid oxidation	(Jouki et al. 2014)
Alginate-chitosan with grapefruit seed extract	Multilayer coatings	Shrimp ( <i>Litopenaeus vannamei</i> )	Reduced the bacterial count and the off-flavor	(Kim et al. 2018b)
Chitosan/gelatin with Ziziphora clinopodioides essential oil and pomegranate peel extract	Films	Fresh shrimp	Decreased counts of bacterial, and population of <i>Listeria monocytogenes</i>	(Shahbazi 2018)
Starfish gelatin with vanillin	Films	Crab sticks	Inhibited the populations of <i>Listeria monocytogenes</i>	(Lee et al. 2016a)

compounds are produced to prolong their shelf life (Table 8.3). The incorporation of grape seed extract and tea polyphenols into chitosan coatings predominantly delayed the degradation of ATP and lipid oxidation of red drum during refrigerated storage (Li et al. 2013). Song et al. (2011b) reported the efficacy of alginate coatings enriched with  $V_c$  and tea polyphenols in inhibiting the growth of total viable counts, reducing chemical spoilage, and improving sensory quality of refrigerated bream compared to uncoated samples. According to Kim et al. (2018b), the multilayer coatings, based on alginate, chitosan, and grapefruit seed extract, were fabricated to reduce the bacterial counts and off-flavor of shrimp stored at 4 °C.

As shown in Table 8.3, the hydrocolloid-based coatings and films with nanoemulsion, nanoencapsulation, and nanocellulose have been created to extend shelf life of meat and seafood products. Dehnad et al. (2014) proved that the application of nanocomposite films based on chitosan and nanocellulose on ground meat decreased lactic acid bacteria population up to 3.1 logarithmic cycles (compared with nylon packaged sample) at 25 °C during 6 days of storage. Noori et al. (2018) showed that the addition of ginger essential oil nanoemulsion into sodium



caseinate coatings caused significant decrease of total aerobic psychrophilic bacteria of refrigerated chicken fillets during 12 days. The chitosan coatings included with nanoencapsulated *Satureja* plant essential oil were developed by Pabast et al. (2018) to improve the microbiological safety and prolong shelf life of lamb meat during chilled storage. Additionally, new plant extracts, as well as hydrocolloids based on non-conventional sources have been developed as potential ingredients of coatings and films (Shahbazi 2018; Jouki et al. 2014; Lee et al. 2016a; Ruiz-Navajas et al. 2015).

Cheese is nutritious food derived from milk. The shelf life of cheese is limited due to the uncontrolled and extensive fungal and bacterial proliferation on its surface. Table 8.4 shows some recent applications of antimicrobial coatings and films based on hydrocolloids in cheese. WPI coatings included with thyme and clove essential oils were produced by Kavas et al. (2015) to prolong the shelf life of semi-hard kashar cheese. The application of this coating on cheese retarded the growth of *Listeria monocytogenes*, *Staphylococcus aureus*, and *Escherichia coli* O157:H7 during 60 days of storage. Nanolaminate coatings based on alginate and lysozyme by LbL technique were fabricated to preserve “Coalho” cheese (Medeiros et al. 2014). After 20 days, coated cheese showed lower values of mass loss, pH, lipidic peroxidation and higher titratable acidity in comparison with uncoated cheese (Medeiros et al. 2014). Kim et al. (2018a, b) wrapped the Mozzarella cheese with chicken bone gelatine films containing cinnamon bark oil (1% w/v) and observed the reduction in the population of *Listeria monocytogenes* on mozzarella cheese during 20 days storage. In the current market, the commercialized hydrocolloid-based coatings, RIOCOBERT and RIOCOBERT PLUS (Becor Barbanza Ltd., A Coruña, Spain) effectively inhibited the growth of fungi on cheese (Fuciños et al. 2017).

For bakery and nuts products, most applications are hydrocolloid-based coatings rather than films. The coatings made from potato starch with potassium sorbate and citric acid were applied to extend shelf life of mini panettone (Ferreira Saraiva et al. 2016). Pinto et al. (2015) coated the cashew nuts with starch-cashew tree gum blend coatings to reduce moisture absorption, lipid oxidation, and the loss of crisp texture of nuts. Apart from that, hydrocolloid-based coatings are an additional method to improve unit operation efficiencies in the food industry. For example, they were applied in frying pre-treatments to reduce oil content in deep-fat fried products, such as chicken breasts (Dragich and Krochta 2010), potato chips (Hua et al. 2015), and fish cake (He et al. 2015). In osmotic dehydration processes of fruits and vegetables, hydrocolloid-based coatings can prevent large solute uptake without noticeably affecting water loss (Rodriguez et al. 2016; Azam et al. 2013).

## 7 Future Perspectives

Although hydrocolloid-based coatings and films have been utilized in food products, their mechanical and water barrier attributes are still weaker compared to those of synthetic plastic materials. Several approaches (e.g., bilayer, multilayer,

**Table 8.4** Recent applications of hydrocolloid-based coatings and films in cheese

Coating/film composites	Form	Food products	Main benefits	References
Water chestnut starch-chitosan containing perilla oil	Coatings	Mongolian cheese	Delayed weight loss and the microbial growth	(Mei et al. 2013)
WPI-guar gum-sunflower oil with natamycin and lactic acid	Coatings	Cheese	Decreased water loss, hardness, and color change, inhibited pathogenic or contaminant microorganisms	(Ramos et al. 2012)
Sodium caseinate-chitosan	Coatings	Cheese	Significantly inhibited the growth of mesophilic bacteria, psychrotrophic, yeasts, and molds	(Moreira et al. 2011a)
Galactomannan with nisin	Coatings	Ricotta cheese	Against <i>Listeria monocytogenes</i>	(Martins et al. 2010)
WPI with thyme and clove essential oils	Coatings	Semi-hard kashar cheese	Significant effect on the antimicrobial activity against <i>Listeria monocytogenes</i>	(Kavas et al. 2015)
WPI with ginger essential oil	Coatings	Kashar cheese	Inhibited the growth of <i>Escherichia coli</i> O157:H7 and <i>Staphylococcus aureus</i>	(Kavas et al. 2016)
Alginate-lysozyme	Nanolaminate coatings	'Coalho' cheese	Lower values of mass loss, pH, lipidic peroxidation, microorganisms' proliferation and higher titratable acidity	(Medeiros et al. 2014)
Sodium caseinate with nisin	Films	Mini red Babybel cheese	Against <i>Listeria innocua</i> during storage at refrigerated temperatures	(Cao-Hoang et al. 2010)
Starch with natamycin and nisin	Films	Port Salut cheese	Controlled <i>Saccharomyces cerevisiae</i> and <i>Listeria innocua</i> growth	(Ollé Resa et al. 2016)
Zein-carnauba wax with lysozyme	Films	Fresh Kashar cheese	A significant reduction in initial <i>Listeria monocytogenes</i> counts	(Ünalán et al. 2013)
Puffer fish skin gelatin with <i>Moringa oleifera</i> Lam. leaf extract	Films	Gouda cheese	Inhibited the <i>Listeria monocytogenes</i> growth, retarded the lipid oxidation	(Lee et al. 2016c)
Chicken bone gelatine with cinnamon bark oil	Films	Mozzarella cheese	Displayed antimicrobial and antioxidant activities, inhibited <i>Listeria monocytogenes</i>	(Kim et al. 2018a)
Red algae with grapefruit seed extract	Films	Cheese	Inhibited the growth of <i>Escherichia coli</i> O157:H7 and <i>Listeria monocytogenes</i> , decreased peroxide and thiobarbituric acid values	(Shin et al. 2012)

crosslinking, and bio-nanocomposite films, etc.) are employed to ameliorate properties of hydrocolloid-based coatings and films. Among them, incorporation of polysaccharide nanofillers into hydrocolloids to produce bio-nanocomposites has gained increasing attention in recent years, due to their edibility, remarkable physical performance, and functional properties (Otoni et al. 2017). Thus, this type of bio-nanocomposites is expected to be a promising area of research in the future.

On the other hand, the nanodelivery systems, such as nanoencapsulation, nanoliposomes, nanoemulsion, and nanolaminate, have emerged to enhance the performance of bioactive agents and improve their effectiveness in preserving food products. Currently, they are developed as the effective tools to augment the functionality of hydrocolloid-based coatings and films (Aloui and Khwaldia 2016). Future research should focus on the development of hydrocolloid coatings and films based on nanodelivery systems as well as their interactions with food products.

As a bottom-up approach, the structure-properties of hydrocolloid coatings and films should be studied further. Practically important properties such as WVP, TS, and EAB must be correlated with molecular structure and mobility in the solid state to further develop the utilization of polysaccharides. For instance, dextran, consisting of  $\alpha$ -1,6 glycosidic linkages, shows a poor film-forming capacity in comparison with pullulan or amylose. In addition, dextran shows the largest molecular mobility in the solid state, followed by pullulan and amylose. The physico-chemical properties and molecular mobility of dextran, pullulan, and amylose in the solid state are quite different from each other because of the different modes of glucosidic linkages (Nishinari et al. 1985, 1992). Overall, hydrocolloids as packaging materials still need scientific research to improve their properties, quality and marketability. Further studies include (1) embracing big data and artificial intelligence (AI) in research and development, e.g., for process simulation, classification, pattern recognition, and transfer learning; (2) developing new techniques, equipment, machines for large-scale industrial implementation and applications.

**Acknowledgements** The author thanks Prof. Loong-Tak Lim of University of Guelph (Guelph, Canada), for his helpful suggestions and review of manuscript.

## References

- Agrawal AM, Pandey P (2015) Scale up of pan coating process using quality by design principles. *J Pharm Sci* 104(11):3589–3611. <https://doi.org/10.1002/jps.24582>
- Ahmad M, Benjakul S, Sumpavapol P, Nirmal NP (2012) Quality changes of sea bass slices wrapped with gelatin film incorporated with lemongrass essential oil. *Int J Food Microbiol* 155(3):171–178. <https://doi.org/10.1016/j.ijfoodmicro.2012.01.027>
- Aloui H, Khwaldia K (2016) Natural antimicrobial edible coatings for microbial safety and food quality enhancement. *Compr Rev Food Sci Food Saf* 15(6):1080–1103. <https://doi.org/10.1111/1541-4337.12226>
- Alves MM, Gonçalves MP, Rocha CMR (2017) Effect of ferulic acid on the performance of soy protein isolate-based edible coatings applied to fresh-cut apples. *LWT Food Sci Technol* 80:409–415. <https://doi.org/10.1016/j.lwt.2017.03.013>

- Andrade RD, Skurtys O, Osorio FA (2012) Atomizing spray systems for application of edible coatings. *Compr Rev Food Sci Food Saf* 11(3):323–337. <https://doi.org/10.1111/j.1541-4337.2012.00186.x>
- Andreuccetti C, Carvalho RA, Grosso CRF (2009) Effect of hydrophobic plasticizers on functional properties of gelatin-based films. *Food Res Int* 42(8):1113–1121. <https://doi.org/10.1016/j.foodres.2009.05.010>
- Arnon H, Zaitsev Y, Porat R, Poverenov E (2014) Effects of carboxymethyl cellulose and chitosan bilayer edible coating on postharvest quality of citrus fruit. *Postharvest Biol Technol* 87:21–26. <https://doi.org/10.1016/j.postharvbio.2013.08.007>
- Arzate-Vázquez I, Chanona-Pérez JJ, Calderón-Domínguez G, Terres-Rojas E, Garibay-Febles V, Martínez-Rivas A, Gutiérrez-López GF (2012) Microstructural characterization of chitosan and alginate films by microscopy techniques and texture image analysis. *Carbohydr Polym* 87(1):289–299. <https://doi.org/10.1016/j.carbpol.2011.07.044>
- ASTM-D3985-02 (2002) Standard test method for oxygen gas transmission rate through plastic film and sheeting using a coulometric sensor. In: Annual book of American standard testing methods. American Society for Testing & Materials, Philadelphia, PA, pp 472–477
- ASTM-D882-91 (1991) Standard test method for tensile properties of thin plastic sheeting. In: Annual book of American standard testing methods. American Society for Testing and Materials, Philadelphia, PA, pp 161–170
- ASTM-E96-92 (1990) Standard test methods for water vapor transmission of materials. In: Annual book of American standard testing methods. American Society for Testing & Materials, Philadelphia, PA, pp 745–754
- Avena-Bustillos RJ, Chiou B, Olsen CW, Bechtel PJ, Olson DA, McHugh TH (2011) Gelation, oxygen permeability, and mechanical properties of mammalian and fish gelatin films. *J Food Sci* 76(7):E519–E524. <https://doi.org/10.1111/j.1750-3841.2011.02312.x>
- Azam M, Haq MA, Hasnain A (2013) Osmotic dehydration of mango cubes: effect of novel gluten-based coating. *Dry Technol* 31(1):120–127. <https://doi.org/10.1080/07373937.2012.727055>
- Azevedo VM, Borges SV, Marconcini JM, Yoshida MI, Neto ARS, Pereira TC, Pereira CFG (2017) Effect of replacement of corn starch by whey protein isolate in biodegradable film blends obtained by extrusion. *Carbohydr Polym* 157:971–980. <https://doi.org/10.1016/j.carbpol.2016.10.046>
- Bigi A, Panzavolta S, Rubini K (2004) Relationship between triple-helix content and mechanical properties of gelatin films. *Biomaterials* 25(25):5675–5680. <https://doi.org/10.1016/j.biomaterials.2004.01.033>
- Bill M, Sivakumar D, Korsten L, Thompson AK (2014) The efficacy of combined application of edible coatings and thyme oil in inducing resistance components in avocado (*Persea americana* Mill.) against anthracnose during post-harvest storage. *Crop Prot* 64:159–167. <https://doi.org/10.1016/j.cropro.2014.06.015>
- Bodnár I, Altíng AC, Verschuere M (2007) Structural effects on the permeability of whey protein films in an aqueous environment. *Food Hydrocoll* 21(5):889–895. <https://doi.org/10.1016/j.foodhyd.2006.11.017>
- Boran G, Regenstein JM (2010) Fish gelatin. In: Taylor SL (ed) *Advances in food and nutrition research*, vol vol 60. Academic Press, Cambridge, pp 119–143. [https://doi.org/10.1016/S1043-4526\(10\)60005-8](https://doi.org/10.1016/S1043-4526(10)60005-8)
- Borges AF, Silva C, Coelho JFJ, Simões S (2015) Oral films: current status and future perspectives: I — Galenical development and quality attributes. *J Control Release* 206:1–19. <https://doi.org/10.1016/j.jconrel.2015.03.006>
- Brown ME, Gallagher PK (2011) *Handbook of thermal analysis and calorimetry: recent advances, techniques and applications*, vol vol 5. Elsevier, New York
- Campos CA, Gerschenson LN, Flores SK (2011) Development of edible films and coatings with antimicrobial activity. *Food Bioprocess Technol* 4(6):849–875. <https://doi.org/10.1007/s11947-010-0434-1>

- Cao-Hoang L, Chaine A, Grégoire L, Waché Y (2010) Potential of nisin-incorporated sodium caseinate films to control *Listeria* in artificially contaminated cheese. *Food Microbiol* 27 (7):940–944. <https://doi.org/10.1016/j.fm.2010.05.025>
- Cazón P, Velazquez G, Ramírez JA, Vázquez M (2017) Polysaccharide-based films and coatings for food packaging: a review. *Food Hydrocoll* 68:136–148. <https://doi.org/10.1016/j.foodhyd.2016.09.009>
- Cerqueira MA, Lima AM, Teixeira JA, Moreira RA, Vicente AA (2009) Suitability of novel galactomannans as edible coatings for tropical fruits. *J Food Eng* 94(3):372–378. <https://doi.org/10.1016/j.jfoodeng.2009.04.003>
- Chen Y, Yang J, Dave RN, Pfeffer R (2009) Granulation of cohesive Geldart group C powders in a Mini-Glatt fluidized bed by pre-coating with nanoparticles. *Powder Technol* 191(1):206–217. <https://doi.org/10.1016/j.powtec.2008.10.010>
- Cheng SZ (2002) *Handbook of thermal analysis and calorimetry: applications to polymers and plastics*, vol vol 3. Elsevier, New York
- Choi WS, Singh S, Lee YS (2016) Characterization of edible film containing essential oils in hydroxypropyl methylcellulose and its effect on quality attributes of ‘Formosa’ plum (*Prunus salicina* L.). *LWT Food Sci Technol* 70:213–222. <https://doi.org/10.1016/j.lwt.2016.02.036>
- Chung Y-C, Chen C-Y (2008) Antibacterial characteristics and activity of acid-soluble chitosan. *Bioresour Technol* 99(8):2806–2814. <https://doi.org/10.1016/j.biortech.2007.06.044>
- Ciannamea EM, Stefani PM, Ruseckaite RA (2014) Physical and mechanical properties of compression molded and solution casting soybean protein concentrate based films. *Food Hydrocoll* 38:193–204. <https://doi.org/10.1016/j.foodhyd.2013.12.013>
- Cosenza VA, Navarro DA, Fissore EN, Rojas AM, Stortz CA (2014) Chemical and rheological characterization of the carrageenans from *Hypnea musciformis* (Wulfen) Lamoroux. *Carbohydr Polym* 102:780–789. <https://doi.org/10.1016/j.carbpol.2013.10.090>
- Crosby AJ, Lee JY (2007) Polymer nanocomposites: the “nano” effect on mechanical properties. *Polym Rev* (Philadelphia, PA) 47(2):217–229. <https://doi.org/10.1080/15583720701271278>
- Cui H, Yuan L, Li W, Lin L (2017) Edible film incorporated with chitosan and *Artemisia annua* oil nanoliposomes for inactivation of *Escherichia coli* O157:H7 on cherry tomato. *Int J Food Sci Technol* 52(3):687–698. <https://doi.org/10.1111/ijfs.13322>
- de Aquino AB, Blank AF, de Aquino Santana LCL (2015) Impact of edible chitosan–cassava starch coatings enriched with *Lippia gracilis* Schauer genotype mixtures on the shelf life of guavas (*Psidium guajava* L.) during storage at room temperature. *Food Chem* 171:108–116. <https://doi.org/10.1016/j.foodchem.2014.08.077>
- De Azeredo HMC, Rosa MF, De Sá M, Souza Filho M, Waldron KW (2014) The use of biomass for packaging films and coatings. In: Waldron K (ed) *Advances in biorefineries*. Woodhead Publishing, Sawston, pp 819–874. <https://doi.org/10.1533/9780857097385.2.819>
- Debeaufort F, Voilley A (2009) Lipid-based edible films and coatings. In: Huber KC, Embuscado ME (eds) *Edible films and coatings for food applications*. Springer, New York, pp 135–168. [https://doi.org/10.1007/978-0-387-92824-1\\_5](https://doi.org/10.1007/978-0-387-92824-1_5)
- Dehnad D, Mirzaei H, Emam-Djomeh Z, Jafari S-M, Dadashi S (2014) Thermal and antimicrobial properties of chitosan–nanocellulose films for extending shelf life of ground meat. *Carbohydr Polym* 109:148–154. <https://doi.org/10.1016/j.carbpol.2014.03.063>
- Dewettinck K, Huyghebaert A (1999) Fluidized bed coating in food technology. *Trends Food Sci Technol* 10(4):163–168. [https://doi.org/10.1016/S0924-2244\(99\)00041-2](https://doi.org/10.1016/S0924-2244(99)00041-2)
- Dhall RK (2013) Advances in edible coatings for fresh fruits and vegetables: a review. *Crit Rev Food Sci Nutr* 53(5):435–450. <https://doi.org/10.1080/10408398.2010.541568>
- Dragich AM, Krochta JM (2010) Whey protein solution coating for fat-uptake reduction in deep-fried chicken breast strips. *J Food Sci* 75(1):S43–S47. <https://doi.org/10.1111/j.1750-3841.2009.01408.x>
- Du H, Hu Q, Yang W, Pei F, Kimatu BM, Ma N, Fang Y, Cao C, Zhao L (2016) Development, physiochemical characterization and forming mechanism of *Flammulina velutipes*

- polysaccharide-based edible films. *Carbohydr Polym* 152:214–221. <https://doi.org/10.1016/j.carbpol.2016.07.035>
- Durrani CM, Donald AM (1995) Physical characterisation of amylopectin gels. *Polym Gels Netw* 3 (1):1–27. [https://doi.org/10.1016/0966-7822\(94\)00005-R](https://doi.org/10.1016/0966-7822(94)00005-R)
- Edible packaging-global market outlook from 2017 to 2023 (2017). <https://www.strategymrc.com/report/edible-packaging-market>. Accessed July 2017
- Emam-Djomeh Z, Moghaddam A, Yasini Ardakani SA (2015) Antimicrobial activity of pomegranate (*Punica granatum* L.) peel extract, physical, mechanical, barrier and antimicrobial properties of pomegranate peel extract-incorporated sodium caseinate film and application in packaging for ground beef. *Packag Technol Sci* 28(10):869–881. <https://doi.org/10.1002/pts.2145>
- Espinoza-Herrera N, Pedroza-Islas R, San Martín-Martínez E, Cruz-Orea A, Tomás SA (2011) Thermal, mechanical and microstructures properties of cellulose derivatives films: a comparative study. *Food Biophys* 6(1):106–114. <https://doi.org/10.1007/s11483-010-9181-0>
- Espitia PJP, Du W-X, Avena-Bustillos RJ, Soares NFF, McHugh TH (2014) Edible films from pectin: physical-mechanical and antimicrobial properties - a review. *Food Hydrocoll* 35:287–296. <https://doi.org/10.1016/j.foodhyd.2013.06.005>
- Fakhouri FM, Martelli SM, Caon T, Velasco JI, Mei LHI (2015) Edible films and coatings based on starch/gelatin: film properties and effect of coatings on quality of refrigerated red crimson grapes. *Postharvest Biol Technol* 109:57–64. <https://doi.org/10.1016/j.postharvbio.2015.05.015>
- Fernández-Pan I, Carrión-Granda X, Maté JI (2014) Antimicrobial efficiency of edible coatings on the preservation of chicken breast fillets. *Food Control* 36(1):69–75. <https://doi.org/10.1016/j.foodcont.2013.07.032>
- Ferreira Saraiva LE, Naponucena LOM, da Silva Santos V, Silva RPD, de Souza CO, Evelyn Gomes Lima Souza I, de Oliveira Mamede ME, Druzian JI (2016) Development and application of edible film of active potato starch to extend mini panettone shelf life. *LWT Food Sci Technol* 73:311–319. <https://doi.org/10.1016/j.lwt.2016.05.047>
- Fishman ML, Coffin DR, Konstance RP, Onwulata CI (2000) Extrusion of pectin/starch blends plasticized with glycerol. *Carbohydr Polym* 41(4):317–325. [https://doi.org/10.1016/S0144-8617\(99\)00117-4](https://doi.org/10.1016/S0144-8617(99)00117-4)
- Franssen L, Krochta J (2003) Edible coatings containing natural antimicrobials for processed foods. In: *Natural antimicrobials for the minimal processing of foods*. Elsevier, New York, pp 250–262
- Fu S, Thacker A, Sperger DM, Boni RL, Buckner IS, Velankar S, Munson EJ, Block LH (2011) Relevance of rheological properties of sodium alginate in solution to calcium alginate gel properties. *AAPS PharmSciTech* 12(2):453–460. <https://doi.org/10.1208/s12249-011-9587-0>
- Fuciños C, Amado IR, Fuciños P, Fajardo P, Rúa ML, Pastrana LM (2017) Evaluation of antimicrobial effectiveness of pimaricin-loaded thermosensitive nanohydrogel coating on Arzúa-Ulloa DOP cheeses. *Food Control* 73:1095–1104. <https://doi.org/10.1016/j.foodcont.2016.10.028>
- Gao C, Pollet E, Avérous L (2017) Properties of glycerol-plasticized alginate films obtained by thermo-mechanical mixing. *Food Hydrocoll* 63:414–420. <https://doi.org/10.1016/j.foodhyd.2016.09.023>
- García LC, Pereira LM, de Luca Sarantópoulos CIG, Hubinger MD (2010) Selection of an edible starch coating for minimally processed strawberry. *Food Bioprocess Technol* 3(6):834–842. <https://doi.org/10.1007/s11947-009-0313-9>
- Gennadios A, Brandenburg AH, Weller CL, Testin RF (1993) Effect of pH on properties of wheat gluten and soy protein isolate films. *J Agric Food Chem* 41(11):1835–1839. <https://doi.org/10.1021/jf00035a006>
- Gennadios A, Weller CL, Hanna MA, Froming GW (1996) Mechanical and barrier properties of egg albumen films. *J Food Sci* 61(3):585–589. <https://doi.org/10.1111/j.1365-2621.1996.tb13164.x>

- Gennadios A, Hanna MA, Kurth LB (1997) Application of edible coatings on meats, poultry and seafoods: a review. *LWT Food Sci Technol* 30(4):337–350. <https://doi.org/10.1006/food.1996.0202>
- Ghanbarzadeh B, Musavi M, Oromiehie AR, Rezayi K, Razmi Rad E, Milani J (2007) Effect of plasticizing sugars on water vapor permeability, surface energy and microstructure properties of zein films. *LWT Food Sci Technol* 40(7):1191–1197. <https://doi.org/10.1016/j.lwt.2006.07.008>
- Ghoshal S, Stapf S, Mattea C (2014) Protein renaturation in the gelatin film formation process. *Appl Magn Reson* 45(2):145–154. <https://doi.org/10.1007/s00723-014-0514-x>
- Giancone T, Torrieri E, Pierro PD, Mariniello L, Moresi M, Porta R, Masi P (2008) Role of constituents on the network formation of hydrocolloid edible films. *J Food Eng* 89(2):195–203. <https://doi.org/10.1016/j.jfoodeng.2008.04.017>
- Gómez-Estaca J, Gavara R, Catalá R, Hernández-Muñoz P (2016) The potential of proteins for producing food packaging materials: a review. *Packag Technol Sci* 29(4–5):203–224. <https://doi.org/10.1002/pts.2198>
- Guckian S, Dwyer C, O'Sullivan M, O'Riordan ED, Monahan FJ (2006) Properties of and mechanisms of protein interactions in films formed from different proportions of heated and unheated whey protein solutions. *Eur Food Res Technol* 223(1):91–95. <https://doi.org/10.1007/s00217-005-0140-9>
- Guo M, Jin TZ, Wang L, Scullen OJ, Sommers CH (2014) Antimicrobial films and coatings for inactivation of *Listeria innocua* on ready-to-eat deli Turkey meat. *Food Control* 40:64–70. <https://doi.org/10.1016/j.foodcont.2013.11.018>
- Han JH (2014) Edible films and coatings: a review. In: Han JH (ed) *Innovations in food packaging*, 2nd edn. Academic Press, San Diego, pp 213–255. <https://doi.org/10.1016/B978-0-12-394601-0.00009-6>
- He S, Franco C, Zhang W (2015) Fish protein hydrolysates: application in deep-fried food and food safety analysis. *J Food Sci* 80(1):E108–E115. <https://doi.org/10.1111/1750-3841.12684>
- Hernandez-Izquierdo VM, Krochta JM (2008) Thermoplastic processing of proteins for film formation—a review. *J Food Sci* 73(2):R30–R39. <https://doi.org/10.1111/j.1750-3841.2007.00636.x>
- Hernández-Muñoz P, Kanavouros A, Ng PKW, Gavara R (2003) Development and characterization of biodegradable films made from wheat gluten protein fractions. *J Agric Food Chem* 51(26):7647–7654. <https://doi.org/10.1021/jf034646x>
- Higuera L, López-Carballo G, Hernández-Muñoz P, Catalá R, Gavara R (2014) Antimicrobial packaging of chicken fillets based on the release of carvacrol from chitosan/cyclodextrin films. *Int J Food Microbiol* 188:53–59. <https://doi.org/10.1016/j.ijfoodmicro.2014.07.018>
- Hosseinnejad M, Jafari SM (2016) Evaluation of different factors affecting antimicrobial properties of chitosan. *Int J Biol Macromol* 85:467–475. <https://doi.org/10.1016/j.ijbiomac.2016.01.022>
- Hu G, Chen J, Gao J (2009) Preparation and characteristics of oxidized potato starch films. *Carbohydr Polym* 76(2):291–298. <https://doi.org/10.1016/j.carbpol.2008.10.032>
- Hua X, Wang K, Yang R, Kang J, Yang H (2015) Edible coatings from sunflower head pectin to reduce lipid uptake in fried potato chips. *LWT Food Sci Technol* 62(2):1220–1225. <https://doi.org/10.1016/j.lwt.2015.02.010>
- Janjarasskul T, Krochta JM (2010) Edible packaging materials. *Annu Rev Food Sci Technol* 1(1):415–448. <https://doi.org/10.1146/annurev.food.080708.100836>
- Jolie RP, Duvetter T, Van Loey AM, Hendrickx ME (2010) Pectin methylesterase and its proteinaceous inhibitor: a review. *Carbohydr Res* 345(18):2583–2595. <https://doi.org/10.1016/j.carres.2010.10.002>
- Jouki M, Mortazavi SA, Yazdi FT, Koocheki A, Khazaei N (2014) Use of quince seed mucilage edible films containing natural preservatives to enhance physico-chemical quality of rainbow trout fillets during cold storage. *Food Sci Hum Wellness* 3(2):65–72. <https://doi.org/10.1016/j.fshw.2014.05.002>



- Karbowiak T, Gougeon RD, Rigolet S, Delmotte L, Debeaufort F, Voilley A (2008) Diffusion of small molecules in edible films: effect of water and interactions between diffusant and biopolymer. *Food Chem* 106(4):1340–1349. <https://doi.org/10.1016/j.foodchem.2007.03.076>
- Kavas G, Kavas N, Saygili D (2015) The effects of thyme and clove essential oil fortified edible films on the physical, chemical and microbiological characteristics of Kasha cheese. *J Food Qual* 38(6):405–412. <https://doi.org/10.1111/jfq.12157>
- Kavas N, Kavas G, Saygili D (2016) Use of ginger essential oil-fortified edible coatings in Kasha cheese and its effects on *Escherichia coli* O157:H7 and *Staphylococcus aureus*. *CYTA J Food* 14(2):317–323. <https://doi.org/10.1080/19476337.2015.1109001>
- Kester JJ, Fennema O (1989) An edible film of lipids and cellulose ethers: barrier properties to moisture vapor transmission and structural evaluation. *J Food Sci* 54(6):1383–1389. <https://doi.org/10.1111/j.1365-2621.1989.tb05118.x>
- Khwalidia K, Banon S, Perez C, Desobry S (2004a) Properties of sodium caseinate film-forming dispersions and films. *J Dairy Sci* 87(7):2011–2016. [https://doi.org/10.3168/jds.S0022-0302\(04\)70018-1](https://doi.org/10.3168/jds.S0022-0302(04)70018-1)
- Khwalidia K, Perez C, Banon S, Desobry S, Hardy J (2004b) Milk proteins for edible films and coatings. *Crit Rev Food Sci Nutr* 44(4):239–251. <https://doi.org/10.1080/10408690490464906>
- Kim KM, Son JH, Kim S-K, Weller CL, Hanna MA (2006) Properties of chitosan films as a function of pH and solvent type. *J Food Sci* 71(3):E119–E124. <https://doi.org/10.1111/j.1365-2621.2006.tb15624.x>
- Kim H, Beak S-E, Yang S-Y, Song KB (2018a) Application of an antimicrobial packaging material from chicken bone gelatine and cinnamon bark oil to mozzarella cheese. *Int J Food Sci Technol* 53(3):619–625. <https://doi.org/10.1111/ijfs.13636>
- Kim J-H, Hong W-S, Oh S-W (2018b) Effect of layer-by-layer antimicrobial edible coating of alginate and chitosan with grapefruit seed extract for shelf-life extension of shrimp (*Litopenaeus vannamei*) stored at 4 °C. *Int J Biol Macromol* 120:1468–1473. <https://doi.org/10.1016/j.ijbiomac.2018.09.160>
- Kumar R, Choudhary V, Mishra S, Varma IK, Mattiason B (2002) Adhesives and plastics based on soy protein products. *Ind Crop Prod* 16(3):155–172. [https://doi.org/10.1016/S0926-6690\(02\)00007-9](https://doi.org/10.1016/S0926-6690(02)00007-9)
- Kunte LA, Gennadios A, Cuppett SL, Hanna MA, Weller CL (1997) Cast films from soy protein isolates and fractions. *Cereal Chem* 74(2):115–118. <https://doi.org/10.1094/cchem.1997.74.2.115>
- Lacroix M, Le Tien C (2005) Edible films and coatings from nonstarch polysaccharides. In: Han JH (ed) *Innovations in food packaging*. Academic Press, London, pp 338–361. <https://doi.org/10.1016/B978-012311632-1/50052-8>
- Lagrain B, Goderis B, Brijs K, Delcour JA (2010) Molecular basis of processing wheat gluten toward biobased materials. *Biomacromolecules* 11(3):533–541. <https://doi.org/10.1021/bm100008p>
- Leceta I, Guerrero P, de la Caba K (2013) Functional properties of chitosan-based films. *Carbohydr Polym* 93(1):339–346. <https://doi.org/10.1016/j.carbpol.2012.04.031>
- LeCorre D, Bras J, Dufresne A (2011) Influence of botanic origin and amylose content on the morphology of starch nanocrystals. *J Nanopart Res* 13(12):7193–7208. <https://doi.org/10.1007/s11051-011-0634-2>
- Lee K-Y, Lee J-H, Yang H-J, Song KB (2016a) Characterization of a starfish gelatin film containing vanillin and its application in the packaging of crab stick. *Food Sci Biotechnol* 25(4):1023–1028. <https://doi.org/10.1007/s10068-016-0165-9>
- Lee K-Y, Lee J-H, Yang H-J, Song KB (2016b) Production and characterisation of skate skin gelatin films incorporated with thyme essential oil and their application in chicken tenderloin packaging. *Int J Food Sci Technol* 51(6):1465–1472. <https://doi.org/10.1111/ijfs.13119>
- Lee K-Y, Yang H-J, Song KB (2016c) Application of a puffer fish skin gelatin film containing *Moringa oleifera* Lam. leaf extract to the packaging of Gouda cheese. *J Food Sci Technol* 53(11):3876–3883. <https://doi.org/10.1007/s13197-016-2367-9>



- Li T, Li J, Hu W, Li X (2013) Quality enhancement in refrigerated red drum (*Sciaenops ocellatus*) filets using chitosan coatings containing natural preservatives. *Food Chem* 138(2):821–826. <https://doi.org/10.1016/j.foodchem.2012.11.092>
- Li K, Zhu J, Guan G, Wu H (2019) Preparation of chitosan-sodium alginate films through layer-by-layer assembly and ferulic acid crosslinking: film properties, characterization, and formation mechanism. *Int J Biol Macromol* 122:485–492. <https://doi.org/10.1016/j.ijbiomac.2018.10.188>
- Lin MG, Lasekan O, Saari N, Khairunniza-Bejo S (2018) Effect of chitosan and carrageenan-based edible coatings on post-harvested longan (*Dimocarpus longan*) fruits. *CYTA J Food* 16 (1):490–497. <https://doi.org/10.1080/19476337.2017.1414078>
- Liu Z (2005) Edible films and coatings from starches. In: Han JH (ed) *Innovations in food packaging*. Academic Press, London, pp 318–337. <https://doi.org/10.1016/B978-012311632-1/50051-6>
- Liu J, Zhan X, Wan J, Wang Y, Wang C (2015) Review for carrageenan-based pharmaceutical biomaterials: Favourable physical features versus adverse biological effects. *Carbohydr Polym* 121:27–36. <https://doi.org/10.1016/j.carbpol.2014.11.063>
- López OV, García MA, Zaritzky NE (2008) Film forming capacity of chemically modified corn starches. *Carbohydr Polym* 73(4):573–581. <https://doi.org/10.1016/j.carbpol.2007.12.023>
- López OV, Zaritzky NE, García MA (2010) Physicochemical characterization of chemically modified corn starches related to rheological behavior, retrogradation and film forming capacity. *J Food Eng* 100(1):160–168. <https://doi.org/10.1016/j.jfoodeng.2010.03.041>
- Lorevice MV, Otoni CG, Moura MR, Mattoso LHC (2016) Chitosan nanoparticles on the improvement of thermal, barrier, and mechanical properties of high- and low-methyl pectin films. *Food Hydrocoll* 52:732–740. <https://doi.org/10.1016/j.foodhyd.2015.08.003>
- Mangavel C, Barbot J, Popineau Y, Guéguen J (2001) Evolution of wheat gliadins conformation during film formation: a fourier transform infrared study. *J Agric Food Chem* 49(2):867–872. <https://doi.org/10.1021/jf0009899>
- Mannozi C, Cecchini JP, Tylewicz U, Siroli L, Patrignani F, Lanciotti R, Rocculi P, Dalla Rosa M, Romani S (2017) Study on the efficacy of edible coatings on quality of blueberry fruits during shelf-life. *LWT Food Sci Technol* 85:440–444. <https://doi.org/10.1016/j.lwt.2016.12.056>
- Maqbool M, Ali A, Alderson PG, Mohamed MTM, Siddiqui Y, Zahid N (2011) Postharvest application of gum arabic and essential oils for controlling anthracnose and quality of banana and papaya during cold storage. *Postharvest Biol Technol* 62(1):71–76. <https://doi.org/10.1016/j.postharvbio.2011.04.002>
- Marsh K, Bugusu B (2007) Food packaging-roles, materials, and environmental issues. *J Food Sci* 72(3):R39–R55. <https://doi.org/10.1111/j.1750-3841.2007.00301.x>
- Martins JT, Cerqueira MA, Souza BWS, Carmo Avides MD, Vicente AA (2010) Shelf life extension of Ricotta cheese using coatings of galactomannans from nonconventional sources incorporating nisin against *Listeria monocytogenes*. *J Agric Food Chem* 58(3):1884–1891. <https://doi.org/10.1021/jf902774z>
- Mauer LJ, Smith DE, Labuza TP (2000) Water vapor permeability, mechanical, and structural properties of edible  $\beta$ -casein films. *Int Dairy J* 10(5):353–358. [https://doi.org/10.1016/S0958-6946\(00\)00061-3](https://doi.org/10.1016/S0958-6946(00)00061-3)
- Medeiros BGDS, Pinheiro AC, Carneiro-da-Cunha MG, Vicente AA (2012a) Development and characterization of a nanomultilayer coating of pectin and chitosan – evaluation of its gas barrier properties and application on ‘Tommy Atkins’ mangoes. *J Food Eng* 110(3):457–464. <https://doi.org/10.1016/j.jfoodeng.2011.12.021>
- Medeiros BGS, Pinheiro AC, Teixeira JA, Vicente AA, Carneiro-da-Cunha MG (2012b) Polysaccharide/protein nanomultilayer coatings: construction, characterization and evaluation of their effect on ‘Rocha’ pear (*Pyrus communis* L.) shelf-life. *Food Bioprocess Technol* 5 (6):2435–2445. <https://doi.org/10.1007/s11947-010-0508-0>
- Medeiros BGDS, Souza MP, Pinheiro AC, Bourbon AI, Cerqueira MA, Vicente AA, Carneiro-da-Cunha MG (2014) Physical characterisation of an alginate/lysozyme nano-laminate coating and

- its evaluation on 'Coalho' cheese shelf life. *Food Bioprocess Technol* 7(4):1088–1098. <https://doi.org/10.1007/s11947-013-1097-5>
- Mei J, Yuan Y, Wu Y, Li Y (2013) Characterization of edible starch–chitosan film and its application in the storage of Mongolian cheese. *Int J Biol Macromol* 57:17–21. <https://doi.org/10.1016/j.ijbiomac.2013.03.003>
- Mendes JF, Paschoalin RT, Carmona VB, Sena Neto AR, Marques ACP, Marconcini JM, Mattoso LHC, Medeiros ES, Oliveira JE (2016) Biodegradable polymer blends based on corn starch and thermoplastic chitosan processed by extrusion. *Carbohydr Polym* 137:452–458. <https://doi.org/10.1016/j.carbpol.2015.10.093>
- Mohebbi M, Ansarifard E, Hasanpour N, Amirouyefi MR (2012) Suitability of Aloe vera and gum tragacanth as edible coatings for extending the shelf life of button mushroom. *Food Bioprocess Technol* 5(8):3193–3202. <https://doi.org/10.1007/s11947-011-0709-1>
- Moreira MR, Pereda M, Marcovich NE, Roura SI (2011a) Antimicrobial effectiveness of bioactive packaging materials from edible chitosan and casein polymers: assessment on carrot, cheese, and salami. *J Food Sci* 76(1):M54–M63. <https://doi.org/10.1111/j.1750-3841.2010.01910.x>
- Moreira MR, Roura SI, Ponce A (2011b) Effectiveness of chitosan edible coatings to improve microbiological and sensory quality of fresh cut broccoli. *LWT Food Sci Technol* 44(10):2335–2341. <https://doi.org/10.1016/j.lwt.2011.04.009>
- Mulvihill DM, Ennis MP (2003) Functional milk proteins: production and utilization. In: Fox PF, McSweeney PLH (eds) *Advanced dairy chemistry—1 proteins: part A/part B*. Springer, Boston, pp 1175–1228. [https://doi.org/10.1007/978-1-4419-8602-3\\_32](https://doi.org/10.1007/978-1-4419-8602-3_32)
- Navarro-Tarazaga ML, Massa A, Pérez-Gago MB (2011) Effect of beeswax content on hydroxypropyl methylcellulose-based edible film properties and postharvest quality of coated plums (Cv. Angeleno). *LWT Food Sci Technol* 44(10):2328–2334. <https://doi.org/10.1016/j.lwt.2011.03.011>
- Nishinari K, Shibuya N, Kainuma K (1985) Dielectric relaxation in solid dextran and pullulan. *Die Makromolekulare Chemie* 186(2):433–438. <https://doi.org/10.1002/macp.1985.021860221>
- Nishinari K, Kohyama K, Shibuya N, Kim KY, Kim NH, Watase M, Tsutsumi A (1992) Molecular motions in cellulose derivatives. In: *Viscoelasticity of biomaterials*, ACS symposium series, vol vol 489. American Chemical Society, Washington, pp 357–369. <https://doi.org/10.1021/bk-1992-0489.ch024>
- Noori S, Zeynali F, Almasi H (2018) Antimicrobial and antioxidant efficiency of nanoemulsion-based edible coating containing ginger (*Zingiber officinale*) essential oil and its effect on safety and quality attributes of chicken breast fillets. *Food Control* 84:312–320. <https://doi.org/10.1016/j.foodcont.2017.08.015>
- Nur Hanani ZA, Beatty E, Roos YH, Morris MA, Kerry JP (2012) Manufacture and characterization of gelatin films derived from beef, pork and fish sources using twin screw extrusion. *J Food Eng* 113(4):606–614. <https://doi.org/10.1016/j.jfoodeng.2012.07.002>
- Ollé Resa CP, Gerschenson LN, Jagus RJ (2016) Starch edible film supporting natamycin and nisin for improving microbiological stability of refrigerated argentinian Port Salut cheese. *Food Control* 59:737–742. <https://doi.org/10.1016/j.foodcont.2015.06.056>
- Otoni CG, Avena-Bustillos RJ, Azeredo HMC, Lorevice MV, Moura MR, Mattoso LHC, McHugh TH (2017) Recent advances on edible films based on fruits and vegetables—a review. *Compr Rev Food Sci Food Saf* 16(5):1151–1169. <https://doi.org/10.1111/1541-4337.12281>
- Pabast M, Shariatifar N, Beikzadeh S, Jahed G (2018) Effects of chitosan coatings incorporating with free or nano-encapsulated Satureja plant essential oil on quality characteristics of lamb meat. *Food Control* 91:185–192. <https://doi.org/10.1016/j.foodcont.2018.03.047>
- Pankaj SK, Bueno-Ferrer C, Misra NN, O'Neill L, Tiwari BK, Bourke P, Cullen PJ (2014) Physicochemical characterization of plasma-treated sodium caseinate film. *Food Res Int* 66:438–444. <https://doi.org/10.1016/j.foodres.2014.10.016>
- Paula GA, Benevides NMB, Cunha AP, de Oliveira AV, Pinto AMB, Morais JPS, Azeredo HMC (2015) Development and characterization of edible films from mixtures of  $\kappa$ -carrageenan,

- t-carrageenan, and alginate. *Food Hydrocoll* 47:140–145. <https://doi.org/10.1016/j.foodhyd.2015.01.004>
- Peretto G, Du W-X, Avena-Bustillos RJ, Berrios JDJ, Sambo P, McHugh TH (2014) Optimization of antimicrobial and physical properties of alginate coatings containing carvacrol and methyl cinnamate for strawberry application. *J Agric Food Chem* 62(4):984–990. <https://doi.org/10.1021/jf4042886>
- Pérez-Gago MB, Krochta JM (2002) Formation and properties of whey protein films and coatings. In: *Protein-based films and coatings*. CRC Press, Boca Raton, pp 159–180
- Pérez-Gago MB, Nadaud P, Krochta JM (1999) Water vapor permeability, solubility, and tensile properties of heat-denatured versus native whey protein films. *J Food Sci* 64(6):1034–1037. <https://doi.org/10.1111/j.1365-2621.1999.tb12276.x>
- Pham GT, Park Y-B, Liang Z, Zhang C, Wang B (2008) Processing and modeling of conductive thermoplastic/carbon nanotube films for strain sensing. *Compos Part B Eng* 39(1):209–216. <https://doi.org/10.1016/j.compositesb.2007.02.024>
- Pinto AMB, Santos TM, Caceres CA, Lima JR, Ito EN, Azeredo HMC (2015) Starch-cashew tree gum nanocomposite films and their application for coating cashew nuts. *LWT Food Sci Technol* 62(1, Part 2):549–554. <https://doi.org/10.1016/j.lwt.2014.07.028>
- Pitak N, Rakshit SK (2011) Physical and antimicrobial properties of banana flour/chitosan biodegradable and self sealing films used for preserving fresh-cut vegetables. *LWT Food Sci Technol* 44(10):2310–2315. <https://doi.org/10.1016/j.lwt.2011.05.024>
- Porta R, Di Pierro P, Rossi-Marquez G, Mariniello L, Kadivar M, Arabestani A (2015) Microstructure and properties of bitter vetch (*Vicia ervilia*) protein films reinforced by microbial transglutaminase. *Food Hydrocoll* 50:102–107. <https://doi.org/10.1016/j.foodhyd.2015.04.008>
- Poverenov E, Rutenberg R, Danino S, Horev B, Rodov V (2014) Gelatin-chitosan composite films and edible coatings to enhance the quality of food products: layer-by-layer vs. blended formulations. *Food Bioprocess Technol* 7(11):3319–3327. <https://doi.org/10.1007/s11947-014-1333-7>
- Prommakool A, Sajjaanantakul T, Janjarasskul T, Krochta JM (2011) Whey protein–okra polysaccharide fraction blend edible films: tensile properties, water vapor permeability and oxygen permeability. *J Sci Food Agric* 91(2):362–369. <https://doi.org/10.1002/jsfa.4194>
- Pushpadass HA, Kumar A, Jackson DS, Wehling RL, Dumais JJ, Hanna MA (2009) Macromolecular changes in extruded starch-films plasticized with glycerol, water and stearic acid. *Starch - Stärke* 61(5):256–266. <https://doi.org/10.1002/star.200800046>
- Qiu X, Chen S, Liu G, Yang Q (2014) Quality enhancement in the Japanese sea bass (*Lateolabrax japonicus*) fillets stored at 4°C by chitosan coating incorporated with citric acid or licorice extract. *Food Chem* 162:156–160. <https://doi.org/10.1016/j.foodchem.2014.04.037>
- Ramos ÓL, Pereira JO, Silva SI, Fernandes JC, Franco MI, Lopes-da-Silva JA, Pintado ME, Malcata FX (2012) Evaluation of antimicrobial edible coatings from a whey protein isolate base to improve the shelf life of cheese. *J Dairy Sci* 95(11):6282–6292. <https://doi.org/10.3168/jds.2012-5478>
- Ramos ÓL, Reinas I, Silva SI, Fernandes JC, Cerqueira MA, Pereira RN, Vicente AA, Poças MF, Pintado ME, Malcata FX (2013) Effect of whey protein purity and glycerol content upon physical properties of edible films manufactured therefrom. *Food Hydrocoll* 30(1):110–122. <https://doi.org/10.1016/j.foodhyd.2012.05.001>
- Ramos-García M, Bosquez-Molina E, Hernández-Romano J, Zavala-Padilla G, Terrés-Rojas E, Alia-Tejagal I, Barrera-Necha L, Hernández-López M, Bautista-Baños S (2012) Use of chitosan-based edible coatings in combination with other natural compounds, to control *Rhizopus stolonifer* and *Escherichia coli* DH5 $\alpha$  in fresh tomatoes. *Crop Prot* 38:1–6. <https://doi.org/10.1016/j.cropro.2012.02.016>
- Rhim J-W, Ng PKW (2007) Natural biopolymer-based nanocomposite films for packaging applications. *Crit Rev Food Sci Nutr* 47(4):411–433. <https://doi.org/10.1080/10408390600846366>
- Robert P, Mangavel C, Renard D (2001) Infrared spectroscopy as applied to glycinin film and gel formation kinetics. *Appl Spectrosc* 55(6):781–787

- Rodriguez A, García MA, Campañone LA (2016) Experimental study of the application of edible coatings in pumpkin sticks submitted to osmotic dehydration. *Dry Technol* 34(6):635–644. <https://doi.org/10.1080/07373937.2015.1069325>
- Rojas-Graü MA, Soliva-Fortuny R, Martín-Belloso O (2009) Edible coatings to incorporate active ingredients to fresh-cut fruits: a review. *Trends Food Sci Technol* 20(10):438–447. <https://doi.org/10.1016/j.tifs.2009.05.002>
- Rossi Marquez G, Di Pierro P, Mariniello L, Esposito M, Giosafatto CVL, Porta R (2017) Fresh-cut fruit and vegetable coatings by transglutaminase-crosslinked whey protein/pectin edible films. *LWT Food Sci Technol* 75:124–130. <https://doi.org/10.1016/j.lwt.2016.08.017>
- Rossmann JM (2009) Commercial manufacture of edible films. In: Huber KC, Embuscado ME (eds) *Edible films and coatings for food applications*. Springer, New York, pp 367–390. [https://doi.org/10.1007/978-0-387-92824-1\\_14](https://doi.org/10.1007/978-0-387-92824-1_14)
- Ruiz-Navajas Y, Viuda-Martos M, Barber X, Sendra E, Perez-Alvarez JA, Fernández-López J (2015) Effect of chitosan edible films added with *Thymus moroderi* and *Thymus piperella* essential oil on shelf-life of cooked cured ham. *J Food Sci Technol* 52(10):6493–6501. <https://doi.org/10.1007/s13197-015-1733-3>
- Saberi B, Golding JB, Marques JR, Pristijono P, Chockchaisawasdee S, Scarlett CJ, Stathopoulos CE (2018) Application of biocomposite edible coatings based on pea starch and guar gum on quality, storability and shelf life of ‘Valencia’ oranges. *Postharvest Biol Technol* 137:9–20. <https://doi.org/10.1016/j.postharvbio.2017.11.003>
- Salvia-Trujillo L, Rojas-Graü MA, Soliva-Fortuny R, Martín-Belloso O (2015) Use of antimicrobial nanoemulsions as edible coatings: impact on safety and quality attributes of fresh-cut Fuji apples. *Postharvest Biol Technol* 105:8–16. <https://doi.org/10.1016/j.postharvbio.2015.03.009>
- Sánchez-González L, Vargas M, González-Martínez C, Chiralt A, Cháfer M (2009) Characterization of edible films based on hydroxypropylmethylcellulose and tea tree essential oil. *Food Hydrocoll* 23(8):2102–2109. <https://doi.org/10.1016/j.foodhyd.2009.05.006>
- Santos AR, da Silva AF, Amaral VCS, Ribeiro AB, de Abreu Filho BA, Mikcha JMG (2016) Application of edible coating with starch and carvacrol in minimally processed pumpkin. *J Food Sci Technol* 53(4):1975–1983. <https://doi.org/10.1007/s13197-016-2171-6>
- Sarengaowa HW, Jiang A, Xiu Z, Feng K (2018) Effect of thyme oil–alginate-based coating on quality and microbial safety of fresh-cut apples. *J Sci Food Agric* 98(6):2302–2311. <https://doi.org/10.1002/jsfa.8720>
- Shahbazi Y (2018) Characterization of nanocomposite films based on chitosan and carboxymethylcellulose containing *Ziziphora clinopodioides* essential oil and methanolic *Ficus carica* extract. *J Food Process Preserv* 42(2):e13444. <https://doi.org/10.1111/jfpp.13444>
- Shen XL, Wu JM, Chen Y, Zhao G (2010) Antimicrobial and physical properties of sweet potato starch films incorporated with potassium sorbate or chitosan. *Food Hydrocoll* 24(4):285–290. <https://doi.org/10.1016/j.foodhyd.2009.10.003>
- Shin YJ, Song HY, Seo YB, Song KB (2012) Preparation of red algae film containing grapefruit seed extract and application for the packaging of cheese and bacon. *Food Sci Biotechnol* 21(1):225–231. <https://doi.org/10.1007/s10068-012-0029-x>
- Shukla R, Cheryan M (2001) Zein: the industrial protein from corn. *Ind Crop Prod* 13(3):171–192. [https://doi.org/10.1016/S0926-6690\(00\)00064-9](https://doi.org/10.1016/S0926-6690(00)00064-9)
- Siew DCW, Heilmann C, Eastaer AJ, Cooney RP (1999) Solution and film properties of sodium caseinate/glycerol and sodium caseinate/polyethylene glycol edible coating systems. *J Agric Food Chem* 47(8):3432–3440. <https://doi.org/10.1021/jf9806311>
- Silva KS, Mauro MA, Gonçalves MP, Rocha CMR (2016) Synergistic interactions of locust bean gum with whey proteins: effect on physicochemical and microstructural properties of whey protein-based films. *Food Hydrocoll* 54:179–188. <https://doi.org/10.1016/j.foodhyd.2015.09.028>
- Siracusa V, Rocculi P, Romani S, Rosa MD (2008) Biodegradable polymers for food packaging: a review. *Trends Food Sci Technol* 19(12):634–643. <https://doi.org/10.1016/j.tifs.2008.07.003>

- Soares NMF, Oliveira MSG, Vicente AA (2015) Effects of glazing and chitosan-based coating application on frozen salmon preservation during six-month storage in industrial freezing chambers. *LWT Food Sci Technol* 61(2):524–531. <https://doi.org/10.1016/j.lwt.2014.12.009>
- Song Y, Zheng Q (2014) Ecomaterials based on food proteins and polysaccharides. *Polym Rev (Philadelphia, PA)* 54(3):514–571. <https://doi.org/10.1080/15583724.2014.887097>
- Song F, Tang D-L, Wang X-L, Wang Y-Z (2011a) Biodegradable soy protein isolate-based materials: a review. *Biomacromolecules* 12(10):3369–3380. <https://doi.org/10.1021/bm200904x>
- Song Y, Liu L, Shen H, You J, Luo Y (2011b) Effect of sodium alginate-based edible coating containing different anti-oxidants on quality and shelf life of refrigerated bream (*Megalobrama amblycephala*). *Food Control* 22(3):608–615. <https://doi.org/10.1016/j.foodcont.2010.10.012>
- Song N-B, Song H-Y, Jo W-S, Song KB (2013) Physical properties of a composite film containing sunflower seed meal protein and its application in packaging smoked duck meat. *J Food Eng* 116(4):789–795. <https://doi.org/10.1016/j.jfoodeng.2013.02.002>
- Song N-B, Lee J-H, Al Mijan M, Song KB (2014) Development of a chicken feather protein film containing clove oil and its application in smoked salmon packaging. *LWT Food Sci Technol* 57(2):453–460. <https://doi.org/10.1016/j.lwt.2014.02.009>
- Song N-B, Lee J-H, Song KB (2015) Preparation of perilla seed meal protein composite films containing various essential oils and their application in sausage packaging. *J Korean Soc Appl Biol Chem* 58(1):83–90. <https://doi.org/10.1007/s13765-015-0031-0>
- Sothornvit R, Krochta JM (2005) Plasticizers in edible films and coatings. In: Han JH (ed) *Innovations in food packaging*. Academic Press, London, pp 403–433. <https://doi.org/10.1016/B978-012311632-1/50055-3>
- Sothornvit R, Pitak N (2007) Oxygen permeability and mechanical properties of banana films. *Food Res Int* 40(3):365–370. <https://doi.org/10.1016/j.foodres.2006.10.010>
- Souza MP, Vaz AFM, Cerqueira MA, Texeira JA, Vicente AA, Carneiro-da-Cunha MG (2015) Effect of an edible nanomultilayer coating by electrostatic self-assembly on the shelf life of fresh-cut mangoes. *Food Bioprocess Technol* 8(3):647–654. <https://doi.org/10.1007/s11947-014-1436-1>
- Subirade M, Kelly I, Guéguen J, Pérolet M (1998) Molecular basis of film formation from a soybean protein: comparison between the conformation of glycinin in aqueous solution and in films. *Int J Biol Macromol* 23(4):241–249. [https://doi.org/10.1016/S0141-8130\(98\)00052-X](https://doi.org/10.1016/S0141-8130(98)00052-X)
- Sutherland IW (1998) Novel and established applications of microbial polysaccharides. *Trends Biotechnol* 16(1):41–46. [https://doi.org/10.1016/S0167-7799\(97\)01139-6](https://doi.org/10.1016/S0167-7799(97)01139-6)
- Szabó B, Süvegh K, Zelkó R (2012) Real time positron annihilation lifetime spectroscopy for the detection of the hydrocolloid gel-film transition of polymers. *Polym Test* 31(4):546–549. <https://doi.org/10.1016/j.polymertesting.2012.02.004>
- Tomadoni B, Moreira MR, Pereda M, Ponce AG (2018) Gellan-based coatings incorporated with natural antimicrobials in fresh-cut strawberries: microbiological and sensory evaluation through refrigerated storage. *LWT Food Sci Technol* 97:384–389. <https://doi.org/10.1016/j.lwt.2018.07.029>
- Treviño-Garza MZ, García S, del Socorro Flores-González M, Arévalo-Niño K (2015) Edible active coatings based on pectin, pullulan, and chitosan increase quality and shelf life of strawberries (*Fragaria ananassa*). *J Food Sci* 80(8):M1823–M1830. <https://doi.org/10.1111/1750-3841.12938>
- Tulamandi S, Rangarajan V, Rizvi SSH, Singhal RS, Chattopadhyay SK, Saha NC (2016) A biodegradable and edible packaging film based on papaya puree, gelatin, and defatted soy protein. *Food Packag Shelf Life* 10:60–71. <https://doi.org/10.1016/j.fpsl.2016.10.007>
- Ünalın İÜ, Arcan I, Korel F, Yemencioğlu A (2013) Application of active zein-based films with controlled release properties to control *Listeria monocytogenes* growth and lipid oxidation in fresh Kashar cheese. *Innov Food Sci Emerg Technol* 20:208–214. <https://doi.org/10.1016/j.ifset.2013.08.004>

- Ustunol Z (2009) Edible films and coatings for meat and poultry. In: Huber KC, Embuscado ME (eds) *Edible films and coatings for food applications*. Springer, New York, pp 245–268. [https://doi.org/10.1007/978-0-387-92824-1\\_8](https://doi.org/10.1007/978-0-387-92824-1_8)
- Valencia-Chamorro SA, Palou L, del Río MA, Pérez-Gago MB (2011) Antimicrobial edible films and coatings for fresh and minimally processed fruits and vegetables: a review. *Crit Rev Food Sci Nutr* 51(9):872–900. <https://doi.org/10.1080/10408398.2010.485705>
- Viebke C, Al-Assaf S, Phillips GO (2014) Food hydrocolloids and health claims. *Bioact Carbohydr Diet Fibre* 4(2):101–114. <https://doi.org/10.1016/j.bcdf.2014.06.006>
- Vieira MGA, da Silva MA, dos Santos LO, Beppu MM (2011) Natural-based plasticizers and biopolymer films: a review. *Eur Polym J* 47(3):254–263. <https://doi.org/10.1016/j.eurpolymj.2010.12.011>
- Wang S, Lu A, Zhang L (2016) Recent advances in regenerated cellulose materials. *Prog Polym Sci* 53:169–206. <https://doi.org/10.1016/j.progpolymsci.2015.07.003>
- Watanabe A, Morita S, Kokot S, Matsubara M, Fukai K, Ozaki Y (2006) Drying process of microcrystalline cellulose studied by attenuated total reflection IR spectroscopy with two-dimensional correlation spectroscopy and principal component analysis. *J Mol Struct* 799(1):102–110. <https://doi.org/10.1016/j.molstruc.2006.03.018>
- Wieser H (2007) Chemistry of gluten proteins. *Food Microbiol* 24(2):115–119. <https://doi.org/10.1016/j.fm.2006.07.004>
- Xiao Q, Lim L-T, Tong Q (2012) Properties of pullulan-based blend films as affected by alginate content and relative humidity. *Carbohydr Polym* 87(1):227–234. <https://doi.org/10.1016/j.carbpol.2011.07.040>
- Xiao Q, Gu X, Tan S (2014a) Drying process of sodium alginate films studied by two-dimensional correlation ATR-FTIR spectroscopy. *Food Chem* 164:179–184. <https://doi.org/10.1016/j.foodchem.2014.05.044>
- Xiao Q, Tong Q, Lim L-T (2014b) Drying process of pullulan edible films forming solutions studied by ATR-FTIR with two-dimensional correlation spectroscopy. *Food Chem* 150:267–273. <https://doi.org/10.1016/j.foodchem.2013.10.122>
- Xiao Q, Lu K, Tong Q, Liu C (2015) Barrier properties and microstructure of pullulan–alginate-based films. *J Food Process Eng* 38(2):155–161. <https://doi.org/10.1111/jfpe.12151>
- Yadav M, Rhee KY, Park SJ (2014) Synthesis and characterization of graphene oxide/carboxymethylcellulose/alginate composite blend films. *Carbohydr Polym* 110:18–25. <https://doi.org/10.1016/j.carbpol.2014.03.037>
- Yang L, Paulson AT (2000) Effects of lipids on mechanical and moisture barrier properties of edible gellan film. *Food Res Int* 33(7):571–578. [https://doi.org/10.1016/S0963-9969\(00\)00093-4](https://doi.org/10.1016/S0963-9969(00)00093-4)
- Yang H, Wen X, Guo S, Chen M, Jiang A, Lai L-S (2015) Physical, antioxidant and structural characterization of blend films based on hsian-tsao gum (HG) and casein (CAS). *Carbohydr Polym* 134:222–229. <https://doi.org/10.1016/j.carbpol.2015.07.021>
- Yang H-J, Lee J-H, Won M, Song KB (2016) Antioxidant activities of distiller dried grains with solubles as protein films containing tea extracts and their application in the packaging of pork meat. *Food Chem* 196:174–179. <https://doi.org/10.1016/j.foodchem.2015.09.020>

# Chapter 9

## Self-assembling Properties



Huiyan Zeng

**Abstract** A simplistic view of food is that food molecules are assembled into hierarchical structures. As the two main components in foods, the self-assembling properties of food proteins and polysaccharides determine the nutritional value, texture, appearance, taste, odour, and shelf-life of foods. In this chapter efforts are first made to provide an overview of the concepts, mechanisms, and forces of self-assembly in a broad context, followed by the specific discussion of the self-assembly of food proteins and polysaccharides. The advancements of the self-assembled nanostructures with various morphologies and functionalities are summarized and discussed to provide a guideline for designing desired food structures and broadening the applications of food proteins and polysaccharides. These self-assemblies may also benefit the health of the consumer, when considering their journey in the body, i.e. the disassembly and reassembly processes. We hope that a better understanding of the self-assembly rules of food proteins and polysaccharides will spark food scientists to develop novel functional foods to meet future consumer demands.

**Keywords** Self-assembly · Proteins · Polysaccharides · Nanostructures · Molecular forces

### 1 Introduction

Self-assembly is a ubiquitous process throughout nature and technology (Whitesides and Boncheva 2002; Whitesides and Grzybowski 2002; Mendes et al. 2013). Nature uses specific self-assembly of molecules to organize elaborate structures that possess unique biological functions (Luo et al. 2016). From ordered protein aggregates (e.g., viral capsids, collagen and actin filaments, flagella), topologically programmed nucleic acids (e.g., DNA duplexes, RNA triplexes), to complicated nucleosomes

---

H. Zeng (✉)  
University of Strasbourg, CNRS, Strasbourg, France  
e-mail: [huiyan.zeng@ics-cnrs.unistra.fr](mailto:huiyan.zeng@ics-cnrs.unistra.fr)



and ribosomes, these self-assembled structures could perform a number of functions, such as genome packaging, structural support, force generation, and information storage and transmission (Goodsell and Olson 2000; Saenger 2008; Luo et al. 2016). An in-depth understanding of molecular self-assembly is important not only to reveal the mechanisms of these beneficial biological processes, but also to provide valuable treatments for human diseases, such as the neurodegenerative diseases that are caused by abnormal protein self-assembly (Dobson 2003; Chiti and Dobson 2006). Self-assembly is also in the forefront of biotechnology and nanotechnology, as it provides an excellent tool to build a broad of complex architectures that cannot be easily achieved by other methods (Lee 2007).

Self-assembly is not a new concept in the food sector, and is omnipresent in both natural and processed foods. Typical examples include the formation of casein micelles in milk, oil-bodies in seeds and starch spherulites in plants, and the gelation of pectins in jelly, micelles in yogurt and soy proteins in tofu (Dickinson and Leser 2007; Ravichandran 2010; Sagalowicz et al. 2017). Two food components, protein and polysaccharide, are the main self-assembly units in the foodstuffs. The assembly of food proteins and polysaccharides has attracted much attention over the past two decades, mainly due to the excellent tech-functionalities of the resultant nanostructures, such as the assembled nanofibrils that form transparent hydrogels at low concentration and room temperature, aggregates that stabilize emulsions and foams, and nanoparticles that deliver drugs and nutrients (Veerman et al. 2003; Kroes-Nijboer et al. 2012; Yao et al. 2015; Hu et al. 2019). In addition, self-assembly is correlated to food texture, taste, and appearance. For instance, the beverage appearance is greatly marred by the self-assembly-induced precipitation. More importantly, as mentioned above, the hierarchical structure of biopolymers is directly linked to their unique biological functions. As such, the elaborate structures generated from the self-assembly of proteins and polysaccharides may bring specific nutritional values or functions to the consumer. All these examples point out that food scientists should have a comprehensive understanding of the self-assembly of proteins and polysaccharides. In this chapter, efforts are made to provide the concepts, mechanisms, and molecular forces for the self-assembly of food proteins and polysaccharides, to summarize and discuss the assembled nanostructures in the food sector, as well as to explain how the self-assembly affects food quality and functions.

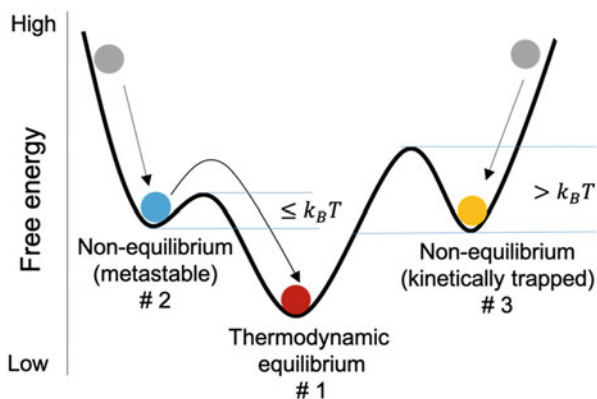
## 2 Physical Aspects of Self-assembly

### 2.1 *Self-assembly*

Self-assembly is a special kind of aggregation whereby this process occurs toward the state of minimum free energy, mainly through non-covalent interactions, such as electrostatic interactions, van der Waals interactions, hydrogen bonding, hydrophobic interactions, metal coordination bonds, and steric and depletion forces (Lindoy and Atkinson 2000; Lee 2007; Ninham and Nostro 2010; Jiang et al. 2011; Padua



**Fig. 9.1** Schematic illustration of Gibbs free energy landscape of the different thermodynamic states in self-assembly process. Adapted with permission from Sorrenti et al. (2017). Copyright 2017 RSC



and Nonthanum 2012; Billon and Borisov 2016; Sundararajan 2016; Wang et al. 2016; Sorrenti et al. 2017). Despite the entropy loss as the ordering of self-assembly building units, the self-assembly is energetically favourable because the entropic cost is greatly offset by the enthalpy gained from the non-covalent interactions (Rajagopal and Schneider 2004; Padua and Nonthanum 2012).

From the thermodynamic point of view, self-assembly is a process that minimizes Gibbs free energy. In general, it brings the entity closer to a thermodynamic equilibrium state (#1 in Fig. 9.1) (Whitesides and Boncheva 2002; Roy et al. 2016; Sorrenti et al. 2017). Many involved intermolecular interactions, as mentioned above, enable the system to explore different configurations (i.e. walk along the energy landscape), and to find the most stable one (Sorrenti et al. 2017). In some cases, the self-assembly process may cause metastable or kinetically trapped states (i.e. non-equilibrium states, #2 and #3 in Fig. 9.1) (Sorrenti et al. 2017). Due to the low energy barrier, the metastable structures will eventually evolve into the thermodynamic equilibrium state, even without any intervention. In contrast, the system will be kinetically trapped in state #3 because of the high energy barrier, if there is no intervention (Wang et al. 2016; Sorrenti et al. 2017). This means that the outcome of the self-assembly process, e.g. the morphology of assembled nanostructures, strongly depends on the experimental parameters and protocols (Sorrenti et al. 2017). In other words, the desired pathway can be rationally selected by appropriate preparation methodologies, resulting in the assemblies with targeted features starting from the same building blocks. This is crucial to develop materials with optimized functionalities (Sorrenti et al. 2017).

From the force point of view, self-assembly can be defined as a delicate balance of the attractive (*driving force*) and repulsive (*opposition force*) intermolecular forces (Whitesides and Boncheva 2002; Lee 2007; Kedracki 2015; Billon and Borisov 2016; Roy et al. 2016). The driving forces bring the self-assembly units together, while opposition forces are in balance with the driving forces (Lee 2007; Kedracki 2015; Billon and Borisov 2016). Besides, many biological and bio-mimetic systems show a unique directionality during self-assembly processes, as well as in many food systems, e.g. the formation of protein nanofibrils and

**Table 9.1** Common forces in self-assembly

Attractive driving forces	Repulsive opposition forces	Directional forces
Electrostatic attraction	Electrostatic repulsion	Electrostatic interaction
Van der Waals interaction	Steric repulsion	Hydrogen bonding
Hydrophobic interaction		Coordination bond
Hydrogen bonding		$\pi$ - $\pi$ stacking
Depletion force		
Coordination bond		
$\pi$ - $\pi$ stacking		

nanotubes, and polysaccharides helices (Graveland-Bikker and de Kruif 2006; Lee 2007; Cao and Mezzenga 2019; Fittolani et al. 2019). The force responsible for these directional self-assembly processes is known as *directional force* or *functional force* (Lee 2007; Kedracki 2015; Billon and Borisov 2016). Hydrogen bond, coordination bond, electrostatic interaction, and  $\pi$ - $\pi$  stacking are the most common directional forces (Lee 2007; Wang et al. 2016). These forces can be a part of a driving or opposition force, but sometimes act exclusively as directional force (Lee 2007).

Therefore, self-assembly is an equilibrium of three classes of forces: driving, opposition, and directional forces, as displayed in Table 9.1 (Lee 2007). The self-assembly process is quite random when only the first two classes of forces are in action. Most of the colloidal self-assembly processes belong to this category. When the third class of forces is involved with the first two classes of forces, the self-assembly processes are directional and often functional, leading to the formation of highly ordered or specific functional structures. In engineering, these three classes of forces can be greatly affected by a number of external parameters, such as pH, ionic strength and type, temperature, solvent type, mechanical treatments (pressure, shear, extension, sonication), or chemical treatments (Lee 2007). Therefore, self-assembly can be triggered, altered, or terminated by controlling these external parameters, thereby managing the desired assembly and the assembled nanostructures.

## 2.2 Forces in Self-assembly

In the self-assembly process, whether it occurs at an atomic-, molecular-, colloidal-, or macro-length scale, the non-covalent forces rather than the chemical forces play vital roles (Lee 2007). Even though these non-covalent forces are weak individually, a large number of such forces in the final can be significant. We first briefly illustrate these forces and then give an example of a combination of two forces—DLVO (Derjaguin–Landau–Verwey–Overbeek) theory.

### 2.2.1 Electrostatic Interaction

Electrostatic interaction appears universally for charged objects. In nonpolar media (e.g. vacuum, air, organic nonpolar liquids), the electrostatic interaction is governed by the Coulomb's law (Lee 2007; Sundararajan 2016). The interaction potential  $U(x)$  between two charges of  $Q_1$  and  $Q_2$  is expressed as:  $U(x) = \frac{Q_1 Q_2}{4\pi\epsilon_0\epsilon x} = \frac{z_1 z_2 e^2}{4\pi\epsilon_0\epsilon x}$ , where  $z_1$  and  $z_2$  are the ionic valence of each charge,  $e$  is the elementary charge,  $\epsilon_0$  is the dielectric permittivity of vacuum,  $\epsilon$  is the relative dielectric permittivity, and  $x$  is the distance between two charges (Lee 2007). Due to  $U(x) \sim x^{-1}$ , the electrostatic interactions in ion-free media can extend over long distance. In polar media (e.g. water, polar organic liquids), free ions in solutions are able to move to oppositely charged interfaces, resulting in the formation of a kind of molecular condenser, known as electrical double layer (Tadros 2013). The thickness of the double layer (i.e. screening length or Debye length) decreases with the increase in free ion concentration, written as  $\kappa^{-1} = \sqrt{\frac{\epsilon_0 \epsilon k_B T}{2 \times 10^3 N_A e^2 I}}$ , here  $I$  is the ionic strength (mol/L),  $k_B$  is the Boltzmann constant,  $T$  is the absolute temperature,  $N_A$  is the Avogadro number. The range of the electrostatic forces is then typically:  $\kappa^{-1} = 10$  nm (at  $I = 1$  mM), 3 nm (at 10 mM), 0.8 nm (at 150 mM), and 0.3 nm (at 1000 mM) at room temperature (Ninham and Nostro 2010). Different from the long-range electrostatic forces in nonpolar media, the electrostatic forces between objects in polar media become short-ranged, or even can be eliminated by increasing salt content due to the screening effect (Ninham and Nostro 2010; Tadros 2013). Therefore, the strength of electrostatic interactions is largely dependent on the solution ionic strength and pH. The flexibility of polymer chain and the charge distribution in polymer chain are also significant factors (Cao et al. 2016a).

### 2.2.2 Van der Waals Interaction

Van der Waals force is generated by dipole or induced-dipole interaction at the atomic and molecular levels, including three contributions: Keesom interaction (dipole–dipole), Debye interaction (dipole–induced dipole), and London interaction (instantaneous induced dipole–induced dipole) (Lindoy and Atkinson 2000; Parsegian 2005; Lee 2007; Ninham and Nostro 2010). All these interactions have a scaling of  $U(x) \sim x^{-6}$ , thus the van der Waals force quickly vanishes at long distances between interacting atoms (Lee 2007; Ninham and Nostro 2010). The van der Waals force between two atoms is weak, but its total collective contribution to molecular interactions can be substantial (Lindoy and Atkinson 2000; Li and Alessandra 2018). For instance, for two identical interacting colloids with a radius of  $R$ , the van der Waals interaction potential is  $U(x) = -\frac{AR}{12x}$ , here  $A$  is Hamaker constant ( $A \approx 3k_B T$  for proteins) (Hamaker 1937; Parsegian 2005; Lee 2007; Israelachvili 2011). Thus, the interaction between two protein monomers could be evident ( $U(x) = k_B T$ ) by considering  $R = 4$  nm and  $x = 1$  nm.

### 2.2.3 Hydrogen Bonding

Hydrogen bond is an attractive force between a hydrogen atom which is covalently bound to an electronegative atom (X-H, donor) and another electronegative atom bearing a lone pair of electrons (Y, acceptor), depicted as X-H...Y (Lindoy and Atkinson 2000; Lee 2007; Ninham and Nostro 2010; Sundararajan 2016). The common hydrogen bond donors include C-H, O-H, N-H, P-H, F-H, Cl-H, Br-H, I-H, while N, O, P, S, F, Cl, Br, I, alkenes, alkynes, aromatic  $\pi$ -clouds are the common acceptors (Lindoy and Atkinson 2000). Hydrogen bond is considered to be a quite strong and directional interaction (Lee 2007). It is generally stronger than the van der Waals interaction, but weaker than covalent and ionic bonds (Lee 2007). The directionality of hydrogen bond results from the hydrogen bond-capable molecules always interacting only through specific sites (Lee 2007). It is a key player in the assembly of protein and polysaccharide systems as almost all constituent units in protein and polysaccharide are capable of forming hydrogen bonding.

### 2.2.4 Hydrophobic Interaction

Hydrophobic interaction describes the energetic preference of nonpolar objects to interact with other nonpolar objects in the presence of aqueous solution (Motiejunas and Wade 2006). This short-range attractive interaction is mainly an entropic effect, but also affected by enthalpy contribution (Motiejunas and Wade 2006; Lee 2007). When a nonpolar molecule is present in the aqueous solution, a highly ordered hydrogen bond network around the nonpolar molecule is formed to minimize the disruption of this nonpolar object, i.e. the formation of a structured water “cage” (Schaeffer 2008). In the process of nonpolar molecular association, the nonpolar molecule system obviously loses its entropy, but the water system gains a significant increase of entropy that overcomes the entropy loss of nonpolar molecules (i.e. total  $\Delta S$  is positive) (Lee 2007; Schaeffer 2008). Moreover, the enthalpy is increased as some of hydrogen bonds that form the “cage” are broken in the association process, but this effect is limited compared to the entropic effect (Lee 2007; Schaeffer 2008). Therefore, the Gibbs free energy change is negative ( $\Delta G = \Delta H - T\Delta S$ ,  $\Delta S =$  large positive value,  $\Delta H =$  small positive value), implying that the hydrophobic effect is spontaneous. Similar to van der Waals forces, hydrophobic interactions are individually weak, but the total contribution to molecular interactions can be significant (Schaeffer 2008). The strength of hydrophobic interaction is associated with the solubility of the nonpolar molecules as well as the quality of the steric match between the molecules (Schaeffer 2008). Most proteins (possessing nonpolar amino acids) and some polysaccharide derivatives (such as MC and HPMC) show a significant hydrophobic character.

### 2.2.5 Steric Repulsion

Steric repulsion is a common force between colloidal particles when water-soluble polymers are tightly adsorbed or grafted onto the surface of colloidal objects (Fig. 9.2a) (Lee 2007). It mainly arises from the loss of configuration entropy when two polymer layers are overlapped (Cooper 2014). Steric repulsion is a long-range force and can reach up to  $\sim 10R_g$  ( $R_g$  is the gyration radius of the polymer chain) (Lee 2007). For effective steric repulsion, water-soluble polymers in the diffuse layer must satisfy the following three requirements: firstly, the polymers should be tightly anchored to the colloidal particles; secondly, part of the polymer chain should extend into the bulk solution; thirdly, there is no significant exposure of the colloidal surface (Cooper 2014).

### 2.2.6 Depletion Attraction

Depletion force is the common force for the colloidal particles considering the presence of non-adsorbing polymers (Fig. 9.2b) (Lee 2007; Lekkerkerker and

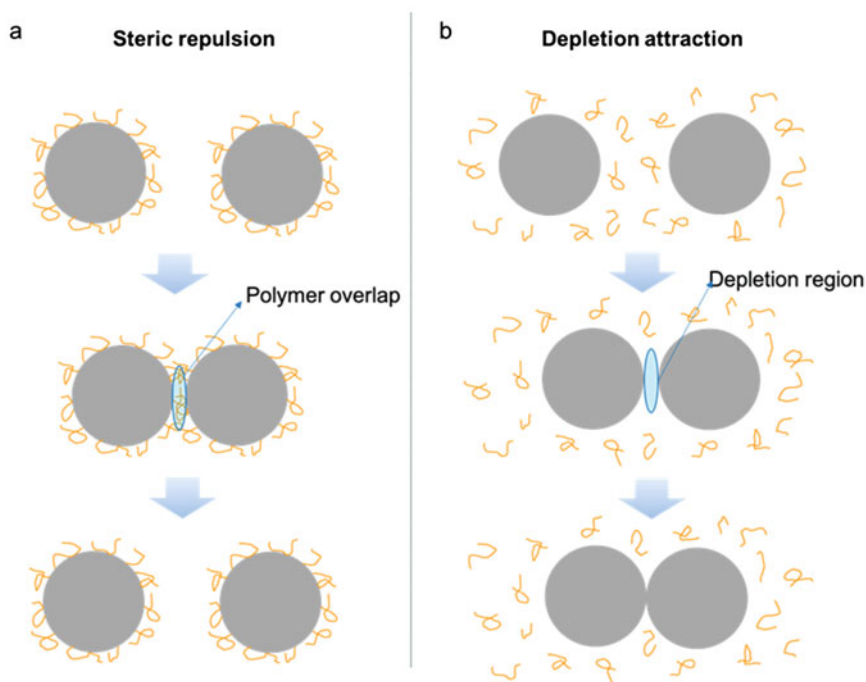


**Fig. 9.2** Schematic illustration of steric repulsion and depletion attraction between two colloidal spheres. (a) Steric repulsion between polymer-adsorbed colloids. (b) Depletion attraction between two colloidal particles in the presence of non-adsorbing polymers or molecules

Tuinier 2011). A depletion region of polymers is generated when the colloidal particles are close enough to each other (smaller than the size of polymers,  $\sim 2R_g$ ), as the polymers are being squeezed out of this region (Lee 2007). The osmotic pressure force that is exerted by the polymers in the outside region (outside of depletion region) exceeds that in the inside region. This, therefore, induces a net attractive force between the colloidal particles (Lee 2007; Lekkerkerker and Tuinier 2011). The depletion force can determine the stability of colloids when there are no other significant attractive forces (Lee 2007). It can be strengthened by increasing polymer concentration and molecular weight (Lee 2007). Colloids with low curvature (e.g. nanorods) experience this attraction more strongly as the depletion attraction scales with the excluded volume of the colloids.

### 2.2.7 DLVO Theory: A Case of the Combination of van der Waals Attraction and Electrostatic Repulsion

The DLVO theory is a useful tool to describe the self-assembly process of charged colloids, which is the combination of two inter-colloidal forces: van der Waals force that acts as the attractive force and electric double-layer interaction as the repulsive force. Their total interaction potential  $U(x)$  can be written as (Adair et al. 2001; Mezzenga and Fischer 2013):

$$U(x) \approx \frac{2\pi\sigma^2 R}{\kappa^2 \epsilon_0 \epsilon} e^{-\kappa x} - \frac{AR}{12x}$$

$\sigma$  and  $R$  are the net surface charge density and radius of colloidal particles, respectively,  $x$  is the separated distance of a pair of colloids. The plots of this equation at different ionic strengths are shown in Fig. 9.3, by considering  $R = 5$  nm,  $\sigma = 20$  mC/m<sup>2</sup>,  $T = 298$  K. The electrostatic force gives a positive term and varies with the solution ionic strength. In contrast, the van der Waals attraction gives a negative term and is independent from ionic strength (Fig. 9.3a) (Adair et al. 2001). The sum of these two forces at different ionic strengths is given in Fig. 9.3b. At low ionic strengths, particles have net repulsion at large and intermediate separations, and the approaching of colloids requires high kinetic energy due to the high energy barrier. Thus, in these cases, colloids are separately suspended in the solution. At high ionic strengths, the energy barrier is lowered and particles can overcome it more easily, leading to the aggregation or self-assembly (Adair et al. 2001).

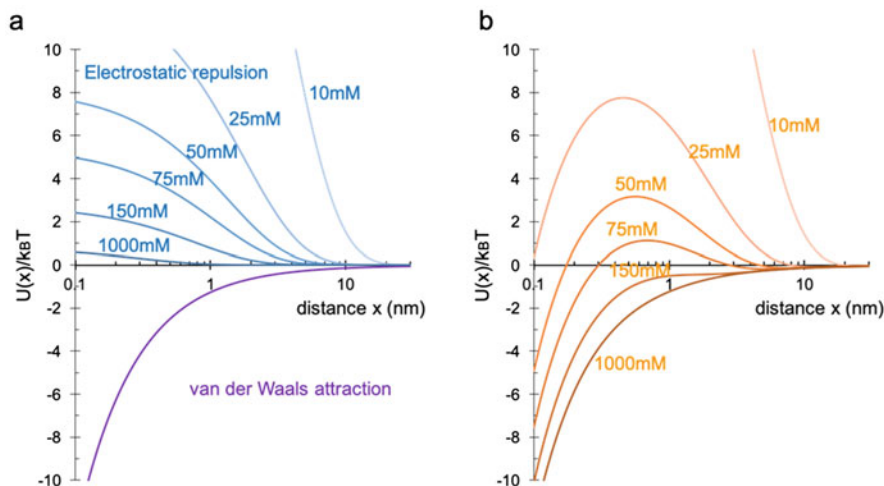


**Fig. 9.3** An example of DLVO interaction potential. (a) Electrostatic repulsion potential versus particle distance  $x$  at different ionic strengths, and van de Waals attraction potential versus particle distance  $x$ . (b) The sum interaction potential of electrostatic and van der Waals forces.  $R = 5$  nm,  $\sigma = 20$  mC/m<sup>2</sup>,  $T = 298$  K are used for the calculation

## 2.3 Self-assembly of Food Proteins and Polysaccharides

### 2.3.1 Protein Self-assembly

Understanding the mechanisms and processes of protein self-assembly is essential to biologists and medical scientists, since it is related to many biological and physiological activities, as mentioned above. The understanding of food protein self-assembly is equally important to food scientists due to a broad range of food-related implications and applications. For instance, protein self-assembly can be harnessed for protein purification through phase separation or crystallization, or can be problematic during storage (Carpenter and Manning 2002; Flickinger 2013; McManus et al. 2016).

Most natural food proteins possess globular or fibrillar conformations (Mezzenga and Fischer 2013; Nicolai 2019). These protein structures result from a combination of the numerous interactions between amino acids, i.e. the self-assembly of polypeptide chain. Depending on the side group, the amino acids in food proteins can be divided into: nonpolar, polar, and ionic, which mainly contribute to hydrophobic interactions, hydrogen bonding, and electrostatic interactions, respectively. In globular conformations, the polypeptide chain is folded into compact spherical shape with most of the nonpolar amino acids buried in the interior, and the polar and ionic amino acids predominately located at the surface (Fig. 9.4a) (Mezzenga and Fischer 2013; Jones 2015; McManus et al. 2016; Cho and Jones 2019). The driving forces for this configuration include the hydrophobic effect as well as other forces, such as hydrogen bonding that contributes to the formation of protein secondary structure

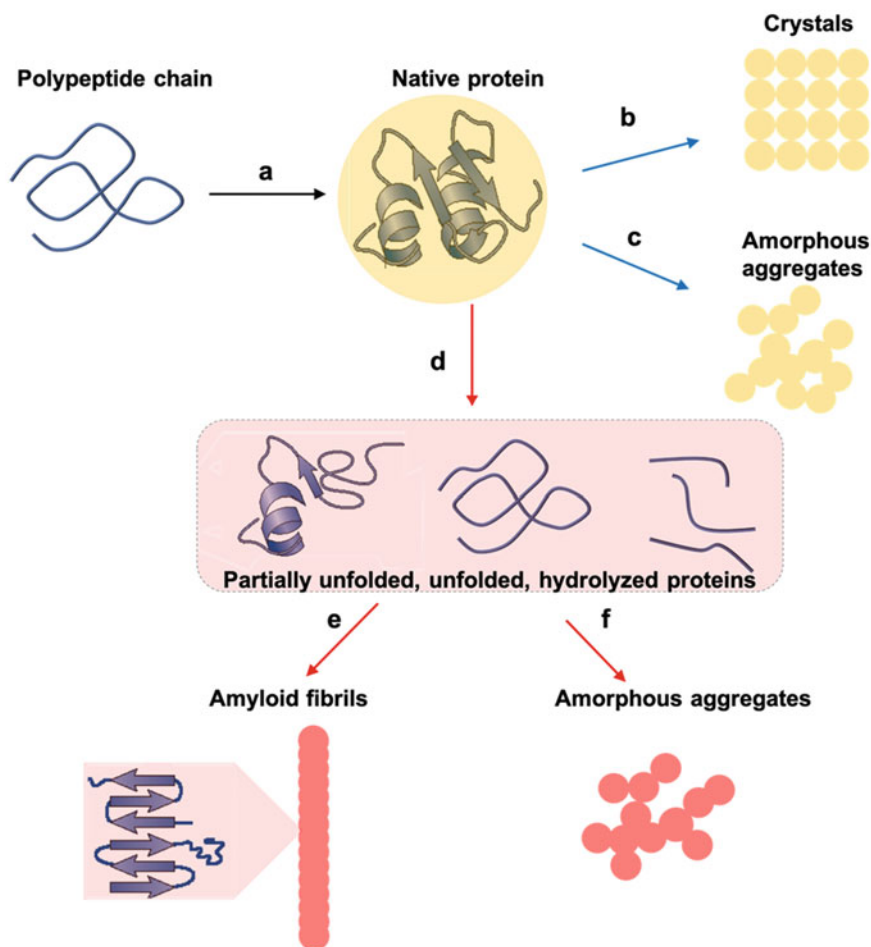


**Fig. 9.4** Schematic illustration of food protein self-assembly and the resultant nanostructures. **(a)** The self-assembly of polypeptide chain into globular proteins. **(b, c)** The self-assembly of natural proteins into crystals **(b)** or amorphous aggregates **(c)**. These processes are often reversible since the protein structure is remained. **(d)** Protein denaturation leads to the (partial) unfolding and and/or hydrolysis of proteins. **(e)** The unfolded and hydrolyzed proteins can further assemble into amyloid fibrils or amorphous aggregates. These processes are often irreversible

( $\alpha$ -helices and  $\beta$ -sheets) (Jones 2015). Indeed, hydrogen bonding is prevalent in proteins by considering all amino acids containing amine- and carbonyl-groups. Fibrous proteins often have specific amino acid sequences that favour twisting of the polypeptide. For example, gelatins are rich in Glycine-X-Y sequence that supports the twisting of gelatin chains with the formation of triple helixes; X and Y are mostly proline and hydroxyl-proline (Russell et al. 2007; Hafidz et al. 2011; Cao et al. 2015; Jones 2015).



Since globular proteins are generally viewed as colloids, a number of models for interpreting colloid self-assembly can be used to understand the self-assembly behaviour of globular proteins. The simplest model is the DLVO model, as discussed above, which could interpret many protein behaviours, such as the aggregation of proteins by adjusting pH or adding salts. However, DLVO cannot explain certain protein behaviour, such as protein crystallization at high salt contents (Piazza 1999; Mezzenga and Fischer 2013). Other studies indicate that the protein aggregation may originate from the presence of depletion forces (Mezzenga and Fischer 2013; McManus et al. 2016). It is worth noting that many models are employed to understand protein self-assembly with varying degree of success, yet no model captures all protein aggregation features (Mezzenga and Fischer 2013). This is possibly caused by the existence of many other forces (e.g. hydrophobic effect, hydrogen bonds, specifically ionic bindings) and effects (e.g., surface charge distributions, molecular recognition) that contribute to the complexity of protein self-assembly (Mezzenga and Fischer 2013). The self-assembly of globular proteins, in native state, can lead to the formation of crystals or amorphous aggregates (Fig. 9.4b and c), and this process is often reversible.

Protein self-assembly could also start from the denatured, unfolded, or hydrolyzed proteins, which is actually more frequently observed in the food systems (Fig. 9.4d). Loss of native structures leads to changes in the capacity of those proteins to interact with each other, and further determine their ability to form supramolecular assemblies (Jones 2015). For instance, the exposure of nonpolar amino acids by unfolding the globular proteins supports the formation of intermolecular forces (Jones 2015; Li et al. 2018). Knowledge of protein characteristics in the chosen environment is essential to the desired assembly, and there are mainly two routes for the protein self-assembly at the denaturation condition: fibrillization and random aggregation, leading to the formation of amyloid fibrils and amorphous aggregates (Fig. 9.4e and f). The most studied condition for triggering this type of self-assembly is heating proteins at various pHs and ionic strengths (van der Linden and Venema 2007; Nicolai and Durand 2013; Jones 2015; Schmitt et al. 2016; Cao and Mezzenga 2019). At pH in the neighbourhood of protein isoelectric point (IEP) or at high ionic strengths, the effective charge of the protein is remarkably suppressed so that amorphous aggregates (i.e. large fractal dimension) generate during thermal treatment, arising from the loss of opposition electrostatic repulsion (right side of Fig. 9.5). As the solution pH leaves from the protein IEP, the effective charge of the protein increases and aggregates become relatively less amorphous (middle of Fig. 9.5). Instead, protein aggregation produces fibrous structures when the pH is significantly far from IEP, since the highly effective charge on the protein surfaces makes them favourable for interactions only among discrete regions on the protein surface (left side of Fig. 9.5). A notable example can be found in  $\beta$ -lactoglobulin protein system. The morphology of protein aggregates remarkably depends on the solution pH: amyloid fibrils and fibrous strands formed at pH 2 and pH 7, respectively (far from  $\beta$ -lactoglobulin IEP); particulates formed at pH 5.2 ( $\approx$  IEP); microgels formed at pH 4.7 and 5.9 (near IEP) (Schmitt et al. 2016).

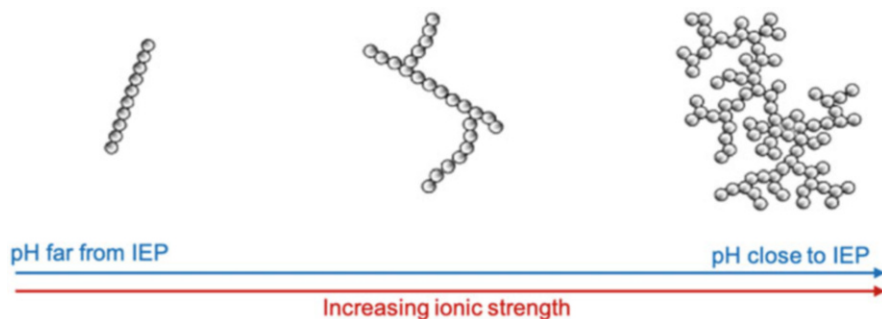


**Fig. 9.5** Schematic representation of the effect of pH and ionic strength on protein self-assembly during heat treatment. Adapted with permission from van der Linden and Venema (2007). Copyright 2007 Elsevier

### 2.3.2 Polysaccharide Self-assembly

Based on the charge nature, polysaccharides can be classified into cationic (chitosan), anionic (alginate, pectin, carrageenan, gellan gum, hyaluronic acid), and neutral (agarose, pullulan, dextran) (Kontogiorgos 2015; Stephen et al. 2016). Despite that most food polysaccharides only consist of 1–3 constituent units, the type of linkages, isomeric forms, esterification, the branching and periodicity of constituent units, and the wide range of molecular weight contribute to their great diversity in structure and property (Kontogiorgos 2015; Stephen et al. 2016). A notable example is that of cellulose and amylose. They have the same repeating unit (glucose), but the different linkage ( $\beta$ -D-(1 $\rightarrow$ 4) in cellulose and  $\alpha$ -D-(1 $\rightarrow$ 4) in amylose), which leads to their extremely different digestion and assembly behaviours. Repulsive interactions in polysaccharide self-assembly often are the steric repulsion and sometimes electrostatic repulsion for charged ones. Attractive forces are the van der Waals interaction, hydrogen bonding, and sometimes the hydrophobic interaction and ionic binding for certain polysaccharides. Hydrogen bonding and ionic binding are the important directional forces in polysaccharide self-assembly.

Similar to food proteins, temperature, pH, and salt are the most common triggers for the self-assembly of food polysaccharides. Either increasing or lowering temperature can induce the self-assembly (Nishinari and Zhang 2004; Stephen et al. 2016). Agaroses, carrageenans, or gellan gums experience the transitions of coil-to-helix and helix-to-super helix in the cooling process, driven by the formation of hydrogen bonding and ionic binding. The helical structures in polysaccharides are still controversial, could be single, double, or triple helices (Fig. 9.6b) (Schefer et al. 2014; Cao et al. 2016b; Stephen et al. 2016; Fittolani et al. 2019). In contrast, methylcellulose and hydroxypropyl methylcellulose are assembled in the heating process, mainly driven by the hydrophobic force. During heating, the solvated cage-like structures (formed through hydrogen bonds between water and cellulose derivatives) are destroyed and thereby hydrophobic regions are exposed, resulting in the

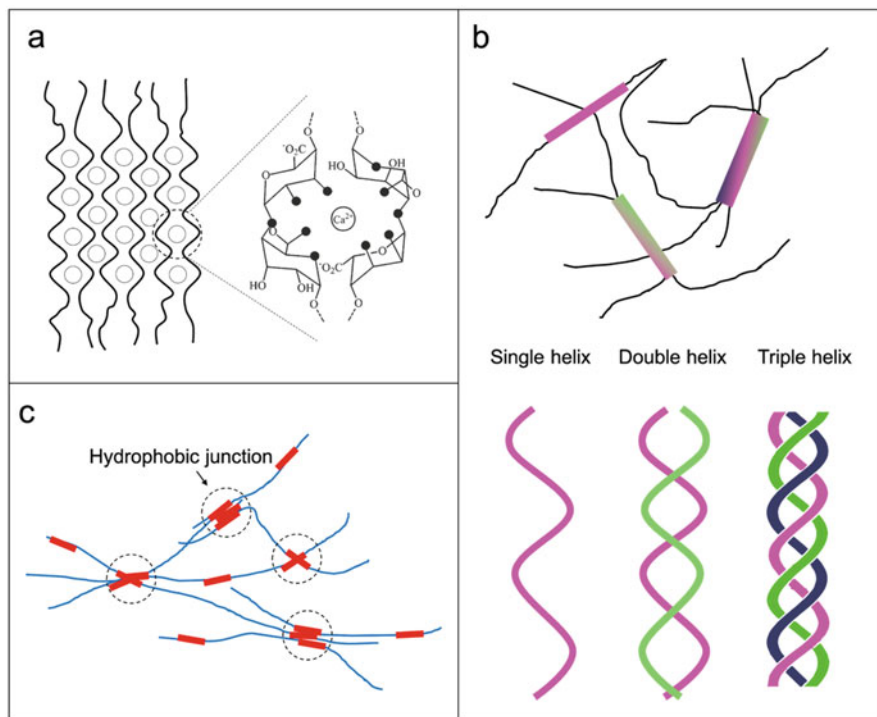


**Fig. 9.6** Typical polysaccharide structures at molecular levels. (a) Left: “egg-box” model of alginate or pectin in the presence of divalent ions, e.g.  $\text{Ca}^{2+}$ ; Right: coordination of  $\text{Ca}^{2+}$  in a cavity created by a pair of guluronate sequences. The open circles represent  $\text{Ca}^{2+}$  ions and the black dots represent the oxygen atoms possibly involved in the coordination with  $\text{Ca}^{2+}$ . Adapted with permission from Fang et al. (2007). Copyright 2007 ACS. (b) Single, double, or triple helical structures in polysaccharides, such as carrageenan (single helix), agarose (double helix), curdlan (triple helix). (c) Hydrophobic association in cellulose derivatives, (e.g. methylcellulose, hydroxypropyl methylcellulose). At relatively high temperatures, the solvated cage-like structures (formed through hydrogen bonds between water and cellulose derivative chains) are destroyed and thereby hydrophobic regions are exposed, causing the formation of hydrophobic junction zones. Adapted with permission from Li et al. (2001). Copyright 2001 ACS

formation of hydrophobic junction zones (Fig. 9.6c) (Li et al. 2001, 2002; Shen et al. 2016).

For ionic polysaccharides, pH and salt not only affect the electrostatic force but also have other important effects. The effect of pH is correlated to the dissociation constant ( $\text{p}K_a$ ). The charge magnitude of ionic polysaccharides depends on the solution pH relative to the  $\text{p}K_a$ . For instance, alginate ( $\text{p}K_a \approx 3.8$ ) is slightly negative (or near neutral) at pH 2 and strongly negative at pH 7, by referring  $\text{pH} - \text{p}K_a = \log_{10}([\text{CO}_2^-]/[\text{CO}_2\text{H}])$ . The protonation of  $\text{COO}^-$  at pH 2 not only weakens the electrostatic repulsion but also enhances the hydrogen bonding due to  $\text{COOH}$  with high hydrogen bond forming ability, resulting in the self-assembly (or gelation) of

alginates at low pH (Draget 2009; Draget et al. 2016). The mechanism for the assembly of chitosan ( $pK_a \approx 6.3$ ) through increasing pH is considered to be similar, i.e. transition of  $NH_3^+$  to  $NH_2$  (Yi et al. 2005; Pillai et al. 2009; Zargar et al. 2015; Shen et al. 2016). Salt plays a vital role in the electrostatic force via altering the Debye screening length, as discussed above. More importantly, some specifically ionic bindings make polysaccharides with a complex self-assembly behaviour. For example, multivalent cations, e.g.  $Ca^{2+}$ , specifically bind to alginate or pectin, causing the formation of an ordered “egg-box” structure (Fig. 9.6a) (Fang et al. 2007). It should be noted that, different from protein systems, the assembly induced by temperature, pH, or salt is often reversible for polysaccharide systems.

### 3 Self-assembled Nanostructures

Nanostructured materials are the forefront of many fields due to their unique and outstanding properties, and self-assembly is broadly considered as a promising approach to produce these nanostructures. In principle, the nanostructures generated from food proteins and polysaccharides could further enrich the versatility of nanostructured materials in terms of category and function due to their nutritional value, biodegradability, biocompatibility, safety, etc. Here we summarize the food protein and polysaccharide nanostructures with different morphologies, and their formation conditions and potential applications.

#### 3.1 Protein Self-assembled Nanostructures

Under certain conditions, proteins can self-assemble into a variety of structures with different sizes and morphologies, including crystals, nanofilaments, nanotubes, and amorphous aggregates. In this part, we will first introduce a naturally assembled protein nanostructure and then discuss the nanostructures produced by the processing.

##### 3.1.1 Natural Self-assembled Nanostructure—Casein Micelles

Milks contain large quantities of protein-based nanostructures, known as casein micelles. These colloidal particles, typically have an average diameter of  $\sim 200$  nm, are naturally assembled from the phosphoproteins—caseins ( $\alpha_{s1}$ -casein,  $\alpha_{s2}$ -casein,  $\beta$ -casein,  $\kappa$ -casein) and calcium phosphate, driven by the forces of hydrogen bonding, ionic bridging, hydrophobic interaction, electrostatic interaction, and van der Waals attraction (Dalgleish 2011; de Kruif et al. 2012; Jones 2015). Within casein micelles, the balance of the hydrophobic and hydrophilic amino acids not only allows formation of this micelle nanostructure, but also helps in retaining the

individual character of the micelles (i.e. adequately stable as a suspension) (Kontogiorgos 2015). Although the composition and forces in casein micelles are well understood, their structure, especially the interior structure, remains a matter of debate (Dalglish 2011; Mezzenga and Fischer 2013). Various models have been proposed, but it is generally agreed that calcium phosphate is responsible for forming salt bridges between phosphoserine residues on the  $\beta$ - and  $\alpha$ -caseins, and  $\kappa$ -casein is predominantly distributed on the micelle surface and contributes to stabilizing micelles (Mezzenga and Fischer 2013; Cho and Jones 2019). Although it is not possible to duplicate the exact assembly of the casein micelles, casein proteins have been demonstrated to assemble micelles-like structures by reincorporating calcium phosphate and citrate ions at milk-relevant contents (Jones 2015). Besides, many methods are available to disassemble and reassemble natural casein micelles, which are useful to create novel nanostructures for controlled delivery purposes (Jones 2015; Cho and Jones 2019).

### 3.1.2 Amorphous Aggregates

Amorphous protein aggregates could be generated from the self-assembly of native proteins (i.e. in a mild condition without the protein denaturation process). This type of aggregates is often reversible due to the lack of significant changes in protein structures and the absence of strong forces. For instance, the clusters formed in high concentration lysozyme protein solution are reversible; the clusters are disassembled by lowering protein concentration (Lu et al. 2008). In contrast, most amorphous aggregates in the food sector are produced by protein unfolding and then assembly, which are generally irreversible because of the significant changes in protein structures and the significant aggregation interactions between proteins. The formation of stable suspensions of amorphous aggregates requires an intermediate surface charge and low protein concentration, otherwise leading to the formation of precipitates or bulk gels (Nicolai and Durand 2013; Schmitt et al. 2016). In most cases, it is not straightforward to form homogeneous nanoaggregates by simply heating globular protein solution. Particularly, Schmitt et al. (Schmitt et al. 2009) found that stable suspensions of roughly spherical protein nanoparticles (with a hydrodynamic radius of  $\sim 200$  nm) can be formed by heating  $\beta$ -lactoglobulin without added salt in two narrow pH ranges (around pH 4.6 and around pH 5.8).

### 3.1.3 Nanofilaments

The formation of filamentous nanostructures needs more specified and stringent conditions than amorphous aggregates. Typically, two common filamentous structures could be produced from food proteins: strand-like objects formed when heating proteins at neutral pH and low salt content; amyloid fibrils formed when heating proteins at low pH and low salt content. These filamentous structures are the promising materials owing to their unique properties. For instance, the high aspect

ratio allows them to form gels or significantly increase solution viscosity at very low protein concentration (Veerman et al. 2003; Kroes-Nijboer et al. 2012).

In the formation of strand-like objects, the intermolecular interactions at certain sites (e.g. disulphide bonds) bring protein monomers together and lead to directional growth, where electrostatic repulsion is in balance with these forces to prevent structure collapse (van der Linden and Venema 2007; Nicolai and Durand 2013; Nicolai et al. 2011). The strands are structurally less ordered than amyloid fibrils due to the fact that the protein chains are confined (low unfolding and hydrolysis extent) (Nicolai and Durand 2013). The resultant strands at neutral pH often have diameters less than 10 nm and lengths between tens and hundreds of nanometres (Nicolai and Durand 2013).

Amyloid fibrils are characteristic with a cross- $\beta$  structure in which continuous hydrogen-bonded  $\beta$ -sheets run along the fibrils (McManus et al. 2016; Chiti and Dobson 2017; Eisenberg and Sawaya 2017). These nanofibrils formed from different proteins are similar: unbranched filamentous structures with a few nanometres in diameter and up to several micrometres in length (McManus et al. 2016; Chiti and Dobson 2017; Eisenberg and Sawaya 2017). Heating proteins at low pH and low ionic strength is often used to prepare food protein amyloid fibrils. In this procedure, the protein monomers are first hydrolyzed and unfolded, and then assembled into amyloid fibrils. Hydrophobic interactions, hydrogen bonding, and sometimes  $\pi$ - $\pi$  stacking are the dominant attractive forces for holding the protein nanofibril structures. In contrast, electrostatic repulsion is the main opposition force to prevent the structure collapse. Indeed, the final fibril morphology is largely affected by the solution ionic strength, since it modulates the strength of electrostatic interactions. Long semiflexible fibrils are generated at low ionic strength, whereas short wormlike fibrils prevail at higher ionic strength (Loveday et al. 2010, 2017; Cao and Mezzenga 2019). This arises from the fact that the strong electrostatic repulsion at low ionic strength leads to the attachment of building blocks to the growing fibrils in a well-ordered arrangement, whereas at higher ionic strength the growth of fibrils is more haphazard and chaotic (Loveday et al. 2017; Cao and Mezzenga 2019). Other factors, such as pH, temperature, protein concentration, stirring speed, co-solvent, and some chemicals could also greatly affect the protein fibrillization process and the final nanofibril morphology (Cao and Mezzenga 2019).

### 3.1.4 Nanotubes

Nanotube is one of the most promising materials from the last century. Carbon nanotubes could be used to build probes and sensors, to store energy and hydrogen gas, and to serve as field emission displays and radiation sources, etc. (Baughman et al. 2002; de Volder et al. 2013). Peptide nanotubes are also of immense interest due to their diverse bio-functionalities which lead to numerous potential applications in nanotechnology as well as in biomedicine (Scanlon and Aggeli 2008; Hamley 2014). Indeed, it has been proved that the nanotube structure provides superior drug

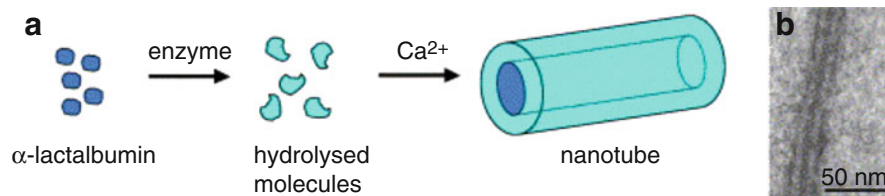


**Fig. 9.7** The formation of  $\alpha$ -lactalbumin nanotubes. (a) Schematic illustration of the self-assembly of partially hydrolyzed  $\alpha$ -lactalbumin into nanotubes in the presence of  $\text{Ca}^{2+}$ . (b) TEM image of negatively stained nanotubes. The dark line in the middle corresponds to the hollow of the nanotube. Reproduced with permission from Graveland-Bikker and de Kruif (2006). Copyright 2006 Elsevier

loading and uptake, and improved release profiles of therapeutics, compared to the spherical counterparts (Geng et al. 2007; Tiwari et al. 2017). Nanotubes, generated from food proteins, could even have new possibilities in food, pharmaceutical, and cosmetic fields, due to their nutritional value, biodegradability, and biocompatibility. Unfortunately, food protein-derived nanotubes are relatively less studied and less of concern. To the best of author's knowledge, food protein nanotubes have so far only been reported for  $\alpha$ -lactalbumin, lysozyme, and albumin (Graveland-Bikker and de Kruif 2006; Lara et al. 2013; Tiwari et al. 2017).

The formation of  $\alpha$ -lactalbumin nanotubes includes two steps: first, the proteins are partially hydrolyzed by enzymes, second, the hydrolyzed proteins are self-assembled into nanotubes in the presence of suitable multivalent ions (Fig. 9.7) (Graveland-Bikker and de Kruif 2006). These assembled nanotubes typically have a diameter of  $\sim 20$  nm and few micrometres in length. The prerequisites to form these nanotube structures are at an intermediate protein concentration and in the presence of appropriate cations. Various di- and tri-valent cations could trigger this self-assembly, including  $\text{Ca}^{2+}$ ,  $\text{Mn}^{2+}$ ,  $\text{Zn}^{2+}$ ,  $\text{Cu}^{2+}$ , and  $\text{Al}^{3+}$ , except  $\text{Ba}^{2+}$  and  $\text{Mg}^{2+}$ .

Lysozyme nanotubes are generated by heating proteins at pH 2 and  $90^\circ\text{C}$  for 30 h (Lara et al. 2013). Under this condition, lysozyme proteins are first hydrolyzed and then assembled into amyloid fibrils with multi-stranded helical ribbon morphology. In the final stage, the helical ribbons progressively closed into nanotubes. Hence, these lysozyme nanotubes can also be recognized as a state of amyloid fibrils. The nanotube diameter is dominated by the initial helical ribbons width and the folding angle, which ranges from  $\sim 40$  to 150 nm. It should be noted that many protein amyloid fibrils possess multi-stranded helical ribbon morphology (Lara et al. 2011), and thereby could be the source to produce nanotube structures.

Albumin nanotubes are formed by heating proteins ( $80\text{--}85^\circ\text{C}$ ) in the presence of glutathione and paclitaxel, which respectively function as the accelerator of protein unfolding and the nucleation core of self-assembly (Tiwari et al. 2017). By exposing buried nonpolar residues, glutathione greatly boosts the interaction of albumin and hydrophobic paclitaxel. Afterwards, the crystallization of the paclitaxels that are



located in the core contributes to the growth of nanotubes. In this case, nanotubes have a diameter of 70–120 nm and length of up to few micrometres.

### ***3.2 Polysaccharide Self-assembled Nanostructures***

The most common function of food polysaccharides is food structuring, which requires the creation of structures up to millimetres or centimetres with specific mechanical properties, that is, the formation of three-dimensional macrostructures (such as bulk gels) (Kontogiorgos 2015; Stephen et al. 2016; Foegeding et al. 2017). Therefore, in food structuring applications, the assembly of polysaccharides involves several length scales, ranging from atomic, molecular, microscopic to macroscopic scales (Kontogiorgos 2015). Current functions related to polysaccharides are not only limited to food structuring, but also include nanoplatforms for targeted delivery and biomedical imaging (Saravanakumar et al. 2012; Debele et al. 2016; Swierczewska et al. 2016). For example, due to the specific cellular recognition of some polysaccharide colloidal nanoparticles, the drug, gene, or nutrient delivery systems derived from these nanoparticles show superior performances (Saravanakumar et al. 2012; Salatin and Yari Khosroushahi 2017). In these applications, individual nanoparticles should be retained and their aggregation must be avoided (Kontogiorgos 2015). Some assembling approaches, e.g., gelation triggered by salt, pH, temperature alteration, electrostatic complexation of opposite charged polysaccharides, have been employed to prepare polysaccharide nanoparticles, but often in a mechanical intervention and/or a low polymer concentration to prevent the bulk gelation. Controlling polysaccharide self-assembly in nanometre length scale is not as easy as that in protein system, because dispersions of polysaccharides in aqueous solutions exhibit very low interfacial tension (Kontogiorgos 2015). Therefore, most of self-assembly-derived polysaccharide nanoparticles are formed by the aid of other methods or chemical modification.

A common approach to produce polysaccharide nanoparticles with controllable size or shape is to first establish the liquid droplets and then self-assemble polysaccharides in these confined droplets (Burey et al. 2008; Shewan and Stokes 2013; Joye and McClements 2014). Extrusion and emulsification always are used to produce these droplets, and the size and shape of nanoparticles are controllable by altering the applied experimental conditions. It should be noted that a “switching” effect can be built into these polysaccharide nanostructures that respond to stimulation *in vitro* or *in vivo*, due to the reversible feature of polysaccharide assembly process (Myrick et al. 2014). Another prominent approach to produce polysaccharide nanoparticles, especially when designing delivery nanoplatforms, is through the assembly of hydrophobic segment-grafted hydrophilic polysaccharides, i.e. the assembly of amphiphilic copolymers, as discussed below (Myrick et al. 2014; Debele et al. 2016; Swierczewska et al. 2016). Such copolymer assembled nanostructures is known as promising drug carriers, and even could lower drug toxicity because the hydrophilic polysaccharide parts are often less absorbed by



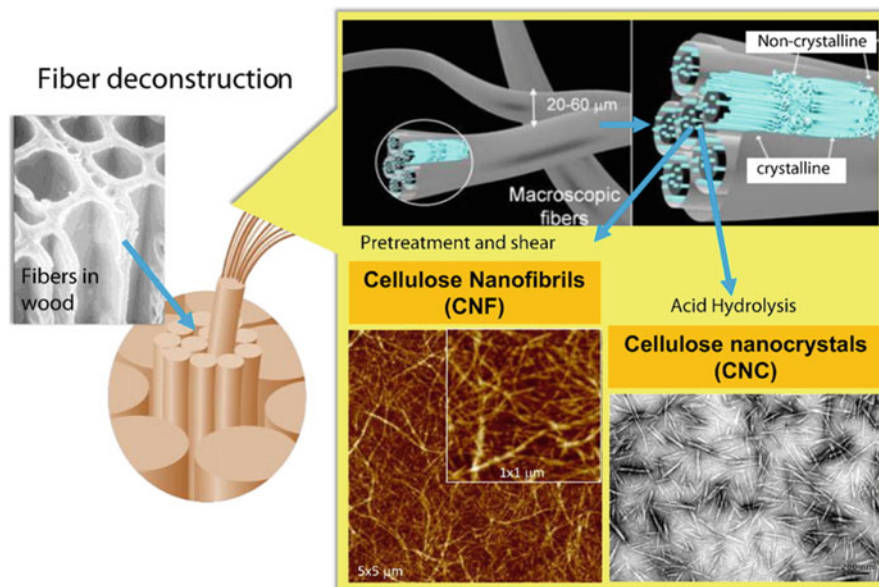


**Fig. 9.8** Schematic illustration of cellulose nanofibrils and nanocrystals produced from fibre cell walls by mechanical and chemical treatments, respectively. Reproduced with permission from Salas et al. (2014). Copyright 2014 Elsevier

normal tissues but can accumulate in cancerous tissues through the enhanced permeability and retention effect (EPR effect) (Myrick et al. 2014; Keservani and Sharma 2018).

Besides the above-mentioned methods, the assembled nanostructures can also be separated from many natural materials since they are already existent in nature but are highly structured. For example, cellulose nanofibrils and cellulose nanocrystals can be dissociated from fibre cell walls by mechanical, chemical, enzymatic treatment, or a combination thereof (Fig. 9.8) (Xu et al. 2013; Salas et al. 2014; Patel 2018). The abundance of OH groups in cellulose chains facilitates the formation of hydrogen bonding, resulting in the assembly into highly ordered structures (i.e. crystalline regions) that alternate with disordered structures (i.e. amorphous regions) (Salas et al. 2014; Patel 2018). Cellulose nanocrystals are usually produced through ultrasonic acid hydrolysis, in which most of the amorphous regions are degraded and the crystalline parts are remained (Salas et al. 2014; Patel 2018). The yielded cellulose nanocrystals often possess a diameter of 10–50 nm and a length of several hundred nm (Habibi et al. 2010; Xu et al. 2013). In contrast, cellulose nanofibrils contain both amorphous and crystalline regions and have a larger aspect ratio than cellulose nanocrystals (Salas et al. 2014; Patel 2018). These cellulose nanostructures have gained great attention in the scientific community, including in food science, due to a wide spectrum of unique properties such as high aspect ratio, excellent mechanical strength and inherent abundance. They can be used to stabilize

emulsions and foams, to prepare hydrogels and aerogels, and to fabricate food-grade packing materials, etc. (Salas et al. 2014; Coffey et al. 2016; Ullah et al. 2016; Patel 2018).

### ***3.3 Protein-co-polysaccharide Self-assembled Nanostructures***

Surfactants (e.g. mono- or diglycerides) have the unique property of self-assembling into a broad range of nanostructures, from micelles and vesicles to membranes and cubic phases, as these molecules possess discrete hydrophobic and hydrophilic moieties (Smart et al. 2008; Jones 2015). Despite that proteins and polysaccharides could self-assemble into several nanostructures as discussed above, these structures are not as diverse and controllable as the specific structures assembled from surface-active agents. This is due to the lack of a significant anisotropic distribution of hydrophobic and hydrophilic moieties in food polymers (Jones 2015). One method to increase this anisotropy is to attach a second component, forming copolymers. A number of chemical techniques could be used to generate these copolymers, but many of them are unfavourable for food formulations (Jones 2015).

Maillard reaction, as one of most common food chemical reactions, is widely used in the food sector to improve food tastes and appearances. It is also an ideal approach to produce food-grade copolymers, typically protein-co-polysaccharide. During Maillard reaction, a reducing end of a polysaccharide and a free amine of a protein are conjugated, with the formation of covalently bonded protein-co-polysaccharide (Kato 2002; Oliver et al. 2006; Jones 2015; de Oliveira et al. 2016). In this type of copolymers, the protein part is often the relatively hydrophobic component that forms the internal phase of micelle-like structures (Fig. 9.9) (Smart et al. 2008; Jones 2015). These food-grade copolymers are the ideal platforms to encapsulate and deliver bioactive compounds. For instance, casein-co-maltodextrin assembled colloids have very high stability, and could reduce the oxidization of encapsulated vitamin D (Markman and Livney 2012; Jones 2015).

## **4 Tech-functionalities**

Proteins and polysaccharides are widely used in the food sector as thickeners, gelling agents, emulsifiers, foam stabilizers, fat replacers, and so on (Phillips and Williams 2009). Self-assembly could happen at different length scales, produce diverse structures, continuum at different time scales (Whitesides and Grzybowski 2002). The appropriate control of self-assembly can produce novel foods and enable new applications. For example, the self-assembly-induced phase separation could produce diverse structures and thus lead to different texture properties. Moreover,

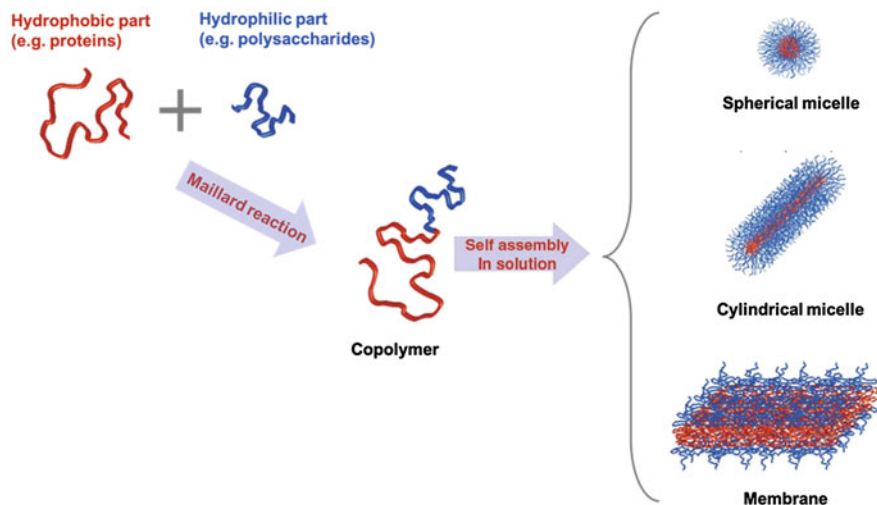


**Fig. 9.9** Different geometries could be produced from protein-co-polysaccharide in selective conditions. Adapted with permission from Smart et al. (2008). Copyright 2008 Elsevier

the assembled nanostructures generally possess better tech-functionalities than the individual proteins and polysaccharides, owing to their specific morphologies and structural alterations (e.g. high aspect ratio and heat resistance for protein nanofibrils). Many examples are mentioned above, such as forming cold-set gels, stabilizing emulsions and foams, and delivering drugs and nutrients. It is worth to note that some polysaccharides are capable of binding with a particular group of receptors at the cell surfaces, thereby can be engineered to prepare desired platforms to enhance the bioavailability of the loaded biomolecules, including food nutrients and bioactive compounds (Schmitt et al. 2016; Swierczewska et al. 2016; Salatin and Yari Khosroushahi 2017).

## 5 Disassembly and Reassembly in the Gastrointestinal Tract

As discussed above, the self-assembly is extremely vital to both natural and processed foods as it determines food appearance, texture, shelf-life, etc. However, the final functions of foods mainly depend on their biological fates in the gastrointestinal tract. As is well known, the macromolecular assembly plays a key role in biological phenomena; analogously, food polymer assembly process in the body certainly affect food functions. Assembly-related processes, such as self-assembly, disassembly, and reassembly, are present in the human digestion and absorption processes. During eating, foods are first broken down in the mouth and then entered into stomach and intestine. Afterwards, foods are degraded into small molecules that

are absorbed by intestinal walls and eventually enter into the bloodstream. The optimal control of the disassembly of food protein and polysaccharide nanostructures can bring not only the basic nutritional value but also other additional functions, e.g., by delivering incorporated bioactive compounds to the targeted sites (McClements et al. 2009; Joye and McClements 2014; McClements 2014; Yao et al. 2015). In contrast, inappropriate disassembly could cause some safety issues. For example, both high-speed (leading to high local concentration) and wrong-site release (such as in the colon altering the gut microbiota) of vitamins will harm the consumer health (McClements and Xiao 2017). Moreover, due to the condition change in the gastrointestinal tract, e.g. pH, the assembled nanostructures could further self-assemble into advanced nanostructures that alter the biological fates of food proteins and polysaccharides by controlling their digestion and absorption abilities. Besides, some degraded molecules can reassemble into nanostructures in the gastrointestinal tract, such as the amyloid fibrils formation in the stimulated gastric condition (Bateman et al. 2011). Understanding the self-assembly, disassembly, and reassembly of food protein and polysaccharide nanostructures during digestion and absorption processes is vital to maximize food nutritional value and improve food quality and even safety.

## 6 Summary, Challenges, and Future Scope

Self-assembly is commonly seen in both natural and processed foods, which is of vital importance to control food quality, functions, and even safety. It can be employed to innovate functional foods, whereas uncontrollable self-assembly may lower food quality and even cause safety issues. Toward the state of minimum free energy and the equilibrium of three classes of forces—driving, opposition, and directional forces, is the basic principle of the self-assembly of proteins and polysaccharides. The specific forces and mechanisms in certain food systems are not well understood, which arises from the complexity of food systems, and requires a deeper investigation in the future by learning from synthetic polymer systems. A variety of protein and polysaccharides nanostructures with unique properties and functionalities, such as micelles, nanofibrils, and nanotubes, could be produced by the self-assembly approach. Yet, some nanostructures are only reported to be generated from a few food sources under very specific experimental conditions. Future research needs to understand the generic feature of these nanostructures, and thereby to extend their sources as well as categories. It is worthy of noticing that many nanostructures, such as amyloid fibrils and amorphous aggregates, are recently considered to be a generic feature of proteins. The self-assembly behaviour of copolymers has been significantly investigated in polymer science but is far from thorough understanding in food science, which calls for more efforts in the future. Milliard reaction is not the only chemical reaction in the field of food chemistry. In addition, an increasing number of food-grade cross-linkers were found in recent years; this may also open the doors to produce protein-co-polysaccharides. In order

to successfully exploit self-assembly in practical applications and to ensure efficient scale-up, a high level of control is also required.

Although some progress has been made in understanding how proteins and polysaccharides assemble into nanostructures and how external factors determine nanostructures properties, studies on how self-, dis-, and re-assembly in gastrointestinal tract control the specific functions of foods are still in the infant stage. They are crucial for human health as these assembly processes can modulate food-body interactions and the biological fate of food components. Know-how on them could provide the guidance to produce foods and generate new functions in food products to benefit the consumer. In summary, future research on the assembly of food polymers and the resultant nanostructures is extremely indispensable.

## References

- Adair J, Suvaci E, Sindel J (2001) Surface and colloid chemistry. In: Cahn R, Flemings M, Ilschner B et al (eds) *Encyclopedia of materials: science and technology*, 2nd edn. Elsevier Inc., pp 1–10
- Bateman L, Ye A, Singh H (2011) Re-formation of fibrils from hydrolysates of  $\beta$ -lactoglobulin fibrils during in vitro gastric digestion. *J Agric Food Chem* 59:9605–9611
- Baughman RH, Zakhidov AA, De Heer WA (2002) Carbon nanotubes - the route toward applications. *Science* 297:787–792
- Billon L, Borisov O (2016) *Macromolecular self-assembly*. Wiley
- Burey P, Bhandari BR, Howes T, Gidley MJ (2008) Hydrocolloid gel particles: formation, characterization, and application. *Crit Rev Food Sci Nutr* 48:361–377
- Cao Y, Mezzenga R (2019) Food protein amyloid fibrils: origin, structure, formation, characterization, applications and health implications. *Adv Colloid Interface Sci* 269:334–356
- Cao Y, Wang L, Zhang K et al (2015) Mapping the complex phase behaviors of aqueous mixtures of  $\kappa$ -carrageenan and type B gelatin. *J Phys Chem B* 119:9982–9992
- Cao Y, Fang Y, Nishinari K, Phillips GO (2016a) Effects of conformational ordering on protein/polyelectrolyte electrostatic complexation: ionic binding and chain stiffening. *Sci Rep* 6:23739
- Cao Y, Li S, Fang Y et al (2016b) Conformational transition of polyelectrolyte as influenced by electrostatic complexation with protein. *Biomacromolecules* 17:3949–3956
- Carpenter JF, Manning MC (2002) *Rational design of stable lyophilized protein formulations: theory and practice*. Springer
- Chiti F, Dobson CM (2006) Protein misfolding, functional Amyloid, and human disease. *Annu Rev Biochem* 75:333–366
- Chiti F, Dobson CM (2017) Protein misfolding, amyloid formation, and human disease: a summary of progress over the last decade. *Annu Rev Biochem* 86:27–68
- Cho Y-H, Jones OG (2019) Assembled protein nanoparticles in food or nutrition applications. In: Toldrá F (ed) *Advances in food and nutrition research*. Academic Press, pp 47–84
- Coffey DG, Bell DA, Henderson A (2016) Cellulose and cellulose derivatives. In: Stephen AM, Phillips GO, Williams PA (eds) *Food polysaccharides and their applications*, 2nd edn. CRC Press, pp 147–180
- Cooper S (2014) *Polymer biomaterials in solution, as interfaces and as solids*. CRC Press
- Dalgleish DG (2011) On the structural models of bovine casein micelles - review and possible improvements. *Soft Matter* 7:2265–2272
- de Kruif CG, Huppertz T, Urban VS, Petukhov AV (2012) Casein micelles and their internal structure. *Adv Colloid Interface Sci* 171:36–52

- de Oliveira FC, dos R Coimbra JS, de Oliveira EB et al (2016) Food protein-polysaccharide conjugates obtained via the Maillard reaction: a review. *Crit Rev Food Sci Nutr* 56:1108–1125
- de Volder MFL, Tawfick SH, Baughman RH, Hart AJ (2013) Carbon nanotubes: present and future commercial applications. *Science* 339:535–539
- Debele TA, Mekuria SL, Tsai H-C (2016) Polysaccharide based nanogels in the drug delivery system: application as the carrier of pharmaceutical agents. *Mater Sci Eng C* 68:964–981
- Dickinson E, Leser ME (2007) Food colloids: self-assembly and material science. Royal Society of Chemistry
- Dobson CM (2003) Protein folding and misfolding. *Nature* 426:884–890
- Draget KI (2009) Alginates. In: Phillips GO, Williams PA (eds) *Handbook of hydrocolloids*, 2nd edn. Woodhead Publishing, pp 807–828
- Draget KI, Moe ST, Skjak-Bræk G, Smidsrød O (2016) Alginates. In: Stephen AM, Phillips GO, Williams PA (eds) *Food polysaccharides and their applications*, 2nd edn. CRC Press, pp 289–334
- Eisenberg DS, Sawaya MR (2017) Structural studies of amyloid proteins at the molecular level. *Annu Rev Biochem* 86:69–95
- Fang Y, Al-Assaf S, Phillips GO et al (2007) Multiple steps and critical behaviors of the binding of calcium to alginate. *J Phys Chem B* 111:2456–2462
- Fittolani G, Seeberger PH, Delbianco M (2019) Helical polysaccharides. *Pept Sci*:e24124
- Flickinger MC (2013) *Downstream industrial biotechnology: recovery and purification*. Wiley
- Foegeding EA, Stieger M, van de Velde F (2017) Moving from molecules, to structure, to texture perception. *Food Hydrocoll* 68:31–42
- Geng Y, Dalhaimer P, Cai S et al (2007) Shape effects of filaments versus spherical particles in flow and drug delivery. *Nat Nanotechnol* 2:249–255
- Goodsell DS, Olson AJ (2000) Structural symmetry and protein function. *Annu Rev Biophys Biomol Struct* 29:105–153
- Graveland-Bikker JF, de Kruif CG (2006) Unique milk protein based nanotubes: food and nanotechnology meet. *Trends Food Sci Technol* 17:196–203
- Habibi Y, Lucia LA, Rojas OJ (2010) Cellulose nanocrystals: chemistry, self-assembly, and applications. *Chem Rev* 110:3479–3500
- Hafidz RNRM, Yaakob CM, Amin I, Noorfaizan A (2011) Chemical and functional properties of bovine and porcine skin gelatin. *Int Food Res J* 18:813–817
- Hamaker HC (1937) The London-van der Waals attraction between spherical particles. *Physica* 4:1058–1072
- Hamley IW (2014) Peptide nanotubes. *Angew Chemie - Int Ed* 53:6866–6881
- Hu J, Yang J, Xu Y, Zhang K, Nishinari K, Phillips GO, Fang Y (2019) Comparative study on foaming and emulsifying properties of different beta-lactoglobulin aggregates. *Food Funct*
- Israelachvili JN (2011) Van der Waals forces between particles and surfaces. In: *Intermolecular and surface forces*. Academic Press, pp 253–289
- Jiang XC, Zeng QH, Chen CY, Yu AB (2011) Self-assembly of particles: some thoughts and comments. *J Mater Chem* 21:16797–16805
- Jones OG (2015) Protein nanostructures. In: Marangoni AG, Pink DA (eds) *Edible nanostructures: a bottom-up approach*. Royal Society of Chemistry, pp 69–113
- Joye IJ, McClements DJ (2014) Biopolymer-based nanoparticles and microparticles: fabrication, characterization, and application. *Curr Opin Colloid Interface Sci* 19:417–427
- Kato A (2002) Industrial applications of Maillard-type protein-polysaccharide conjugates. *Food Sci Technol Res* 8:193–199
- Kedracki D (2015) DNA-copolymers structure formation: beyond self-assembly. University of Geneva
- Keservani RK, Sharma AK (2018) *Nanodispersions for drug delivery*. CRC Press
- Kontogiorgos V (2015) Polysaccharide nanostructures. In: Marangoni AG, Pink DA (eds) *Edible nanostructures: a bottom-up approach*. Royal Society of Chemistry, pp 41–68

- Kroes-Nijboer A, Venema P, van der Linden E (2012) Fibrillar structures in food. *Food Funct* 3:221–227
- Lara C, Adamcik J, Jordens S, Mezzenga R (2011) General self-assembly mechanism converting hydrolyzed globular proteins into giant multistranded amyloid ribbons. *Biomacromolecules* 12:1868–1875
- Lara C, Handschin S, Mezzenga R (2013) Towards lysozyme nanotube and 3D hybrid self-assembly. *Nanoscale* 5:7197–7201
- Lee YS (2007) *Self-assembly and nanotechnology: a force balance approach*. Wiley
- Lekkerkerker HNW, Tuinier R (2011) *Colloids and the depletion interaction*. Springer
- Li T, Alessandra M (2018) *Pharmaceutical crystals: science and engineering*. Wiley
- Li L, Thangamathesvaran PM, Yue CY et al (2001) Gel network structure of methylcellulose in water. *Langmuir* 17:8062–8068
- Li L, Shan H, Yue CY et al (2002) Thermally induced association and dissociation of methylcellulose in aqueous solutions. *Langmuir* 18:7291–7298
- Li C, Qin R, Liu R et al (2018) Functional amyloid materials at surfaces/interfaces. *Biomater Sci* 6:462–472
- Lindoy LF, Atkinson I (2000) *Self-assembly in supramolecular systems*. Royal Society of Chemistry
- Loveday SM, Wang XL, Rao MA et al (2010) Tuning the properties of  $\beta$ -lactoglobulin nanofibrils with pH, NaCl and CaCl<sub>2</sub>. *Int Dairy J* 20:571–579
- Loveday SM, Anema SG, Singh H (2017)  $\beta$ -Lactoglobulin nanofibrils: the long and the short of it. *Int Dairy J* 67:35–45
- Lu PJ, Zaccarelli E, Ciulla F et al (2008) Gelation of particles with short-range attraction. *Nature* 453:499–503
- Luo Q, Hou C, Bai Y et al (2016) Protein assembly: versatile approaches to construct highly ordered nanostructures. *Chem Rev* 116:13571–13632
- Markman G, Livney YD (2012) Maillard-conjugate based core-shell co-assemblies for nanoencapsulation of hydrophobic nutraceuticals in clear beverages. *Food Funct* 3:262–270
- McClements DJ (2014) *Nanoparticle- and microparticle-based delivery systems: encapsulation, protection and release of active compounds*. CRC Press
- McClements DJ, Xiao H (2017) Is nano safe in foods? Establishing the factors impacting the gastrointestinal fate and toxicity of organic and inorganic food-grade nanoparticles. *NPJ Sci Food* 1:6
- McClements DJ, Decker EA, Park Y, Weiss J (2009) Structural design principles for delivery of bioactive components in nutraceuticals and functional foods. *Crit Rev Food Sci Nutr*
- McManus JJ, Charbonneau P, Zaccarelli E, Asherie N (2016) The physics of protein self-assembly. *Curr Opin Colloid Interface Sci* 22:73–79
- Mendes AC, Baran ET, Reis RL, Azevedo HS (2013) Self-assembly in nature: using the principles of nature to create complex nanobiomaterials. *Wiley Interdiscip Rev Nanomed Nanobiotechnol* 5:582–612
- Mezzenga R, Fischer P (2013) The self-assembly, aggregation and phase transitions of food protein systems in one, two and three dimensions. *Reports Prog Phys* 76:046601
- Motiejunas D, Wade RC (2006) Structural, energetic, and dynamic aspects of ligand-receptor interactions. In: *Comprehensive medicinal chemistry II*. Elsevier Inc., pp 193–212
- Myrick JM, Vendra VK, Krishnan S (2014) Self-assembled polysaccharide nanostructures for controlled-release applications. *Nanotechnol Rev* 3:319–346
- Nicolai T (2019) Gelation of food protein-protein mixtures. *Adv Colloid Interface Sci* 270:147–164
- Nicolai T, Durand D (2013) Controlled food protein aggregation for new functionality. *Curr Opin Colloid Interface Sci* 18:249–256
- Nicolai T, Britten M, Schmitt C (2011)  $\beta$ -Lactoglobulin and WPI aggregates: formation, structure and applications. *Food Hydrocoll* 25:1945–1962
- Ninham BW, Nostro PL (2010) *Molecular forces and self assembly: in colloid, nano sciences and biology*. Cambridge University Press

- Nishinari K, Zhang H (2004) Recent advances in the understanding of heat set gelling polysaccharides. *Trends Food Sci Technol* 15:305–312
- Oliver CM, Melton LD, Stanley RA (2006) Creating proteins with novel functionality via the Maillard reaction: a review. *Crit Rev Food Sci Nutr* 46:337–350
- Padua GW, Nonthantum P (2012) Material components for nanostructures. In: Padua GW, Wang Q (eds) *Nanotechnology research methods for food and bioproducts*. Wiley-Blackwell, pp 5–17
- Parsegian VA (2005) *Van der Waals Forces: a handbook for biologists, chemists, engineers, and physicists*. Cambridge University Press
- Patel AR (2018) Functional and engineered colloids from edible materials for emerging applications in designing the food of the future. *Adv Funct Mater* 1806809:1–34
- Phillips GO, Williams PA (2009) *Handbook of hydrocolloids*, 2nd edn. Woodhead Publishing
- Piazza R (1999) Interactions in protein solutions near crystallisation: a colloid physics approach. *J Cryst Growth* 196:415–423
- Pillai CKS, Paul W, Sharma CP (2009) Chitin and chitosan polymers: chemistry, solubility and fiber formation. *Prog Polym Sci* 34:641–678
- Rajagopal K, Schneider JP (2004) Self-assembling peptides and proteins for nanotechnological applications. *Curr Opin Struct Biol* 14:480–486
- Ravichandran R (2010) Nanotechnology applications in food and food processing: innovative green approaches, opportunities and uncertainties for global market. *Int J Green Nanotechnol Phys Chem* 1:72–96
- Roy A, Shrivastava SL, Mandal SM (2016) Self-assembled carbohydrate nanostructures: synthesis strategies to functional application in food. In: *Novel approaches of nanotechnology in food*. Academic Press, pp 133–164
- Russell JD, Dolphin JM, Koppang MD (2007) Selective analysis of secondary amino acids in gelatin using pulsed electrochemical detection. *Anal Chem* 79:6615–6621
- Saenger W (2008) *Principles of nucleic acid structure*. Springer Science & Business Media
- Sagalowicz L, Michel M, Blank I et al (2017) Self-assembly in food — a concept for structure formation inspired by nature. *Curr Opin Colloid Interface Sci* 28:87–95
- Salas C, Nypelö T, Rodriguez-Abreu C et al (2014) Nanocellulose properties and applications in colloids and interfaces. *Curr Opin Colloid Interface Sci* 19:383–396
- Salatin S, Yari Khosroushahi A (2017) Overviews on the cellular uptake mechanism of polysaccharide colloidal nanoparticles. *J Cell Mol Med* 21:1668–1686
- Saravanakumar G, Jo DG, Park JH (2012) Polysaccharide-based nanoparticles: a versatile platform for drug delivery and biomedical imaging. *Curr Med Chem* 19:3212–3229
- Scanlon S, Aggeli A (2008) Self-assembling peptide nanotubes. *Nano Today* 3:22–30
- Schaeffer L (2008) The role of functional groups in drug-receptor interactions. In: Wermuth CG (ed) *The practice of medicinal chemistry*, 3rd edn. Elsevier/Academic Press, pp 464–480
- Schefer L, Adamcik J, Mezzenga R (2014) Unravelling secondary structure changes on individual anionic polysaccharide chains by atomic force microscopy. *Angew Chemie - Int Ed* 53:5376–5379
- Schmitt C, Bovay C, Vuilliomenet AM et al (2009) Multiscale characterization of individualized  $\beta$ -lactoglobulin microgels formed upon heat treatment under narrow pH range conditions. *Langmuir* 25:7899–7909
- Schmitt C, Bovay C, Kolodziejczyk E et al (2016) Functional dairy protein-based aggregates for designing food formulations. In: Williams PA, Phillips GO (eds) *Gums and stabilisers for the food industry 18 - hydrocolloid functionality for affordable and sustainable global food solutions*. Royal Society of Chemistry, pp 321–330
- Shen X, Shamshina JL, Berton P et al (2016) Hydrogels based on cellulose and chitin: fabrication, properties, and applications. *Green Chem* 18:53–75
- Shewan HM, Stokes JR (2013) Review of techniques to manufacture micro-hydrogel particles for the food industry and their applications. *J Food Eng* 119:781–792
- Smart T, Lomas H, Massignani M et al (2008) Block copolymer nanostructures. *Nano Today* 3:38–46



- Sorrenti A, Leira-Iglesias J, Markvoort AJ et al (2017) Non-equilibrium supramolecular polymerization. *Chem Soc Rev* 46:5476–5490
- Stephen AM, Phillips GO, Williams PA (2016) *Food polysaccharides and their applications.*, 2nd edn. CRC Press
- Sundararajan PR (2016) *Physical aspects of polymer self-assembly.* Wiley
- Swierczewska M, Han HS, Kim K et al (2016) Polysaccharide-based nanoparticles for theranostic nanomedicine. *Adv Drug Deliv Rev* 99:70–84
- Tadros T (2013) *Encyclopedia of colloid and interface science.* Springer
- Tiwari AP, Joshi MK, Maharjan B et al (2017) Formation of lipophilic drug-loaded human serum albumin nanofibers with the aid of glutathione. *Chem Eng J* 313:753–758
- Ullah H, Santos HA, Khan T (2016) Applications of bacterial cellulose in food, cosmetics and drug delivery. *Cellulose* 23:2291–2314
- van der Linden E, Venema P (2007) Self-assembly and aggregation of proteins. *Curr Opin Colloid Interface Sci* 12:158–165
- Veeraman C, Baptist H, Sagis LMC, van der Linden E (2003) A new multistep Ca<sup>2+</sup>-induced cold gelation process for  $\beta$ -lactoglobulin. *J Agric Food Chem* 51:3880–3885
- Wang J, Liu K, Xing R, Yan X (2016) Peptide self-assembly: thermodynamics and kinetics. *Chem Soc Rev* 45:5589–5604
- Whitesides GM, Boncheva M (2002) Beyond molecules: self-assembly of mesoscopic and macroscopic components. *Proc Natl Acad Sci U S A* 99:4769–4774
- Whitesides GM, Grzybowski B (2002) Self-assembly at all scales. *Science* 295:2418–2421
- Xu X, Liu F, Jiang L et al (2013) Cellulose nanocrystals vs. Cellulose nanofibrils: a comparative study on their microstructures and effects as polymer reinforcing agents. *ACS Appl Mater Interfaces* 5:2999–3009
- Yao M, McClements DJ, Xiao H (2015) Improving oral bioavailability of nutraceuticals by engineered nanoparticle-based delivery systems. *Curr Opin Food Sci* 2:14–19
- Yi H, Wu LQ, Bentley WE et al (2005) Biofabrication with chitosan. *Biomacromolecules* 6:2881–2894
- Zargar V, Asghari M, Dashti A (2015) A review on chitin and chitosan polymers: structure, chemistry, solubility, derivatives, and applications. *ChemBioEng Rev* 2:204–226

# Chapter 10

## Flavour Delivery



Matthias Schultz

**Abstract** Flavourings are usually complex blends of solid or liquid compounds that need to be turned into a format useful to the food or beverage manufacturer. They often require protection during processing, transport, and storage to make sure that the consumer has a delightful and authentic flavour experience during food and beverage consumption. Flavour delivery systems provide flavourings in liquid format as emulsions or in dry format embedded in a solid matrix or core-shell capsule.

Food hydrocolloids play an indispensable role in the development and production of flavour delivery systems due to their emulsifying, viscosifying, glass forming, film forming, and other functionalities. The use of food hydrocolloids in flavour delivery systems is reviewed in this chapter mainly considering the scientific literature of the last two decades. Emphasis is put on the role of food hydrocolloids for the different technologies currently used to produce flavour delivery systems and on the structural concepts which their performance is based on. Interaction between hydrocolloids and flavouring compounds often influences flavour partitioning and release, and thorough knowledge is needed to perfectly balance the composition of the flavouring.

Current trends such as consumption of healthier food, changing life style, and labelling transparency are impacting the way flavour delivery systems are being designed.

**Keywords** Flavourings · Flavour delivery · Dry flavours · Beverage emulsions · Flavour release

---

M. Schultz (✉)  
Givaudan International SA, Kempthal, Switzerland  
e-mail: [matthias.schultz@givaudan.com](mailto:matthias.schultz@givaudan.com)

## 1 Introduction

### 1.1 *Flavour and Flavourings*

During consumption of food and beverages substances causing aroma or taste sensations impart the perception of flavour. Aroma perception is commonly triggered by the contact of compounds released from food and beverages with receptors in the nose. These compounds can enter the nose either directly from the headspace over the food or beverage (orthonasal perception) or through the oral cavity (retronasal perception). Taste molecules interact with receptors on the tongue or in the oral cavity and cause sensations like sweet, sour, salty, bitter, and umami. Despite being mostly related to the senses of smell and taste, flavour perception also involves textural, visual, and motorial aspects, all processed in a variety of brain systems (Fig. 10.1) to make flavour perception one of the most complex human behaviours (Shepherd 2006).

Substances imparting flavour perception by the senses are called flavourings. Flavourings can be liquid or dry substances. They can be single chemical compounds (like vanillin) as well as complex blends of materials of natural (e.g., essential oils, plant extracts, juice concentrates) and/or synthetic origin. Their chemical diversity is vast (Uhleemann and Reiß 2010); often they are complex blends of compounds displaying a huge variety of physicochemical properties such as melting, boiling and flash points, solubility, volatility, partitioning coefficients, and chemical reactivity (Table 10.1). Being given a range of just 16 flavouring compounds, a flavourist would be able to compose different fruit flavourings by changing the ratio of these compounds (Table 10.1, Grab 1998). The flavouring concentrate represents the complete flavour profile in the most concentrated form, but is often diluted with a carrier (ethanol in the case of the examples in Table 10.1). In practice, however, flavourings are often not created by using only individual chemical substances, but contain essential oils, botanical extracts, and the like (Wright 2010).

### 1.2 *Flavour Delivery and Flavour Delivery Systems*

Only a perfectly balanced composition at the point of flavour release immediately before or during consumption will deliver an authentic flavour profile. The process between preparation of a flavouring by a flavour company and contact with the consumer's receptors, however, can take from a few weeks to several years (Fig. 10.2).

Any changes in composition caused by untimely release or the reaction of flavouring constituents during blending, packaging, transport, storage, application into food or beverage products and cooking, baking, frying or other food preparation steps will change the composition of the flavouring and affect flavour perception. Turning a flavouring into the right format for application into food or beverages

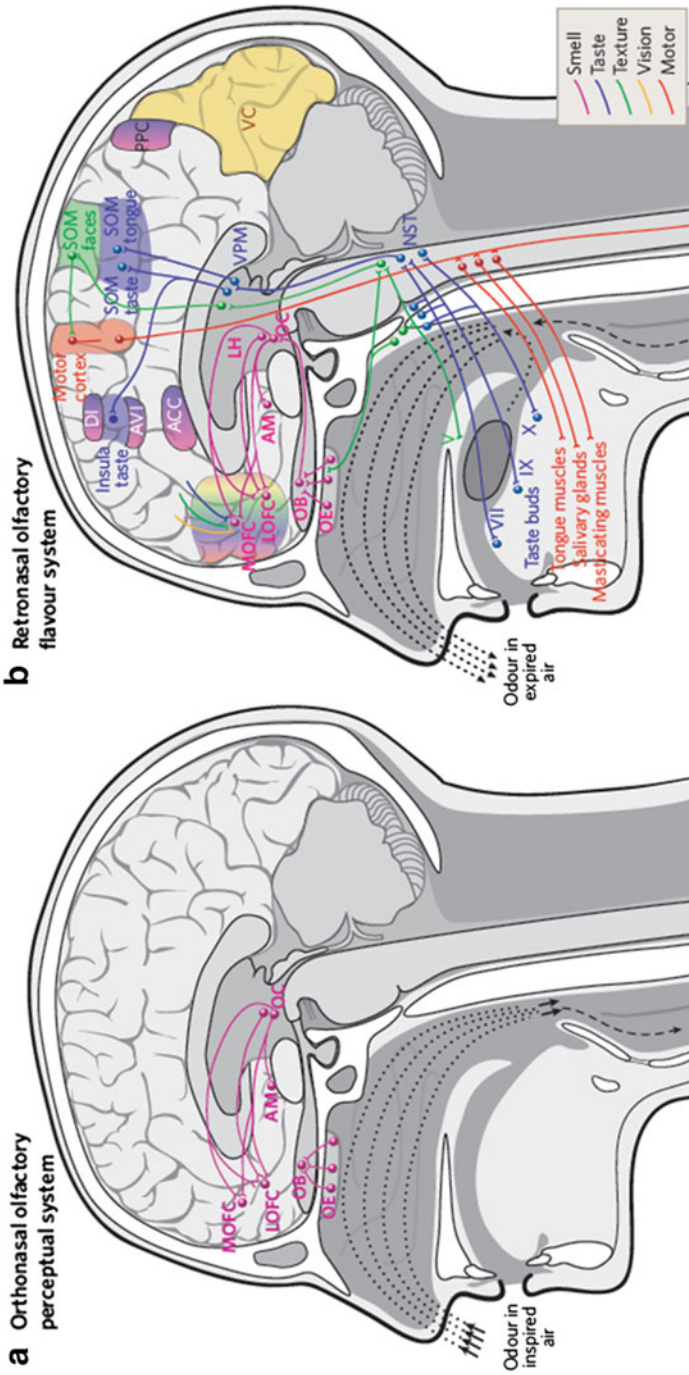


**Fig. 10.1** The dual olfactory system, **a** Brain systems involved in aroma perception during orthonasal olfaction (sniffing in), **b** Brain systems involved in aroma perception during retronasal perception (breathing out), with food in the oral cavity. Air flows indicated by dashed and dotted lines; dotted lines indicate air carrying odour molecules. ACC, accumbens; AM, amygdala; AVI, anterior ventral insular cortex; DI, dorsal insular cortex; LH, lateral hypothalamus; LOFC, lateral orbitofrontal cortex; MOFC, medial orbitofrontal cortex; NST, nucleus of the solitary tract; OB, olfactory bulb; OC, olfactory cortex; OE, olfactory epithelium; PPC, posterior parietal cortex; SOM, somatosensory cortex; V, VII, IX, X, cranial nerves; VPM, primary visual cortex; VC, ventral posterior medial thalamic nucleus (Reprinted with permission from Shepherd 2006, Copyright Springer Nature)

**Table 10.1** Examples of simple flavouring compositions, data from Grab (1998); physical data: log octanol-water partitioning coefficients ( $\log P_{ow}$ ) calculated by ChemDraw<sup>®</sup> Professional (Perkin Elmer 2019), boiling temperatures ( $T_b$ ) from Reineccius (1994)

Flavouring compound	Apple	Banana	Pear	Pineapple	$\log P_{ow}$	$T_b$
	parts by weight					°C (at mm Hg)
<i>Alcohols</i>						
1-Butanol	30	5	30	1	0.97	117–118
2-Methyl butanol	30	5	50	5	1.37	
1-Hexanol	30	5	40		1.80	156–157
<i>Esters</i>						
Amyl acetate	50	10	20	5	1.62	149
Isoamyl acetate	5	150	5	5	1.53	143
Ethyl butyrate	5	40	10	10	1.37	120
Amyl butyrate	5	30	20	20	2.69	185–186
Heptyl acetate	5	5	100	5	2.45	192–193
Ethyl 2-methylbutyrate	5	10	5	20	1.93	132–133
Allyl caproate	5	5	5	120	2.55	180–188
Citronellyl acetate	5	5	40	1	3.05	119–121 (15 mm)
<i>Aldehydes</i>						
Hexanal	100	1	5	1	1.33	130–131
(E)-2-Hexenal	100	10	30	5	1.31	47–48 (17 mm)
Benzaldehyde	0.1	0.2	0.2	0.1	1.78	179
<i>Others</i>						
Vanillin	1	30	1	30	1.27	170 (15 mm)
Eugenol	0.1	2	0.2	0.1	2.57	254
<i>Solvent added to make up to 1000 parts by weight</i>						
Ethanol	693.8	686.8	638.6	770.8	0.07	64

(e.g., an instantly soluble powder or sufficiently stable emulsion), protecting it from adverse changes and releasing it at the right point in time is accomplished by capturing it in a flavour delivery system. For better protection of the flavouring, especially against oxidation, a physical barrier might be erected between the flavouring and the environment. For example, liquid flavouring droplets are embedded in a solid polysaccharide matrix or in a core-shell capsule. Such systems are referred to as flavour encapsulation systems. Hence, flavour delivery systems commonly bridge the gap between the flavouring and food and beverages, enabling food manufacturers to more easily apply flavourings in their products with optimum protection and performance, and providing the desired consumer experience (Schultz and Ringgenberg 2008; Bouquerand et al. 2012; Ubbink 2013).

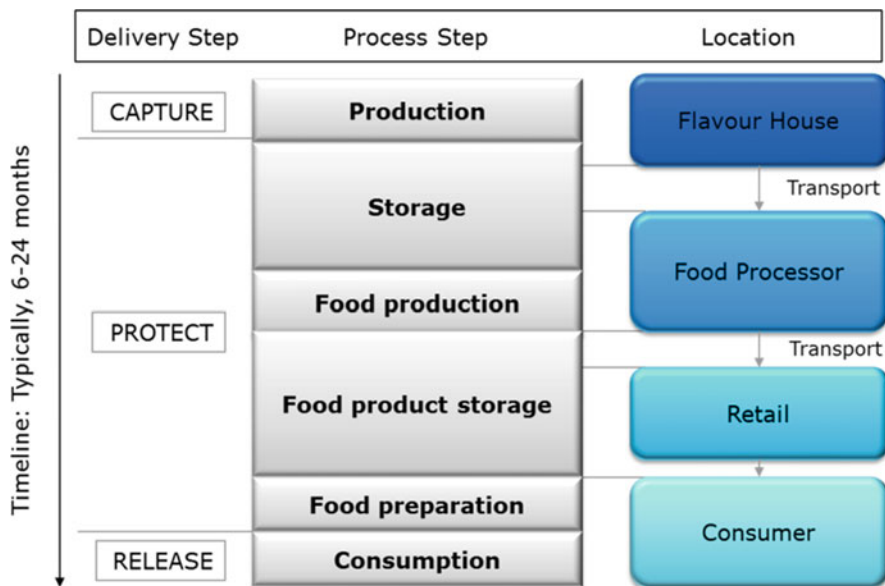


Fig. 10.2 The journey of a flavouring from the flavour house to the consumer

Table 10.2 Flavour encapsulation technology overview

Technology	Particle size		Flavour load <sup>a</sup>		Release mechanism
	Min	Max	Min	Max	
	µm	µm	wt%	wt%	
Extrusion	200	2000	8–10	15	Dissolution
Spray drying	20	100	20	25	Dissolution
Multi-stage spray drying	50	150	20	25	Dissolution
Fluid bed granulation	200	2000	10–15	20	Dissolution
Coacervation	20	800	40	70	Breakage, diffusion
Submerged nozzle	800	5000	70	90	Breakage, dissolution

<sup>a</sup>Flavour load = wt% of flavourings in the delivery system

### 1.3 Flavour Delivery Technologies

Table 10.2 presents an overview of the most important technologies to manufacture solid flavour delivery systems together with their main characteristics. A useful comparison of technologies and principles for product design and process engineering has also been published by Uhlemann et al. (2002), Doorn and Campanile (2006), Madene et al. (2006), Uhlemann and Reiß (2010), Bouquerand et al. (2012), and Ubbink (2013).

For the preparation of flavour powders the flavouring is usually dissolved or emulsified in a carrier material melt (for extrusion) or solution (e.g., for spray

drying). Almost all technologies require a subsequent drying step to remove excess water. In order to homogeneously distribute the particles with other powder food or powder beverage constituents, subsequent powder blending is often required. Food hydrocolloids play an important role as emulsifiers and wall or matrix materials capturing and protecting the flavouring (Sect. 2).

Water soluble liquid flavourings for beverages and liquid foods can often be applied in highly concentrated form and do not need a flavour delivery system. In some cases, solvents are added to mediate the generation of a homogeneous solution of individual constituents and facilitate application. In case the flavour is no longer sufficiently soluble in the food or beverage application, a flavour emulsion is produced that can be easily diluted, e.g. in a beverage. Again, food hydrocolloids are an integral part of such emulsions and act as emulsifiers and stabilizers (Sect. 3).

The desired mechanism by which the flavouring substances should be released (e.g., dissolution, diffusion, mechanical breakage, instant or delayed release) during food and beverage consumption (Sect. 4) plays a role when selecting the most suitable technology for a specific application.

## **2 Functionality of Hydrocolloids in Dry Flavour Delivery Systems**

### ***2.1 General Concepts of Matrix Encapsulation***

A matrix surrounding flavouring droplets in powder particles needs to fulfil certain criteria to be efficient. It needs to be stable against environmental conditions, in particular against humidity, have good mechanical resistance and be dense enough to prevent even the smallest flavouring molecules from permeating out and reactants like oxygen molecules from permeating into the particle (Quellet et al. 2001). Dry flavour delivery systems usually need to dissolve in water immediately, since typical applications they are blended in—like instant beverages, soups and sauces—all need to dissolve rapidly.

Food hydrocolloids fulfil certain tasks to contribute to the functionality of dry flavour delivery systems (Bouquerand et al. 2012). First, a certain reduction of interfacial tension is often needed to achieve homogeneous distribution of the flavouring in the matrix carrier solution as finely dispersed droplets. Hydrocolloids like octenyl succinate modified starches or acacia gum are commonly employed, but other emulsifiers are also possible. Second, to provide the mechanical and protective carrier properties of the matrix material, carbohydrates are used and processed in a way to solidify them in their amorphous state during drying. Traditionally, starch hydrolysis products are widely used to form a dense, glassy matrix. Being of comparatively high molecular weight carbohydrate macromolecules leave voids in the matrix structure that can facilitate permeation. Hence, third, and for oxidation sensitive flavourings in particular, lower molecular weight molecules usually not

being hydrocolloids are added to further densify the matrix. We will have a more thorough look at hydrocolloid emulsifiers and matrix materials in the following sections.

### 2.1.1 Emulsifiers

Emulsifiers need to facilitate formation of flavouring droplets during emulsification and stabilize them for the time between spray feed preparation and the drying step. This could cover a period of time between several minutes and a few days. Hence, the stability requirements for feed emulsions are lower than for beverage emulsions (see Sect. 3.2.1), which require several months of stability. Therefore, for feed emulsions, it is easier to compromise between emulsifier performance and cost. Traditionally, acacia gum, also known as gum arabic, is used. In particular, gum derived from trees of the species *Acacia seyal* shows sufficient performance for dried products. In some cases, acacia gum is used as both emulsifier and wall material (Bertolini et al. 2001; Fang et al. 2005).

Alternatively, several types of starches modified by reaction with octenyl succinic anhydride (OSA) are used as a very efficient emulsifier. The introduction of the hydrophobic octenyl chain to the hydrophilic starch molecule provides the amphiphilicity required for interfacial activity. Furthermore, the efficiency of octenyl succinate modified starches is very much affected by other structural parameters like the degree of branching (DB), degree of octenyl succinate substitution (DS), and the distribution of octenyl chains in the macromolecule (Fig. 10.3, Sweedman et al. 2013; Tizzotti et al. 2013; Zasytkin and Porzio 2004).

Proteins have been proposed and tested as emulsifiers for the production of flavour powders; however, a few disadvantages have prevented proteins from broad application. They often have limited solubility in the pH range used to prepare feed emulsions, and tend to react with some flavouring constituents, especially aldehydes. They can, however, be useful for the encapsulation of other food ingredients (Reineccius 2019).

Other polysaccharides such as sugar beet pectin (Paramita et al. 2010), cellulose derivatives (Zhou et al. 2018), and modified guar gum (Sarkar et al. 2013) have been tested as emulsifiers for feed emulsions for dry flavours. Often, their interfacial activity is not sufficient due to their hydrophilic character unless they are chemically modified or have a fraction of protein bound to polysaccharide chains providing amphiphilic functionality such as in sugar beet pectin (Williams et al. 2005).

### 2.1.2 Matrix Materials

Starch hydrolysis products such as dextrans, maltodextrins, and glucose syrups are commonly categorized by a parameter called dextrose equivalent (DE) which is a measure of the reducing power of a material relative to that of glucose (being assigned a reducing power of 100). That means the larger the DE the shorter the



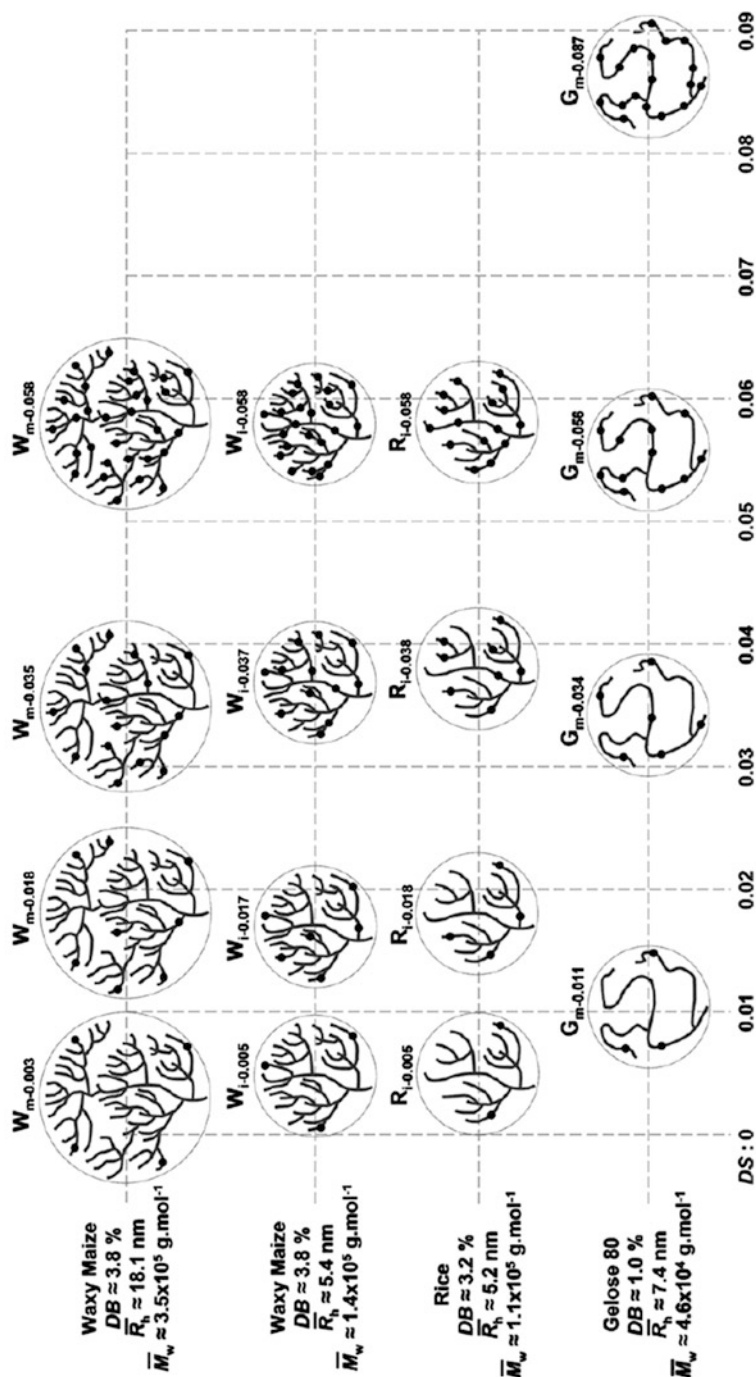


**Fig. 10.3** Schematic representations of OSA-modified starches used by Tizzotti et al. (2013), ● = grafted OSA groups, DS = degree of substitution, DB = degree of branching,  $R_h$  = hydrodynamic radius of gyration,  $\bar{M}_w$  = weight average molecular weight,  $W_{m-x}$ ,  $W_{i-x}$ ,  $R_{i-x}$  and  $G_{m-x}$ : W, R and G stand for Waxy Maize, Rice or Gelose 80, respectively. Subscripts i and m indicate the alcohol used during the acid hydrolysis reaction (isopropanol or methanol, respectively) (Reprinted with permission from Tizzotti et al. 2013, Copyright Elsevier B.V.)

polymer chain and the lower the molecular weight. Starch hydrolysates with DE values below 20 are referred to as maltodextrins, while those with DE greater than 20 are typically referred to as glucose syrups, glucose solids, or corn syrup solids. Being derived from natural products, they all have a comparatively broad molecular weight distribution, often with a certain amount of oligomers present (White Jr. et al. 2003).

Starch hydrolysis products play an outstanding role as matrix materials as they unify a number of advantageous properties including good water solubility, comparatively low viscosity and high glass transition temperature. The former two are important to dissolve them at rather high solid content, reducing the amount of water that needs to be removed during the drying process.

The concept of glass transition temperature,  $T_g$  (Liu et al. 2006), is especially important to produce powders with low hygroscopicity, which is, in turn, related to desirable transport, storage stability and powder flow properties. When being dried, starch hydrolysis products solidify in an amorphous state, also referred to as glassy state. Glass formers undergo a second order phase transition at  $T_g$  where they turn from a brittle and hard glass into a somewhat rubbery, viscoelastic material. The rate of mass transport within the rubbery state is much greater than in the glassy state. Hence, at and above  $T_g$ , integrity of the powder is no longer maintained.  $T_g$  is a function of DE as well as of the water activity,  $a_w$ , in a powder. Careful control of  $T_g$  and  $a_w$  is of huge practical importance, as low DE materials have a beneficially high  $T_g$ . However, due to their high molecular weight they form a more permeable matrix, causing lower retention of volatile chemicals and limited oxidative protection of the flavouring compared to matrices with a mixture of low and high molecular weight polymers.

Research on the relationship between maltodextrin molecular weight and glass transition temperature has been reported by Avaltroni et al. (2004). An increase in  $a_w$  results in a reduction of  $T_g$  as the water has a plasticizing effect on the carbohydrate matrix (Fig. 10.4). This may have devastating consequences if the  $T_g$  is reduced down to the transport or storage temperature of a powder, leading to the formation of lumps or agglomeration of the powder into a solid block. On the other hand, drying a powder down to very low  $a_w$  may considerably increase drying time and manufacturing cost. Normand et al. (2019) studied water diffusion in the 18 DE maltodextrin/water system and the drying kinetics by collecting the evaporated water through a condenser.

The concept of free volume has been introduced to better explain the occurrence of voids in the structure of glassy carbohydrates (Roussanova et al. 2013). Positron Annihilation Lifetime Spectroscopy (PALS) was found useful to measure free volume in maltooligomer matrices (Roussanova and Alam 2013). The plasticizing properties of water and substances like glycerol have also been determined (Roussanova et al. 2014).

A common approach to densify carbohydrate matrices is the addition of small molecular weight molecules to fill the subnanometer-size voids in the glassy matrix. Typical materials are sucrose, maltose, and trehalose, which work well to substantially improve oxidative stability of flavourings, but again reduce  $T_g$  (Sillick and

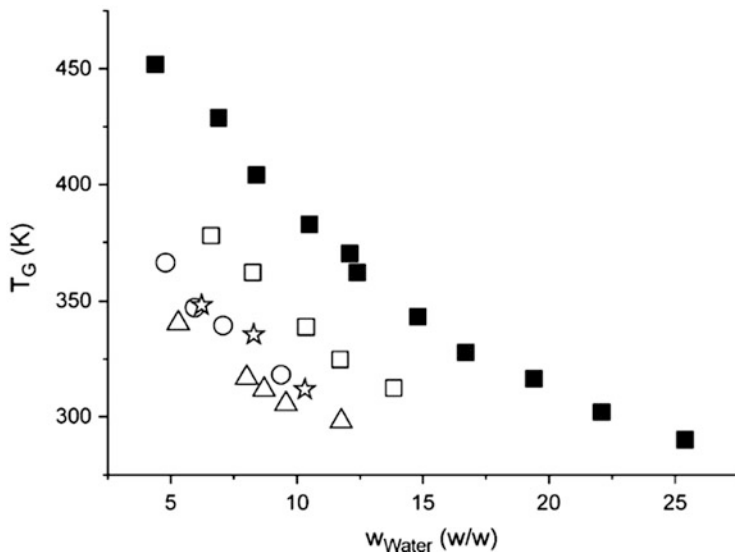


**Fig. 10.4**  $T_g$  measured for maltodextrins as a function of the water content of the sample. Open scatters: squares DE = 2, circles DE = 10, triangles DE = 19, stars mixture of DE = 2 and DE = 19. Solid squares: used from the literature (Benczédi et al. 1998) for extruded starch (Reprinted with permission from Avaltroni et al. 2004, Copyright Elsevier B.V.)

Gregson 2010). Therefore, thorough knowledge of the material science of carbohydrate glasses is a prerequisite for the successful development of dry flavour delivery systems (Fig. 10.5).

More recently, in studies of hydrophobically-modified starch-sucrose blends using wide-angle x-ray scattering and PALS, partial amorphous-amorphous phase separation in the powders was detected (Tedeschi et al. 2016) and confirmed by Dynamic Scanning Calorimetry (DSC) and  $^1\text{H}$  solid state NMR (Hughes et al. 2018). The temperature dependence of the local free volume as a function of blend composition and water content results in complex phase separation behaviour (Hughes et al. 2016).

Other matrix materials have been tested, but have not found broad application due to performance, cost or labelling issues. However, as in recent years the use of materials like maltodextrins has become less preferred due to increasing sensitivity of consumers regarding food ingredients that they are less familiar with, it is expected that other materials will gain importance as matrix materials.

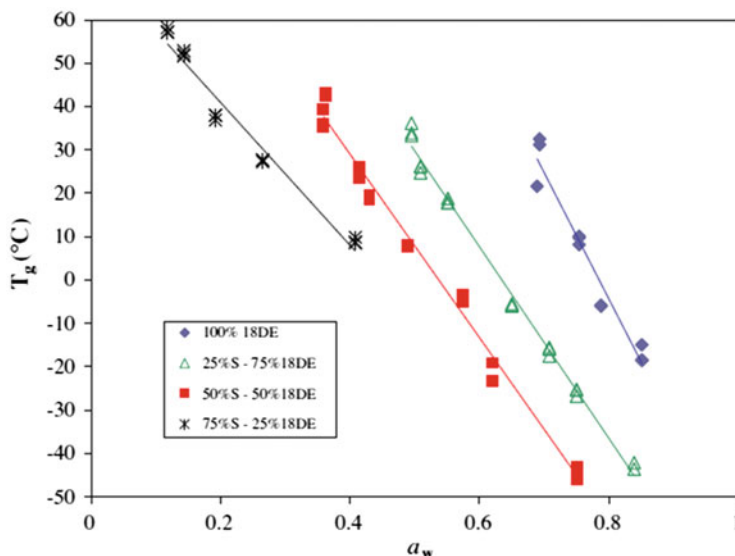


**Fig. 10.5** Trends of  $T_g$  vs.  $a_w$  for selected sucrose (S)/18 DE maltodextrin blends (Reprinted with permission from Sillick and Gregson 2010. Copyright Elsevier B.V.)

## 2.2 Use of Food Hydrocolloids to Produce Dry Flavour Delivery Systems

### 2.2.1 Extrusion

Extrusion is a general term for processes which include the transport of a comparatively viscous material under pressure through a die. The die configuration defines the shape and size of the extrudate. Typical extrusion technologies for flavour encapsulation are melt injection, also known as ram extrusion, and melt extrusion, a process carried out in a screw or twin-screw extruder (Porzio 2008; Tackenberg and Kleinebudde 2015; Lazou and Krokida 2017).

#### Ram Extrusion

This is the older process where a sugar or corn syrup solids melt is blended with the flavour, the system is pressurized by a gas and injected through a die into a bath of cold solvent (usually isopropanol) where the melt immediately solidifies and is broken into particles by rapid agitation (Porzio 2008). Thus, particles with a shape described as rods, threads or strands are obtained (Fig. 10.6a). Hydrocolloids do not play a major role in this process, although addition of hydrocolloids is discussed in the literature to modify certain properties and produce matrices with a specific functionality. For example, the use of agar has been described in a matrix further

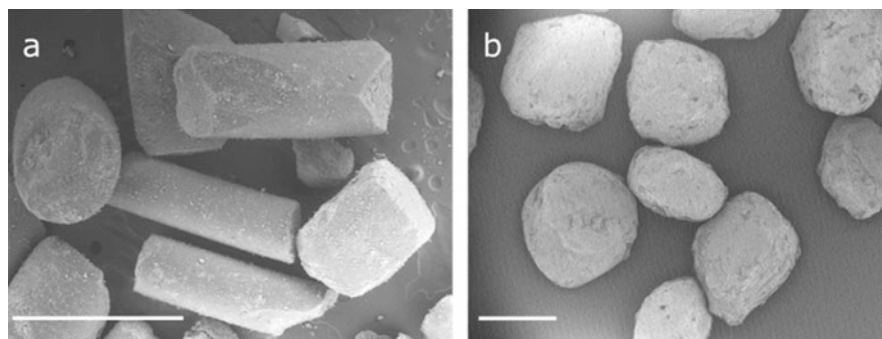


**Fig. 10.6** Scanning Electron Microscopy (SEM) images of extruded particles prepared by **a** ram and **b** twin-screw extrusion, scale bars 1 mm

containing maltodextrins or starch hydrolysates and flavouring compounds such as cinnamic aldehyde or menthol to produce soft-gelled particles when dispersed in water with good flavour retention (McIver et al. 2002).

#### Screw or Twin-screw Extrusion

In this process, a carbohydrate polymer matrix is molten or plasticized in an extruder and conveyed by a screw or co-rotating twin-screws to the die. A liquid flavouring can be added at the inlet feed or at any stage during the extrusion process, and, if needed, be emulsified in the presence of an emulsifier. Single-screw extruders are rarely described, whereas twin-screw extruders with co-rotating screws have become common to produce flavour delivery systems (Porzio 2008; Tackenberg and Kleinebudde 2015). A broader variety of shapes is possible due to different die configurations (Fig. 10.6b). Carbohydrate polymer matrices play an important role here and are used as such or in combination with low molecular weight sugars or sugar alcohols (Tackenberg et al. 2014). Recent reviews have been published by Tackenberg and Kleinebudde (2015) and Castro et al. (2016a).

In a series of articles, Tackenberg et al. (2015a, b) describe the encapsulation of orange terpenes in maltodextrin matrices. They studied the variation of sucrose, water, and orange terpene content in the extrusion matrix to assess the influence of feed composition and processing parameters on crystalline content,  $T_g$ , orange terpene retention and limonene content in the orange terpenes. Good encapsulation efficiency and storage stability are confirmed under optimum conditions. Castro et al. (2016b) varied the DE of maltodextrins in a melt extrusion process using different plasticisers (water, glycerol, sorbitol) and found no linear dependence between maltodextrin DE and glass transition temperature in extrudates.

Compared with spray dried systems, a main disadvantage of extrudates is their comparatively low flavouring load. Snyder and Zhang (2017) aimed to increase the load of cold pressed orange oil in a matrix containing maltodextrin and octenyl

succinate modified starch by varying the DE of the maltodextrins. The lower the DE the higher was the retained orange oil after extrusion. The maximum retained oil value for an optimum composition and screw configuration was in the range of 12–15 wt%.

Native starches have been studied as extrusion matrices as well. Emin and Schuchmann (2013) simulated the flow of plasticized maize starch during extrusion processing by Computational Flow Dynamics. The results suggest that a strong increase in zero shear viscosity has no influence on the flow, whereas a slight change in viscosity at the shear thinning region leads to significant increase in pressure drop along the mixing zone of the extruder. Simulation results were validated quantitatively by experimental data.

### 2.2.2 Spray Drying

For many years, spray drying has been the work horse technology to encapsulate flavourings in a glassy carbohydrate matrix (Porzio 2007). Typically, a feed solution is prepared by dissolving or emulsifying a flavouring into a carrier solution and using an atomizer disk or pressure nozzle to spray from the top into the chamber of a spray drier. Hot air is blown from the bottom of the dryer that evaporates the water in the spray droplets within a very short period of time, and a glassy matrix is formed wherein the flavouring molecules are dissolved or finely dispersed as droplets. Particle diameters of the dry powder are small (Fig. 10.7a, b), typically in the range between 20 and 100  $\mu\text{m}$  (Fang and Bhandari 2012; Ré 1998).

In order to increase the flowability and wettability of the powder, spray drying can be combined with an agglomeration step. In a so-called multi-stage drier, the finest particles are returned into the drying chamber and more feed emulsion is sprayed onto their surface. In addition, an internal or external fluid bed can be applied for further agglomeration, and particle diameters of 50–150  $\mu\text{m}$  are commonly obtained (Fig. 10.7c, d).

As for delivery systems prepared by extrusion (Sect. 2.2.1), there is a range of requirements for well performing spray dried flavour powders. These include mechanical (physical) stability, long-term flavour (chemical) stability through adequate protection in a sufficiently dense matrix, consistent powder integrity during transport and storage at varying temperatures and limited hygroscopicity. These properties are related to physical and structural parameters such as water activity, bulk density, and glass transition temperature that need to be carefully controlled. Besides thorough understanding of the spray drying process parameters, the composition of the powder matrices surrounding the flavouring molecules or droplets is key, and hydrocolloids play a major role. Cost and energy consumption considerations are becoming more and more important as well.

Within the last decades a multitude of materials including many hydrocolloids has been tested for their capability to form matrix materials and some reviews are available (Soottitantawat et al. 2015; Reineccius and Yan 2016; Jafari et al. 2008;

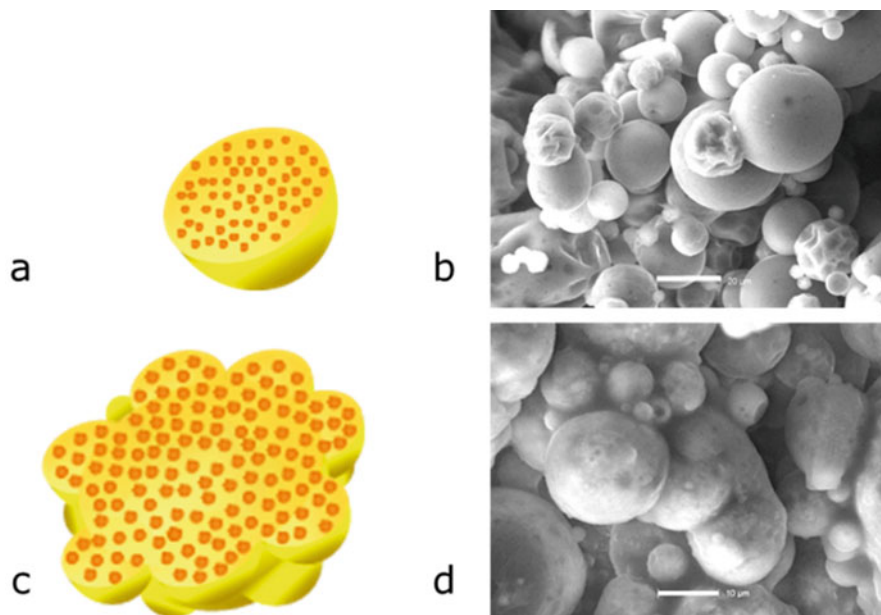


**Fig. 10.7** Schematic and SEM images of spray and multistage spray dried particles, **a** spray dried particle: flavour droplets (orange) embedded in a glassy carbohydrate matrix (yellow), **b** SEM image of spray dried particles, scale bar 20  $\mu\text{m}$ , **c** multistage spray dried particle (colours same as in **a**), **d** SEM image of multistage dried particles, scale bar 10  $\mu\text{m}$

Gharsallaoui et al. 2007). The mechanisms of permeation of flavouring and oxygen molecules through the matrix are still under investigation.

Upon ageing a glassy system moves toward equilibrium below  $T_g$ , a process called structural relaxation occurs, resulting in a decrease of energy and free volume and an increase of structural order. Enthalpy relaxation times of spray dried carbohydrate matrices containing volatile flavour compounds were determined by differential and isothermal calorimetric methods and correlated with flavour retention and formation of oxidation products (Sahni et al. 2015). Greater enthalpy relaxation time appears to be well correlated with better stability and may become a useful predictor of stability for both loss of volatile flavouring compounds and oxidation.

High solid content in the feed solution or emulsion is important to keep drying times short (less water to be evaporated), to limit exposure of volatile or thermolabile flavouring compounds to heat (reducing flavouring losses) and for cost reasons (reduced manufacturing cost at high throughput). However, an increase in the content of dissolved materials in the feed is often limited by their solubility or viscosity. Consequently, hydrocolloids that have excellent solubility while keeping suspension viscosity low are most preferred. Not surprisingly, maltodextrins with a DE of 5–20 work well and are comparatively well studied. Great care was taken in the characterization of the maltodextrin-water system using  $T_g$  as a measure to avoid stickiness of spray dried powders (Roos and Karel 1991; Normand et al. 2013). The



effect of DE on the properties of lime oil spray dried particles has been studied by Campelo et al. (2017). High DE was found to be better for oil retention and encapsulation efficiency. In a study to develop a model for shelf life prediction of orange oil, the oxidation stability was found to increase with increasing DE of the encapsulation matrix, but led to decreased humidity resistance (Subramaniam et al. 2013). By adding high DE carbohydrates, mono- or disaccharides, a compromise has to be found to produce a shelf-stable product.

Acacia gum is often combined with maltodextrins mainly for its emulsifying properties. In some cases, it is used as the sole encapsulation material (Bertolini et al. 2001). When compared with other wall materials, it has been found to display better protecting properties (Krishnan et al. 2005), but the results often depend on the quality of the gum, the specific flavouring and the stability testing conditions.

Other hydrocolloids are more rarely used. Depolymerized guar gum has been reported as partial replacement for acacia gum in the encapsulation of mint oil (Sarkar et al. 2012). Blends of acacia gum with xanthan have also been used (Outuki et al. 2016).

### 2.2.3 Freeze Drying and Vacuum Drying

Despite its huge importance for the production of instant coffee, freeze drying has not found wide application for the encapsulation of flavourings mainly due to the immense energy input needed and the related processing costs. A solution of matrix material is first frozen followed by direct sublimation of water under reduced pressure (Fang and Bhandari 2012).

Vacuum drying is mainly used in the production of the so-called process or reaction flavours (Kerler et al. 2010), but in some instances for flavour encapsulation as well. A high solid content dispersion is spread as a thin film in trays, occasionally foamed to accelerate drying under vacuum. The resulting cake is milled to obtain a free flowing powder (Ubbink 2013).

### 2.2.4 Fluidized-Bed Technologies

For flavour encapsulation in a fluidized bed a batch of solid particles is fluidized in a chamber by blowing air through them. In some equipment configurations, moving part of the equipment contributes to efficient fluidization. As a result, the particles behave and move like a fluid. A layer of encapsulated flavouring can be generated on the surface of the particles by spraying flavour dissolved or emulsified in a carrier solution into the fluid bed and evaporating the remaining solvent in the hot air stream. There are different fluid bed geometries available in either batch or continuous mode (Meiners 2012; Guignon et al. 2002; Teunou and Poncelet 2002). Batch granulators can, e.g., be equipped with rotor, Wurster or top spray inserts. Additional layers around the particles can be added in a subsequent coating step to further modify the functionality of the particles (Fig. 10.8).



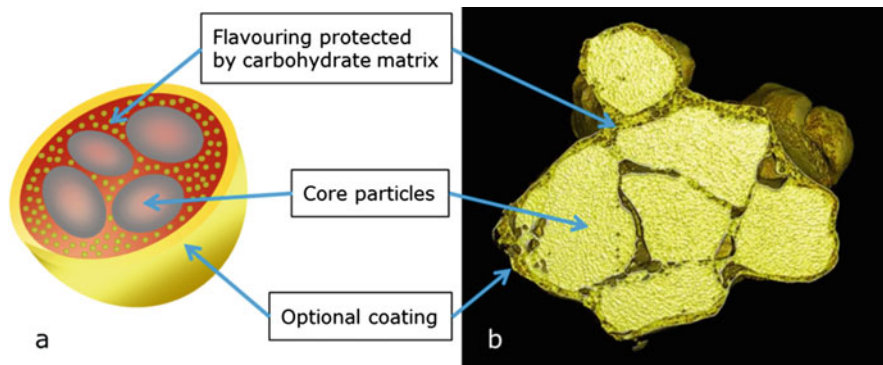


**Fig. 10.8** Cross section of a particle produced by fluidized-bed granulation, **a** schematic sketch, **b** X-ray microtomography image, image width 1.5 mm

The size of the resulting granules depends mainly on the size of the core material, typical particle diameters are between 500  $\mu\text{m}$  and several millimetres. They are useful in applications where larger particles are required such as tea bags or visual, in part coloured cues are desirable such as in confectionery, hard boiled, and chewy candy products.

Any food grade material that can be fluidized may serve as core material. Typical core materials used by the flavour industry are amorphous or crystalline mono-, di-, and oligosaccharides, food acids, plant leaves, fibres, and fruit pieces. Hydrocolloids are rarely used as core materials, but play a role as matrix material in the flavour layer protecting the flavouring by forming a glassy matrix as described for the technologies above.

Materials for the outer coating around the flavour layer include fats and waxes, but hydrocolloids are rather useful as well. Cellulose derivatives have found broad application. Nienaltowska et al. (2009) studied the coating quality of three water soluble cellulose derivatives—methyl cellulose, carboxymethyl cellulose, and hydroxypropyl cellulose, using glass beads as a core material. The concentration of the coating solutions and the related viscosity had a profound effect on coating quality.

Spray dried particles can be further agglomerated and coated in fluidized-bed equipment. In one study (Turchiuli and Dumoulin 2013), the flavour/carrier emulsion was spray dried. Then the fine powders ( $<30 \mu\text{m}$ ) were agglomerated in a fluidized bed with hot air by top spraying water or water/flavour/carrier emulsion. Then agglomerates were coated with a dry thin layer of emulsion.

### 2.2.5 Coacervation

Coacervation is a phase separation phenomenon in polymer solutions triggered by changes of temperature and/or pH. In simple coacervation, a polymer phase

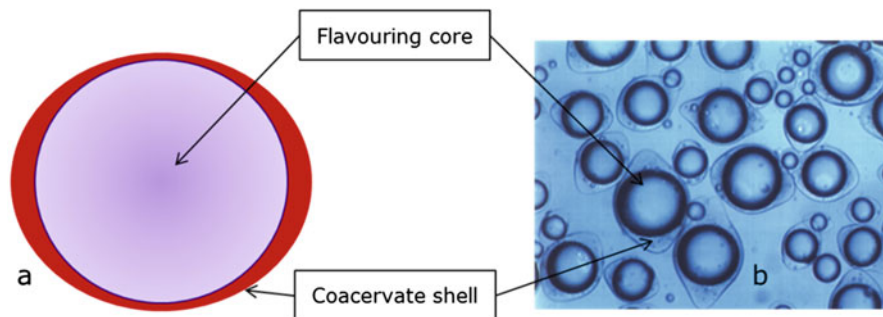


**Fig. 10.9** Coacervate beads, **a** schematic sketch, **b** microscope image, image width about 500  $\mu\text{m}$

separates from a pure solvent phase. Complex coacervation is more commonly used for flavour encapsulation (Thies 2007; Xiao et al. 2014). Typically, an ionic macromolecule with interfacial activity is used to emulsify a hydrophobic flavouring in an aqueous medium. An oppositely charged polymer is present or added which after adjusting temperature and pH accordingly combines with the first polymer at the interface of the oil droplets forming a coacervate phase around the droplet. The shell can be turned insoluble by adding a cross-linking agent generating water insoluble core-shell capsules with the lemon shape typical for products made by coacervation (Fig. 10.9).

Hydrocolloids are useful polymers for complex coacervation. There are certain requirements for optimum performance in forming coacervate phases. Both coacervation partners should have about approximately equal but opposite charge at a pH where each of them alone is completely soluble (Schmitt and Turgeon 2011). Chitosan is among the few positively charged polysaccharides at acid pH and has hence been studied for coacervation processes (Liu et al. 2013; Han et al. 2013; Butstraen and Salaün 2014), although it is considered food grade in only some regional markets. Chitosan has, however, a few disadvantages related to solubility and the mechanical properties of the resulting capsules. Instead usually proteins are being used, gelatin in particular, as the positively charged coacervation partner (Schmitt and Turgeon 2011). There is a broader choice of anionic hydrocolloids for complex coacervation, among them acacia gum (Leclercq et al. 2009a; Yeo et al. 2005), pectin (Silva et al. 2012), agar (Singh et al. 2007), carboxymethyl cellulose (Lv et al. 2012), and alginate (Devi and Kakati 2013). Many combinations of proteins and coacervates are possible. Detailed overviews were published by Schmitt et al. (2009) and Xiao et al. (2014).

Dardelle and Erni (2014) have studied the interplay of wetting phenomena and fluid viscoelasticity in coacervate/oil/water systems. Coacervate shells containing gelatin can also be easily cross-linked using aldehydes such as glutaraldehyde or enzymes like transglutaminase (Dardelle et al. 2011).

Direct encapsulation of complex blends of flavourings in coacervate capsules is difficult to achieve since some constituents of the blends partition between the oil core of the later coacervate capsule and the aqueous phase in which coacervation

occurs (Reineccius 2019). An approach to overcome this problem is to produce dry coacervate capsules with a neutral oil core, and then load them with flavour by spontaneous partitioning of the flavour into the oil cores through the coacervate shell (Wieland and Soper 2008; Leclercq et al. 2009b).

### 2.2.6 Other Technologies to Produce Insoluble Capsules

There are other technologies to prepare insoluble core shell or matrix capsules for the encapsulation of flavourings. The possibility to cross-link alginate or pectin capsules by dripping or jetting them into a bath containing calcium ions is used in a variety of processes. Alginates are derived from seaweed mainly as a sodium salt. They are structurally characterized by their molecular mass and the ratio of guluronic and mannuronic acid subunits (the G/M ratio) in the polymer. A high G/M ratio provides the basis for efficient cross-linking by calcium ions in a so-called egg-box type structure (Draget 2008). Pectins also form cross-linked gels with bivalent cations, and are characterized by their molecular mass and their content of methoxy or amide substituents in the glucopyranose rings (Endreß and Christensen 2009). Low methoxy content or high amide group content is necessary for them to be efficiently cross-linked by bivalent cations. Combinations of alginates and pectins can be used for formation of matrix or core-shell capsules.

In the simplest approach, a flavouring is emulsified into an alginate or pectin solution, and the emulsion is just dripped through a syringe into a calcium chloride bath (Petzold et al. 2014). More sophisticated nozzles such as vibrated two-fluid nozzles allow for the preparation of core-shell capsules with oil in the core and a polysaccharide as the shell. There are methods for making narrow size-distribution capsule cores using vibrating nozzles (Brandenberger and Widmer 1998), piezo driven drop formation in submerged nozzles (Böhmer et al. 2006), electrostatic extrusion (Lević et al. 2016) or microfluidic channels (Amici et al. 2008). All these methods have in common that they find applications in the pharmaceutical and cosmetic industries where small batches are produced and rather expensive ingredients are encapsulated. The days of the production of flavour delivery systems by such techniques at a sufficiently large scale are, however, still to come.

Yeast cells were used as thermo-stable flavour delivery systems (Normand et al. 2005; Dardelle et al. 2007). Their cell walls consist of external  $\beta$ -glucan and mannoprotein layers and were found permeable to both small polar and apolar molecules in aqueous solution. The reticulated  $\beta$ -glucan network plays the role of a skeleton, whereas the external protein layer acts like a sieve with a mesh-size evolving with the water content.

### 3 Functionality of Food Hydrocolloids in Beverage Emulsions

#### 3.1 *General Concepts in the Development of Beverage Emulsions*

Beverage emulsions are oil-in-water emulsions delivering flavour, in most cases cloudiness, and in some cases additional ingredients like colours, juices, juice concentrates or vitamins in the final beverage. For the convenience of the beverage manufacturer, the emulsion is supplied as a beverage concentrate that needs to be only diluted with water, sweetener, and food acid to provide the final soft drink, energy drink, flavoured water, squash or syrup, depending on the dilution ratio. Flavourings which are highly water soluble do not need to be emulsified and are often supplied as such or diluted in a solvent. Citrus flavourings—from orange, lemon, lime, mandarin, tangerine, and similar fruits—containing essential oils are not sufficiently soluble in the ready to drink beverage and hence need to be emulsified, unless the least soluble ingredients are removed, which often has adverse consequences for an authentic flavour profile.

Industry requirements for food hydrocolloids in beverage emulsions have been reviewed (Schultz 2010). Dickinson (2009) lists some important performance related requirements such as fast reduction of interfacial tension at the oil–water interface, strong adherence to the interface once they are adsorbed, and protection of newly formed droplets against flocculation and coalescence. There are additional needs arising from quality assurance, economical, regulatory, and consumer perception considerations. Those include constant quality and performance, regulatory acceptance, reasonable and constant price, and consumer acceptance.

Beverage emulsions are oil-in-water emulsions with a typical oil content of 5–25%. The oil phase consists of the flavouring and, in emulsions for cloudy beverages, of the so-called weighting agents. Weighting agents such as glycerol esters of different types of tree rosin or sucrose acetate isobutyrate increase the density of the oil phase to bring it closer to that of the water phase in order to delay creaming of oil droplets and ring formation in the emulsion and beverage. In case an oil soluble colorant, e.g. a carotenoid, is included, it also needs to be dissolved in the oil phase. Optionally, antioxidants like tocopherols or butylated hydroxyanisole may be part of the oil phase. The water phase contains emulsifiers and, in part, stabilizers, water soluble colorants and typically a preservative system. Traditionally, sodium benzoate or potassium sorbate are added as preservatives in combination with citric acid to convert benzoate and sorbate into the corresponding acids that imply the preserving functionality.

The emulsions are in general produced by separately preparing the water and oil phases to completely dissolving all the ingredients in each. During a pre-homogenisation step the oil phase is slowly added to the water phase under high shear, followed by a subsequent high-pressure homogenisation step that can apply one or more passes through a high-pressure homogenizer. For emulsions for

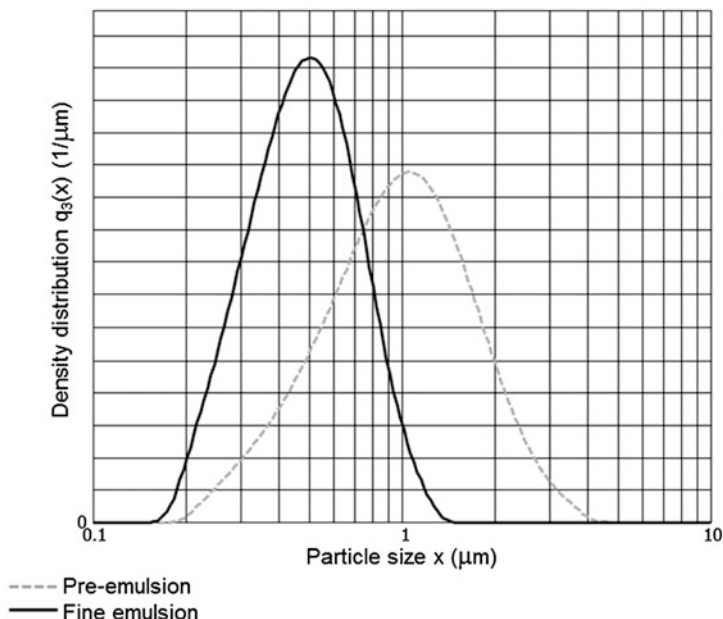


**Fig. 10.10** Typical droplet size distributions of emulsions after high-shear (pre)homogenisation (dashed curve) and high-pressure homogenisation (solid curve)

cloudy beverages the emulsion droplet diameter is reduced from below about 5 μm after pre-homogenisation down to 300–800 nm (Fig. 10.10). Droplets in this size range identical with the wavelength range of visible light provide optimum cloudiness in the beverage by effective light scattering.

Recent overviews of beverage emulsion materials science and technology are available (Given Jr. 2009; Schultz 2010; Piorkowski and McClements 2014; Dickinson 2018).

## 3.2 Hydrocolloids Used in Beverage Emulsions

### 3.2.1 Hydrocolloids as Emulsifiers

Dickinson (2018) has summarized why and which hydrocolloid emulsifiers work well in food emulsions. Besides having surface activity resulting in the reduction of interfacial tension and interfacial adsorption at a timescale relevant for emulsion preparation, they should not be prone to strong aggregation and gelation. Only a small number of hydrocolloids satisfy these requirements in a way that makes them useful as primary emulsifiers, whereas many hydrocolloids are good stabilizers due to their functionality as thickeners and viscosifiers.

## Acacia gum

Acacia gum, for the application as emulsifier and stabilizer in beverage emulsions, is harvested from *Acacia senegal* trees as the exudate produced by the tree to close wounds of natural origin or from tapping. It is a complex polysaccharide whose exact structure is still under debate (Al-Assaf et al. 2005; Renard et al. 2006; Sanchez et al. 2008; Mahendran et al. 2008; Williams and Phillips 2009; Atgié et al. 2019). When fractionated by Size Exclusion Chromatography, a high molecular weight arabinogalactan-protein fraction constituting about 10 wt% of the gum was identified and found to be mainly responsible for its emulsifying properties. The largest fraction, 85–90 wt% of the gum, despite containing some protein as well, is mainly arabinogalactan and contributes to the stabilizing properties of the gum. The smallest fraction, mainly peptides, makes another 1–2 wt% of the whole gum. Much effort has been spent to assure consistent gum quality for beverage emulsions—a challenging task due to the dependence of the exact composition of the gum on climate, soil, age of trees, and other factors (Al-Assaf et al. 2003). The content of the emulsifying arabinogalactan-protein fraction is an important but not the only parameter.

In an attempt to bind more protein to polysaccharides to increase the content of the arabinogalactan-protein fraction, acacia gum was subjected to a physical treatment in dry form at elevated temperature. The resulting gum showed improved emulsifying efficiency and has since then been commercialized (Al-Assaf et al. 2007).

Another more recent development is chemically modified *A. seyal* gum to get its performance closer to that of gum from *A. senegal* (Bi et al. 2017). As for starch, a hydrophobic octenyl chain can be introduced to the polysaccharide chains of the gum structure (Shi et al. 2017). Indeed, a strong improvement of emulsifying power can be achieved, although the treated gum loses its natural reputation due to the chemical modification step.

## Ghatti gum

Another tree exudate with excellent emulsifying properties is gum ghatti collected from *Anogeissus latifolia* trees growing in India (Al-Assaf et al. 2009). Compared with acacia gum the protein content is higher (Ido et al. 2008) and more evenly distributed throughout the gum's molecular structure. The component of gum ghatti adsorbed at the oil–water interface has higher surface coverage and the amount of gum ghatti adsorbed is more than three times that of acacia gum (Katayama et al. 2018). Consequently, gum ghatti can be used at lower concentrations than acacia gum (Ido et al. 2008; Al-Assaf et al. 2008) and would be expected to play an increasingly important role if regulatory admittance in major markets could be achieved.

## Octenyl Succinate Modified Starch

Like for flavour powders, octenyl succinate modified starch plays an important role as emulsifier in beverage emulsions (Trubiano 1995; Viswanathan 1999). However, different starch properties are desirable than for spray dry emulsions. While modified starches for spray dry feed emulsions should provide low viscosity to maximize the solid content in the feed, it is generally desirable for modified starches for beverage emulsions to provide higher viscosities to the water phase, contributing to long-term stabilization of the emulsions. Hydrolysed starches from waxy maize or corn are good substrates for chemical modification due to their high content of amylopectin and their good and almost complete solubility (Zhao et al. 2018b). Starches of different origin are also being studied (Jain et al. 2019). Compared with acacia gum, the interfacial tension is more efficiently decreased and smaller emulsion oil droplet diameters can be obtained at comparable pressures during homogenisation (Qian et al. 2011). However, the formed interfacial layers have lower shear elasticity than those formed by acacia gum (Erni et al. 2007).

## Sugar Beet Pectin

Pectins are polysaccharides that display little interfacial activity unless they contain substantial amounts of protein (Funami et al. 2006; Williams et al. 2005). One such pectin is isolated from sugar beet and was studied as emulsifier in beverage emulsions (Bai et al. 2017). The emulsifying efficiency was found to be good, however, only small amounts could be applied due to the very high molecular weight and high viscosity.

## Other Food Hydrocolloid Emulsifiers

Many other hydrocolloids have been proposed as emulsifiers for beverage emulsions, among them corn fibre gum (Yadav et al. 2009; Bai et al. 2017), mesquite gum (Román-Guerrero et al. 2009), fenugreek gum (Huang et al. 2001; Kaltsa et al. 2016), and spruce galactoglucomannan (Mikkonen et al. 2009). None of them has, however, yet found broad industrial application for the emulsification of flavours.

### 3.2.2 Hydrocolloids as Emulsion Stabilizers

Guar gum and carboxymethyl cellulose have been tested as emulsion stabilizers alone and in combination by Izadi and Emam Djomeh (2015). A combination of 0.5% guar gum and 0.2 wt% carboxymethyl cellulose was found to work best. However, long-term stability tests have not been reported and stability would be expected to be low due to comparatively large particle size. Nevertheless, a range of

hydrocolloids, due to their thickening and viscosifying properties, can considerably stabilize beverage emulsions.

Xanthan gum has been used in combination with acacia gum in orange oil emulsions (Mirhosseini et al. 2008a). Xanthan as well as tragacanth gums can stabilize emulsions due to the formation of a phase separated microstructure containing oil rich compartments (Moschakis et al. 2005; Drakos and Kiosseoglou 2006). Furthermore, the shear thinning properties of xanthan gum contribute to stabilization; the structure is maintained as long as the emulsion is not subjected to high shear or heavy movement.

Given that many flavours in beverage emulsions contain essential citrus oils the use of citrus pectin as a stabilizer deserves attention from a labelling perspective. The emulsifying capacity of citrus pectins of different origin has been studied (Akhtar et al. 2002; Leroux et al. 2003; Schmidt et al. 2015, 2017; Zhao et al. 2018a), however, its combination with conventional emulsifiers appears more promising (Verkempinck et al. 2018).

## 4 Flavour Release

While flavourings need to be captured and protected during processing, transport and storage, efficient release is required at the point of consumption. For foods and beverages containing dry delivery systems fast and complete dissolution is required in the food or beverage product immediately before consumption or in the oral cavity. Aroma perception depends on the availability of flavouring molecules in the gas phase; hence, the partitioning of flavouring molecules from the food matrix plays an important role and is influenced by the interaction with food components such as hydrocolloids and fat. Taste is perceived in the oral cavity only if the taste molecules reach the receptors on the tongue.

### 4.1 *Flavour Release from Delivery Systems*

While instantly soluble flavour powders release the flavour upon dilution into the water phase and from there into the gas phase, water insoluble capsules display release by diffusion in an aqueous environment or by mechanical disruption, e.g. when chewing. The effects of texture and structure on the retention of aroma compounds during processing and storage and on the aroma release and perception during consumption were reviewed by de Roos (2003). The release of cherry and peppermint flavouring compounds encapsulated by melt extrusion was measured by Gunning et al. (1999). The effects of water content and temperature variation on the release into the headspace over the extruded powders were studied. The largest amounts of release occurred when the matrix was above its glass transition temperature.



Release from gelatin/acacia gum coacervate capsules was measured by monitoring the headspace of a vessel containing the capsules to proton transfer reaction mass spectrometry (PTR-MS). No effects of cross-linking or wall/core ratio on volatile release in hot water could be found for any of the volatiles studied. When comparing real-time release of the prepared coacervates to a spray dried equivalent, there was no difference in the release from hot water but the release was slower when coacervates were added to ambient-temperature water. Volatile release was primarily determined by compound partition coefficients (oil/water and water/air) and temperature (Leclercq et al. 2009b).

In some specific applications prolonged or delayed release is desirable, e.g. in chewing gum. This can be achieved by hydrocolloid and other coatings added to granulates (see Sect. 2.2.4) that take time to first dissolve the coating before the flavour is released. Sequential flavour release from foods like chewing gums, confectionery products or bars are possible by combining fast with delayed release systems.

Flavourings included in emulsions and pastes are released into the headspace upon consumption, but the process is far from being simple due to partitioning of flavouring compounds in the water and oil or fat phase (de Roos 2000; Taylor and Linforth 2001) or interaction with food components, e.g. fat and protein phases in dairy products (Mao et al. 2017).

Very few publications deal with flavour release from typical beverage emulsions with hydrocolloid emulsifiers and stabilizers whereas there is ample literature on release from emulsions stabilized with small molecular weight emulsifiers and surfactants. Mirhosseini et al. (2008b) study the influence of main emulsion components (acacia gum, xanthan gum, and orange oil) on the release of target volatile flavour compounds released from a model orange beverage (diluted orange beverage emulsion) into the headspace.

## 4.2 *Flavour Release from Food*

Flavour release from food products and their sensory perception has been widely studied (van Ruth and Roozen 2010). This section only deals with food systems where food hydrocolloids play a role. Polysaccharides affect retention, release, and perception of flavourings, e.g. the viscosity and swelling ability of a hydrocolloid influences the release of flavour molecules from the matrix. In a study of the release from polysaccharide films of cellulose derivatives, fast dissolving polysaccharides were found to result in a quick burst of flavour at high intensity that tapered more quickly whereas slowly dissolving films gave a slower onset and a more consistent release over time (Cook et al. 2018).

Release of 20 flavour compounds from xanthan thickened food model systems with different viscosities were studied (Bylaite et al. 2005). Limonene and some of the esters and aldehydes exhibited decreased air-liquid partitioning coefficients in the presence of xanthan, indicating that the release of these volatile aroma

compounds was reduced due to interaction with the xanthan matrix. The release of 43 flavour compounds was reported from viscous solutions containing  $\lambda$ -carrageenan and sucrose (Bylaite et al. 2004). No overall effect of  $\lambda$ -carrageenan was found, except with the most hydrophobic compounds. Analysis of flavour release under non-equilibrium conditions, however, revealed a suppressing effect of  $\lambda$ -carrageenan on the release rates of aroma compounds, and the extent of decrease in release rates was dependent on the physicochemical characteristics of the aroma compounds, with the largest effect for the most volatile compounds.  $\iota$ - and  $\kappa$ -carrageenans did not appear to cause a significant difference in odour intensity for flavour molecules of different chemical classes, except for ethyl hexanoate, which was found to be retained by  $\iota$ -carrageenan. Nevertheless, in-mouth aroma perception was significantly different between the two systems (Juteau et al. 2004). The influence of food composition and temperature on the release of a strawberry flavouring in a system simulating yoghurt with a fruit preparation syrup has also been described (Nongonierma et al. 2006). Agar gels were used as encapsulating medium for limonene (Piazza and Benedetti 2010). The flavour binding capacity of amylose, a major component of starches is also well known (Conde-Petit et al. 2006; Arvisenet et al. 2002; Yeo et al. 2016). Flavour-protein interactions and their influence on flavour release and flavour perception are described by Wang and Arntfield (2017).

Control of flavour release is important when fat is reduced in certain foods. In part, hydrocolloids are added as thickeners to products to compensate for the loss of thickness and texture. Arancibia et al. (2015) demonstrated that thickener type and concentration and fat content significantly affect *in vivo* aroma release from a fat reduced dairy dessert. The delivery to the nasal cavity of the most lipophilic compound (linalool) mainly depended on fat content while thickener type and concentration mainly affected the release of the least lipophilic compound (cis-3-hexen-1-ol).

Such interactions between flavourings and other food ingredients constitute a challenge for the formulation of the flavouring. Flavourists as well as flavour delivery experts need to be aware to balance the ratio of individual compounds. In an exemplary article, Yang et al. (2011) describe reformulating a commercial strawberry flavouring that delivered a highly acceptable flavour in a pectin-sucrose gel, but did not perform as well in a chewy candy containing sugar, protein and fat.

## 5 Summary and Outlook

Development and innovation in the flavour industry will continue to be driven by the demand of consumers for fresh and authentic eating and drinking experiences. Flavour delivery systems seen as the essential bridge between the flavourings and food and beverages will play a key role. Delivery systems allow capturing, protecting, and releasing flavourings, and food hydrocolloids play an indispensable role for all these functionalities.

In a recent article (Givaudan Science and Technology Team 2017), three key areas have been identified to be important to be successful in the highly competitive area of designing state of the art flavour delivery systems. First, the growing need to replace chemically modified ingredients with natural substances and those that are more label-friendly. Second, the industry must develop a foundational understanding of how these materials behave in flavour applications; and finally, it must also improve the efficiency and sustainability of processing technologies:

When it comes to the material basis of delivery systems, customers are always keen to make more appealing declarations on the end product labels. As an example, modified starches have historically been used as encapsulation matrices in spray drying thanks to the solubility in water and the ability to form a robust encapsulating matrix around the flavour. The challenge is now to either develop natural starch-based materials, which can provide the same performance, or research alternative materials from different sources.

A scientific approach to the understanding of how materials behave is also essential. While much is already known, there is work to be done to close the gaps in the existing knowledge, for example to pinpoint how specific flavours might be best protected in an encapsulation matrix.

There is also room to improve the cost effectiveness and sustainability of processing technologies, such as using less water and working at lower temperatures in the drying processes, which would save energy and reduce the CO<sub>2</sub> footprint.

The introduction of new functional hydrocolloids is often restricted by legislative hurdles and lack of consumer acceptance. Materials only processed by physical methods with a natural and healthy reputation will be preferred and most successful in the market. Natural materials (McClements et al. 2017), dietary fibres (Gidley and Yakubov 2019), and plant proteins (Wang and Arntfield 2017) have the potential to replace traditional emulsifiers and encapsulation materials in case there are labelling, performance and cost benefits. Sustainability concerns will play an increasing role; sourcing and supply including the use of food processing side streams will also become more important.

## References

- Akhtar M, Dickinson E, Mazoyer J, Langendorff V (2002) Emulsion stabilizing properties of depolymerized pectin. *Food Hydrocolloids* 16:249–256
- Al-Assaf S, Katayama T, Phillips GO, Sasaki Y, Williams PA (2003) Quality control of gum arabic. *Foods Food Ingredients J Jpn* 208:771–780
- Al-Assaf S, Phillips GO, Williams PA (2005) Studies on acacia exudate gums. Part I: the molecular weight of *Acacia senegal* gum exudate. *Food Hydrocolloids* 19:647–660
- Al-Assaf S, Phillips GO, Aoki H, Sasaki Y (2007) Characterization and properties of *Acacia senegal* (L.) Willd. var. *senegal* with enhanced properties (*Acacia (sen) SUPER GUM™*): Part 1 – controlled maturation of *Acacia senegal* var. *senegal* to increase viscoelasticity, produce a hydrogel form and convert a poor into a good emulsifier. *Food Hydrocolloids* 21:319–328
- Al-Assaf S, Amar V, Phillips GO (2008) Characterisation of gum ghatti and comparison with gum arabic. In: Williams PA, Phillips GO (eds) *Gums and stabilisers for the food industry* 14. RSC Publishing, Cambridge, pp 280–290

- Al-Assaf S, Phillips GO, Amar V (2009) Gum ghatti. In: Phillips GO, Williams PA (eds) Handbook of hydrocolloids, 2nd edn. Woodhead Publishing, Oxford, pp 477–494
- Amici E, Tetradis-Meris G, de Torres CP, Jousse F (2008) Alginate gelation in microfluidic channels. *Food Hydrocolloids* 22:97–104
- Arancibia C, Castro C, Jublot L, Costell E, Bayarri S (2015) Colour, rheology, flavour release and sensory perception of dairy desserts. Influence of thickener and fat content. *LWT - Food Sci Technol* 62:408–416
- Arvisenet G, Le Bail P, Voilley A, Cayot N (2002) Influence of physicochemical interactions between amylose and aroma compounds on the retention of aroma in food-like matrices. *J Agric Food Chem* 50:7088–7093
- Atgié M, Garrigues JC, Chennevière A, Masbernat O, Roger K (2019) Gum Arabic in solution: composition and multi-scale structures. *Food Hydrocolloids* 91:319–330
- Avaltroni F, Bouquerand P-E, Normand V (2004) Maltodextrin molecular weight distribution influence on the glass transition temperature and viscosity in aqueous solutions. *Carbohydr Polym* 58:323–334
- Bai L, Huan S, Li Z, McClements DJ (2017) Comparison of emulsifying properties of food-grade polysaccharides in oil-in-water emulsions: gum arabic, beet pectin, and corn fiber gum. *Food Hydrocolloids* 66:144–153
- Benczédi D, Tomka I, Escher F (1998) Thermodynamics of amorphous starch-water systems. 1. Volume fluctuations. *Macromolecules* 31:3055–3061
- Bertolini AC, Siani AG, Grosso CRF (2001) Stability of monoterpenes encapsulated in gum arabic by spray-drying. *J Agric Food Chem* 49:780–785
- Bi B, Yang H, Fang Y, Nishinari K, Phillips GO (2017) Characterization and emulsifying properties of  $\beta$ -lactoglobulin-gum Acacia *Seyal* conjugates prepared via the Maillard reaction. *Food Chem* 214:614–621
- Böhmer MR, Schroeders R, Steenbakkens JAM, de Winter SHPM, Duineveld PA, Lub J, Nijssen WPM, Pikkemaat JA, Stapert HR (2006) Preparation of monodisperse polymer particles and capsules by ink-jet printing. *Colloids Surf A: Physicochem Eng Asp* 289:96–104
- Bouquerand P-E, Dardelle G, Erni P, Normand V (2012) An industry perspective on the advantages and disadvantages of different flavor delivery systems. In: Garti N, McClements DJ (eds) Encapsulation technologies and delivery systems for food ingredients and nutraceuticals. Woodhead Publishing, Cambridge, pp 453–487
- Brandenberger H, Widmer F (1998) A new multinozzle encapsulation immobilization system to produce uniform beads of alginate. *J Biotechnol* 63:73–80
- Butstraen C, Salaün F (2014) Preparation of microcapsules by complex coacervation of gum Arabic and chitosan. *Carbohydr Polym* 99:608–616
- Bylaite E, Ilgunaité Ž, Meyer AS, Adler-Nissen J (2004) Influence of  $\lambda$ -carrageenan on the release of systematic series of volatile flavor compounds, from viscous food model systems. *J Agric Food Chem* 52:3542–3549
- Bylaite E, Adler-Nissen J, Meyer AS (2005) Effect of xanthan on flavor release from thickened viscous food model systems. *J Agric Food Chem* 53:3577–3583
- Campelo PH, do Carmo EL, Zacarias RD, Yoshida MI, Ferraz VP, da Barros Fernandes RV, Botrel DA, Borges SV (2017) Effect of dextrose equivalent on physical and chemical properties of lime essential oil microparticles. *Ind Crop Prod* 102:105–114
- Castro N, Durrieu V, Raynaud C, Rouilly A, Rigal L, Quillet C (2016a) Melt extrusion encapsulation of flavours: a review. *Polym Rev* 56:137–186
- Castro N, Durrieu V, Raynaud C, Rouilly A (2016b) Influence of DE-value on the physicochemical properties of maltodextrin for melt extrusion processes. *Carbohydr Polym* 144:464–473
- Conde-Petit B, Escher F, Nuessli J (2006) Structural features of starch-flavor complexation in food model systems. *Trends Food Sci Technol* 17:227–235
- Cook SL, Methven L, Parker JK, Khutorianskiy VV (2018) Polysaccharide food matrices for controlling the release, retention and perception of flavours. *Food Hydrocolloids* 79:253–216

- Dardelle G, Erni P (2014) Three-phase interactions and interfacial transport phenomena in coacervate/oil/water systems. *Adv Colloid Interface Sci* 206:79–91
- Dardelle G, Normand V, Steenhoudt M, Bouquerand P-E, Chevalier M, Baumgartner P (2007) Flavour-encapsulation and flavour-release performances of a commercial yeast-based delivery system. *Food Hydrocolloids* 21:953–960
- Dardelle G, Subramaniam A, Normand V (2011) Determination of covalent cross-linker efficacy of gelatin strands using calorimetric analyses of the gel state. *Soft Matter* 7:3315–3322
- de Roos KB (2000) Physicochemical models of flavor release from foods. *ACS Symp Ser* 763:126–141
- de Roos KB (2003) Effect of texture and microstructure on flavour retention and release. *Int Dairy J* 13:593–605
- Devi N, Kakati DK (2013) Smart porous microparticles based on gelatin/sodium alginate polyelectrolyte complex. *J Food Eng* 117:193–204
- Dickinson E (2009) Hydrocolloids as emulsifiers and emulsion stabilizers. *Food Hydrocolloids* 23:1473–1482
- Dickinson E (2018) Hydrocolloids acting as emulsifying agents – how do they do it? *Food Hydrocolloids* 78:2–14
- Doom L, Campanile F (2006) Encapsulation of food ingredients: principles and applications for flavours. In: Phillips GO, Williams PA (eds) *Gums and stabilisers for the food industry* 13. Royal Society of Chemistry, Cambridge, pp 268–274
- Dragnet KI (2008) Alginates. In: Phillips GO, Williams PA (eds) *Handbook of hydrocolloids*, 2nd edn. Woodhead Publishing, Oxford, pp 807–828
- Drakos A, Kiosseoglou V (2006) Stability of acidic egg white protein emulsions containing xanthan gum. *J Agric Food Chem* 54:10164–10169
- Emin MA, Schuchmann HP (2013) Analysis of the dispersive mixing efficiency in a twin-screw extrusion processing of starch based matrix. *J Food Eng* 115:132–143
- Endreß H-U, Christensen SH (2009) Pectins. In: Phillips GO, Williams PA (eds) *Handbook of hydrocolloids*, 2nd edn. Woodhead Publishing, Oxford, pp 274–297
- Erni P, Windhab EJ, Gunde R, Graber M, Pfister B, Parker A, Fischer P (2007) Interfacial rheology of surface-active polymers: Acacia senegal gum versus hydrophobically modified starch. *Biomacromolecules* 8:3458–3466
- Fang Z, Bhandari B (2012) Spray drying, freeze drying and related processes for food ingredient and nutraceutical encapsulation. In: Garti N, McClements DJ (eds) *Encapsulation technologies and delivery systems for food ingredients and nutraceuticals*. Woodhead Publishing, Cambridge, pp 73–109
- Fang X, Shima M, Adachi S (2005) Effects of drying conditions on the oxidation of linoleic acid encapsulated with gum arabic by spray-drying. *Food Sci Technol Res* 11:380–384
- Funami T, Zhang G, Noda S, Nakauma M, Asai I, Al-Assaf S, Phillips GO (2006) Does pectin emulsification mechanism operate via an AGP (arabinogalactan protein) type fraction? *Foods Food Ingredients J Jpn* 211:255–263
- Gharsallaoui A, Roudaut G, Chambin O, Voilley A, Saurel R (2007) Applications of spray-drying in microencapsulation of food ingredients: an overview. *Food Res Int* 40:1107–1121
- Gidley MJ, Yakubov GE (2019) Functional categorisation of dietary fibre in foods: beyond ‘soluble’ vs ‘insoluble’. *Trends Food Sci Technol* 86:563–568
- Givaudan Science and Technology Team (2017) Harnessing the potential of F&F delivery systems. *Perfumer Flavorist* 42:42–47
- Given PS Jr (2009) Encapsulation of flavors in emulsions for beverages. *Curr Opin Colloid Interface Sci* 14:43–47
- Grab W (1998) Blended flavourings. In: Ziegler E, Ziegler H (eds) *Flavourings*. Wiley-VCH, Weinheim, pp 348–386
- Guignon B, Duquenoy A, Dumoulin ED (2002) Fluid bed encapsulation of particles: principles and practice. *Dry Technol* 20:419–447

- Gunning YM, Gunning PA, Kemsley EK, Parker R, Ring SG, Wilson RH, Blake A (1999) Factors affecting the release of flavor encapsulated in carbohydrate matrixes. *J Agric Food Chem* 47:5198–5205
- Han GT, Yang ZM, Peng Z, Wang G, Zhou M, Pang YX, Li PW (2013) Preparation and properties analysis of slow-release microcapsules containing patchouli oil. *Adv Mater Res* 641:935–938
- Huang X, Kakuda Y, Cui W (2001) Hydrocolloids in emulsions: particle size distribution and interfacial activity. *Food Hydrocolloids* 15:533–542
- Hughes D, Tedeschi C, Leuenberger B, Roussanova M, Coveney A, Richardson A, Bönisch GB, Alam MA, Ubbink J (2016) Amorphous-amorphous phase separation in hydrophobically-modified starch-sucrose blends II. Crystallinity and local free volume investigation using wide-angle X-ray scattering and positron annihilation lifetime spectroscopy. *Food Hydrocolloids* 58:316–323
- Hughes DJ, Bönisch GB, Zwick T, Schäfer C, Tedeschi C, Leuenberger B, Martini F, Mencarini B, Geppi M, Alam MA, Ubbink J (2018) Phase separation in amorphous hydrophobically modified starch-sucrose blends: glass transition, matrix dynamics and phase behaviour. *Carbohydr Polym* 199:1–10
- Ido T, Ogasawara T, Katayama T, Sasaki Y, Al-Assaf S, Phillips GO (2008) Emulsification properties of GATIFOLIA (gum ghatti) used for emulsions in food products. *Foods Food Ingredients J Jpn* 213:365–371
- Izadi SH, Emam Djomeh Z (2015) Formulation development and physicochemical characterisation of model beverage emulsions stabilised by guar gum and carboxymethyl cellulose. *Qual Assur Saf Crops Foods* 7:697–705
- Jafari SM, Assadpoor E, He Y, Bhandari B (2008) Encapsulation efficiency of food flavours and oils during spray drying. *Dry Technol* 26:816–835
- Jain S, Winuprasith T, Suphantharika M (2019) Design and synthesis of modified and resistant starch-based oil-in-water emulsions. *Food Hydrocolloids* 89:153–162
- Juteau A, Tournier C, Guichard E (2004) Influence of type and amount of gelling agent on flavour perception: physicochemical effect or interaction between senses? *Flavour Fragrance J* 19:483–490
- Kaltsa O, Yanniotis S, Mandala I (2016) Stability properties of different fenugreek galactomannans in emulsions prepared by high-shear and ultrasonic method. *Food Hydrocolloids* 52:487–496
- Katayama T, Ido T, Sasaki Y, Ogasawara T, Al-Assaf S, Phillips GO (2018) Characteristics of the adsorbed component of gum ghatti responsible for its oil-water interface advantages. *Foods Food Ingredients J Jpn* 213:372–376
- Kerler J, Winkel C, Davidek T, Blank I (2010) Basic chemistry and process conditions for reaction flavours with particular focus on Maillard-type reactions. In: Taylor AJ, Linforth RST (eds) *Food flavour technology*, 2nd edn. Blackwell Publishing, Oxford, pp 51–88
- Krishnan S, Kshirsagar AC, Singhal RS (2005) The use of gum arabic and modified starch in the microencapsulation of a food flavoring agent. *Carbohydr Polym* 62:309–315
- Lazou A, Krokida MK (2017) Extrusion for microencapsulation. In: Krokida MK (ed) *Thermal and nonthermal encapsulation methods*. CRC Press, Boca Raton, pp 137–171
- Leclercq S, Harlander KR, Reineccius GA (2009a) Formation and characterization of microcapsules by complex coacervation with liquid or solid aroma cores. *Flavour Fragrance J* 24:17–24
- Leclercq S, Milo C, Reineccius GA (2009b) Effects of cross-linking, capsule wall thickness, and compound hydrophobicity on aroma release from complex coacervate microcapsules. *J Agric Food Chem* 57:1426–1432
- Le Roux J, Langendorff V, Schick G, Vaishnav V, Mazoyer J (2003) Emulsion stabilizing properties of pectin. *Food Hydrocolloids* 17:455–462
- Lević S, Pajić Lijaković I, Dorević V, Rac V, Rakić V, Šolević Knudsen T, Pavlović V, Bugarski B, Nedović V (2016) Characterization of sodium alginate/d-limonene emulsions and respective calcium alginate/d-limonene beads produced by electrostatic extrusion. *Food Hydrocolloids* 45:111–123

- Liu Y, Bhandari B, Zhou W (2006) Glass transition and enthalpy relaxation of amorphous food saccharides: a review. *J Agric Food Chem* 54:5701–5717
- Liu J, Liu C, Liu Y, Chen M, Hu Y, Yang Z (2013) Study on the grafting of chitosan–gelatin microcapsules onto cotton fabrics and its antibacterial effect. *Colloids Surf B: Biointerfaces* 109:103–108
- Lv Y, Zhang X, Abbas S, Karangwa E (2012) Simplified optimization for microcapsule preparation by complex coacervation based on the correlation between coacervates and the corresponding microcapsule. *J Food Eng* 111:225–233
- Madene A, Jacquot M, Scher J, Desobry S (2006) Flavour encapsulation and controlled release - a review. *Int J Food Sci Technol* 41:1–21
- Mahendran T, Williams PA, Phillips GO, Al-Assaf S, Baldwin TC (2008) New insights into the structural characteristics of the arabinogalactan-protein (AGP) fraction of gum arabic. *J Agric Food Chem* 56:9269–9276
- Mao L, Roos YH, Biliaderis CD, Miao S (2017) Food emulsions as delivery systems for flavor compounds: a review. *Crit Rev Food Sci Nutr* 57:3173–3187
- McClements DJ, Bai L, Chung C (2017) Recent advances in the utilization of natural emulsifiers to form and stabilize emulsions. *Annu Rev Food Sci Technol* 8:205–236
- McIver RC, Vlad F, Golding RA Jr, Leichsenring TD, Benczedi D (2002) Encapsulated flavour and/or fragrance composition. US Patent 6,932,982
- Meiners JA (2012) Fluid bed microencapsulation and other coating methods for food ingredient and nutraceutical bioactive compounds. In: Garti N, McClements DJ (eds) *Encapsulation technologies and delivery systems for food ingredients and nutraceuticals*. Woodhead Publishing, Cambridge, pp 151–176
- Mikkonen KS, Tenkanen M, Cooke P, Xu C, Rita H, Willför S, Holmbom B, Hicks KB, Yadav MP (2009) Mannans as stabilizers of oil-in-water beverage emulsions. *LWT – Food Sci Technol* 42:849–855
- Mirhosseini H, Tan CP, Hamid NSA, Yusof S (2008a) Optimization of the contents of Arabic gum, xanthan gum and orange oil affecting turbidity, average particle size, polydispersity index and density in orange beverage emulsion. *Food Hydrocolloids* 22:1212–1223
- Mirhosseini H, Tan CP, Hamid NSA, Yusof S (2008b) Effect of Arabic gum, xanthan gum and orange oil on flavor release from diluted orange beverage emulsion. *Food Chem* 107:1161–1172
- Moschakis T, Murray BS, Dickinson E (2005) Microstructural evolution of viscoelastic emulsions stabilised by sodium caseinate and xanthan gum. *J Colloid Interface Sci* 284:714–728
- Nienaltowska K, Depypere F, Dewettinck K, Van Der Meeren P, Ronsse F, Pieters JG (2009) Water-soluble cellulose derivatives as coating agents in fluidized bed processing. *Part Sci Technol* 27:389–403
- Nongonierma AB, Springett M, Le Quéré J-L, Cayot P, Voilley A (2006) Flavour release at gas/matrix interfaces of stirred yoghurt models. *Int Dairy J* 16:102–110
- Normand V, Dardelle G, Bouquerand P-E, Nicolas L, Johnston D (2005) Flavor encapsulation in yeasts: multitechnique approach for characterization of the release mechanism. *J Agric Food Chem* 53:7532–7543
- Normand V, Subramaniam A, Donnelly J, Bouquerand P-E (2013) Spray drying: thermodynamics and operating conditions. *Carbohydr Polym* 97:489–495
- Normand V, Armanet L, McIver RC, Bouquerand P-E (2019) Water diffusion in the semi-liquid state during industrial candy preparation. *Food Biophys* 14:193–204
- Outuki PM, de Francisco LMB, Hoscheid J, Bonifácio KL, Barbosa DS, Cardoso MLC (2016) Development of arabic and xanthan gum microparticles loaded with an extract of *Eschweilera nana* Miars leaves with antioxidant capacity. *Colloids Surf A: Physicochem Eng Asp* 499:103–112
- Paramita V, Furuta T, Yoshii H (2010) Microencapsulation efficacy of d-limonene by spray drying using various combinations of wall materials and emulsifiers. *Food Sci Technol Res* 16:365–372
- PerkinElmer Informatics Inc. (2019) ChemDraw® Professional Software, Version 15.0.0.106

- Petzold G, Gianelli MP, Bugueño G, Celan R, Pavez C, Orellana P (2014) Encapsulation of liquid smoke flavoring in ca-alginate and ca-alginate-chitosan beads. *J Food Sci Technol* 51:183–190
- Piazza L, Benedetti S (2010) Investigation on the rheological properties of agar gels and their role on aroma release in agar/limonene solid emulsions. *Food Res Int* 43:269–276
- Piorkowski DT, McClements DJ (2014) Beverage emulsions: recent developments in formulation, production and applications. *Food Hydrocolloids* 42:5–41
- Porzio M (2007) Spray drying. *Perfumer Flavorist* 32:34–39
- Porzio M (2008) Melt injection and melt extrusion. *Perfumer Flavorist* 33:48–53
- Qian C, Decker EA, Xiao H, McClements DJ (2011) Comparison of biopolymer emulsifier performance in formation and stabilization of orange oil-in-water emulsions. *J Am Oil Chem Soc* 88:47–55
- Quellet C, Schudel M, Ringgenberg R (2001) Flavors & fragrance delivery systems. *Chimia* 55:421–426
- Ré MI (1998) Microencapsulation by spray drying. *Dry Technol* 16:1195–1236
- Reineccius GA (ed) (1994) Source book of flavors, 2nd edn. Chapman and Hall, New York
- Reineccius G (2019) Use of proteins for the delivery of flavours and other bioactive compounds. *Food Hydrocolloids* 86:62–69
- Reineccius GA, Yan C (2016) Factors controlling the deterioration of spray dried flavourings and unsaturated lipids. *Flavour Fragrance J* 31:5–21
- Renard D, Lavenant-Gourgeon L, Ralet M-C, Sanchez C (2006) *Acacia senegal* gum: continuum of molecular species differing by their protein to sugar ratio, molecular weight, and charges. *Biomacromolecules* 7:2637–2649
- Román-Guerrero A, Orozco-Villafuerte J, Pérez-Orozco JP, Cruz-Sosa F, Jiménez-Alvarado R, Vernon-Carter EJ (2009) Application and evaluation of mesquite gum and its fractions as interfacial film formers and emulsifiers of orange peel-oil. *Food Hydrocolloids* 23:708–713
- Roos Y, Karel M (1991) Water and molecular weight effects on glass transitions in amorphous carbohydrates and carbohydrate solutions. *J Food Sci* 56:1676–1681
- Roussenova M, Alam MA (2013) PALS: a unique probe for the molecular organisation of biopolymer matrices. *J Phys: Conf Ser* 443:012044
- Roussenova M, Townrow S, Murith M, Ubbink J, Alam A (2013) Molecular packing of carbohydrate oligomer encapsulants - a free volume perspective. *Mater Sci Forum* 733:96–99
- Roussenova M, Andrieux J-C, Alam MA, Ubbink J (2014) Hydrogen bonding in maltooligomer-glycerol-water matrices: relation to physical state and molecular free volume. *Carbohydr Polym* 102:566–575
- Sahni EK, Thakur M, Chaney MA, Sherman G, Siegel DP, Pikal MJ (2015) Dynamics in polysaccharide glasses and their impact on the stability of encapsulated flavors. *Food Biophys* 11:20–33
- Sanchez C, Schmitt C, Kolodziejczyk E, Lapp A, Gaillard C, Renard D (2008) The acacia gum arabinogalactan fraction is a thin oblate ellipsoid: a new model based on small-angle neutron scattering and ab initio calculation. *Biophys J* 94:629–639
- Sarkar S, Gupta S, Variyar PS, Sharma A, Singhal RS (2012) Irradiation depolymerized guar gum as partial replacement of gum Arabic for microencapsulation of mint oil. *Carbohydr Polym* 90:1685–1694
- Sarkar S, Gupta S, Variyar PS, Sharma A, Singhal RS (2013) Hydrophobic derivatives of guar gum hydrolyzate and gum Arabic as matrices for microencapsulation of mint oil. *Carbohydr Polym* 95:177–182
- Schmidt US, Schmidt K, Kurz T, Endreß H-U, Schuchmann HP (2015) Pectins of different origin and their performance in forming and stabilizing oil-in-water-emulsions. *Food Hydrocolloids* 46:59–66
- Schmidt US, Schütz L, Schuchmann HP (2017) Interfacial and emulsifying properties of citrus pectin: interaction of pH, ionic strength and degree of esterification. *Food Hydrocolloids* 62:288–298



- Schmitt C, Turgeon SL (2011) Protein/polysaccharide complexes and coacervates in food systems. *Adv Colloid Interface Sci* 167:63–70
- Schmitt C, Aberkane L, Sanchez C (2009) Protein-polysaccharide complexes and coacervates. In: Phillips GO, Williams PA (eds) *Handbook of hydrocolloids*, 2nd edn. Woodhead Publishing, Oxford, pp 420–476
- Schultz M (2010) Industry requirements for hydrocolloids in beverage emulsions. In: Phillips GO, Williams PA (eds) *Gums and stabilisers for the food industry 15*. Royal Society of Chemistry, Cambridge, pp 257–266
- Schultz M, Ringgenberg R (2008) Emulsifying flavours into beverages. *Foods Food Ingredients J Jpn* 213:206–214
- Shepherd GM (2006) Smell images and the flavour system in the human brain. *Nature* 444:316–321
- Shi Y, Li C, Zhang L, Huang T, Ma D, Tu Z-c, Wang H, Xie H, Zhang N-h, Ouyang B-l (2017) Characterization and emulsifying properties of octenyl succinate anhydride modified *Acacia seyal* gum (gum arabic). *Food Hydrocolloids* 65:10–16
- Sillick M, Gregson C (2010) Critical water activity of disaccharide/maltodextrin blends. *Carbohydr Polym* 79:1028–1033
- Silva DF, Favaro-Trindade CS, Rocha GA, Thomazini M (2012) Microencapsulation of lycopene by gelatin–pectin complex coacervation. *J Food Process Preserv* 36:185–190
- Singh SS, Bohidar HB, Bandyopadhyay S (2007) Study of gelatin–agar intermolecular aggregates in the supernatant of its coacervate. *Colloids Surf B* 57:29–36
- Snyder D, Zhang J (2017) High load flavor particles. WO Patent Application 2017203006
- Soottitawat A, Partanen R, Neoh TL, Yoshii H (2015) Encapsulation of hydrophilic and hydrophobic flavors by spray drying. *Jpn J Food Eng* 16:37–52
- Subramaniam A, Veazey RL, Schober A, Rada A, Rong Y, van Sleetuwen RMT, Golding R, Zhang S, Normand V (2013) Orange oil stability in spray dry delivery systems. *Carbohydr Polym* 97:352–357
- Sweedman MC, Tizzotti MJ, Schäfer C, Gilbert RG (2013) Structure and physicochemical properties of octenyl succinic anhydride modified starches: a review. *Carbohydr Polym* 92:905–920
- Tackenberg MW, Kleinebudde P (2015) Encapsulation of liquids via extrusion - a review. *Curr Pharm Des* 21:5815–5828
- Tackenberg MW, Thommes M, Schuchmann HP, Kleinebudde P (2014) Solid state of processed carbohydrate matrices from maltodextrin and sucrose. *J Food Eng* 129:30–37
- Tackenberg MW, Krauss R, Schuchmann HP, Kleinebudde P (2015a) Encapsulation of orange terpenes investigating a plasticisation extrusion process. *J Microencapsul* 32:408–417
- Tackenberg MW, Krauss R, Marmann A, Thommes M, Schuchmann HP, Kleinebudde P (2015b) Encapsulation of liquids using a counter rotating twin screw extruder. *Eur J Pharm Biopharm* 89:9–17
- Taylor AJ, Linforth RST (2001) Modelling flavour release through quantitative structure property relationships (QSPR). *Chimia* 55:448–452
- Tedeschi C, Leuenberger B, Ubbink J (2016) Amorphous-amorphous phase separation in hydrophobically-modified starch-sucrose blends I. Phase behavior and thermodynamic characterization. *Food Hydrocolloids* 58:75–88
- Teunou E, Poncelet D (2002) Batch and continuous fluid bed coating - review and state of the art. *J Food Eng* 53:325–340
- Thies C (2007) Microencapsulation of flavors by complex coacervation. In: Lakkis JM (ed) *Encapsulation and controlled release technologies in food systems*. Blackwell Publishing, Oxford, pp 149–170
- Tizzotti MJ, Sweedman MC, Schäfer C, Gilbert RG (2013) The influence of macromolecular architecture on the critical aggregation concentration of large amphiphilic starch derivatives. *Food Hydrocolloids* 31:365–374
- Trubiano PC (1995) The role of specialty food starches in flavour emulsions. In: Ho C-T, Tan C-T, Tong C-H (eds) *Flavor technology – physical chemistry, modification, and process*, ACS Symposium Series 610. American Chemical Society, Washington, pp 199–209

- Turchiuli C, Dumoulin E (2013) Aroma encapsulation in powder by spray drying, and fluid bed agglomeration and coating. In: Yanniotis S, Taoukis P, Stoforos N, Karathanos V (eds) *Advances in food process engineering research and applications*. Food Engineering Series. Springer, Boston, pp 255–265
- Ubbink J (2013) Flavour delivery systems. In: Kirk-Othmer encyclopedia of chemical technology. Wiley Online Library. <https://doi.org/10.1002/0471238961.0612012221020209.a01.pub2>, John Wiley & Sons
- Uhlemann J, Reiß I (2010) Product design and process engineering using the example of flavors. *Chem Eng Technol* 33:199–212
- Uhlemann J, Schleifenbaum B, Bertram H-J (2002) Flavor encapsulation technologies: an overview including recent developments. *Perfumer Flavorist* 27:52–61
- van Ruth S, Roozen JP (2010) Delivery of flavours from food matrices. In: Taylor AJ, Linforth R (eds) *Food flavour technology*, 2nd edn. Blackwell Publishing, Oxford, pp 190–206
- Verkempinck SHE, Kyomugasho C, Salvia-Trujillo L, Denis S, Bourgeois M, Van Loey AM, Hendrickx ME, Grauwet T (2018) Emulsion stabilizing properties of citrus pectin and its interactions with conventional emulsifiers in oil-in-water emulsions. *Food Hydrocolloids* 85:144–157
- Viswanathan A (1999) Effect of degree of substitution of octenyl succinate starch on the emulsification activity on different oil phases. *J Environ Polym Degrad* 7:191–196
- Wang K, Arntfield SD (2017) Effect of protein-flavour binding on flavour delivery and protein functional properties: a special emphasis on plant-based proteins. *Flavour Fragrance J* 32:92–101
- White DR Jr, Hudson P, Adamson JT (2003) Dextrin characterization by high-performance anion-exchange chromatography-pulsed amperometric detection and size-exclusion chromatography-multi-angle light scattering-refractive index detection. *J Chromatogr A* 997:79–85
- Wieland RB, Soper CJ (2008) Encapsulation method. WO 2006119660 A1
- Williams PA, Phillips GO (2009) Gum arabic. In: Phillips GO, Williams PA (eds) *Handbook of hydrocolloids*, 2nd edn. Woodhead Publishing, Oxford, pp 252–273
- Williams PA, Sayers C, Viebke C, Senan C, Mazoyer J, Boulenguer P (2005) Elucidation of the emulsification properties of sugar beet pectin. *J Agric Food Chem* 53:3592–3597
- Wright J (2010) Creating and formulating flavours. In: Taylor AJ, Linforth R (eds) *Food flavour technology*, 2nd edn. Blackwell Publishing, Oxford, pp 1–23
- Xiao Z, Liu W, Zhu G, Zhou R, Niu Y (2014) A review of the preparation and application of flavour and essential oils microcapsules based on complex coacervation technology. *J Sci Food Agric* 94:1482–1494
- Yadav MP, Johnston DB, Hicks KB (2009) Corn fiber gum: new structure/function relationships for this potential beverage flavour stabilizer. *Food Hydrocolloids* 23:1488–1493
- Yang N, Linforth RST, Walsh S, Brown K, Hort J, Taylor AJ (2011) Feasibility of reformulating flavours between food products using in vivo aroma comparisons. *Flavour Fragrance J* 26:107–115
- Yeo Y, Bellas E, Firestone W, Langer R, Kohane DS (2005) Complex coacervates for thermally sensitive controlled release of flavor compounds. *J Agric Food Chem* 53:7518–7525
- Yeo L, Thompson DB, Peterson DG (2016) Inclusion complexation of flavour compounds by dispersed high-amylose maize starch (HAMS) in an aqueous model system. *Food Chem* 199:393–400
- Zasytkin D, Porzio M (2004) Glass encapsulation of flavours with chemically modified starch blends. *J Microencapsul* 21:385–397
- Zhao S, Gao W, Tian G, Zhao C, Dimarco-Crook C, Fan B, Li C, Xiao H, Lian Y, Zheng J (2018a) Citrus oil emulsions stabilized by citrus pectin: the influence mechanism of citrus variety and acid treatment. *J Agric Food Chem* 66:12978–12988
- Zhao S, Tian G, Zhao C, Lu C, Bao Y, Liu X, Zheng J (2018b) Emulsifying stability properties of octenyl succinic anhydride (OSA) modified waxy starches with different molecular structures. *Food Hydrocolloids* 85:248–256

Zhou Y, Yin X, Chen J, Feng D, Zhu L (2018) Encapsulation efficiency and release of citral using methylcellulose as emulsifier and interior wall material in composite polysaccharide microcapsules. *Adv Polym Technol* 37:3199–3209

# Chapter 11

## Encapsulation and Targeted Release



Bin Liu, Lulu Jiao, Jingjing Chai, Cheng Bao, Ping Jiang, and Yuan Li

**Abstract** This chapter described the definition of encapsulation and food delivery systems/food carriers, benefits for encapsulation, and various delivery systems classified by structure and function. Firstly, the classification of food bioactive compounds and the reason for encapsulation were discussed. Later, the structure classified delivery systems of core–shell carriers, Pickering emulsions, complex coacervates, gels, and self-assemblies of cross-linked biopolymer were described. Due to the delivery of bioactive compounds via the oral route is restricted by various physiological barriers including harsh gastrointestinal (GI) pH conditions, enzymes in GI, the mucus layer, and the epithelium, intelligent delivery systems are promising strategies to protect bioactive molecules from degradation and improve their bioavailability. Then the novel intelligent carriers that are responsive to the oral route, pH, enzymes, and cell receptors were discussed. Next, the cellular uptake mechanisms of food carriers were summarized and analyzed. In addition, the gastrointestinal in vitro and in vivo models to evaluate the function of the carriers were compared, and the applications of carriers in different types of food were reviewed and analyzed. Finally, the future design and development trends and practical applications of the carriers are prospected. This comprehensive multidisciplinary chapter provides useful guidelines and inspirations for the design of intelligent carrier systems, which were exploited for the encapsulation of bioactive compounds and improving their low solubility, poor stability, and low bioavailability during the processing, storage, and orally uptake.

**Keywords** Intelligent delivery systems · Food colloid-based carriers · Encapsulation · Food bioactive compounds · Bioavailability

---

B. Liu · L. Jiao · J. Chai · C. Bao · P. Jiang · Y. Li (✉)  
College of Food Science and Nutritional Engineering, China Agricultural University, Beijing,  
People's Republic of China  
e-mail: [yuanli@cau.edu.cn](mailto:yuanli@cau.edu.cn)

## 1 Introduction

Great attention has been paid to bioactive compounds derived from foods over the past few decades since they may be beneficial to the health by decreasing the risks of numerous disorders, including obesity, cancer, diabetes, and cardiovascular diseases (CVDs) (Oh 2016). Such beneficial effects can be attributed to their effects against inflammation, cancer, oxidation, hypertension, and hyperlipidemia, apart from the fundamental nutritional effects. Such food-originated bioactive compounds cover phytochemicals (Velderrain-Rodríguez et al. 2014), proteins (Dhaval et al. 2016), bioactive peptides (Dhaval et al. 2016), vitamins (Katouzian and Jafari 2016), bioactive polysaccharides (PLS, Jiang et al. 2016), and fatty acids (FAs, Kruk et al. 2016). Such compounds show high sensitivity to diverse environmental stimuli, including heat, light, oxygen, and low pH in the processing and storage processes (Gleeson et al. 2016). Besides, more efforts should be made to manage the problems occurring when bioactive ingredients are administered orally. For instance, some consumers discover the unpleasant flavor of certain bioactive ingredients when they are administered orally. Besides, hydrophobic compounds are poorly soluble, which greatly prevents them from being dissolved into the water medium and absorbed in the gastrointestinal tract of human body. However, such compounds are unstable in the processing and storage conditions (like heat, oxygen, and light exposure), which decreases their functional efficiency. Generally, many of the bioactive ingredients display low absorption rates via small intestinal epithelium. Foods will be digested and degraded in acidic environment by a variety of enzymes (pepsin, amylase, pancreatin) and by the mucus barriers that cover the GI tract luminal epithelium (Chen et al. 2011). Besides, only limited food ingredients can diffuse through the intestinal mucus or permeate across the intestinal epithelium, which has seriously impeded their bioavailability. On the other hand, food ingredients can hardly be absorbed by cells even though they permeate the intestinal mucus. Only limited polyphenols can be absorbed in cells based on the carrier-regulated transport, which is related to the mechanism of “multiple-drug resistance”. There are multiple glycoprotein efflux pumps on epithelial cells, which function to pump the polyphenols absorbed back to intestinal lumen (Chan et al. 2004).

For overcoming the above-mentioned problems, a number of delivery systems based on food colloids are synthesized, which can mask the unpleasant compound taste, dissolve the hydrophobic compounds in water through combining them in the food hydrocolloid milk protein microcapsules, protect against the harmful environment, and improve the permeability across the epithelial and intestinal mucus (Livney 2010). Numerous micro/nanocapsules delivery systems constructed based on food colloids are able to resist the decomposition of bioactive ingredients in GI tract. The above-mentioned systems have different structures and sizes and are utilized to change the cargo release kinetics as well as target delivery to typical sites. Certain carriers that can penetrate the intestinal mucus are able to rapidly transport bioactive ingredients through intestinal mucus, as a result, they are markedly absorbed to the systemic circulation when they are administered orally

(Lundquist and Artursson 2016). Nonetheless, certain carriers prepared by mucoadhesive biomaterials will increase the compound retention time in intestines and elevate the corresponding local concentrations near epithelial cell surface (Saura-Calixto et al. 2007). Recently, delivery systems synthesized based on food colloids become more and more functionalized. But to obtain the more intelligent carriers, factors including oral cavity responsiveness, enzymes, intestinal pH, overcoming of intestinal mucus barriers, and physiological biorecognition must be taken into account in the design of a sophisticated delivery system. The compound food hydrogels coacervation system has been synthesized to deliver flavor compounds orally, so as to extend the food retention time and to elevate the sensory perception (Zhang et al. 2015). Layer-by-layer carriers based on polysaccharide hydrogel can respond to intestinal pH, which prevent the decomposition of encapsulated compounds and release these compounds into small intestine (Shi et al. 2017). Polysaccharide/polyaminoacid hydrogel for colon-specific delivery systems assists in the release of encapsulated compounds by means of the colonic dextranase-mediated degradation (Casadei et al. 2008). For carriers responsive to receptor that target the intestinal cells, they markedly enhance the absorption of encapsulated compounds by cells (Tian et al. 2016). Besides, the food hydrocolloid soy/milk liposomes that can penetrate the intestinal mucus efficiently promote cargo absorption because they can rapidly penetrate the mucus barriers to reach the epithelial cells (Li et al. 2017a). In comparison, the mucoadhesive carriers constructed based on food colloid can interact with mucus, thus realizing the extended release of the encapsulated compounds (Sheng et al. 2015). As a result, the intelligent delivery systems synthesized based on food colloids become more and more important, which offer the efficient platforms to apply these bioactive ingredients in food industry and to promote their effects and bioavailability.

## 2 The Encapsulation Technology Developed for Sensitive Bioactive Compounds

### 2.1 *Factors Influencing the Stability and Bioavailability of Bioactive Compounds*

The most important types of bioactive compounds were summarized in Fig. 11.1 (Taiz et al. 2015; Bao et al. 2019). As shown in Fig. 11.1, the bioactive ingredients displayed include bioactive peptides (casein, carnosine,  $\alpha$ -lactalbumin, angiotensin-converting enzyme (ACE)), polyunsaturated fatty acids (PUFAs, such as EPA, ARA, DHA), bioactive polysaccharides (grifolan, lentinan), polyphenols (resveratrol, curcumin, tea polyphenols, anthocyanin, quercetin), minerals (Ca, Fe, Zn), vitamins (VB<sub>6</sub>, VC, VD, VE), and others including isoflavone, carotenoids, isothiocyanates, sitosterol, alkaloids, terpenes, and lignin (not presented in Fig. 11.1) (Taiz et al. 2015). Such bioactive ingredients are suggested to be

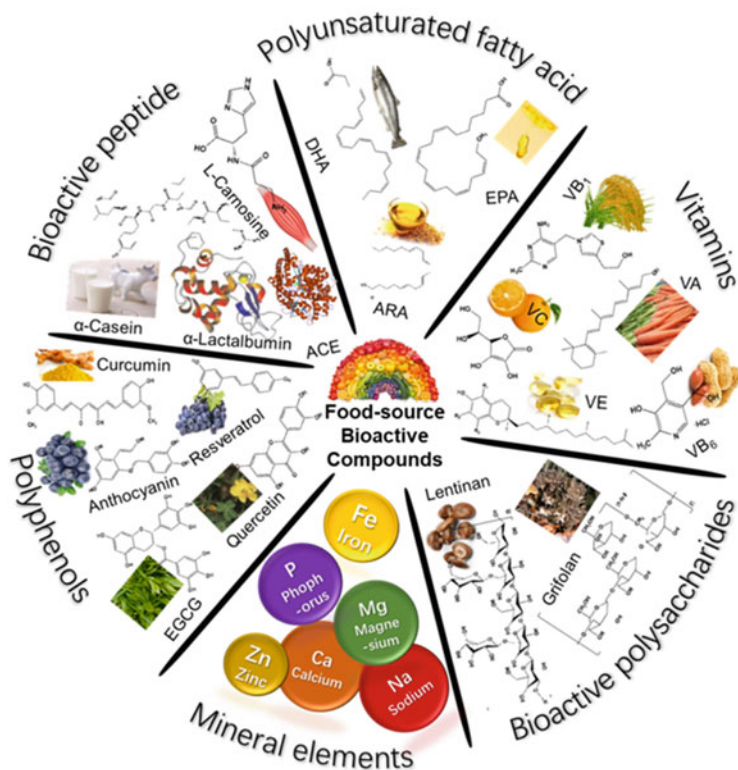


**Fig. 11.1** Overview of food-sourced bioactive compounds. Important types of bioactive ingredients were summarized, including polyphenols (e.g., curcumin, resveratrol, epigallocatechin gallate (EGCG), quercetin, anthocyanin), polyunsaturated fatty acid (e.g., docosahexaenoic acid (DHA), eicosapentaenoic acid (EPA), arachidonic acid (ARA)), vitamins (e.g., vitamin C (VC), vitamin A (VA), vitamin E (VE)), bioactive polysaccharides (e.g., lentinan, grifolan), bioactive peptides (e.g.,  $\alpha$ -casein, L carnosine,  $\alpha$ -lactalbumin) and mineral elements (e.g., Zn, Fe, Mg, Ca, Na, P) (Bao et al. 2019). Reproduction with permission from (Bao et al. 2019), Copyright 2020 ELSEVIER. Order Number: 4958630740831

beneficial to human health (Table 11.1). For instance, flavonoids including apigenin and quercetin show potent antitumor activities (Batra and Sharma 2013); omega-3 PUFAs can be adopted to reduce the risk of cardiovascular diseases (CVDs) (Richard et al. 2009); carotenoids like astaxanthin and  $\beta$ -carotene can scavenge the free radicals (Nagao 2009); while bioactive polypeptides including peptidyl dipeptidase A have antihypertensive effect (Corvol et al. 1995); and the plants- and algae-derived polysaccharides have excellent anti-inflammatory activity (Liu et al. 2015a).

Food nutraceuticals can hardly be adsorbed by cells, which has severely affected their bioavailability in vivo because their absorption in the human body is only achieved when they penetrate the GI barriers. In addition, numerous environmental stimuli have affected the stability of bioactive ingredients. This section analyzed the vital factors that affected bioactive ingredient absorption, as displayed in Table 11.1.

**Table 11.1** The summary of physiological function, absorption mechanisms, and environmental influencing factors for bioactive compounds including vitamins, polyphenols, polypeptides, polysaccharides, and unsaturated fatty acids. Reproduction with permission from (Bao et al. 2019), Copyright 2020 ELSEVIER. Order Number: 4958630740831

Bioactive compounds	Function	Influence Factors	Absorption mechanisms in small intestine	Ref.
$\beta$ -Carotene	Antioxidant, anticancer, immune enhancement and anti-obesity activities, prevention of cardiovascular diseases	Light, heat	By passive diffusion and/or transporter-mediated processes	(Wang 1994)
Omega-3 polyunsaturated fatty acid	Essential for humans and animals to treat and prevent atherosclerosis and cardiovascular diseases	Heat, light	Carrier-mediated transport	(Yang et al. 2017)
Quercetin	Prevention of oxidative stress-related chronic diseases	Heat, alkali	Passive diffusion and/or transporter-mediated processes	(Day et al. 2003)
Curcumin	Antioxidant, anti-inflammatory, anticancer, antiviral, and antibacterial activities	Heat, light, Fe	Passive diffusion, P-glycoprotein pump-mediated transportation	(Wang et al. 2017)
Resveratrol	Anticancer, antioxidant, antiaging, anti-frailty, anti-inflammatory, anti-allergenic activities	Heat, light	Passive diffusion and/or transporter-mediated processes	(Gambini et al. 2015)
Vitamin D	Facilitating calcium absorption to build-up bone preventing cancer and cardiovascular diseases	Light, acid	Passive diffusion and/or receptor-mediated transport	(Reboul et al. 2011)
Vitamin C	Action as coenzyme or prosthetic group which is important to metabolic activity of human body	Heat, light, humidity	Na <sup>+</sup> -dependent transporters-mediated transportation	(Bianchi et al. 1986)
Vitamin A	Essential to the formation of visual chromophore and hormone which maintain the vision and promote body growth; strengthen immunity and scavenge free radicals	Light, acid, heat, humidity	As the form of retinol via the chylomicron/lymphatic route or flowed into the portal vein circulation by the lipid transporter	(Harrison 2012)

(continued)



**Table 11.1** (continued)

Bioactive compounds	Function	Influence Factors	Absorption mechanisms in small intestine	Ref.
Vitamin E	Antioxidant, anticancer, antiaging activity	Heat, light, humidity	Passive diffusion, receptor-mediated transport	(Reboul 2017)
Casein peptides	Lowering the blood pressure by angiotensin-converting enzyme (ACE)-inhibitory peptides	High enzymatic degradation, short half-life	Vesicle-mediated transcellular transport	(Shen and Matsui 2017)
Soybean $\beta$ -Conglycinin	Anti-hypocholesterolemic, anti-hypoglycemic, antioxidant, and prebiotic effects	Easy oxidation, easy hydrolysis	Carrier-mediated transport, receptor-mediated transport	(Chen et al. 1995)
Astragalus polysaccharides	Triggering non-specific reaction of the immune system, and have antimicrobial, anti-hypocholesterolemic, anti-hypoglycemic antioxidant, and prebiotic effects	Stickiness, low solubility	Carrier-mediated transport, passive diffusion	(Cheng et al. 2011)
Fungal polysaccharides	Immunomodulating, anticancer, antimicrobial, hypocholesterolemia, hypoglycemic, and health-promoting properties	Heat, light, humidity	Clathrin-mediated endocytosis	(Giavasis 2014)

First of all, a variety of environmental stimuli can affect the bioactive ingredient stability, like light, strong acid, oxygen, and heat. For instance, carotenoids have antioxidant ability, which is achieved by the active conjugated double bonds that can be oxidized and broken easily (Wang 1994). Moreover, the interactions between carotenoids and other food ingredients, like fats and proteins, can decrease their antioxidant ability (Ranhotra et al. 1995). Curcumin shows high sensitivity to heat, light, and acid, since they are three tightly associated lipophilic moieties constituted by certain double bonds and phenolic groups (Heger et al. 2014). On the other hand, the harsh GI tract environment is also a major factor that affects bioavailability. For instance, the degradation rates of hydroxycinnamoyl acid and flavonoids are 80% and 84% in the *in vitro* GI tract, while that of vitamin C is 91% under intestinal digestion conditions (Vallejo et al. 2004). Further, digestive enzymes, like trypsin in intestine and pepsin in stomach, are also able to decompose peptides and proteins, resulting in the decreased activity (Layer and Gröger 1993). Particularly, the

bioactive ingredients are digested or broken before they can exert their functions. Therefore, digestion in GI tract also represents a physiological barrier that should be managed to improve ingredient uptake. Mucus layer is the last barrier of absorption, and it covers the surface of the whole GI tract. Mucus is mainly made up of lipids, glycoproteins, along with the sloughed cellular materials (Abdulkarim et al. 2015). It may serve as an intelligent semipermeable membrane, which allows for numerous nutritional substances exchange in the meantime of preventing pathogen or bacterium permeation onto the surfaces of epithelial cells (Cone 2009). Nonetheless, only little amount of food ingredients can penetrate the mucus, which possibly suppresses the availability and absorption of these compounds in enterocytes. Typically, hydrophobic bioactive ingredients have been reported to interact with mucin proteins, thereby slowing down their penetration across the mucus (Liu et al. 2015b).

In this regard, it is of great necessity to design a measure for managing the above problems (Li et al. 2015b). Encapsulation technique has been developed rapidly, and used widely applied in many areas such as pharmaceutical and food industries. In food industries, encapsulation refers to the process where core material microparticles are packed in the wall material for the formation of capsules. Encapsulation means to isolate the active ingredients in food products with the building blocks of food-grade biopolymers, and it is identified as an efficient approach for masking the unpleasant taste and improving stability and solubility of orally administered functional ingredients. In the field of food industry, encapsulation systems have been widely used for solving the formulation issues induced by the low active ingredient stability (incompatibility of the active ingredients with the food matrix), or for controlling active ingredient release or improving the nutrient bioavailability (Ubbink and Krüger 2006). The encapsulation approach is used for protecting bioactive compounds (micronutrients, nutraceuticals, polyphenols, antioxidants, and enzymes), protecting these compounds from the harsh environment during the finished applications, and controlling cargo release at specific sites. The encapsulation technology is adopted in food industry for maintaining excellent properties and quality, including taste, texture, water solubility, stability, and color strength in the processing and storage processes. For bioactive compounds, their absorption rate is tightly associated with the water solubility, but most of them are hydrophobic, giving rise to the poor absorption in GI tract. At present, the Pickering emulsions, complex coacervates, cross-linked polymer gels, core-shell-structured microcapsules, together with the self-assembled structures, have been extensively utilized for enhancing the stability, bioavailability, and water solubility of the encapsulated compounds (Fig. 11.2). The important food delivery systems based on encapsulation techniques classified by structure are presented in the section below.

## ***2.2 The Food Delivery Systems Classified by Structure***

The delivery systems for food bioactive compounds played a vital part in the food sector. Natural biopolymers, including lipids, proteins, and polysaccharides, are

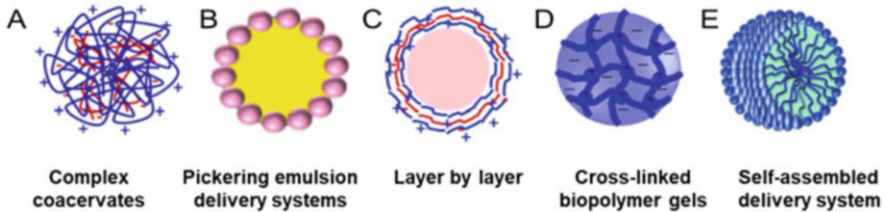


**Fig. 11.2** The delivery systems classified by their building structures including (a) complex coacervates capsules, (b) Pickering emulsion delivery systems, (c) core-shell capsules made by layer-by-layer techniques, (d) cross-linked polymer gels, and (e) self-assembled nanocapsules (Bao et al. 2019). Reproduction with permission from (Bao et al. 2019), Copyright 2020 ELSEVIER. Order Number: 4958630740831

often used as wall materials for preparing novel capsules. The food delivery systems can be built by various structures such as Pickering emulsions, complex coacervates, cross-linked biopolymer gels, core-shell-structured microcapsules, along with the self-assembled structures (Fig. 11.2). Those carriers will be discussed in this section.

### 2.2.1 Complex Coacervates

Two Dutch physicists named Kruyt and Bun Enberg de Jong created the term of “complex coacervate” for discriminating it from the one-single polymer coacervate. Complex coacervate stands for the phenomenon where phase separation occurs when two polymers with opposite charges are added into water (Sing 2017). The formation of complex coacervates was driven by the discharge of counterions with low molecular weight (MW) that conjugated with charged groups on large molecules and entropy gained during this process (Pergushov et al. 2012). Typically, the most extensively synthesized complex coacervates consist of proteins with positive charges and polysaccharides with negative charges (De Kruif et al. 2004). Among the earliest diverse polysaccharides with negative charges, acacia gum (AG) is involved in the coacervation with  $\beta$ -lactoglobulin ( $\beta$ -lg) with positive charges (Schmitt et al. 2001).

Complex coacervates can form the insoluble films that may be additionally synthesized as microcapsules. Many studies have been conducted to investigate the delivery systems constructed based on the protein-polysaccharide complex coacervates. The casein hydrolysate was encapsulated in complex coacervation formed by soybean protein isolate (SPI)/pectin (Mendanha et al. 2009), of which the solubility and stability were improved, and the bitter taste was masked. It is also reported that, the whey protein isolates (WPI)-GA complex coacervate can be utilized for the encapsulation of *L. paracasei subsp. paracasei* in yogurts without changing the texture. It is an efficient carrier used to deliver probiotics to the intestine (Bosnea et al. 2017). According to the above studies, complex coacervate is a candidate food carrier to improve bioactive components for their stability. The

charge screening effect of the 150 nM physiological salt can result in complex coacervates capsule dissociation, while cross-linking can manage such problem.

### 2.2.2 Pickering Emulsion Delivery Systems

In recent years, wide attention has been paid to the particle-stabilized Pickering emulsions at food grade because of their excellent colloidal stability. To be specific, Pickering emulsions are stabilized with the solid colloidal particles but not the biopolymers or small molecular surfactants. Those particles utilized for stabilizing Pickering emulsions should be partially wetted by the aqueous and oil phases (Chevalier and Bolzinger 2013). There is a contact angle  $\theta$  for the colloidal particles absorbed onto the interface between oil and water for characterizing solid particle wettability. The contact angle of water-in-oil (W/O) emulsions produced in the presence of residual hydrophobic particles in oil phase is over  $90^\circ$ ; on the contrary, that of oil-in-water (O/W) emulsions produced in the presence of residual hydrophilic particles mainly in aqueous phase is  $<90^\circ$  (Binks 2002; Williams et al. 2014). Typically, emulsions stabilized by colloidal particles are extensively investigated to examine whether they can be utilized as the delivery systems of food ingredients, and they are usually classified as 3 types: (1) polysaccharides with hydrophobic modification: the nanospheres constructed based on amphiphilic starch are suggested to be effective on stabilizing Pickering emulsions (Tan et al. 2012). Besides, both modified starch (MS) and microcrystalline cellulose (MCC) are utilized for preparing the highly stable Pickering emulsions. Additionally, compared with MS particles, the MCC particles can better improve the lipid stability to resist oxidation, since they can produce a thick layer surrounding oil droplets, thus preventing lipid oxidization (Kargar et al. 2012). The vitamin E (VE as in L283) stability is suggested to be markedly improved when it is encapsulated to the modified tapioca starch nanocapsules. At 60 days after storage under the temperature of  $35^\circ\text{C}$ , the vitamin E retention rate is about 1/2 of the original value (Hategekimana et al. 2015). (2) Pickering particles prepared based on protein: specifically, zein, the plant protein with water insolubility, is used for stabilizing Pickering emulsions. Feng and colleagues used sodium caseinate (NaCas) to modify zein nanoparticles (NPs) on the surface, and discovered that the resultant nanocomplexes performed better in stabilizing the O/W Pickering emulsions relative to the unmodified ones (Feng and Lee 2016). (3) Miscellaneous Pickering particles: Colloidal particles can be utilized to stabilize the colloidosome-based Pickering emulsions by using those self-assembled particles at the interfaces, and the modified products show superb embedding together with controlled-release characteristics. Curcumin is encapsulated into the chitosan-tripolyphosphate NPs-stabilized Pickering emulsions (Shah et al. 2016). As a result, the Pickering emulsions become the prospective systems used to engineer the functional interfaces within the food emulsions. They show relative anti-coalescence stability because the Pickering particles have great desorption energy. However, it requires a long time for the equilibration of the rigid Pickering particles shell in the process of production, making it difficult to obtain emulsion with expected droplet

size (Berton-Carabin and Schroën 2015). For solving the above problems, soft particles including whey protein nanogels can be adopted to be the emulsifiers to make emulsions, which is a novel way to generate the uniform size of emulsion droplets (Wu et al. 2015).

### 2.2.3 Core-Shell Microcapsules Delivery System Prepared by Layer-by-Layer Technique

As the novel colloidal structure in the encapsulation and controlled release of bioactive ingredients, the multilayer microparticles synthesized by the layer-by-layer (LbL) assembly technology have received wide attention (Tong et al. 2012). Notably, the LbL deposition approach forms a specific structure that has tailored functionality on the basis of weak interaction across the interacting polymers (Costa and Mano 2014). The LbL assembly approach has been utilized to prepare the three-layered microcapsules with the use of octenyl succinic anhydride (OSA)-starch, soy protein isolate, and chitosan as the wall materials. Three-layer microcapsules display reduced encapsulation rate in comparison with the one- or two-layer counterparts, but they show the procedural controlled-release behavior (Noshad et al. 2015). The poly (L-glutamic acid) (PLGA) with negative charges and poly (L-lysine) (PLL) with positive charges were assembled onto the oxidized starch microgel particle surfaces through the LbL assembly technology, and the resultant PLL/PLGA-coated starch microgels are found to efficiently reduce lysozyme release within the 0.05 M NaCl solution, which also prevent gel particle degradation via the action of  $\alpha$ -amylase (Li et al. 2012). Nonetheless, there may be certain drawbacks, like the difficulties in regulating the synthesis process usually accompanied with aggregation, and assembly dissociation because of salt sensitivity, which have restricted their applications (Guzmán et al. 2017). Besides, the introduction of other inter-layer covalent cross-links may stabilize the LbL structure (Han et al. 2017).

### 2.2.4 Cross-Linked Biopolymer Gels

Polymer gels can be produced through the intermolecular or intramolecular biopolymer cross-links connected based on polymer chains. In general condition, both physical (non-covalent bonds) and chemical (covalent bonds) cross-links can be used to form biopolymer network. Of them, chemical cross-linking is extensively utilized in various fields, such as microsphere preparation, double-layer cross-linking, and food starch modification. The modified food starch using sodium tripolyphosphate (STPP) combined with sodium trimetaphosphate (STMP) in the alkaline environment has enhanced activity of  $\alpha$ -amylase to restrict swelling and to resist decomposition (Woo and Seib 2002). Further, the introduction of transglutaminase at food grade into the gelatin-maltodextrin microspheres leads to superb activity in the protection of probiotic lactic acid bacteria that are subjected to the simulated GI tract environment (Nawong et al. 2016).

In potato starch, the TEMPO ((2,2,6,6-Tetramethylpiperidin-1-yl)oxyl)-oxidation can be applied in the selective oxidation of primary alcohol groups located at the sixth position in hexose unit to the carboxyl groups. Such method achieves a controlled oxidation degree of 30–100%, and the resultant toxicity is negligible (Li et al. 2009; Jiang et al. 2018). For the charged neutral polysaccharides, such an oxidation process can enhance the controlled-release property and charge density (Li et al. 2011). For instance, for oxidized starch microgels cross-linked with STMP, they exhibit a great loading capacity for anthocyanins (Wang et al. 2013) and proteins with positive charges (Zhao et al. 2015a). Besides, they can regulate  $\beta$ -carotene release especially under the intestinal conditions (Wang et al. 2015a, b). Oxidized starch microgels cross-linked with glycerol diglycidyl ether are reported to regulate lysozyme release and uptake (Zhao et al. 2015a). In addition, the oxidized konjac glucomannan microspheres are synthesized through the cross-linking of  $\text{Fe}^{3+}$  (Chen et al. 2014; Chen et al. 2016), and they may be decomposed and release anthocyanins in sequence under the intestinal conditions (Lu et al. 2015). As the non-covalent cross-linker, tannic acid has been utilized for preparing the hollow zein NPs that have enhanced resistance to the simulated intestinal digestion compared with the non-crosslinked samples. But, cross-linked polymers are linked with the disadvantage of absorption of excessive water, while this is undesired in food processing. In some cases, the cross-linking agents will develop side reactions with bioactive compounds existing within the hydrogel matrix (Maitra and Shukla 2014). Further, these compounds involved may show the uncontrolled pulsed release driven by diffusion. Therefore, a more controllable and cleaner process of cross-linking should be developed in the near future.

### 2.2.5 Self-Assembled Delivery Systems

Recently, wide attention has been paid to the self-assembly based delivery systems (Song et al. 2015). Self-assembly occurs spontaneously, which helps to organize the biopolymers to micro/nanostructures with clear boundary by means of non-covalent interactions (such as Van der Waals forces, hydrogen bonding,  $\pi$ - $\pi$  interactions, and electrostatic forces) in the absence of any other external intervention (Mendes et al. 2013). It should be noted that, this spontaneous process on the basis of the reversible and weak bonds or interactions can result in the formation of different nanostructures because of the “self-error-correcting” and “self-checking” processes controlled thermodynamically (Baek et al. 2015). For instance,  $\alpha$ -lactalbumin is partly hydrolyzed to amphiphilic peptides, which contributes to the self-assembly to nanomicelles that are 20 nm in size on average (Li et al. 2017b). The prepared nanomicelles can be used to load curcumin at the hydrophobic core and deliver curcumin to tumor sites specifically. Numerous natural biopolymers in foods, including proteins and polysaccharides, are found to generate the self-assembled structure by themselves or with additional functional molecules (Song et al. 2015).

In the case of food biopolymers, self-assembly possibly takes place under the conditions mentioned below. (1) Polysaccharides self-assembly delivery systems:

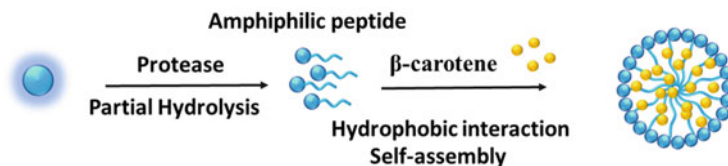


**Fig. 11.3** The illustration of micelles loaded with  $\beta$ -carotene.  $\alpha$ -Lactalbumin was partially hydrolyzed into amphiphilic peptides, which self-assembled into micelles. During this process  $\beta$ -carotene can be loaded into the micelles core via hydrophobic interaction (Du et al. 2019). Reproduction with permission from (Du et al. 2019), Copyright 2020 ELSEVIER. Order Number: 4958631460919

the self-assembled starch NPs can be used to efficiently enhance starch nanocomposite film thermostability on the basis of the short amylose (Jiang et al. 2016). It is reported that, when linoleic acid is conjugated with hydroxyethyl cellulose, a novel amphiphilic cellulose derivative can be generated, which can self-assemble to spherical nanomicelles in water. Such resultant micelles show a great efficiency in encapsulating hydrophobic components, thus enhancing the  $\beta$ -carotene solubility as well as bioavailability (Yang et al. 2016). (2) Protein self-assembly delivery systems: the amphiphilic peptides acquired by the partial hydrolysis of  $\alpha$ -lactalbumin are able to self-assemble into micelles for encapsulating  $\beta$ -carotene and curcumin at the hydrophobic core (Li et al. 2017b; Du et al. 2019). The schematic illustration of  $\alpha$ -lactalbumin nanomicelles loaded with  $\beta$ -carotene was shown in Fig. 11.3 (Du et al. 2019). Besides, the negatively charged  $\alpha$ -lactalbumin nanomicelles are able to deliver multiple antioxidants such as anthocyanins and curcumin with enhanced synergistic cellular antioxidant activity (Jiang et al. 2018). When vitamin D is encapsulated into the  $\beta$ -lactoglobulin self-assembled capsules, its absorption and solubility are improved (Górska et al. 2012). (3) Liposomes: microbubbles loaded with DOX (doxorubicin)-liposome can be generated spontaneously according to the ultrasound-mediated self-assembly approach, and the resultant products can target cancer cells. On the other hand, hydrophilic polyethylene glycol (PEG) modification, ursolic acid (UA) can be successfully loaded using the soya lecithin-based self-assembled liposomes. Such self-assembled liposomes modified with PEG efficiently enhance UA stability and reduce its release (Zhao et al. 2015b). In addition, Lee and colleagues discovered that, lipid anion reverse self-assembly took place within the diluted oil through integrating the saturated phospholipid, 1,2-dimyristoyl-sn-glycero-3-phosphocholine (DMPC), and the divalent or trivalent cations. The above lipid anions are stable for few weeks, which can be utilized for encapsulating bioactive components (Lee et al. 2013). For instance, the degradation of curcumin within GI tract is prevented through liposomes encapsulation, which can markedly increase its plasma level, suggesting the promoted bioavailability and bioactivity (Takahashi et al. 2009).

To sum up, these delivery systems can serve as the candidate measures to improve the solubility, stability as well as bioavailability of bioactive components. Table 11.2 summarizes the benefits, mechanisms of formation and assessed models



**Table 11.2** Comparisons of the encapsulated compounds, mechanisms of formation, benefits, and assessed models applied in investigating the absorption and digestion behaviors of a variety of carrier systems. Reproduction with permission from (Bao et al. 2019), Copyright 2020 ELSEVIER. Order Number: 4958630740831

Structures	Encapsulated compounds	Formation mechanisms	Used models	Benefits	Ref.
Complex coacervation	$\beta$ -Carotene	Electrostatic interactions	Simulated GI fluid model	Improved stability, and antioxidant activity	(Schmitt et al. 2001)
Pickering emulsion	Vitamin E	Particles absorption at the oil–water interfaces	TIM models	Improved stability	(Williams et al. 2014)
Spray drying	Carotenoids	Atomization at an elevated temperature	TIM models	Improve solubility and stability	(Ye et al. 2010)
Layer-by-layer	Polypeptide	Weak interaction of the interacting polymers	Simulated GI fluid model	Slow down the enzymolysis	(Costa and Mano 2014)
Cross-linked biopolymer gels	$\beta$ -Carotene	Intra- or intermolecular physical or chemical cross-links of biopolymers	Cell culture models	High storage stability and improved cellular uptake	(Tian et al. 2016)
Self-assembly	Curcumin	Non-covalent interactions	Simulated GI fluid model	Improve solubility and bioavailability	(Qiu et al. 2014)
Self-assembly	Insulin	Emulsion template	Cell culture and animal models	Improve pharmacological availability	(Shan et al. 2015)

for those above technologies for diverse components. Therefore, the appropriate encapsulation technology may be screened for some compounds with diverse properties.

### 3 The Different Delivery Systems Classified by Function

Based on the above analysis, food carrier systems can be used to enhance bioactive compound stability and solubility, yet there are numerous challenges to be solved when food ingredients are delivered orally, like the ionic strength, pH, mucus barriers, and enzymes within GI tract. Such problems have great influences on carrier properties and thus the bioactive compound bioavailability. Bioaccessibility refers to the proportion of components released from the food substrate into GI tract, and this helps to facilitate the intestinal uptake (Saura-Calixto et al. 2007). Besides, bioavailability can accurately indicate the effective use of bioactive compounds



indeed absorbed via enterocytes and then entering into the blood circulation. Research on bioaccessibility mainly emphasizes the digestion *in vitro*, while bioavailability focuses on the absorption *in vivo*. For the sake of improving food ingredient oral bioavailability, more efforts are needed to develop the advanced carrier systems to deliver bioactive compounds on demand and release them at the appropriate time and site. To enhance the responsiveness to intestinal pH value, retention performance, mucus penetration, and cell absorption of bioactive compounds, it is needed to design the more advanced carriers.

In addition, the smart delivery systems for the controlled release of encapsulated compounds at suitable time and site through targeted site-specific delivery are in greater and greater demands. At the same time, oral bioavailability is markedly improved by the use of carriers that have improved mucus-penetrating capacity and increased epithelial cell absorption efficiency (Ezhilarasi et al. 2013). Based on the previous descriptions regarding the microenvironments for different parts in GI tract, the smart carriers with responsive to the GI tract (including mouth, stomach, colon, and small intestine) environmental changes should be designed (Table 11.3). Typically, the smart food delivery systems can be classified as different types based on their speciality, including pH-responsive, oral-responsive, targeted-delivery, enzyme-responsive, mucoadhesive carriers, and mucus-penetrating (Fig. 11.4) (Chai et al. 2018). Firstly, the complex coacervation system can be developed for the controlled release of flavor compounds in the mouth, so as to extend the food retention time while increasing sensory perception (Zhang et al. 2015). Besides, the intestinal pH-responsive carriers can be utilized for protecting the encapsulated compounds transported into the stomach and releasing these compounds into the small intestine when the carriers are degraded in the intestine (Garinot et al. 2007). Colon-specific carriers have been synthesized for releasing the encapsulated compounds after the carriers are degraded by the microbial enzymes in the colon including dextranase. The ligand-conjugated carriers significantly enhance cell absorption through the receptor-regulated endocytosis (Jiang et al. 2014). Mucus-penetrating carriers rapidly penetrate into the mucus barriers and reach the epithelial cells at an increased level, leading to the enhanced encapsulated compound uptake relative to the free compounds (Li et al. 2017a). Besides, mucoadhesive carriers may stay stably in the mucus for a long period and allow for the controlled release of encapsulated compounds (Sheng et al. 2015). The next section will elaborate each type of carrier.

### ***3.1 Oral-Responsive Delivery Systems***

Generally, flavor compounds include the volatile and sensitive molecules like ketones, aldehydes, or additional phytochemicals (Wu et al. 2016). The delivery technique is extensively applied in the field of flavor encapsulation for enhancing some pleasant flavors while masking the unfavorable ones. For food flavor compounds, their excessively high volatility promotes them to retain in foods for an

**Table 11.3** The comparison of structure, responsive mechanisms, and effect for various responsive delivery systems. Reproduction with permission from (Chai et al. 2018), Copyright 2020 ELSEVIER. Order Number: 4958621407796

Responsiveness	Structure	Responsive mechanisms	Effect	References
Oral responsive	Pickering emulsion Complex coacervation	Promote the stability of flavor compounds during storage. Have a burst release in the mouth triggered by amylase, temperature, or pH	Have an on-demand release in mouth. Prolong their retention time and provide the desired sensory experience	(Doyennette et al. 2014; Zhang et al. 2015)
pH responsive	Complex coacervation Spray drying Layer-by-layer Self-assembly	The structure remained contact at acidic pH but ruptured at intestinal neutral pH	Increase their stability at acidic and digestive enzymatic conditions. Prevent the early release at stomach. Specifically arrive to small intestine for further absorption	(Ezhilarasi et al. 2013; Liu et al. 2016b)
Enzyme responsive	Pickering emulsion Layer-by-layer	The wall materials such as resistant starch or konjac glucomannan can be degraded by colonic microorganism enzymes such as dextranase	Release specifically in the colon for therapy. Work as the prebiotics	(Kumar et al. 2017; Situ et al. 2014; Zeeb et al. 2015)
Receptor targeting	Cross-linked biopolymer gels	Coupling a targeting molecule at the surface of carriers, then the carriers will have an enhanced uptake via receptor-mediated endocytosis	Improve the cellular uptake as well as the absorption of bioactive compounds	(Jiang et al. 2014; Yun et al. 2013)
Mucus-Penetrating	Layer-by-layer Complex coacervation	Quickly and deeply penetrate through the mucus barriers with reduced interaction with mucin network	Transport across the epithelium and arrive to the epithelial cells for absorption and then largely enter the systemic circulation	(Iglesias et al. 2017; Lai et al. 2009)
Mucoadhesive	Layer-by-layer	Increase the interaction between the carriers and the mucus layer, then prolong the retention time of the carriers on mucus	Have a prolonged and sustained release manner	(Sheng et al. 2015; Shrestha et al. 2015)

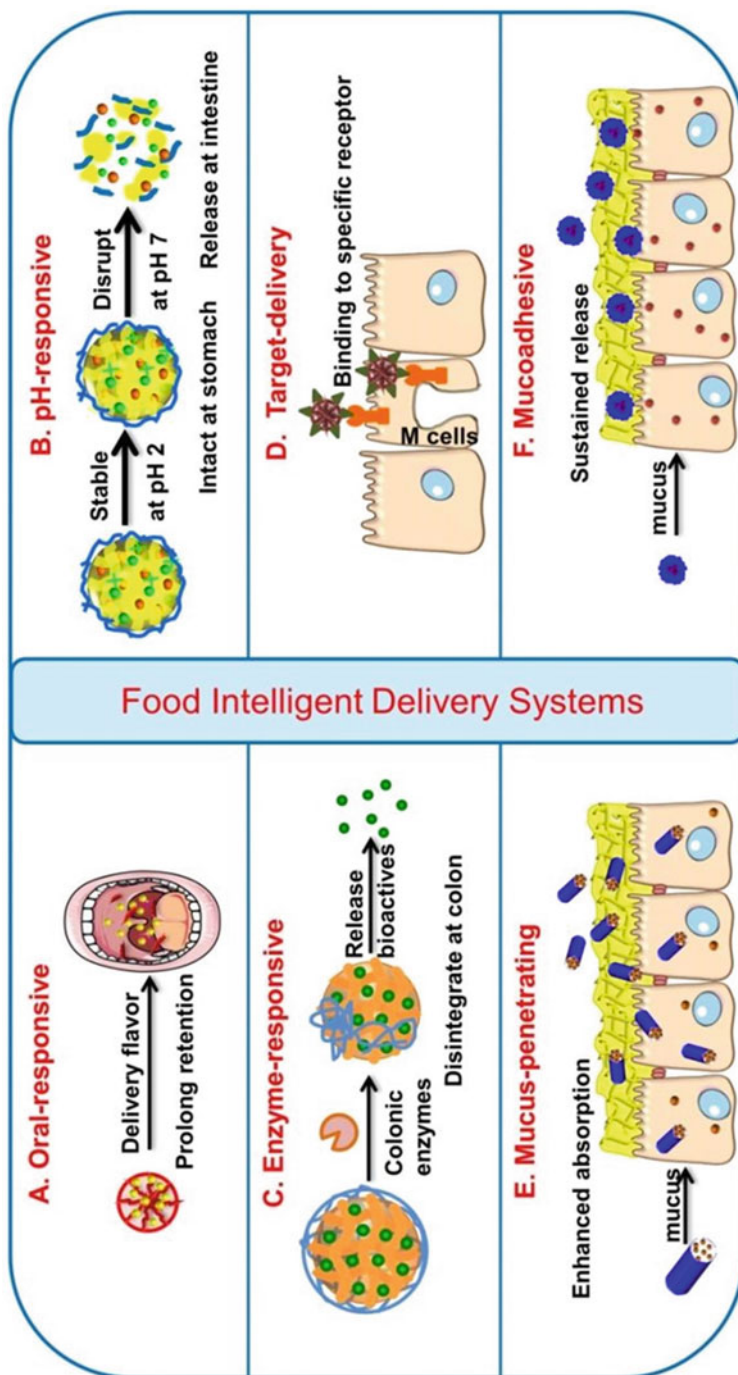


**Fig. 11.4** The illustration of various food intelligent systems. (a) Oral-responsive carriers: prolong the flavor retention; (b) pH-responsive carriers: keep stable at stomach pH but release specifically at intestinal pH 7; (c) Enzyme-responsive carriers: degraded by colonic enzymes and release specifically in colon; (d) Targeted-delivery carriers: a targeting molecule conjugated with carrier, which increases the biorecognition with the receptor at the cell surface; (e) Mucus penetrating carriers: penetrate through the mucus barriers and arrive to the epithelial cells and (f) Mucoadhesive carriers: have a sustained release manner (Chai et al. 2018). Reproduction with permission from (Chai et al. 2018), Copyright 2020 ELSEVIER. Order Number: 4958621407796

extended period. Their flavor contents may decrease because of the early release in the process of storage. Typically, encapsulation mainly aims to embed the bioactive components to the delivery systems for reducing their evaporation while enhancing chemical stability and solubility in the storage process. Meanwhile, carriers may be used to release the bioactive components at suitable sites, like in the mouth (McClements 2017). Currently, the carrier systems are put forward to encapsulate the flavor components in food substrates, which allow for the controlled and responsive release in the mouth. For example, the aromatic menthol and menthone are encapsulated to the amylose  $\alpha$ -helix by means of the hydrogen bonding, thus forming the saliva amylase-responsive starch/flavor complexes. In the process of storage before and after oral absorption, the flavor is well preserved and slowly released into the oral cavity when it is absorbed. As suggested by studies on the simulated saliva fluid release, due to the gradual hydrolysis of starch by the saliva  $\alpha$ -amylase, the aroma experiences controlled release from the complexes, which also retains for a long time in the mouth (Ades et al. 2012). Additionally, a starch-based Pickering emulsion is synthesized for encapsulating curcumin, which increases the resistance to oxygen and heat during storage. Moreover, the starch-based Pickering emulsion shows high susceptibility to  $\alpha$ -amylase within the simulated saliva fluid, resulting in the early encapsulated curcumin release (Wang et al. 2014). The multilayer emulsions stabilized by whey protein isolate (WPI)-pectin can be utilized to be the carrier for delivering the volatile flavor compounds into the mouth. In the mouth, hydrophobic volatiles, including heptanone, pentanone and ethyl butyrate, will be released. Meanwhile, the WPI and pectin with negative charges repulse each other at pH 7.0, giving rise to the weak interaction between them (Benjamin et al. 2013). McClements and colleagues used the casein/alginate complex coacervation hydrogel to encapsulate the lipophilic bioactive components. Typically, delivery systems at food grade can efficiently protect the lipid droplets in the storage process, but they will release lipid droplets in the oral cavity because the hydrogel particles are dissociated at pH 7.0 (Zhang et al. 2015). In addition, hydrogel particles constituted by caseinate and gelatine can be adopted for encapsulating the polyunsaturated lipids to resist oxidation in the process of storage, yet they can be released in the oral cavity through gelatine melting under body temperature (Zhang et al. 2015). The textural properties perceived are determined by particle size, shape, and hardness, while the palate can detect particles  $>ca$  10  $\mu$ m in size (Engelen et al. 2005). Therefore, controlling the oral delivery carriers size  $<10$   $\mu$ m is of great importance. On the other hand, the association of carriers with tongue mucus layer must also be considered.

Moreover, oral delivery systems can also be utilized to mask the unpleasant flavor in foods. For instance, Jaleh and colleagues prepared the lipid nanocapsules covered by the carbohydrate biopolymers (low methoxypectin, alginate, and chitosan,) that contained hesperetin. As suggested by sensory analysis, the synthesized nanocapsules markedly shielded the bitter taste of hesperetin (Fathi and Varshosaz 2013). In addition, carriers loaded with phenobarbital constructed on the basis of microemulsions (MEs) to deliver components in the mouth can reduce the bitter taste of phenobarbital (Monteagudo et al. 2014). The SPI/gelatin complexes-based

microcapsules prepared by spray drying can be utilized to diminish the bitter taste of casein hydrolysate (Favaro-Trindade et al. 2010). On the other hand, to reduce the unpleasant garlic flavor, the  $\beta$ -lactoglobulin microcapsules have been designed for the encapsulation of thiosulfinate allicin (Wilde et al. 2016). Further, the oral delivery systems may be utilized to investigate the sensory perception as well as oral processing. For instance, the starch NPs loaded with vanillin constructed according to the electrospray approach are utilized for investigating the vanillin taste perception after vanillin is taken. The findings suggest that, starch NPs can enhance the vanillin flavor perception in the oral cavity because the saliva amylase is gradually degraded in the mouth (Ege et al. 2017). Furthermore, the carboxymethyl cellulose-based delivery systems allow for the taste perception and controlled release of sodium in the mouth, thus balancing the sodium flavor (Aditya et al. 2017).

### 3.2 pH-Responsive Delivery Systems

Various probiotics, peptides, proteins, vitamins, and polyphenols can be easily decomposed under the acidic environment containing numerous digestive enzymes, including pepsin in GI tract. Such environment will induce great loss of compounds before they reach the small intestine. After such components are appropriately encapsulated, their degradation by the enzymes and acids in stomach can be prevented (Ezhilarasi et al. 2013). Thereafter, those compounds encapsulated will be maintained in stomach and released into the small intestine, thus increasing the specific bioaccessibility. Consequently, functional microcapsules must be responsive to the neutral pH in intestine; in addition, the early decomposition or release at acidic enzymatic conditions in the stomach must be prevented, thus facilitating the intestine-specific release.

The delivery system responsive to pH is extensively investigated previously. Typically, complex coacervation using WPI/gum Arabic (GA) is adopted for delivering the alive probiotics (*L. paraplantarum B1* and *L. paracasein E6*), and this approach contributes to maximally retaining the probiotic viability in comparison with free cells within the simulated gastric fluid. The interaction of WPI with GA changes from attraction to repulsion, as a result, the controlled release of cells can be tuned at pH 7.0 (Bosnea et al. 2014). Nonetheless, the pH-responsive coacervate capsules also have certain limitations, since they are instable at great physiological salt level of about 150 mM. Polymers with opposite charges can dissociate at this salt level because of the charge screening effect. This problem can be potentially managed by cross-linking between polymers with opposite charges. Notably, the oxidized starch microspheres cross-linked with  $\text{Fe}^{3+}$  and encapsulated with  $\beta$ -carotene can preserve the stabilized structure within the simulated gastric fluid (pH < 2.0) and efficiently enhance bioactive component release within the simulated intestinal fluid (pH 7.0) (Wang et al. 2015b). The akin pH-responsive effects can also be detected in the starch hydrogels-encapsulated nano-emulsion loaded with  $\beta$ -carotene (Wang et al. 2015a). The oxidized Konjac glucomannan (OKGM)

microspheres coated with chitosan (CS), where anthocyanins and  $\beta$ -carotene are introduced at the same time, are responsive to the pH value in the intestine (Shi et al. 2017). These microspheres are stable in the acidic stomach ( $\text{pH} < 2.0$ ), which will be destroyed to release the antioxidants loaded at neutral pH in the intestine ( $\text{pH} 7.0$ ), thus attaining intestine-specific release. Furthermore, the dual bioactive components are loaded onto the CS-OKGM microspheres; as a result, microspheres have synergistic antioxidant ability and increased thermostability. Typically, the double-network microspheres constituted by oxidized polysaccharides cross-linked with  $\text{Fe}^{3+}$ /CS oligosaccharides cross-linked with glutaraldehyde also display similar responsiveness (Lu et al. 2015). Nonetheless, the cross-linked polymer hydrogels also have certain drawbacks, since they frequently absorb excessive water, while this goes against food processing. Because of the potent hydrophobic interactions and hydrogen bonds of polyphenols with human serum albumin (HSA), HSA encapsulation markedly improves polyphenol stability under slight alkaline and neutral pH conditions (Li et al. 2015a). (–)-Epigallocatechin-3-gallate (EGCG) accounts for vital antioxidant isolated based on the tea extracts, yet it has poor solubility and stability. In this regard, it is of great importance to encapsulate EGCG for delivery and improving its stability. By adopting the emulsion solvent diffusion approach, the encapsulated EGCG is stabilized under acidic condition ( $\text{pH} 1.2$ ) in the stomach or the rat small intestine. Additionally, the encapsulated EGCG can be released at the pH condition in the intestine and maintained stable at that in the stomach (Onoue et al. 2011). For probiotics, their survival ability within host GI tract greatly affects their activity. Tremendous probiotics are stable in the digestive tract. But the large amounts of bile salts and highly acidic environment in stomach leads to the decreased bacterial survival rate. A variety of delivery systems synthesized to encapsulate probiotics can enhance the viability of bacteria. For instance, some study has successfully synthesized the new intestine-specific carrier constituted by one—encapsulated  $\text{Ca}^{2+}$ -alginate core encapsulated with Lactobacillus-casein as well as one composite shell consisting of  $\text{Ca}^{2+}$ -alginate/protamine, which effectively protects the encapsulated Lactobacillus casein under the acidic gastric condition, but the compound is released into small intestine rapidly because the core–shell structure is rapidly degraded (Mei et al. 2014). Additionally, the hydrogel microspheres consisting of the ethylenediaminetetraacetic acid-calcium-alginate (EDTA- $\text{Ca}^{2+}$ -Alg) system have been successfully synthesized and used to be the pH-responsive carrier to deliver Lactobacillus rhamnosus ATCC 53103 into the oral cavity. The prepared system can protect probiotics against the acidic environment in the stomach, but it is slowly gastric released into the intestine with collapsed gel structure at  $\text{pH} 7.0$ – $8.0$  (Zheng et al. 2017).

### 3.3 *Enzymatically-Responsive Delivery Systems*

A variety of enzymes, including  $\beta$ -mannanase and dextranases, can be produced by colonic microflora existing in GI tract. As a result, microcapsules responsive to

colonic enzymes may be potentially used as the colon-specific delivery systems (Pérez-Esteve et al. 2015). Typically, in terms of the colon-specific delivery, Konjac glucomannans (KGM) are the frequently utilized food polysaccharides. For instance, it is reported that KGM-hydroxypropyl methylcellulose capsules can be used for the specific delivery of 5-aminosalicylic acid to colon, due to its effect on avoiding gastric fluid degradation and release in the colon because of colonic  $\beta$ -mannanase degradation (Zhang et al. 2014). Besides, the KGM-xanthan gum (XG) based carrier system is degraded via the colonic  $\beta$ -mannanase but not small intestinal one and it shows the controlled-release feature for the embedded compounds (Alvarez-Manceñido et al. 2008). The bioactive compounds-loaded dextran hydrogel shows high stability within GI tract at physiological conditions, which is specifically released in colon only because of colonic microbial dextranase-mediated degradation (Hovgaard and Brøndsted 1995). The glycidyl methacrylate dextran (GMD) and poly acrylic acids (PAA) based hydrogels are also responsive to dextranase. The embedded 5-aminosalicylic acid is only slightly released at both intestinal and gastric pH values, but it is rapidly released from PAA/GMD hydrogels because of colonic dextranase-mediated glycosidic bond hydrolysis (Kim and Oh 2005). On the other hand, the CS-coated liposomes (chitosomes) have been designed to be responsive to pancreatic lipase in releasing the carotenoids encapsulated. The CS layer controls lipase permeability into liposomes present within the small intestine, which thereby shows the controlled-release feature (Tan et al. 2016). It is interesting that, the lipid digestion kinetics may be adjusted via the carrier systems because digestive lipase shows controlled approachability to oil encapsulated lipids; consequently, they may be utilized for designing the low-calorie foods. For instance, Zeeb and colleagues (Zeeb et al. 2015) discovered that lipid digestion was adjusted through changing the microcapsule layer number that covered the oil droplets. For the double-layer O/W emulsions, their colloidal stability is enhanced, which thereby facilitates lipase to penetrate the layer and change the encapsulated lipids to monoacylglycerols and free fatty acids. Nonetheless, in the primary single layer emulsion, coalescence or flocculation takes place when it is in the stomach environment; therefore, oil is digested at a slow rate within small intestine because the surface area exposed decreases. The stable and small emulsion droplets may seem to have a higher digestion rate. It should be noted that, wall materials (restricted to certain cleavable polysaccharides specific to intestinal amylase or colonic microbial enzymes) are the key factors limiting carriers responsive to intestinal enzymes. In addition, protein only is not appropriate in this application because the protein has been totally hydrolyzed under the gastric conditions.

### ***3.4 Biorecognition by Specific Receptors Delivery System***

Coupling targeted molecules (like peptide ligands) on carrier surfaces may contribute to the interaction between the molecule with surface receptors in targeted tissue. Such approach can be used to efficiently enhance bioactive compound absorption in



cells, in particular for certain immunomodulatory compounds (Yun et al. 2013). For instance, as the new M cell-homing peptide ligand, CKSTHPLSC (CKS9) peptide is cross-linked with CS NPs and the resultant product can efficiently deliver compounds to the follicle-associated epithelium (FAE) in Peyer's patches. CKS9 peptide has markedly improved transcytotic property and binding affinity to M cells; besides, the specific localization to FAE in Peyer's patches can be realized in vivo (Yoo et al. 2010). On the other hand, the solid lipid nanoparticles (SLNs) modified by CSKSSDYQC (CSK) can be used to be the candidate carriers to transport hydrophobic drugs, like atorvastatin calcium (ATC), and they are synthesized through cross-linking peptide ligand CSK with the stearic acid. Specifically, the SLNs modified by CSK peptide display potent ability to penetrate the mucus into intestinal cell monolayer and it also significantly enhances the bioavailability of ATC (Tian et al. 2016). RGD (Arg-Gly-Asp), which is also a peptide ligand, can be covalently bonded onto the PEGylated PLGA-based NPs loaded with antigen to specifically target the human M cells. Besides, the RGD-conjugated NPs evidently promoted compounds to penetrate human FAEs (co-cultures), since RGD ligand interacts with  $\beta$ 1 integrin on the co-culture apical surface. Studies in vivo also suggested that RGD-conjugated NPs are especially enriched into M cells (Garinot et al. 2007). Additionally, a seven-peptide (namely, Histidine-Alanine-Isoleucine-Tyrosine-Proline-Arginine-Histidine, HAIYPRH) that specific to transferrin receptor (TfR) is used to cover the poly (ethylene glycol)-block-poly ( $\epsilon$ -caprolactone) (PEG-b-PCL) micelle cores loaded with coumarin 6, so as to prepare the targeted NPs (Du et al. 2013). As a result, the synthesized NPs markedly elevate the cell absorption rate and penetrate cells via the specific clathrin-regulated mechanism associated with the receptor-regulated mechanism. Moreover, FQS peptide (FQSIYpIK), which represents a receptor with high level of conservation that is expressed in intestinal epithelium, exclusively binds to integrin avb3 receptor. Cross-linking FQS-TMC with the insulin-loaded NPs constituted based on the poly(lactide-co-glycolide acid)-monomethoxy-poly(polyethylene glycol) (PLGA-mPEG) improves the cell absorption rate and promotes glucose-lowering effect (Liu et al. 2016a). Such specific delivery systems have been extensively utilized in the field of pharmaceuticals, but they are rarely applied in the food industry. The green and safe methods like enzymatic modification to conjugate the ligands onto carriers must be taken into consideration in food applications.

### ***3.5 Mucus-Penetrating and Mucoadhesive Delivery Systems***

The mucus layer acts as a barrier for the uptake of bioactive compounds and the transport of carriers. It can trap the foreign particles because of its adhesion and steric hindrance and remove them in few seconds to few hours at the anatomical site (Dunnhaupt et al. 2015). The EGCG-loaded liposomes are found to show increased interactions with the human intestinal mucus compared with the  $\beta$ -carotene-loaded liposomes, since the hydrophobic bioactive compounds have certain influence on the



mucus layer rheological characteristics, which cannot be achieved by hydrophilic bioactive compounds. The co-culture systems consisting of Caco-2 (mucus-free) as well as Caco-2/HT29-MTX (mucus secretory cells) were adopted for investigating the interactions between mucus and liposome (Li et al. 2017a). Recently, the “mucus-penetrating particle” (MPP) (Lai et al. 2009) systems enable the efficient penetration of delivery systems into mucus layers and maximally reach the absorption membrane, since such vehicles rapidly deliver compounds to the systemic circulation via the epithelium. Using the electrically neutral and hydrophilic PEG to decorate the surface of NPs that had weak interaction with mucus can be a possible strategy to cope with this problem. PEG is the extensively utilized hydrophilic polymer, which has been usually utilized in coating NPs for improving their ability to penetrate the mucus. For example, Li and colleagues analyzed how the chain length (500–5000) of PEG-modifying micelles affected the oral bioavailability and membrane permeability in the delivery of trans-retinoic acid (ATRA), indicating that ATRA-PEG micelles with the PEG chain length of 1000 contributed to attaining superior oral bioavailability (Li et al. 2015a). The dextran–protamine (DEX-Prot) complex-modified nano-sized lipid carrier can offer the charge-neutral surface, which thus facilitates its diffusion into the intestinal mucus (Lai et al. 2009). In addition, different polymers, including DEX, cyclodextrin (HPBCD), aminodextran (ADEX), PEG, and mannose-amine (MA) modified NPs are compared for their mucus permeability. As a result, the MA-decorated NPs showed the maximal penetration into mucus layer (Iglesias et al. 2017). Moreover, carriers should be further designed for overcoming the lysosomal enzymes-mediated intracellular degradation. Certain proteases existing in endosomes may trigger the degradation of proteins, thereby resulting in complete carrier degradation as well as bioactive component tracking inside the lysosomes. It is necessary to design such carriers for escaping from lysosome, delivering them to cytoplasm and subsequently entering into the blood circulation.

Notably, the mucoadhesive delivery system represents the oral delivery approach frequently utilized to deliver components with poor absorption. It mainly functions to prolong the retention time as well as accumulation on mucus and to release the components near the absorption site (Dünnhaupt et al. 2011). On the other hand, the thiolated polymers, including conjugated poly(acrylates), thiol groups, CS, and the deacetylated gellan gum derivatives, may also interact with the mucus glycoprotein subdomains with abundant cysteine through the disulphide bonds, thus improving the mucoadhesion (Leitner et al. 2003). Palazzo and colleagues (Palazzo et al. 2017) compared the low-molecular-weight (LMW) CS-coated poly(isobutyl cyanoacrylate) (PIBCA) NPs with the reduced glutathione (GSH)- and glycol chitosan (GCS)-modified *N*-acetyl cysteine (NAC) for their mucoadhesive properties. As a result, the GCS-GSH-coated PIBCA NPs showed the optimal mucoadhesive properties. Additionally, it is found that the CS polymer-coated solid lipid NPs markedly enhance the curcumin oral bioavailability (Ramalingam et al. 2016). Besides, the mucoadhesive CS-coated porous silicon (Si) nanocarriers have also been synthesized to release two peptides, namely, the glucagon-like peptide-1 together with the dipeptidyl peptidase-4 (DPP4). The nanocarriers loaded

with two compounds may release the encapsulated peptides and have improved mucoadhesion because of the CS surface modification (Shrestha et al. 2015). *N*-trimethyl chitosan chloride (TMC), a kind of mucoadhesive polymer displaying biocompatibility, is utilized for nanocarriers modification, thus improving the specific mucoadhesive performance. For instance, the TMC-coated poly(lactide-co-glycoside acid) (PLGA) NPs (TMC-PLGA NPs) have been developed and used to deliver insulin in the mouth. When TMC-PLGA NPs are administered orally, they prevent the enzyme-mediated degradation of insulin within GI tract and extend the retention time of insulin at the absorption site, which is ascribed to TMC's mucoadhesive performance (Sheng et al. 2015). More attention should be paid to strategies for preventing the intestine-specific carriers from adhering to the gastric mucus.

#### 4 The Mechanisms of Cellular Uptake of Carriers

Generally speaking, many bioactive compounds cannot be efficiently absorbed via the epithelium. For instance, hydrophobic compounds can be usually absorbed by means of simple passive diffusion. In addition, vitamin A (VA) can be absorbed by way of bile salt micelle transport, while polyphenols can be absorbed through the carrier-regulated transport. However, the presence of efflux pump P-gp in epithelial cells may contribute to pumping back the absorbed polyphenols into the lumen, which thus largely restrict their absorption by cells. As a result, it is necessary to use the delivery carriers for managing the problem of poor bioactive compound absorption because of the restricted cell absorption. In other words, the delivery carriers can increase the absorption of bioactive compounds. Carriers may be developed to penetrate deep into the mucus layer in the meantime of improving the transmembrane permeability into the epithelium. Besides, carriers also deliver excessive components in each package and then actively enter into cells. Further, carriers also cope with the potential impacts of efflux pumps. Carriers show different cell absorption pattern from that of bioactive compounds; as a result, it is necessary to understand the different mechanisms between carriers and cell absorption before a carrier system is designed and applied. The NPs passive transcellular transport takes place by the non-specific permeability pathways, which is extremely restricted because NPs have large size (Ramesan and Sharma 2009). In addition, the energy-dependent mechanisms may also be applied in transporting NPs by means of active transport, and it is efficient relative to passive transport (Chen et al. 2011). On the other hand, active transcellular transport can be divided as 4 diverse mechanisms, including macropinocytosis, phagocytosis, caveolin-regulated endocytosis, and clathrin-regulated endocytosis (Fig. 11.5). Of them, the phagocytosis and endocytosis pathways may possibly take place within M cells. Besides, the clathrin-regulated endocytosis, caveolin-regulated endocytosis, micropinocytosis, and endocytosis represent the major pathways related to NP absorption by enterocytes, which are complicated and may take place through several routes; as

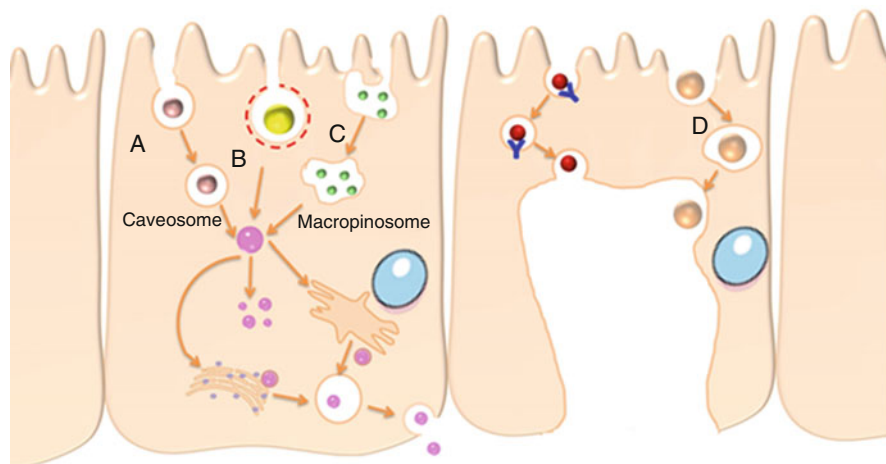


**Fig. 11.5** The different active transcellular transport mechanisms of cellular internalization for foreign delivering particles. (a) Caveolae-mediated endocytosis depends on a multidomain GTPase-dynamin. (b) Clathrin-mediated endocytosis is a widely shared pathway of nanoparticle internalization. (c) Macropinocytosis displays a poor selectivity for engulfing nanoparticles and the extracellular milieu. (d) Phagocytosis is an actin-based pathway taking place primarily in professional phagocytes. The figure was modified according to reference (Yu et al. 2016) Reproduction with permission from (Chai et al. 2018), Copyright 2020 ELSEVIER. Order Number: 4958621407796

a result, the new NPs are greatly needed to enhance transcytosis (Yu et al. 2016). For example, the soybean Bowman–Birk inhibitor NPs loaded with curcumin (Liu et al. 2017) can be detected in the clathrin-regulated endocytosis pathway. Moreover, the amphiphilic co-dendrimer porous graphitized carbon (PGC) NPs loaded with honokiol are mostly absorbed through the clathrin- and caveolae-regulated endocytosis (Guo et al. 2017). Generally, enterocytes specifically absorb NPs with the size of <math><100\text{ nm}</math>, whereas the M cells in Peyer’s patches are more likely to absorb NPs > 500 nm in size (Chen et al. 2013).

Hydrophilic bioactive components are mostly transported by the paracellular pathway. But there are intercellular tight junctions (TJs), as a result, there is a quite limited intercellular space (about 1 nm), thereby significantly restricting the diffusion of bioactive components. TJs represent the vital barriers limiting the intercellular permeation, particularly for the high-molecular-weight (HMW) components (Ramesan and Sharma 2009). For the sake of speeding up the paracellular transport rate, it is an efficient approach to open TJs. NPs cross-linked with *N*-trimethyl CS chloride (TMC) are suggested to efficiently open TJs in a reversible way and enhance insulin uptake in the mouth (Sheng et al. 2015).

## 5 The Evaluation of Carriers by Digestion and Absorption Models

For screening the appropriate carriers to deliver diverse bioactive compounds, multiple models *in vitro* have been utilized for evaluating the delivery performances. The *in vitro* simulated GI model has frequently been used to evaluate the uptake and digestion of bioactive components together with the corresponding delivery systems, which do not require human or animal experiment. The *in vitro* GI models are associated with the advantages of cost-effectiveness, great reproducibility, and time-saving property; as a result, they are extensively used for research in the pharmaceutical and functional food fields. Such models have offered the fundamental information before the *in vivo* experiments are performed (Kong and Singh 2010). At present, the existing *in vitro* models are the simulated GI fluid model, SHIME model, INFOGEST models, HGS model, and TIM model. In addition, the *in vivo* animal bioavailability model and *in vitro* Caco-2 monolayer cell model are constructed based on living systems. Further, we also conclude the representative digestion and uptake models, and compare the corresponding merits and demerits, as presented in Table 11.4. Typically, the simulated GI fluid model represents the multi-stage stimulator that is reported for the first time, which can be utilized for investigating factors that affect food ingredient digestion, including enzymatic activity, ionic components, applied mechanical stresses, and digestion time (Boisen and Eggum 1991). In addition, the SHIME model represents the multi-stage simulator designed for investigating the association of food ingredients with colonic microbial composition. It has been extensively used to study in the pharmaceutical, nutrition, micro-ecology, and general safety assessment fields and to examine the digestion and efficacy behaviors of nutraceuticals as well as their bioaccessibility (Alander et al. 1999). The TIM model is also extensively used to research in the pharmaceutical and food industries for studying the uptake and interactions of nutrients, drugs, and functional components. Additionally, the food digestion site, the nutrient uptake rate, and the association of inhibiting factors with stimulating ones may be studied using the TIM model as well (Ribnicky et al. 2014). Moreover, the HGS model contributes to mimicking the digestion process in human body and study those changes in gastric contents and food components in the food digestion process. In addition, it can also be used to study food and nutrient degradation kinetics affected by physiological conditions including enzyme production, acid, and mechanical contraction. According to the COST Infogest international network, the general standardized and practical static digestion model appropriate for foods on the basis of physiological conditions is put forward, namely, the INFOGEST model, and it can be used to investigate different endpoints and is modified for accommodating the more specific requirements (Minekus et al. 2014). As the *in vitro* cell model, the Caco-2 cell monolayer can be used for investigating the apparent permeability (Papp) for reflecting nutrient uptake by enterocytes (Sambuy et al. 2005). However, the Caco-2 monolayer model does not represent the actual *in vivo* condition, so the nutrition oral bioavailability must be assessed through calculating

**Table 11.4** The comparison of various GI digestion absorption models. Reproduction with permission from (Bao et al. 2019), Copyright 2020 ELSEVIER. Order Number: 4958630740831

Type of models	Application	Advantage	Disadvantages	Ref.
Simulated GI fluid method	Simulate the GI fluid environment and digestion time, and analyze the stability of food during digestion at the stomach condition	Easy to build up and cost-saving	The mechanical forces and the fluid mechanics that food encountered cannot be reproduced in the stomach	(Kong and Singh 2010)
The simulated human intestinal microbial ecosystem (SHIME)	Study the interaction and composition of microbial community in colon microbiota	The kinetics of chyme pass through the GI tract can be simulated	The interaction between probiotics and the host cannot be imitated	(Kontula et al. 1998)
TNO's gastro-intestinal model (TIM)	Monitor the place where food digested, evaluate the availability of nutrients absorption and the interactions of food between stimulating and inhibiting factors	Comprehensively simulate the process of digestion, and the process is controllable	Absence of feedback from the central nervous system and specific hormone releases for controlling the gastric, intestinal motility and secretions, mucosal cells and immune system	(Yoo and Chen 2006)
Human gastric simulator (HGS)	Study the digestion of foods in stomach	A more accurate stomach wall movement can be simulated, and the gastric secretion and emptying are controllable	Lack of intestinal conditions	(Kong and Singh 2010)
Cell culture models	Predict the permeability and mechanism of food compounds across the small intestinal cell monolayer	Easy to build and standardize, require small amount of sample reflect the absorption on the cell level	Lack of mucus barrier allows compounds easy access to the apical cell membrane, neglect other complex factors in vivo	(Sambuy et al. 2005)
Animal models	Study the bio-availability of nutrients in vivo	Offer a living system imitating the full dynamic physiological and physiochemical events during the absorption, distribution, and metabolism	Time-consuming, costly, and sometimes inhumane	(Boxenbaum 1982)

the pharmacokinetics of blood nutrient contents at consecutive time intervals when they are administered to animals (Bursztyka et al. 2008).

## 6 The Application of Carriers in Different Types of Food

Numerous requirements should be met in the preparation of carriers. Firstly, carriers must be of stability and will not release those encapsulated compounds ahead of time in the stomach but release them in the intestine. Secondly, easy diffusion of carriers across the intestinal mucus layer should be guaranteed, so that they rapidly reach the surface of enterocytes and will not be removed by mucus renewal. Besides, the charge-neutral and hydrophilic components can easily penetrate the mucus (Shan et al. 2015). Particularly, nanocapsules are able to directly enter into small intestinal epithelium by active transport. As a result, this significantly improves the bioavailability of the encapsulated bioactive components in such delivery systems. Besides, these nanocapsules may also open TJs between epithelial cells in a reversible manner, thus enhancing bioactive compound delivery via the paracellular pathway (Dodane and Vilivalam 1998). When the bioactive compounds are delivered, TJs will return back to the physiological status (Li et al. 2015a). Moreover, carrier size also represents a factor that affects the penetration into mucus and the opening of TJs. Carriers of a smaller size can rapidly penetrate the mucus barriers while reversibly opening TJs, thereby releasing bioactive compounds to the capillary blood (Patel and Champavat 2015). Further, the associations of nanocapsules conjugated with target ligands with typical receptors on the surface of epithelial cells can promote bioactive compound absorption (Jiang et al. 2018).

A variety of sensitive food component delivery systems are synthesized to mask the unpleasant flavors, which thus increase the water solubility of these components, protect them against the harmful external environment, and improve their penetration into intestinal mucus as well as epithelial cells (Augustin and Hemar 2009). Different technologies are designed in recent years to prepare the food delivery systems. Initially, complex coacervates, which are constituted by polysaccharides and proteins, have been the widely used conventional technology used to fabricate microcapsules (de Kruif et al. 2004). Proteins including whey protein (Weinbreck et al. 2003), zein (Chen and Subirade 2009), casein (Mendanha et al. 2009), and gelatin (Saravanan and Rao 2010), or carbohydrates including chitosan (Espinosa-Andrews et al. 2007) and pectin (Saravanan and Rao 2010) are extensively used to be the constructing materials. Thereafter, the cross-linked polysaccharides- and proteins-based hydrogel microparticles have aroused increasing attention due to their water swellability and great loading capacity (McClements 2017). Then, the Pickering emulsions are also developed to be the new delivery systems to load hydrophobic components because of the excellent long-time emulsification stability on the surface of small surfactants (Chevalier and Bolzinger 2013). Additionally, the food-resourced Pickering particulate stabilizers are adopted for improving the bioavailability of lipophilic bioactive compounds, which including lipids,

nutraceuticals, or the oil-soluble vitamins (McClements 2018). In recent years, great attention has been paid to self-assembled NPs due to their numerous merits, including the ability of penetration into mucus, high cell absorption and controlled release compared with the conventional delivery systems (Ezhilarasi et al. 2013). Different bioactive compounds have diverse chemical structures (lipophilic or hydrophilic), sensitivity, and biological functions. For instance, a majority of polyphenolic compounds possess the unfavorable flavors or tastes, among which, some are lipophilic, thus limiting their wide application. Typically, the encapsulation technology can be used to load polyphenols, which efficiently mitigate the above drawbacks, such as freeze drying, spray, crystallization, coacervation, liposome, complexation, and emulsion entrapment (Fang and Bhandari 2010). Most vitamins, including vitamin A, D, E, and K, have low solubility and oxidation sensitivity, thus restricting their actual application. On the whole, it is of great significance to develop an approach for overcoming the above problems while enhancing bioactive component bioavailability. Micro- or nano-emulsion and nano-encapsulation can markedly enhance their water stability and dispersibility (Gonnet et al. 2010). The polyunsaturated fatty acids (PUFAs), like EPA and DHA, can be easily oxidized. The encapsulation technology may be adopted for inhibiting the degradation of these compounds while retaining the resultant product quality (Holser 2011). Numerous bioactive peptides and proteins show high susceptibility to degradation, but they are poorly absorbed within GI tract; in addition, microparticles and NPs may be utilized for encapsulating, retaining, protecting, and specifically delivering the bioactive proteins to the intestine (McClements 2018).

A number of carrier systems are proposed to deliver bioactive compounds (Ezhilarasi et al. 2013). Meanwhile, most carrier systems can be utilized to promote the hydrophobic compound solubility; for example, the successful encapsulation of procyanidin in zein NPs is achieved, thus evidently enhancing the procyanidin solubility within the water solutions (Zou et al. 2012). The application of molecular co-assembly or self-assembly technique in encapsulating vitamin D (VD) into  $\beta$ -lactoglobulin markedly increases the VD solubility. For  $\beta$ -lactoglobulin nanocapsules encapsulated with linoleic acid, their solubility increases by 33–45% (Górska et al. 2012); while for albumin NPs encapsulated with CoQ10, their aqueous solubility evidently increases (Matsushita et al. 2013). Certain bioactive components, including USFAs and vitamins, are unstable in the presence of oxygen, light, or heat. In this case, the encapsulation technique can be utilized in the food industry for encapsulating, protecting, and releasing many bioactive components. For instance, investigators succeed in encapsulating vitamin E (VE) to the modified tapioca starch nanocapsules, which remarkably enhances the VE stability. At 60 days after storage under the temperature of 4–35 °C, VE attains a retention rate of about 50% of the original value, along with good solubility (Hategekimana et al. 2015). Amphiphilic peptides can be acquired by hydrolyzing caseins and they can co-assemble to the micellar NPs. By means of hydrophobic interactions, it is possible to incorporate VD to the hydrophobic cores, thus markedly improving the thermostability (Haham et al. 2012). Vitamin C (VC) represents another unstable vitamin in the presence of heat, light, and oxygen (Bendich et al. 1986). For VC



encapsulates with the inorganic layer  $\text{SiO}_2$  shell, its stability is 95%, but that for the non-encapsulated VC is just lower than 10% at 4 weeks later (Yang et al. 2003). Besides, forming nanocomplexes may also enhance the USFA stability. Nanocapsules constructed based on  $\beta$ -lactoglobulin and pectin protect DHA against degradation; to be specific, just about 5–10% loss is detected over 100 h under 40 °C in comparison with 80% loss reported for the non-encapsulated DHA (Zimet and Livney 2009). Bioactive compounds are associated with off-target effect and low stability at physiological conditions (enzymes, pH, together with intestinal mucus barrier) within the GI tract, which results in their poor bioavailability and bioaccessibility. There are many obstacles preventing the nanocarriers loaded with bioactive compounds from arriving at the target site because of the complex physiological environment in human body.

## 7 Future Prospects

As a result, it is necessary to develop the intelligent delivery systems for protecting and transporting bioactive compounds to target sites. The GI condition-responsive intelligent carriers may also be synthesized for the specific release of compounds in the intestine under the following conditions: microbial enzymes, neutral pH, epithelial cell mucus barriers, and specific receptors. Typically, it is possible to deliver bioactive compounds to specific intestinal sites where they can be further absorbed and utilized. At present, many reviewers have focused on investigating whether such compounds are stable under the simulated harsh GI conditions but neglect their real bioavailability and stability *in vivo*. Nonetheless, further practical models are needed because of the existence of factors such as cell absorption, mucus barriers, metabolism, and transport mechanisms, which facilitates to the accurate evaluation on the bioavailability and stability of encapsulated bioactive compounds. For the high-load intelligent designs, compound stability within GI tract, facile diffusion into the intestinal mucus layers, enhanced cell absorption, and cell junction opening must be taken into full consideration. The research directions in the future are the hydrogel- and self-assembled NPs-based multifunctional nanocarriers with simultaneous responsiveness to physiological environment (including enzymes, pH value, as well as intestinal mucus barrier) within GI tract. More efforts are needed to explore the nano-sized delivery systems that efficiently promote the stability, bioavailability, and sensory perception. For such delivery systems, their toxicity *in vivo* must be studied from the perspectives of biodistribution, metabolism, and cell viability. The analysis in this section contributes to developing the more sophisticated carrier systems to prevent disease and promote health. As found in this chapter, intelligent delivery systems can be utilized for the effective improvement of bioactive compound bioavailability and quality within functional foods in the future, which shed more lights on the design of intelligent carriers.



## References

- Abdulkarim M, Agulló N, Cattoz B, Griffiths P, Bernkop-Schnürch A, Borros SG, Gumbleton M (2015) Nanoparticle diffusion within intestinal mucus: three-dimensional response analysis dissecting the impact of particle surface charge, size and heterogeneity across polyelectrolyte, pegylated and viral particles. *Eur J Pharm Biopharm* 97:230–238. <https://doi.org/10.1016/j.ejpb.2015.01.023>
- Ades H, Kesselman E, Ungar Y, Shimoni E (2012) Complexation with starch for encapsulation and controlled release of menthone and menthol. *LWT Food Sci Technol* 45(2):277–288. <https://doi.org/10.1016/j.lwt.2011.08.008>
- Aditya NP, Espinosa YG, Norton IT (2017) Encapsulation systems for the delivery of hydrophilic nutraceuticals: food application. *Biotechnol Adv* 35(4):450–457. <https://doi.org/10.1016/j.biotechadv.2017.03.012>
- Alander M, De Smet I, Nollet L, Verstraete W, von Wright A, Mattila-Sandholm T (1999) The effect of probiotic strains on the microbiota of the simulator of the human intestinal microbial ecosystem (SHIME). *Int J Food Microbiol* 46(1):71–79. [https://doi.org/10.1016/S0168-1605\(98\)00182-2](https://doi.org/10.1016/S0168-1605(98)00182-2)
- Alvarez-Manceño F, Landin M, Martínez-Pacheco R (2008) Konjac glucomannan/xanthan gum enzyme sensitive binary mixtures for colonic drug delivery. *Eur J Pharm Biopharm* 69(2):573–581. <https://doi.org/10.1016/j.ejpb.2008.01.004>
- Augustin MA, Hemar Y (2009) Nano- and micro-structured assemblies for encapsulation of food ingredients. *Chem Soc Rev* 38(4):902–912. <https://doi.org/10.1039/B801739P>
- Baek K, Hwang I, Roy I, Shetty D, Kim K (2015) Self-assembly of nanostructured materials through irreversible covalent bond formation. *Acc Chem Res* 48(8):2221–2229. <https://doi.org/10.1021/acs.accounts.5b00067>
- Bao C, Jiang P, Chai JJ, Jiang YM, Li D, Bao WE, Liu BX, Liu B, Nordec W, Li Y (2019) The delivery of sensitive food bioactive ingredients: absorption mechanisms, influencing factors, encapsulation techniques and evaluation models. *Food Res Int* 120:130–140. <https://doi.org/10.1016/j.foodres.2019.02.024>
- Batra P, Sharma AK (2013) Anti-cancer potential of flavonoids: recent trends and future perspectives. *3 Biotech* 3(6):439–459. <https://doi.org/10.1007/s13205-013-0117-5>
- Bendich A, Machlin LJ, Scandurra O, Burton GW, Wayner DDM (1986) The antioxidant role of vitamin C. *Adv Free Radic Biol Med* 2(2):419–444. [https://doi.org/10.1016/S8755-9668\(86\)80021-7](https://doi.org/10.1016/S8755-9668(86)80021-7)
- Benjamin O, Silcock P, Beauchamp J, Buettner A, Everett DW (2013) Volatile release and structural stability of  $\beta$ -lactoglobulin primary and multilayer emulsions under simulated oral conditions. *Food Chem* 140(1):124–134. <https://doi.org/10.1016/j.foodchem.2013.02.043>
- Berton-Carabin CC, Schroën K (2015) Pickering emulsions for food applications: background, trends, and challenges. *Annu Rev Food Sci Technol* 6(1):263–297. <https://doi.org/10.1146/annurev-food-081114-110822>
- Bianchi J, Wilson FA, Rose RC (1986) Dehydroascorbic acid and ascorbic acid transport systems in the Guinea pig ileum. *Am J Phys* 250(4):461–468. <https://doi.org/10.1152/ajpgi.1986.250.4.G461>
- Binks BP (2002) Particles as surfactants-similarities and differences. *Curr Opin Colloid Interface Sci* 7(1):21–41. [https://doi.org/10.1016/S1359-0294\(02\)00008-0](https://doi.org/10.1016/S1359-0294(02)00008-0)
- Boisen S, Eggum BO (1991) Critical evaluation of *in vitro* methods for estimating digestibility in simple-stomach animals. *Nutr Res Rev* 4:141–162. <https://doi.org/10.1079/nrr19910012>
- Bosnea LA, Moschakis T, Biliaderis CG (2014) Complex coacervation as a novel microencapsulation technique to improve viability of probiotics under different stresses. *Food Bioprocess Technol* 7(10):2767–2781. <https://doi.org/10.1007/s11947-014-1317-7>
- Bosnea LA, Moschakis T, Biliaderis CG (2017) Microencapsulated cells of *Lactobacillus paracasei subsp. paracasei* in biopolymer complex coacervates and their function in a yogurt matrix. *Food Funct* 8(2):554–562. <https://doi.org/10.1039/C6FO01019A>

- Boxenbaum H (1982) Interspecies scaling, allometry, physiological time, and the ground plan of pharmacokinetics. *J Pharmacokinet Biopharm* 10(2):201–225. <https://doi.org/10.1007/BF01062336>
- Bursztyka J, Perdu E, Tulliez J, Debrauwer L, Delous G, Canlet C, De Sousa G, Rahmani R, Benfenati E, Cravedi J-P (2008) Comparison of genistein metabolism in rats and humans using liver microsomes and hepatocytes. *Food Chem Toxicol* 46(3):939–948. <https://doi.org/10.1016/j.fct.2007.10.023>
- Casadei MA, Pitarresi G, Calabrese R, Paolicelli P, Giammona G (2008) Biodegradable and pH-sensitive hydrogels for potential colon-specific drug delivery: characterization and *in vitro* release studies. *Biomacromolecules* 9(1):43–49. <https://doi.org/10.1021/bm700716c>
- Chai J, Jiang P, Wang P, Jiang Y, Li D, Bao WE, Yuan QP, Ren FZ, Li Y (2018) The intelligent delivery systems for bioactive compounds in foods: physicochemical and physiological conditions, absorption mechanisms, obstacles and responsive strategies. *Trends Food Sci Technol* 78:144–154. <https://doi.org/10.1016/j.tifs.2018.06.003>
- Chan LMS, Lowes S, Hirst BH (2004) The ABCs of drug transport in intestine and liver: efflux proteins limiting drug absorption and bioavailability. *Eur J Pharm Sci* 21(1):25–51. <https://doi.org/10.1016/j.ejps.2003.07.003>
- Chen L, Subirade M (2009) Elaboration and characterization of soy/zein protein microspheres for controlled nutraceutical delivery. *Biomacromolecules* 10(12):3327–3334. <https://doi.org/10.1021/bm900989y>
- Chen H-M, Muramoto K, Yamauchi F (1995) Structural analysis of antioxidative peptides from soybean .beta.-Conglycinin. *J Agric Food Chem* 43(3):574–578. <https://doi.org/10.1021/jf00051a004>
- Chen M-C, Sonaje K, Chen K-J, Sung H-W (2011) A review of the prospects for polymeric nanoparticle platforms in oral insulin delivery. *Biomaterials* 32(36):9826–9838. <https://doi.org/10.1016/j.biomaterials.2011.08.087>
- Chen M-C, Mi F-L, Liao Z-X, Hsiao C-W, Sonaje K, Chung M-F, Hsu L-W, Sung H-W (2013) Recent advances in chitosan-based nanoparticles for oral delivery of macromolecules. *Adv Drug Deliv Rev* 65(6):865–879. <https://doi.org/10.1016/j.addr.2012.10.010>
- Chen X, Wang S, Lu M, Chen Y, Zhao L, Li W, Yuan Q, Norde W, Li Y (2014) Formation and characterization of light-responsive TEMPO-oxidized konjac glucomannan microspheres. *Biomacromolecules* 15(6):2166–2171. <https://doi.org/10.1021/bm500327m>
- Chen Y, Zhao H, Liu X, Li Z, Liu B, Wu J, Shi M, Norde W, Li Y (2016) TEMPO-oxidized konjac glucomannan as appliance for the preparation of hard capsules. *Carbohydr Polym* 143:262–269. <https://doi.org/10.1016/j.carbpol.2016.01.072>
- Cheng Y, Tang K, Wu S, Liu L, Qiang C, Lin X, Liu B (2011) Astragalus polysaccharides lowers plasma cholesterol through mechanisms distinct from statins. *PLoS One* 6(11):1–9. <https://doi.org/10.1371/journal.pone.0027437>
- Chevalier Y, Bolzinger M-A (2013) Emulsions stabilized with solid nanoparticles: pickering emulsions. *Colloids Surf A Physicochem Eng Asp* 439:23–34. <https://doi.org/10.1016/j.colsurfa.2013.02.054>
- Cone RA (2009) Barrier properties of mucus. *Adv Drug Deliv Rev* 61(2):75–85. <https://doi.org/10.1016/j.addr.2008.09.008>
- Corvol P, Williams TA, Soubrier F (1995) [18] Peptidyl dipeptidase a: angiotensin I-converting enzyme. In: *Methods in enzymology*, vol vol 248. Academic Press, Cambridge, pp 283–305. [https://doi.org/10.1016/0076-6879\(95\)48020-X](https://doi.org/10.1016/0076-6879(95)48020-X)
- Costa RR, Mano JF (2014) Polyelectrolyte multilayered assemblies in biomedical technologies. *Chem Soc Rev* 43(10):3453–3479. <https://doi.org/10.1039/C3CS60393H>
- Day AJ, Gee JM, DuPont MS, Johnson IT, Williamson G (2003) Absorption of quercetin-3-glucoside and quercetin-4'-glucoside in the rat small intestine: the role of lactase phlorizin hydrolase and the sodium-dependent glucose transporter. *Biochem Pharmacol* 65(7):1199–1206. [https://doi.org/10.1016/s0006-2952\(03\)00039-x](https://doi.org/10.1016/s0006-2952(03)00039-x)

- De Kruif CG, Weinbreck F, de Vries R (2004) Complex coacervation of proteins and anionic polysaccharides. *Curr Opin Colloid Interface Sci* 9(5):340–349. <https://doi.org/10.1016/j.cocis.2004.09.006>
- Dhaval A, Yadav N, Purwar S (2016) Potential applications of food derived bioactive peptides in management of health. *Int J Pept Res Ther* 22(3):377–398. <https://doi.org/10.1007/s10989-016-9514-z>
- Dodane V, Vilivalam VD (1998) Pharmaceutical applications of chitosan. *Pharm Sci Technol Today* 1(6):246–253. [https://doi.org/10.1016/S1461-5347\(98\)00059-5](https://doi.org/10.1016/S1461-5347(98)00059-5)
- Doyennette M, Deleris I, Feron G, Guichard E, Souchon I, Trelea IC (2014) Main individual and product characteristics influencing in-mouth flavor release during eating masticated food products with different textures: mechanistic modelling and experimental validation. *J Theor Biol* 340:209–221. <https://doi.org/10.1016/j.jtbi.2013.09.005>
- Du W, Fan Y, Zheng N, He B, Yuan L, Zhang H, Wang X, Wang J, Zhang X, Zhang Q (2013) Transferrin receptor specific nanocarriers conjugated with functional 7peptide for oral drug delivery. *Biomaterials* 34(3):794–806. <https://doi.org/10.1016/j.biomaterials.2012.10.003>
- Du Y, Bao C, Huang J, Jiang P, Jiao L, Ren F, Li Y (2019) Improved stability, epithelial permeability and cellular antioxidant activity of  $\beta$ -carotene via encapsulation by self-assembled  $\alpha$ -lactalbumin micelles. *Food Chem* 271:707–714. <https://doi.org/10.1016/j.foodchem.2018.07.216>
- Dünnhaupt S, Barthelmes J, Hombach J, Sakloetsakun D, Arkhipova V, Bernkop-Schnürch A (2011) Distribution of thiolated mucoadhesive nanoparticles on intestinal mucosa. *Int J Pharm* 408(1):191–199. <https://doi.org/10.1016/j.ijpharm.2011.01.060>
- Dünnhaupt S, Kammona O, Waldner C, Kiparissides C, Bernkop-Schnürch A (2015) Nano-carrier systems: strategies to overcome the mucus gel barrier. *Eur J Pharm Biopharm* 96:447–453. <https://doi.org/10.1016/j.ejpb.2015.01.022>
- Ege ZR, Akan A, Oktar FN, Kalkandelen C, Gunduz O (2017) Production of starch nanoparticles by electrospraying as a delivery system for vanillin. In: 2017 medical technologies national congress (Tiptekno). IEEE, 4 pp. <https://doi.org/10.1109/tiptekno.2017.8238095>
- Engelen L, van der Bilt A, Schipper M, Bosman F (2005) oral size perception of particles: effect of size, type, viscosity and method. *J Texture Stud* 36(4):373–386. <https://doi.org/10.1111/j.1745-4603.2005.00022.x>
- Espinosa-Andrews H, Báez-González JG, Cruz-Sosa F, Vernon-Carter EJ (2007) Gum Arabic–chitosan complex coacervation. *Biomacromolecules* 8(4):1313–1318. <https://doi.org/10.1021/bm0611634>
- Ezhilarasi PN, Karthik P, Chhanwal N, Anandharamakrishnan C (2013) Nanoencapsulation techniques for food bioactive components: a review. *Food Bioprocess Technol* 6(3):628–647. <https://doi.org/10.1007/s11947-012-0944-0>
- Fang Z, Bhandari B (2010) Encapsulation of polyphenols – a review. *Trends Food Sci Technol* 21(10):510–523. <https://doi.org/10.1016/j.tifs.2010.08.003>
- Fathi M, Varshosaz J (2013) Novel hesperetin loaded nanocarriers for food fortification: production and characterization. *J Funct Foods* 5(3):1382–1391. <https://doi.org/10.1016/j.jff.2013.05.006>
- Favaro-Trindade CS, Santana AS, Monterrey-Quintero ES, Trindade MA, Netto FM (2010) The use of spray drying technology to reduce bitter taste of casein hydrolysate. *Food Hydrocoll* 24(4):336–340. <https://doi.org/10.1016/j.foodhyd.2009.10.012>
- Feng Y, Lee Y (2016) Surface modification of zein colloidal particles with sodium caseinate to stabilize oil-in-water pickering emulsion. *Food Hydrocoll* 56:292–302. <https://doi.org/10.1016/j.foodhyd.2015.12.030>
- Gambini J, Ingles M, Olaso G, Lopez-Grueso R, Bonet-Costa V, Gimeno-Mallench L, Mas-Bargues C, Abdelaziz KM, Gomez-Cabrera MC, Vina J, Borrás C (2015) Properties of resveratrol: *in vitro* and *in vivo* studies about metabolism, bioavailability, and biological effects in animal models and humans. *Oxid Med Cell Longev* 2015:1–13. <https://doi.org/10.1155/2015/837042>

- Garinot M, Fiévez V, Pourcelle V, Stoffelbach F, des Rieux A, Plapied L, Theate I, Freichels H, Jérôme C, Marchand-Brynaert J, Schneider Y-J, Prétat V (2007) PEGylated PLGA-based nanoparticles targeting M cells for oral vaccination. *J Control Release* 120(3):195–204. <https://doi.org/10.1016/j.jconrel.2007.04.021>
- Giavasis I (2014) Bioactive fungal polysaccharides as potential functional ingredients in food and nutraceuticals. *Curr Opin Biotechnol* 26:162–173. <https://doi.org/10.1016/j.copbio.2014.01.010>
- Gleeson JP, Ryan SM, Brayden DJ (2016) Oral delivery strategies for nutraceuticals: delivery vehicles and absorption enhancers. *Trends Food Sci Technol* 53:90–101. <https://doi.org/10.1016/j.tifs.2016.05.007>
- Gonnet M, Lethuaut L, Boury F (2010) New trends in encapsulation of liposoluble vitamins. *J Control Release* 146(3):276–290. <https://doi.org/10.1016/j.jconrel.2010.01.037>
- Górska A, Szulc K, Ostrowska-Ligeza E, Wirkowska-Wojdyła M (2012) Using binding feature of  $\beta$ -lactoglobulin to bind cholecalciferol. *Zywn Nauka Technol Jakosc* 2(81):99–106. <https://doi.org/10.15193/zntj/2012/81/099-106>
- Guo Y, Zhao Y, Wang T, Zhao S, Qiu H, Han M, Wang X (2017) Honokiol nanoparticles stabilized by oligoethylene glycols codendrimer: *in vitro* and *in vivo* investigations. *J Mater Chem B* 5(4):697–706. <https://doi.org/10.1039/C6TB02416E>
- Guzmán E, Mateos-Maroto A, Ruano M, Ortega F, Rubio RG (2017) Layer-by-layer polyelectrolyte assemblies for encapsulation and release of active compounds. *Adv Colloid Interf Sci* 249:290–307. <https://doi.org/10.1016/j.cis.2017.04.009>
- Haham M, Ish-Shalom S, Nodelman M, Duek I, Segal E, Kustanovich M, Livney YD (2012) Stability and bioavailability of vitamin D nanoencapsulated in casein micelles. *Food Funct* 3(7):737–744. <https://doi.org/10.1039/C2FO10249H>
- Han B, Ma T, Vergara JH, Palmese GR, Yin J, Lee D, Han L (2017) Non-additive impacts of covalent cross-linking on the viscoelastic nanomechanics of ionic polyelectrolyte complexes. *RSC Adv* 7(84):53334–53345. <https://doi.org/10.1039/C7RA08514A>
- Harrison EH (2012) Mechanisms involved in the intestinal absorption of dietary vitamin A and provitamin A carotenoids. *BBA-Mol Cell Biol L* 1821(1):70–77. <https://doi.org/10.1016/j.bbali.2011.06.002>
- Hategekimana J, Masamba KG, Ma J, Zhong F (2015) Encapsulation of vitamin E: effect of physicochemical properties of wall material on retention and stability. *Carbohydr Polym* 124:172–179. <https://doi.org/10.1016/j.carbpol.2015.01.060>
- Heger M, van Golen RF, Broekgaarden M, Michel MC (2014) The molecular basis for the pharmacokinetics and pharmacodynamics of curcumin and its metabolites in relation to cancer. *Pharmacol Rev* 66(1):222–307. <https://doi.org/10.1124/pr.110.004044>
- Holser R (2011) Encapsulation of polyunsaturated fatty acid esters with solid lipid particles. *Lipid Insights* 5:1–5. <https://doi.org/10.4137/LPI.S7901>
- Hovgaard L, Brøndsted H (1995) Dextran hydrogels for colon-specific drug delivery. *J Control Release* 36(1):159–166. [https://doi.org/10.1016/0168-3659\(95\)00049-E](https://doi.org/10.1016/0168-3659(95)00049-E)
- Iglesias T, López de Cerain A, Irache JM, Martín-Arbella N, Wilcox M, Pearson J, Azqueta A (2017) Evaluation of the cytotoxicity, genotoxicity and mucus permeation capacity of several surface modified poly(anhydride) nanoparticles designed for oral drug delivery. *Int J Pharm* 517(1):67–79. <https://doi.org/10.1016/j.ijpharm.2016.11.059>
- Jiang T, Singh B, Li H-S, Kim Y-K, Kang S-K, Nah J-W, Choi Y-J, Cho C-S (2014) Targeted oral delivery of BmpB vaccine using porous PLGA microparticles coated with M cell homing peptide-coupled chitosan. *Biomaterials* 35(7):2365–2373. <https://doi.org/10.1016/j.biomaterials.2013.11.073>
- Jiang S, Liu C, Wang X, Xiong L, Sun Q (2016) Physicochemical properties of starch nanocomposite films enhanced by self-assembled potato starch nanoparticles. *LWT Food Sci Technol* 69:251–257. <https://doi.org/10.1016/j.lwt.2016.01.053>
- Jiang P, Huang J, Bao C, Jiao L, Zhao H, Du Y, Fazheng R, Li Y (2018) Enzymatically partially hydrolyzed  $\alpha$ -lactalbumin peptides for self-assembled micelle formation and their application

- for coencapsulation of multiple antioxidants. *J Agric Food Chem* 66(49):12921–12930. <https://doi.org/10.1021/acs.jafc.8b03798>
- Kargar M, Fayazmanesh K, Alavi M, Spyropoulos F, Norton IT (2012) Investigation into the potential ability of pickering emulsions (food-grade particles) to enhance the oxidative stability of oil-in-water emulsions. *J Colloid Interface Sci* 366(1):209–215. <https://doi.org/10.1016/j.jcis.2011.09.073>
- Katouzian I, Jafari SM (2016) Nano-encapsulation as a promising approach for targeted delivery and controlled release of vitamins. *Trends Food Sci Technol* 53:34–48. <https://doi.org/10.1016/j.tifs.2016.05.002>
- Kim I-S, Oh I-J (2005) Drug release from the enzyme-degradable and pH-sensitive hydrogel composed of glycidyl methacrylate dextran and poly(acrylic acid). *Arch Pharm Res* 28(8):983–987. <https://doi.org/10.1007/BF02973887>
- Kong FB, Singh RP (2010) A human gastric simulator (HGS) to study food digestion in human stomach. *J Food Sci* 75(9):E627–E635. <https://doi.org/10.1111/j.1750-3841.2010.01856.x>
- Kontula P, Jaskari J, Nollet L, De Smet I, von Wright A, Poutanen K, Mattila-Sandholm T (1998) The colonization of a simulator of the human intestinal microbial ecosystem by a probiotic strain fed on a fermented oat bran product: effects on the gastrointestinal microbiota. *Appl Microbiol Biotechnol* 50(2):246–252. <https://doi.org/10.1007/s002530051284>
- Kruk J, Szymańska R, Nowicka B, Dłużewska J (2016) Function of isoprenoid quinones and chromanols during oxidative stress in plants. *New Biotechnol* 33(5, Part B):636–643. <https://doi.org/10.1016/j.nbt.2016.02.010>
- Kumar B, Kulanthaivel S, Mondal A, Mishra S, Banerjee B, Bhaumik A, Banerjee I, Giri S (2017) Mesoporous silica nanoparticle based enzyme responsive system for colon specific drug delivery through guar gum capping. *Colloids Surf B: Biointerfaces* 150:352–361. <https://doi.org/10.1016/j.colsurfb.2016.10.049>
- Lai SK, Wang Y-Y, Hanes J (2009) Mucus-penetrating nanoparticles for drug and gene delivery to mucosal tissues. *Adv Drug Deliv Rev* 61(2):158–171. <https://doi.org/10.1016/j.addr.2008.11.002>
- Layer P, Gröger G (1993) Fate of pancreatic enzymes in the human intestinal lumen in health and pancreatic insufficiency. *Digestion* 54:10–14. <https://doi.org/10.1159/000201097>
- Lee H-J, Woo HG, Greenwood TA, Kripke DF, Kelsoe JR (2013) A genome-wide association study of seasonal pattern mania identifies NF1A as a possible susceptibility gene for bipolar disorder. *J Affect Disord* 145(2):200–207. <https://doi.org/10.1016/j.jad.2012.07.032>
- Leitner VM, Walker GF, Bernkop-Schnürch A (2003) Thiolated polymers: evidence for the formation of disulphide bonds with mucus glycoproteins. *Eur J Pharm Biopharm* 56(2):207–214. [https://doi.org/10.1016/S0939-6411\(03\)00061-4](https://doi.org/10.1016/S0939-6411(03)00061-4)
- Li Y, de Vries R, Slaghek T, Timmermans J, Cohen Stuart MA, Norde W (2009) Preparation and characterization of oxidized starch polymer microgels for encapsulation and controlled release of functional ingredients. *Biomacromolecules* 10(7):1931–1938. <https://doi.org/10.1021/bm900337n>
- Li Y, Kleijn JM, Cohen Stuart MA, Slaghek T, Timmermans J, Norde W (2011) Mobility of lysozyme inside oxidized starch polymer microgels. *Soft Matter* 7(5):1926–1935. <https://doi.org/10.1039/C0SM00962H>
- Li Y, Norde W, Kleijn JM (2012) Stabilization of protein-loaded starch microgel by polyelectrolytes. *Langmuir* 28(2):1545–1551. <https://doi.org/10.1021/la204014q>
- Li Z, Han X, Zhai Y, Lian H, Zhang D, Zhang W, Wang Y, He Z, Liu Z, Sun J (2015a) Critical determinant of intestinal permeability and oral bioavailability of pegylated all trans-retinoic acid prodrug-based nanomicelles: chain length of poly(ethylene glycol) corona. *Colloids Surf B: Biointerfaces* 130:133–140. <https://doi.org/10.1016/j.colsurfb.2015.03.036>
- Li Z, Jiang H, Xu C, Gu L (2015b) A review: using nanoparticles to enhance absorption and bioavailability of phenolic phytochemicals. *Food Hydrocoll* 43:153–164. <https://doi.org/10.1016/j.foodhyd.2014.05.010>

- Li Y, Arranz E, Guri A, Corredig M (2017a) Mucus interactions with liposomes encapsulating bioactives: interfacial tensiometry and cellular uptake on Caco-2 and cocultures of Caco-2/HT29-MTX. *Food Res Int* 92:128–137. <https://doi.org/10.1016/j.foodres.2016.12.010>
- Li Y, Li W, Bao W, Liu B, Li D, Jiang Y, Wei W, Ren F (2017b) Bioinspired peptosomes with programmed stimuli-responses for sequential drug release and high-performance anticancer therapy. *Nanoscale* 9(27):9317–9324. <https://doi.org/10.1039/C7NR00598A>
- Liu J, Willför S, Xu C (2015a) A review of bioactive plant polysaccharides: biological activities, functionalization, and biomedical applications. *Bioact Carbohydr Diet Fibre* 5(1):31–61. <https://doi.org/10.1016/j.bcdf.2014.12.001>
- Liu M, Zhang J, Shan W, Huang Y (2015b) Developments of mucus penetrating nanoparticles. *Asian J Pharm Sci* 10(4):275–282. <https://doi.org/10.1016/j.ajps.2014.12.007>
- Liu C, Shan W, Liu M, Zhu X, Xu J, Xu Y, Huang Y (2016a) A novel ligand conjugated nanoparticles for oral insulin delivery. *Drug Deliv* 23(6):2015–2025. <https://doi.org/10.3109/10717544.2015.1058433>
- Liu W, Chen XD, Cheng Z, Selomulya C (2016b) On enhancing the solubility of curcumin by microencapsulation in whey protein isolate via spray drying. *J Food Eng* 169:189–195. <https://doi.org/10.1016/j.jfoodeng.2015.08.034>
- Liu C, Cheng F, Yang X (2017) Fabrication of a soybean Bowman–Birk inhibitor (BBI) nanodelivery carrier to improve bioavailability of curcumin. *J Agric Food Chem* 65(11):2426–2434. <https://doi.org/10.1021/acs.jafc.7b00097>
- Livney YD (2010) Milk proteins as vehicles for bioactives. *Curr Opin Colloid Interface Sci* 15(1):73–83. <https://doi.org/10.1016/j.cocis.2009.11.002>
- Liu M, Li Z, Liang H, Shi M, Zhao L, Li W, Chen Y, Wu J, Wang S, Chen X, Yuan Q, Li Y (2015) Controlled release of anthocyanins from oxidized konjac glucomannan microspheres stabilized by chitosan oligosaccharides. *Food Hydrocoll* 51:476–485. <https://doi.org/10.1016/j.foodhyd.2015.05.036>
- Lundquist P, Artursson P (2016) Oral absorption of peptides and nanoparticles across the human intestine: opportunities, limitations and studies in human tissues. *Adv Drug Deliv Rev* 106:256–276. <https://doi.org/10.1016/j.addr.2016.07.007>
- Maitra J, Shukla VK (2014) Cross-linking in hydrogels—a review. *Am J Polym Sci* 4(2):25–31. <https://doi.org/10.5923/j.ajps.20140402.01>
- Matsushita N, Oshima T, Takahashi H, Baba Y (2013) Enhanced water dispersibility of coenzyme Q10 by complexation with albumin hydrolysate. *J Agric Food Chem* 61(25):5972–5978. <https://doi.org/10.1021/jf4003297>
- McClements DJ (2017) Recent progress in hydrogel delivery systems for improving nutraceutical bioavailability. *Food Hydrocoll* 68:238–245. <https://doi.org/10.1016/j.foodhyd.2016.05.037>
- McClements DJ (2018) Encapsulation, protection, and delivery of bioactive proteins and peptides using nanoparticle and microparticle systems: a review. *Adv Colloid Interf Sci* 253:1–22. <https://doi.org/10.1016/j.cis.2018.02.002>
- Mei L, He F, Zhou R-Q, Wu C-D, Liang R, Xie R, Ju X-J, Wang W, Chu L-Y (2014) Novel intestinal-targeted Ca-alginate-based carrier for pH-responsive protection and release of lactic acid bacteria. *ACS Appl Mater Interfaces* 6(8):5962–5970. <https://doi.org/10.1021/am501011j>
- Mendanha DV, Molina Ortiz SE, Favaro-Trindade CS, Mauri A, Monterrey-Quintero ES, Thomazini M (2009) Microencapsulation of casein hydrolysate by complex coacervation with SPI/pectin. *Food Res Int* 42(8):1099–1104. <https://doi.org/10.1016/j.foodres.2009.05.007>
- Mendes AC, Baran ET, Reis RL, Azevedo HS (2013) Self-assembly in nature: using the principles of nature to create complex nanobiomaterials. *Wiley Interdiscip Rev Nanomed Nanobiotechnol* 5(6):582–612. <https://doi.org/10.1002/wnan.1238>
- Minckus M, Almingier M, Alvito P, Ballance S, Bohn T, Bourlieu C, Carrière F, Boutrou R, Corredig M, Dupont D, Dufour C, Egger L, Golding M, Karakaya S, Kirkhuis B, Le Feunteun S, Lesmes U, Macierzanka A, Mackie A, Marze S, McClements DJ, Ménard O, Recio I, Santos CN, Singh RP, Vegarud GE, Wickham MSJ, Weitschies W, Brodtkorb A (2014) A standardised



- static *in vitro* digestion method suitable for food – an international consensus. *Food Funct* 5 (6):1113–1124. <https://doi.org/10.1039/C3FO60702J>
- Monteagudo E, Langenheim M, Salerno C, Buontempo F, Bregni C, Carlucci A (2014) Pharmaceutical optimization of lipid-based dosage forms for the improvement of taste-masking, chemical stability and solubilizing capacity of phenobarbital. *Drug Dev Ind Pharm* 40 (6):783–792. <https://doi.org/10.3109/03639045.2013.787536>
- Nagao A (2009) Absorption and function of dietary carotenoids. In: Yoshikawa T (ed) *Food factors for health promotion*, Forum of nutrition, vol vol 61. Karger Publishers, Berlin, pp 55–63. <https://doi.org/10.1159/000212738>
- Nawong S, Oonsivilai R, Boonkerd N, Truelstrup Hansen L (2016) Entrapment in food-grade transglutaminase cross-linked gelatin–maltodextrin microspheres protects *Lactobacillus spp.* during exposure to simulated gastro-intestinal juices. *Food Res Int* 85:191–199. <https://doi.org/10.1016/j.foodres.2016.04.041>
- Noshad M, Mohebbi M, Shahidi F, Koocheki A (2015) Effect of layer-by-layer polyelectrolyte method on encapsulation of vanillin. *Int J Biol Macromol* 81:803–808. <https://doi.org/10.1016/j.ijbiomac.2015.09.012>
- Oh YS (2016) Bioactive compounds and their neuroprotective effects in diabetic complications. *Nutrients* 8(8):472. <https://doi.org/10.3390/nu8080472>
- Onoue S, Ochi M, Yamada S (2011) Development of (–)-epigallocatechin-3-gallate (EGCG)-loaded enteric microparticles with intestinal mucoadhesive property. *Int J Pharm* 410 (1):111–113. <https://doi.org/10.1016/j.ijpharm.2011.03.020>
- Palazzo C, Trapani G, Ponchel G, Trapani A, Vauthier C (2017) Mucoadhesive properties of low molecular weight chitosan- or glycol chitosan- and corresponding thiomers-coated poly (isobutylcyanoacrylate) core-shell nanoparticles. *Eur J Pharm Biopharm* 117:315–323. <https://doi.org/10.1016/j.ejpb.2017.04.020>
- Patel J, Champavat V (2015) Toxicity of nanomaterials on the gastrointestinal tract. *Biointeract Nanomater* 3:259–283
- Pérez-Esteve É, Ruiz-Rico M, Martínez-Máñez R, Barat JM (2015) Mesoporous silica-based supports for the controlled and targeted release of bioactive molecules in the gastrointestinal tract. *J Food Sci* 80(11):E2504–E2516. <https://doi.org/10.1111/1750-3841.13095>
- Pergushov DV, Müller AHE, Schacher FH (2012) Micellar interpolyelectrolyte complexes. *Chem Soc Rev* 41(21):6888–6901. <https://doi.org/10.1039/C2CS35135H>
- Qiu L, Li Z, Qiao M, Long M, Wang M, Zhang X, Tian C, Chen D (2014) Self-assembled pH-responsive hyaluronic acid–g-poly(L-histidine) copolymer micelles for targeted intracellular delivery of doxorubicin. *Acta Biomater* 10(5):2024–2035. <https://doi.org/10.1016/j.actbio.2013.12.025>
- Ramalingam P, Yoo SW, Ko YT (2016) Nanodelivery systems based on mucoadhesive polymer coated solid lipid nanoparticles to improve the oral intake of food curcumin. *Food Res Int* 84:113–119. <https://doi.org/10.1016/j.foodres.2016.03.031>
- Ramesan RM, Sharma CP (2009) Challenges and advances in nanoparticle-based oral insulin delivery. *Expert Rev Med Devices* 6(6):665–676. <https://doi.org/10.1586/erd.09.43>
- Ranhotra GS, Gelroth JA, Langemeier J, Rogers DE (1995) Stability and contribution of beta carotene added to whole wheat bread and crackers. *Cereal Chem* 72(2):139–141
- Reboul E (2017) Vitamin E bioavailability: mechanisms of intestinal absorption in the spotlight. *Antioxidants (Basel)* 6(4):95. <https://doi.org/10.3390/antiox6040095>
- Reboul E, Goncalves A, Comera C, Bott R, Nowicki M, Landrier J-F, Jourdeuil-Rahmani D, Dufour C, Collet X, Borel P (2011) Vitamin D intestinal absorption is not a simple passive diffusion: evidences for involvement of cholesterol transporters. *Mol Nutr Food Res* 55 (5):691–702. <https://doi.org/10.1002/mnfr.201000553>
- Ribnicky DM, Roopchand DE, Oren A, Grace M, Poulev A, Lila MA, Havenaar R, Raskin I (2014) Effects of a high fat meal matrix and protein complexation on the bioaccessibility of blueberry anthocyanins using the TNO gastrointestinal model (TIM-1). *Food Chem* 142:349–357. <https://doi.org/10.1016/j.foodchem.2013.07.073>

- Richard D, Bausero P, Schneider C, Visioli F (2009) Polyunsaturated fatty acids and cardiovascular disease. *Cell Mol Life Sci* 66(20):3277. <https://doi.org/10.1007/s00018-009-0085-4>
- Sambuy Y, De Angelis I, Ranaldi G, Scarino ML, Stamatii A, Zucco F (2005) The Caco-2 cell line as a model of the intestinal barrier: influence of cell and culture-related factors on Caco-2 cell functional characteristics. *Cell Biol Toxicol* 21(1):1–26. <https://doi.org/10.1007/s10565-005-0085-6>
- Saravanan M, Rao KP (2010) Pectin–gelatin and alginate–gelatin complex coacervation for controlled drug delivery: influence of anionic polysaccharides and drugs being encapsulated on physicochemical properties of microcapsules. *Carbohydr Polym* 80(3):808–816. <https://doi.org/10.1016/j.carbpol.2009.12.036>
- Saura-Calixto F, Serrano J, Goñi I (2007) Intake and bioaccessibility of total polyphenols in a whole diet. *Food Chem* 101(2):492–501. <https://doi.org/10.1016/j.foodchem.2006.02.006>
- Schmitt C, Sanchez C, Lamprecht A, Renard D, Lehr C-M, de Kruif CG, Hardy J (2001) Study of  $\beta$ -lactoglobulin/acacia gum complex coacervation by diffusing-wave spectroscopy and confocal scanning laser microscopy. *Colloids Surf B: Biointerfaces* 20(3):267–280. [https://doi.org/10.1016/S0927-7765\(00\)00200-9](https://doi.org/10.1016/S0927-7765(00)00200-9)
- Shah BR, Li Y, Jin W, An Y, He L, Li Z, Xu W, Li B (2016) Preparation and optimization of pickering emulsion stabilized by chitosan-tripolyphosphate nanoparticles for curcumin encapsulation. *Food Hydrocoll* 52:369–377. <https://doi.org/10.1016/j.foodhyd.2015.07.015>
- Shan W, Zhu X, Liu M, Li L, Zhong J, Sun W, Zhang Z, Huang Y (2015) Overcoming the diffusion barrier of mucus and absorption barrier of epithelium by self-assembled nanoparticles for oral delivery of insulin. *ACS Nano* 9(3):2345–2356. <https://doi.org/10.1021/acs.nano.5b00028>
- Shen W, Matsui T (2017) Current knowledge of intestinal absorption of bioactive peptides. *Food Funct* 8(12):4306–4314. <https://doi.org/10.1039/c7fo01185g>
- Sheng J, Han L, Qm J, Ru G, Li R, Wu L, Cui D, Yang P, He Y, Wane J (2015) *N*-trimethyl chitosan chloride-coated PLGA nanoparticles overcoming multiple barriers to oral insulin absorption. *ACS Appl Mater Interfaces* 7(28):15430–15441. <https://doi.org/10.1021/acsami.5b03555>
- Shi M, Bai J, Zhao L, Yu X, Liang J, Liu Y, Nord W, Li Y (2017) Co-loading and intestine-specific delivery of multiple antioxidants in pH-responsive microspheres based on TEMPO-oxidized polysaccharides. *Carbohydr Polym* 157:858–865. <https://doi.org/10.1016/j.carbpol.2016.10.057>
- Shrestha N, Shahbazi M-A, Araújo F, Mäkilä E, Raula J, Kauppinen EI, Salonen J, Sarmiento B, Hirvonen J, Santos HA (2015) Multistage pH-responsive mucoadhesive nanocarriers prepared by aerosol flow reactor technology: a controlled dual protein-drug delivery system. *Biomaterials* 68:9–20. <https://doi.org/10.1016/j.biomaterials.2015.07.045>
- Sing CE (2017) Development of the modern theory of polymeric complex coacervation. *Adv Colloid Interf Sci* 239:2–16. <https://doi.org/10.1016/j.cis.2016.04.004>
- Situ W, Chen L, Wang X, Li X (2014) Resistant starch film-coated microparticles for an oral colon-specific polypeptide delivery system and its release behaviors. *J Agric Food Chem* 62(16):3599–3609. <https://doi.org/10.1021/jf500472b>
- Song G-B, Xu J, Zheng H, Feng Y, Zhang W-W, Li K, S-s G, Li K, Zhang H (2015) Novel soluble dietary fiber–tannin self-assembled film: a promising protein protective material. *J Agric Food Chem* 63(24):5813–5820. <https://doi.org/10.1021/acs.jafc.5b00192>
- Taiz L, Zeiger E, Møller IM, Murphy A (2015) *Plant physiology and development*. Sinauer Associates, Sunderland, MA
- Takahashi M, Uechi S, Takara K, Asikin Y, Wada K (2009) Evaluation of an oral carrier system in rats: bioavailability and antioxidant properties of liposome-encapsulated curcumin. *J Agric Food Chem* 57(19):9141–9146. <https://doi.org/10.1021/jf9013923>
- Tan Y, Xu K, Liu C, Li Y, Lu C, Wang P (2012) Fabrication of starch-based nanospheres to stabilize pickering emulsion. *Carbohydr Polym* 88(4):1358–1363. <https://doi.org/10.1016/j.carbpol.2012.02.018>



- Tan C, Feng B, Zhang X, Xia W, Xia S (2016) Biopolymer-coated liposomes by electrostatic adsorption of chitosan (chitosomes) as novel delivery systems for carotenoids. *Food Hydrocoll* 52:774–784. <https://doi.org/10.1016/j.foodhyd.2015.08.016>
- Tian Q, Ding F, Guo L, Wang J, Wu F, Yu Y (2016) Targeted solid lipid nanoparticles with peptide ligand for oral delivery of atorvastatin calcium. *RSC Adv* 6(42):35901–35909. <https://doi.org/10.1039/C6RA02371A>
- Tong W, Song X, Gao C (2012) Layer-by-layer assembly of microcapsules and their biomedical applications. *Chem Soc Rev* 41(18):6103–6124. <https://doi.org/10.1039/C2CS35088B>
- Ubbink J, Krüger J (2006) Physical approaches for the delivery of active ingredients in foods. *Trends Food Sci Technol* 17(5):244–254. <https://doi.org/10.1016/j.tifs.2006.01.007>
- Vallejo F, Gil-Izquierdo A, Pérez-Vicente A, García-Viguera C (2004) *In vitro* gastrointestinal digestion study of broccoli inflorescence phenolic compounds, glucosinolates, and vitamin C. *J Agric Food Chem* 52(1):135–138. <https://doi.org/10.1021/jf0305128>
- Velderrain-Rodríguez G, Palafox-Carlos H, Wall-Medrano A, Ayala-Zavala J, Chen CO, Robles-Sánchez M, Astiazaran-García H, Alvarez-Parrilla E, González-Aguilar G (2014) Phenolic compounds: their journey after intake. *Food Funct* 5(2):189–197. <https://doi.org/10.1039/c3fo60361j>
- Wang XD (1994) Absorption and metabolism of beta-carotene. *J Am Coll Nutr* 13(4):314–325. <https://doi.org/10.1080/07315724.1994.10718416>
- Wang Z, Li Y, Chen L, Xin X, Yuan Q (2013) A study of controlled uptake and release of anthocyanins by oxidized starch microgels. *J Agric Food Chem* 61(24):5880–5887. <https://doi.org/10.1021/jf400275m>
- Wang MS, Chaudhari A, Pan Y, Young S, Nitin N (2014) Controlled release of natural polyphenols in oral cavity using starch pickering emulsion. *MRS Proc* 1688:7–11. <https://doi.org/10.1557/opl.2014.482>
- Wang S, Chen X, Shi M, Zhao L, Li W, Chen Y, Lu M, Wu J, Yuan Q, Li Y (2015a) Absorption of whey protein isolated (WPI)-stabilized  $\beta$ -carotene emulsions by oppositely charged oxidized starch microgels. *Food Res Int* 67:315–322. <https://doi.org/10.1016/j.foodres.2014.11.041>
- Wang S, Chen Y, Liang H, Chen Y, Shi M, Wu J, Liu X, Li Z, Liu B, Yuan Q, Li Y (2015b) Intestine-specific delivery of hydrophobic bioactives from oxidized starch microspheres with an enhanced stability. *J Agric Food Chem* 63(39):8669–8675. <https://doi.org/10.1021/acs.jafc.5b03575>
- Wang YH, Ke XM, Zhang CH, Yang RP (2017) Absorption mechanism of three curcumin constituents through in situ intestinal perfusion method. *Braz J Med Biol Res* 50(11):e6353. <https://doi.org/10.1590/1414-431X20176353>
- Weinbreck F, de Vries R, Schrooyen P, de Kruijff CG (2003) Complex coacervation of whey proteins and gum Arabic. *Biomacromolecules* 4(2):293–303. <https://doi.org/10.1021/bm025667n>
- Wilde SC, Keppler JK, Palani K, Schwarz K (2016)  $\beta$ -lactoglobulin as nanotransporter for allixin: sensory properties and applicability in food. *Food Chem* 199:667–674. <https://doi.org/10.1016/j.foodchem.2015.12.055>
- Williams M, Armes SP, Verstraete P, Smets J (2014) Double emulsions and colloidosomes-in-colloidosomes using silica-based pickering emulsifiers. *Langmuir* 30(10):2703–2711. <https://doi.org/10.1021/la500219m>
- Woo KS, Seib PA (2002) Cross-linked resistant starch: preparation and properties. *Cereal Chem* 79(6):819–825. <https://doi.org/10.1094/CCHEM.2002.79.6.819>
- Wu J, Shi M, Li W, Zhao L, Wang Z, Yan X, Norde W, Li Y (2015) Pickering emulsions stabilized by whey protein nanoparticles prepared by thermal cross-linking. *Colloids Surf B: Biointerfaces* 127:96–104. <https://doi.org/10.1016/j.colsurfb.2015.01.029>
- Wu Y, Shen J, Larcinese-Hafner V, Erni P, Ouali L (2016) Hybrid microcapsules with tunable properties via pickering emulsion templates for the encapsulation of bioactive volatiles. *RSC Adv* 6(104):102595–102602. <https://doi.org/10.1039/C6RA21338C>

- Yang JH, Lee SY, Han YS, Park KC, Choy JH (2003) Efficient transdermal penetration and improved stability of L-ascorbic acid encapsulated in an inorganic nanocapsule. *Bull Kor Chem Soc* 24(4):499–503
- Yang Y, Guo Y, Sun R, Wang X (2016) Self-assembly and  $\beta$ -carotene loading capacity of hydroxyethyl cellulose-graft-linoleic acid nanomicelles. *Carbohydr Polym* 145:56–63. <https://doi.org/10.1016/j.carbpol.2016.03.012>
- Yang T, Moresi L, Müller RD, Gurnis M (2017) Oceanic residual topography agrees with mantle flow predictions at long wavelengths. *Geophys Res Lett* 44(21):10, 896–810, 906. <https://doi.org/10.1002/2017GL074800>
- Ye M, Kim S, Park K (2010) Issues in long-term protein delivery using biodegradable microparticles. *J Control Release* 146(2):241–260. <https://doi.org/10.1016/j.jconrel.2010.05.011>
- Yoo JY, Chen XD (2006) GIT physicochemical modeling - a critical review. *Int J Food Eng* 2 (4):182–190. <https://doi.org/10.2202/1556-3758.1144>
- Yoo M-K, Kang S-K, Choi J-H, Park I-K, Na H-S, Lee H-C, Kim E-B, Lee N-K, Nah J-W, Choi Y-J, Cho C-S (2010) Targeted delivery of chitosan nanoparticles to peyer's patch using M cell-homing peptide selected by phage display technique. *Biomaterials* 31(30):7738–7747. <https://doi.org/10.1016/j.biomaterials.2010.06.059>
- Yu M, Yang Y, Zhu C, Guo S, Gan Y (2016) Advances in the transepithelial transport of nanoparticles. *Drug Discov Today* 21(7):1155–1161. <https://doi.org/10.1016/j.drudis.2016.05.007>
- Yun Y, Cho YW, Park K (2013) Nanoparticles for oral delivery: targeted nanoparticles with peptidic ligands for oral protein delivery. *Adv Drug Deliv Rev* 65(6):822–832. <https://doi.org/10.1016/j.addr.2012.10.007>
- Zeeb B, Weiss J, McClements DJ (2015) Electrostatic modulation and enzymatic cross-linking of interfacial layers impacts gastrointestinal fate of multilayer emulsions. *Food Chem* 180 (2):257–264. <https://doi.org/10.1016/j.foodchem.2015.02.048>
- Zhang C, Chen J-D, Yang F-Q (2014) Konjac glucomannan, a promising polysaccharide for ODDS. *Carbohydr Polym* 104:175–181. <https://doi.org/10.1016/j.carbpol.2013.12.081>
- Zhang Z, Zhang R, Decker EA, McClements DJ (2015) Development of food-grade filled hydrogels for oral delivery of lipophilic active ingredients: pH-triggered release. *Food Hydrocoll* 44:345–352. <https://doi.org/10.1016/j.foodhyd.2014.10.002>
- Zhao L, Chen Y, Li W, Lu M, Wang S, Chen X, Shi M, Wu J, Yuan Q, Li Y (2015a) Controlled uptake and release of lysozyme from glycerol diglycidyl ether cross-linked oxidized starch microgel. *Carbohydr Polym* 121:276–283. <https://doi.org/10.1016/j.carbpol.2015.01.002>
- Zhao T, Liu Y, Gao Z, Gao D, Li N, Bian Y, Dai K, Liu Z (2015b) Self-assembly and cytotoxicity study of PEG-modified ursolic acid liposomes. *Mater Sci Eng C* 53:196–203. <https://doi.org/10.1016/j.msec.2015.04.022>
- Zheng H, Gao M, Ren Y, Lou R, Xie H, Yu W, Liu X, Ma X (2017) An improved pH-responsive carrier based on EDTA-Ca-alginate for oral delivery of lactobacillus rhamnosus ATCC 53103. *Carbohydr Polym* 155:329–335. <https://doi.org/10.1016/j.carbpol.2016.08.096>
- Zimet P, Livney YD (2009) Beta-lactoglobulin and its nanocomplexes with pectin as vehicles for  $\omega$ -3 polyunsaturated fatty acids. *Food Hydrocoll* 23(4):1120–1126. <https://doi.org/10.1016/j.foodhyd.2008.10.008>
- Zou T, Li Z, Percival SS, Bonard S, Gu L (2012) Fabrication, characterization, and cytotoxicity evaluation of cranberry procyanidins-zein nanoparticles. *Food Hydrocoll* 27(2):293–300. <https://doi.org/10.1016/j.foodhyd.2011.10.002>

# Chapter 12

## Replacement of Fat or Starch



**Cuixia Sun and Yapeng Fang**

**Abstract** A growing public demand for low-calorie foods is stimulating the researchers and food manufacturers to develop reduced-calorie products due to the recognized adverse effects of high energy diet on human health. Fat and starch are two condensed sources of energy, and reducing their intake is a major dietary goal for the consumer. Currently a variety of available technological options have been applied to decrease the content of fat or starch in foods. The development of food hydrocolloids-based fat or starch replacers is one of the most important approaches for fat or starch reduction because their functionalities allow them to mimic the oral and flow properties of fat or starch. However, the replacement of fat or starch is not trivial because both of them play important roles in determining the nutritional, physical, chemical, and sensory characteristics of foods. How to achieve the replacement of fat while matching as close as possible all the characteristics of full-fat foods remains a major challenge. This chapter describes the main challenges for the reduction of fat from the viewpoint of flavour perception and texture quality. Two strategies for fat replacement are involved, including food formulation optimization and food structure design. Various hydrocolloids-based formulations created for the purpose of starch replacement are introduced and the associated principles discussed. The commercially available fat replacers and their applications in different food products are presented.

**Keywords** Fat · Starch · Replacement · Challenges · Strategies

---

C. Sun · Y. Fang (✉)

Department of Food Science and Technology, School of Agriculture and Biology, Shanghai Jiao Tong University, Shanghai, China

e-mail: [ypfang@sjtu.edu.cn](mailto:ypfang@sjtu.edu.cn)

## 1 Introduction

High calorie food intake is associated with the increased prevalence of numerous chronic diseases, including obesity, type 2 diabetes, hypertension, cancers, gall bladder disease, and coronary heart disease. Fat and starch are two major sources of calories in many processed food products. High levels of certain types of triacylglycerols in the blood have been related to coronary heart disease and obesity (Bray et al. 2004; Han et al. 2016). Rapid digestion of starch causes a sudden rise in blood glucose level, which has been linked to diabetes and obesity (Lustig et al. 2012; Svihus and Hervik 2016). Based on the growing awareness about the adverse effects of high caloric products through nutrition and health claims, reducing fat or starch intake is becoming a major dietary goal for the consumer. In addition, our ever more sedentary life styles serve as a driving force to decline the consumption of high-energy foods.

The World Health Organization (2003) recommends a daily intake of total fat no more than 30% of dietary energy, of which <10% should be saturated fatty acids. The UK Food Standards Agency (2008) published its Saturated Fat and Energy Intake Programme and recommends that the saturated fat consumption should be reduced from 13.3% of dietary energy to 11%. The 2015–2020 Dietary Guidelines for Americans emphasize the restriction of trans and saturated fats intake and recommend the consumption of low-fat or fat-free foods (DeSalvo et al. 2016). Food reformulation to reduce the content of fat was included in nutrition action plans of many European countries (Belc et al. 2019). The United States Code of Federal Regulations (2014) defines low-fat food as: ‘The food has a reference amount customarily consumed >30 g and contains 3 g or less of fat per reference amount customarily consumed (RACC); or the food has a reference amount customarily consumed of 30 g or less and contains 3 g or less of fat per RACC and per 50 g of food’. In the USA, a low-fat cheese must contain 6 g or less of fat per 100 g of cheese, while a reduced-fat cheese requires at least a 25% reduction in fat level from the traditional fat level of the referenced variety. Fat-free cheese is defined as that with <0.5 g fat per 100 g of cheese (Johnson 2011).

In such a context, researchers and the food industry are highly sensitive to consumer perceptions and demands for low-calorie foods. However, the replacement of fat or starch is not trivial because both of them play important roles in determining the nutritional, physical, chemical, and sensory characteristics of foods. For example, as shown in Fig. 12.1, fat not only provides a concentrated source of energy, but also supplies essential fatty acids and fat-soluble vitamins (A, D, E, and K). Fat reduction would result in loss of nutritional benefits or even an unbalanced diet (Colmenero 2000). Besides, fat provides structure in baked goods, influences the storage stability, and affects the observed lightness of food products owing to the impact of the fat droplets on light scattering (Chung et al. 2013a). A direct removal or simple replacement of fat without compensation for specific functions would cause a considerable change in the organoleptic characteristics of foods, leading to a poor food quality. For instance, inulin addition at levels of 100% in cake

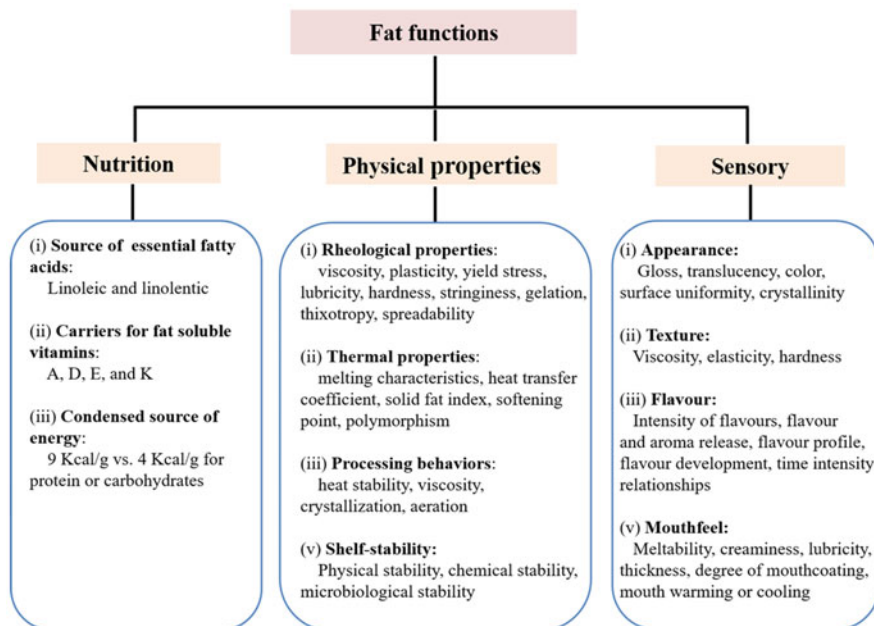


**Fig. 12.1** Functions of fat in food products

formulations resulted in remarkable loss of different quality attributes, including higher water activity and baking loss, lower volume, harder texture, darker colour, and highly asymmetrical shape (Majzoobi et al. 2018). Starch granules are often used in food products to provide desirable texture attributes, such as ‘thickness’, and contribute to the physicochemical properties of foods, including the volume, viscosity, gelation, and stability (Ai and Jane 2015). Any ingredients to replace starch granules should be able to simulate such characteristics normally provided by conventional starch granules and meanwhile should contribute less calories and lower glycemic index (McClements et al. 2017).

Consequently, a number of considerations need to be taken into account for the feasibility of fat- or starch-reduced products in order to maintain the desired physicochemical and sensory attributes of original foods. In this chapter, major challenges for the development of low-fat or low-starch foods are discussed from the aspects of scientific problems and technical limitations. A variety of hydrocolloids-based formulations developed for the purpose of fat or starch replacement are introduced and the associated principles discussed. The commercially available fat replacers and their applications in different food products are presented.

## 2 Challenges for Fat or Starch Replacement

Based on either omission or replacement of fat or starch, a variety of available technological options have been involved to quantitatively reduce fat or starch content and qualitatively modify the fatty acid profiles. For example, food reformulation is one of the most important approaches to remove, reduce, and/or replace different components in order to develop healthy products. However, food is a typically complex colloid system with common characteristics of multiphase, multicomponent, and multiscale. Fat droplets and starch granules vary considerably in their size, shape, charge, and behaviour and endow foods with many desirable functions. Therefore, they are difficult to replace.

### 2.1 Challenges for Fat Replacement

The elimination or reduction of fat in foods evidently modifies its composition and structure and also the expected interactions among components, giving rise in most cases to clearly perceptible changes in flavour and/or texture. Moreover, although most taste compounds do not dissolve in fats, when fat content is reduced, the salty, sweet, sour, and umami tastes will be weakened and the bitter taste enhanced (Metcalf and Vickers 2002).

#### 2.1.1 Flavour Concerns

Sensory preference for fat appears to be a universal human trait because fat contributes to numerous sensory characteristics of fatty products, including appearance, texture, flavour and aroma, and mouthfeel. Flavour as one of the most-important attributes determines consumer selection and satisfaction with fat-reduced foods. Reduction or elimination of fat directly affects the processes of flavour release and perception, modifies the signals received by the brain on consuming a particular food, and may partially determine its acceptance or rejection.

#### Flavour Distribution and Release

The term 'flavour' refers to volatile components that are sensed by aroma receptors in the nose and non-volatile components that are sensed by taste receptors in the mouth (Taylor and Linforth 1996). The overall perceived flavour of a food product usually involves the integration of information from mouthfeel, taste, and aroma during mastication (González-Tomás et al. 2008). As an extremely complicated process, flavour perception is dependent on a combination of physicochemical, biological, and psychological phenomenon, which is perhaps the most multisensory

of our everyday experiences (Spence 2015). Fat functions as flavour precursors, and reducing fat content influences both the distribution of the flavour and the kinetics of flavour release (McClements and Demetriades 1998). The type and concentration of flavour molecules mainly determine the perceived flavour. For nonpolar flavour, decreasing fat content would increase in the aqueous phase flavour concentration, leading to an intense initial taste perception (Roberts et al. 2003). Even if the amount of flavour compounds is rebalanced in fat-reduced foods to provide the same maximum aroma intensity as the full-fat products, the low-fat alternatives still fail to match the same perception. The major reason is that fat has an impact on time-intensity profile of lipophilic flavour release. The sustained aroma release relies on the hydrophobicity and fat content of the product, that is, the higher the hydrophobicity and fat content, the slow the aroma release into the aqueous phase (de Roos 2006). In full-fat products, a rich flavour sensation is perceived because flavour compounds with various degrees of hydrophobicity are released at different rates. On the contrary, in reduced-fat products, lower amount of fat is insufficient to retain the aroma compounds and thus causes quick flavour disappearance and lack of richness (van Ruth et al. 2002).

### Flavour–Ingredients Interactions

Food matrix ingredients such as proteins, polysaccharides, and lipids can interact with flavour compounds (Guichard 2002). Modification of the food formulation by using fat replacers would change such interaction and thus alter the flavour perception. The development of fat-reduced products with desired flavour will be only possible if the knowledge of flavour-ingredients interactions has been well understood (Plug and Haring 1994). Flavour-binding behaviour of fat replacers results in lower volatilities in aqueous systems, which may explain the decreased flavour intensity in fat-reduced foods (Godshall 1997; Fischer and Widder 1997). For example, proteins like  $\beta$ -lactoglobulin, casein, gelatin, and egg albumin can interact with flavour compounds by reversible or irreversible binding, causing lower volatilities in water phase (Maier 1970). More research is required to explore the mechanisms of flavour–ingredients interactions and the location of the binding sites, which can provide the necessary information for the selection of suitable fat replacers in the development of fat-reduced food products.

#### 2.1.2 Texture Concerns

Texture is another important sensory attribute to assess food quality, such as being hard or soft, cold or warm, oily or juicy, elastic or flaky, heavy, viscous, or smooth. If the texture attribute fails to meet our expectations, we may reject the food regardless of the quality of flavour (Engelen and de Wijk 2012). Fat is an important contributor to texture in different types of foods, such as thickness of liquid foods (Villegas and Costell 2007), consistency of semisolids (Tárrega and Costell 2006), and firmness of

solids (Kavas et al. 2004). Fat content has obvious impacts on the food texture in different ways because fat droplets impart many textural characteristics such as the viscosity, afterfeel, lubrication, and melting or cooling mouthfeel. Fat reduction usually results in a dramatic decrease in viscosity, leading to the lower perceived thickness. The common approach is to add biopolymer or biopolymer mixture to the aqueous phase to enhance its viscosity. However, biopolymer molecules are not able to mimic all of the textural characteristics. Particularly, fat has distinctive thermal properties because of its unique melting point, which contributes the creamy mouthfeel after the melting of fat crystals at room temperature (Weenen 2005). It was reported that heat transfer between foods and the oral surface may be an important factor for fat perception. The perceived food temperature is associated with fat content, for example, high fat products were perceived as warmer than low-fat products (Weenen et al. 2003). Therefore, the sensory difference of foods with different fat contents can be detected based on the fact that lips and tongue are highly sensitive with the temperature changes (Prinz et al. 2007).

Moreover, numerous sensory characteristics of food emulsions are related to their rheological properties such as elasticity, viscosity, and viscoelasticity. For example, the fatty, creamy, smooth, and thick texture of full-fat products is related to the bulk rheology, thin-film rheology, and colloidal interaction between food and oral surface (Malone et al. 2003). Removal of fat causes textural problems in reduced or low-fat ice creams, such as coarseness and iciness, crumbly body, shrinkage, and flavour defects (Akalin et al. 2008). Cakes presented significantly increased hardness, elasticity, and decreased specific volume as fat replacement increased above 65%, leading to lower scores on taste and flavour (Psimouli and Oreopoulou 2013). Fat reduction is likely to reduce the degree of shear-thinning behaviour, which may have important implications for the mouthfeel and texture of the product. Therefore, a thorough understanding of the rheological behaviours and colloidal properties of foods would provide guidelines for the design of products with the replacement of fat or starch but without quality loss.

Overall, the functional properties of lipids that must be reproduced include organoleptic properties, the ability to dissolve lipid-soluble flavours, aeration, aroma, emulsification, flavour, heat stability, and spreadability. Translating idea into reality is not a simple task. Hydrocolloids-based fat replacers are generally polar water-soluble compounds, so it is difficult for them to replace some of the nonpolar functional characteristics of fats, such as lipid-soluble flavour-carrying capacity.

## ***2.2 Challenges for Starch Replacement***

Starch granules are widely used in foods to create desirable textural attributes because of its preferable characteristics such as gelling, thickening, and aqueous solubility. The viscosity is a determining factor for the application of starch in food products to obtain desirable rheological characteristics (Sarkar et al. 2013).



Therefore, the challenge for starch replacement is how to develop a food ingredient with similar functional attributes as starch granules.

### 2.2.1 Pasting and Gel Texture Properties Control

The replacement of starch with non-starch hydrocolloids influences the properties of a starch-based paste, gel, or food product. Mixing gelatin (0.5 wt%) with pectin (0.01 wt%) formed the hydrogel particles with similar dimensions to swollen starch granules, and these hydrogel microspheres were shown to have similar rheological attributes as starch pastes (Wu et al. 2014). However, the unsolved technical and scientific question is that the physicochemical properties of gelatin are highly susceptible to temperature because it forms a gel at low temperatures. By the increase of corn starch citrate (CSC) substitution level, the textural parameters of wheat starch gels were decreased, such as firmness, cohesiveness, springiness, gumminess, and chewiness (Hedayati and Niakousari 2018). Addition of glutamic acid or lysine increased gelatinization temperatures of the cross-linked potato starches and decreased the  $G'$  and  $G''$  moduli of the modified starch gels while accelerated the retrogradation process (Gałkowska and Juszcak 2019), which may cause undesirable changes to food and mostly affect the bakery products. The substitution of kudzu and lotus starches with soybean soluble polysaccharide (SSPS) reduced the hardness of the starch/SSPS gels, and the mixtures of starch/SSPS yielded more liquid-like behaviour than the controls did (Liu et al. 2019). The modified pasting and gel texture properties may change the sensory properties of the end product. Therefore, how to control the stability and quality of starch-based foods is the key point for starch replacement. In addition, the amylose content positively correlated with its cohesiveness and stringiness (Zhang et al. 2019), and amylopectin molecular size significantly contributes to gel viscoelasticity (Li et al. 2019). Consequently, the pasting and gel texture properties of starch-based foods would be influenced after starch being replaced by the non-starch hydrocolloids.

### 2.2.2 Interactions Control

The compositions of starch-based foods are generally complicated, and the interactions of starch with various food components such as proteins and lipids have been extensively reported. The challenge of starch replacement lies in the understanding of the interaction mechanisms of starch and non-starch food constituents to achieve desirable quality of low-starch foods. Starch–protein interactions affect the rheological, pasting, gelatinization, textural, and physicochemical properties of food systems (Villanueva et al. 2015). In general, the inclusion of proteins increased water absorption capacity, water absorption index, water solubility index, and swelling power, decreased the viscosity of gels, and increased their stability, with the effect being more conspicuous for SPI incorporation (Villanueva et al. 2018). The interaction between starch and whey protein mainly through hydrogen bonds restricted

the swelling process of starch granule while accelerated recrystallization after cold storage (Yang et al. 2019). Complexes between amylose and lipids may significantly modify the properties and functionality of starch. For example, the solubility of starch in water is reduced, and the gelatinization temperature is increased after the complexation with lipids (Copeland et al. 2009). Lipids may prevent gelatinization by inhibiting hydration of amylopectin chains and retard retrogradation, which affects starch digestibility (Henry 2009). Starch/carrageenan interactions are especially involved in dairy products where gelling properties are of primary importance (Huc et al. 2014). The lower carrageenan charge density, the higher the interaction between starch and carrageenan (Lascombes et al. 2017). Formation of starch gel is hindered by the presence of cationic polysaccharide and, therefore, the retrogradation of starch at very early stage can be delayed by addition of chitosan. However, long-term retrogradation was slightly increased (Raguzzoni et al. 2016).

Overall, a universal starch substitute does not exist. All of the macromolecule replacers contribute to distinct properties suitable for replicating a limited number of functions in particular food products.

### **3 Strategies for Fat Replacement**

The traditional dietary advice is to replace fat with low-calorie fruits, vegetables, and grains, which has not been very effective for reducing fat consumption. Direct fat removal was evolved as the first strategy to comply with nutritional recommendations in the 1980s, which worked well for milk, some dairy products, certain processed meat, but not much else. The approach to fat replacement has changed in the twenty-first century. Formulation optimization emerged as the second strategy to reduce fat content in foods, which is one of the most important approaches to replace fat in modern food technology. The food reformulation refers to the development of a range of functional ingredients as fat replacers to reduce fat intake. There are two large groups of fat replacers: fat substitutes and fat mimetics. In general, lipid-based fat replacers are fat substitutes, and protein- or carbohydrate-based fat replacers are fat mimetics (Sandrou and Arvanitoyannis 2000). In addition, processing technology is the third fat replacement strategy by varying processing conditions (pH, pressure, ionic strength, time and temperature, mixing order, stirring speed, etc.) to cause interactions in ingredients or to modify functionalities.

#### ***3.1 Food Formulation Optimization***

Ideally, fat mimetics should be safe, inexpensive, low calorie, suitable for cooking applications, yet provide the sensory equivalent of fat texture and flavour, and maintain the eating quality of foods. The majority of fat mimetics belong to the groups of polysaccharide and protein hydrocolloids because their functionalities

allow them to mimic the oral and flow properties of fat. For example, viscosity enhancement potential is an important feature in the use of hydrocolloids as emulsifying, stabilizing, and bodying agents in low-fat foods. Hydrocolloids as fat mimetics are able to augment the lubrication of aqueous fluids through the three lubrication regimes via both viscosity modification and by adsorbing to hydrophobic substrates (Stokes et al. 2011). Hydrocolloids-based fat replacers are usually divided into protein-based, carbohydrate-based, and lipid-based.

### 3.1.1 Protein-Based Fat Replacers

Protein-based fat mimetics are typically produced from egg, milk, whey, soy, or wheat proteins. Using proteinaceous ingredients to replace fat in food emulsions is mainly because of their emulsifying and stabilizing capacities. The particle size of hydrocolloids is important in determining both the taste and mouthfeel of fats in fat-replaced products. Food particles  $<3 \mu\text{m}$  in diameter are not detected by the oral cavity, and instead the substance feels creamy and smooth. The minimum size of particles above which humans detect the grittiness depends on the hardness and the shape of particles (Engelen et al. 2005). Therefore, proteins are often microparticulated by applying a high shearing force during heating of the proteins. The obtained small spherical (0.1–2.0  $\mu\text{m}$  diameter) protein gel particles are perceived in the mouth and taste buds as similar to fat with a creamy, smooth texture. Gelatin is commonly used in low-fat yoghurts due to its melting behaviour at body temperature, as it forms a thermoreversible gel (Alting et al. 2009). The representative microparticulated whey proteins (MWP) have been produced and applied in food systems as fat replacers since the 1980s due to its soft lubrication characteristics. MWP increases the lightness and viscosity of products, and almost all of the MWP-based systems have a creamy white appearance similar to sauces and dressings, indicating their potential application in the manufacture of reduced-fat foods (Chung and McClements 2014). For example, the improved texture and rheological properties of low-fat yoghurt were obtained when whey proteins were added as microparticles rather than conventional whey protein ingredients such as whey protein isolate (Torres et al. 2018). In addition, the complex of MWP and high-methoxyl pectin was prepared as a novel fat mimetic in low-fat mayonnaise (Fig. 12.2), and two possible hypotheses were proposed to explain the interaction and distribution of MWP, pectin, and droplets (Sun et al. 2018): (1) in low-fat mayonnaise (upper figure of Fig. 12.2), MWP particles were adsorbed on the surface of oil droplets by hydrophobic interaction and formed thick and viscous films, and pectin formed coatings around interfacial proteins to inhibit flocculation of oil droplets. (2) in non-fat mayonnaise (lower figure of Fig. 12.2), MWP evenly distributed among the stable three-dimensional network formed by pectin molecules, and the stable structure of fat mimetic was maintained by hydrogen bonding, electrostatic force, and van der Waals interactions (Gentès et al. 2010).

It was observed that the friction levels attained with MWP and dairy fat (DF) at typical speeds involved in oral processing were comparable, hence demonstrating

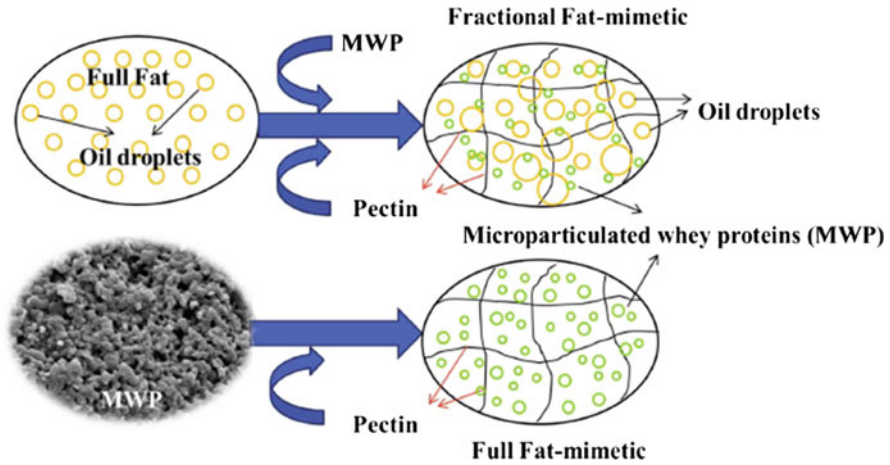


**Fig. 12.2** Schematic representation of interaction among microparticulated whey protein, pectin, and oil in low-fat and non-fat mayonnaises. Reproduction with permission from (Sun et al. 2018), Copyright 2018 Elsevier

the capability of MWP in skim milk dispersions to imitate DF in fluid milk-based systems from a lubrication point of view (Olivares et al. 2019). Compared with MWP, superfine MWP (sMWP) exhibited more stable liquid behaviours (Sun et al. 2015a) and could maintain creamy mouthfeel better due to high dispersion stability of sMWP–pectin–xanthan gum gel mixtures (Sun et al. 2016). In addition, a novel group of fat globular mimetics (FGMs) was prepared by coating calcium carbonate particles with a layer of casein–maltodextrin conjugates. Such FGMs were stable in skim milk during 10-day storage at 5 °C, and increased the desirable turbidity and viscosity of skim milk, which can be used to simultaneously reduce fat and increase calcium contents of food products (Qu and Zhong 2017).

Animal proteins are rich in necessary nutrients, particularly the essential amino acids needed for human body. However, they may have a strong allergic effect and are not suitable to produce food requiring heat treatment, because high temperatures induce irreversible denaturation of protein, altering the structure of the final product (Jing et al. 2011). Besides, the consumption of animal proteins would cause problems associated with biodiversity, land use, water use, climate, human health, and animal welfare (Aiking 2011). Natural plant proteins show similar physicochemical properties to animal proteins like water binding capacity and can serve as fat substitutes in low-calorie food. Soy proteins are increasingly important in the human diet because of reported beneficial effects on nutrition and health, including lowering plasma cholesterol, prevention of cancer, diabetes, and obesity, and protection against bowel and kidney disease (Friedman and Brandon 2001). The addition of soy protein isolate improved the textural properties of chopped low-fat pork batters and lowered the cooking loss (Gao et al. 2015). Soy protein hydrolysates (SPH) and their blends with xanthan gum (SPH/XG) is an alternative choice as a fat replacer in the production of reduced-fat ice cream since 50% fat-substituted ice cream with

SPH/XG (96:4) had an appearance, taste, and texture similar to that of 10% full-fat ice cream (Liu et al. 2018a). The major limitation of proteins as fat replacers is the occurrence of molecular interactions between proteins and some volatile compounds, giving rise to unbalanced or even unacceptable sensory profiles (Kühn et al. 2006).

### 3.1.2 Carbohydrate-Based Fat Replacers

Carbohydrates are typical fat replacers due to their molecular diversity that gives rise to various structural and physicochemical properties. For example, carbohydrate-based fat replacers bind water into a gel-type structure, resulting in lubrication and flow properties similar to those of fat. Cookies prepared from wheat flour by 15% supplementation of carbohydrate-based fat replacers showed better attributes in terms of colour and texture, which were judged to be the best by the panellists (Majeed et al. 2017). Compared with the relatively limited available choices for protein-based fat replacers, carbohydrate-based fat replacers include a much larger family of materials, which can be categorized into digestible polysaccharides (starch) and non-digestible polysaccharides (gums and cellulose).

#### Digestible Starch

Among the carbohydrate-based fat replacers, starch is one of the most frequently used ingredients as it is relatively inexpensive and readily available and capable of replacing numerous attributes (O'Connor and O'Brien 2011). There are two hypotheses for starch-based fat replacer to mimic the mouthfeel and texture characteristics of fat. One is that starch would form a three-dimensional gel network structure, and the water trapped in the gel could provide a fat-like sensation (Alexander 1995). The other is that the starch could form spherulites with similar size to fat globules (2–10  $\mu\text{m}$ ) during heating and cooling treatment, which provide the lubricating mouthfeel of fat (Singh et al. 2010). Amylose plays an important role in the simulation mechanism of starch-based fat replacer because amylose contributed to the gel structure of starch-based fat replacer (Yang and Xu 2007). With the increasing amylose ratio, spherulites of 2–10  $\mu\text{m}$  diameter, similar to fat globules in size, started to appear with the increasing amylose ratio, and the potato starch with 85% amylose ratio presented the better creamy texture (Hu et al. 2019). Starch-based fat replacers have been applied in a wide variety of low-fat food products including cheeses, sausages, yoghurt, mayonnaise, and frozen desserts (Peng and Yao 2017). The concentrations of starch frequently used as fat replacer in cheese normally ranges from 0.5 to 1.5% (Diamantino et al. 2014).

Different types of starches may present different behaviours as fat replacers. Compared to native starches, the modified starches produced high paste viscosity values and showed low retrogradation rates, which can be regarded as promising fat replacers in cheese (Diamantino et al. 2019). Starch granules remain even after

heating the aqueous starch suspension, but heating at temperatures higher than 130 °C leads to complete molecular dissociation (Hanselmann et al. 1996). Starch–water systems can be classified into three states: the intact granular state, the melted state, and the solution state. When aqueous potato starch suspensions were heated and then cooled, spreadable particle gels were obtained with a spherulite morphology and a cream-like texture, which is currently applied as a fat mimetic (Steeneken and Woortman 2009). Citric acid treated sweet potato starch showed fat mimetic properties as its melting temperature (51.44 °C) was close to the melting point of fat (Surendra Babu et al. 2016). The pasting viscosity of the octenyl succinic anhydride (OSA) modified mung bean starches (OSA-MS) was found to be higher when compared with native starch, and cakes prepared from 30% OSA-MS were found to be highly acceptable by their overall quality score including the best texture, desirable colour, and mouthfeel (Punia et al. 2019). For acidified milk gels (yoghurt) with pregelatinized (PG), and both pregelatinized and chemically modified starches, viscosity/texture values were similar to or higher than those found for full-fat milk gel (Bravo-Núñez et al. 2019). The corn starch nanocrystals (CSNC) are regarded as a useful fat replacer/stabilizer for an O/W model emulsion because its addition resulted in a more solid-like behaviour of the emulsions due to the formation of nanocrystal network in the continuous phase (Javidi et al. 2019). However, one of the potential disadvantages of starch-based fat replacer is that it contains calories, so its overconsumption may lead to problems with overweight and diabetes (Lustig et al. 2012). Some of these problems may be overcome by using resistant starch (Parada and Aguilera 2011).

### Non-digestible Cellulose Derivatives

Cellulose derivatives show different solubility, emulsifying property, and gelation characteristics, and they can reassociate with each other to form aggregates that can be used as fat replacers. Typically, 60–70% of the cellulose microcrystals are <0.2 mm long, which can form an insoluble dispersion in water. Methylcellulose (MC) and hydroxypropyl methylcellulose (HPMC) have been used to stabilize air bubbles, provide lubricity and creaminess, and entrap moisture in a variety of foods, such as salad dressings and biscuits (Laguna et al. 2014). Microcrystalline cellulose (MCC) is an uncharged biopolymer with a crystalline structure and could form a filled particle gel network. Therefore, MCC provides a fat-like mouthfeel and a softer texture (Fig. 12.3a) when it is added to the ground beef without causing a disturbance of the protein network. Since carboxymethyl cellulose (CMC) at high concentrations (>0.5 wt%) is thermodynamically incompatible with meat proteins, it is not a suitable fat replacer because it weakened the connections within the protein network (Gibis et al. 2015). As shown in Fig. 12.3b, cellulose nanofibrils (CNFs) at concentrations of 0.15 and 0.3 wt% were incorporated into low-fat (5 wt%) and standard ice cream formulations (10 wt%), which improved the sensory properties of low-fat samples, even after heat shocking the specimens (Velásquez-Cock et al. 2019).

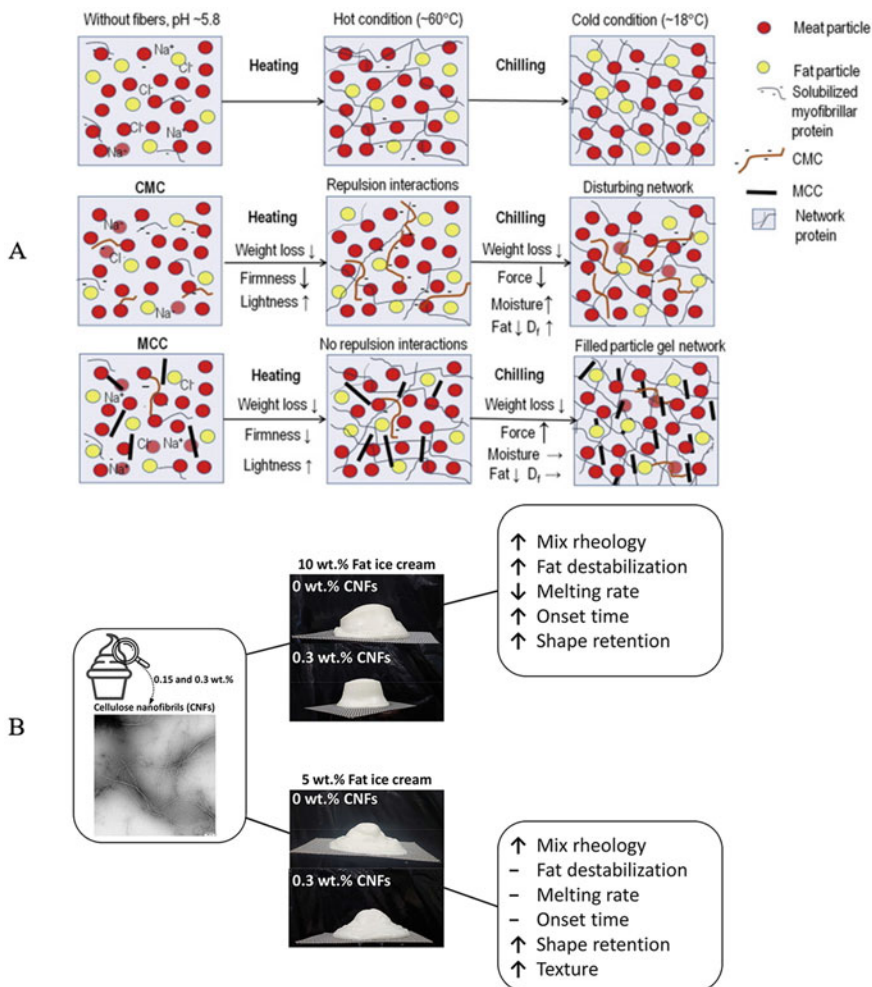


**Fig. 12.3** (a) Suggested mechanisms of interaction of meat proteins with CMC and MCC ( ) and (b) effect of cellulose nanofibrils (CNFs) at concentrations of 0.15 and 0.3 wt % on the physicochemical properties of low-fat (5 wt%) and standard ice cream formulations (10 wt%). (a) Reproduction with permission from (Gibis et al. 2015), Copyright 2015 Elsevier. (b) Reproduction with permission from (Velásquez-Cock et al. 2019), Copyright 2019 Elsevier

### Non-digestible Inulin

Inulin, typically derived from chicory root, belongs to a class of carbohydrates known as fructans (Kaur and Gupta 2002). As a non-digestible dietary fibre, inulin can remain stable during processing and successive heat treatment. It is widely used in replacing dietary fat in baked products, providing nearly the same sensory characters as of full-fat products while giving only 25–35% energy as compared to



digestible carbohydrates (Keenan et al. 2014). Such fat-substituting property is based on its ability to stabilize the structure of the aqueous phase, which creates an improved creaminess. A creamy mouthfeel is achieved when inulin is used as a fat replacer in dairy products due to its interactions with whey protein and caseinate (Karaca et al. 2009). Long chain inulin microcrystals could aggregate each other, interact with water, and eventually agglomerate creating a gel network, thus altering the product texture and providing a fat-like mouthfeel (Bayarri et al. 2011). The consumer study revealed that 15% fat replacement by inulin provided acceptable biscuits, but higher replacement decreased the overall acceptability (Laguna et al. 2014). Inulin addition (2–7%) to replace fat in fresh caprine milk cheese provided a creamier mouthfeel and added a reasonable flavour with softening effect (Salvatore et al. 2014). Fermented chicken sausages made with inulin as a partial oil replacement persisted stable without any significant loss of physicochemical, microbiological, and sensory characteristics during storage at 4 °C for 45 days (Menegas et al. 2013). It was found that inulin fortification of low-fat set yoghurt significantly reduced syneresis by 59% over full-fat control yoghurt (Rudra et al. 2017). What is more, inulin has promising gut health properties due to its prebiotic nature and may increase absorption of nutrients such as calcium. Therefore, it is recommended as a reasonably high-level fat replacer in crackers, cakes, biscuits, and muffins (Shoaib et al. 2016).

#### Other Non-digestible Gums

The performance of gums as fat replacers is determined mainly by their distinct chemical composition and structure (Saha and Bhattacharya 2010). The principles that are taken into account in applying gum as a fat mimetic include the rheological properties of the gel it forms, the effects of temperature and shearing forces on the functional properties of the gum, and its compatibility with other ingredients in the foods. Xanthan gum and carrageenan had large spheres of hydration, provided slipperiness and viscosity, and mimicked the continuous phase of mayonnaise (De Ruiter and Rudolph 1997). Locust bean gum (LBG) formed non-dissolved microparticles at relatively high concentrations ( $\geq 0.4\%$ ), trapping fat droplets within its hydrogel particles and helping balance the flavour profile of reduced-fat products (Chung et al. 2013b). Water-extracted okra gum was found to be effective to make an ice cream comparable with full-fat ice cream and was used to replace the fat in ice cream at 0, 22, 44, 55, 88, and 100% to produce super premium (18% fat), premium (14% fat), regular (10% fat), economy (8% fat), low-fat (2% fat), and zero-fat (0% fat) ice cream (Aziz et al. 2018). The substitution of fat with okra gum increased the viscous modulus ( $G''$ ) of the ice cream, and up to 55% replacement of fat was feasible to achieve satisfactory ice cream properties (Aziz et al. 2018). Addition of tragacanth gum (*A. gossypinus* and *A. compactus*) to sausage formulation effectively reduced cooking loss and enhanced oxidative stability, and 0.5% tragacanth (*A. gossypinus*) showed an acceptable sensory score of the sausage formulation, suggesting its potential to be a fat replacer in the reduced-fat sausages (Abbasi et al.



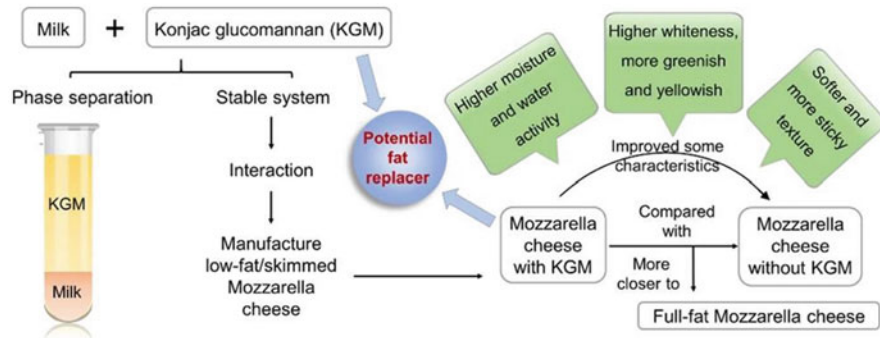


**Fig. 12.4** Schematic representation of KGM addition as a potential replacer in Mozzarella cheese. Reproduction with permission from (Dai et al. 2018), Copyright 2018 Elsevier

2019). The addition of pectin in ice cream can cause an increase in viscosity, overrun, and hardness and a decrease in meltdown of the ice cream. When 0.72% pectin (w/w) was incorporated into ice cream, a prototype product of ice cream with 45% lower fat content compared to the control was prepared (Zhang et al. 2018). Konjac glucomannan (KGM) as a natural polysaccharide also exhibits functional properties as a potential fat replacer in dairy products. As shown in Fig. 12.4, KGM addition in cheese affected the lightness, increased the moisture, lowered firmness, and increased the stickiness, and such changes were closer to those of full-fat cheese, suggesting KGM could improve some characteristics of the fat-reduced Mozzarella cheeses (Dai et al. 2018). Mozzarella cheese with konjac had lower firmness but higher meltability and less scorching in pizza bake and exhibited a denser casein matrix with coalesced fat globules (Dai et al. 2019). Sodium alginate was used to modify the textural and microstructural properties of low-fat Cheddar cheese up to 91% fat reduction (Khanal et al. 2018).

### 3.1.3 Combination Systems

Individual fat mimetic has limitations in its ability to cover the full functions of fat. The combination of different fat replacers may show synergistic interactions and provide better fat-like qualities which are not easy to achieve by individual fat replacers (Sikora et al. 2008). For example, single carbohydrate-based and protein-based fat mimetics may suffer from several sensory and functional limitations such as poor stability and undesirable mouthfeel. The simultaneous addition of protein and polysaccharides may induce intermolecular interactions that modify or generate more desirable functional properties (Gulão et al. 2016).

### Protein–Polysaccharide Combination

A combination of polydextrose with MWP is the most suitable fat replacers for soft-type cookies (Zoulias et al. 2000). The MWP in combination with either modified starch or locust bean gum (LBG), with or without fat droplets (5%), could be used as fat mimetics to modulate the texture, appearance, and stability of emulsion-based food products with reduced calorie such as sauces, mayonnaise, dressings, and dips (Chung et al. 2014). A nonheated whey protein–high methoxyl pectin mixture can be used as fat replacer in the skim milk formulations, which yielded a yoghurt texture resembling the full-fat counterpart because the associative interaction of whey proteins with pectin suppressed whey protein aggregation while maintaining the structuring effects of denatured whey protein in yoghurt (Krzeminski et al. 2014). Biopolymer-based hydrogel particles consisting of a protein-rich core and a pectin-rich shell were formed by using a segregation–aggregation phase separation method. Such particles may be suitable as texture modifiers and fat replacers since they scattered light strongly to give the hydrogel suspensions a milky white appearance and also led to an appreciable increase in viscosity or gel-like characteristics (Duval et al. 2015). The mixtures of soy protein isolate (SPI) and cellulose nanofibre (CNF) with a higher CNF proportion showed increased viscosity, storage modulus, and loss modulus and a higher tendency of gelation. The targeted low fat, low calorie, anti-melting, and similar textural taste were achieved when SPI–CNF complex gels with an SPI:CNF ratio of 7:1 were added to ice cream as a fat replacer (Fig. 12.5), in which 10% fat was replaced (Sun et al. 2015b).

### Polysaccharide–Polysaccharide Combination

Polysaccharides such as pectin and alginates can interact with each other to form more or less permanent junction zones, providing yield stress and gel structure. Maltodextrin and xanthan gum yielded increased moisture, hardness, and chewiness in 66% FR (fat replacer) muffins (Khouryieh et al. 2005). The mixtures of guar gum

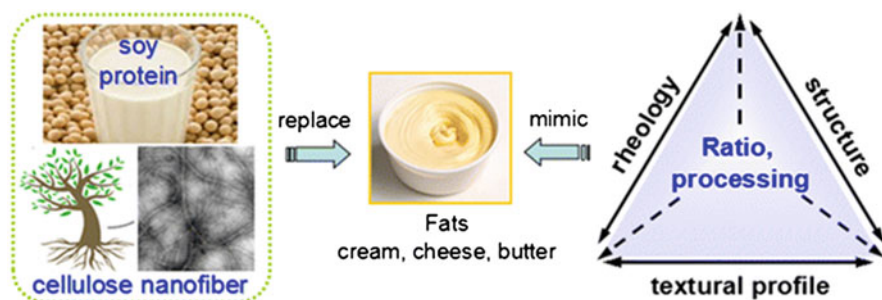


**Fig. 12.5** Soy protein isolate/cellulose nanofibre complex gels as fat substitutes in dairy products. Reproduction with permission from (Sun et al. 2015b), Copyright 2015 Springer Nature

(GG) and xanthan gum or citrus fibre simulated the function of oil emulsions and made the low-fat mayonnaise score the same as the full-fat counterpart with sensory panels (Su et al. 2010). Synergistic interaction between xanthan and pregel corn starch and also between xanthan and GG was identified by data analysis (Rahmati et al. 2015). The addition of xanthan gum and GG in low-fat cheese softened the structure by interfering the casein–casein interaction and cellulose particles that function similar to fat globules (Murtaza et al. 2017). Polydextrose and GG were successful fat replacers in biscuits at a relatively high level of FR (70%), with an increase in perceived taste, flavour, and consumer acceptance (Chugh et al. 2013). The combination of gum arabic at concentrations of <75 ppm with GG in the concentration range of 75–170 ppm provided the softest texture of low-fat Iranian white cheese (Lashkari et al. 2014). The blend of GG and basil seed gum yielded better creaminess in low-fat ice cream than GG alone (Javidi et al. 2016). Four combination sets of carboxymethyl cellulose, gum arabic, carrageenan, and xanthan were used as fat replacers in Labneh (semi-solid yoghurt with high solid content 23–25%), suggesting Labneh water holding capacity in the following order: xanthan > gum arabic > carrageenan > carboxymethyl cellulose (Saleh et al. 2018). Mixture of  $\kappa$ -carrageenan, locust bean, and xanthan gums has been added to milk to make cheese. Majeed et al. (2017) explored the combined potential of pectin and banana powder as carbohydrate-based fat replacers in cookies, suggesting that the fat content was reduced from 29.82% to 17.07% by using 15% such complex fat replacers. Upon using different concentrations of hydrocolloids, low-fat cheese showed a significant increase in the physiochemical characteristics, yield, and moisture. Furthermore, organoleptic properties obtained were both highly acceptable and comparable to full-fat cheese (Alnemr et al. 2016). The hybrid hydrogel prepared from sodium alginate and pectin by combining both physical and chemical cross-linking methods using citric acid as the cross linker was proved to reduce up to 50 vol% fat content in chocolate with the highest melting resistance (80 °C) (Francis and Ramalingam 2019).

### 3.1.4 Lipid-Based Fat Replacers

Lipid-based fat replacers are either chemically synthesized or derived from conventional fats and oils by enzymatic modification. They are usually stable at cooking and frying temperatures.

#### Emulsions

Wheat gluten-stabilized high internal phase emulsions (HIPEs) could be promising substitutes for mayonnaise because HIPEs and mayonnaise might have similar sensory property and perceived texture such as creaminess, smoothness, and sliminess (Liu et al. 2018b). Concentrated emulsions prepared by adding a fish gelatin-gum arabic mixture at pH 5.0 and 3.6 to olive oil at W:O = 30:70 (w/w) were

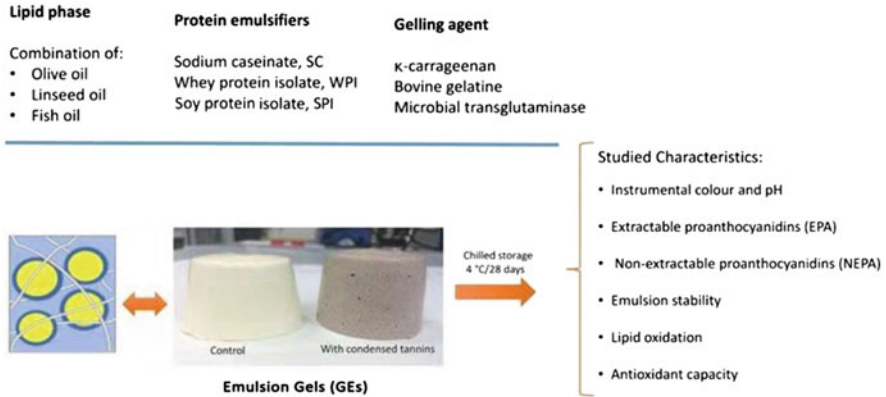


**Fig. 12.6** Emulsion gels prepared with different protein emulsifiers and gelling agents. Reproduction with permission from (Freire et al. 2018), Copyright 2018 Elsevier

designed as novel fat replacers in reduced-fat (15% fat) and low-fat (6% fat) Cheddar cheeses (Anvari and Joyner 2018). Micron to nano-sized fat emulsions prepared from sodium caseinate and anhydrous butter were used as a source of fat in low-fat Cheddar without affecting much the texture, chemical and bio-chemical properties of cheese (Khanal et al. 2019). Food-grade emulsion (O/W) gels (Fig. 12.6) formulated with a lipid phase rich in n-3 fatty acids and different emulsifiers (sodium caseinate, whey protein isolate, and soy protein isolate) showed solid-like structure and their overall appearance is good enough to be used as animal fat replacers with a lower fat content (Freire et al. 2018). A multiple emulsion refers to the coexisting of water-in-oil and oil-in-water morphologies within the same system (Dickinson 2011). Multiple emulsions of water-in-oil-in-water (W/O/W) are particularly suitable for reducing the fat content of products because some of the fat within the droplets is replaced by water (Lobato-Calleros et al. 2008). However, it is difficult to ensure that the multiple emulsions have sufficient stability for commercial applications (Chung et al. 2016). Multiple emulsions (W/O/W) prepared with olive oil and sodium caseinate (SC) by two-step emulsification procedure resulted in reduced lipid, increased protein content, and modified fatty acid composition and were noted as promising constituents for beef fat replacement (Serdaroğlu et al. 2016). Multiple emulsions (W/O/W) with an average droplet size of 32  $\mu\text{m}$  containing native beetroot juice as inner water phase, sunflower oil as oil phase, and 0.5% whey protein isolate as outer water phase were used to replace fat (11%) in meat products and also to enhance the product colour (Eisinaite et al. 2017). The emulsion gel (EG) prepared with gelling agents (chia flour and/or soy protein isolate, inulin, carrageenan, sodium caseinate, and sodium tripolyphosphate) resulted in a solid-like fat replacer, which was utilized as an animal fat replacer to prepare soft Bologna sausage (de Souza Paglarini et al. 2019).

## Structured Oils

Unsaturated vegetable oils are often used to reduce saturated fats content in meat products, which improves the fatty acid profiles and also helps in product stability (Siraj et al. 2015). Oil structuring, or oleogelation, is the process in which edible liquid oil is immobilized in a three-dimensional gel network of gelators, conferring solid-fat functionality to liquid oils (Co and Marangoni 2012). This technology is relatively simple since it refers to the transformation of a liquid oil into a ‘gel-like’ structure with visco-elastic properties. The schematic representation is shown in Fig. 12.7 (Jiang et al. 2018). Unlike polymers used for hydrogels, such oleogels utilize small, amphiphilic molecules that self-assemble via non-covalent interactions forming fibrillar or platelet crystals (Patel and Dewettinck 2016). The interactions are responsible for gelation, including hydrogen bonding,  $\pi$ - $\pi$  stacking, electrostatic and van der Waals interactions (Okesola et al. 2015).

Over the past decade, oleogels have made significant strides towards emulating desired sensory traits while maintaining healthy nutritional profile of the oil. In recent years, structuring techniques for liquid oils have received considerable attention in different fields including food science. Oleogel technology has shown strong potential as a way to replace hard-stock fats in meat products. Sunflower oil oleogels structured with monoglycerides and phytosterols at 15:5 weight ratio were used to replace 50% of the pork backfat in frankfurter sausages without significantly compromising their physicochemical, textural, and sensorial characteristics, at the same time providing an enriched polyunsaturated fatty acids lipid profile (Kouzounis

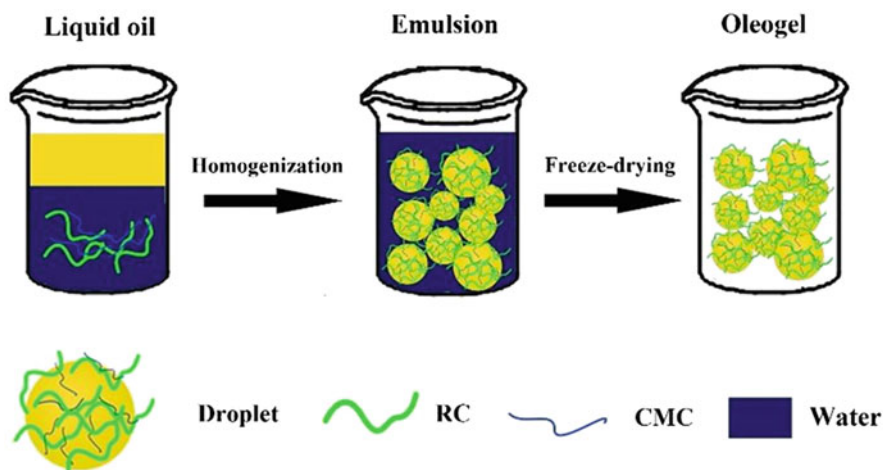


**Fig. 12.7** Schematic representation of the process where liquid oil is first used to prepare an oil-in-water emulsion stabilized by regenerated cellulose (RC) and carboxymethyl cellulose (CMC), followed by freeze-drying to selectively evaporate the water phase, where further shearing of the dried oil results in the formation of an oleogel. Reproduction with permission from (Jiang et al. 2018), Copyright 2018 Elsevier

et al. 2017). Ethylcellulose (EC) oleogels have been used to replace colloidal fat crystal networks comprised of saturated fat of frankfurters (Zetzel et al. 2012). A lipid combination made with olive, linseed, and fish oils stabilized in a konjac gel matrix was created to reduce pork backfat in pork patties (Salcedo-Sandoval et al. 2015). Canola oil was structured with foam-structured hydroxypropyl methylcellulose (HPMC) into solid-like oleogels. Such an HPMC oleogel was used as an animal fat replacer for saturated fat-reduced meat patty, and the highest sensory acceptability was obtained at a 50% replacement level (Oh et al. 2019). Oleogels appeared to be the most successful fat replacer in cake, with no changes to the sensory qualities at 100% fat replacement (Kim et al. 2017). Overall, the novel approach of structuring liquid oils would be one of the most promising ways to develop healthy lipid meat products, which makes it possible to create a solid-like material rich in monounsaturated fatty acid (MUFA) and polyunsaturated fatty acid (PUFA) and with reduced saturated fatty acid (SFA) levels and zero *trans* fatty acids (Jimenez-Colmenero et al. 2015). In addition, as solid-fat replacer, the constructed structured oil systems can be used in both water-free (shortenings, chocolates, and chocolate pastes) and water-containing (cooked meat products, margarine, and spreads) products.

### 3.2 Food Structure Design

While fat replacers have been applied in the development of reduced-fat products, an attractive strategy for fat reduction is created based on the fundamental structure–function relationship of food ingredients (Fig. 12.8a) (Campbell et al. 2017). Structural design principles can be used to mimic some of the desirable physicochemical, sensory, and physiologic attributes normally associated with fat droplets. A variety of approaches based on structural design principles that can be used in emulsion-based products are highlighted in Fig. 12.8b (McClements 2015). For example, the control of microstructure and physical properties of biopolymer hydrogel particles can be achieved through modulation of electrostatic interactions, which could be used to manipulate food formulations to achieve desirable physicochemical or sensory properties (Chung and McClements 2015).

The potential of controlled aggregation has been used to improve texture properties for reduced-fat products since the aggregation of emulsion droplets forms a three-dimensional network that inhibits droplet movement and leads to increased viscosity and even gel-like structure (Mao and McClements 2011, 2012). The principle to control emulsion aggregation is through regulating interfacial properties of the emulsion droplets and induce electrostatic attraction between the colloidal particles (Mao and McClements 2013). By carefully controlling the pH below, above, or equal to the protein's isoelectric point (pI), respectively, the protein-stabilized emulsion droplets carry positive, negative, or neutral charges. Thus, droplets self-aggregation can be induced due to the oppositely charged biopolymers (Wu et al. 2013a). The interactions between negatively charged polysaccharide and positively charged protein interactions allow efficient approaches to construct food

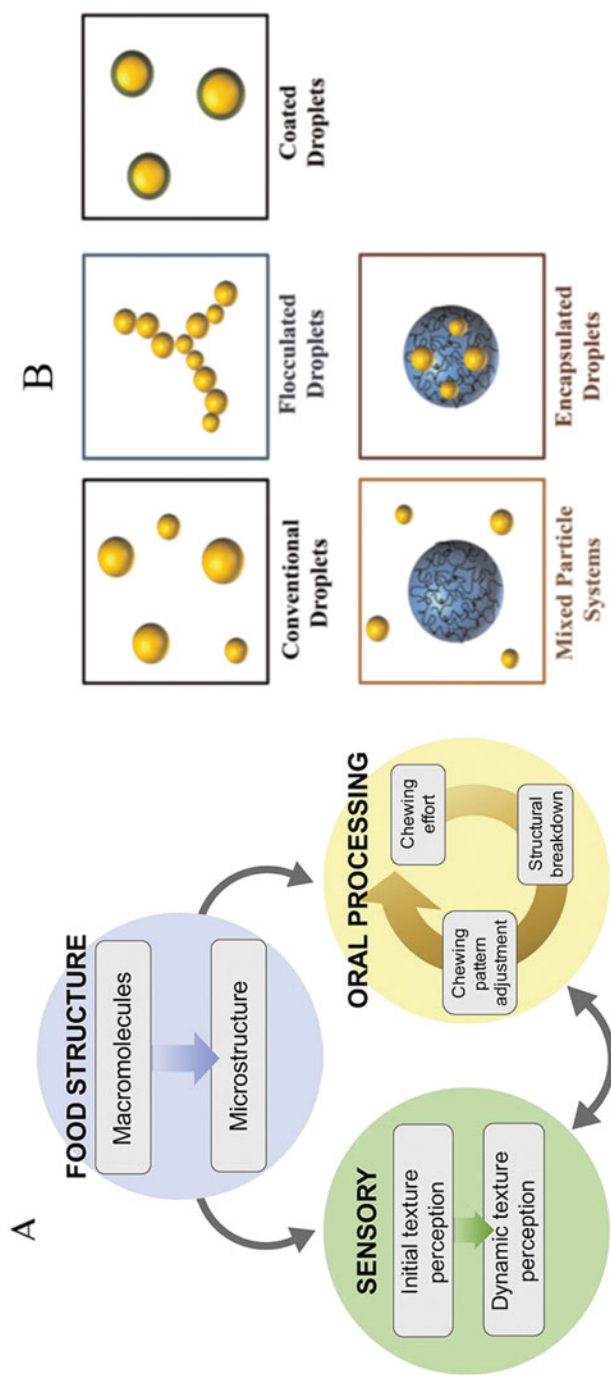


**Fig. 12.8** (a) The relationships among food structure, oral processing, sensory perception and (b) structural design principles to create reduced-fat emulsion-based products with physicochemical attributes similar to conventional products. (a) Reproduction with permission from (Campbell et al. 2017), Copyright 2017 Elsevier. (b) Reproduction with permission from (McClements 2015), Copyright 2015 Oxford University Press



structures and improve the stability and textural properties of semi-solid food colloids (Le et al. 2017). Based on controlled aggregation, model reduced-calorie food emulsions consisting of fat droplets (5 wt%), starch granules (4 wt%), and xanthan gum (0–0.02 wt%) were developed with desirable textural and optical properties at pH 3, and the structural organization of the fat droplets could be regulated by altering xanthan levels (Wu and McClements 2015a). Alternatively, ions such as calcium can be added to induce aggregation of negatively charged droplets, and paste-like materials were produced when the fat droplets formed a three-dimensional network at a high calcium concentration (Wu et al. 2013b). Casein–maltodextrin conjugates produced smaller fat globule mimetics and increased the desirable turbidity and viscosity of skim milk (Qu and Zhong 2017).

## 4 Strategies for Starch Replacement

High consumption of digestible starch is linked to a number of diet-related diseases. There is an increasing interest in the development of starch mimetics. Based on the important physicochemical properties and sensory attributes of foods, starch mimetics should have at least two essential attributes, being capable of effectively enhancing the viscosity of solutions and giving a desirable mouthfeel to foods such as thickness and creaminess (Rao 2014). Food hydrocolloids with a relatively low calorie density are suitable for creating reduced-calorie starch mimetics as they often contain large quantities of water, therefore increase the viscosity of starch pastes, influence the retrogradation rate, and prevent the syneresis of starch (Dolz et al. 2006).

### 4.1 Non-starch Polysaccharides

Non-starch polysaccharides can interact with starch and impart desired functionality to the resultant blend for oriented application (Yoshimura et al. 1999; Funami 2009; BeMiller 2011; Mahmood et al. 2017). *Mesona chinensis* polysaccharide (MCP) can improve the thermal stability in the early stage of pasting and enhance the rheological properties of wheat starch (Liu et al. 2018c). The addition of gums (xanthan gum, flaxseed gum, konjac glucomannan, or tamarind seed gum) to starch resulted in softer binary gels, which are effective in retarding retrogradation of starches (Pongsawatmanit et al. 2013; Liu and Xu 2019). The presence of basil seed gum (BSG) led to greater water binding capacity and greater water absorption index of the starch compared to the free-gum systems and also led to a rise in the viscoelasticity ( $G'$  and  $G''$ ) and hardness of the final gels (Matia-Merino et al. 2019). The addition of pectin increased the storage modulus ( $G'$ ) and loss modulus ( $G''$ ) of corn starch while resulted in a decrease in the starch susceptibility to  $\alpha$ -amylase and promoted a remarkable reduction in the fraction of rapidly digested starch (Ma et al. 2019).



Modified starch can be replaced by inulin as prebiotic encapsulant matrix of lipophilic bioactive compounds (Zabot et al. 2016). Inulin at low concentrations can effectively restrain the retrogradation of wheat starch (Luo et al. 2017). Rice starch (RS) can be also partially replaced by inulin because it affects the pasting, thermal, and rheological properties of RS (Wang et al. 2019). Barley sourced beta glucan ( $\beta$ G) and microcrystalline cellulose (MCC) could replace starch in meat emulsions. The maximum inclusion level of MCC and  $\beta$ G that has been previously tested without detrimentally affecting colour and textural properties of meat emulsions was 2% (Schuh et al. 2013) and 3% (Mejia et al. 2018), respectively. The combination of  $\beta$ G (1.5%) and MCC (1.5%) to replace starch resulted in beef emulsions with less calories, greater insoluble fibre content, and appropriate technological properties (Mejia et al. 2019).

## 4.2 Hydrocolloid Microgels

Hydrocolloid microgels have been attracting much attention to produce low-calorie foods (Norton et al. 2006). Hydrocolloids microgels fabricated by complexation of cationic proteins and anionic polysaccharides through electrostatic attraction showed a strong potential to be starch mimetic. Gelatin-pectin-based starch mimetics have been developed, and the size and morphology of such starch mimetic could be controlled through manipulation of gelatin/pectin ratio. For example, gelatin at a fixed concentration of 0.5 wt% can form micro-sized translucent spheroids when interacting with 0.01 wt% pectin at pH 5, and these hydrogel particles showed similar dimensions, shape, and rheological properties as swollen starch granules (Wu et al. 2014). The ionic strength should also be controlled during gelatin–pectin complex formation, as a too high salt content perturbed the gelatin–pectin interactions through electrostatic screening and ion binding effects (Wu and McClements 2015b). The cross-linking altered the microstructure and rheology of the microgels under simulated oral processing conditions. The melt-in-the-mouth behaviour of the hydrocolloid microgels could be made to be similar to that of starch granules by controlling the degree of cross-linking (Wu and McClements 2015c). In addition, the gelatin–pectin microgels designed to dissociate around body temperature may be useful for imitating the melting properties and/or thickening properties of starch granules in the mouth, which is also particularly helpful for the development of elderly foods with improved swallowing ease under oral conditions. Electrostatic complexation of gelatin and modified (OSA) starch shows potential to modify texture of food products, suggesting their feasibility to replace starch granules in foods (Wu and McClements 2015d).

## 5 Commercially Available Fat Replacers

Limited studies have been specifically focused on the development of starch mimetics though there are lots of reports about the design of biopolymer-based hydrogel particles, so commercial starch mimetics are limited. As a result, commercial fat replacers are mainly introduced in this part.

Fat-reduction ingredients fall into three categories: carbohydrate-based, protein-based, and lipid-based, in which carbohydrate-based fat replacers are the most common. Examples of commercially available fat replacers and their applications and functional properties are shown in Table 12.1 (Mattes 1998). In some cases, the Food and Drug Administration (FDA) has approved fat-reduction ingredients as food additives, including carrageenan, olestra, and polydextrose. In other instances, fat-reduction ingredients are 'generally recognized as safe' (GRAS). Most carbohydrate-based fat replacers are GRAS substances. For example, oatrim gel made from whole oat flour behaves like shortening, being solid at room and body temperatures and liquid at cooking temperatures, and imparts fat-like qualities such as creaminess, moisture retention, bulking, and texture. Oatrim is heat stable in cooking and baking applications and can replace fat in foods such as frozen desserts, salad dressings, soups, cheeses, baked goods, meats, and skim milk. Besides, Oatrim also contains beta glucan, so it offers double health benefit by replacing the fat and increasing the soluble fibre content of foods (Hahn 1997).

Protein-based fat replacers are not as many as carbohydrate-based ingredients, but they have a wide range of applications. Commercially available protein-based fat replacers are Simplese and Dairy Lois, which are derived from whey protein concentrates and are generally regarded as safe (Yazici and Akgun 2004). This category of fat mimetics is suitable for use in dairy products, salad dressings, frozen desserts, and table spreads. For instance, Dairy Lois incorporated at 5% by weight has been used to develop an ice cream containing 1% fat.

Lipid-based fat replacers often provide the closest taste and cooking properties of fat. Salatrim belongs to a group of structured triacylglycerols and has been used as a fat mimetic in reduced-calorie food products for many years because it provides approximately half of the calories and has similar physicochemical and organoleptic properties as those of conventional fats (Smith et al. 1994). A great concentration of undigested fat within the lower gastrointestinal tract (GIT) remained, indicating that Salatrim may be an effective fat replacer due to its ability to suppress hunger and increase fullness (Sørensen et al. 2008). Olestra is a sucrose polyester, in which the ester bonds are not hydrolysed by lipase in the human GIT because of steric hindrance effects. As a result, Olestra is not absorbed by the body and is specially designed to be a zero-calorie fat substitute to replace triglyceride oils in products such as fried foods, snacks, breads, and fillings (Bimal and Guonong 2006). However, Olestra may disturb the absorption of fat-soluble vitamins and may be linked to undesirable GIT symptoms, so its used amount is limited by FDA (Prince and Welschenbach 1998).

**Table 12.1** Commercially available fat replacers and their applications

Fat replacer	Trade name	Applications	Functions
Protein-based (microparticulated protein, modified whey protein concentrate)	Simplese, Dairy Lois, K-Blazer, Veri-lo, Power-pro, Versapro, Ultra-Baketm, Ultra-Freezetm, Lita	Dairy products, salad-dressing, margarine- and mayonnaise-type products, baked goods, coffee creamer, soups, and sauces	Mouthfeel, creaminess, viscosity
Lipid-based	Caprenin, Salatrim, Dur-Lo, ECT-25, Olestra	Confections, baked goods, dairy products	Mouthfeel, stability
Cellulose	Avicel cellulose gel, Methocel, Solka-Floc, Just Fiber	Dairy products, sauces, frozen desserts, salad dressings	Water retention, texturizer, stabilizer, mouthfeel, clouding agents
Dextrins	Amylum, N-Oil, Stalex	Salad dressings, puddings, spreads, dairy products, frozen desserts	Gelling, thickening, stabilizing, texturizer
Maltodextrins	CrystaLean, Lorelite, Lycadex, Malitrin, Oatrim, Stalex, nu-trim	Baked goods, dairy products, salad dressings, sauces, spreads, frostings, fillings, beverages	Gelling, thickening, stabilizing, texturizer
Gums (guar gum, gum arabic, locust bean gum, xanthan gum, carrageenan, pectin)	Kelcogel, Keltrol, Viscarin, Novagel, Jaguar, Fibrex, Splendid, Grindsted	Salad dressings, formulated foods such as desserts and processed meats	Water retention, texturizer, thickener, mouthfeel, gelling, stabilizer
Inulin	Raftiline, Fruitafit, Fibruline	Yoghurt, cheese, frozen desserts, baked goods, fillings, whipped cream, fibre supplements	
Fibre	Opta TM, Oat Fiber, Snowite, Ultracel TM, Z-Trim	Baked goods, meats, spreads, extruded products	Heat stable
Starch and modified starch	Amalean I and II, N-Lite, Fairnex TMVA15 and VA 20, Instant StellarTM, Pure-Gel, Sta-SlimiTM, OptaGread	Dairy products, processed meats, salad dressings, baked goods, frozen desserts	Bodying agents, gelling, thickening, texture modifiers

Reproduction with permission from (Mattes 1998), Copyright 1998 Elsevier

## 6 Future Perspective

Nowadays, healthiness and beauty are common interests among people. Reducing calorie consumption is a major goal for the consumer. Consequently, both food manufactures and researchers are sparing no effort to develop reduced-fat/starch food products. The key point is that the replacement of fat or starch should contribute

low or even zero calorie to food products and should be nondetrimental to their organoleptic qualities.

Many low-fat products have been based on the use of a wide variety of biopolymers, especially hydrocolloids. More basic knowledge of physical, rheological, chemical, and sensory characteristics, functionality, and fat or starch interactions with other ingredients is required as to formulating these bases. Further studies are needed on new food-grade ingredients as potential replacers of fat or starch. Other approaches are available based upon the use of manufacturing and preparation procedures that can help to achieve desired product properties such as colour, texture, and water- and fat-holding abilities. A thorough understanding of the physicochemical properties and molecular interactions of food-grade ingredients is necessary for developing innovative fat reduction strategies such as utilizing structural design approach to control the macroscopic properties.

Currently, the consumer's unwillingness to give up high-energy foods suggests that there is a considerable potential market for frequently consumed foods such as meats which have been reformulated to produce health benefits. It is believed that in near future, people would adapt to a low-fat or low-starch diet based on the development of novel advanced technologies for the replacement of fat or starch.

## References

- Abbasi E, Amini Sarteshnizi R, Ahmadi Gavlighi H, Nikoo M, Azizi MH, Sadeghinejad N (2019) Effect of partial replacement of fat with added water and tragacanth gum (*Astragalus gossypinus* and *Astragalus compactus*) on the physicochemical, texture, oxidative stability, and sensory property of reduced fat emulsion type sausage. *Meat Sci* 147:135–143. <https://doi.org/10.1016/j.meatsci.2018.09.007>
- Ai Y, Jane JL (2015) Gelatinization and rheological properties of starch. *Starch-Stärke* 67:213–224. <https://doi.org/10.1002/star.201400201>
- Aiking H (2011) Future protein supply. *Trends Food Sci Technol* 22(2–3):112–120. <https://doi.org/10.1016/j.tifs.2010.04.005>
- Akalın AS, Karagözlü C, Ünal G (2008) Rheological properties of reduced-fat and low-fat ice cream containing whey protein isolate and inulin. *Eur Food Res Technol* 227(3):889–895. <https://doi.org/10.1007/s00217-007-0800-z>
- Alexander RJ (1995) Fat replacers based on starch. *Cereal Foods World* 40(5):249–262. <https://doi.org/10.1021/bp00033a016>
- Alnemr T, Helal A, Hassan A, Elsaadany K (2016) Utilizing the functions of hydrocolloids as fat mimetic to enhance the properties of low-fat domiati cheese. *J Food Process Technol* 7(11):637. <https://doi.org/10.4172/2157-7110.1000637>
- Alting AC, Van de Velde F, Kanning MW, Burgering M, Mulleners L, Sein A, Buwalda P (2009) Improved creaminess of low-fat yoghurt: the impact of amyломaltase-treated starch domains. *Food Hydrocoll* 23(3):980–987. <https://doi.org/10.1016/j.foodhyd.2008.07.011>
- Anvari M, Joyner HS (2018) Concentrated emulsions as novel fat replacers in reduced-fat and low-fat Cheddar cheeses. Part 1. Rheological and microstructural characterization. *Int Dairy J* 86:76–85. <https://doi.org/10.1016/j.idairyj.2018.06.017>
- Aziz NS, Sofian-Seng N-S, Yusop SM, Kasim KF, Mohd Razali NS (2018) Functionality of okra gum as a novel carbohydrate-based fat replacer in ice cream. *Food Sci Technol Res* 24(3):519–530. <https://doi.org/10.3136/fstr.24.519>

- Bayarri S, González-Tomás LU, Hernando I, Lluch MA, Costell E (2011) Texture perceived on inulin-enriched low-fat semisolid dairy desserts. Rheological and structural basis. *J Texture Stud* 42(3):174–184. <https://doi.org/10.1111/j.1745-4603.2010.00280.x>
- Belc N, Smeu I, Macri A, Vallauri D, Flynn K (2019) Reformulating foods to meet current scientific knowledge about salt, sugar and fats. *Trends Food Sci Technol* 84:25–28. <https://doi.org/10.1016/j.tifs.2018.11.002>
- BeMiller JN (2011) Pasting, paste, and gel properties of starch–hydrocolloid combinations. *Carbohydr Polym* 86(2):386–423. <https://doi.org/10.1016/j.carbpol.2011.05.064>
- Bimal C, Guonong Z (2006) Olestra: a solution to food fat? *Food Rev Intl* 22(3):245–258. <https://doi.org/10.1080/87559120600694705>
- Bravo-Núñez Á, Pando V, Gómez M (2019) Physically and chemically modified starches as texturisers of low-fat milk gels. *Int Dairy J* 92:21–27. <https://doi.org/10.1016/j.idairyj.2019.01.007>
- Bray GA, Paeratakul S, Popkin BM (2004) Dietary fat and obesity: a review of animal, clinical and epidemiological studies. *Physiol Behav* 83(4):549–555. <https://doi.org/10.1016/j.physbeh.2004.08.039>
- Campbell CL, Wagoner TB, Foegeding EA (2017) Designing foods for satiety: the roles of food structure and oral processing in satiation and satiety. *Food Struct* 13:1–12. <https://doi.org/10.1016/j.foostr.2016.08.002>
- Chugh B, Singh G, Kumbhar BK (2013) Development of low-fat soft dough biscuits using carbohydrate-based fat replacers. *Int J Food Sci* 2013:1–12. <https://doi.org/10.1155/2013/576153>
- Chung C, McClements DJ (2014) Structure–function relationships in food emulsions: improving food quality and sensory perception. *Food Struct* 1(2):106–126. <https://doi.org/10.1016/j.foostr.2013.11.002>
- Chung C, McClements DJ (2015) Controlling microstructure and physical properties of biopolymer hydrogel particles through modulation of electrostatic interactions. *J Food Eng* 158:13–21. <https://doi.org/10.1016/j.jfoodeng.2015.02.028>
- Chung C, Degner B, McClements DJ (2013a) Physicochemical characteristics of mixed colloidal dispersions: models for foods containing fat and starch. *Food Hydrocoll* 30(1):281–291. <https://doi.org/10.1016/j.foodhyd.2012.06.008>
- Chung C, Degner B, McClements DJ (2013b) Designing reduced-fat food emulsions: locust bean gum–fat droplet interactions. *Food Hydrocoll* 32(2):263–270. <https://doi.org/10.1016/j.foodhyd.2013.01.008>
- Chung C, Degner B, McClements DJ (2014) Development of reduced-calorie foods: microparticulated whey proteins as fat mimetics in semi-solid food emulsions. *Food Res Int* 56:136–145
- Chung C, Smith G, Degner B, McClements DJ (2016) Reduced fat food emulsions: physicochemical, sensory, and biological aspects. *Crit Rev Food Sci Nutr* 56(4):650–685. <https://doi.org/10.1080/10408398.2013.792236>
- Co ED, Marangoni AG (2012) Organogels: an alternative edible oil-structuring method. *J Am Oil Chem Soc* 89(5):749–780. <https://doi.org/10.1007/s11746-012-2049-3>
- Colmenero FJ (2000) Relevant factors in strategies for fat reduction in meat products. *Trends Food Sci Technol* 11(2):56–66. [https://doi.org/10.1016/S0924-2244\(00\)00042-X](https://doi.org/10.1016/S0924-2244(00)00042-X)
- Copeland L, Blazek J, Salman H, Tang MC (2009) Form and functionality of starch. *Food Hydrocoll* 23(6):1527–1534. <https://doi.org/10.1016/j.foodhyd.2008.09.016>
- Dai S, Jiang F, Corke H, Shah NP (2018) Physicochemical and textural properties of mozzarella cheese made with konjac glucomannan as a fat replacer. *Food Res Int* 107:691–699. <https://doi.org/10.1016/j.foodres.2018.02.069>
- Dai S, Jiang F, Shah NP, Corke H (2019) Functional and pizza bake properties of Mozzarella cheese made with konjac glucomannan as a fat replacer. *Food Hydrocoll* 92:125–134. <https://doi.org/10.1016/j.foodhyd.2019.01.045>

- de Roos KB (2006) How lipids influence flavor perception. In: *Food lipids*, vol 920. American Chemical Society Publications, Washington, DC, pp 145–158. <https://doi.org/10.1021/bk-2005-0920.ch012>
- De Ruiter GA, Rudolph B (1997) Carrageenan biotechnology. *Trends Food Sci Technol* 8 (12):389–395. [https://doi.org/10.1016/s0924-2244\(97\)01091-1](https://doi.org/10.1016/s0924-2244(97)01091-1)
- de Souza Paglarini C, de Figueiredo Furtado G, Honório AR, Mokarzel L, da Silva Vidal VA, Ribeiro APB, Cunha RL, Pollonio MAR (2019) Functional emulsion gels as pork back fat replacers in Bologna sausage. *Food Struct* 20:100105. <https://doi.org/10.1016/j.foostr.2019.100105>
- DeSalvo KB, Olson R, Casavale KO (2016) Dietary guidelines for Americans. *JAMA* 315 (5):457–458. <https://doi.org/10.1001/jama.2015.18396>
- Diamantino VR, Beraldo FA, Sunakozawa TN, Penna ALB (2014) Effect of octenyl succinylated waxy starch as a fat mimetic on texture, microstructure and physicochemical properties of Minas fresh cheese. *LWT Food Sci Technol* 56(2):356–362. <https://doi.org/10.1016/j.lwt.2013.12.001>
- Diamantino VR, Costa MS, Taboga SR, Vilamaior PSL, Franco CML, Penna ALB (2019) Starch as a potential fat replacer for application in cheese: behaviour of different starches in casein/starch mixtures and in the casein matrix. *Int Dairy J* 89:129–138. <https://doi.org/10.1016/j.idairyj.2018.08.015>
- Dickinson E (2011) Double emulsions stabilized by food biopolymers. *Food Biophys* 6(1):1–11. <https://doi.org/10.1007/s11483-010-9188-6>
- Dolz M, Hernandez MJ, Delegido J (2006) Oscillatory measurements for salad dressings stabilized with modified starch, xanthan gum, and locust bean gum. *J Appl Polym Sci* 102(1):897–903. <https://doi.org/10.1002/app.24125>
- Duval S, Chung C, McClements DJ (2015) Protein-polysaccharide hydrogel particles formed by biopolymer phase separation. *Food Biophys* 10(3):334–341. <https://doi.org/10.1007/s11483-015-9396-1>
- Eisinaite V, Juraite D, Schroën K, Leskauskaitė D (2017) Food-grade double emulsions as effective fat replacers in meat systems. *J Food Eng* 213:54–59. <https://doi.org/10.1016/j.jfoodeng.2017.05.022>
- Engelen L, de Wijk RA (2012) Oral processing and texture perception. In: *Food oral processing: fundamentals of eating and sensory perception*. Wiley-Blackwell, Oxford, pp 159–176. <https://doi.org/10.1002/9781444360943.ch8>
- Engelen L, Van Der Bilt A, Schipper M, Bosman F (2005) Oral size perception of particles: effect of size, type, viscosity and method. *J Texture Stud* 36(4):373–386. <https://doi.org/10.1111/j.1745-4603.2005.00022.x>
- Fischer N, Widder S (1997) How proteins influence food flavor. *Food Technol* 51(1):68–70. <https://doi.org/10.1177/108201329700300608>
- Food Standards Agency (2008) Saturated fat and energy intake programme. <http://www.food.gov.uk/multimedia/pdfs/satfatprog>
- Francis FP, Ramalingam C (2019) Hybrid hydrogel dispersed low fat and heat resistant chocolate. *J Food Eng* 256:9–17. <https://doi.org/10.1016/j.jfoodeng.2019.03.012>
- Freire M, Cofrades S, Pérez-Jiménez J, Gómez-Estaca J, Jiménez-Colmenero F, Bou R (2018) Emulsion gels containing n-3 fatty acids and condensed tannins designed as functional fat replacers. *Food Res Int* 113:465–473. <https://doi.org/10.1016/j.foodres.2018.07.041>
- Friedman M, Brandon DL (2001) Nutritional and health benefits of soy proteins. *J Agric Food Chem* 49(3):1069–1086. <https://doi.org/10.1021/jf0009246>
- Funami T (2009) Functions of food polysaccharides to control the gelatinization and retrogradation behaviors of starch in an aqueous system in relation to the macromolecular characteristics of food polysaccharides. *Food Sci Technol Res* 15:557–568. <https://doi.org/10.3136/fstr.15.557>
- Gąkowska D, Juszcak L (2019) Effects of amino acids on gelatinization, pasting and rheological properties of modified potato starches. *Food Hydrocoll* 92:143–154. <https://doi.org/10.1016/j.foodhyd.2019.01.063>

- Gao XQ, Kang ZL, Zhang WG, Li YP, Zhou GH (2015) Combination of  $\kappa$ -carrageenan and soy protein isolate effects on functional properties of chopped low-fat pork batters during heat-induced gelation. *Food Bioprocess Technol* 8(7):1524–1531. <https://doi.org/10.1007/s11947-015-1516-x>
- Gentès MC, St-Gelais D, Turgeon SL (2010) Stabilization of whey protein isolate-pectin complexes by heat. *J Agric Food Chem* 58(11):7051–7058. <https://doi.org/10.1021/jf100957b>
- Gibis M, Schuh V, Weiss J (2015) Effects of carboxymethyl cellulose (CMC) and microcrystalline cellulose (MCC) as fat replacers on the microstructure and sensory characteristics of fried beef patties. *Food Hydrocoll* 45:236–246. <https://doi.org/10.1016/j.foodhyd.2014.11.021>
- Godshall MA (1997) How carbohydrates influence food flavor. *Food Technol* 51:63–67. <https://doi.org/10.1177/108201329700300608>
- González-Tomás L, Bayarri S, Taylor AJ, Costell E (2008) Rheology, flavour release and perception of low-fat dairy desserts. *Int Dairy J* 18(8):858–866. <https://doi.org/10.1016/j.idairyj.2007.09.010>
- Guichard E (2002) Interactions between flavor compounds and food ingredients and their influence on flavor perception. *Food Rev Intl* 18(1):49–70. <https://doi.org/10.1081/FRI-120003417>
- Gulão EDS, de Souza CJ, Andrade CT, Garcia-Rojas EE (2016) Complex coacervates obtained from peptide leucine and gum arabic: formation and characterization. *Food Chem* 194:680–686. <https://doi.org/10.1016/j.foodchem.2015.08.062>
- Hahn NI (1997) Replacing fat with food technology. *J Acad Nutr Diet* 97(1):15–16. [https://doi.org/10.1016/S0002-8223\(97\)00007-2](https://doi.org/10.1016/S0002-8223(97)00007-2)
- Han SH, Nicholls SJ, Sakuma I, Zhao D, Koh KK (2016) Hypertriglyceridemia and cardiovascular diseases: revisited. *Korean Circ J* 46:135–144. <https://doi.org/10.4070/kcj.2016.46.2.135>
- Hanselmann R, Burchard W, Ehrat M, Widmer HM (1996) Structural properties of fractionated starch polymers and their dependence on the dissolution process. *Macromolecules* 29:3277–3282. <https://doi.org/10.1021/ma951452c>
- Hedayati S, Niakousari M (2018) Microstructure, pasting and textural properties of wheat starch-corn starch citrate composites. *Food Hydrocoll* 81:1–5. <https://doi.org/10.1016/j.foodhyd.2018.02.024>
- Henry J (2009) Processing, manufacturing, uses and labeling of fats in the food supply. *Ann Nutr Metab* 55(1–3):273–300. <https://doi.org/10.1159/000229006>
- Hu Y, Li C, Regenstein JM, Wang L (2019) Preparation and properties of potato amylose-based fat replacer using super-heated quenching. *Carbohydr Polym* 223:115020. <https://doi.org/10.1016/j.carbpol.2019.115020>
- Huc D, Maignon A, Barey P, Desprairies M, Mauduit S, Sieffermann JM, Michon C (2014) Interactions between modified starch and carrageenan during pasting. *Food Hydrocoll* 36:355–361. <https://doi.org/10.1016/j.foodhyd.2013.08.023>
- Javidi F, Razavi SMA, Behrouzian F, Alghooneh A (2016) The influence of basil seed gum, guar gum and their blend on the rheological, physical and sensory properties of low fat ice cream. *Food Hydrocoll* 52:625–633. <https://doi.org/10.1016/j.foodhyd.2015.08.006>
- Javidi F, Razavi SMA, Mohammad Amini A (2019) Corn starch nanocrystals as a potential fat replacer in reduced fat O/W emulsions: a rheological and physical study. *Food Hydrocoll* 90:172–181. <https://doi.org/10.1016/j.foodhyd.2018.12.003>
- Jiang Y, Liu L, Wang B, Sui X, Zhong Y, Zhang L, Mao Z, Xu H (2018) Cellulose-rich oleogels prepared with an emulsion-templated approach. *Food Hydrocoll* 77:460–464. <https://doi.org/10.1016/j.foodhyd.2017.10.023>
- Jimenez-Colmenero F, Salcedo-Sandoval L, Bou R, Cofrades S, Herrero AM, Ruiz-Capillas C (2015) Novel applications of oil-structuring methods as a strategy to improve the fat content of meat products. *Trends Food Sci Technol* 44(2):177–188. <https://doi.org/10.1016/j.tifs.2015.04.011>
- Jing H, Yap M, Wong PY, Kitts DD (2011) Comparison of physicochemical and antioxidant properties of egg-white proteins and fructose and inulin Maillard reaction products. *Food Bioprocess Technol* 4(8):1489–1496. <https://doi.org/10.1007/s11947-009-0279-7>



- Johnson ME (2011) Cheese: low-fat and reduced-fat cheese. In: Encyclopedia of dairy science. Academic Press, New York, pp 833–842. <https://doi.org/10.1016/B978-0-12-374407-4.00098-4>
- Karaca OB, Güven M, Yasar K, Kaya S, Kahyaoglu T (2009) The functional, rheological and sensory characteristics of ice creams with various fat replacers. *Int J Dairy Technol* 62(1):93–99. <https://doi.org/10.1111/j.1471-0307.2008.00456.x>
- Kaur N, Gupta AK (2002) Applications of inulin and oligofructose in health and nutrition. *J Biosci* 27(7):703–714. <https://doi.org/10.1007/BF02708379>
- Kavas G, Oysun G, Kinik O, Uysal H (2004) Effect of some fat replacers on chemical, physical and sensory attributes of low-fat white pickled cheese. *Food Chem* 88(3):381–388. <https://doi.org/10.1016/j.foodchem.2004.01.054>
- Keenan DF, Resconi V, Kerry JP, Hamill RM (2014) Modelling the influence of inulin as a fat substitute in comminuted meat products on their physico-chemical characteristics and eating quality using a mixture design approach. *Meat Sci* 96(3):1384–1394. <https://doi.org/10.1016/j.meatsci.2013.11.025>
- Khanal BKS, Bhandari B, Prakash S, Liu D, Zhou P, Bansal N (2018) Modifying textural and microstructural properties of low fat Cheddar cheese using sodium alginate. *Food Hydrocoll* 83:97–108. <https://doi.org/10.1016/j.foodhyd.2018.03.015>
- Khanal BKS, Budiman C, Hodson MP, Plan MR, Prakash S, Bhandari B, Bansal N (2019) Physico-chemical and biochemical properties of low fat Cheddar cheese made from micron to nano sized milk fat emulsions. *J Food Eng* 242:94–105. <https://doi.org/10.1016/j.jfoodeng.2018.08.019>
- Khouryieh HA, Aramouni FM, Herald TJ (2005) Physical and sensory characteristics of no-sugar-added/low-fat muffin. *J Food Qual* 28(5–6):439–451. <https://doi.org/10.1111/j.1745-4557.2005.00047.x>
- Kim JY, Lim J, Lee J, Hwang HS, Lee S (2017) Utilization of oleogels as a replacement for solid fat in aerated baked goods: physicochemical, rheological, and topographic characterization. *J Food Sci* 82(2):445–452. <https://doi.org/10.1111/1750-3841.13583>
- Kouzounis D, Lazaridou A, Katsanidis E (2017) Partial replacement of animal fat by oleogels structured with monoglycerides and phytosterols in frankfurter sausages. *Meat Sci* 130:38–46. <https://doi.org/10.1016/j.meatsci.2017.04.004>
- Krzeminski A, Prell KA, Busch-Stockfisch M, Weiss J, Hinrichs J (2014) Whey protein–pectin complexes as new texturising elements in fat-reduced yoghurt systems. *Int Dairy J* 36(2):118–127. <https://doi.org/10.1016/j.idairyj.2014.01.018>
- Kühn J, Considine T, Singh H (2006) Interactions of milk proteins and volatile flavor compounds: implications in the development of protein foods. *J Food Sci* 71(5):72–82. <https://doi.org/10.1111/j.1750-3841.2006.00051.x>
- Laguna L, Primo-Martín C, Varela P, Salvador A, Sanz T (2014) HPMC and inulin as fat replacers in biscuits: sensory and instrumental evaluation. *LWT Food Sci Technol* 56(2):494–501. <https://doi.org/10.1016/j.lwt.2013.12.025>
- Lascombes C, Agoda-Tandjawa G, Boulenguer P, Le Garnec C, Gilles M, Mauduit S, Bary P, Langendorff V (2017) Starch-carrageenan interactions in aqueous media: role of each polysaccharide chemical and macromolecular characteristics. *Food Hydrocoll* 66:176–189. <https://doi.org/10.1016/j.foodhyd.2016.11.025>
- Lashkari H, Madadlou A, Alizadeh M (2014) Chemical composition and rheology of low-fat Iranian white cheese incorporated with guar gum and gum arabic as fat replacers. *J Food Sci Technol* 51(10):2584–2591. <https://doi.org/10.1007/s13197-012-0768-y>
- Le XT, Rioux LE, Turgeon SL (2017) Formation and functional properties of protein-polysaccharide electrostatic hydrogels in comparison to protein or polysaccharide hydrogels. *Adv Colloid Interf Sci* 239:127–135. <https://doi.org/10.1016/j.cis.2016.04.006>
- Li H, Lei N, Yan S, Yang J, Yu T, Wen Y, Wang J, Sun B (2019) The importance of amylopectin molecular size in determining the viscoelasticity of rice starch gels. *Carbohydr Polym* 212:112–118. <https://doi.org/10.1016/j.carbpol.2019.02.043>



- Liu J, Xu B (2019) A comparative study on texture, gelatinisation, retrogradation and potential food application of binary gels made from selected starches and edible gums. *Food Chem* 296:100–108. <https://doi.org/10.1016/j.foodchem.2019.05.193>
- Liu R, Wang L, Liu Y, Wu T, Zhang M (2018a) Fabricating soy protein hydrolysate/xanthan gum as fat replacer in ice cream by combined enzymatic and heat-shearing treatment. *Food Hydrocoll* 81:39–47. <https://doi.org/10.1016/j.foodhyd.2018.01.031>
- Liu X, Guo J, Wan Z-L, Liu Y-Y, Ruan Q-J, Yang X-Q (2018b) Wheat gluten-stabilized high internal phase emulsions as mayonnaise replacers. *Food Hydrocoll* 77:168–175. <https://doi.org/10.1016/j.foodhyd.2017.09.032>
- Liu S, Lin L, Shen M, Wang W, Xiao Y, Xie J (2018c) Effect of *Mesona chinensis* polysaccharide on the pasting, thermal and rheological properties of wheat starch. *Int J Biol Macromol* 118:945–951. <https://doi.org/10.1016/j.ijbiomac.2018.06.178>
- Liu D, Li Z, Fan Z, Zhang X, Zhong G (2019) Effect of soybean soluble polysaccharide on the pasting, gels, and rheological properties of kudzu and lotus starches. *Food Hydrocoll* 89:443–452. <https://doi.org/10.1016/j.foodhyd.2018.11.003>
- Lobato-Calleros C, Sosa-Perez A, Rodriguez-Tafoya J, Sandoval-Castilla O, Perez-Alonso C, Vernon-Carter EJ (2008) Structural and textural characteristics of reduced-fat cheese-like products made from W1/O/W2 emulsions and skim milk. *LWT Food Sci Technol* 41:1847–1856. <https://doi.org/10.1016/j.lwt.2008.01.006>
- Luo D, Li Y, Xu B, Ren G, Li P, Li X, Ren G, Li P, Li X, Han S, Liu J (2017) Effects of inulin with different degree of polymerization on gelatinization and retrogradation of wheat starch. *Food Chem* 229:35–43. <https://doi.org/10.1016/j.foodchem.2017.02.058>
- Lustig RH, Schmidt LA, Brindis CD (2012) Public health: the toxic truth about sugar. *Nature* 482:27–29. <https://doi.org/10.1038/482027a>
- Ma S, Zhu P, Wang M (2019) Effects of konjac glucomannan on pasting and rheological properties of corn starch. *Food Hydrocoll* 89:234–240. <https://doi.org/10.1016/j.foodhyd.2018.10.045>
- Mahmood K, Kamilah H, Shang PL, Sulaiman S, Ariffin F, Alias AK (2017) A review: interaction of starch/non-starch hydrocolloid blending and the recent food applications. *Food Biosci* 19:110–120. <https://doi.org/10.1016/j.fbio.2017.05.006>
- Maier HG (1970) Volatile flavoring substances in foodstuffs. *Angew Chem Int Ed Engl* 9 (12):917–926. <https://doi.org/10.1002/anie.197009171>
- Majeed M, Anwar S, Khan MU, Asghar A, Shariati MA, Semykin V, Fazel M (2017) Study of the combined effect of pectin and banana powder as carbohydrate based fat replacers to develop low fat cookies. *Foods Raw Mater* 5(2):62–69. <https://doi.org/10.21603/2308-4057-2017-2-62-69>
- Majzoobi M, Mohammadi M, Mesbahi G, Farahnaky A (2018) Feasibility study of sucrose and fat replacement using inulin and rebaudioside A in cake formulations. *J Texture Stud* 49 (5):468–475. <https://doi.org/10.1111/jtxs.12330>
- Malone M, Appelqvist I, Norton I (2003) Oral behaviour of food hydrocolloids and emulsions. Part 1. Lubrication and deposition considerations. *Food Hydrocoll* 17(6):763–773. [https://doi.org/10.1016/S0268-005X\(03\)00097-3](https://doi.org/10.1016/S0268-005X(03)00097-3)
- Mao Y, McClements DJ (2011) Modulation of bulk physicochemical properties of emulsions by hetero-aggregation of oppositely charged protein-coated lipid droplets. *Food Hydrocoll* 25 (5):1201–1209. <https://doi.org/10.1016/j.foodhyd.2010.11.007>
- Mao Y, McClements DJ (2012) Modulation of emulsion rheology through electrostatic heteroaggregation of oppositely charged lipid droplets: influence of particle size and emulsifier content. *J Colloid Interface Sci* 380:60–66. <https://doi.org/10.1016/j.jcis.2012.05.007>
- Mao Y, McClements DJ (2013) Modulation of food texture using controlled heteroaggregation of lipid droplets: principles and applications. *J Appl Polym Sci* 130(6):3833–3841. <https://doi.org/10.1002/app.39631>
- Matia-Merino L, Prieto M, Roman L, Gómez M (2019) The impact of basil seed gum on native and pregelatinized corn flour and starch gel properties. *Food Hydrocoll* 89:122–130. <https://doi.org/10.1016/j.foodhyd.2018.10.005>

- Mattes RD (1998) Position of the American Dietetic Association: fat replacers. *J Am Diet Assoc* 98:463–468. [https://doi.org/10.1016/s0002-8223\(98\)00105-9](https://doi.org/10.1016/s0002-8223(98)00105-9)
- McClements DJ (2015) Reduced-fat foods: the complex science of developing diet-based strategies for tackling overweight and obesity. *Adv Nutr* 6(3):338S–352S. <https://doi.org/10.3945/an.114.006999>
- McClements DJ, Demetriades K (1998) An integrated approach to the development of reduced-fat food emulsions. *Crit Rev Food Sci Nutr* 38(6):511–536. <https://doi.org/10.1080/10408699891274291>
- McClements DJ, Chung C, Wu BC (2017) Structural design approaches for creating fat droplet and starch granule mimetics. *Food Funct* 8(2):498–510. <https://doi.org/10.1039/c6fo00764c>
- Mejia SMV, de Francisco A, Barreto PLM, Damian C, Zibetti AW, Mahecha HS, Bohrer BM (2018) Incorporation of  $\beta$ -glucans in meat emulsions through an optimal mixture modeling systems. *Meat Sci* 143:210–218. <https://doi.org/10.1016/j.meatsci.2018.05.007>
- Mejia SMV, de Francisco A, Bohrer BM (2019) Replacing starch in beef emulsion models with  $\beta$ -glucan, microcrystalline cellulose, or a combination of  $\beta$ -glucan and microcrystalline cellulose. *Meat Sci* 153:58–65. <https://doi.org/10.1016/j.meatsci.2019.03.012>
- Menegas LZ, Pimentel TC, Garcia S, Prudencio SH (2013) Dry-fermented chicken sausage produced with inulin and corn oil: physicochemical, microbiological, and textural characteristics and acceptability during storage. *Meat Sci* 93(3):501–506. <https://doi.org/10.1016/j.meatsci.2012.11.003>
- Metcalf KL, Vickers ZM (2002) Taste intensities of oil-in-water emulsions with varying fat content. *J Sens Stud* 17:379–390. <https://doi.org/10.1111/j.1745-459X.2002.tb00354.x>
- Murtaza MS, Sameen A, Huma N, Hussain F (2017) Influence of hydrocolloid gums on textural, functional and sensory properties of low fat cheddar cheese from buffalo milk. *Pak J Zool* 49(1):27–34. <https://doi.org/10.17582/journal.pjz/2017.49.1.27.34>
- Norton IT, Frith WJ, Ablett S (2006) Fluid gels, mixed fluid gels and satiety. *Food Hydrocoll* 20:229–239. <https://doi.org/10.1016/j.foodhyd.2004.03.011>
- O'Connor TP, O'Brien NM (2011) Butter and other milk fat products fat replacers. In: *Encyclopedia of dairy science*. Academic Press, New York, pp 528–532. <https://doi.org/10.1016/B978-0-12-374407-4.00330-7>
- Oh I, Lee J, Lee HG, Lee S (2019) Feasibility of hydroxypropyl methylcellulose oleogel as an animal fat replacer for meat patties. *Food Res Int* 122:566–572. <https://doi.org/10.1016/j.foodres.2019.01.012>
- Okesola BO, Vieira VM, Cornwell DJ, Whitelaw NK, Smith DK (2015) 1,3:2,4-Dibenzylidene-D-sorbitol (DBS) and its derivatives-efficient, versatile and industrially-relevant low-molecular-weight gelators with over 100 years of history and a bright future. *Soft Matter* 11(24):4768–4787. <https://doi.org/10.1039/C5SM00845J>
- Olivares ML, Shahrivar K, de Vicente J (2019) Soft lubrication characteristics of microparticulated whey proteins used as fat replacers in dairy systems. *J Food Eng* 245:157–165. <https://doi.org/10.1016/j.jfoodeng.2018.10.015>
- Parada J, Aguilera JM (2011) Starch matrices and the glycaemic response. *Food Sci Technol Int* 17(3):187–204. <https://doi.org/10.1177/1082013210387712>
- Patel AR, Dewettinck K (2016) Edible oil structuring: an overview and recent updates. *Food Funct* 7(1):20–29. <https://doi.org/10.1039/c5fo01006c>
- Peng X, Yao Y (2017) Carbohydrates as fat replacers. *Annu Rev Food Sci Technol* 8(1):331–351. <https://doi.org/10.1146/annurev-food-030216-030034>
- Plug H, Haring P (1994) The influence of flavour-ingredient interactions on flavour perception. *Food Qual Prefer* 5:95–102. [https://doi.org/10.1016/0950-3293\(94\)90013-2](https://doi.org/10.1016/0950-3293(94)90013-2)
- Pongsawatmanit R, Chantaro P, Nishinari K (2013) Thermal and rheological properties of tapioca starch gels with and without xanthan gum under cold storage. *J Food Eng* 117:333–341. <https://doi.org/10.1016/j.jfoodeng.2013.03.010>
- Prince DM, Welschenbach MA (1998) Olestra: a new food additive. *J Am Diet Assoc* 98:565–569. [https://doi.org/10.1016/S0002-8223\(98\)00126-6](https://doi.org/10.1016/S0002-8223(98)00126-6)

- Prinz JF, Huntjens LAH, de Wijk RA, Engelen L, Polet IA (2007) Is fat perception a thermal effect? *Percept Mot Skills* 104(2):381–386. <https://doi.org/10.2466/PMS.104.2.381-386>
- Psimouli V, Oreopoulou V (2013) The effect of fat replacers on batter and cake properties. *J Food Sci* 78(10):C1495–C1502. <https://doi.org/10.1111/1750-3841.12235>
- Punia S, Siroha AK, Sandhu KS, Kaur M (2019) Rheological and pasting behavior of OSA modified mungbean starches and its utilization in cake formulation as fat replacer. *Int J Biol Macromol* 128:230–236. <https://doi.org/10.1016/j.ijbiomac.2019.01.107>
- Qu B, Zhong Q (2017) Casein-maltodextrin conjugate as an emulsifier for fabrication of structured calcium carbonate particles as dispersible fat globule mimetics. *Food Hydrocoll* 66:61–70. <https://doi.org/10.1016/j.foodhyd.2016.12.022>
- Raguzzoni JC, Delgadillo I, da Silva JAL (2016) Influence of a cationic polysaccharide on starch functionality. *Carbohydr Polym* 150:369–377. <https://doi.org/10.1016/j.carbpol.2016.05.024>
- Rahmati NF, Tehrani MM, Daneshvar K, Koocheki A (2015) Influence of selected gums and pregelatinized corn starch on reduced fat mayonnaise: modeling of properties by central composite design. *Food Biophys* 10(1):39–50. <https://doi.org/10.1007/s11483-014-9356-1>
- Rao MA (2014) Rheology of fluid, semisolid, and solid foods. Springer, Boston, MA, pp 161–229. <https://doi.org/10.1021/jf025646k>
- Roberts DD, Pollien P, Watzke B (2003) Experimental and modeling studies showing the effect of lipid type and level on flavor release from milk-base liquid emulsions. *J Agric Food Chem* 51:189–195. <https://doi.org/10.1021/jf025646k>
- Rudra SG, Nath P, Kaur C, Basu S (2017) Rheological, storage stability and sensory profiling of low-fat yoghurt fortified with red capsicum carotenoids and inulin. *J Food Process Preserv* 41(4):e13067–e13076. <https://doi.org/10.1111/jfpp.13067>
- Saha D, Bhattacharya S (2010) Hydrocolloids as thickening and gelling agents in food: a critical review. *J Food Sci Technol* 47(6):587–597. <https://doi.org/10.1007/s13197-010-0162-6>
- Salcedo-Sandoval L, Cofrades S, Ruiz-Capillas C, Carballo J, Jiménez-Colmenero F (2015) Konjac-based oil bulking system for development of improved-lipid pork patties: technological, microbiological and sensory assessment. *Meat Sci* 101:95–102. <https://doi.org/10.1016/j.meatsci.2014.11.010>
- Saleh M, Al-Baz F, Al-Ismael K (2018) Effects of hydrocolloids as fat replacers on the physico-chemical properties of produced Labneh. *J Texture Stud* 49(1):113–120. <https://doi.org/10.1111/jtxs.12296>
- Salvatore E, Pes M, Mazzarello V, Pirisi A (2014) Replacement of fat with long-chain inulin in a fresh cheese made from caprine milk. *Int Dairy J* 34(1):1–5. <https://doi.org/10.1016/j.idairyj.2013.07.007>
- Sandrou DK, Arvanitoyannis IS (2000) Low-fat/calorie foods: current state and perspectives. *Crit Rev Food Sci Nutr* 40(5):427–447. <https://doi.org/10.1080/10408690091189211>
- Sarkar S, Gupta S, Variyar PS, Sharma A, Singhal RS (2013) Hydrophobic derivatives of guar gum hydrolyzate and gum arabic as matrices for microencapsulation of mint oil. *Carbohydr Polym* 95(1):177–182. <https://doi.org/10.1016/j.carbpol.2013.02.070>
- Schuh V, Allard K, Herrmann K, Gibis M, Kohlus R, Weiss J (2013) Impact of carboxymethyl cellulose (CMC) and microcrystalline cellulose (MCC) on functional characteristics of emulsified sausages. *Meat Sci* 93(2):240–247. <https://doi.org/10.1016/j.meatsci.2012.08.025>
- Serdaroğlu M, Öztürk B, Ürgü M (2016) Emulsion characteristics, chemical and textural properties of meat systems produced with double emulsions as beef fat replacers. *Meat Sci* 117:187–195. <https://doi.org/10.1016/j.meatsci.2016.03.012>
- Shoib M, Shehzad A, Omar M, Rakha A, Raza H, Sharif HR, Shakeel A, Ansari A, Niazi S (2016) Inulin: properties, health benefits and food applications. *Carbohydr Polym* 147:444–454. <https://doi.org/10.1016/j.carbpol.2016.04.020>
- Sikora M, Badrie N, Deisingh AK, Kowalski S (2008) Sauces and dressings: a review of properties and applications. *Crit Rev Food Sci Nutr* 48(1):50–77. <https://doi.org/10.1080/10408390601079934>

- Singh J, Lelane C, Stewart RB, Singh H (2010) Formation of starch spherulites: role of amylose content and thermal events. *Food Chem* 121(4):980–989. <https://doi.org/10.1016/j.foodchem.2010.01.032>
- Siraj N, Shabbir MA, Ahmad T, Sajjad A, Khan MR, Khan MI, Butt MS (2015) Organogelators as a saturated fat replacer for structuring edible oils. *Int J Food Prop* 18(9):1973–1989. <https://doi.org/10.1080/10942912.2014.951891>
- Smith RE, Finley JW, Leveille GA (1994) Overview of SALATRIM: a family of low-calorie fats. *J Agric Food Chem* 42(2):432–434. <https://doi.org/10.1021/jf00038a036>
- Sørensen LB, Cueto HT, Andersen MT, Bitz C, Holst JJ, Rehfeld JF, Astrup A (2008) The effect of salatrim, a low-calorie modified triacylglycerol, on appetite and energy intake. *Am J Clin Nutr* 87(5):1163–1169. <https://doi.org/10.1039/b518127e>
- Spence C (2015) Multisensory flavor perception. *Cell* 161(1):24–35. <https://doi.org/10.1016/j.cell.2015.03.007>
- Steeneken PA, Woortman AJ (2009) Superheated starch: a novel approach towards spreadable particle gels. *Food Hydrocoll* 23(2):394–405. <https://doi.org/10.1016/j.foodhyd.2008.01.006>
- Stokes JR, Macakova L, Chojnicka-Paszu A, de Kruif CG, de Jongh HHJ (2011) Lubrication, adsorption, and rheology of aqueous polysaccharide solutions. *Langmuir* 27:3474–3484. <https://doi.org/10.1021/la104040d>
- Su HP, Lien CP, Lee TA, Ho JH (2010) Development of low-fat mayonnaise containing polysaccharide gums as functional ingredients. *J Sci Food Agric* 90(5):806–812. <https://doi.org/10.1002/jsfa.3888>
- Sun C, Wu T, Liu R, Liang B, Tian Z, Zhang E, Zhang M (2015a) Effects of superfine grinding and microparticulation on the surface hydrophobicity of whey protein concentrate and its relation to emulsions stability. *Food Hydrocoll* 51:512–518. <https://doi.org/10.1016/j.foodhyd.2015.05.027>
- Sun L, Chen W, Liu Y, Li J, Yu H (2015b) Soy protein isolate/cellulose nanofiber complex gels as fat substitutes: rheological and textural properties and extent of cream imitation. *Cellulose* 22(4):2619–2627. <https://doi.org/10.1007/s10570-015-0681-4>
- Sun C, Liu R, Wu T, Liang B, Shi C, Cong X, Hou T, Zhang M (2016) Combined superfine grinding and heat-shearing treatment for the microparticulation of whey proteins. *Food Bioprocess Technol* 9(2):1–9. <https://doi.org/10.1007/s11947-015-1629-2>
- Sun C, Liu R, Liang B, Wu T, Sui W, Zhang M (2018) Microparticulated whey protein-pectin complex: a texture-controllable gel for low-fat mayonnaise. *Food Res Int* 108:151–160. <https://doi.org/10.1016/j.foodres.2018.01.036>
- Surendra Babu A, Parimalavalli R, Jagannadham K, Sudhakara Rao J, Shalini Gaur R (2016) Fat mimicking properties of citric acid treated sweet potato starch. *Int J Food Prop* 19(1):139–153. <https://doi.org/10.1080/10942912.2015.1020390>
- Svihus B, Hervik AK (2016) Digestion and metabolic fates of starch, and its relation to major nutrition-related health problems: a review. *Starch-Stärke* 68:302–313. <https://doi.org/10.1002/star.201500295>
- Tárrega A, Costell E (2006) Effect of inulin addition on rheological and sensory properties of fat-free starch-based dairy desserts. *Int Dairy J* 16(9):1104–1112. <https://doi.org/10.1016/j.idairyj.2005.09.002>
- Taylor AJ, Linforth RST (1996) Flavour release in the mouth. *Trends Food Sci Technol* 7(12):444–448. [https://doi.org/10.1016/S0924-2244\(96\)10046-7](https://doi.org/10.1016/S0924-2244(96)10046-7)
- Torres IC, Amigo JM, Knudsen JC, Tolkach A, Mikkelsen BØ, Ipsen R (2018) Rheology and microstructure of low-fat yoghurt produced with whey protein microparticles as fat replacer. *Int Dairy J* 81:62–71. <https://doi.org/10.1016/j.idairyj.2018.01.004>
- United States Code of Federal Regulations (2014) Title 21. Nutrient content claims for fat, fatty acid, and cholesterol content of foods. 101.62. <http://www.gpo.gov/fdsys/pkg/CFR-2014-title21-vol2/pdf/CFR-2014-title21-vol2-chapI.pdf>

- van Ruth SM, de Vries G, Geary M, Giannouli P (2002) Influence of composition and structure of oil-in-water emulsions on retention of aroma compounds. *J Sci Food Agric* 82:1028–1035. <https://doi.org/10.1002/jsfa.1137>
- Velásquez-Cock J, Serpa A, Vélez L, Gañán P, Hoyos CG, Castro C, Duizer L, Goff HD, Zuluaga R (2019) Influence of cellulose nanofibrils on the structural elements of ice cream. *Food Hydrocoll* 87:204–213. <https://doi.org/10.1016/j.foodhyd.2018.07.035>
- Villanueva M, Mauro RR, Collar C, Ronda F (2015) Acidification of protein-enriched rice starch doughs: effects on breadmaking. *Eur Food Res Technol* 240(4):783–794. <https://doi.org/10.1007/s00217-014-2384-8>
- Villanueva M, De Lamo B, Harasym J, Ronda F (2018) Microwave radiation and protein addition modulate hydration, pasting and gel rheological characteristics of rice and potato starches. *Carbohydr Polym* 201:374–381. <https://doi.org/10.1016/j.carbpol.2018.08.052>
- Villegas B, Costell E (2007) Flow behaviour of inulin–milk beverages. Influence of inulin average chain length and of milk fat content. *Int Dairy J* 17(7):776–781. <https://doi.org/10.1016/j.idairyj.2006.09.007>
- Wang R, Wan J, Liu C, Xia X, Ding Y (2019) Pasting, thermal, and rheological properties of rice starch partially replaced by inulin with different degrees of polymerization. *Food Hydrocoll* 92:228–232. <https://doi.org/10.1016/j.foodhyd.2019.02.008>
- Weenen H (2005) Effects of structure breakdown on creaminess in semisolid foods. *Food Lipids* 920:119–132. <https://doi.org/10.1021/bk-2005-0920.ch010>
- Weenen H, Van Gemert LJ, Van Doorn JM, Dijksterhuis GB, De Wijk RA (2003) Texture and mouthfeel of semisolid foods: commercial mayonnaises, dressings, custard desserts and warm sauces. *J Texture Stud* 34(2):159–179. <https://doi.org/10.1111/j.1745-4603.2003.tb01373.x>
- WHO (2003) Diet, nutrition and the prevention of chronic diseases: report of a joint WHO. World Health Organization. <https://doi.org/10.1046/j.1365-2648.2003.02792.x>
- Wu BC, McClements DJ (2015a) Design of reduced-fat food emulsions: manipulating microstructure and rheology through controlled aggregation of colloidal particles and biopolymers. *Food Res Int* 76:777–786. <https://doi.org/10.1016/j.foodres.2015.06.034>
- Wu BC, McClements DJ (2015b) Functional hydrogel microspheres: parameters affecting electrostatic assembly of biopolymer particles fabricated from gelatin and pectin. *Food Res Int* 72:231–240. <https://doi.org/10.1016/j.foodres.2015.02.028>
- Wu BC, McClements DJ (2015c) Development of hydrocolloid microgels as starch granule mimetics: hydrogel particles fabricated from gelatin and pectin. *Food Res Int* 78:177–185. <https://doi.org/10.1016/j.foodres.2015.10.020>
- Wu BC, McClements DJ (2015d) Microgels formed by electrostatic complexation of gelatin and OSA starch: potential fat or starch mimetics. *Food Hydrocoll* 47:87–93. <https://doi.org/10.1016/j.foodhyd.2015.01.021>
- Wu BC, Degner B, McClements DJ (2013a) Microstructure & rheology of mixed colloidal dispersions: influence of pH-induced droplet aggregation on starch granule–fat droplet mixtures. *J Food Eng* 116(2):462–471. <https://doi.org/10.1016/j.jfoodeng.2012.12.020>
- Wu BC, Degner B, McClements DJ (2013b) Creation of reduced fat foods: influence of calcium-induced droplet aggregation on microstructure and rheology of mixed food dispersions. *Food Chem* 141(4):3393–3401. <https://doi.org/10.1016/j.foodchem.2013.06.044>
- Wu BC, Degner B, McClements DJ (2014) Soft matter strategies for controlling food texture: formation of hydrogel particles by biopolymer complex coacervation. *J Phys Condens Matter* 26(46):464104. <https://doi.org/10.1088/0953-8984/26/46/464104>
- Yang Y, Xu S (2007) Roles of components of rice-based fat substitute in gelation. *Food Res Int* 40(9):1155–1160. <https://doi.org/10.1016/j.foodres.2007.06.010>
- Yang C, Zhong F, Douglas Goff H, Li Y (2019) Study on starch-protein interactions and their effects on physicochemical and digestible properties of the blends. *Food Chem* 280:51–58. <https://doi.org/10.1016/j.foodchem.2018.12.028>

- Yazici F, Akgun A (2004) Effect of some protein based fat replacers on physical, chemical, textural, and sensory properties of strained yoghurt. *J Food Eng* 62(3):245–254. [https://doi.org/10.1016/S0260-8774\(03\)00237-1](https://doi.org/10.1016/S0260-8774(03)00237-1)
- Yoshimura M, Takaya T, Nishinari K (1999) Effects of xyloglucan on the gelatinization and retrogradation of corn starch as studied by rheology and differential scanning calorimetry. *Food Hydrocoll* 13:101–111. [https://doi.org/10.1016/S0268-005X\(98\)00075-7](https://doi.org/10.1016/S0268-005X(98)00075-7)
- Zabot GL, Silva EK, Azevedo VM, Meireles MAA (2016) Replacing modified starch by inulin as prebiotic encapsulant matrix of lipophilic bioactive compounds. *Food Res Int* 85:26–35. <https://doi.org/10.1016/j.foodres.2016.04.005>
- Zetzl AK, Marangoni AG, Barbut S (2012) Mechanical properties of ethylcellulose oleogels and their potential for saturated fat reduction in frankfurters. *Food Funct* 3(3):327–337. <https://doi.org/10.1039/c2fo10202a>
- Zhang H, Chen J, Li J, Wei C, Ye X, Shi J, Chen S (2018) Pectin from citrus canning wastewater as potential fat replacer in ice cream. *Molecules* 23(4):925–936. <https://doi.org/10.3390/molecules23040925>
- Zhang M, Sun C, Li Q (2019) Interaction between the polysaccharides and proteins in semisolid food systems. In: Varelis P, Melton L, Shahidi F (eds) *Encyclopedia of food chemistry*. Elsevier, Oxford, pp 439–445. <https://doi.org/10.1016/b978-0-08-100596-5.21474-1>
- Zoulias EI, Oreopoulou V, Tzia C (2000) Effect of fat mimetics on physical, textural and sensory properties of cookies. *Int J Food Prop* 3(3):385–397. <https://doi.org/10.1080/10942910009524643>

# Chapter 13

## Structuring for Elderly Foods



**Makoto Nakauma and Takahiro Funami**

**Abstract** For the elderlies with reduced eating capability, food texture should be modified from rheological, colloidal, and tribological aspects to make it comfortable to eat for them. In aged society, formulation/structure design for food texture for the elderlies is now one of the most important tasks in the food industry. This chapter aims to provide readers with relevant knowledge for the industrial implementation of the texture design of elderly foods. Firstly, usefulness of polysaccharides as a texture modifier will be summarized, and with presenting commercial examples in Japan, it is indicated that the manipulation of polysaccharides is the most practical way for the product development. Secondary, mechanical criteria for texture of elderly foods in Japan will be reviewed with comparison to the global standards. Although Texture Profile Analysis is the base for the mechanical measurements in Japanese standardization, some cautions should be required in the test operation and data analysis. As advanced texture assessment, the progress of mechanical and physiological tests will be also explained. Thirdly, since the intake of too much salt/sugar is the major concern for consumers including the elderlies, strategy for release control of aroma and taste through food structure design will be shown. Interesting phenomenon from our findings is that inhomogeneous spatial distribution of aroma can enhance not only aroma perception but also the eating behavior, which can be favorable for the elderlies with reduced sensing and eating capability.

**Keywords** Elderly foods · Dysphagia · Texture design · Criteria · Release

---

M. Nakauma (✉) · T. Funami  
San-Ei Gen F.F.I., Toyonaka, Osaka, Japan  
e-mail: [m-nakauma@saneigenffi.co.jp](mailto:m-nakauma@saneigenffi.co.jp)



## 1 Introduction

Texture is a sensory property (Szczesniak 2002) as defined by the International Organization for Standardization (1994) and thus should be evaluated by human. As defined by ISO, texture is associated with all the mechanical, geometrical, and surface attributes of a food. Hence, food texture is a multiplex of physicochemical properties perceived by human in a series of food oral processing.

Texture is the most important element of food palatability (Szczesniak and Kleyn 1963), especially for staple foods such as rice, noodle, bread, and meat, where texture dominates more than 30% of palatability (Nishinari 1996). Texture can also modify the flavor perception (Clark 2002; Morris 1993) because how a food is broken down in the mouth and how the broken food is mixed with saliva both relate to the flavor release from the food and influence its perception through retronasal pathway (Baek et al. 1999; Boland et al. 2006; Repoux et al. 2012). Also, texture can modify the digestion and absorption behaviors of nutriment and minerals on a similar principle to the flavor release (Nakauma et al. 2012, 2014).

Texture is important for safety of eating and is emphasized in recent aged society (Nishinari 2009). Changes in human physiology with aging can reduce some eating capabilities through the depression of muscle and organ activities (Mioche 2004; Sako 2005), saliva secretion (Sako 2005; Shern et al. 1993; Shin et al. 2015), and sensitivity to taste and aroma (Arey et al. 1935; Doty 1989; Sako 2005). The design of the elderlies-friendly food formulation is required to the food industry, and safe swallowing for dysphagia patients should be a priority as aspiration in such patients can cause death in the worst case through pneumonia (Nishinari et al. 2011). As for reduction of the swallowing capability with aging, prolonged swallow response due to a delay in laryngeal closure (Clavé et al. 2006) may cause the misleading. To prevent the misleading, food or food bolus should flow at moderate velocity through the pharyngeal phase, not at very high or very low one, as one cohesive bolus with low adhesiveness and high lubricity. Dysphagia is managed in most cases using texture-controlled foods, which are thickened or gelled (Clavé et al. 2006; Logemann 1998; Quinchia et al. 2011). To the author's understanding, food texture design has been done empirically in both food manufactures and hospital/nursing-care facilities, and more scientific-based approach should be necessary for the future. This chapter covers essential elements for food texture design for the elderlies, followed by the illustration of industrially feasible way for the goal and the trend of production development in Japan. New approach for texture evaluation will be also elaborated for more advanced strategy in the future.



## 2 Use of Polysaccharides as a Texture Modifier in Elderly Foods

Polysaccharides are frequently used as a texture modifier in processed food products, and this is also the key technology for the development of elderly foods. Polysaccharides used in the food industry are all natural as their sources are found in seeds, tree sap, seaweeds, microorganism, etc. in nature (Funami 2011). Polysaccharides serve a variety of purposes in processed food products due to their capabilities of thickening, gelling, water holding, dispersing, stabilizing, film forming, and foaming (Funami 2011). Through these functions, mechanical, geometrical, and surface properties can change, and food texture is modified as a result.

In Japan, various types of processed food products are being marketed for the elderly. Representatives are semi-solidified (either thickened or gelled) enteral nutrition, water-supply jelly, and nutrition-supply jelly as a ready-to-eat product. Also, instant gelling agent for pasted/pureed foods and dysphagia thickener are both for supplement purpose working through small addition to existing foods and distributed commercially in a dry powder form. The terms “jelly,” “gelling,” and “thickener” all relate directly to the polysaccharide functions.

Semi-solidified enteral nutrition can reduce the complication risks encountered in feeding of thin liquid enteral nutrition via an enteral tube or percutaneous endoscopic gastrostomy. These risks include the secondary aspiration caused by gastroesophageal reflux, local skin infection by the leakage from gastrostomy, bed sore by prolonged feeding time, and diarrhea by rapid absorption and dumping (Goda 2008). By selection and combination of polysaccharides, the intensity and quality of viscosity can be modified to achieve smooth flow through the tube and controlled feeding speed for the prevention of diarrhea and reflux (Tanishima et al. 2009). This type of enteral nutrition uses representatively agar, pectin, carrageenan, and xanthan gum and is gaining the market share in Japan (Nakauma et al. 2012, 2014). Regarding water-supply jelly, the creation of new texture has been tried by polysaccharide technology to mimic not only texture but also appearance of real fruits (Funami 2013). Appearance can enhance human appetite as one of the dominant attributes for food palatability. It has been reported recently that the visual food recognition can influence on swallowing function (Kamiya et al. 2015). This study demonstrates that a larger amount of saliva secretion was found when subjects saw the pictures of normal diets compared to those of corresponding blended foods. Another advantage of using polysaccharides instead of real fruits lies in the feasibility of calorie and nutrition controls. For example, control of potassium intake is essential for patients with kidney dialysis treatment, and this type of food products is flexible in changing the formulation. Instant gelling agent is used for shape retention and the prevention of syneresis for pasted and pureed foods (Funami 2013). Foods, including cooked rice, fish, meat, and vegetable, are pasted together with the gelling agent and water or soup if necessary. By remolding to the original shape, people can recognize what they are eating. Polysaccharides which hydrate or dissolve in water without heating are preferably used in this type of gelling agent.

### 3 Usefulness of Xanthan Gum as Dysphagia Thickener

Low viscosity liquids can be aspirated by dysphagia patients (Nishinari et al. 2011). To prevent this, dysphagia thickener, called *toromi* in Japan, is used at hospital and nursing-care facilities. Dysphagia thickener contains polysaccharides as a main ingredient, where xanthan gum has been recently replacing modified starch (Funami et al. 2006, 2009). Dysphagia thickener is usually stirred manually to disperse them in liquid foods like water, tea, juice, soup, etc. Dysphagia thickener should have functions of no lumping, rapid viscosity increase, stable viscosity upon storage, and usability in a wide range of liquid foods even under weak stirring conditions. The thickener should also provide preferable organoleptic properties with liquid foods, including cohesive texture and no off-flavor. Xanthan gum meets these requirements and must be practically the best choice (Funami et al. 2006).

Most polysaccharides, not limited to xanthan, hydrate quickly in water and thus form lumps easily. Lumping is the most unfavorable for dysphagia thickener. When this happens, textural homogeneity cannot be ensured, and this adverse effect against good dispersion should be eliminated by powder processing, mostly granulation. Here, the relationship between dispersibility and viscosity enhancement can be described as a seesaw in which when one is improved, the other is deteriorated (Funami et al. 2006). For good balance of these two attributes, technical know-how in a granulation process should be necessary, including optimization of certain operation conditions (e.g., inlet air temperature and volume, liquid spray rate and amount) or usage of certain co-agents in a liquid spray, either of which aims to control the speed of polysaccharide hydration.

Xanthan solutions are fluid, but from rheological point of view, they behave like a solid or gel (Nakauma et al. 2011). As shown in Fig. 13.1, xanthan solutions have

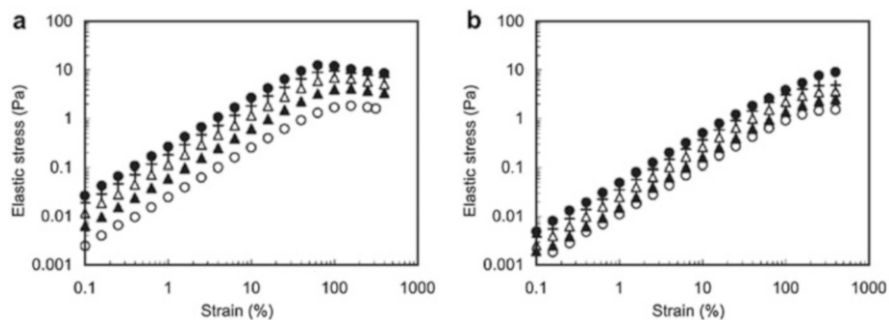


**Fig. 13.1** Elastic stress (storage modulus  $\times$  strain) of xanthan gum and locust bean gum solutions at 20 °C plotted as function of strain. Concentrations of polysaccharide: 0.3, 0.45, 0.6, 0.75 and 0.9% for xanthan gum (a) and 0.5, 0.6, 0.7, 0.75, and 0.8% for locust bean gum (b), represented by open circles, closed triangles, open triangles, crosses, and closed circles in increasing order for each polysaccharide. The yield stress and strain were estimated from the maximum point in the curve. For the experimental details, see Nakauma et al. (2011), *Food Hydrocolloids* 25, 1165–1173. Reproduction with permission from (Nakauma et al. 2011), Copyright 2010 Elsevier Ltd

elastic character represented by yield stress in contrast to locust bean gum. Yield stress was detected as the peak in Fig. 13.1, in which the data from strain-dependence of dynamic viscoelasticity were replotted. The yield stress is a stress at which the flow begins (Bourne 2002a), relating to the degree of the internal binding force. Thus, the yield stress can present cohesiveness of food bolus. It has been believed for a long time that the flow speed of liquid food bolus through the pharyngeal phase is moderated by thickening and that shear viscosity can only determine the flow behavior; the higher the viscosity, the slower the flow speed can be through the pharyngeal phase. Whether it is always true or not and which shear rate should be used for viscosity measurement to obtain the best correlation with physiological flow behavior should be of research interest. For the first question, the answer must be NO when the results from our recent studies (Nakauma et al. 2011; Funami et al. 2017) are considered. Elasticity should not be negligible or rather important in explaining physiological flow behavior of food bolus. This is supported by Chen and Lolivret (2011), who concluded that extensional stretch ability should be one of the most important mechanical parameters for swallowing ease. For the second question, the maximum shear rate was expected to range between  $400 \text{ s}^{-1}$  (Meng et al. 2005) and 3000 or even larger  $180,000 \text{ s}^{-1}$  (Nicosia and Robbins 2001) depending on the type of simulation. However, it is still quite difficult to estimate such an *in vivo* parameter *in silico* due to the irregularity of oral geometry.

As a non-invasive *in vivo* measurement, acoustic analysis was performed to investigate the correlation with sensory evaluation (Funami 2011; Nakauma et al. 2011). From the acoustic analysis, time required for food bolus to transfer through the pharyngeal phase ( $t_2$ ) decreases with increasing xanthan concentration although steady shear viscosity is increased (Fig. 13.2). This may be consistent with the ultrasonic pulse Doppler measurement, elucidating that velocity spectra are narrower in the distribution range with increasing concentration of food polysaccharide thickeners (Kumagai et al. 2009). Also,  $t_2$  is well correlated with perceived intensities of cohesiveness and swallowing ease (Fig. 13.3). Bolus from xanthan solutions flows through the pharyngeal phase as one coherent bolus with small variation of flow velocity, and this flow behavior leads to a greater sensation of swallowing ease. For swallowing ease, “structured fluid” or “weak gel” should be a preferable food structure from rheological point of view (Nakauma et al. 2011). This food structure can be represented rheologically by yield stress of approx. 7.0–9.0 Pa and steady shear viscosity of approx. 0.9–1.2 Pas at  $10 \text{ s}^{-1}$  (Nakauma et al. 2011). Also, it is reported that non-Newtonian fluids, representatively xanthan solutions with showing shear-thinning behavior (Nishinari et al. 2011), are safer to swallow than Newtonian fluids with lower aspiration risk (Meng et al. 2005). The preference of non-Newtonian fluids for safe swallowing refers to the need of elasticity to ensure the mechanical cohesiveness of food bolus rather than the issue of shear rate dependence (Funami et al. 2012).

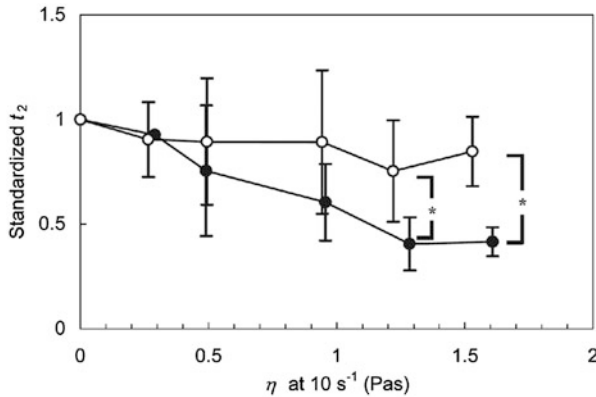


**Fig. 13.2** Duration  $t_2$  in swallowing polysaccharide solutions as a function of steady shear viscosity  $\eta$  at  $10 \text{ s}^{-1}$ . Both mechanical and in vivo measurements were carried out at  $20^\circ \text{C}$ . Closed circles: xanthan gum; open circles: locust bean gum. Serving volume of polysaccharide solutions was 15 mL. Each datum was standardized with that for control (water). Data with asterisk are significantly different between xanthan gum and locust bean gum at  $p < 0.05$ . For the experimental details, see Nakauma et al. (2011), *Food Hydrocolloids* 25, 1165–1173. Reproduction with permission from (Nakauma et al. 2011), Copyright 2010 Elsevier Ltd

#### 4 Working Mechanical Criteria for Elderly Foods in Japan and Comparison to the Global Standards

Representative Japanese standards to define the mechanical criteria of elderly foods will be presented. As a national standard issued by the Consumer Affairs Agency, “Foods for swallowing difficulty” has three-level classification and defines the range of mechanical properties for each classification (Nishinari et al. 2013, 2019a). “Universal Design Foods” ([http://www.udf.jp/about\\_udf/section\\_01.html](http://www.udf.jp/about_udf/section_01.html)) is an industry standard issued by the Japan Care Food Conference, in which food manufactures and food ingredient/package companies are involved. It has four-level classification differed by mastication difficulty. “Dysphagia Foods Pyramid” is a standard proposed by a nutrition manager of a famous hospital and has five-level classification by swallowing difficulty. It is similar to the national standard in that both use hardness, adhesiveness, and cohesiveness as a mechanical parameter (Sakai 2007). Mechanical criteria presented in these standards are served as a guideline mainly for food manufactures in producing processed foods, not for hospital and nursing-care facilities. This is because the measurement apparatus is neither inexpensive nor suitable for on-site use.

Mechanical hardness, adhesiveness, and cohesiveness, adopted in “Foods for swallowing difficulty” and “Dysphagia Foods Pyramid,” are measured by two-bite analyses called TPA (Texture Profile Analysis). TPA uses a universal testing machine such as Instron, and in TPA profiling, a food sample is compressed twice in a reciprocal manner for mimicking human jaw action during food consumption. Based on the resultant force-time curve, hardness is determined by the force peak in

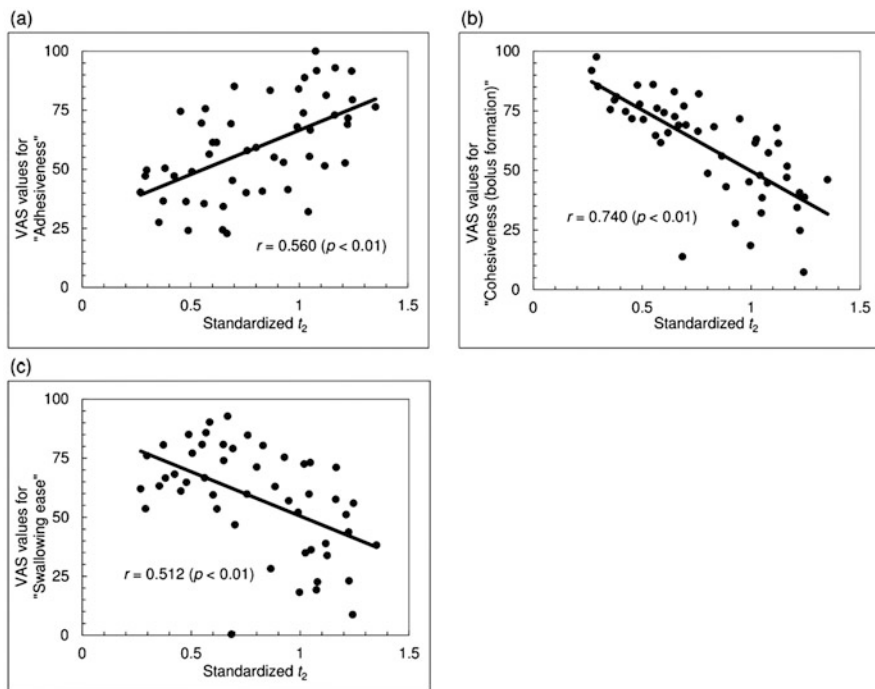


**Fig. 13.3** Correlation between the duration  $t_2$  and the score of each sensory attribute in swallowing polysaccharide solutions. Serving volume of polysaccharide solutions was 15 mL. (a) perceived adhesiveness; (b) perceived cohesiveness; (c) perceived swallowing ease. Duration  $t_2$  was standardized with the corresponding data for water. For the experimental details, see Nakauma et al. (2011), *Food Hydrocolloids* 25, 1165–1173. Reproduction with permission from (Nakauma et al. 2011), Copyright 2010 Elsevier Ltd

the first bite cycle, adhesiveness by the negative force area during the first bite, and cohesiveness by the ratio of the positive force areas under the first and the second bites (Bourne 2002b). This was originally developed for measurements of solid or semi-solid foods (Szczesniak and Hall 1975), but now the TPA measurement is expanded to less hard and more fluid foods. This generates one major difference from the original; a support of a container or cup to “pour” the food sample is needed for TPA measurements, which is not the case of solid or semi-solid foods as they can stand alone. The size of plunger is smaller than that of test sample, which is another difference from the original. Due to these differences, some difficulties in operation and data analysis have been highlighted (Nouchi et al. 2012; Nishinari et al. 2013; Brenner and Nishinari 2014). In principle, TPA parameters cannot be compared among food samples of different viscoelastic natures, and the TPA founder concerned about the misinterpretation of TPA parameters obtained from the measurement of liquid foods in a cup (Szczesniak and Bourne 1998). Although there is no doubt as to the utility of TPA parameters in presenting food texture, we should be

**Table 13.1** New grouping of thickening led by the Japanese Society of Dysphagia Rehabilitation

	Level 1 Mildly thick	Level 2 Moderately thick	Level 3 Extremely thick
Features (in swallowing)	<ul style="list-style-type: none"> <li>• Appropriate to express by “drink”</li> <li>• Spreadable in the mouth</li> <li>• Not concerned for some liquids depending on the kind, taste, and temperature</li> <li>• Large force unnecessary in swallowing</li> <li>• Easy to swallow through a straw</li> </ul>	<ul style="list-style-type: none"> <li>• Viscous to be detected</li> <li>• Appropriate to express by “drink”</li> <li>• Smooth but not so spreadable in the mouth</li> <li>• Cohesive on the tongue</li> <li>• Perceiving a resistance to swallow through a straw</li> </ul>	<ul style="list-style-type: none"> <li>• Apparently viscous to be detected</li> <li>• Easy to form bolus</li> <li>• Appropriate to express by “eat” using a spoon</li> <li>• Difficult to swallow through a straw</li> </ul>
Feature (in appearance)	<ul style="list-style-type: none"> <li>• Easy to slide on spoon surface when tilted</li> <li>• Flowing rapidly through in-between forks</li> <li>• Trace of flow on cup surface when tilted to pour off</li> </ul>	<ul style="list-style-type: none"> <li>• Slidable on spoon surface when tilted</li> <li>• Flowing slowly through in-between forks</li> <li>• Thin film formation on cup surface when tilted to put off</li> </ul>	<ul style="list-style-type: none"> <li>• Shape retention and resistant to slide on spoon surface when tilted</li> <li>• Cannot flow through in-between forks</li> <li>• Not flowing out of cup when tilted or flowing slowly as one cohesive bolus</li> </ul>
Viscosity <sup>a</sup> (mPa·s)	50–150	150–300	300–500
LST value <sup>b</sup> (mm)	36–43	32–36	30–32

<sup>a</sup>Measuring at  $50\text{s}^{-1}$  at  $20\text{ }^{\circ}\text{C}$

<sup>b</sup>Pouring 20 mL sample into a cylinder of 30 mm in diameter, drawing it up, and measuring the length of the spread after 30 s for determination of Line Spread Value. Reproduction with permission from (Funami 2016), Copyright 2016 Wiley Periodicals, Inc

cautious about their validities or physical meanings in discussing TPA results (Nishinari and Fang 2018; Nishinari et al. 2019b).

As shown, multiple standards are working in parallel in Japan, showing some complexity. Under the leadership of the Japanese Society of Dysphagia Rehabilitation (JSDR), these standards were integrated. A novel classification of dysphagia foods has been proposed by JSDR, in which new five classes are identified with no mechanical criteria. Interchangeability of these new five classes with previous three standards has been also indicated in the JSDR standard. JSDR has also proposed a new grouping of thickening (Table 13.1). Viscosity should be measured at a fixed shear rate of  $50\text{ s}^{-1}$ , which is harmonized with American standard National Dysphagia Diets; NDD (Cichero et al. 2013), and the choice of this shear rate is based on Wood’s report (Wood 1968). Line Spread Test, which is similar to USDA Consistometer (Bourne 2002c) and converts rheological measures for fluids expressed in viscosity mPas to distance mm (Cichero et al. 2013), is also adopted

**Table 13.2** International terminology of thickened liquids (cite from Curr Phys Med Rehabil Rep (2013) 1:280–291

Country	< “Water-like”			“Pudding-like” >	
USA (NDD)[45]	Thin (1-50 cP <sup>a</sup> )		Nectar-Like (51-350 cP <sup>a</sup> )	Honey-like (351-1750 cP <sup>a</sup> )	Spoon-thick (>1750cP <sup>a</sup> )
United Kingdom[44]	Thin	Naturally thick fluid	Thickened fluid – stage 2	Thickened fluid 1	Thickened fluid – Stage 3
Australia[6]	Regular	-	Level 150 – Mildly thick	Level 400 – moderately thick	Level 900 – Extremely thick
Ireland[40]	Regular	Grade 1 – Very mildly thick	Grade 2 – Mildly thick	Grade 3 – Moderately thick	Grade 4 – Extremely thick
Japan (JSDR; scheme)[41]	Less mildly thick (< 50 mPa.s <sup>a</sup> )	Mildly thick (50-150 mPa.s <sup>a</sup> )	Moderately thick (150-300 mPa.s <sup>a</sup> )	Extremely thick (300-500 mPa.s <sup>a</sup> )	Over Extremely thick (> 500 mPa.s <sup>a</sup> )
Canada	Regular/ Thin/ Clear		Nectar / Stage 1 / Level 1 / >250cP / 51-350 cP	Honey / Stage 2 / Level 2 / > 800 cP / 351-1750cP / Default Thick	Pudding / Spoon thick / Stage 3 / Level 3 / > 2000 cP / > 1750 cP
Denmark[46]	Normal	Chocolate milk	Syrup	Jelly	
Spain	Thin			Medium	Full protection/thick/pudding
Netherlands	Thin		‘Thickened’		Pudding-like
Brazil	Normal or thin	Thicker liquid		Nectar or Honey	Paste or Creamy (Homogenous or Heterogenous)
Sweden[43]	Liquids	Thickened liquids			

<sup>a</sup>Shear rate 50 s<sup>-1</sup>, both cP and mPa.s are used in the literature as the unit of viscosity, 1 cP = 1 mPa.s. Reproduction with permission from (Cichero et al. 2013), Copyright the Authors 2013. This article is published with open access at Springerlink.com

as more convenient and less expensive method. JSDR can be the most advanced specification which provides measurable indication. We can see both similarities and differences when compared to the terminology and viscosity guideline used in other countries (Table 13.2). Regarding the terminology, real fluid foods, including nectar, honey, pudding, chocolate milk, syrup, and jelly are used for viscosity classification in some standards like USA, Canada, Denmark, etc. In Australia, Ireland, and also JSDR standards, predicative presentation of thickness such as mildly thick, moderately thick, or extremely thick are used. However, these terms mean ambiguously if the definition is lacking as the image of thickness perceived by the terms depends on personal cognition. Therefore, subjective measures with physical meaning are necessary to get consensus and to remove the bias caused by the terminological ambiguity. As a subjective measure, NDD, JSDR, and Canada (maybe) use shear viscosity at 50 s<sup>-1</sup>, but this is not in the case for other countries. It is necessary to install the instrument like viscometer for measurement of viscosity. This may cost a lot for hospitals and care homes and can be one of the reasons for this inhomogeneity. To secure the patient safety and to enhance inter-professional collaboration, international initiative was led by an independent and non-profit entity; the International Dysphagia Diet Standardisation Initiative (IDDSI).

As a noticeable activity, IDDSI developed a new set of standardized terminology and definition for the description of texture of modified foods and thickened fluids in 2016 (Lam and Cichero 2016; Cichero et al. 2017). The IDDSI framework consists of a continuum of 8 levels (0–7), identified by numbers, text labels, and color codes. Levels 0–4 represent fluid foods, levels 3–7 represent solid or semi-solid foods, and

levels 3 and 4 at the intermediate and apply to both. The IDDSI flow test was proposed for the measurements of fluid foods, in which a 10-ml syringe is used. In this test, the syringe is filled with 10 ml fluid food, and the fluid food is allowed to flow freely by gravity for 10 s. The IDDSI level of the fluid food is determined by reading the remaining volume after the gravity flow for 10 s. The larger the volume, the thicker the sample is. This test is for categorizing the texture of fluid foods (i.e., thickness) in simple and practical manner and can be utilized universally with low cost (Su et al. 2018; Yokote et al. 2017; Steele et al. 2018). Although the IDDSI test requires the measurements under ambient conditions where foods and beverages are usually consumed, it is desirable from scientific point of view to perform the test under a temperature-controlled condition because the viscosity of fluid foods depends strongly on temperature. Texture of solid or semi-solid foods is often represented by hardness, and hardness is usually determined mechanically on a texture analyzer, which compresses or extend test sample coaxially. However, this may cost a lot for hospitals and care homes as in the case of viscometer, leading to the difficulty in installation. A practical test using a fork or spoon has been previously recommended as part of the United Kingdom dysphagia diet standard for assessment of foods with the IDDSI Levels 5–7. In this test, force or pressure is applied to a food sample with a fork, and deformation behavior of the food sample is observed. In order to standardize the force applied, the IDDSI fork test recommends that the fork should be pressed onto the food sample by placing the thumb onto the bowl of the fork (base of the prongs), and pressing just hard enough to cause blanching of the thumbnail. Blanching occurs when the pressure overcomes mean arterial blood pressure and has been quantified at approx. 17 kPa. Details are described in the following URL;

[http://ftp.iddsi.org/Documents/Testing\\_Methods\\_IDDSI\\_Framework\\_Final\\_31\\_July2019.pdf](http://ftp.iddsi.org/Documents/Testing_Methods_IDDSI_Framework_Final_31_July2019.pdf)

This pressure corresponds closely to a typical tongue pressure during swallowing (Fei et al. 2013; Youmans and Stierwalt 2006). Descriptions and testing methods have been also developed using chopsticks (indirect as in the case of fork) and fingers (direct) instead of fork.

## 5 Mechanical Simulation of Palatal Reduction

Two oral strategies for food size reduction in the mouth are known; mastication (or chewing) and palatal reduction. Palatal reduction involves squeezing and tongue-(hard) palate compression, and the elderlies like to use palatal reduction, particularly those with mastication difficulty. Solid or semi-solid foods are usually reduced to suitable particle sizes by mastication and/or palatal reduction, followed by incorporation of the right amount of saliva to form coherent bolus (Chen 2009; Hutchings and Lillford 1988; Prinz and Lucas 1995). Rheological properties change dramatically from the original food (prior to oral processing) during formation of food bolus (Chen 2009). Bolus rheology is gaining interest in relation to food texture perception



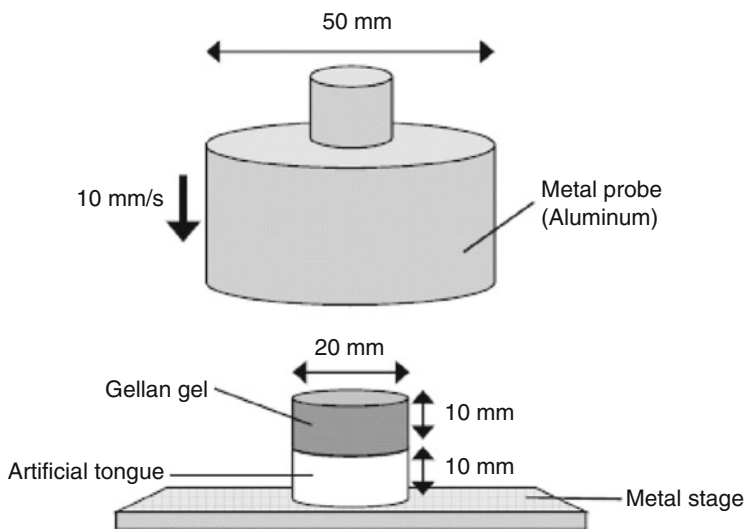


**Fig. 13.4** Setup and standard operation condition of instrumental compression test using artificial (simulated) tongue as a substrate. Reproduction with permission from (Ishihara et al. 2014), Copyright 2014 Wiley Periodicals, Inc

(Ishihara et al. 2011b). Easiness to form bolus and suitability of bolus to the elderly's oral physiology should be the key for the formulation or texture design of elderly foods.

In a series of food oral management, a food is deformed slightly by tongue-palate compression at the initial stage for recognition of texture (Arai and Yamada 1993) and for determination of subsequent oral strategy for size reduction. That is, when a food is soft enough to be fractured by tongue-palate compression, the tongue works continuously for size reduction, whereas mastication is initiated when a food is too strong to be fracture by tongue-palate compression. To mimic tongue-palate compression, an *in vitro* food texture assessment system has been developed, where a food sample (in a cylindrical shape of 20 mm in diameter and 10 mm in height) is compressed between hard non-deformable plate (50 mm in diameter) and artificial tongue from a soft material (i.e., silicone rubber of the same shape and size as the food sample) on a conventional uniaxial compression apparatus (Ishihara et al. 2013) (Fig. 13.4). Young's modulus of artificial tongue corresponds to apparent elastic modulus determined at approx. 20% strain. It is concluded from their study using agar gels as food samples that when an artificial tongue with the Young's modulus of approx. 55 kPa is used as substrate, the fracture profile of a food sample predicts the human oral strategy for size reduction. That is, when a food sample is broken down by compression on the system, tongue-palate compression will be the main oral strategy for size reduction, whereas mastication will be when the food sample is not broken down on the system (Table 13.3). The assessment system uses the compression (crosshead) speed at 10 mm/s and the same size of crosshead as the food sample. Young's modulus of artificial tongue lies between that of human (healthy young

**Table 13.3** Fracture profile of agar gels during compression on artificial tongue in relation to human oral strategy for size reduction

	Artificial tongue		
	S40 (18.3 kPa)	S50 (54.9 kPa)	S60 (113.0 kPa)
Agar gel			
A3 (14.7 kPa)	F 8/0	F 8/0	F 8/0
A4 (17.5 kPa)	F 7/1	F 7/1	F 7/1
A5 (53.5 kPa)	N 3/5	F 3/5	F 3/5
A6 (97.9 kPa)	N 0/8	N 0/8	F 0/8

Symbols F and N represent that agar gels did not fracture upon compression on each artificial tongue up to 50% strain of the combination of agar gel and artificial tongue, respectively. Slash data below the symbol represent the number of subjects who used the tongue-palate compression for size reduction (upper) and the number of subjects who used mastication for size reduction (lower). Figures in parenthesis represent apparent elastic modulus of either agar gel or artificial tongue. Reproduction with permission from (Funami 2016), Copyright 2016 Wiley Periodicals, Inc

adults) tongue in relaxation; 12.2 kPa and in a tension state; 122.5 kPa (Ishihara et al. 2013).

Subsequent study confirmed the robustness and the limitation of the assessment system using gellan gum gels in wider mechanical range (Ishihara et al. 2014). It is concluded from their study that operation conditions should be modified in some cases, which may linked to physiological changes in tongue-palate compression upon food texture. In details, some behavioral modulations may occur during consumption of highly deformable gels. These include the tongue-palate compression speed and tongue excitation. The first factor can be recreated by decreasing the crosshead speed from 10 to 5 mm/s in associated with the stress relaxation, a phenomenon of energy dissipation increased at lower deformation speed (Luyten and van Vliet 1995). The second factor can be recreated by increasing the Young's modulus of artificial tongue from approx. 55 to approx. 110 kPa. The slope of the curve from tongue pressure measurement (tongue pressure versus time) during the first size reduction is almost independent of physical properties (texturally brittle or deformable) or consistency (soft or hard) of polysaccharide gels (Hori et al. 2015). Based on this finding, it should be reasonable that decreased speed of tongue-palate compression gives rise to increased tongue pressure. Decrease in the crosshead speed or increase in the Young's modulus of artificial tongue in evaluating highly deformable samples should be also reasonable. Usage of artificial tongue of larger size can be an option as surface contact area between the food sample and the tongue will be enlarged when the food sample is highly deformable. In relation to "highly deformable," it is suggested that the mode to decide oral strategy for size reduction should depend on the fracture strain of food, and its boundary can be at approx. 60%–70% (Ishihara et al. 2014). The oral strategy for size reduction can be decided

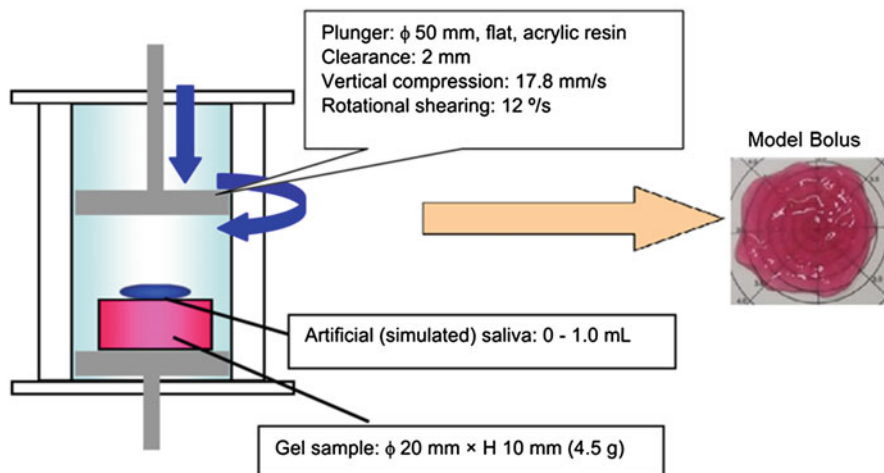


**Fig. 13.5** Mechanical mouth-simulator for model bolus formation. Reproduction with permission from (Ishihara et al. 2011a), Copyright 2010 Elsevier Ltd

by sensing the difference in strain of food relative to the tongue perceived dynamically during oral processing (Kohyama 2015). Fracture strain is a dominant mechanical parameter which can govern the decision of oral strategy for size reduction (Arai and Yamada 1993), and this is the same as the determination of the biting speed (Mioche and Peyron 1995). These are all in line with the results from Ishihara et al. (2013, 2014).

Mechanical mouth-simulator is useful to collect simulated food bolus as shown in Fig. 13.5 (Funami 2011; Ishihara et al. 2011a, 2011b). This simulator, originally developed for flavor analysis, works in a closed system, allowing the process of a food sample in the presence of artificial (simulated) saliva. Human saliva is two orders of magnitude lower than that of water in the boundary friction coefficient (Bongaerts et al. 2007), and the lubrication of food bolus is determined by the miscibility with saliva. This is why the saliva incorporation in bolus rheology and tribology is important (Torres et al. 2019). With regard to deformation, a food sample is compressed with shear on the simulator, which recreate the tongue movement during food consumption; 10 cycles of vertical compression at 17.8 mm/s with 2.0 mm-clearance and simultaneous rotational shearing at rate of 12°/s. In studies by Ishihara et al. (2011a, 2011b), four gel samples prepared using two different gelling agents at two different consistencies were processed mechanically to obtain simulated food bolus. Gels can be base for dysphagia foods due to their versatile viscoelastic character (Funami 2011), and thus gel samples were used as a model food. For example, gels from the mixture of low-acylated gellan gum and psyllium seed gum have more deformable (plastic) texture than that of gellan single gels due to the effects of psyllium seed gum, and water-holding capacity of the mixture gels is also increased (Ishihara et al. 2011c). As shown in Fig. 13.6, the frequency-dependence of dynamic mechanical loss tangent of stimulated bolus from

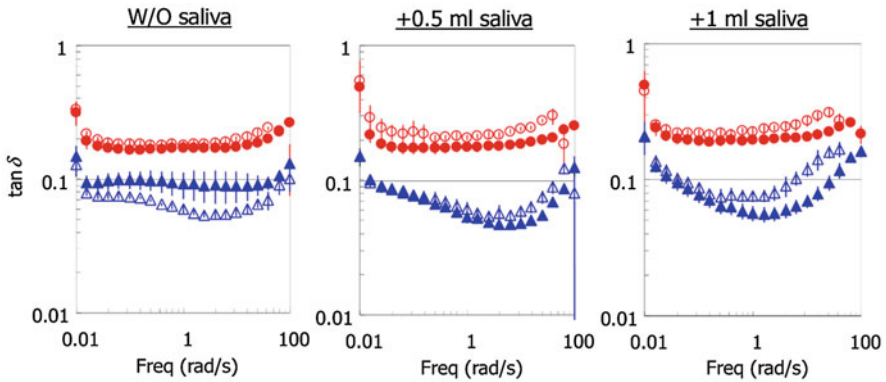


**Fig. 13.6** Frequency-dependence of dynamic mechanical loss tangent for model bolus. Measurements were carried out at 20 °C at a fixed strain of 1%. Open circles: 1.0% SAN SUPPORT® (a mixture of de-acylated gellan gum and psyllium seed gum); closed circle: 1.5% SAN SUPPORT®; open triangle: 0.075% gellan gum; closed triangle: 0.15% gellan gum. Data are presented as means  $\pm$  SD of triplicate. For the experimental details, see Ishihara et al. (2011a), *Food Hydrocolloids* 25, 1016–1024. Reproduction with permission from (Funami 2016), Copyright 2016 Wiley Periodicals, Inc

the mixture gels is almost independent of the addition level of simulated saliva, whereas the bolus form gellan single gel is dependent on. Here, mechanical loss tangent presents how a sample is elastic or viscous, and the smaller the parameter, the more elastic the sample is. The mixture gels are less influenced by the saliva secretion in bolus formation and exhibit rheologically weak gel property, assumedly leading to a comfortableness of eating for the elderlies.

## 6 Progress of In Vivo Physiological Tests as Advanced Texture Assessment

Although rheological measurements reveal the mechanical and related microstructural properties of foods, the reality and the complexity of oral experience can be oversimplified (Peleg 2006). The deviation is due to the lack of salivation (Stokes 2012) and the use of stiff materials (Peleg 2006), for instance. Limitations of rheological measurements in identification of food texture, causing inconsistency between both results, are explained by at least two reasons; temporal difference in judgement and the complexity/simplicity of sensing between instrument and human (Kohyama 2015). Another explanation should be from Peleg (2006) indicating that the sensory response to a mechanical (or acoustic) stimulus should be expressed not as a characteristic ‘value’, i.e. as a mean relative or an absolute score, but as a distribution of the terms used by those who sense them. Therefore, in vivo human physiological measurements should be introduced to reconcile instrumental

measures (Foster et al. 2011; Koç et al. 2013; Wilkinson et al. 2000), where non-invasive sensors attached to human subjects are used to monitor the organ and muscle signals related to food oral processing for tracing the dynamic changes of food texture. A various kinds of in vivo measurements are often used for texture assessment, involving palatal pressure measurements (Nakazawa and Togashi 2000; Takahashi and Nakazawa 1991, 1992), electromyography (Kohyama et al. 1998, 2005b, 2005c, 2007), biting force measurements (Kohyama and Nishi 1997; Kohyama et al. 1997, 2001, 2003, 2005a), and ultrasonic pulse Doppler methods (Kumagai et al. 2009; Nakazawa et al. 2000). In terms of dynamics, in vivo measurements lie between instrumental measurements and sensory evaluations, and understanding on the dynamic changes of foods during oral processing should be the key for texture studies (Chen 2009). From this perspective, in vivo measurements should be utilized more in this research area. As a model food/beverage for texture studies, polysaccharide gels/sols are useful because of their controllable rheological properties without significantly affecting other organoleptic properties, particularly flavor and appearance (Peleg 2006).

### **6.1 Tongue Pressure Measurement**

As the tongue plays a crucial role in a series of food oral processing, it is physiologically reasonable to link its movement to food texture. Two literatures published recently, relating to tongue pressure measurement during food oral processing and its usefulness for food texture study, are highlighted. In these two literatures, effects of food texture on tongue movement were investigated using a novel sensing system and polysaccharide gels as a model food (Hori et al. 2015; Yokoyama et al. 2014). They indicated potential usage of tongue pressure measurement for elucidation of the dynamics of food oral processing and for visualization of food-tongue interaction. T-shaped sensor sheet with five measuring channels is the main part of the sensing system (Fig. 13.7), which makes it possible to monitor tongue pressure in real time on an electrical transducer (from resistance to electrical current). This device has been developed by Osaka University research team, which specializes the design of the palatal plate particularly for tongue cancer patients (Hori et al. 2009). Their idea to apply this device to food science is novel utilizing its features beneficial for texture study. The sensor sheet has only 0.1 mm thickness with various sizes, and its mechanical flexibility realizes easy adaptation to the oral shape and does not change the oral physiology nor interfere with the occlusion. In addition, the sensor sheet does not cover the whole area of the palate and thus does not interfere with taste, aroma, and texture perceptions. The sensor sheet does not interfere with natural eating behavior of human, and this can be the greatest advantage over a conventional system using a small balloon-shaped probe called a manometer (Shaker et al. 1988). Using this sensing system, temporal and spatial distribution patterns of tongue pressure during food oral processing were elucidated (Hori et al. 2015; Yokoyama et al. 2014). Polysaccharide gels were used as a test sample with

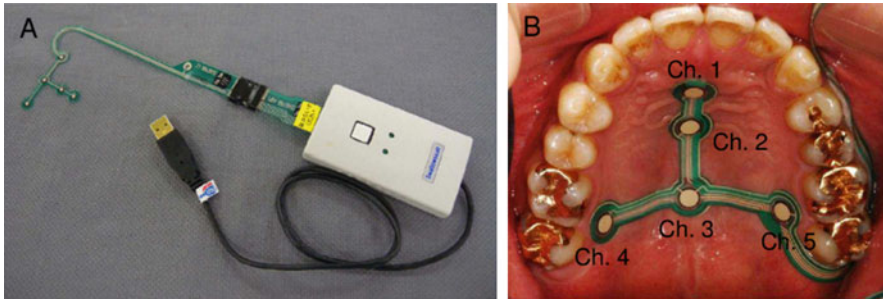


**Fig. 13.7** Tongue pressure sensing system (a) and location of sensor points (b). The lengths between Ch. 1 and Ch. 3 were 23, 25.5, 28 mm for Small, Medium, Large size of sensor sheet respectively. Those between Ch. 4 and Ch. 5 were 35, 38, 41 mm for S, M, L size. Reproduction with permission from (Hori et al. 2015), Copyright 2014 Elsevier Ltd

various textures by using different gelling agents; low-acylated gellan gum, and the mixture of low-acylated gellan gum and psyllium seed gum. By changing polysaccharide concentration, gels of three different hardness values (defined here as the stress at 67% strain); approx. 1600, 5500, and 12,000 Pa were prepared. Texture of the gellan single gel is brittle (Morris 2006) with detectable syneresis, particularly at low concentrations. For the mixture gel, syneresis is not detective due to the function of psyllium seed gum, which also increases textural deformability (Ishihara et al. 2011c). When subjects were asked to eat the gel samples by compressing them between the tongue and the hard palate (i.e., squeezing), temporal pattern of tongue pressure during squeezing did not change substantially upon gel texture, presenting the first onset at the mid-median part (Ch. 2), followed by the anterior-median (Ch. 1), the posterior-median (Ch. 3) parts, and the circumferential parts (Chs. 4 and 5) in this order for each type of gel sample (Fig. 13.8). However, differences were noted in offset between the two gel samples. As a result, duration of squeezing for texturally deformable gels (i.e., the mixture gels) tended to become shorter than that for texturally brittle gels (i.e., gellan single gels) when the gel hardness was lower, whereas vice versa when the gel hardness was higher. Spatial distribution pattern of the tongue pressure during squeezing changed upon gel texture; the maximum amplitudes at Chs. 1 and 2 were larger than those at Chs. 4 and 5 for gellan single gels, whereas no marked difference was found between channels for the mixture gels (Fig. 13.9). Consequently, human eating behavior can be visualized by tongue movement, which changes upon food texture. Foods in the form of weak gels, emulsions, and fluids are eaten by squeeze between the tongue and the palate during oral processing, and in these cases, texture relates to thin film rheological behaviors of foods as well as the bulk properties (Malone et al. 2003), including mayonnaise (Giasson et al. 1997) and chocolate (Luengo et al. 1997). The combination of both shear and squeeze flow is more realistic representation for tongue movement during food oral processing (Stokes 2012). The influence of polysaccharides' conformation and structure on lubrication has been presented (Garrec and Norton 2012, 2013; Malone et al. 2003), and effects of polysaccharides on food

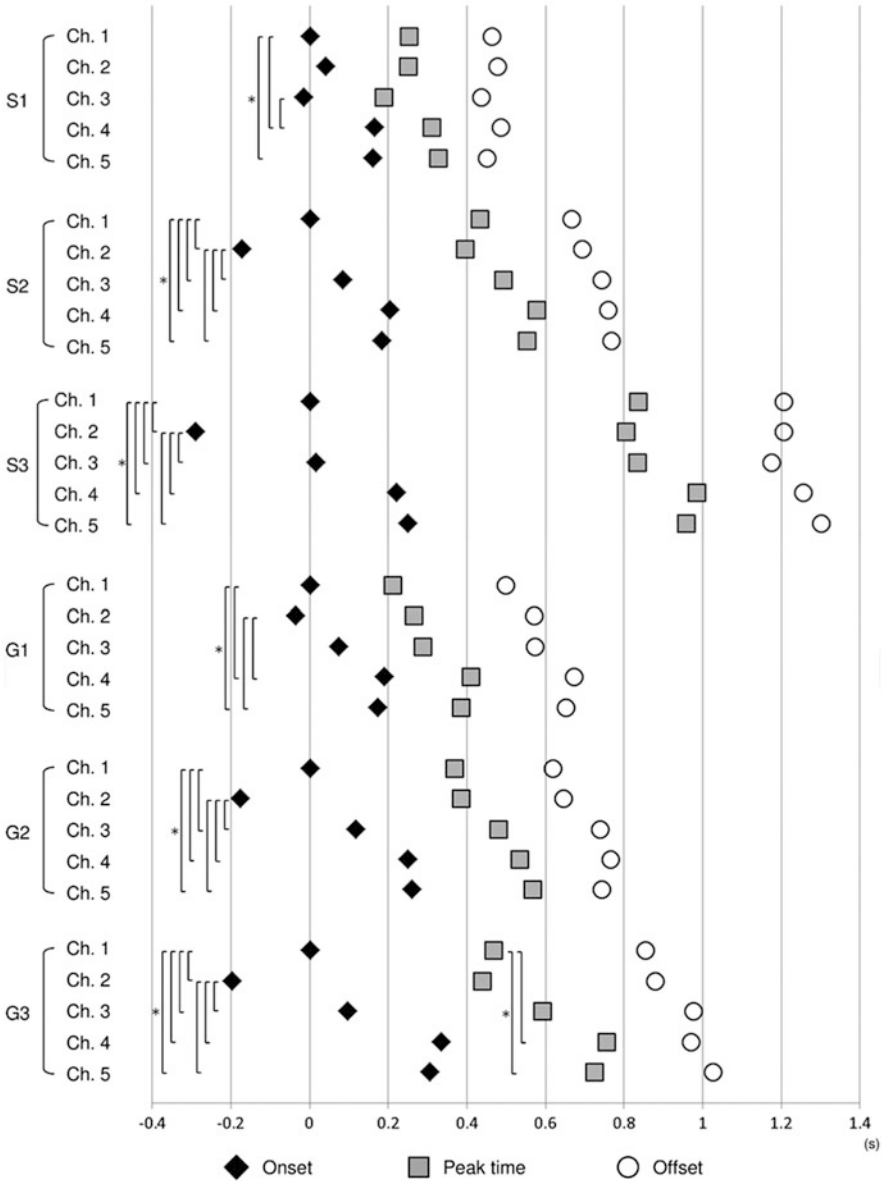


**Fig. 13.8** Time sequences of tongue pressure during the initial squeeze. The time “0” was set as the onset of Ch. 1. \*:  $p < 0.05$  (Kruskale–Wallis test and post hoc test with Bonferroni correction). S1–3 presents texturally deformable gel samples from the mixture of low-acylated gellan gum and psyllium gum with increased consistency in order, whereas G1–3 presents texturally brittle gel samples from low-acylated gellan gum with increased consistency in order. When the number is the same, consistency of the gel sample is equivalent between both types of gel sample. Reproduction with permission from (Hori et al. 2015), Copyright 2014 Elsevier Ltd



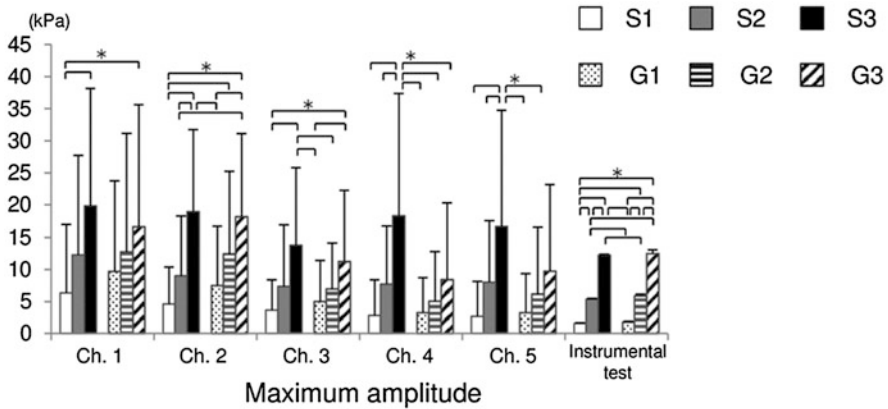


**Fig. 13.9** The maximum amplitude of tongue pressure at each channel during the initial squeeze. \*:  $p < 0.05$  (one-way ANOVA test and Tukey's post hoc test). Reproduction with permission from (Hori et al. 2015), Copyright 2014 Elsevier Ltd

texture, including creaminess, smoothness, sliminess, and thickness, should be investigated by tribological approaches (See Chap. 7 in this book). From these perspectives, it is expected that tongue pressure measurement will be facilitated and emphasized in food texture study.

## 6.2 Electromyography

Electromyography (EMG) has a long history of usage in food science area (Dea et al. 1988; Boyar and Kilcast 1986) and has gained the status as one of the most popular *in vivo* measurements for food texture (Espinosa and Chen 2012; Funami et al. 2014). Relationship of some EMG variables with mechanical properties from instrumental test or texture perception from sensory evaluation has been investigated a lot, and some representative investigations will be reviewed briefly in this section.

Eight kinds of solid foods in a wide range of physicochemical properties were selected as a test food (i.e., dry hard bread, elastic konjac gel, dry sausage, soft candy, raw radish, pickled radish, boiled carrot, and raw carrot), and nine independent parameters were chosen from 28 physicochemical parameters (i.e., stress at 10%, 50%, 70%, or 90% compression strain, breaking stress, cohesiveness, adhesiveness, density, and moisture content) (Kohyama et al. 2008). It is concluded that the mechanical properties under larger deformation should correlate well to EMG variables. Results from other studies using buckwheat noodles (Kohyama et al. 2010) and gummy candies (Hayakawa et al. 2009) support this conclusion. When the correlation with EMG variables is studied for solid foods which needs mastication, it would be recommended in general to see the mechanical properties of food sample under large deformation conditions, sometimes beyond the fracture point.



High correlation can be found between EMG variables and mechanical properties under extremely deformation condition regardless of rheological nature of food sample; elastic or plastic since the upper and lower teeth almost reach contact during mastication for each type of sample. EMG can also detect food oral process at the early stage, it would be necessary to further investigate why there is hardly seen a good correlation between EMG parameters and sensory evaluation in small deformation ranges. It is not clear whether the sensitivity of EMG is not high enough or human did not care about small deformation.

All these studies used relatively hard foods consumed by mastication or chewing for size reduction, but similar principle can be applied to relatively soft foods which do not necessarily require mastication. From this perspective, EMG measurements were performed for foods which are soft enough to be processed with the tongue-palate compression (Ishihara et al. 2011c). In this study, polysaccharide gels from either low-acylated gellan gum or the mixture of low-acylated gellan gum and psyllium seed gum were fed to young healthy adult subjects, and the correlation between EMG variables and mechanical properties was investigated. For each gelling agent, gels of different hardness; approx. 1000 and 4000 Pa determined as the compression stress at 67% strain were prepared by changing polysaccharide concentration, and 15 g for each gel was served to the subjects. As mentioned, there was a texture difference between both types of gel (i.e., brittle or deformable). It is concluded that whole sequence of food oral processing is prolonged and that EMG activity of the suprahyoid musculature increases by increasing hardness for each type of gel. EMG activity of the suprahyoid musculature is well correlated to the compression load at extremely large strain conditions (e.g., 90% strain) and to sensory perceived hardness. This is similar to another study using gelatin gels, which are different in rheological natures; elastic or plastic and are processed by mastication, where the duration of the whole sequence and EMG activity of the masseter and the temporalis increase with Instron hardness represented as the compression stress at 50% strain (Foster et al. 2006). In summary, mechanical properties at large strains relate to physiological response during food oral processing regardless the oral strategy for size reduction; mastication or tongue-palate compression.

## **7 Release Control of Flavor and the Effects on Human Eating Behavior**

Using food gels as a feeding sample, it was found that perceived flavor (including strawberry aroma and sucrose) intensity increased as their fracture strain decreased (Morris 1993). Another study showed that overall flavor (including aroma and sweetener but not specified) intensity decreased linearly with increasing hardness (i.e., rupture force) of food gels (Clark 2002). However, a highly cohesive gel was exceptional and positioned below the linear regression line when compared at

equivalent hardness. Whereas gelatin gel was positioned upward the linear regression line when compared at equivalent hardness, representing increased flavor intensity due to lower melting temperature of the gels. Thermal property and water-holding capacity (i.e., syneresis) are also essential attributes in determining flavor release (Nishinari 2006), while the effect of free diffusion may be relatively low compared to the effect of external deformation through compression and fracture (Wang et al. 2014). As a rheological parameter, fracture strain presents perceived flavor intensity better than fracture stress, which should be reasonable when food breakdown during oral processing is considered. Foods with smaller fracture strain and more brittle texture collapse at an early stage of oral processing and disintegrate into smaller particles. This rupture behavior of foods can lead to increased surface exposed area of food bolus in the mouth, stimulating perceived intensity of flavor via contact with saliva. It has been reported (Weel et al. 2002) that significant changes in aroma intensity are observed between different concentrations of whey protein gels though nosespace aroma concentration is independent of their hardness; the lower the gel hardness, the higher the aroma intensity is. Based on this finding, it can be said that aroma perception is determined by texture rather than the aroma release although biological mechanism is not still clear. It has been also confirmed that perceived aroma intensity is more influenced by the release rate than by the release amount of the aroma compound (Baek et al. 1999). Using gelatin gels sweetened with sucrose and flavored with furfuryl acetate, no significant differences are found in the maximum in-nose volatile concentration between different concentrations of gelatin gels. The amount of volatile present does not correlate with the sensory analysis, while the rate of volatile release shows good correlation. As these, release rate of aroma is associated with the degree of food breakdown in the mouth, demonstrating the importance of dynamic (not static) analysis of aroma release for high correlation with sensory data.

Regarding flavor perception, It has been indicated that inhomogeneous spatial distribution of tastants like sweetness (Holm et al. 2009; Mosca et al. 2010, 2013) and saltiness (Mosca et al. 2013; Noort et al. 2010, 2012) for solid foods increase perceived taste intensity, and similar effect can be expected also for liquid foods. Adaptation occurs when exposed continuously to taste stimulus for extended period of time, leading to elevated threshold particularly at high doses, and in this context, the effect of inhomogeneous spatial distribution can be attributed to prevention of adaptation (Meiselman 1972). That is, discontinuous taste stimulus helps recovery from adaptation and enhances taste perception during oral processing. In contrast, there are few reports found on the similar effects of aroma inhomogeneous distribution. Using polysaccharide gels as a feeding sample, effects of inhomogeneous spatial distribution of aroma on its perceived intensity and also eating behavior have been investigated (Nakao et al. 2013). The sample architecture used in their study is illustrated in Fig. 13.10, where the degree of aroma inhomogeneity is variable by changing aroma concentrations in both the matrix and the dispersed gels with keeping the overall aroma concentration constant within one whole gel sample. This situation presents inhomogeneous spatial distribution of aroma. In their study (Nakao et al. 2013), there was no difference in the mechanical properties between the

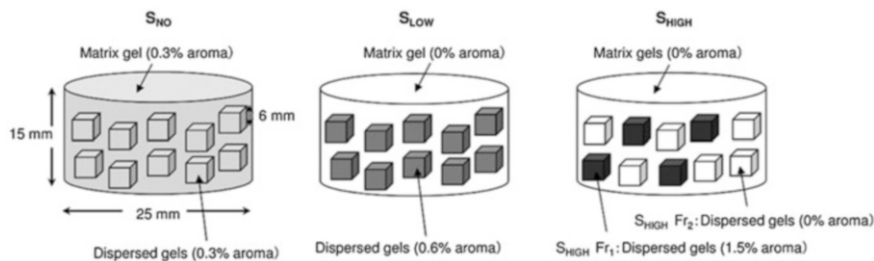


**Fig. 13.10** Schematic drawings of structured gels used.  $S_{NO}$ : homogeneous spatial of aroma, where both the dispersed and the matrix gels contained 0.3% aroma compounds;  $S_{LOW}$ : the lower degree of inhomogenous spatial distribution of aroma, where all dispersed gels contained 0.6% aroma compounds (0.3% in total);  $S_{HIGH}$ : the higher degree of inhomogenous spatial distribution of aroma, where 40% of the dispersed gels contained 1.5% aroma compounds ( $S_{HIGH} FR_1$ ) and remaining 60% of the dispersed gels did not contain aroma compounds ( $S_{HIGH} FR_2$ ) (0.3% in total). Reproduction with permission from (Nakao et al. 2013), Copyright 2013 Wiley Periodicals, Inc

gel samples tested, and also all gel samples were soft enough to be processed by tongue-palate compression for size reduction without chewing. Under these experimental conditions, perceived aroma intensity increased with increasing degree of aroma inhomogeneity. Also, increase in the degree of aroma inhomogeneity increased both duration of oral processing and activity of the suprahyoid musculature, a group of muscles active for jaw opening and also tongue movement (Kohyama et al. 2010; Palmer et al. 1992; Shiozawa et al. 1999a, 1999b; Taniguchi et al. 2008), decreased particle size of expectorated bolus before swallowing, and increased saliva content in the bolus (Fig. 13.11). These results indicate the importance of food structure design for enhancement of perceived aroma intensity and human eating behavior. In relation to the interaction between texture and aroma during food oral processing, a hypothesis is that texture perception on consistency or hardness and eating behavior can be changed by the degree of aroma inhomogeneity (Funami et al. 2016). That is, the higher the aroma inhomogeneity, the less the perceived hardness of foods can be even if a similar effort should be necessary for consumption, and eating behavior can be less consistency-dependent as aroma inhomogeneity is greater. In their study (Funami et al. 2016), the same sample architecture as Nakao et al. (2013) was used but with three different consistency levels of the gel samples. Their finding from surface EMG is that EMG variables; duration and activity of the suprahyoid musculature generally increase with consistency at each degree of aroma inhomogeneity, accompanied with decreased intensity of aroma and taste perception. Another important finding is that as aroma inhomogeneity is greater, increases in the EMG variables are less consistency-dependent, and the intensity of perceived hardness is lower for eating effort (Fig. 13.12). No interaction is found in the EMG variables between consistency and aroma inhomogeneity. From these results, change of aroma inhomogeneity can be a strategy for food product development which promotes oral processing without loading too much for eating, particularly for elderly and dysphagia patients.

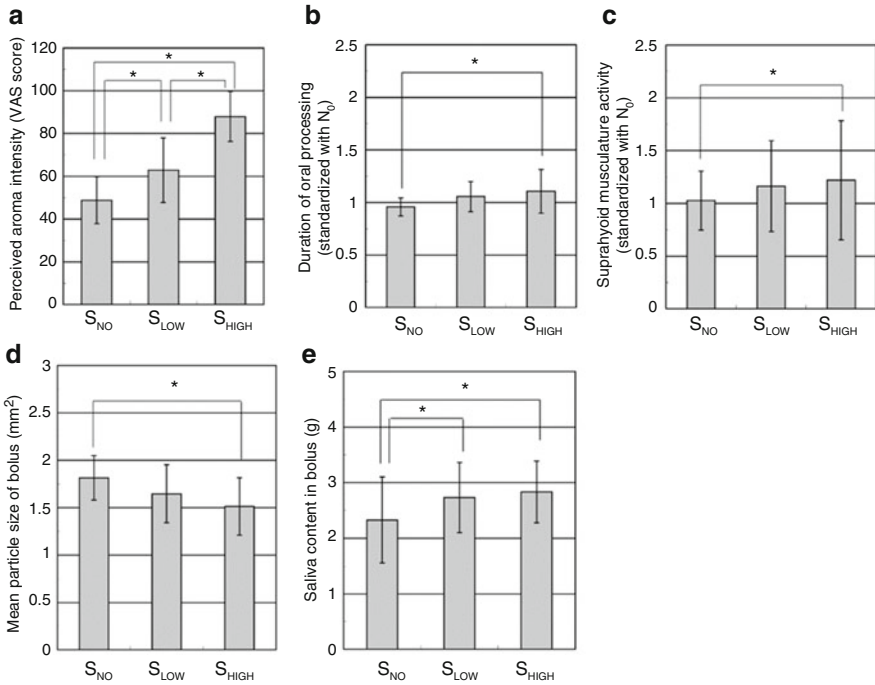


**Fig. 13.11** Effect of the degree of aroma inhomogeneity on variables associated with food oral processing. (a): Perceived aroma intensity; (b): electromyography duration of oral processing; (c): electromyography suprahyoid musculature activity; (d): mean particle size of bolus; (e): saliva content in bolus. Six subjects of 32.0 years old on average participated in tests. Data were presented means  $\pm$  SD of the six subjects. Data with asterisk are significantly different ( $p < 0.05$ ). Reproduction with permission from (Nakao et al. 2013), Copyright 2013 Wiley Periodicals, Inc

## 8 Conclusion

In this chapter, essential elements for formulation design of elderly foods were described along with introduction of recent product developments in Japan. Use of food polysaccharides can be the most practical and reasonable way for texture creation and optimization of elderly foods, but this should be evidenced scientifically. For texture design of elderly foods, both *in vivo* measurements and bolus rheology should be novel approach by taking human physiological response during eating and drinking into account. For the goal, food scientists/technologists are urgently required to work more closely with medical doctors, dentists, dietitians, and therapists to contribute to improved quality of life for the elderlies from dietary aspect.

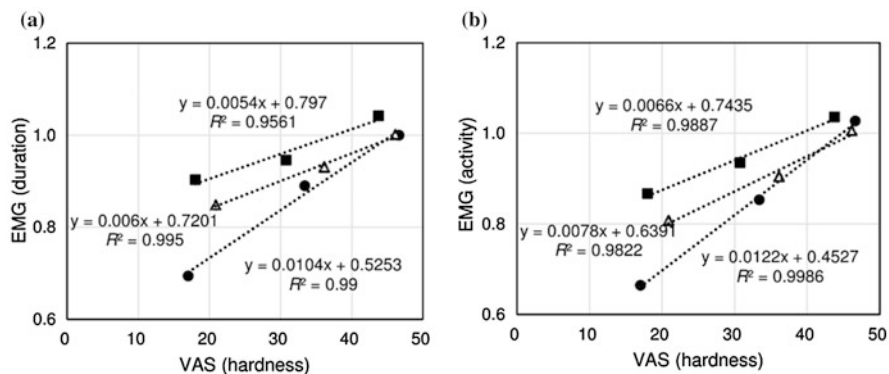


**Fig. 13.12** Relationship between sensory and EMG variables. Liner regression analysis was done for the same degree of aroma inhomogeneity with various consistencies. **(a)** Electromyography duration of oral processing as a function of VAS score of perceived hardness; **(b)** electromyography activity of the suprahyoid musculature as a function of VAS score of perceived hardness. Closed circle: homogeneous spatial distribution of aroma; open triangle: the lower degree of inhomogeneous spatial distribution of aroma; closed squares: the higher degree of inhomogeneous spatial distribution of aroma. Reproduction with permission from (Funami et al. 2016), Copyright 2015 Elsevier Ltd

## References

- Arai E, Yamada Y (1993) Effect of the texture of food on the masticatory process. *Jpn J Oral Biol* 35:312–322
- Arey LB, Tremaine MG, Monzingo FL (1935) The numerical and topographical relations of taste buds to human circumvallate papillae throughout the life span. *Anat Rec* 64:9–25
- Baek I, Linforth RST, Blake A, Taylor AJ (1999) Sensory perception is related to the rate of change of volatile concentration in-nose during eating of model gels. *Chem Senses* 24:155–160
- Boland AB, Delahunty CM, van Ruth SM (2006) Influence of the texture of gelatin gels and pectin gels on strawberry flavour release and perception. *Food Chem* 96:452–460
- Bongaerts JHH, Rossetti D, Stokes JR (2007) The lubricating properties of human whole saliva. *Tribol Lett* 27:277–287
- Bourne MC (2002a) Chapter 3: physics and texture. In: Bourne MC (ed) *Food texture and viscosity: concept and measurement*, 2nd edn. Academic Press, New York, pp 59–106
- Bourne MC (2002b) Chapter 4: principles of objective texture measurement. In: Bourne MC (ed) *Food texture and viscosity: concept and measurement*, 2nd edn. Academic Press, New York, pp 107–188
- Bourne MC (2002c) Chapter 5: practice of objective texture measurement. In: Bourne MC (ed) *Food texture and viscosity: concept and measurement*, 2nd edn. Academic Press, New York, pp 189–233
- Boyar MM, Kilcast D (1986) Review food texture and dental science. *J Texture Stud* 17 (3):221–252
- Brenner T, Nishinari K (2014) A note on instrumental measures of adhesiveness and their correlation with sensory perception. *J Texture Stud* 45:74–79
- Chen J (2009) Food oral processing - a review. *Food Hydrocoll* 23:1–25
- Chen J, Lolivret L (2011) The determining role of bolus rheology in triggering a swallowing. *Food Hydrocoll* 25:325–332

- Cichero JAY, Steele C, Duivesteyn J, Clave P, Chen J, Kayashita J, Dantas R, Lecko C, Speyer R, Lam P, Murray J (2013) The need for international terminology and definitions for texture-modified foods and thickened liquids used in dysphagia management: foundations of a global initiative. *Curr Phys Med Rehabil Rep* 1:280–291
- Cichero JA, Lam P, Steele CM, Hanson B, Chen J, Dantas RO et al (2017) Development of international terminology and definitions for texture-modified foods and thickened fluids used in dysphagia management: the IDDSI framework. *Dysphagia* 32:293–314
- Clark R (2002) Influence of hydrocolloids on flavour release and sensory-instrumental correlations. In: Phillips GO, Williams PA (eds) *Gums and stabilizers for the food industry* 11. Royal Society of Chemistry, Cambridge, pp 217–224
- Clavé P, De Kraa M, Arreole V, Girvent M, Farre R, Palomera E, Serra-Prat M (2006) The effect of bolus viscosity on swallowing function in neurogenic dysphagia. *Aliment Pharmacol Ther* 24:1385–1394
- Dea ICM, Eves A, Morris ER (1988) Relationship of electromyographic evaluation of semi-fluid model food systems with dynamic shear viscosity. In: Phillips GO, Wedlock DJ, Williams PA (eds) *Gums and stabilisers for the food industry* 4. Royal Society of Chemistry, Cambridge, pp 241–246
- Doty RL (1989) Influence of age and age-related diseases on olfactory function. *Ann N Y Acad Sci* 561:76–86
- Espinosa YG, Chen J (2012) Applications of electromyography (EMG) technique for eating studies. In: Chen J, Engelen L (eds) *Food oral processing fundamentals of eating and sensory perception*. Blackwell Publishing, Chichester, pp 289–317
- Fei T, Polacco RC, Hori SE, Molfenter SM, Peladeau-Pigeon M, Tsang C, Steele CM (2013) Age-related differences in tongue-palate pressures for strength and swallowing tasks. *Dysphagia* 28:575–581
- Foster K, Woda A, Peyron MA (2006) Effect of texture of plastic and elastic model foods on the parameters of mastication. *J Neurophysiol* 95:3469–3479
- Foster KD, Grigor JMV, Cheong JN, Yoo MJY, Brounlund JE, Morgenstern P (2011) The role of oral processing in dynamic sensory perception. *J Food Sci* 76:R49–R61
- Funami T (2011) Next target for food hydrocolloid studies: texture design of foods using hydrocolloid technology. *Food Hydrocoll* 25:1904–1914
- Funami T (2013) Use of gelling agents for elderly foods. In: *Stabilization and functionality of gels, application development for the next generation*. Technical Information Institute, Tokyo, pp 395–401 (in Japanese)
- Funami T (2016) The formulation design of elderly special diets. *J Texture Stud* 47:313–322
- Funami T, Tsutsumino T, Kishimoto K (2006) Thickening and gelling agents used for dysphagia thickeners and diets. *J Cook Sci Jpn* 39:233–239 (in Japanese)
- Funami T, Tobita M, Hoshi M, Toyama Y, Sato N, Konno S, Hikita H, Ito S, Yoshihira K, Fujisaki T (2009) Methods for measuring the mechanical properties of dysphagia thickening agents: the usefulness of texture profile analysis. *Jpn J Dysphagia Rehabil* 13:10–19 (in Japanese with English summary)
- Funami T, Ishihara S, Nakauma M, Kohyama K, Nishinari K (2012) Texture design for products using food hydrocolloids. *Food Hydrocoll* 26:412–420
- Funami T, Ishihara S, Kohyama K (2014) Use of electromyography in measuring food texture. In: Dar YL, Light JM (eds) *Food texture design and optimization*. Wiley-Blackwell, Oxford, pp 283–307
- Funami T, Nakao S, Isono M, Ishihara, Nakauma M (2016) Effects of food consistency on perceived intensity and eating behavior using soft gels with varying aroma inhomogeneity. *Food Hydrocoll* 52:896–905
- Funami T, Matsuyama S, Ikegami A, Nakauma M, Hori K, Ono T (2017) *In vivo* measurement of swallowing by monitoring thyroid cartilage movement in healthy subjects using thickened liquid samples and its comparison with sensory evaluation. *J Texture Stud* 48:494–506

- Garrec DA, Norton IT (2012) The influence of hydrocolloid hydrodynamics on lubrication. *Food Hydrocoll* 26:389–397
- Garrec DA, Norton IT (2013) Kappa carrageenan fluid gel material properties. Part 2: tribology. *Food Hydrocoll* 33:160–167
- Giasson S, Israelachvili J, Yoshizawa H (1997) Thin film morphology and tribology study of mayonnaise. *J Food Sci* 62:640–652
- Goda F (2008) Problems and their solutions for gastrostomy tube feeding of semi-solid nutrients. *J JSPEN* 23:235–241 (in Japanese)
- Hayakawa F, Kazami Y, Fujimoto S, Kikuchi H, Kohyama K (2009) Time-intensity analysis of sourness of commercially produced gummy jellies available in Japan. *Food Sci Technol Res* 15:75–82
- Holm K, Wendin K, Hermansson AM (2009) Sweetness and texture perceptions in structured gelatin gels with embedded sugar rich domains. *Food Hydrocoll* 23:2388–2393
- Hori K, Ono T, Tamine K, Kondo J, Hamanaka S, Maeda Y et al (2009) Newly developed sensor sheet for measuring tongue pressure during swallowing. *J Prosthodont Res* 53:28–32
- Hori K, Hayashi H, Yokoyama S, Ono T, Ishihara S, Magara J, Taniguchi H, Funami T, Maeda Y, Inoue M (2015) Comparison of mechanical analysis and tongue pressure analyses during squeezing and swallowing gels. *Food Hydrocoll* 44:145–155
- Hutchings JB, Lillford PJ (1988) The perception of food texture—the philosophy of the breakdown path. *J Texture Stud* 19:103–115
- International Organization for Standardization (1994) ISO 11036: sensory analysis—methodology—texture profile
- Ishihara S, Nakauma M, Funami T, Odake S, Nishinari K (2011a) Swallowing profiles of food polysaccharide gels in relation to bolus rheology. *Food Hydrocoll* 25:1016–1024
- Ishihara S, Nakauma M, Funami T, Odake S, Nishinari K (2011b) Viscoelastic and fragmentation characters of model bolus from polysaccharide gels after instrumental mastication. *Food Hydrocoll* 25:1210–1218
- Ishihara S, Nakauma M, Funami T, Tanaka T, Nishinari K, Kohyama K (2011c) Electromyography during oral processing in relation to mechanical and sensory properties of soft gels. *J Texture Stud* 42:254–267
- Ishihara S, Nakao S, Nakauma M, Funami T, Hori K, Ono T, Kohyama K, Nishinari K (2013) Compression test of food gels on artificial tongue and its comparison with human test. *J Texture Stud* 44:104–114
- Ishihara S, Isono M, Nakao S, Nakauma M, Funami T, Hori K, Ono T, Kohyama K, Nishinari K (2014) Instrumental uniaxial compression test of gellan gels of various mechanical properties using artificial tongue and its comparison with human oral strategy for the first size reduction. *J Texture Stud* 45:354–366
- Kamiya M, Ota K, Morishima K, Sawa S, Kondo I (2015) Examination of the effect of visual food perception on swallowing. *Jpn J Dysphagia Rehabil* 19:24–32 (in Japanese with English summary)
- Koç H, Vinyard CJ, Essick GK, Forgeding EA (2013) Food oral processing: conversion of food structure to textural perception. *Annu Rev Food Sci Technol* 4:237–266
- Kohyama K (2015) Oral sensing of food properties. *J Texture Stud* 46:138–151
- Kohyama K, Nishi M (1997) Direct measurement of biting pressures for crackers using a multiple-point sheet sensor. *J Texture Stud* 28(6):605–617
- Kohyama K, Nishi M, Suzuki T (1997) Measuring texture of crackers with a multiple-point sheet sensor. *J Food Sci* 62:922–925
- Kohyama K, Ohtsubo K, Toyoshima H, Shiozawa K (1998) Electromyographic study on cooked rice with different amylose contents. *J Texture Stud* 29:101–113
- Kohyama K, Sakai T, Azuma T, Mizuguchi T, Kimura I (2001) Pressure distribution measurement in biting surimi gels with molars using a multiplepoint sheet sensor. *Biosci Biotechnol Biochem* 65:2597–2603

- Kohyama K, Sasaki T, Dan H (2003) Active stress during compression testing of various foods measured by a multiple-point sheet sensor. *Biosci Biotechnol Biochem* 67:1492–1498
- Kohyama K, Hatakeyama E, Dan H, Sasaki T (2005a) Effects of sample thickness on bite force for raw carrots and fish gels. *J Texture Stud* 36:157–173
- Kohyama K, Nakayama Y, Watanabe H, Sasaki T (2005b) Electromyography of eating apples: influence of cooking, cutting, and peeling. *J Food Sci* 70:S257–S261
- Kohyama K, Yamaguchi M, Kobori C, Nakayama Y, Hayakawa F, Sasaki T (2005c) Mastication effort estimated by electromyography for cooked rice of differing water content. *Biosci Biotechnol Biochem* 69:1669–1676
- Kohyama K, Sawada H, Nonaka M, Kobori C, Hayakawa F, Sasaki T (2007) Textural evaluation of rice cake by chewing and swallowing measurements on human subjects. *Biosci Biotechnol Biochem* 71:358–365
- Kohyama K, Sasaki T, Hayakawa F (2008) Characterization of food physical properties by the mastication parameters measured by electromyography of the jaw-closing muscles and mandibular kinematics in young adults. *Biosci Biotechnol Biochem* 72:1690–1695
- Kohyama K, Hanyu T, Hayakawa F, Sasaki T (2010) Electromyographic measurement of eating behaviors for buckwheat noodles. *Biosci Biotechnol Biochem* 74:56–62
- Kumagai H, Tashiro A, Hasegawa A, Kohyama K, Kumagai H (2009) Relationship between flow properties of thickener solutions and their velocity through the pharynx measured by the ultrasonic pulse Doppler method. *Food Sci Technol Res* 15:203–210
- Lam P, Cichero J (2016) International food for the elderly conference—congratulations from the international dysphagia diet standardisation initiative. *J Texture Stud* 47:373–374
- Logemann JA (1998) Evaluation and treatment of swallowing disorders, 2nd edn. Pro-Ed, Austin, TX
- Luengo G, Tsuchiya M, Heuberger M, Israelachvili J (1997) Thin film rheology and tribology of chocolate. *J Food Sci* 62:767–772
- Luyten H, van Vliet T (1995) Fracture properties of starch gels and their rate dependency. *J Texture Stud* 26:281–298
- Malone ME, Appelqvist IAM, Norton IT (2003) Oral behavior of food hydrocolloids and emulsions. Part I. Lubrication and deposition considerations. *Food Hydrocoll* 17:763–773
- Meiselman HL (1972) Human taste perception. *CRC Crit Rev Food Technol* 3:89–119
- Meng Y, Rao MA, Datta AK (2005) Computer simulation of the pharyngeal bolus transport of Newtonian and non-Newtonian fluids. *T I Chem Eng Lond Part C* 83:297–305
- Mioche L (2004) Mastication and food texture perception: variation with age. *J Texture Stud* 35:145–158
- Mioche L, Peyron MA (1995) Bite force displayed during assessment of hardness in various texture contexts. *Arch Oral Biol* 40:415–423
- Morris ER (1993) Rheological and organoleptic properties of food hydrocolloids. In: Nishinari K, Doi E (eds) *Food hydrocolloids, structures, properties, and functions*. Plenum Press, New York, pp 201–210
- Morris VJ (2006) Bacterial polysaccharides. In: Stephen AM, Phillips GO, Williams PA (eds) *Food polysaccharides and their applications*, 2nd edn. CRC Press, Boca Raton, FL, pp 413–454
- Mosca AC, van de Velde F, Bult JHF, van Boekel MAJS, Stieger M (2010) Enhancement of sweetness intensity in gels by inhomogeneous distribution of sucrose. *Food Qual Prefer* 21:837–842
- Mosca AC, Bult JHF, Stieger M (2013) Effect of spatial distribution of tastants on taste intensity, taste intensity fluctuation and consumer preference of (semi-) solid food products. *Food Qual Prefer* 28:182–187
- Nakao S, Ishihara S, Nakauma M, Funami T (2013) Inhomogeneous spatial distribution of aroma compounds in food gels for enhancement of perceived aroma intensity and muscle activity during oral processing. *J Texture Stud* 44:289–300
- Nakauma M, Ishihara S, Funami T, Nishinari K (2011) Swallowing profiles of food polysaccharide solutions with different flow behaviors. *Food Hydrocoll* 25:1165–1173



- Nakauma M, Tanaka R, Ishihara S, Funami T, Nishinari K (2012) Elution of sodium caseinate from agar-based gel matrixes in simulated gastric fluids. *Food Hydrocoll* 27:427–437
- Nakauma M, Nakao S, Ishihara S, Funami T (2014) Elution profile of sodium caseinate in simulated gastric fluids using an in vitro stomach model from semi-solidified enteral nutrition. *Food Hydrocoll* 36:294–300
- Nakazawa F, Togashi M (2000) Evaluation of food texture by mastication and palatal pressure, jaw movement and electromyography. In: Nishinari K (ed) *Hydrocolloids part 2 fundamentals and applications in food, biology, and medicine*. Elsevier, Amsterdam, pp 473–483
- Nakazawa F, Ohno M, Morita A, Takahashi J (2000) Ultrasonic measurement of the velocity through the pharynx of swallowed rice boiled with differing water content. *J Home Econ Jpn* 51:1067–1071 (in Japanese)
- Nicosia MA, Robbins J (2001) The fluid mechanics of bolus ejection from the oral cavity. *J Biomech* 34:1537–1544
- Nishinari K (1996) New texture modifiers for foods, interactions among different food hydrocolloids and their potential of application. *Kagaku Seibutsu* 34:197–204 (in Japanese)
- Nishinari K (2006) Polysaccharide rheology and in-mouth perception. In: Stephen AM, Phillips GO, Williams PA (eds) *Food polysaccharides and their applications* 2nd ed. CRC Press, Boca Raton, FL, pp 541–588
- Nishinari K (2009) Texture and rheology in food and health. *Food Sci Technol Res* 15:99–106
- Nishinari K, Fang Y (2018) Perception and measurement of food texture: solid foods. *J Texture Stud* 49:160–201
- Nishinari K, Takemasa M, Su L, Michiwaki Y, Mizunuma H, Ogoshi H (2011) Effect of shear thinning on aspiration-toward making solutions for judging the risk of aspiration. *Food Hydrocoll* 25:1737–1743
- Nishinari K, Kohyama K, Kumagai H, Funami T, Bourne MC (2013) Parameters of texture profile analysis. *Food Sci Technol Res* 19:519–521
- Nishinari K, Turcanu M, Nakauma M, Fang Y (2019a) Role of the viscosity and cohesiveness in safe swallowing. *NPJ Sci Food* 3(1):5
- Nishinari K, Fang Y, Rosenthal A (2019b) Human oral processing and texture profile analysis parameters: bridging the gap between the sensory evaluation and the instrumental measurements. *J Texture Stud* 50:369–380
- Noort MWJ, Bult JHF, Stieger M, Hamer RJ (2010) Saltiness enhancement in bread by inhomogeneous spatial distribution of sodium chloride. *J Cereal Sci* 52:378–386
- Noort MWJ, Bult JHF, Stieger M (2012) Saltiness enhancement by taste contrast in bread prepared with encapsulated salt. *J Cereal Sci* 55:218–225
- Nouchi Y, Ajiki Y, Tobitsuka K, Sasaki T, Kohyama K (2012) Bite-speed effects in two-bite texture analysis. *Nippon Shokuhin Kagaku Kogaku Kaishi* 59:96–103 (in Japanese with English summary)
- Palmer JB, Rodin NJ, Lala G, Crompton AW (1992) Coordination of mastication and swallowing. *Dysphagia* 7:187–200
- Peleg M (2006) On fundamental issues in texture evaluation and texturization—a view. *Food Hydrocoll* 20:405–414
- Prinz JF, Lucas PW (1995) Swallow thresholds in human mastication. *Arch Oral Biol* 40:401–403
- Quinchia LA, Valencia C, Partal P, Franco JM, Brito-de Fuente E, Gallegos C (2011) Linear and non-linear viscoelasticity of puddings for nutritional management of dysphagia. *Food Hydrocoll* 25:586–593
- Repoux M, Laboure H, Courcoux P, Andriot I, Semmon E, Yven C, Feron G, Guichard E (2012) Combined effect of cheese characteristics and food oral processing on in vivo aroma release. *Flavour Frag J* 27:414–423
- Sakai M (2007) Chapter 4: mechanical properties of dysphagia diets. In: Egashira F, Kayashita J (eds) *Stepwise swallowing diets* recipe 125. Ishiyaku Publishers, Tokyo, pp 25–32 (in Japanese)
- Sako N (2005) Changes in physiological functions with aging. In: Nishinari K, Ogoshi H, Kohyama K, Yamamoto T (eds) *Handbook for food creation*. Science Forum, Tokyo, pp 111–118 (in Japanese)

- Shaker R, Cook IJ, Dodds WJ, Hogan WJ (1988) Pressure-flow dynamics of the oral phase of swallowing. *Dysphagia* 3:79–84
- Sherm RJ, Fox PC, Li SH (1993) Influence of age on the secretory rates of the human minor salivary glands and whole saliva. *Arch Oral Biol* 38:755–761
- Shin S, Fujita H, Ito T (2015) Comparison of the elderly and the young about the number of swallows during nighttime sleep and resting saliva or swallowing reflex while awake. *Jpn J Dysphagia Rehabil* 19:63–68 (in Japanese with English summary)
- Shiozawa K, Kohyama K, Yanagisawa K (1999a) Influence of ingested food texture on jaw muscle and tongue activity during mastication in humans. *Jpn J Oral Biol* 41:27–34
- Shiozawa K, Kohyama K, Yanagisawa K (1999b) Food bolus texture and tongue activity just before swallowing in human mastication. *Jpn J Oral Biol* 41:297–302
- Steele CM, Namasivayam-MacDonald AM, Guida BT, Cichero JA, Duivesteyn J, Hanson B et al (2018) Creation and initial validation of the international dysphagia diet standardisation initiative functional diet scale. *Arch Phys Med Rehabil* 99(5):934–944
- Stokes JR (2012) Oral rheology. In: Chen J, Engelen L (eds) *Food oral processing fundamentals of eating and sensory perception*. Blackwell Publishing, Chichester, pp 227–263
- Su M, Zheng G, Chen Y, Xie H, Han W, Yang Q et al (2018) Clinical applications of IDDSI framework for texture recommendation for dysphagia patients. *J Texture Stud* 49:2–10
- Szczesniak AS (2002) Texture is a sensory property. *Food Qual Prefer* 13:215–225
- Szczesniak AS, Bourne M (1998) Letter to the editor, issues pertaining to the texture profile analysis. *J Texture Stud* 29:vii–viii
- Szczesniak AS, Hall BJ (1975) Application of the general foods texturometer to specific food products. *J Texture Stud* 6:117–138
- Szczesniak AS, Kleyn DH (1963) Consumer awareness of texture and other food attributes. *Food Technol* 17:74–77
- Takahashi J, Nakazawa F (1991) Palatal pressure patterns of gelatin gels in the mouth. *J Texture Stud* 22:1–11
- Takahashi J, Nakazawa F (1992) Effects of dimensions of agar and gelatin gels on palatal pressure patterns. *J Texture Stud* 23:139–152
- Taniguchi H, Tsukada T, Ootaki S, Yamada Y, Inoue M (2008) Correspondence between food consistency and suprahyoid muscle activity, tongue pressure, and bolus transit times during the oropharyngeal phase of swallowing. *J Appl Physiol* 105:791–799
- Tanishima Y, Fujita T, Suzuki Y, Kawasaki N, Nakayoshi T, Tsuboi K, Omura N (2009) Effects of half-solid nutrients on gastroesophageal reflux in beagle dogs with or without cardioplasty and intrathoracic cardiopexy. *J Surg Res* 161:272–277
- Torres O, Yamada A, Rigby NM, Hanawa T, Kawano Y, Sarkar A (2019) Gellan gum: a new member in the dysphagia thickener family. *Biotribology* 17:8–18
- Wang Z, Yang K, Brenner T, Kikuzaki H, Nishinari K (2014) The influence of agar gel texture on sucrose release. *Food Hydrocoll* 36:196–203
- Weel KGC, Boelrijk AEM, Alting AC, van Mil PJJM, Burger JJ, Gruppen H et al (2002) Flavor release and perception of flavored whey protein gels: perception is determined by texture rather than by release. *J Agric Food Chem* 50:5149–5155
- Wilkinson C, Dijksterhuis GB, Minekus M (2000) From food structure to texture. *Trends Food Sci Technol* 11(12):442–450
- Wood FW (1968) Psychophysical studies on the consistency of liquid foods. In *rheology and texture of food stuffs*. S.C.I. monograph 27. Science Research, London, pp 40–49
- Yokote Y, Takata N, Yamagata Y, Kayashita J (2017) A comparison of viscosity classifications between the Japanese dysphagia diet 2013 criteria and the international dysphagia diet standardisation initiative. *EC Nutr* 10:185–194
- Yokoyama S, Hori K, Tamine K, Fujiwara S, Inoue M, Maeda Y et al (2014) Tongue pressure modulation for initial gel consistency in a different oral strategy. *PLoS One* 9:e91920
- Youmans SR, Stierwalt JA (2006) Measures of tongue function related to normal swallowing. *Dysphagia* 21:102–111

# Chapter 14

## Bioactivities



Kang Liu, Xue-Ying Li, Jian-Ping Luo, and Xue-Qiang Zha

**Abstract** Polysaccharides and proteins are representative natural biomacromolecules existing in animals, plants, and microorganisms. They are attracting a great attention of scholars worldwide due to their various healthy functions, such as immunomodulation, anti-tumor, anti-oxidative, hypoglycemic, and hypolipidemic activities. Besides the strong bioactivity, these natural polysaccharides and proteins are non-toxic and show no side effects. In recent decades, a large number of bioactive polysaccharides and proteins with different structure and bioactivity from natural resources have been extracted, purified, and characterized. The aim of this chapter is to summarize the bioactivities, active mechanisms, structure features, structure–activity relationships of natural polysaccharides, proteins, and their derivatives. Moreover, this chapter also presented the applications of some active natural biopolymers in foods and medicines.

**Keywords** Polysaccharide · Protein · Bioactivity · Structure–activity relationship

### 1 Introduction

The food hydrocolloid is an edible soft matter system, which determines the texture and flavor characteristics of food products (Van der Sman and Van der Goot 2009). In food processing, various food materials such as polysaccharides, proteins, lipids, emulsifiers, sugars, minerals, and water are often mixed and fabricated. Among these ingredients, polysaccharides and proteins are the most used materials, which not only acting as “building blocks” for designing food hydrocolloids, but also providing interface-stabilizing properties via the interaction with other molecules (Wijaya et al. 2017).

---

K. Liu · X.-Y. Li · J.-P. Luo · X.-Q. Zha (✉)  
School of Food and Biological Engineering, Hefei University of Technology, Hefei, China  
e-mail: zhaxueqiang@hfut.edu.cn

Polysaccharide is defined as carbohydrate polymers consisting of different monosaccharide linked by glycosidic bonds (Xie et al. 2016). Protein is a macromolecular compound, which is formed by the binding of peptide chains composed of amino acids. In recent decades, many natural polysaccharides and proteins have been extracted and purified from plants, animals, and microorganisms. In addition to the properties of food hydrocolloids, these natural macromolecules also possess many bioactivities, such as anti-tumor, immunomodulation, anti-oxidative, hypoglycemic, and hypolipidemic (Cho et al. 2015). Therefore, this chapter mainly introduces the bioactivities of natural hydrocolloids, including anti-tumor, immunomodulation, anti-oxidation, antimicrobial, hypoglycemic, and hypolipidemic effects. Moreover, the applications of these natural biomacromolecules in functional foods and medicines are presented in this chapter.

## 2 Bioactivities

In recent years, natural polysaccharides and proteins extracted from different materials have attracted increasing attention because of their wide bioactivities, such as anti-oxidation, immunomodulation, anti-tumor, antimicrobial, hypoglycemic, and hypolipidemic effects. Moreover, more and more evidence indicated that most of these bioactivities of polysaccharides and proteins are related to the immune system.

### 2.1 *Anti-Tumor*

Cancer is a group of diseases involving abnormal cell growth with the potential to invade or spread to other parts of the body. According to the report released by the World Health Organization (WHO) 2018, cancer is one of the main causes of human death worldwide. Although there are many different types of antineoplastic drugs in clinic, these drugs not only have limited efficacy, but also have strong side effects. Since *Lentinan* was first recognized to have anti-tumor efficacy (Chihara et al. 1969), more and more studies on natural polysaccharides used in cancer treatment have been carried out in vitro and in vivo.

Up to date, a series of human carcinoma cell lines have been employed to investigate the anticancer activity of polysaccharides, such as the lung cancer cell line (A549 cell), the cervical carcinoma cell line (Hela cell), the gastric carcinoma cell line (BGC-823 cell), the breast carcinoma cell line (MCF-7 cell), the colon cancer cell line (HCT116 cell and HT29 cell), and the liver cancer cell line (HepG2 cell). In addition, some mouse-derived cancer cell lines were also used to evaluate the activity of polysaccharides. It has been suggested that the anti-tumor mechanisms of polysaccharides were possibly attributed to their inhibition of tumor cell proliferation, initiation of tumor cell apoptosis, and activation of immune system to kill tumor cells (Zong et al. 2012).

It has been reported that polysaccharides from *Dendrobium* (Yu et al. 2018), *Astragalus* (Zhai et al. 2018), *Lentinus edodes* (Ya 2017), *Ganoderma lucidum* (Mohan et al. 2017), and *Portulaca Oleracea L.* (Zhao et al. 2016) exhibited good inhibitory effects on HeLa cells proliferation. These anti-proliferation effects might be related to the increase in autophagic activity of HeLa cells via regulating the expression of some key proteins in mitochondria-mediated signaling pathway, such as beclin1, LC3, and p62 (Zhai et al. 2018). Polysaccharides extracted from *Houttuynia cordata* (Han et al. 2018), *Tremella* (Shi et al. 2018), *Sargassum integerrimum* (Liu et al. 2016), *Pleurotus nebrodensis* (Cui et al. 2016), *Auricularia polytricha* (Yu et al. 2014) exhibited strong activity to resist the proliferation of human A549 cells. Lin et al. (2018) reported that *Hedyotis diffusa* polysaccharides could induce the apoptosis of A549 cells via regulating caspase-3-dependent mitochondrial pathway. Wu et al. (2017) found that polysaccharide from *Glehnia littoralis* could inhibit A549 cell proliferation and migration via decreasing the expression of PCNA, leading to cell cycle arrested in S and G2/M phase. Luo et al. (2016) also found that *coix* polysaccharides had the function to inhibit the migration and invasion of A549 cells via down-regulating the expression of S100A4. S100A4, a member of the S100 family, is a sort of calcium binding protein with EF double helix domain. The S100A4 expresses in kinds of tumor and stem cells of human rather than normal somatocytes.

HepG2 is an immortalized cell line consisting of human liver carcinoma cells. It has been reported that polysaccharides extracted from *Phormidium versicolor* (Belhaj et al. 2018), *Ganoderma lucidum* (Yang et al. 2017), *Lentinus edodes* (Zhao et al. 2017), *Antrodia camphorata* (Li et al. 2009a, b), *Grifola frondosa* (Wang et al. 2013) showed strong ability to prevent the proliferation of HepG2 cells. Li et al. (2013a) reported that polysaccharide from *Phellinus linteus* could induce S-phase arrest in HepG2 cells via decreasing calreticulin expression and activating the P27kip1-cyclin A/D1/E-CDK2 pathway. Shen et al. (2014) found that polysaccharide from *Ganoderma lucidum mycelia* could induce HepG2 cells apoptosis via regulating the expression of miRNAs. Some algae polysaccharides have been proved to possess broad-spectrum antineoplastic effects. For instance, polysaccharides from *Sargassum plagiophyllum* and *Sargassum pallidum* showed strong inhibitory effects on the proliferation of HepG2 cells, A549 cells, and MGC-803 cells in vitro (Ye et al. 2008; Suresh et al. 2013).

$\beta$ -glucans, a type of the most abundant polysaccharides in the cell wall of bacteria and fungus, are glucose polymers linked by 1 $\rightarrow$ 3 linear  $\beta$ -glycosidic bond (Chan et al. 2009). Over the last half-century, fungi-derived  $\beta$ -glucans have received great attention because of the potential medical and edible value all over the world. Lentinan is a representative  $\beta$ -glucan. It has been widely proved to have therapeutic effect on many kinds of tumors. In clinical trials, compared to chemotherapy alone, the addition of lentinan to standard chemotherapy could relieve the pain and prolong survival in patients with gastric cancer (Oba et al. 2009), pancreatic cancer (Shimizu et al. 1999), colorectal cancer (Hazama et al. 2009), liver cancer (Ina et al. 2016), breast Cancer (Taguchi 1983). A large number of cell and animal experiments have also proved these anti-tumor effects. For instance, lentinan has ability to inhibit

proliferation and differentiation of cancer cells, such as human autologous tumor cell line (K562 cell) (Tani et al. 1993), human gastric cancer cell line (BGC823 cell) (Zhao et al. 2013), human pancreatic cancer cell line (BXPC-3 cell) (Qian et al. 2018), human cervical cancer cell line (Hela cell) (Qian et al. 2018), human breast cancer cell line (MCF-7 cell) (Yi et al. 2018), non-small cell lung cancer (Wang et al. 2020), human bladder cancer cell line (T24) (Bao et al. 2015), liver cancer cell line (H22 cell) (Yamamoto et al. 1989). Animal experiments demonstrated that lentinan could inhibit colitis-associated cancer (CAC) development via regulating TLR4/NF-kappaB signaling-mediated inflammatory responses in model mice (Liu et al. 2018).

$\beta$ -glucans have also been reported to kill cancer cells directly. The anticancer mechanisms of these polysaccharides are mainly dependent on the ability of enhancement of host immune system, increase in the antioxidant capacity of host, up-regulation of phase I and phase II enzymes in metabolic transformation, and the detoxification of mutagenic compounds (Vannucci et al. 2013). Masuda et al. (2013) reported that both oral administration and intraperitoneal injection of  $\beta$ -glucans from *Grifola frondosa* could inhibit tumor growth via regulating the systemic immune response. Moreover, the possible mechanism was revealed that the *Grifola frondosa*  $\beta$ -glucans can induce systemic tumor-antigen specific T cell response via dectin-1-dependent activation of DCs, enhance the infiltration of the activated T cells into the tumor, and decrease number of tumor-caused immunosuppressive cells such as myeloid-derived suppressor cells and regulatory T cells, thus leading to the anti-tumor activity. Yeast  $\beta$ -glucans, extracted from by-product yeast of beer production, have been known to exhibit anti-tumor activities by potentiating host immunity (Suphantharika et al. 2003).

In recent years, a large number of anticancer peptides have been identified from plant-derived proteins. For instance, corn peptides can induce the apoptosis of HepG2 cells by increasing caspase-3 expression (Díaz-Gómez et al. 2018). The lunasin peptide from soybean has the ability to resist skin cancer (Hernandez-Ledesma et al. 2009). The potato protein was found to suppress the proliferation of mouse melanoma B16 cells (Sun et al. 2013). Kannan et al. have extracted a pentapeptide (Glu-Gly-Arg-Pro-Arg) from rice bran and proved that it had the ability against the proliferation of colon cancer cells (Kannan et al. 2010). It has been reported that peptides derived from fish proteins have the inhibitory effect on MCF-7 cells in a dose-dependent manner (Hsu et al. 2011). Nongonierma and FitzGerald (2016) also found that milk protein-derived peptides exhibited anti-proliferative activity to tumor cells.

## 2.2 Immunoregulation

The immune system is a complex network of cells, tissues, and organs that work together to protect the body from harmful substances and organisms and defend against disease. However, when the immune system is disorder, autoimmune

**Table 14.1** Immunomodulatory effects of some polysaccharides on macrophages

Source	Mice type	Cell type	Effects on immune cells	References
<i>Ganoderma atrum</i>	–	RAW264.7	Phagocytosis ↑, NO ↑, TNF-α↑, IL-1β ↑	Yu et al. (2013)
<i>Dendrobium officinale</i>	–	RAW264.7	Phagocytosis ↑, NO ↑	Xia et al. (2012)
<i>Astragalus membranaceus</i>	H22 tumor-bearing mice	H22	IL-2↑, IL-12↑ TNF-α ↑, IL-10↓	Yang et al. (2013)
<i>Mushroom sclerotia</i>	Male BALB/c mice and athymic BALB/c nude mice	–	IL-13↑, IL-17↑, IFN-γ↑	Wong et al. (2011)
<i>Grifola frondosa</i>	–	HepG-2	NO ↑, TNF-α↑, IL-1β ↑	Mao et al. (2015)
<i>Inonotus obliquus</i>	–	SGC-7901	TNF-α↑,	Fan et al. (2012a, b)
<i>Porphyra haitanensis</i>	A BALB/c murine	RAW264.7 DC Tregs	Phagocytosis ↑, TNF-α ↑, NO↑, IL-10↑, IL-6↑	Liu et al. (2017a, b)
<i>Dictyophora indusiata</i>	–	RAW 264.7	TNF-α↑, NO↑,(IL)-6↑	Liao et al. (2015)
<i>Ganoderma lucidum</i>	–	CD	–	Lai et al. (2010)
<i>Prunella vulgaris</i>	–	RAW 264.7	NO↑, TNF-α↑, (IL)-6↑	Li et al. (2015)
<i>Longan pulp</i>	–	Splenic cells	Proliferation↑	Yi et al. (2012)
<i>Cordyceps sinensis</i>	–	RAW 264.7	TNF-α↑, (IL)-6↑, IL-10↑, IL-1α↑	Wu et al. (2014)
<i>Panax Ginseng</i>	–	DC	Proliferation↑, IL-12 ↑, TNF-α↑	Kim et al. (2010)
<i>Laminaria japonica</i>	–	RAW264.7	NO↑, TNF-α↑, IL-1β↑, IL-6↑, IL-10 ↑	Fang et al. (2015)

diseases, inflammatory diseases, and cancer will happen in the body. Many natural polysaccharides have exhibited the ability to affect the immune system via modulating the immune functions including ROS production, cytokine/chemokine production, cell proliferation, and so on (Table 14.1). Therefore, polysaccharide is considered as a potential immunomodulator with great development prospects (Schepetkin and Quinn 2006). Figure 14.1 shows the possible signaling pathways involved in macrophage activation by polysaccharides (Schepetkin and Quinn 2006). It is known that the anti-tumor activity of polysaccharide is partly related to the enhancement of immune system.

The host defense mechanism consists of innate immunity and adaptive immunity, where the innate immunity is the first line of defense mediated the initial protection against infections. It is known that the innate immune system mainly contains macrophages, monocytes, granulocytes, and humoral elements. Among these

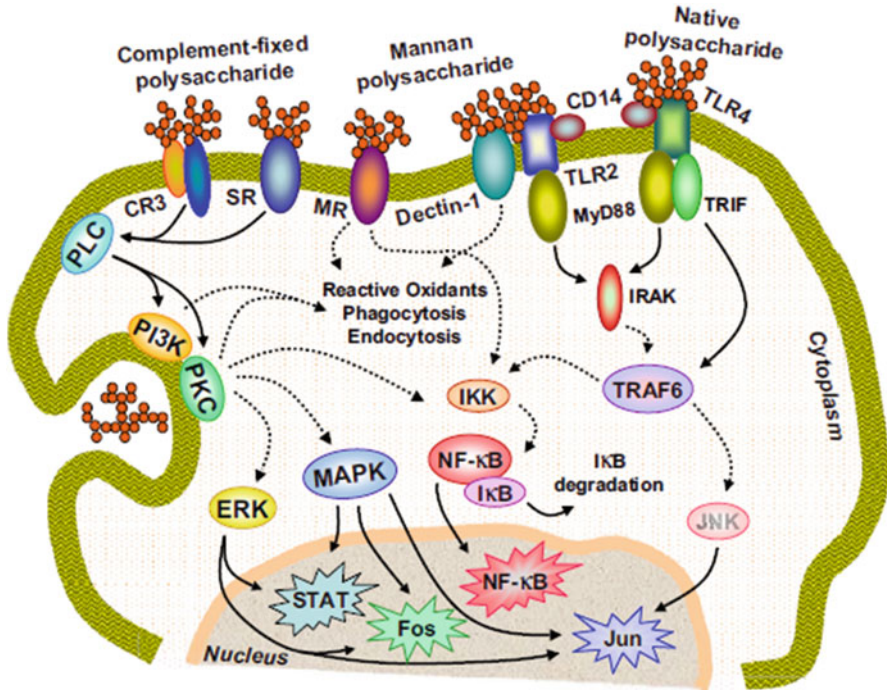


**Fig. 14.1** Schematic model of potential signaling pathways involved in macrophage activation by polysaccharides. Reproduction with permission from (Schepetkin and Quinn 2006), Copyright 2006 Elsevier

components, macrophages are reported to exhibit various biological functions, such as chemotaxis, surveillance, phagocytosis, and destruction of targeted organisms, indicating the macrophages activation might be a hopeful strategy to resist diseases (José et al. 2007). It has been reported that *Juniperus scopolorum* polysaccharides could increase macrophage cytotoxic activity against tumor cells and microorganisms, activate phagocytic activity, and enhance the secretion of cytokines and chemokines, such as tumor necrosis factor (TNF- $\alpha$ ), interleukin (IL)-1, IL-6, IL-8, IL-12, interferon gamma (IFN- $\gamma$ ), and IFN-2 (Chen et al. 2010a, b; Schepetkin et al. 2005). Polysaccharide from *Lycium barbarum* could activate macrophages via regulating the transcription factors AP-1 and NF- $\kappa$ B to induce TNF- $\alpha$  production and up-regulating the expression of MHC class II costimulatory molecules, resulting in the enhancement of innate immunity (Chen et al. 2008). Those phenomena indicated that macrophage activation is required for the activation of innate immune system (Plüddemann et al. 2011). For these events, the pattern recognition receptors (PRRs) are required for these cells to recognize stimulators, triggering the activation of signaling pathways and the synthesis of pro-inflammatory cytokines (Kumar et al. 2011). Toll-like receptors (TLRs), the important PRRs, are existed on plasma membrane (Kawai and Akira 2010). It has been reported that macrophage activation



induced by polysaccharides involves TLRs mediated recognition (Li et al. 2011). Figueiredo et al. (2012) have evidenced that TLR2 and TLR4 were the receptors involved in the recognition of *fungus* polysaccharides. Ferwerda et al. (2008) reported that the *saccharomyces cerevisiae* cell wall polysaccharide (Zymosan) has function to induce macrophages to release cytokines by the recognition of TLR2, TLR4, and Dectin-1. Nuclear factor  $\kappa$ B (NF- $\kappa$ B) and mitogen-activated protein kinases (MAPK) are the key proteins in the downstream signaling pathway of TLR, which play important role in the host defenses via regulating the expression of multiple inflammatory and immune genes (DiDonato et al. 2012). With respect to MAPKs, mammalian cells expressed three representative MAPK pathways, containing C-Jun-N-terminal kinase (JNK), extracellular signal regulated kinase (ERK1/2), and p38. In recent years, the immunostimulatory activity mechanisms of polysaccharides have been widely studied. Results suggested that the regulation of intracellular signaling pathways is essential for the activation of macrophages (Diao et al. 2014; Zhang et al. 2014; Maeda et al. 2012). Extracellular polysaccharide LBP32 from *Bacillus sp.* strain was reported to inhibit LPS-induced production of pro-inflammatory cytokines via attenuating the phosphorylation of P38 and JNK, but not ERK1/2 (Diao et al. 2014). *Lycium barbarum* polysaccharide (LBPF4-OL) was found to have the ability to promote the secretion of TNF- $\alpha$  and IL-1 $\beta$  via inhibiting JNK and ERK1/2 MAPK phosphorylation and increasing the phosphorylation of p38-MAPK (Zhang et al. 2014). The sulfated polysaccharide SP1 from *Caulerpa lentillifera* had the function to activate macrophages and enhance NO production via regulating NF- $\kappa$ B and P38 MAPK signaling pathways (Maeda et al. 2012). These results demonstrated that various polysaccharides can exert their biological activities through regulating different signaling pathways. The inflammatory response has been reported to be highly dependent on MAPK signaling pathways via activating its downstream cytosolic proteins and nuclear transcriptional factors (Arthur and Ley 2013). NF- $\kappa$ B is a ubiquitous transcription factor, which plays a critical role in the host defenses via regulating the expression of multiple inflammatory and immune genes (DiDonato et al. 2012). In unstimulated cells, NF- $\kappa$ B locates in cytoplasm and combines with inhibitory proteins to form an inactive trimer (p50-p65-I $\kappa$ B). When cells are stimulated, I $\kappa$ Bs will be phosphorylated by I $\kappa$ B kinase, leading to I $\kappa$ B degradation and translocation of NF- $\kappa$ B to the nucleus for binding to its cognate DNA in the regulation region of a variety of genes (He et al. 2013). It has been reported that the ability of some polysaccharides to activate macrophages is dependent on their level to the activation of NF- $\kappa$ B pathway (Zhang et al. 2011; Yu et al. 2013).

Lymphocyte is considered as a mediator of innate and adaptive immunity. Shriner et al. (2010) reported that *pneumococcal polysaccharide* could stimulate the proliferation of IL-7-driven B lymphocytes, regulate their cytokine production, and restore impaired T cell by immune response. Among the specialized cell subsets of the innate immune system, DCs are the critical sensors via expressing various pattern recognition receptors (Steinman and Banchereau 2007). In particular, TLRs and cytosolic sensors for DNA and RNA recognition expressed by DCs use endogenous host elements carrying microbial components (such as the alarmin HMGB1),

pathogen associated molecular patterns, and/or nucleic acids to stimulate intrinsic apoptotic pathways to generate protective immune responses (Peng et al. 2005; Poeck et al. 2008; Besch et al. 2009). During this process, polysaccharide was found to regulate the immunity via inducing DC maturation. For example, *Astragalus* polysaccharides could induce the differentiation of DCs to CD11c<sup>high</sup>CD45RB<sup>low</sup> DCs by shifting of Th2 to Th1, resulting in the enhancement of T lymphocyte immune function in vitro (Liu et al. 2011a). *Achyranthes bidentata* polysaccharide was reported to enhance DC maturation and function, supplying extra IL-12 and MHC class II molecules to up-regulating antigen presentation, activating CD4+ T cell, and thus leading to an enhancement of DC-CD4+ T cell (Zou et al. 2011). Meng et al. (2011) reported that polysaccharides from *Ganoderma lucidum* could promote effective activation of murine DCs in the immune response via up-regulating the expression of CD86, CD40, and MHC II and down-regulation of acid phosphatases.

In the past decades, the structure–activity relationships of immunomodulatory polysaccharides have been studied, indicating the interaction of immunostimulatory polysaccharides with cell receptors may trigger signaling pathways and thereby result in the induction of gene transcription (Ferreira et al. 2015a, b). A *Houttuynia cordata* pectic polysaccharide (HCP-2) with a linear chain of 1,4-linked  $\alpha$ -D-galacturonic acid residues has been reported to increase the secretion of MIP-1 $\alpha$ , MIP-1 $\beta$ , TNF- $\alpha$ , IL-1 $\beta$ , and RANTES in human peripheral blood mononuclear cells via regulating TLR-4 mediated signaling (Cheng et al. 2014). Bose et al. (2014) reported that 1,3-linked  $\beta$ -D-glucans could activate innate immune functions via regulating Dectin-1 and CR3 mediated signaling pathways. SR has been shown to be the pattern recognition receptor of fucoïdan. Guo et al. (2009) found that a 1,3-linked glucan from spores could be recognized by dectin-1 on macrophages and thereby possess the biological activities. These results suggested that what is polysaccharide's pattern recognition receptor might be determined by the structure of polysaccharide. Lo et al. (2007) suggested that galactose, mannose, xylose, and arabinose played an important role in the stimulation of macrophages, but not glucose. The residues of 1,4-lined  $\beta$ -D-Rhap and 1,5-lined  $\alpha$ -L-Araf were reported to be important for lymphocytes activation (Yang et al. 2012). The 1,4-linked mannose and glucose was reported to be the important elements for macrophages activation by a purified *Laminaria japonica* polysaccharide LJP-31 (Fang et al. 2015).

In recent years, some immunomodulatory peptides have been prepared from food proteins (Agyei and Danquah 2012). Otani et al. (2003) reported that phosphopeptides from casein could stimulate gastrointestinal tracts of mice to release immunoglobulin A. Pan et al. (2013a) revealed that peptide from milk protein exhibits immunomodulatory property in ICR mice. After modification with dicarbonyl methylglyoxyl, ovalbumin has the ability to stimulate immune cells to release tumor necrosis factor (TNF) alpha (Fan et al. 2003). The immunogenic ovalbumin peptides have been employed to enhance the immune response of different cancer patients (Vidovic et al. 2002; Goldberg et al. 2003). Some fish protein-derived immune peptides have also been identified in recent years (Yang

et al. 2009; Hou et al. 2016). Sheu et al. (2004) have separated an immunomodulatory protein from the Jew's Ear mushroom *Auricularia polytricha*. Some peptides extracted from macroalgae were also reported to exhibit immunomodulatory activity via regulating the nuclear factor kappa B (NF- $\kappa$ B) pathway (Ahn et al. 2011).

### 2.3 Anti-Oxidation

Oxidative damage of biomolecules triggers not only physiological process of aging, but also causes various physiological functional disorders, leading to serious health problem ultimately (Harman 1993). In theory, antioxidants might have a positive effect on our health because they have ability to clear free radicals from human body. As is well known, free radicals can attack macromolecules such as proteins, membrane lipids, and DNA, leading to many health problems (i.e., cancer, neurodegenerative diseases, and diabetes mellitus) via damaging cells and tissues (Lim et al. 2014). Reactive nitrogen species (RNS) and reactive oxygen species (ROS) are free radicals that are formed during the normal metabolism of cells, which can be removed by cellular anti-oxidative defense systems, such as glutathione peroxidase (GSH-Px) and superoxide dismutase (SOD). Under normal physiological conditions, the generation and elimination of RNS and ROS are balanced. Once this balance is broken, either by the overproduction of ROS and RNS, or by the damage in anti-oxidative system, oxidative stress will occur (Klaus et al. 2011; Sun et al. 2010). In food industries, some synthetic commercial antioxidants such as tertbutylhydroquinone (TBHQ), butylated hydroxytoluene (BHT), butylated hydroxyanisole (BHA), and propyl gallate (PG) have been extensively used to reduce the oxidation and peroxidation damage. However, these antioxidants have potential hazards to human health (Nagaoka et al. 2010). Therefore, screening antioxidants from natural resources is always a hot topic (Peña-Ramos and Xiong 2002). Natural polysaccharides have attracted extensive attention and are proposed to be the potential resource of novel antioxidants due to their low toxicity and excellent anti-oxidation. Algal polysaccharides have been demonstrated as a scavenger of free radicals for the prevention of oxidative damage in vivo (Cristina Diaz et al. 2017).

In general, the polysaccharide eliminates free radicals through four aspect, including: (1) Hydrogen atoms on the structure of polysaccharides react with free radicals to form water, and the single electrons generated by the reaction can be further reduced. (2) Polysaccharides capture free radicals produced in lipid reactions or chelate with metal ions, which are important factors for the formation of free radicals. (3) Polysaccharides enhance the activity of some antioxidant enzymes. (4) Polysaccharides indirectly achieve antioxidant effect by regulating immunity. As shown in Table 14.2,  $\beta$ -glucan extracted from mushrooms and yeast have been reported to be the potential antioxidants. Three polysaccharides isolated from *Ganoderma lucidum* (GLP-H, GLP-V, and GLP-F) were found to possess the stronger radical scavenging activities (Fan et al. 2012a, b). *Astragalus*

**Table 14.2** Antioxidants activity of  $\beta$ -glucan

Source	Antioxidant activity	References
<i>Jinqian mushroom</i>	ABT radical scavenging activity was 63.96% at 5 mg/mL DPPH scavenging ratio was 89.84% at 5 mg/mL Iron chelating effect was 14.06% at 5 mg/mL Hydroxyl radical scavenging activity was 24.30% at 5 mg/mL	Liu et al. (2014a, b)
<i>Polyporus dermatopus</i>	Hydroxyl radicals inhibition was 96% at 267 $\mu$ g/mL Lipid peroxidation inhibition was 42.9% at 67 $\mu$ g/mL Superoxide inhibition was 83.3% at 67 $\mu$ g/mL	Dore et al. (2014)
<i>Saccharomyces cerevisiae</i>	Decreasing the formation of RBARS in LPS stimulated human blood platelets Decreasing the formation of O <sub>2</sub> in LPS stimulated human blood platelets	Saluk et al. (2013)
<i>Geastrum saccatum mushroom</i>	Inhibition of the formation of hydroxyl radicals in a dose-dependent manner	Guerra Dore et al. (2007)
<i>Pleurotus ostreatus</i>	The antioxidant enzymes activity, ferric reducing activity, and ascorbate concentration in human red blood cells hemolysates were markedly increased	Pietrzycka et al. (2006)
<i>Lentinus edodes</i>	Inhibition of lipid peroxidation, as well as a strong hydroxyl radical scavenging activity and superoxide radical scavenging activity	Feng et al. (2010)
<i>Yeast</i>	The level of glutathione was replenished and myeloperoxidase activity was suppressed in a rat model of sepsis	Sener et al. (2005)

Reproduction with permission from (Nie et al. 2018), Copyright 2018 Elsevier

polysaccharides were reported to inhibit the generation of ROS via suppressing the NF- $\kappa$ B signal pathway (Xue et al. 2015). When the mice were orally administrated with extracellular polysaccharides of *Morchella esculenta*, the activity of SOD and GSH-Px were elevated in the blood, heart, liver, spleen, and kidney of mice (Meng 2010).

It has been reported that some compounds such as proteins, peptides, pigments, polyphenols, and flavones could bind to polysaccharides. Compared to the polysaccharides, these complexes have stronger antioxidant activity. For instance, the antioxidant effects of tea polysaccharides (TPS)-protein conjugates are dose-dependent on the protein content (Nie et al. 2008). In addition, the in vivo and in vitro antioxidant activities of crude tea polysaccharides were found to be better than that of tea polysaccharide fraction, which can be interpreted by the relatively higher proportion of tea pigments, vitamins, tea polyphenols, and other antioxidant components in the cruder fractions (Zhou et al. 2007). Moreover, Zhang et al. (2016a, b, c) suggested that the antioxidant activity of polysaccharides from *Ganoderma atrum* (PSG) was depended on the content of phenolic compounds/proteins.

It is a fact that the antioxidant activity of polysaccharides is closely correlated with their structural parameters, such as solubility, degree of substitution, degree of

branching, molecular weight, monosaccharide composition, solution conformation, and functional groups. Jing et al. (2009) reported that phosphorylated modification could enhance the ability of fucoidan to scavenge hydroxyl and superoxide radicals. The possible mechanism might be that the phosphate is a polyelectrolyte group and could activate the hydrogen atom of the anomeric carbon.

The acetylated modification was reported to enhance the ability of mushroom *Inonotus obliquus* polysaccharides to inhibit lipid peroxidation via affecting the conformation of polysaccharides (Ma et al. 2012). The carboxymethylated modification can increase the water solubility and antioxidant activity of  $\beta$ -(1,3)-glucan from the sclerotium of *Poria coco* via changing the flexibility of polysaccharides chain (Wang and Zhang 2006). Molecular weight was an important factor that can influence the antioxidant ability of polysaccharides. Yan et al. (2009) used an acidic solution to hydrolyze the exopolysaccharide from *Cordyceps sinensis*, giving a degraded exopolysaccharide. Results showed that the degraded products had much higher antioxidant activity than that of original polysaccharide.

## 2.4 Antimicrobial

$\beta$ -glucans are ubiquitously found in both bacterial and fungal cell walls and have been implicated in the initiation of antimicrobial immune response. It has been proved that the (1 $\rightarrow$ 3)- $\beta$ -D glucan with (1 $\rightarrow$ 6)- $\beta$ -D branches could act as antimicrobial agent in vivo (Ferreira et al. 2015a, b). Hetland et al. (2000) obtained a soluble branched  $\beta$ -(1,3)-glucan (SSG) from the culture broth of the fungus *Sclerotinia sclerotiorum* IFO9395. Results exhibited that the oral administration of SSG could help the mice to resist the infection of *Streptococcus pneumoniae* sero type 4 and 6B. Faccin et al. (2007) reported that  $\beta$ -glucan from the fruiting body of *Agaricus brasiliensis* mushrooms exhibited an antiviral activity against poliovirus typ1 in HEp-2 cells. Peter et al. found that oral administration of  $\beta$ -glucan (glucan phosphate, scleroglucan, and laminarin) at a dose of 1 mg/kg/day could enhance the survival of mice infected with *S. aureus* or *Candida albicans*. In Sharma's study (Sharma et al. 2015), it was found that both extracellular polysaccharide (EPS) and intracellular polysaccharides (IPS) extracted from *Cordyceps* species exhibited obvious antimicrobial activities against all pathogenic microorganism tested. Moreover, IPS showed stronger antimicrobial activity than that of EPS. The polysaccharides extracted from *Ganoderma* species have also been proved to exhibit spectral antimicrobial activity (Table 14.3). It has been found that the acidic polysaccharide CS-F2 from green tea had a selective anti-adhesive activity against some pathogenic bacteria and strongly inhibited the growth of gastric and skin pathogenic bacteria.

More and more evidences exhibited that some proteins and their derived peptides from plants, mammals, insects, and bacteria also have antimicrobial activity against eukaryotes, fungi, bacteria, and viruses (Zhu et al. 2019). The first antimicrobial peptide was found from the moth *Hyalophora cecropia* in 1981 (Steiner et al. 1981). A lectin-like peptide from red lentil seeds exhibited antimicrobial activity against

**Table 14.3** The antimicrobial activity of polysaccharides

Specie	Microorganisms used	Type of assay	References
<i>Ganoderma lucidum</i>	<i>Bacillus subtilis</i> , <i>Bacillus cereus</i> , <i>Erwinia carotovora</i> , <i>Escherichia coli</i> , <i>Penicillium digitatum</i> , <i>Botrytis cinerea</i>	In vitro	Bai et al. (2008)
<i>Ganoderma applanatum</i>	<i>Acrobacter aerogenes</i> , <i>Acitenobacter aerogenes</i> , <i>Arthrobacter citreus</i> , <i>Bacillus brevis</i> , <i>B. subtilis</i> , <i>Corynebacterium insidiosum</i> , <i>Clostridium pasteurianum</i> , <i>Escherichia coli</i> , <i>Micrococcus roseus</i> , <i>Mycobacterium phlei</i> , <i>Proteus vulgaris</i> , <i>Sarcina lutea</i> St	In vitro	Bhattacharyya et al. (2006)
<i>Ganoderma formosanum</i>	<i>Listeria monocytogenes</i>	In vivo	Wang et al. (2011)
Glucans	<i>Staphylococcus aureus</i> or <i>Candida albicans</i>	In vitro	Rice et al. (2005)
<i>Schizophyllum</i>	<i>Salmonella enterica serovar</i>	In vivo	Chen et al. (2008)
Oat	Herpes simplex virus 1	In vivo	Murphy et al. (2009)

*Mycosphaerella arachidicola* (Wang and Ng 2007). The defensin PDC1 peptide, a fermentation product of corn using *Pichia pastoris* and *Escherichia coli* as the mixed strain, has an ability to inhibit the growth of *Fusarium graminearum* (Kant et al. 2009). Using *Bacillus subtilis* sck-2 to ferment soybean paste, a peptide was obtained and exhibited antibacterial activity against *Bacillus cereus* (Yeo et al. 2012). These antimicrobial peptides can be considered as the good candidates for food antiseptics.

## 2.5 Hypoglycemic

Diabetes mellitus (DM) is a group of metabolic disorders characterized by high blood sugar levels over a prolonged period. Symptoms of high blood sugar mainly include frequent urination, increased thirst, and increased hunger. If not treated in time, diabetes will cause many complications. Acute complications include hyperosmolar hyperglycemic state, diabetic ketoacidosis, or death. Serious long-term complications include cardiovascular disease, chronic kidney disease, foot ulcers, stroke, and damage to the eyes. According to the International Diabetes Federation (IDF) in 2017, an estimated 425 million individuals are living with DM. At present, the main treatment of diabetes is oral hypoglycemic drugs and insulin injection. However, long-term use of these drugs could lead to insulin resistance and other side effects. Thus, it is quite necessary to develop helpful, innocuous, and inexpensive drugs for DM patients. As the non-toxic biological

**Table 14.4** The anti-diabetic effects of polysaccharides

Source	Model	Effects and mechanisms	References
<i>Opuntia dillenii</i>	STZ mice	Protecting the liver from peroxidation damage, maintaining tissue function, improving the sensitivity and response of target cells in diabetic mice to insulin	Zhao et al. (2011)
<i>Tremella aurantia</i>	KK-Ay mice	Reducing levels of insulin, total cholesterol and triglyceride in the mice blood, decreasing the level of plasma lipoperoxide	Kiho et al. (2001)
<i>Phellinus linteus</i>	NOD mice	Inhibiting the development of autoimmune diabetes by regulating cytokine expression	Kim et al. (2010)
<i>Morus alba fruit</i>	T2DM mice	Repairing of damaged pancreatic tissues of diabetic rats.	Jiao et al. (2017)
<i>Lycium barbarum</i>	T2DM mice	Increasing insulinogenic index	Cai et al. (2011)
<i>Pleurotus ostreatus</i>	STZ mice	Reducing the risk of oxidative damage by increasing catalase (CAT), glutathione peroxidase (GSH-Px) and superoxide dismutase (SOD) activities and decreasing malonaldehyde (MDA) level	Zhang et al. (2016a, b, c)
<i>Portulaca oleracea L.</i>	Alloxan-induced diabetic mice	Controlling blood glucose, and modulating the metabolism of glucose and blood lipid in diabetes mellitus mice	Li et al. (2009a, b)
<i>Corn silk</i>	T2DM	Regulating the levels of serum lipid profile, decreasing the levels of glycated serum protein, non-esterified fatty acid	Pan et al. (2017)
<i>Hedysarum polybotrys</i>	Alloxan-induced diabetic mice	Increasing insulin secretion, inhibiting lipid peroxidation, promoting the sensitivity to insulin, suppressing gluconeogenesis, and reducing the biosynthesis fatty acid, cholesterol, and cell cytokines related to insulin resistance	Hu et al. (2010)
<i>Taxus cuspidata</i>	STZ mice	Increasing the body weight of diabetic mice, and reversing the decrease of SOD and the increase of thiobarbituric acid reactive substances (TBARS) in kidney and liver of diabetic mice	Zhang et al. (2012)
<i>Ganoderma lucidum</i>	T2DM	Down-regulation of the hepatic glucose regulated enzyme mRNA levels via AMPK activation, improvement of insulin resistance and decrease of epididymal fat/BW ratio	Xiao et al. (2016)

macromolecules, natural polysaccharides were observed to have positive effects to treat DM (Huie and Di 2004; Zhou et al. 2007). Table 14.4 presents the anti-diabetic effects of different polysaccharides.

A polysaccharide (CSP-1) from *Cordyceps sinensis* consists of glucose, mannose, and galactose in a molar ratio of 1:0.6:0.75, and exhibited a significant drop in blood glucose level in both normal and streptozotocin (STZ)-diabetic animals. These results could be related to the increase in blood insulin level via the release of insulin from the residual pancreatic cells and/or CSP-1-induced the reduction of insulin



metabolism in body (Li et al. 2006a, b). Another two purified polysaccharides (CS-F30 and CS-F10) from *Cordyceps sinensis mycelia* was also proved to have hypoglycemic effects on mice (Kiho et al. 1996, 1999). Compared to CSP-1, these two polysaccharides have different monosaccharide composition. In recent years, the hypoglycemic effect of tea polysaccharides (TPS) has also attracted much attention. Chen et al. (2010a, b) reported that the oral administration of TPS at 150 mg/kg/day can significantly reduce the blood glucose level in non-obese diabetic (NOD) mice. From TPS, two water-soluble polysaccharide fractions of TFP-1 and TFP-2 were obtained. The average molecular weight was determined to be  $15.9 \times 10^4$  and  $1.12 \times 10^4$  Da, respectively. Results showed that continuous administration of TFP-2 could dose-dependently decrease the blood glucose level in alloxan-induced diabetic mice by inhibiting  $\alpha$ -amylase and  $\alpha$ -glucosidase (Han et al. 2011a, b). Zhou et al. (2007) isolated a crude tea polysaccharides (CTP) and a tea polysaccharide fraction (TPF) from green tea. It was found that CTP and TPF have hypoglycemic effects on alloxan-induced diabetic mice. The hypoglycemic action of polysaccharides from oolong tea and black tea has also been investigated. Results exhibited that these tea polysaccharides could alleviate the diabetic mice and improve diabetes symptoms, indicating tea polysaccharides have good effects on the prevention of hyperglycemia (Nie et al. 2011).

Food-derived peptides have been reported to have antagonistic effects against glucose-dependent insulinotropic polypeptide (GIP) and glucagon-like peptide-1 (GLP-1) in type 2 diabetes via inhibiting the activity of Dipeptidyl peptidase IV (DPP-IV) (Matteucci and Giampietro 2009). So far, this active peptide has been isolated from corn, milk, soybean, rice, and other foods (Zhu et al. 2019; Mochida et al. 2010; Hira et al. 2009; Sanjukta and Rai 2016). The dipeptides and tripeptides isolated from whey proteins have been used as competitive inhibitors to interact with DPP-IV substrates (Gunnarsson et al. 2006). Recently, more attention have been paid on the application of marine bioactive peptides to treat type 2 diabetes. The peptides from *Porphyra dioica* were observed to have the inhibitory effect on DPP-IV (Stack et al. 2017). Three polypeptides (ILAP, LLAP, and MAGVDHI) with similar bioactivity were also isolated from macroalga *Palmaria palmata* (Harnedy et al. 2015).

## 2.6 Hypolipidemic

Hyperlipidemia is a lipid metabolic disorder characterized by the enhancement of blood total cholesterol (TC), low-density lipoprotein (LDL), very low-density lipoprotein-cholesterol (VLDL-C) and triglyceride (TG), with a concomitant decrease in the level of high-density lipoprotein-cholesterol (HDL-C) in the plasma. With the improvement of people's living standard and the change of dietary structure, the incidence of hyperlipidemia is increasing year by year (Chan et al. 2009). Hyperlipidemia is one of the main risk factors for inducing cardiovascular diseases, such as hypertension, atherosclerosis, and coronary heart disease (Rosenson et al. 2002).



In a meanwhile, lipid accumulation in liver (steatosis) can result in oxidative stress and inflammation, leading to the damage of liver (Esposito et al. 2002). Thus, how to reduce lipid level is one of most important clinical problems. At the present time, statins, nicotinic acid, and its derivatives are the most common lipid-lowering prescribed drugs. Although these drugs help in lowering lipids, their side effects are also enormous, such as headache, muscle pain, and nausea. Moreover, the long-term use of these drugs can increase the risk of type 2 diabetes (Hsu et al. 2015). In recent decades, more and more evidences exhibited that natural polysaccharides had the function to low lipids. For instance, *Enteromorpha prolifera* polysaccharides exhibited a high hypolipidemic action in high fat rats via decreasing the plasma LDL-C, TC, and TG levels and increasing HDL-C level (Teng et al. 2013). *Ganoderma lucidum*  $\beta$ -glucan was also reported to decrease the TC, TG, and LDL-C levels in the serum of diabetic mice, whereas the HDL-C level was increased (Li et al. 2011). Recently, significant in vivo studies testing, the efficacy of cereal  $\beta$ -glucans using animal and human subjects has led to health claims for this material in many industrialized countries. The soluble dietary fibers (i.e.,  $\beta$ -glucan from cereal grains) are well accepted to be the polysaccharides with the ability to lower lipids (Pomeroy et al. 2001). Therefore, adding  $\beta$ -glucan-rich fiber products in the daily diet is now considered as an effective approach to lower lipids. Extensive efforts have been made to establish the relationship between the structure of cereal  $\beta$ -glucans and reduction of LDL-C levels (Lazaridou and Biliaderis 2004; Li et al. 2006a, b). Cereal  $\beta$ -glucans are linear homopolysaccharides formed by the linkage of  $\beta$ -D-glucopyranosyl units via (1 $\rightarrow$ 4)- $\beta$ -linkage and separated by single (1 $\rightarrow$ 3)- $\beta$ -linkages. They are the main component of water-soluble dietary fibers from cereals. The physiological activity of soluble  $\beta$ -glucan from cereal is closely related to its unique structure of (1 $\rightarrow$ 3)(1 $\rightarrow$ 4)- $\beta$ -D-glucan. It was concluded that the LDL-C lowering effect and the ability to control blood glucose of cereal  $\beta$ -glucan may depend on its viscosity in solution, which is controlled by the  $M_w$ , structure, and concentration in the intestine (Wood 2007).

It has been reported that  $\beta$ -glucan can bind to the bile acid in intestinal lumen. This combination would reduce the circulation of bile acid liver and further stimulate the production of more bile acids from cholesterol. Moreover,  $\beta$ -glucan could be fermented in the large bowel by colonic bacteria, and producing the short-chain fatty acids. The short-chain fatty acids could be absorbed by portal vein, and inhibit hepatic cholesterol synthesis via regulating the activity of HMG-CoA reductase (a rate-limiting enzyme required for cholesterol biosynthesis), or increasing catabolism of LDL-cholesterol. Another phenomenon was observed that  $\beta$ -glucan reduced the concentration of postprandial serum insulin by delaying gastric emptying, leading to the inhibition of hepatic cholesterol production. It was also reported that  $\beta$ -glucan could interfere with the absorption of dietary fat via increasing intestinal viscosity (Bell et al. 1999).

## 2.7 Other Activities

Besides the healthy benefits mentioned above, some other bioactivities of polysaccharides and protein-related compounds have been studied in recent years, including antidiarrheal, anti-fatigue, anti-tussive, anti-analgesia, anti-allergic, and anti-dyszoospermia activities. Baek et al. (2010) evaluated the anti-diarrhea effect of *ginseng* polysaccharides in vitro using the model of rotavirus infection. Results showed that two pectic ginseng polysaccharides dose-dependently rescued the cell viability from rotavirus infection. Moreover, the prevention of polysaccharide on rotavirus was attributed to the inhibitory effects of rotaviral attachment to cells. In recent years, the anti-fatigue effect of polysaccharides extracted from different materials is gradually accepted by people (Jing et al. 2009). Pimentel et al. (2019) demonstrated that macroalgae-derived peptides and enzymes have protective effects on skin via eliminating free radicals and promoting moisture.

## 3 Structure Features

Chemical structure is the basis of polysaccharides and to exert their biological activity, including monosaccharide composition, monosaccharide arranging order, anomeric carbon configuration, glycoside bond types, branches, substituted groups, and the spatial conformation. It has been reported that most bioactive polysaccharides are mainly composed of glucose, fucose, galactose, arabinose, mannose, xylose, ribose, glucuronic acid, and galacturonic acid. According to the published literatures, the fungal derived polysaccharides have been found to be  $\alpha$ -mannan,  $\beta$ -glucans and hetero- $\beta$ -glucans,  $\alpha$ -mannan- $\beta$ -glucan complexes, heteroglycans, glycopeptides or glycoprotein and proteoglycan. The polysaccharides extracted from plants mainly include glucans, glucomannans, heteroglycans, arabinans, arabinogalactan, pectins, rhamnogalacturonan, and their sulfated or acetylated forms. Animal polysaccharides are mainly composed of glycosaminoglycan and sulfated glycosaminoglycan.

Although it is quite difficult to determine the structural variability of polysaccharides from different resources, a series of analytical methods have been established to achieve this. The high performance liquid chromatography (HPLC) is often performed to determine the molecular weight of polysaccharides. The infrared spectroscopy (IR), ultraviolet spectroscopy (UV), gas chromatography-mass spectrometry, NMR spectroscopy, periodate oxidation, partial acid hydrolysis, methylation, and periodate oxidation-Smith degradation are the common methods to analyze structural features of polysaccharides (Yang et al. 2009).

The chemical structure of natural polysaccharides is very complex. Table 14.5 showed the structure features of some polysaccharides extracted from different species. In most cases, one material could contain a variety of polysaccharides with different structures. Moreover, the same species growing in different places

**Table 14.5** Structure features of polysaccharides from various sources. Reproduction with permission from (Nie et al. 2018), Copyright 2018 Elsevier

Source	Mw (Da)	Monosaccharide composition	Backbone	References
<i>Pleurotus florida</i>	180,000	Glucose	(1→6)-linked-β-D-Glcp (1→3,6)-linked-β-D-Glcp	Maji et al. (2012)
<i>Auricularia polytricha</i>	120,000	Glucose	1,3-β-glucan 1,3-α-glucan 1,4-α-glucan	Song and Du (2012)
<i>Cistanche Deserticola Y. Ma</i>	10,000	Glucose	1,4-linked-α-D-glucan	Dong et al. (2007)
<i>Cordyceps sinensis</i>	–	Glucose, Mannose, Galactose	(1→4)-linked-α-D-Glcp	Nie et al. (2011)
<i>Ganoderma lucidum</i>	83,000	Rhamnose, Galactose, Glucose	1,4-linked-α-D-Glcp 1,6-linked-β-D-Glcp	Bao et al. (2002a, b)
<i>Ganoderma lucidum</i>	200,000	Glucose, Mannose	1,3-, 1,4-, 1,6-linked-β-D-Glcp 1,6-linked-β-D-Manp	Bao et al. (2002a, b)
<i>Ophiopogon japonicus</i>	35,200	Arabinose, Glucose, Galactose	1,4-linked-Glcp 1,6-linked-Glcp 1,4,6-linked-Glcp	Chen et al. (2011)
<i>Lentinus squarrosulus (Mont.) Singer</i>	196,000	Galactose, Glucose, Fucose	(1→4)-linked-α-D-Glcp (1→6)-linked-β-D-Glcp (1→4,6)-linked-D-Glcp (1→3,6)-linked-D-Glcp	Bhunia et al. (2010)
<i>Dendrobium huoshanense</i>	73,000	Glucose, Galactose, Xylose	1,4-linked-β-D-Glcp 1,6-linked-β-D-Glcp 1,4,6-linked-β-D-Glcp	Pan et al. (2013b)
<i>Radix Astragali</i>	1334,000	Rhamnose, Glucose, Arabinose, Galactose, Galactose acid	1,4-linked-α-Glcp 1,4-linked-α-GalAp6Me 1,2,4-linked-Rhap 1,3,6-linked-β-Galp	Yin et al. (2012)

could contain different polysaccharides. It is also reported that the polysaccharides in different organs of the same species is also different in the structures. It has been observed that polysaccharides extracted from the spores of *Ganoderma lucidum* possessed a backbone of (1–3)-β-linked glucans (Bao et al. 2001). However, the backbone of fruit bodies polysaccharides was composed of 1,3-linked glucose, 1,6-linked glucose, 1,6-linked mannose, 1,4-linked glucose, and 1,6-linked galactose (Bao et al. 2002a, b).

For the preparation of natural polysaccharides, the extraction methods and extraction parameters are also critical factors affecting polysaccharide's structures and properties. For instance, Palacios et al. compared the effects of different extraction methods on the structure of polysaccharides from *Pleurotus ostreatus* mushroom. Results showed that the polysaccharides extracted by cold-water mainly

consisted of 1–3- $\alpha$ -linked and 1–6- $\alpha$ -linked galactose. The polysaccharide extracted by hot-water was mainly composed of 1–4- $\alpha$ -linked glucose. However, the fraction extracted by hot-aqueous NaOH was mainly composed of 1–3- $\beta$ -linked and 1–6- $\beta$ -linked glucose (Palacios et al. 2012).

In addition to the natural factors, chemical modification can also change the polysaccharide's structure, leading to the variation of physicochemical properties and bioactivities (Fiorito et al. 2018). According to the published literatures, the acetylation, carboxymethylation, sulfation, phosphorylation, alkylation, and selenization have been employed to modify the structure of polysaccharides (Prashanth and Tharanathan 2007). Moreover, some modified polysaccharides have been developed into drug delivery systems (Shah et al. 2011).

In addition to the natural factors, polysaccharide derivatives also contribute to the structural diversity, which can also be classified as a semisynthetic polysaccharide. It has been reported that the effective chemical modification of this natural structure could improve the bioactivities and some key parameters, including solubility, bioavailability, and pharmacokinetics (Fiorito et al. 2018). Chemical modification can control the final structure of polysaccharides, and thus determining the specific biological functions. In addition, the chemical modification of polysaccharide structure mainly utilizes the polysaccharide's reactive groups, such as hydroxyl, carboxyl, and amino groups, to chemically introduce new functional groups. Chemical modification of polysaccharide includes sulfation, carboxymethylation, acetylation, alkylation, phosphorylation, and selenization. Some semisynthetic polysaccharides have been developed into various drug delivery systems.

In recent years, a large number of studies have been carried out on the structure–activity relationship of polysaccharides. Results exhibited that the activity of polysaccharides was mainly related to the molecular weight, chemical structure, and physical properties (Jin et al. 2012). The (1,3)- $\beta$ -D-glucan from *Poria cocos* sclerotium is a water-insoluble polysaccharide and exhibited low bioactivity. After carboxymethylation, both the water solubility and bioactivity were enhanced (Wang et al. 2009). Di et al. (2017) reported that sulfated polysaccharides from *Gracilaria rubra* exerted immunologic activity by promoting the proliferation of RAW264.7 cells. Moreover, the activity was improved with the decrease of polysaccharide molecular weight. Chen et al. (2015) demonstrated that sulfated polysaccharide from *Ganoderma atrum* has the strongest immunological activity when the molecular weight was intermediate ( $4.0 \times 10^{-6}$  Da). Zhang et al. (2005) found that the physicochemical property and steric conformation of polysaccharides from *Poria cocos* mycelia were changed by the introduction of sulfate groups, leading to the changes in the bioactivity of polysaccharides. Similarly, sulfated modification changed the structure and conformation of polysaccharides from *Hypsizygus marmoreus*, enhancing the ability of anticancer and immunity (Bao et al. 2010). The substitution degree of substituent groups also has a great influence on the biological activity of polysaccharides. For instance, chitosan with different substitution degree of sulfuric acid group exhibited different strength of immunoregulation ability (Yang et al. 2018). Liu et al. (2017a, b) investigated the structure–activity relationship of selenium-containing polysaccharide. Results showed that the

anti-diabetic activity was improved with the increase of selenium content of *Catathelasma ventricosum* polysaccharide with triple helical structure. However, when the tri-helical structure was damaged, the anti-diabetic effect was decreased. With respect to the structure–activity relationship of proteins, it has been reported that the bioactivity of proteins was highly related to its structure characteristics, such as amino acid composition, amino acid sequence, molecular weight, and hydrophobicity (Silva et al. 2017).

## 4 Application

Because natural polysaccharides have wide biological activities and low toxicity, some of them have been successfully applied in fields of drugs and foods (Table 14.6). In the field of drugs, some polysaccharides such as Lentinan, *Astragalus* polysaccharide, Ginseng polysaccharide, Poria polysaccharide, and Chondroitin have been developed into injections, tablets, and capsules. In the field of foods, some polysaccharides have been used as the additives to endow new nutritional and healthy functions of foods. For instance, *Lycium barbarum* polysaccharides (LBPs) have been processed into different forms of functional foods, such as Goji beverage, Goji wine, Goji tea, Goji oral liquid, Goji tablet, Goji capsule, and Goji granules. Among these healthy foods, the Goji capsule and Goji oral liquid were popular in the public. Long-term use of Goji capsule and Goji oral liquid can enhance the immunity, improve sleep, protect liver, and reduce fatigue (Wu et al. 2018).

Proteins are the important components in foods. Since soybean protein isolate was produced in large-scale in 1958, the application of food protein becomes more and more pluralistic. In the field of traditional foods, the soybean protein, milk protein, egg protein, meat protein, and nut protein have been applied in beverage food, baby food, baked food, pastry, and meat products. In the field of non-traditional foods, the protein has been used as a main component to prepare reproduced foods and simulated foods, such as soybean protein beef, plant protein chicken, vegetarian ham, vegetarian sausage, and imitation meat hamburger. Moreover, food protein widely applied in cosmetics and biomedicine.

## 5 Conclusions and Future Prospects

In recent decades, the research of bioactive polysaccharides has made some important progress and has been widely used in pharmaceutical, biochemical cosmetic, and functional food industries. However, due to the limitations of existing experimental methods and the complexity of their structure, research about polysaccharides is still far behind than that of proteins and nucleic acids. Although the functional properties of polysaccharides have been widely studied, the mechanism of their actions is still unknown. One of the main reasons is that the structural

**Table 14.6** Practical Applications of Polysaccharides

Applications areas	Polysaccharides	Practical applications	Bioactivities	References
Clinical drugs and medicines	<i>Astragalus polysaccharide</i>	Astragalus polysaccharide injection	Immunomodulation; Antioxidant; Anti-hypertensive	Xu (2012) Zhang et al. (2016a, b, c)
	<i>Ginseng polysaccharide</i>	Ginseng polysaccharide injection	Anti-tumor immunity	Xu (2015)
	<i>Lentinan polysaccharide</i>	Lentinan injection; Lentinan capsules	Immunomodulation; Anti-tumor	Wang (2012) Wang et al. (2013)
	<i>Poria polysaccharide</i>	Poria polysaccharide oral solution	Anti-gastric cancer	Yang et al. (2017) Hou and Luo (2017)
	<i>Chondroitin sulfate</i>	Chondroitin sulfate tablets; chondroitin sulfate capsules	Anti-arthritis; Anti-angiocardopathy	Gacci et al. (2015) Liu et al. (2014a, b)
	<i>Fucoidan</i>	Active pharmaceutical ingredient; Antivirus drugs	Hypolipidemic; Antivirus	Wu and Yang (2010) Mandal et al. (2007)
	<i>Ganoderma atrum polysaccharide</i>	Hypoglycemic drugs	Hypoglycemic	Zhu et al. (2013)
	<i>Heparin</i>	Anticoagulant drugs	Anticoagulant	Bai and Ahsan (2009) Dong and Fang (2001)
Food industry	<i>Exopolysaccharides</i>	Fermented dairy products	Anti-ulcer; Immunomodulation; Anti-tumor	Yang et al. (2010)
	<i>Soybean soluble polysaccharide</i>	Yogurt; Milk beverage	Anti-hypertensive; Reduce weight; Hypoglycemic	Ron et al. (2010) Nakamura et al. (2006)
	<i>Red ginseng polysaccharide</i>	Noodles, bread, or cake making	Immunomodulation; Anti-tumor	Yu et al. (2012)
	<i>Carrageenan</i>	Desserts (ice cream and puddings)	Antivirus	Prajapati et al. (2014)
Cosmetics industry	<i>Hyaluronic acid</i>	Sodium hyaluronate injection	Moisture absorption and moisture retention	Zhang et al. (2008)
	<i>Aloe polysaccharides</i>	Aloe Vera gel	Anti-aging; Versatile skin care	Takahashi et al. (2009)
	<i>Marine algae polysaccharides</i>	Marine algae deep moisturizing cream	Anti-radiation; Whitening and moisturizing	Moore (2002)

diversity and heterogeneity of natural polysaccharides hamper the research and product development. Moreover, the polysaccharides extracted from the same raw material by different preparation methods often have different compositions. Therefore, the preparation process of polysaccharides needs to be standardized. To reveal the structure–activity relationship is always the focus of polysaccharides research, which will disclose the structural basis for polysaccharides to perform their healthy functions. This is not only necessary to screen and design high-active polysaccharides, but also have important theoretical guiding significance to study the medicinal mechanism of polysaccharides. In addition, because polysaccharides have a wide range of biological activities, they will have broad application prospects in functional foods in the future. Therefore, it is also necessary to strengthen the research on the activity development and mechanism of polysaccharides.

## References

- Agyei D, Danquah MK (2012) Rethinking food-derived bioactive peptides for antimicrobial and immunomodulatory activities. *Trends Food Sci Technol* 23:62–69
- Ahn G, Park E, Lee WW et al (2011) Enzymatic extract from *Ecklonia cava* induces the activation of lymphocytes by IL-2 production through the classical NF- $\kappa$ B pathway. *Mar Biotechnol* 13:66–73
- Arthur JSC, Ley SC (2013) Mitogen-activated protein kinases in innate immunity. *Nat Rev Immunol* 13(9):679–692
- Baek SH, Lee JG, Park SY et al (2010) Pectic polysaccharides from *Panax ginseng* as the antirotavirus principals in ginseng. *Biomacromolecules* 11(8):2044–2052
- Bai D, Chang NT, Li DH et al (2008) Antiblastic activity of *Ganoderma lucidum* polysaccharides. *Acta Agric Bor Sin* 23(S1):282–285
- Bai S, Ahsan F (2009) Synthesis and evaluation of pegylated dendrimeric nanocarrier for pulmonary delivery of low molecular weight heparin. *Pharm Res* 26:539–548
- Bao HH, Wonseok C, You SG (2010) Effect of sulfated modification on the molecular characteristics and biological activities of polysaccharides from *Hypsizigus marmoreus*. *Biosci Biotech Bioch* 74:1408–1414
- Bao L, Wang Y, Ma R et al (2015) Apoptosis-inducing effects of *lentinan* on the proliferation of human bladder cancer T24 cells. *Pak J Pharm Sci* 28(5):1595–1600
- Bao X, Liu C, Fang J et al (2001) Structural and immunological studies of a major polysaccharide from spores of *Ganoderma lucidum* (fr.) karst. *Carbohydr Res* 332(1):67–74
- Bao XF, Wang XS, Dong Q et al (2002a) Structural features of immunologically active polysaccharides from *Ganoderma lucidum*. *Phytochemistry* 59(2):175–181
- Bao XF, Zhen Y, Ruan L et al (2002b) Purification, characterization, and modification of T lymphocyte-stimulating polysaccharide from spores of *Ganoderma lucidum*. *Chem Pharm Bull* 50(5):623–629
- Belhaj D, Athmouni K, Ahmed MB et al (2018) Polysaccharides from *Phormidium versicolor* (NCC466) protecting HepG2 human hepatocellular carcinoma cells and rat liver tissues from cadmium toxicity: evidence from in vitro and in vivo tests. *Int J Biol Macromol* 113:813–820
- Bell S, Goldman VM, Bistrrian BR et al (1999) Effect of  $\beta$ -glucan from oats and yeast on serum lipids. *Crit Rev Food Sci* 39(2):189–202
- Besch R, Poeck H, Hohenauer T et al (2009) Proapoptotic signaling induced by RIG-I and MDA-5 results in type I interferon-independent apoptosis in human melanoma cells. *J Clin Invest* 119(8):2399–2411

- Bhattacharyya C, De S, Basak A et al (2006) Antimicrobial activities of some *Basidiomycetous fungi*. *J Mycopathol Res* 44:129–135
- Bhunia SK, Dey B, Maity KK et al (2010) Structural characterization of an immunoenhancing heteroglycan isolated from an aqueous extract of an edible mushroom, *Lentinus squarrosulus* (mont.) singer. *Carbohydr Res* 345(17):2542–2549
- Bose N, Wurst LR, Chan AS et al (2014) Differential regulation of oxidative burst by distinct beta-glucan-binding receptors and signaling pathways in human peripheral blood mononuclear cells. *Glycobiology* 24:379–391
- Cai X, Wang YF, Mao FF et al (2011) Hypoglycemic and hyperglycemia-prevention effects of crude tea flower polysaccharide. *Mod Food Sci Technol* 27:262–266
- Chan G, Chan W, Sze D (2009) The effects of beta-glucan on human immune and cancer cells. *J Hematol Oncol* 2(1):25
- Chen JR, Yang ZQ, Hu TJ et al (2010a) Immunomodulatory activity in vitro and in vivo of polysaccharide from *Potentilla anserina*. *Fitoterapia* 81(8):1117–1124
- Chen KL, Weng BC, Chang MT et al (2008) Direct enhancement of the phagocytic and bactericidal capability of abdominal macrophage of chicks by beta-1, 3-1, 6-glucan. *Poult Sci* 87:2242–2249
- Chen X, Jin J, Tang J et al (2011) Extraction, purification, characterization and hypoglycemic activity of a polysaccharide isolated from the root of *Ophiopogon japonicus*. *Carbohydr Polym* 83(2):749–754
- Chen XQ, Lin Z, Ye Y et al (2010b) Suppression of diabetes in non-obese diabetic (NOD) mice by oral administration of water-soluble and alkali-soluble polysaccharide conjugates prepared from green tea. *Carbohydr Polym* 82:28–33
- Chen Y, Zhang H, Wang Y et al (2015) Sulfated modification of the polysaccharides from *Ganoderma atrum* and their antioxidant and immunomodulating activities. *Food Chem* 186:231–238
- Cheng BH, Chan JYW, Chan BCL et al (2014) Structural characterization and immunomodulatory effect of a polysaccharide HCP-2 from *Houttuynia cordata*. *Carbohydr Polym* 103:244–249
- Chihara G, Maeda Y, Hamuro J et al (1969) Inhibition of mouse sarcoma 180 by polysaccharides from *Lentinus edodes* (Berk.) sing. *Nature* 222:687–688
- Cho CW, Han CJ, Rhee YK et al (2015) *Cheonggukjang* polysaccharides enhance immune activities and prevent cyclophosphamide-induced immunosuppression. *Int J Biol Macromol* 72:519–525
- Cristina Diaz A, Laura Espino M, Arzoz NS et al (2017) Free radical scavenging activity of extracts from seaweeds *Macrocystis pyrifera* and *Undaria pinnatifida*: applications as functional food in the diet of prawn *Artemesia longinaris*. *Lat Am J Aquat Res* 45(1):104–112
- Cui H, Wu S, Shang Y et al (2016) *Pleurotus nebrodensis* polysaccharide (PN50G) evokes A549 cell apoptosis by the ROS/AMPK/PI3K/AKT/mTOR pathway to suppress tumor growth. *Food Funct* 7(3):1616–1627
- Di T, Chen G, Sun Y et al (2017) Antioxidant and immunostimulating activities in vitro of sulfated polysaccharides isolated from *Gracilaria rubra*. *J Funct Foods* 28:64–75
- Diao Y, Xin Y, Zhou Y et al (2014) Extracellular polysaccharide from *Bacillus sp. strain* LBP32 prevents LPS-induced inflammation in RAW 264.7 macrophages by inhibiting NF- $\kappa$ B and MAPKs activation and ROS production. *Int Immunopharmacol* 18(1):12–19
- Díaz-Gómez J, Ortiz-Martínez M, Aguilar O et al (2018) Antioxidant activity of zein hydrolysates from zein species and their cytotoxic effects in a hepatic cell culture. *Molecules* 23(2):312–326
- DiDonato JA, Mercurio F, Karin M (2012) NF- $\kappa$ B and the link between inflammation and cancer. *Immunol Rev* 246(1):379–400
- Dong Q, Fang J (2001) Structural elucidation of a new arabinogalactan from the leaves of *Nerium indicum*. *Carbohydr Res* 332(1):109–114
- Dong Q, Yao J, Fang JN et al (2007) Structural characterization and immunological activity of two cold-water extractable polysaccharides from *Cistanche deserticola* Y. C. Ma. *Carbohydr Res* 342(10):1343–1349



- Dore C, Alves M, Santos M et al (2014) Antioxidant and anti-inflammatory properties of an extract rich in polysaccharides of the mushroom *Polyporus dermatopus*. *Antioxidants (Basel)* 3 (4):730–744
- Esposito K, Nappo F, Marfella R et al (2002) Inflammatory cytokine concentrations are acutely increased by hyperglycemia in humans: role of oxidative stress. *Circulation* 106(16):2067
- Faccin LC, Benati F, Rincão VP et al (2007) Antiviral activity of aqueous and ethanol extracts and of an isolated polysaccharide from *Agaricus brasiliensis* against poliovirus type I. *Lett Appl Microbiol* 45:24–28
- Fan L, Ding S, Ai L et al (2012a) Antitumor and immunomodulatory activity of water-soluble polysaccharide from *inonotus obliquus*. *Carbohydr Polym* 90(2):870–874
- Fan L, Li J, Deng K et al (2012b) Effects of drying methods on the antioxidant activities of polysaccharides extracted from *Ganoderma lucidum*. *Carbohydr Polym* 87(2):1849–1854
- Fan X, Subramaniam R, Weiss MF et al (2003) Methylglyoxal-bovine serum albumin stimulates tumor necrosis factor alpha secretion in RAW 264.7 cells through activation of mitogen-activating protein kinase, nuclear factor kappaB and intracellular reactive oxygen species formation. *Arch Biochem Biophys* 409:274–286
- Fang Q, Wang JF, Zha XQ et al (2015) Immunomodulatory activity on macrophage of a purified polysaccharide extracted from *Laminaria japonica*. *Carbohydr Polym* 134:66–73
- Feng Y, Li W, Wu X et al (2010) Rapid and efficient microwave-assisted sulfate modification of *lentinan* and its antioxidant and antiproliferative activities in vitro. *Carbohydr Polym* 82 (3):605–612
- Ferreira IC, Heleno SA, Reis FS et al (2015a) Chemical features of *ganoderma* polysaccharides with antioxidant, antitumor and antimicrobial activities. *Phytochemistry* 114:38–55
- Ferreira SS, Passos CP, Madureira P et al (2015b) Structure-function relationships of immunostimulatory polysaccharides: a review. *Carbohydr Polym* 132:378–396
- Ferwerda G, Meyer-Wentrup F, Kullberg BJ et al (2008) Dectin-1 synergizes with TLR2 and TLR4 for cytokine production in human primary monocytes and macrophages. *Cell Microbiol* 10 (10):2058–2066
- Figueiredo RT, Bittencourt VCB, Lopes LCL et al (2012) Toll-like receptors (TLR2 and TLR4) recognize polysaccharides of *Pseudallescheria boydii* cell wall. *Carbohydr Res* 356:260–264
- Fiorito S, Epifano F, Prezioso F et al (2018) Selenylated plant polysaccharides: a survey of their chemical and pharmacological properties. *Phytochemistry* 153:1–10
- Gacci M, Saleh O, Giannessi C et al (2015) Sodium hyaluronate and chondroitin sulfate replenishment therapy can improve nocturia in men with post-radiation cystitis: results of a prospective pilot study. *BMC Urol* 15(1):1–6
- Goldberg J, Shrikant P, Mescher MF (2003) In vivo augmentation of tumor-specific CTL responses by class I/peptide antigen complexes on microspheres (large multivalent immunogen). *J Immunol* 170:228–235
- Guerra Dore CMP, Azevedo TCG, De Souza MCR et al (2007) Antiinflammatory, antioxidant and cytotoxic actions of  $\beta$ -glucan-rich extract from *Geastrum saccatum* mushroom. *Int Immunopharmacol* 7:1160–1169
- Gunnarsson PT, Winzell MS, Deacon CF et al (2006) Glucose-induced incretin hormone release and inactivation are differently modulated by oral fat and protein in mice. *Endocrinology* 147 (7):3173–3180
- Guo L, Xie J, Ruan Y et al (2009) Characterization and immunostimulatory activity of a polysaccharide from the spores of *Ganoderma lucidum*. *Int Immunopharmacol* 9:1175–1182
- Han K, Jin C, Chen H et al (2018) Structural characterization and anti-A549 lung cancer cells bioactivity of a polysaccharide from *Houttuynia cordata*. *Int J Biol Macromol* 120:288–296
- Han Q, Yu QY, Shi J et al (2011a) Molecular characterization and hypoglycemic activity of a novel water soluble polysaccharide from tea (*Camellia sinensis*) flower. *Carbohydr Polym* 86:797–805

- Han QA, Yu QY, Shi JA et al (2011b) Structural characterization and antioxidant activities of 2 water soluble polysaccharide fractions purified from tea (*Camellia sinensis*) flower. *J Food Sci* 76:462–471
- Harman D (1993) Free radical involvement in aging pathophysiology and therapeutic implications. *Drug Aging* 3(1):60–80
- Harnedy PA, O’Keeffe M, FitzGerald R (2015) Purification and identification of dipeptidyl peptidase (DPP) IV inhibitory peptides from the macroalga *Palmaria palmata*. *Food Chem* 172:400–406
- Hazama S, Watanabe S, Ohashi M et al (2009) Efficacy of orally administered superfine dispersed lentinan ( $\beta$ -1,3-glucan) for the treatment of advanced colorectal cancer. *Anticancer Res* 29 (7):2611–2617
- He L, Ji P, Cheng J et al (2013) Structural characterization and immunostimulatory activity of a novel protein-bound polysaccharide produced by *Hirsutella sinensis* Liu, Guo, Yu & Zeng. *Food chem* 141(2):946–953
- Hernandez-Ledesma B, Hsieh CC, De Lumen BO (2009) Lunasin, a novel seed peptide for cancer prevention. *Peptides* 30(2):426–430
- Hetland G, Ohno N, Aaberge IS et al (2000) Protective effect of  $\beta$ -glucan against systemic *Streptococcus pneumoniae* infection in mice. *FEMS Immuno Med Mic* 27:111–116
- Hira T, Mochida T, Miyashita K et al (2009) GLP-1 secretion is enhanced directly in the ileum but indirectly in the duodenum by a newly identified potent stimulator, zein hydrolysate, in rats. *Am J Physiol Gastroint Liver Physiol* 297(4):G663–G671
- Hou H, Fan Y, Wang S et al (2016) Immunomodulatory activity of Alaska Pollock hydrolysates obtained by glutamic acid biosensor-artificial neural network and the identification of its active central fragment. *J Funct Foods* 24:37–47
- Hou WT, Luo JB (2017) The study of the compound *poria* polysaccharide oral liquid on the antitumor activity and immune regulation function. *Pharm Clin Chin Mat Med* 33(2):78–81
- Hsu K, Li-Chan E, Jao C (2011) Antiproliferative activity of peptides prepared from enzymatic hydrolysates of tuna dark muscle on human breast cancer cell lines MCF-7. *Food Chem* 126:617–622
- Hsu SY, Lee WJ, Chong K et al (2015) Laparoscopic bariatric surgery for the treatment of severe hypertriglyceridemia. *Asian J Surg* 38(2):96–101
- Hu F, Li X, Zhao L et al (2010) Antidiabetic properties of purified polysaccharide from *Hedysarum polybotrys*. *Can J Physiol Pharm* 88(1):64–72
- Huie C, Di X (2004) Chromatographic and electrophoretic methods for lingzhi pharmacologically active components. *J Chromatogr B* 812(1–2):241–257
- Ina K, Furuta R, Kataoka T et al (2016) P1-035 chemo-immunotherapy using *lentinan* for the treatment of inoperable gastric cancer with multiple liver metastases. *Ann Oncol* 27(suppl 7): vii94
- Jiao Y, Wang X, Jiang X et al (2017) Antidiabetic effects of *Morus alba* fruit polysaccharides on high-fat diet- and streptozotocin-induced type 2 diabetes in rats. *J Ethnopharmacol* 199:119–127
- Jin ML, Zhao K, Huang QS et al (2012) Isolation, structure and bioactivities of the polysaccharides from *Angelica sinensis* (Oliv.) Diels: a review. *Carbohydr Polym* 89(3):713–722
- Jing L, Cui G, Feng Q et al (2009) Orthogonal test design for optimization of the extraction of polysaccharides from *Lycium barbarum* and evaluation of its anti-athletic fatigue activity. *J Med Plants Res* 3(5):433–437
- José ML, Castro R, Arranz JA et al (2007) Immunomodulating activities of acidic sulphated polysaccharides obtained from the seaweed *Ulva rigida* C. Agardh. *Int Immunopharmacol* 7 (7):879–888
- Kannan A, Hettiarachchy NS, Lay JO et al (2010) Human cancer cell proliferation inhibition by a pentapeptide isolated and characterized from rice bran. *Peptides* 31(9):1629–1634
- Kant P, Liu WZ, Pauls KP (2009) PDC1, a corn defensin peptide expressed in *Escherichia coli* and *Pichia pastoris* inhibits growth of *Fusarium graminearum*. *Peptides* 30(9):1593–1599

- Kawai T, Akira S (2010) The role of pattern-recognition receptors in innate immunity: update on toll-like receptors. *Nat Immunol* 11(5):373–384
- Kiho T, Kochi M, Usui S et al (2001) Antidiabetic effect of an acidic polysaccharide (TAP) from *tremella aurantia* and its degradation product (TAP-H). *Biol Pharm Bull* 24(12):1400–1403
- Kiho T, Ookubo K, Usui S et al (1999) Structural features and hypoglycemic activity of a polysaccharide (CS-F10) from the cultured mycelium of *Cordyceps sinensis*. *Biol Pharm Bull* 22(9):966–970
- Kiho T, Yamane A, Hui J et al (1996) Polysaccharides in fungi. xxxvi. hypoglycemic activity of a polysaccharide (CS-F30) from the cultural mycelium of *Cordyceps sinensis* and its effect on glucose metabolism in mouse liver. *Biol Pharm Bull* 19(2):294–296
- Kim HM, Kang JS, Kim JY et al (2010) Evaluation of antidiabetic activity of polysaccharide isolated from *Phellinus linteus* in non-obese diabetic mouse. *Int Immunopharmacol* 10(1):72–78
- Klaus A, Kozarski M, Niksic M et al (2011) Antioxidative activities and chemical characterization of polysaccharides extracted from the *basidiomycete* schizophyllum commune. *LWT- Food Sci Technol* 44(10):2005–2011
- Kumar H, Kawai T, Akira S (2011) Pathogen recognition by the innate immune system. *Int Rev Immunol* 30(1):16–34
- Lai CY, Hung JT, Lin HH et al (2010) Immunomodulatory and adjuvant activities of a polysaccharide extract of *Ganoderma lucidum* in vivo and in vitro. *Vaccine* 28(31):4945–4954
- Lazaridou A, Biliaderis CG (2004) Cryogelation of cereal  $\beta$ -glucans: structure and molecular size effects. *Food Hydrocolloid* 18(6):933–947
- Li C, Huang Q, Fu X et al (2015) Characterization, antioxidant and immunomodulatory activities of polysaccharides from *Prunella vulgaris* linn. *Int J Biol Macromol* 75:298–305
- Li F, Li Q, Gao D et al (2009a) Preparation and antidiabetic activity of polysaccharide from *Portulaca oleracea* L. *Afr J Biotechnol* 8(4):569–573
- Li F, Zhang Y, Zhong Z et al (2011) Antihyperglycemic effect of *Ganoderma lucidum* polysaccharides on streptozotocin-induced diabetic mice. *Int J Mol Sci* 12(12):6135–6145
- Li SL, Huang ZN, Hsieh HH et al (2009b) The augmented anti-tumor effects of *Anrodia camphorata* co-fermented with Chinese medicinal herb in human hepatoma cells. *Am J Chin Med* 37(4):771–783
- Li SP, Zhang GH, Zeng Q et al (2006a) Hypoglycemic activity of polysaccharide with antioxidation isolated from cultured *Cordyceps mycelia*. *Phytomedicine* 13(6):428–433
- Li W, Wang Q, Cui SW et al (2006b) Elimination of aggregates of (1 $\rightarrow$ 3) (1 $\rightarrow$ 4)- $\beta$ -d-glucan in dilute solutions for light scattering and size exclusion chromatography study. *Food Hydrocolloid* 20:361–368
- Li YG, Ji DF, Zhong S et al (2013a) Polysaccharide from *Pellinus linteus* induces S-phase arrest in HepG2 cells by decreasing calreticulin expression and activating the P27kip1-cyclin A/D1/E-CDK2 pathway. *J Ethnopharmacol* 150(1):187–195
- Li YG, Ji DF, Zhong S et al (2013b) Polysaccharide from *Pellinus linteus* induces S-phase arrest in HepG2 cells by decreasing calreticulin expression and activating the P27kip1-cyclin A/D1/E-CDK2 pathway. *J Ethnopharmacol* 150(1):187–195
- Liao W, Luo Z, Liu D et al (2015) Structure characterization of a novel polysaccharide from *Dictyophora indusiata* and its macrophage immunomodulatory activities. *J Agric Food Chem* 63(2):535–544
- Lim JY, Kim OK, Lee J et al (2014) Protective effect of the standardized green tea seed extract on uvb-induced skin photoaging in hairless mice. *Nutr Res Pract* 8(4):398–403
- Lin L, Cheng K, Xie Z et al (2018) Purification and characterization a polysaccharide from *Hedyotis diffusa* and its apoptosis inducing activity toward human lung cancer cell line A549. *Int J Biol Macromol* 122:64–71
- Liu G, Kuang S, Wu S et al (2016) A novel polysaccharide from *Sargassum integerrimum* induces apoptosis in A549 cells and prevents angiogenesis in vitro and in vivo. *Sci Rep* 6:26722
- Liu QM, Xu SS, Li L et al (2017a) In vitro and in vivo immunomodulatory activity of sulfated polysaccharide from *Porphyra haitanensis*. *Carbohydr Polym* 165:189–196

- Liu QY, Yao YM, Zhang SW et al (2011a) *Astragalus* polysaccharides regulate T cell-mediated immunity via CD11chighcd45RBlow DCs in vitro. *J Ethnopharmacol* 136(3):457–464
- Liu QY, Yao YM, Zhang SW et al (2011b) *Astragalus* polysaccharides regulate T cell-mediated immunity via CD11chighcd45RBlow DCs in vitro. *J Ethnopharmacol* 136(3):457–464
- Liu Y, Du YQ, Wang JH et al (2014a) Structural analysis and antioxidant activities of polysaccharide isolated from *jinqian mushroom*. *Int J Biol Macromol* 64:63–68
- Liu Y, Liu Y, Jiang H et al (2014b) Preparation, antiangiogenic and antitumoral activities of the chemically sulfated glucan from *Pellinus ribis*. *Carbohydr Polym* 106:42–48
- Liu Y, You Y, Li Y et al (2017b) The characterization, selenylation and antidiabetic activity of mycelial polysaccharides from *Catathelasma ventricosum*. *Carbohydr Polym* 174:72–81
- Liu Y, Zhao J, Zhao Y et al (2018) Therapeutic effects of lentinan on inflammatory bowel disease and colitis-associated cancer. *J Cell Mol Med* 23(2):1–11
- Lo TCT, Jiang YH, Chao AL et al (2007) Use of statistical methods to find the polysaccharide structural characteristics and the relationships between monosaccharide composition ratio and macrophage stimulatory activity of regionally different strains of *Lentinula edodes*. *Anal Chim Acta* 584:50–56
- Luo C, Luo C, Wang X et al (2016) Molecular inhibition mechanisms of cell migration and invasion by *coix* polysaccharides in A549 NSCLC cells via targeting S100A4. *Mol Med Rep* 15(1):309–316
- Ma L, Chen H, Zhang Y et al (2012) Chemical modification and antioxidant activities of polysaccharide from mushroom *inonotus obliquus*. *Carbohydr Polym* 89(2):371–378
- Maeda R, Ida T, IHARA H et al (2012) Immunostimulatory activity of polysaccharides isolated from *Caulerpa lentillifera* on macrophage cells. *Biosci Biotech Bioch* 76(3):501–505
- Maji PK, Sen IK, Behera B et al (2012) Structural characterization and study of immunoenhancing properties of a glucan isolated from a hybrid mushroom of *pleurotus florida* and *lentinula edodes*. *Carbohydr Res* 358:110–115
- Mandal P, Mateu CG, Chattopadhyay K et al (2007) Structural features and antiviral activity of sulphated fucans from the *brown seaweed cystoseira indica*. *Antivir Chem Chemother* 18(3):153–162
- Mao GH, Ren Y, Feng WW et al (2015) Antitumor and immunomodulatory activity of a water-soluble polysaccharide from *grifola frondosa*. *Carbohydr Polym* 134:406–412
- Masuda Y, Inoue H, Ohta H et al (2013) Oral administration of soluble  $\beta$ -glucans extracted from, *grifola frondosa*, induces systemic antitumor immune response and decreases immunosuppression in tumor-bearing mice. *Int J Cancer* 133(1):108–119
- Matteucci E, Giampietro O (2009) Dipeptidyl peptidase-4 (CD26): knowing the function before inhibiting the enzyme. *Curr Med Chem* 16:2943–2951
- Meng FY (2010) Extraction optimization and in vivo antioxidant activities of exopolysaccharide by *morchella esculenta* SO-01. *Bioresour Technol* 101(12):4564–4569
- Meng J, Hu X, Shan F et al (2011) Analysis of maturation of murine dendritic cells (DCs) induced by purified *ganoderma lucidum* polysaccharides (GLPs). *Int J Biol Macromol* 49(4):693–699
- Mochida T, Hira T, Hara H (2010) The corn protein, zein hydrolysate, administered into the ileum attenuates hyperglycemia via its dual action on glucagon-like peptide-1 secretion and dipeptidyl peptidase-IV activity in rats. *Endocrinology* 151(7):3095–3104
- Mohan K, Padmanaban AM, Uthayakumar V et al (2017) Anti-cancer effect of the polysaccharide extract from the *ganoderma lucidum* against hela cell lines. *Bangladesh J Pharmacol* 12(1):56–57
- Moore A (2002) The biochemistry of beauty. *EMBO Rep* 3(8):714–717
- Murphy EA, Davis JM, Carmichael MD et al (2009) Benefits of oat  $\beta$ -glucan and sucrose feedings on infection and macrophage antiviral resistance following exercise stress. *Am J Phys* 297:1188–1194
- Nagaoka M, Shibata H, Kimura-Takagi I et al (2010) Anti-ulcer effects and biological activities of polysaccharides from *marine algae*. *Biofactors* 12:267–274

- Nakamura A, Yoshida R, Maeda H et al (2006) The stabilizing behaviour of *soybean* soluble polysaccharide and pectin in acidified milk beverages. *Int Dairy J* 16(4):361–369
- Nie S, Xie M, Fu Z et al (2008) Study on the purification and chemical compositions of tea glycoprotein. *Carbohydr Polym* 71(4):626–633
- Nie SP, Cui SW, Phillips AO et al (2011) Elucidation of the structure of a bioactive hydrophilic polysaccharide from *cordyceps sinensis* by methylation analysis and nmr spectroscopy. *Carbohydr Polym* 84(3):894–899
- Nie SP, Cui SW, Xie MY (2018) *Bioactive polysaccharides*. Elsevier, Amsterdam, pp 1–141
- Nongonierma AB, FitzGerald RJ (2016) Strategies for the discovery, identification and validation of milk protein-derived bioactive peptides. *Trends Food Sci Technol* 50:26–43
- Oba K, Kobayashi M, Matsui T et al (2009) Individual patient based meta-analysis of lentinan for unresectable/recurrent gastric cancer. *Anticancer Res* 29(7):2739–2745
- Otani H, Nakano K, Kawahara T (2003) Stimulatory effect of a dietary casein phosphopeptide preparation on the mucosal IgA response of mice to orally ingested lipopolysaccharide from *Salmonella typhimurium*. *Biosci Biotech Bioch* 67(4):729–735
- Palacios I, García-Lafuente A, Guillamón E et al (2012) Novel isolation of water-soluble polysaccharides from the fruiting bodies of *pleurotus ostreatus* mushrooms. *Carbohydr Res* 358:72–77
- Pan DD, Wu Z, Liu J et al (2013a) Immunomodulatory and hypoallergenic properties of milk protein hydrolysates in ICR mice. *J Dairy Sci* 96(8):4958–4964
- Pan LH, Feng BJ, Wang JH et al (2013b) Structural characterization and anti-glycation activity in vitro of a water-soluble polysaccharide from *dendrobium huoshanense*. *J Food Biochem* 37(3):313–321
- Pan Y, Wang C, Chen Z et al (2017) Physicochemical properties and antidiabetic effects of a polysaccharide from corn silk in high-fat diet and streptozotocin-induced diabetic mice. *Carbohydr Polym* 164:370–378
- Peña-Ramos EA, Xiong YL (2002) Antioxidative activity of whey protein hydrolysates in a liposomal system. *J Dairy Sci* 84(12):2577–2583
- Peng GY, Guo Z, Kuniwa Y, Voo KS et al (2005) Toll-like receptor 8-mediated reversal of CD4+ regulatory T cell function. *Science* 309(5739):1380–1384
- Pietrzycka A, Stepniewski M, Waszkielewicz AM et al (2006) Effect of vita glucan on some antioxidant parameters of the human blood in vitro study. *Acta Pol Pharm* 63(6):547
- Pimentel FB, Alves RC, Harnedy PA et al (2019) Macroalgal-derived protein hydrolysates and bioactive peptides: enzymatic release and potential health enhancing properties. *Trends Food Sci Technol* 93:106–124
- Plüddemann A, Mukhopadhyay S, Gordon S (2011) Innate immunity to intracellular pathogens: macrophage receptors and responses to microbial entry. *Immunol Rev* 240(1):11–24
- Poeck H, Besch R, Maihoefer C et al (2008) 5'-triphosphate-sirna: turning gene silencing and rig-i activation against melanoma. *Nat Med* 14(11):1256–1263
- Pomeroy S, Tupper R, Cehun-Aders M et al (2001) Oat  $\beta$ -glucan lowers total and LDL-cholesterol. *Aust J Nutr Diet* 58:51–55
- Prajapati VD, Maheriya PM, Jani GK et al (2014) Carrageenan: a natural seaweed polysaccharide and its applications. *Carbohydr Polym* 105:97–112
- Prashanth KVH, Tharanathan RN (2007) Chitin/chitosan: modifications and their unlimited application potential—an overview. *Trends Food Sci Technol* 18(3):117–131
- Qian Y, Wang D, Fan M et al (2018) Effects of intrinsic metal ions of lentinan with different molecular weights from *Lentinus edodes* on the antioxidant capacity and activity against proliferation of cancer cells. *Int J Biol Macromol* 120:73–81
- Rice PJ, Adams EL, Ozment-Skelton T et al (2005) Oral delivery and gastrointestinal absorption of soluble glucans stimulate increased resistance to infectious challenge. *J Pharmacol Exp Ther* 314:1079–1086

- Ron N, Zimet P, Bargarum J et al (2010) Beta-lactoglobulin-polysaccharide complexes as nanovehicles for hydrophobic nutraceuticals in non-fat foods and clear beverages. *Int Dairy J* 20:686–693
- Rosenson RS, Otvos JD, Freedman DS (2002) Relations of lipoprotein subclass levels and low-density lipoprotein size to progression of coronary artery disease in the pravastatin limitation of atherosclerosis in the coronary arteries (plac-i) trial. *Am J Cardiol* 90(2):89–94
- Saluk J, Bijak M, Ponczek MB et al (2013) (1→3)- $\beta$ -d-glucan reduces the damages caused by reactive oxygen species induced in human platelets by lipopolysaccharides. *Carbohydr Polym* 97(2):716–724
- Sanjukta S, Rai AK (2016) Production of bioactive peptides during soybean fermentation and their potential health benefits. *Trends Food Sci Technol* 50:1–10
- Schepetkin IA, Faulkner CL, Nelson-Overton LK et al (2005) Macrophage immunomodulatory activity of polysaccharides isolated from *Juniperus scopolorum*. *Int Immunopharmacol* 5 (13–14):1783–1799
- Schepetkin IA, Quinn MT (2006) Botanical polysaccharides: macrophage immunomodulation and therapeutic potential. *Int Immunopharmacol* 6(3):317–333
- Sener G, Toklu H, Ercan F et al (2005) Protective effect of  $\beta$ -glucan against oxidative organ injury in a rat model of sepsis. *Int Immunopharmacol* 5(9):1387–1396
- Shah N, Shah T, Amin A (2011) Polysaccharides: a targeting strategy for colonic drug delivery. *Expert Opin Drug Deliv* 8:779–796
- Sharma SK, Gautam N, Atri NS (2015) Optimized extraction, composition, antioxidant and antimicrobial activities of exo and intracellular polysaccharides from submerged culture of *cordyceps cicadae*. *BMC Complement Altern Med* 15(1):446
- Shen J, Park HS, Xia YM et al (2014) The polysaccharides from fermented *ganoderma lucidum* mycelia induced miRNAs regulation in suppressed HepG2 cells. *Carbohydr Polym* 103:319–324
- Sheu F, Chien PJ, Chien AL et al (2004) Isolation and characterization of an immunomodulatory protein (APP) from the Jew's Ear mushroom *Auricularia polytricha*. *Food Chem* 87(4):593–600
- Shi X, Wei W, Wang N (2018) *Tremella* polysaccharides inhibit cellular apoptosis and autophagy induced by *Pseudomonas aeruginosa* lipopolysaccharide in A549 cells through sirtuin 1 activation. *Oncol Lett* 15:9609–9616
- Shimizu K, Watanabe S, Watanabe S et al (1999) Efficacy of oral administered superfine dispersed lentinan for advanced pancreatic cancer. *Hepato-Gastroenterology* 56(89):240–244
- Shriner AK, Liu H, Sun G et al (2010) IL-7-dependent B lymphocytes are essential for the anti-polysaccharide response and protective immunity to *streptococcus pneumoniae*. *J Immunol* 185 (1):525–531
- Silva FGDE, Hernández-Ledesma B, Amigo L et al (2017) Identification of peptides released from flaxseed (*Linum usitatissimum*) protein by Alcalase®; hydrolysis: antioxidant activity. *LWT Food Sci Technol* 76:140–146
- Song G, Du Q (2012) Structure characterization and antitumor activity of an  $\alpha\beta$ -glucan polysaccharide from *auricularia polytricha*. *Food Res Int* 45(1):381–387
- Stack J, Tobin PR, Gietl A et al (2017) Seasonal variation in nitrogenous components and bioactivity of protein hydrolysates from *Porphyra dioica*. *J Appl Phycol* 29:2439–2450
- Steiner H, Hultmark D, Engstrom A et al (1981) Sequence and specificity of two antibacterial proteins involved in insect immunity. *Nature* 292(5820):246–248
- Steinman RM, Banchereau J (2007) Taking dendritic cells into medicine. *Nature* 449:419–426
- Sun Y, Jiang L, Wei D (2013) Partial characterization, in vitro antioxidant and antiproliferative activities of patatin purified from potato fruit juice. *Food Funct* 4:1502–1511
- Sun Y, Li X, Yang J et al (2010) Water-soluble polysaccharide from the fruiting bodies of *chroogomphis rutilus* (Schaeff.: Fr.) o. k. miller: isolation, structural features and its scavenging effect on hydroxyl radical. *Carbohydr Polym* 80(3):720–724

- Sun Y, Li X, Yang J et al (2010) Water-soluble polysaccharide from the fruiting bodies of *Chroogomphus rutilus* (Schaeff.: Fr.) O. K. Miller: isolation, structural features and its scavenging effect on hydroxyl radical. *Carbohydr Polym* 80(3):720–724
- Suphantharika M, Khunrae P, Thanardkit P et al (2003) Preparation of spent brewer's yeast  $\beta$ -glucans with a potential application as an immunostimulant for black tiger shrimp, *Penaeus monodon*. *Bioresour Technol* 88(1):55–60
- Suresh V, Senthilkumar N, Thangam R et al (2013) Separation, purification and preliminary characterization of sulfated polysaccharides from *Sargassum plagiophyllum* and its in vitro anticancer and antioxidant activity. *Process Biochem* 48(2):364–373
- Taguchi T (1983) Effects of lentinan in advanced or recurrent cases of gastric, colorectal, and breast cancer. *Gan To Kagaku Ryoho* 10(2):387–393
- Takahashi M, Kitamoto D, Asikin Y et al (2009) Liposomes encapsulating *aloe vera* leaf gel extract significantly enhance proliferation and collagen synthesis in human skin cell lines. *J Oleo Sci* 58(12):643–650
- Tani M, Tanimura H, Yamaue H et al (1993) Augmentation of lymphokine-activated killer cell activity by lentinan. *Anticancer Res* 13(5):1773–1776
- Teng Z, Qian L, Zhou Y (2013) Hypolipidemic activity of the polysaccharides from *enteromorpha prolifera*. *Int J Biol Macromol* 62:254–256
- Van der Sman R, Van der Goot A (2009) The science of food structuring. *Soft Matter* 5(3):501–510
- Vannucci L, Krizan J, Sima P et al (2013) Immunostimulatory properties and antitumor activities of glucans (review). *Int J Oncol* 43(2):357–364
- Vidovic D, Graddis T, Chen F et al (2002) Antitumor vaccination with HER-2-derived recombinant antigens. *Int J Cancer* 102:660–664
- Wang CL, Meng M, Liu SB et al (2013) A chemically sulfated polysaccharide from *grifola frondosa* induces HepG2 cell apoptosis by notch1-NF- $\kappa$ B pathway. *Carbohydr Polym* 95(1):282–287
- Wang CL, Pi CC, Kuo CW et al (2011) Polysaccharides purified from the submerged culture of *Ganoderma formosanum* stimulate macrophage activation and protect mice against *Listeria monocytogenes* infection. *Biotechnol Lett* 33:2271–2278
- Wang GJ (2012) A systematic research on lentinan injection preparation quality standard. The Second Military Medical University, Shanghai
- Wang HX, Ng TB (2007) An antifungal peptide from red lentil seeds. *Peptides* 28(3):547–552
- Wang X, Wang Y, Zhou Q et al (2020) Immunomodulatory effect of Lentinan on aberrant T subsets and cytokines profile in non-small cell lung cancer patients. *Pathol Oncol Res* 26(1):499–505
- Wang Y, Zhang L (2006) Chain conformation of carboxymethylated derivatives of (1  $\rightarrow$ 3)- $\beta$ -D-glucan from *poria cocos sclerotium*. *Carbohydr Polym* 65(4):504–509
- Wang YJ, Yu YZ, Mao JW (2009) Carboxymethylated D-glucan derived from *Poria cocos* with biological activities. *J Agric Food Chem* 57(22):10913–10915
- Wijaya W, Patel AR, Setiowati AD et al (2017) Functional colloids from proteins and polysaccharides for food applications. *Trends Food Sci Technol* 68:56–69
- Wood PJ (2007) Cereal  $\beta$ -glucans in diet and health. *J Cereal Sci* 46:230–238
- Wong KH, Lai CKM, Cheung PCK (2011) Immunomodulatory activities of mushroom sclerotial polysaccharides. *Food Hydrocolloid* 25(2):150–158
- Wu DT, Guo H, Lin S et al (2018) Review of the structural characterization, quality evaluation, and industrial application of, *lycium barbarum*, polysaccharides. *Trends Food Sci Technol* 79:171–183
- Wu DT, Meng LZ, Wang LY et al (2014) Chain conformation and immunomodulatory activity of a hyperbranched polysaccharide from *cordyceps sinensis*. *Carbohydr Polym* 110:405–414
- Wu J, Chen J, Song Z et al (2017) Anticancer activity of polysaccharide from *glehnia littoralis* on human lung cancer cell line A549. *Int J Biol Macromol* 106:464–472
- Wu Q, Yang BX (2010) Observation on effect of combined use of fucoidan polysaccharide sulfate and benazepril for treatment of early diabetic nephropathy. *Clin J Med Off* 38(5):743–745

- Xia L, Liu X, Guo H et al (2012) Partial characterization and immunomodulatory activity of polysaccharides from the stem of *dendrobium officinale* (Tiepishihu) in vitro. *J Funct Foods* 4 (1):294–301
- Xiao C, Wu Q, Zhang J et al (2016) Antidiabetic activity of *ganoderma lucidum* polysaccharides F31 down-regulated hepatic glucose regulatory enzymes in diabetic mice. *J Ethnopharmacol* 196:47–57
- Xie JH, Jin ML, Morris GA et al (2016) Advances on bioactive polysaccharides from medicinal plants. *Crit Rev Food Sci* 60:S60–S84
- Xu J (2012) Effects of *astragalus* polysaccharide combined with Megestrol on life quality improvement of patients with advanced malignant tumor. *Chin Trad Herb Drug* 43 (7):1385–1386
- Xu JD (2015) Effect of *ginseng* polysaccharide injection combined with chemotherapy on immune function and therapeutic of the patients with advanced gastric cancer. *Cent South Pharm* 13 (3):316–321
- Xue H, Gan F, Zhang Z et al (2015) *Astragalus* polysaccharides inhibits pcv2 replication by inhibiting oxidative stress and blocking NF- $\kappa$ B pathway. *Int J Biol Macromol* 81:22–30
- Ya GW (2017) A *Lentinus edodes* polysaccharide induces mitochondrial-mediated apoptosis in human cervical carcinoma HeLa cells. *Int J Biol Macromol* 103:676–682
- Yamamoto S, Takatori K, Ohmoto K et al (1989) NK activity and T cell subsets in percutaneous ethanol injection therapy of liver cancer-effect of lentinan with combined use. *Gan To Kagaku Ryoho* 16(9):3291–3294
- Yan JK, Li L, Wang ZM et al (2009) Acidic degradation and enhanced antioxidant activities of exopolysaccharides from *cordyceps sinensis* mycelial culture. *Food Chem* 117(4):641–646
- Yang B, Xiao B, Sun T (2013) Antitumor and immunomodulatory activity of *astragalus membranaceus* polysaccharides in H22 tumor-bearing mice. *Int J Biol Macromol* 62 (11):287–290
- Yang R, Zhang Z, Pei X et al (2009) Immunomodulatory effects of marine oligopeptide preparation from chum Salmon (*Oncorhynchus keta*) in mice. *Food Chem* 113(2):464–470
- Yang Y, Xing R, Liu S et al (2018) Immunostimulatory effects of sulfated chitosans on RAW 264.7 mouse macrophages via the activation of PI3K/Akt signaling pathway. *Int J Biol Macromol* 108:1310–1321
- Yang Y, Zhang MW, Liao ST et al (2012) Structural features and immunomodulatory activities of polysaccharides of *longan* pulp. *Carbohydr Polym* 87:636–643
- Yang Z, Li S, Zhang X et al (2010) Capsular and slime-polysaccharide production by *lactobacillus rhamnosus* jaas8 isolated from chinese sauerkraut: potential application in fermented milk products. *J Biosci Bioeng* 110(1):53–57
- Yang Z, Wu F, Yang H et al (2017) Endocytosis mechanism of a novel proteoglycan, extracted from *ganoderma lucidum*, in HepG2 cells. *RSC Adv* 7(66):41779–41786
- Ye H, Wang K, Zhou C et al (2008) Purification, antitumor and antioxidant activities in vitro of polysaccharides from the *brown seaweed sargassum pallidum*. *Food Chem* 111(2):428–432
- Yeo IC, Lee NK, Hahm YT (2012) Genome sequencing of *Bacillus subtilis* SC-8, antagonistic to the *Bacillus cereus* group, isolated from traditional Korean fermented-soybean. *Food J Bacteriol* 194:536–537
- Yi W, Zhang P, Hou J et al (2018) Enhanced response of tamoxifen toward the cancer cells using a combination of chemotherapy and photothermal ablation induced by lentinan-functionalized multi-walled carbon nanotubes. *Int J Biol Macromol* 120:1525–1532
- Yi Y, Zhang MW, Liao ST et al (2012) Structural features and immunomodulatory activities of polysaccharides of *longan* pulp. *Carbohydr Polym* 87(1):636–643
- Yin JY, Lin HX, Nie SP et al (2012) Methylation and 2d nmr analysis of arabinoxylan from the seeds of *plantago asiatica*. *Carbohydr Polym* 88(4):1395–1401
- Yu J, Sun R, Zhao Z et al (2014) *Auricularia polytricha* polysaccharides induce cell cycle arrest and apoptosis in human lung cancer A549 cells. *Int J Biol Macromol* 68:67–71



- Yu L, Yue H, Liu Y et al (2012) Effect of red *ginseng* polysaccharide on bread quality. *Sci Technol Food Ind* 24:332–338
- Yu Q, Nie SP, Li WJ et al (2013) Macrophage immunomodulatory activity of a purified polysaccharide isolated from *ganoderma atrum*. *Phytother Res* 27(2):186–191
- Yu W, Ren Z, Zhang X et al (2018) Structural characterization of polysaccharides from *dendrobium officinale* and their effects on apoptosis of HeLa cell line. *Molecules* 23(10):2484
- Zhai QL, Hu XD, Xiao J et al (2018) *Astragalus* polysaccharide may increase sensitivity of cervical cancer HeLa cells to cisplatin by regulating cell autophagy. *China J Chin Mat Med* 43(4):805–812
- Zhang D, Meng H, Yang HS (2012) Antidiabetic activity of *taxus cuspidata* polysaccharides in streptozotocin-induced diabetic mice. *Int J Biol Macromol* 50(3):720–724
- Zhang H, Cui SW, Nie SP et al (2016a) Identification of pivotal components on the antioxidant activity of polysaccharide extract from *ganoderma atrum*. *Bioact Carbohydr Diet Fib* 7(2):9–18
- Zhang L, Chen L, Xu X et al (2005) Comparison on chain stiffness of a water-insoluble (1→3)- $\alpha$ -d-glucan isolated from *Poria cocos* mycelia and its sulfated derivative. *Carbohydr Polym* 59:257–263
- Zhang WQ, Huang YS, Zhi XX (2008) Application of hyaluronic acid to clinical medicine. *J Clin Rehabil Tissue Eng Res* 12(23):4515–4518
- Zhang XR, Zhou WX, Zhang YX et al (2011) Macrophages, rather than t and b cells are principal immunostimulatory target cells of *lycium barbarum L.* polysaccharide LBPF4-OL. *J Ethnopharmacol* 136(3):465–472
- Zhang XR, Qi CH, Cheng JP et al (2014) *Lycium barbarum* polysaccharide LBPF4-OL may be a new toll-like receptor 4/MD2-MAPK signaling pathway activator and inducer. *Int Immunopharmacol* 19(1):132–141
- Zhang Y, Hu T, Zhou HL et al (2016b) Antidiabetic effect of polysaccharides from *pleurotus ostreatus* in streptozotocin-induced diabetic rats. *Int J Biol Macromol* 83:126–132
- Zhang Y, Wang L, Du MN (2016c) Research progress on treatment of tumor with *Astragalus* polysaccharides for injection. *Drug Eval Res* 39(6):1092–1094
- Zhao L, Xiao Y, Xiao N (2013) Effect of lentinan combined with docetaxel and cisplatin on the proliferation and apoptosis of BGC823 cells. *Tumor Biol* 34(3):1531–1536
- Zhao LY, Lan QJ, Huang ZC et al (2011) Antidiabetic effect of a newly identified component of *opuntia dillenii* polysaccharides. *Phytomedicine* 18(8–9):661–668
- Zhao R, Zhang T, Ma B et al (2016) Antitumor activity of *Portulaca Oleracea L.* polysaccharide on HeLa cells through inducing TLR4/NF- $\kappa$ B signaling. *Nutr Cancer* 69(1):131–139
- Zhao YM, Yang JM, Liu YH et al (2017) Ultrasound assisted extraction of polysaccharides from *lentinus edodes* and its anti-hepatitis B activity in vitro. *Int J Biol Macromol* 107:2217–2223
- Zhou X, Wang D, Sun P et al (2007) Effects of soluble tea polysaccharides on hyperglycemia in alloxan-diabetic mice. *J Agric Food Chem* 55(14):5523–5528
- Zhu BY, He H, Hou T (2019) A comprehensive review of corn protein-derived bioactive peptides: production, characterization, bioactivities, and transport pathways. *Compr Rev Food Sci Food Saf* 18:329–345
- Zhu K, Nie S, Li C et al (2013) A newly identified polysaccharide from *ganoderma atrum* attenuates hyperglycemia and hyperlipidemia. *Int J Biol Macromol* 57:142–150
- Zong A, Cao H, Wang F (2012) Anticancer polysaccharides from natural resources: a review of recent research. *Carbohydr Polym* 90:1395–1410
- Zou Y, Meng J, Chen W et al (2011) Modulation of phenotypic and functional maturation of murine dendritic cells (DCS) by purified *achyrantes bidentata* polysaccharide (ABP). *Int Immunopharmacol* 11(8):1103–1108

# Chapter 15

## Dietary Fibers: Structural Aspects and Nutritional Implications



**Bin Zhang, Shaokang Wang, Santad Wichienchot, Qiang Huang, and Sushil Dhital**

**Abstract** Along with the brief outline of the definition evolution of dietary fibers, this chapter focuses on how the physical and chemical structures of fibers are related to the health effects. The role of fiber in the human digestive tract including oral, gastric, small intestinal, and large intestinal phases is also discussed. Our further emphasis is on the colonic microbial fermentation performance and health implications of dietary fibers. Fibers with higher water holding capacity or viscosity are desirable for slowing down the metabolic response (e.g., post prandial blood glucose

---

B. Zhang (✉)

School of Food Science and Engineering, Guangdong Province Key Laboratory for Green Processing of Natural Products and Product Safety, South China University of Technology, Guangzhou, China

Department of Applied Biology and Chemical Technology, The Hong Kong Polytechnic University, Hung Hom, Kowloon, Hong Kong, China

Overseas Expertise Introduction Center for Discipline Innovation of Food Nutrition and Human Health (111 Center), Guangzhou, China

e-mail: [zhangb@scut.edu.cn](mailto:zhangb@scut.edu.cn)

S. Wang

School of Food Science and Engineering, Guangdong Province Key Laboratory for Green Processing of Natural Products and Product Safety, South China University of Technology, Guangzhou, China

S. Wichienchot

Center of Excellence in Functional Foods and Gastronomy, Faculty of Agro-Industry, Prince of Songkla University, Hat Yai, Songkhla, Thailand

Q. Huang

School of Food Science and Engineering, Guangdong Province Key Laboratory for Green Processing of Natural Products and Product Safety, South China University of Technology, Guangzhou, China

Overseas Expertise Introduction Center for Discipline Innovation of Food Nutrition and Human Health (111 Center), Guangzhou, China

S. Dhital

Department of Chemical Engineering, Monash University, Clayton Campus, Clayton, VIC, Australia

level), whereas the fibers with slow fermentation throughout the colon and higher level of butyrate/propionate production are considered ideal for colonic health. Thus foods that have the balance of viscous and slowly fermentable fibers are considered beneficial in terms of overall nutrition and health. Although role of fibers in small intestine is well studied and known, how the fiber specificity can modulate the gut microbial ecology for desired health benefits still needs further research investigation.

**Keywords** Dietary fiber · Definition · Chemical structure · Fermentation performance · Health implications

## 1 Definition, Structure, and Analysis of Dietary Fiber

### 1.1 What Is Dietary Fiber?

Definition of dietary fiber has a very long history. Several progressions are made on defining the dietary fiber, yet no single consensus definition of dietary fiber is agreed. Hipsley (1953) first introduced the term “dietary fiber (DF).” In 2001, the American Association of Cereal Chemists International (now Cereals & Grains Association) proposed a definition and is most widely accepted. DF is defined as “the edible parts of plants or analogous carbohydrates that are resistant to digestion and absorption in the human small intestine with complete or partial fermentation in the large intestine.” Thus, the term included non-starch polysaccharides (e.g., cellulose, pectin, gums), resistant oligosaccharides (e.g., fructooligosaccharides, galactooligosaccharides), and other carbohydrates (e.g., resistant starch (RS), resistant dextrin). Moreover, the non-carbohydrate-based polymers (e.g., lignin) and some animal origin carbohydrates (e.g., chitin, hyaluronan, chondroitin sulfate) are also considered in this definition. In 2006, the Japanese Association for Dietary Fiber Research defined as “dietary components which are not digested and/or absorbed in the human small intestine and which exert physiological effect that are useful in maintaining good health via the gastrointestinal tract”(Kiriya et al. 2006). In 2009, Codex Alimentarius Commission, an international body that sets guidelines for national regulatory authorities, defined DF as carbohydrate polymers with at least ten monomer units, which cannot be hydrolyzed by the enzymes in the small intestine. Three categories were set as follows: (1) Edible carbohydrate polymers existing in food as ingredients, (2) Carbohydrate polymers prepared from raw food ingredients by different processing methods, including physical, enzymatic, and chemical methods; beneficial metabolic effects were tested and approved. (3) Carbohydrate polymers which are synthesized but proven by scientific evidence with healthy effects to the host (Alimentarius 2010). Most recently, US Food and Drug Administration (FDA) published the official definition for the first time that defines the DF as “non-digestible soluble and insoluble carbohydrates (with 3 or more monomeric units) and lignin that are intrinsic and intact in plants; isolated or

synthetic non-digestible carbohydrates (with 3 or more monomeric units) determined by the FDA to have physiological effects that are beneficial to human health.” In the recent rule, USFDA (2016) clearly mentioned that fibers that are naturally present in the food and associated with food matrices (intrinsic) with no relevant components removed or destroyed during processing (intact) do not need to be approved to be quantified as dietary fiber. However, the externally added dietary fiber needs to be approved by FDA before listing them as dietary fiber or making any nutrient content or health claim. This definition is dramatically different from the previous definition, in a sense, the definition specifies that the added dietary fiber (except that are approved by FDA), though technically is fiber but do not necessarily provide the physiological benefits so are excluded from the approved list of fibers. The FDA has identified psyllium husk, beta-glucan soluble fiber, guar gum, locust bean gum, cellulose, pectin, and hydroxypropyl methylcellulose as the non-digestible carbohydrates that can be added into the food or food formulations as dietary fiber. However, widely accepted fiber such as “inulin” is not in the list of approved fiber, so foods that have additional inulin will not be able to make fiber claims (Dhital et al. 2018).

## ***1.2 Structure and Physicochemical Properties of Dietary Fibers***

Dietary fibers can be categorized in different ways such as structure and solubility. According to solubility, dietary fibers are normally identified as either soluble or insoluble DFs. Insoluble dietary fiber (IDF) mainly consists of cell wall components, such as cellulose, lignin, hemicellulose. While soluble dietary fiber (SDF) mainly contains non-cellulosic polysaccharides, such as beta-glucans, gums, pectin, pentosans, and mucilage (Chawla and Patil 2010). The molecular/chemical structure is the key to understanding whether the dietary fiber is soluble in water. Chemical structures of common dietary fibers are given in Table 15.1, which shows that dietary fibers are composed of linked monosaccharide units. Physical properties (e.g., solubility) of dietary fiber is determined more by the inter- and intra-chain linkages than the nature of the monosaccharide units, which can be defined by comparing two forms of the water-soluble  $\beta$ -glucan and insoluble poly-D-cellulose. Cellulose is a homopolymer of  $\beta$ -1-4-linked glucose, whereas  $\beta$ -glucans have mixed  $\beta$ -(1-3) and  $\beta$ -(1-4) linkages. The regularity of cellulose can be realized by adopting crystalline structures with hydrogen bonds and thus formed the ordered insoluble structure. On the other hand, the irregular structure of the  $\beta$ -glucans prevents the formation of ordered crystalline structures, so the water soluble fibers could be achieved. Besides, branched structures are unable to adopt ordered crystalline structures, and they are also soluble (arabinoxylans in cereals). However, the ester bond between ferulic acid moieties “cross-links” the multiple chains making them insoluble. Thus based on the degree of crosslinking, the arabinoxylan (AX) can be soluble (e.g., in endosperm cell

**Table 15.1** Chemical structure of selected dietary fibers

Dietary fiber	Chemical structure	Dietary fiber	Chemical structure
<i>Pectin</i>		<i>Hemicelluloses</i>	
Homogalacturonan	Linear $\alpha$ -(1,4) GalA units partially methylated and acetylated	Arabinoxylan	$\beta$ -(1,4) Xyl units as the backbone with side chains of Ara units via $\alpha$ -(1,2), $\alpha$ -(1,3), and $\alpha$ -(1,5). Gal, GluA, and FerA units may also be present in the branched points
Rhamnogalacturonan-I	Linear $\alpha$ -(1,4) GalA and $\alpha$ -(1,2) Rha units	Xylan	$\beta$ -(1,4)-D-xylose
Rhamnogalacturonan-II	Linear $\alpha$ -(1,4) GalA units branched with Api, Ara, AceA, Dha, Fuc, Gal, GluA, Kdo, Rha, Xyl	Xyloglucan	$\beta$ -(1,4) Glu units as the backbone with single unit side chains of $\alpha$ -(1,6) Xyl. Gal, and Fuc may also be present in the branched point
Pectic galactan	$\beta$ -(1,4) Gal, $\beta$ -(1,6) Gal, $\alpha$ -(1,4) Ara unit	Glucomannan	Linear or slightly branched backbone chain of $\beta$ -(1,4) Man and $\beta$ -(1,4) Glu
Arabinogalactan-type I	$\beta$ -(1,4)-D-galactose	Galactomannan	Linear or slightly branched backbone chain of $\beta$ -(1,4) Man moreover, $\beta$ -(1,4) Glu with side chains of $\alpha$ -(1,6) Gal
Arabinogalactan-type II	$\beta$ -(1,3)- and $\beta$ -(1,6)-D-galactose	$\beta$ -Glucan	Repeating linear polymer of two $\beta$ -(1,4) Glu alternated with $\beta$ -(1,3) Glu units
Arabinan	$\alpha$ -(1,5), (1,3) Moreover, $\alpha$ -(1,2) Ara units	Galactoglucomannan	$\beta$ -(1,4)-D-mannose, $\beta$ -(1,4)-D-glucose
$\beta$ -1,4-D-Galactan	$\beta$ -1,4-D-galactose	Mannan	$\beta$ -(1,4)-D-mannose
$\beta$ -1,3-D-Galactan	$\beta$ -1,3-D-galactose	Arabinogalactan (proteoglycan)	$\beta$ -(1,6)-D-galactose. Linked to peptides
<i>Cellulose</i>	Linear $\beta$ -(1,4) Glu units	<i>Gums</i>	
<i>Polyfructans</i>		Carrageenan	Sulfated galactans, units of $\beta$ -(1,3) Gal and $\alpha$ -(1,4) linked 3,6 anhydro Gal
Inulin	$\beta$ -(2,1) Fru	Alginate	Linear $\beta$ -(1,4) ManA and $\alpha$ -(1,4) GluA
Levan	$\beta$ -(2,6) Fru	Locust bean gum	$\beta$ -(1,4)-D-mannose
<i>Chitin</i>	$\beta$ -(1,4)-N-acetyl-D-glucosamine	Furcellaran	D-galactose, D-galactose-sulfate, 3,6-anhydro-D-

(continued)

**Table 15.1** (continued)

Dietary fiber	Chemical structure	Dietary fiber	Chemical structure
			galactose, 3,6-anhydro-D-galactose-2-sulfate
<i>Chitosan</i>	$\beta$ -(1,4)-D-glucosamine and $\beta$ -(1,4)-N-acetyl-D-glucosamine	Agar	Heterogenous product: mainly $\beta$ -D-galactose and 3,6-anhydro- $\alpha$ -L-galactose, which alternate through 1,4 and 1,3 linkages
<i>Lignin</i>	Polyphenols, Syringyl alcohol, Guaiacyl alcohol, and p-coumaryl alcohol	Gum Arabic	$\beta$ -(1,3)-D-galactose
<i>Resistant starch</i>	$\alpha$ -(1,4)-D-glucose units with few $\alpha$ -(1,6)-D-glucose branches	Gum Guarani (guar)	$\beta$ -(1,4)-D-mannose
		Xanthan gum	$\beta$ -(1,4)-D-glucose

Abbreviations used: *AceA* acetic acid, *Ara* arabinose, *Api* apiose, *Dha* 3-deoxy-D-lyxo-2-heptulosaric acid, *FerA* ferulic acid, *Fru* fructose, *Fuc* fucose, *Gal* galactose, *GalA* galacturonic acid, *Glu* glucose, *GluA* glucuronic acid, *Kdo* 3-deoxy-D-manno-2-octulosonic acid, *Man* mannose, *Man A* mannuronic acid, *Rha* rhamnose, *Xyl* xylose

walls of oat and barley) or insoluble (e.g., in wheat bran and wheat endosperm cell walls) (Gartaula et al. 2018). Dietary fibers with charged groups (e.g.,  $\text{COO}^-$  or  $\text{SO}_3^{3-}$ ) such as the pectin and carrageenan are also water soluble, due to the electrostatic repulsion preventing the molecules from being closely packed together in an ordered structure (Oakenfull et al. 2001).

Solubility is also closely related to other physicochemical properties of dietary fibers, such as water holding capacity and viscosity. Generally, strongly hydrophilic properties existed in the polysaccharide constituents (monosaccharides) of dietary fibers. Water is conserved on the void spaces in the molecular structure or the hydrophilic sites (Mudgil and Barak 2013). Gel-forming or viscosity ability is linked with the capacity to absorb water and form a gelatinous mass. It is attributed to the physical interactions between polysaccharide molecules in solution, and the molecules become entangled. Generally, the viscosity of solution is mainly caused by water-soluble fibers. Gels were obtained from soluble fibers, and the viscosity and bulk of the contents of the gastrointestinal tract could increase. It was well reported that gels have good viscoelastic properties and could respond both elastic behavior and viscous behavior in human gastrointestinal tract. This viscoelastic behavior is responsible for the delayed gastric emptying of foods rich in fibers. Soluble fibers increase bulk (gelling) property, whereas insoluble fibers increase the mass (water holding or absorption) of the luminal content. However, the classification of dietary fibers as “soluble” or “insoluble” may not be sufficient to explain the functionality of dietary fibers (Gidley and Yakubov 2019). For instance, a large amount of dietary

fiber in foods is either soluble (e.g., cereal endosperm flours), or highly hydrated but insoluble (e.g., fruits and cereal brans).

## **2 Roles of Dietary Fiber in the Digestive Tract**

### ***2.1 The Oral and Gastric Processing of Dietary Fiber***

Mouth and stomach play crucial roles in the mechanical and enzymatic breakdown of food structure as well as in appetite regulation. The mechanical process in mouth facilitates the structural breakdown of food, which further disintegrates the fiber into more softer and homogenous boluses, which can be easily swallowed and pass through the esophagus before reaching to stomach. Only a small amount of macronutrients can be digested, including hydrolysis of starch (Brownlee 2014). However, the bio-accessibility of nutrients could be improved through the plant cell walls' mechanical breakdown during mastication (Ellis et al. 2004), and is possibly to change the taste perception of these foods.

The end-product of oral processing, i.e., food bolus, enters the stomach and mixes with gastric secretions. Dietary fibers have a significant impact on gastric processing events, as the physical structure and material profiles of plant-based food bolus could be determined, hence the dilution, transport along with mixing profile of the stomach could be affected. For instance, the gastric emptying can be slowed down when dietary fibers form gel in the acid conditions in the large intestine, and the timescale of nutrient delivery along with perceived satiety can be prolonged. For example, oat porridge has a higher satiety index as well as glycemic response compared to white bread. This is solely due to the bulking property of oats in the stomach increasing the gastric retention time. Set micellar casein as another example. Through acidification, micellar casein in milk can be converted from a thin liquid to a solid, thus it can be delivered from mouth to stomach. This process leads to the less rapidly digested properties of the casein fraction of milk when compared to whey protein fraction (without gelation under gastric condition) (Gidley 2013).

### ***2.2 Small Intestine Digestion and Dietary Fiber***

The small intestine is the primary site for digestion and absorption of nutrients such as dietary carbohydrates, lipids, proteins as well as micronutrients. Although a minor physical degradation on molecular size may occur in the small intestine, dietary fibers remain intact in the small intestine but play an essential role in modulating small intestinal behavior of plant-based food, such as passage rate and enzyme digestion process. It was well suggested that the absorption and digestion as well as bolus transport in human small intestine can be influenced as a function of physicochemical profiles belong to soluble DF, including water holding capacity,

organic compound entrapment, and viscosity (Bach Knudsen 2001). Generally, soluble DFs with high viscosity are linked with slow transit time through stomach and small intestine. The increase in viscosity and bulky forming is usually associated with the high molecular size and branching structures, as well as the ability to tie endogenous compounds such as bile acids and enzymes (Mackie et al. 2016). Absorption and digestion of dietary substrates could also be slowed down as a function of the capacities of organic compound entrapment or viscosity of DF. For example, it may affect the digestion by reducing the nutrient diffusion and bioavailability through the small intestine as a result of the viscosity and diluting of bolus compounds by adding non-digestible material (Innami et al. 2000).

Insoluble fiber does not dissolve in water but retains its structure. The influence of insoluble DF on nutrients digestibility in the small intestine is summed up in two hypotheses: (1) A higher absorption and digestion could occur when the nutrient properties of the bolus at the start stage of the small intestine are changed due to the prolonged retention time in the stomach. For example, insoluble DF in the bolus starts the degradation partially in the stomach and increases the solubilization, which speeds up the motion of food through the gut and increases the digestibility in the small intestine (Wilfart et al. 2007). (2) The digestion process could be changed due to the water and nutrients absorption ability of insoluble DF (Taghipoor et al. 2014). For example, insoluble DFs were proven to improve the access of the enzymes to the substrates by enhancing the propulsive contraction effects of the small intestine, which has a positive impact on digestion and absorption (Choct et al. 2000). Insoluble DFs also play a significant role by increasing the mass of luminal content forming feces in the colon.

### 3 Gut Microbial Fermentation of Dietary Fibers in the Colon

Because of the restriction of human-specific enzymes, only a few  $\alpha$ -glucosidic linkages (e.g.,  $\alpha$ -1,2,  $\alpha$ -1,3,  $\alpha$ -1,4,  $\alpha$ -1,6 bonds) present in a subset of carbohydrates can be degraded in the upper gastrointestinal tract. A complex microbial community, defined as gut microbiota, inhabits in the human gut. Human gut microbiota consist of at least  $10^{14}$  microorganisms belonging to over 1000 species, of which, members of Firmicutes (~60–65%), Bacteroidetes (~20–25%), Actinobacteria (~3%), and Proteobacteria (~5–10%) are the most common bacteria at the phylum level. Gut bacteria have more catabolic enzymes and advanced metabolic systems to ferment DFs for an energy source. The fermentation rate and end products of the fermentation are essential in providing the metabolic, immunologic, and protective functions. Gut microbiota, thus, can be perceived as a “digestive partner” or an “additional digestive organ” that has offered connection with human host and that provide healthy benefits.



### **3.1 Fermentation Rate**

During fermentation, the number of metabolites (normally gases and SCFAs) usually decreased from the proximal colon to the distal colon. Thus, a slow fermentation and metabolism of fiber are more preferable, and the requirements of energy of the distal colon could be realized (Rose et al. 2010; Williams et al. 2011a). It was generally accepted that the critical factors determining fermentation rate contain physical form and chemical structure of dietary fibers (Gidley 2013). In vitro fermentation models present a good way to investigate how gut microbiota use specific fiber and measure the quantity of metabolites and microbiota changes after fermentation, which has important implications for food nutrition. Here, we compared the in vitro fermentation profiles using human fecal inocula for a wide range of dietary fibers in Table. 15.2. Chemical structure of dietary fibers includes monosaccharide and linkage compositions, monosaccharide arrangements, molecular size, complexity, etc., and shows a considerable effect on the fermentation rate, particularly for soluble DFs. In general, soluble DFs are fermented faster and to a greater extent than insoluble fibers, and over-consumption might positively linked with some bad effects accompanied by fast fermentation rate, including eructation, bloating and flatulence (Hamaker and Tuncil 2014). Fermentation rate is also closely related to the physical form of fibers such as particle size (Day et al. 2012), and solubility (Williams et al. 2011b).

### **3.2 Short-Chain Fatty Acids Production and Related Gut Bacteria Growth**

DFs are major substrates of microbial fermentation leading to SCFA production. Generally, acetate, propionate, and butyrate are the main SCFAs produced, mainly in the proximal colon at very high concentrations (70–140 mM) and but distal colon at lower concentrations (20–70 mM) (Wong et al. 2006). The molar ratios of acetate, propionate, and butyrate from fiber fermentation normally are 60:25:15, respectively (Tan et al. 2014). SCFAs show excellent physiological activity, especially propionic and butyric acids. Except providing energy for the colon epithelial cells, the stimulation of the secretion of PYY and GLP-1 as well as the suppression of the primary inflammation of endothelial cells is an important function of SCFA (Topping and Lockett 2016). Acetate, a potential appetite-regulating agent, links to the blood–brain barrier and could reduce appetite through the function of a central homeostatic mechanism. Propionate is largely metabolized in the liver where it is possibly used as a glucogenic substrate, thus the related cholesterol synthesis could also be suppressed (Hassan Younes et al. 1995). Butyrate is the primary energy source for colonocytes and could hinder the proliferation of cancer cells, and accelerate differentiation of cancer cell apoptosis without affecting normal epithelial cell differentiation and proliferation (Comalada et al. 2006).

**Table 15.2** In vitro fermentation performance of various dietary fibers using human fecal inocula

Dietary fiber	Fermentation rate	SCFA molar ratio	Microbiota composition changes	References
Resistant starch type 2 (native starch granules)	Slow	Acetate↑ Butyrate↑	<i>Bifidobacterium</i> ↑, <i>Blautia</i> ↓, <i>Dorea</i> ↓, <i>Bacteroides</i> ↓	(Plongbunjong et al. 2017; Yang et al. 2013)
Resistant starch type 3 (retrograded starches)	Slow	Acetate↑ Butyrate↑	<i>Bifidobacterium</i> ↑	(Plongbunjong et al. 2017; Arcila and Rose 2015; Jonathan et al. 2012)
Resistant starch type 4 (chemically modified starches)	Slow	Acetate↑ Butyrate↑	<i>Bifidobacteria</i> ↑	(Bae et al. 2013; Thompson et al. 2011)
Arabinoxylan	Fast	Acetate↑ Butyrate↑	<i>Bacteroides</i> ↑, <i>Coprococcus</i> ↑, <i>Faecalibacterium</i> ↑	(Yang et al. 2013; Chen et al. 2017; Rumpagaporn et al. 2015)
Xyloglucan	Fast	Propionate↑ Butyrate↑	<i>Lachnospiraceae</i> ↑, <i>Bacteroides</i> ↑	(Tuncil et al. 2017)
Inulin	Fast	Acetate↑ Butyrate↑	<i>Bacteroides</i> ↓, <i>Bifidobacterium</i> ↑, <i>Catenibacterium</i> ↑, <i>Collinsella</i> ↑, <i>Dorea</i> ↓	(Yang et al. 2013)
Pectin	Fast	Acetate↑ Propionate↓ Butyrate↑	<i>Bacteroides</i> ↓, <i>Bifidobacterium</i> ↑, <i>Dorea</i> ↓, <i>Parabacteroides</i> ↓, <i>Lachnospira</i> ↑, <i>Clostridium</i> ↑, <i>Sutterella</i> ↑	(Yang et al. 2013; Bang et al. 2018; Ferreira-Lazarte et al. 2018; Jonathan et al. 2012)
Guar gum	Fast	Acetate↑ Propionate↓ Butyrate↑	<i>Roseburia</i> ↑	(Yang et al. 2013; Jonathan et al. 2012)
Glucomannan	Slow	Acetate↑ Propionate↑ Butyrate↓	N/A <sup>a</sup>	(Jonathan et al. 2012)
β-Glucan	Fast	Acetate↑ Butyrate↑	<i>Coprobacillus</i> ↑, <i>Dorea</i> ↓, <i>Lactobacillus</i> ↑, <i>Enterococcus</i> ↑	(Jonathan et al. 2012; Hughes et al. 2008)
Cellulose	Very limited	Acetate↑ Butyrate↑	<i>Bacteroides</i> sp. ↑, <i>Ruminococcus</i>	(Jonathan et al. 2012; Chassard et al. 2010)

(continued)

**Table 15.2** (continued)

Dietary fiber	Fermentation rate	SCFA molar ratio	Microbiota composition changes	References
			sp.↑, <i>Enterococcus</i> sp.↑	
Fructooligosaccharides	Fast	Acetate↑ Butyrate↑	<i>Lactobacilli</i> ↑, <i>Prevotella</i> ↑	(Jonathan et al. 2012; Chen et al. 2017; Li et al. 2015)
Galactooligosaccharides	Fast	Propionate↑ Butyrate↑	<i>Bifidobacteria</i> ↑	(Li et al. 2015)

<sup>a</sup>N/A not available

Type and structure of cereal dietary fibers can regulate the yield and molar ratio of metabolites SCFAs as well as certain bacteria promotion during the gut microbial fermentation. For instance, it was well documented that  $\beta$ -glucans and grain-derived xylans could promote the SCFAs concentration during fermentation, particularly butyric acid (Bach Knudsen 2015), whereas the fermentation of arabinose is associated with increased production of acetic acid (Hu et al. 2013). Compared with non-starch polysaccharides, in vitro and in vivo fermentation of RS (especially RS type III) usually results in a significant increase in butyrate production (Plongbunjong et al. 2017; Tan et al. 2014).

In regard to bacterial types, propionic acid was found to be positively correlated with *Ruminococcus obeum*, *Bacteroides* spp., *Megasphaera elsdenii*, *Roseburia inulinivorans*, *Phascolarctobacterium succinatutens*, *Dialister* spp., *Veillonella* spp., *Coprococcus catus*, *Salmonella* spp., etc. (Bindels et al. 2012; Louis et al. 2014). Butyrate can be produced by a series of bacteria, including *Eubacterium hallii*, *Coprococcus eutactus*, *Coprococcus catus*, *Faecalibacterium prausnitzii*, *Eubacterium rectale*, *Anaerostipes* spp., *Roseburia* spp., etc. (Duncan et al. 2002). The intake of dietary fibers could improve the metabolic interactions among various bacterial species through the cross-feeding process, which means the SCFAs produced from fermentation by one bacterial group could provide substrates for the growth of other bacteria.

The metabolic consequences of fermenting dietary substrates by gut microbiota may be influenced by single culture composition. Some bacteria may grow through cross-feeding, whereas pH value and nutrient shifts may inhibit the growth of other species in the microbial community.

The fermentation of dietary fibers results in the acidic environment in the gastrointestinal tract, which could change the microbial communities composition. For example, the acidic conditions are more preferable to the growth of butyrate-producers such as *Roseburia* spp., while inhibit the proliferation of the acid sensitive bacteria such as *Bacteroides* (Walker et al. 2005; Duncan et al. 2009). The ratio of *Firmicutes/Bacteroides* could be used as an indicator which represents health status for diabetes and obesity.

## 4 The Role of Dietary Fiber in Health and Disease

Adequate DF intake is often considered an essential component of healthy diets. The positive influence of healthy diets arises not only from the low-calorie components but also from the partially or fully fermentability of DFs and their microbiota response in the colon. Nutritional and potential health benefits can be provided by diets which contain a wide range of DFs. These include active competition against pathogenic organisms, regular bowel movement, short-chain fatty acid production which provides energy for colonocyte cells, avoidance of cancer-promoting metabolites as well as toxic from protein fermentation. Some particular DFs stimulate on specific groups of bacteria such as *Akkermansia muciniphila*, bifidobacteria, and lactobacilli with beneficial host effects such as strengthen gut barrier, anti-inflammation, and immune function (Gidley 2013). In the absence of dietary fibers or other luminal energy sources, gut microbiota will turn to large intestinal mucus as an energy source before attacking the underlying mucosa caused by gut-leak (Brownlee 2011).

The interplay between DF, microbiota, and health conditions is complex. Both genetic background and individual profiles (e.g., lifestyle, diets) affect microbial composition. Apart from this, products of microbial fermentation also play a major role in the microbiota composition shift and the immunological barrier function and final health effect of the host. The DF metabolism by microbiota is an example of the symbiotic connection between the host and the microbiota preventing dysbiosis. Microbiota rely on DFs as a carbon source for bacteria growth, and DFs involved in regulating the microbiota composition during the fermentation process. The relationship offers an option for dietary regulation of the microbiota because metabolism and microbial growth depend on substrate availability, such as the content, chemical/physical structures of dietary fibers consumed by the host.

Due to the expanded development of molecular techniques, including metagenomics and 16S rRNA sequencing, the numerous studies focus on the relationship between diets and gut microbiota. It was reported that diet patterns contribute a lot to host gut microbiota composition (almost 60%), and dietary fiber as well as animal diets make up larger proportions. Several reports suggested the bacterial diversity in our gut is decreasing due to the consumption of westernized food, which is related to the increase of metabolic diseases as well as allergic and autoimmune diseases (Bach 2002). The westernized diets are rich in animal protein compared to complex carbohydrates. Even though the trend of adding fiber to processed foods has increased, most food manufacturers prefer to add soluble fiber compared to complex insoluble fiber (Redgwell and Fischer 2005). As explained in previous sections, the soluble fibers are fermented quickly in the proximal colon. This leads to a decrease in metabolic and physiological activity in the distal colon opening the door for colon disorders (Leach 2007). In a recent report, Martínez et al. (2015) characterized the fecal microbial structure, diversity profiles, and assembly processes in United States residents and rural Papua New Guineans. The results showed that Papua New Guineans harbor communities with vastly different

abundance properties, greater bacterial diversity, lower inter-individual difference, and bacterial lineages undetectable in US residents. It is suggested that a lower intake of plant-derived carbohydrates and dietary fiber along with the unhealthy lifestyle are affecting “microbial diversity” in westernized societies. In the short term, the increase in consumption of diets rich in dietary fiber as well as whole grains substantially increases the diversity of fecal microbiota in rats (Sonnenburg et al. 2016) and humans (Tap et al. 2015). Thus, switching to a high and complex fiber diet can help to replenish the lost microbial diversity in our gut, leading to improved metabolic and immunological health. The following sub-sections describe the relationship between dietary fiber and some common chronic and metabolic diseases.

#### ***4.1 Constipation***

Constipation is the passing of hard, dry stools that may be infrequent or difficult to pass. Up to 30% of people experience constipation which can be chronic, sometimes severe, and have significant and often debilitating influences on quality of life (Tack et al. 2011). Constipation can be caused by many different factors. However, a poor diet and an unhealthy lifestyle are two risk factors for constipation. Lack of fiber in the diet makes the stool hard that is unable to pass (move) through the colon. The accumulation of hard stool may lead to more serious illness and often require immediate medical attention. However, constipation can be alleviated if the diet is rich in soluble fiber (that softens stool), and insoluble fiber (that adds stool bulk). Adequate fiber intake (at least 25 g/day) was recommended by the Academy of Nutrition and Dietetics, as fibers from a wide range of plant foods could contribute to laxation through a series of ways, such as promotion of stool frequency, increase of fecal biomass, and reduction in intestinal transit time (Dahl and Stewart 2015).

#### ***4.2 Irritable Bowel Syndrome***

A most common gastrointestinal disease, named irritable bowel syndrome (IBS), generally occurred in people no more than 45 years old. A great number of people (10–15%) are being affected by IBS, and between the ages of 20 and 30 is the age of high incidence. Also, it was well recorded that IBS is twice as common in males as it is in females (Lovell and Ford 2012). A person who has had unexplained discomfort more than 3 times during the past 3 months might be diagnosed as IBS. Four categories can be listed as follow: IBS with diarrhea, IBS with constipation, mixed IBS alternating constipation and diarrhea, and unsubtyped with a milder degree of abnormal stool consistency.

Food ingredients may cause IBS symptoms, and reasonable diet management can alleviate related symptoms. It is widely believed that increased fiber consumption may help to promote long-term alleviation of IBS symptoms because of fiber's

multiple roles in promoting digestive health. However, the report about fibers' function on IBS showed by the American College of Gastroenterology is still inconsistent and is specific for each fiber type (Ford et al. 2014). The study showed that bran (water-insoluble fiber) lowered the risk by only 10%, whereas psyllium (water-soluble fiber) resulted in a significant 17% reduction in IBS. A systematic summary and meta-analysis (1299 participants; 4.1–40 g fiber/day; 3–16 weeks) suggested that soluble fiber plays a pivotal role in alleviating the symptoms of IBS and reducing the risks of harm (Nagarajan et al. 2015). Highly fermentable and short-chain soluble dietary fiber (oligosaccharides) could result in rapid gas production that might cause abdominal bloating/distension, flatulence, and abdominal pain/discomfort in patients with IBS. Conversely, moderately fermentable dietary fiber (long-chain, intermediate viscous, and soluble) such as psyllium can lead to a low gas production and the inhibition of the associated symptoms.

### ***4.3 Colorectal Cancer***

Colorectal cancer accounts for the fourth highest number of deaths of any cancer worldwide. Except for the genetic factors, diet and lifestyle are still believed to be the significant factors that can delay or prevent the occurrence of this condition. Adequate fiber in the diet is associated with a lower risk of colorectal cancer.

A dose-response meta-analysis (16 prospective studies; 1,985,552 participants; 4.5–26 years of follow-up; 14,514 colorectal cancer cases) found a significantly lower risk of colorectal cancer (10%) for each 10 g/day intake of total fiber and cereal fiber and a 17% reduction for each three servings (90 g/day) of whole grain daily with further reductions at higher intake (Aune et al. 2011). Several plausible mechanisms have been proposed to explain the hypothesis, including the increase in stool bulk, decreasing transit time, and diluting fecal carcinogens, thus reducing the contact between carcinogens and the lining of the colorectum (Lipkin et al. 1999). Also, bacterial fermentation of fiber generates short-chain fatty acids production, which might be linked with the protective effects against colorectal cancer.

### ***4.4 Inflammatory Bowel Disease***

Inflammatory bowel disease (IBD) is an umbrella term to describe disorders that involve chronic inflammation of digestive tract, with Crohn's disease and ulcerative colitis being the most dominant prominent types. This disease is accompanied by a damaged large intestinal epithelium along with a compromised barrier function. Active inflammatory bowel disease are generally related to dysbiosis and dietary intake of indigestible fibers, whereas a reduced risk of inflammatory bowel disease is positively corrected with the high intake of plant-based dietary. However, it is still unclear whether dietary fiber intake positively or negatively impacts disease

progression and symptomology in IBD patients, and there is evidence that the active inflammation experienced in IBD is, at least in part, due to the low-fiber intake and inappropriate immune response to the luminal gut microbiota.

Crohn's disease patients always related to the high level of the phylum Proteobacteria and a decreased level of the phyla Firmicutes and Bacteroidetes. The Crohn's and Colitis Foundation of America Partners Internet cohort dietary survey (1619 participants in remission; dietary intake and disease activity index survey; 6 months) reported that a higher fiber intake during remission is linked to disease remission (Brotherton et al. 2016).

A meta-analysis of observational studies (two cohort studies, one nested case-control study and five case-control studies) indicated that higher fiber intake significantly decreased Crohn's disease risk (56%) and ulcerative colitis risk by 20% (Liu et al. 2015). Several mechanisms support increased fiber intake to reduce the risk of inflammatory bowel disease by (1) improving the health of colonic microflora, which can regulate colonic immune response and maintain immune homeostasis; (2) promoting direct anti-inflammatory effects through the production of butyrate by fermenting fibers, which is known to improve colon endothelial condition; (3) regulating the protective response of aryl hydrocarbon receptors to the pathogenesis of inflammatory bowel disease; and (4) reducing C-reactive protein levels associated with increased risk of Crohn's disease (Liu et al. 2015; Jiao et al. 2015).

#### 4.5 Obesity and Diabetes

Nowadays, both developing and industrialized countries are troubled by the epidemic of obesity. A wide range of factors may influence obesity, but epidemiological and clinical studies have proved the link of low-fiber consumption and increased risk of metabolic conditions such as obesity. It has been shown that adequate fiber in the daily diet could reduce excessive food intake and depot fat storage by increasing the effort involved in eating, interfering slightly with the efficiency of energy absorption, promoting intestinal satiety, slowing rate of food ingestion, and decreasing the caloric density of the diet (Van Itallie 1978). Further, a cycle is established; people with lower fiber intake have reduced microbial diversity, which is associated with reduced satiety and increase appetite. It is agreed that individuals with lower microbial diversity have higher body lipid content, insulin resistance, and lower-grade systemic inflammation than individuals with higher microbial diversity (Makki et al. 2018). Overweight and obese people tend to eat more low-fiber refined foods, which are more metabolic; the number of bacteria producing butyrate decreases, in particular, *F. prausnitzii*; increases inflammation-promoting effects, such as mucus degradation and endotoxin production such as lipopolysaccharides (LPS) (Brahe et al. 2016; Miquel et al. 2013). On the contrary, a high fiber-rich foods intake could lead to a more diverse microbiota bacterial genes functions, including metabolism of cofactors and vitamins, cell motility, and increased abundance of *Bifidobacterium* species and butyrate-producing bacteria such as *F. prausnitzii*, a

symbol of a healthy microbiota due to its anti-inflammatory activity (Brahe et al. 2016; Furet et al. 2010). SCFAs are the most probable fiber-related microbiota metabolites linked to leanness and obesity. High fiber content could contribute to protecting against obesity, as the SCFA's ability to act as ligands of free fatty acids receptors, which increases secretion and expression of satiety hormones glucagon-like peptide 1 or peptide YY and leptin from adipocytes (Blaut 2015; Chambers et al. 2015).

Diabetes is the result of an increased level of circulating blood glucose associated with insufficient insulin to utilize the glucose in cells. Therefore, a diet with high glycemic index (high digestible starch and low fiber) is associated with an increased risk of diabetes (Sluijs et al. 2012). Overweight and obesity are the initial risk factors for diabetes, because low-grade inflammation increases to tissues involved in metabolic regulation, such as liver, adipose tissue, and muscle, interfering with cellular insulin signaling, leading to insulin resistance. This low-grade inflammation and insulin resistance are associated with an imbalance of colonic microflora. Proteobacteria are significantly abundant in diabetic in comparison with healthy persons and positively associated with plasma glucose (Larsen et al. 2010). Two other studies also reported that diabetic subjects were characterized by a decrease of the level of Clostridiales bacteria (*Faecalibacterium prausnitzii* and *Roseburia* species), which generate butyrate (Moreno-Indias et al. 2014; Weitkunat et al. 2017). Hence, it is tempting to speculate that whereas the incidence rate of obesity is resulted by reduced fiber intake, lack of butyrate-producing and fiber-degrading bacteria may predispose to type 2 diabetes.

## 5 Conclusions and Future Direction

There is a consensus that dietary fibers have great potential to improve or maintain balanced health and wellbeing. Dietary fiber's beneficial effect on health almost uniquely depends on the modulation of digestive processes, which largely depends upon the intrinsic property of the fiber. In summary, fiber-enriched foods are less calorific and often need to more oral processing such as chewing. This slows down the food intake. On the other hand, fiber increases the bulk in the stomach and lowers the gastric emptying rate. In the small intestine, fiber interferes with the absorption of nutrients such as glucose as well as increases the peristalsis (foods moves faster). In the colon, fiber increases the fecal mass and also provides the carbon source of proliferation of bacteria. The metabolic products of bacterial fermentation of fiber are known to affect the immune system and the neuroendocrine system positively. By now, there is no question on the importance of fiber and food authorities around the globe are encouraging the public to consume at least 25 g of fiber from a variety of sources. However, there is still a lack of a universal definition of fiber. Further, the effect of processing on the nutritional functionality of fiber needs to be clearer. It is also necessary to establish proper models to speculate microbial composition and



metabolites in both health and disease people with intake of different dietary fibers, and verify the effectiveness as well as feasibility of the model through in vivo study.

**Acknowledgements** We thank the National Natural Science Foundation of China (31701546) and the 111 Project (B17018) for financial support. Bin Zhang thanks the Hong Kong Scholar Program (XJ2019049), Pearl River Talent Recruitment Program of Guangdong Province (2017GC010229), and the Pearl River Nova Program of Guangzhou (201906010079).

## References

- Alimentarius C (2010) (CODEX) guidelines on nutrition labeling CAC/GL 2–1985 as last amended 2010
- Arcila JA, Rose DJ (2015) Repeated cooking and freezing of whole wheat flour increases resistant starch with beneficial impacts on in vitro fecal fermentation properties. *J Funct Foods* 12:230–236. <https://doi.org/10.1016/j.jff.2014.11.023>
- Aune D, Chan DS, Lau R, Vieira R, Greenwood DC, Kampman E, Norat T (2011) Dietary fiber, whole grains, and risk of colorectal cancer: systematic review and dose-response meta-analysis of prospective studies. *BMJ* 343:d6617. <https://doi.org/10.1136/bmj.d6617>
- Bach J-F (2002) The effect of infections on susceptibility to autoimmune and allergic diseases. *New Engl J Med* 347:911–920. <https://doi.org/10.1056/NEJMr020100>
- Bach Knudsen KE (2001) The nutritional significance of “dietary fibre” analysis. *Anim Feed Sci Technol* 90(1):3–20. [https://doi.org/10.1016/S0377-8401\(01\)00193-6](https://doi.org/10.1016/S0377-8401(01)00193-6)
- Bach Knudsen KE (2015) Microbial degradation of whole-grain complex carbohydrates and impact on short-chain fatty acids and health. *Adv Nutr* 6(2):206–213. <https://doi.org/10.3945/an.114.007450>
- Bae C-H, Park M-S, Ji G-E, Park H-D (2013) Effects of phosphorylated cross-linked resistant corn starch on the intestinal microflora and short chain fatty acid formation during in vitro human fecal batch culture. *Food Sci Biotechnol* 22(6):1649–1654. <https://doi.org/10.1007/s10068-013-0262-y>
- Bang SJ, Kim G, Lim MY, Song EJ, Jung DH, Kum JS, Nam YD, Park CS, Seo DH (2018) The influence of in vitro pectin fermentation on the human fecal microbiome. *AMB Express* 8(1):98. <https://doi.org/10.1186/s13568-018-0629-9>
- Bindels LB, Porporato P, Dewulf EM, Verrax J, Neyrinck AM, Martin JC, Scott KP, Buc Calderon P, Feron O, Muccioli GG, Sonveaux P, Cani PD, Delzenne NM (2012) Gut microbiota-derived propionate reduces cancer cell proliferation in the liver. *Br J Cancer* 107(8):1337–1344. <https://doi.org/10.1038/bjc.2012.409>
- Blaut M (2015) Gut microbiota and energy balance: role in obesity. *Proc Nutr Soc* 74(3):227–234. <https://doi.org/10.1017/S0029665114001700>
- Brahe LK, Astrup A, Larsen LH (2016) Can we prevent obesity-related metabolic diseases by dietary modulation of the gut microbiota? *Adv Nutr* 7(1):90–101. <https://doi.org/10.3945/an.115.010587>
- Brotherton CS, Martin CA, Long MD, Kappelman MD, Sandler RS (2016) Avoidance of fiber is associated with greater risk of Crohn’s disease flare in a 6-month period. *Clin Gastroenterol Hepatol* 14(8):1130–1136. <https://doi.org/10.1016/j.cgh.2015.12.029>
- Brownlee IA (2011) The physiological roles of dietary fiber. *Food Hydrocoll* 25(2):238–250. <https://doi.org/10.1016/j.foodhyd.2009.11.013>
- Brownlee I (2014) The impact of dietary fiber intake on the physiology and health of the stomach and upper gastrointestinal tract. *Bioact Carbohydr Diet Fibre* 4(2):155–169. <https://doi.org/10.1016/j.bcdf.2014.09.005>

- Chambers ES, Morrison DJ, Frost G (2015) Control of appetite and energy intake by SCFA: what are the potential underlying mechanisms? *Proc Nutr Soc* 74(3):328–336. <https://doi.org/10.1017/S0029665114001657>
- Chassard C, Delmas E, Robert C, Bernalier-Donadille A (2010) The cellulose-degrading microbial community of the human gut varies according to the presence or absence of methanogens. *FEMS Microbiol Ecol* 74(1):205–213. <https://doi.org/10.1111/j.1574-6941.2010.00941.x>
- Chawla R, Patil GR (2010) Soluble dietary fiber. *Compr Rev Food Sci Food Saf* 9(2):178–196. <https://doi.org/10.1111/j.1541-4337.2009.00099.x>
- Chen T, Long W, Zhang C, Liu S, Zhao L, Hamaker BR (2017) Fiber-utilizing capacity varies in *Prevotella*- versus *Bacteroides*-dominated gut microbiota. *Sci Rep* 7(1):2594. <https://doi.org/10.1038/s41598-017-02995-4>
- Choct M, Bedford MR, Partridge GG (2000) Enzymes in farm animal nutrition. In: *Enzyme supplementation of poultry diets based on viscous cereals*. CABI, Wallingford, pp 145–160. <https://doi.org/10.1079/9780851993935.0145>
- Comalada M, Bailon E, de Haro O, Lara-Villoslada F, Xaus J, Zarzuelo A, Galvez J (2006) The effects of short-chain fatty acids on colon epithelial proliferation and survival depend on the cellular phenotype. *J Cancer Res Clin Oncol* 132(8):487–497. <https://doi.org/10.1007/s00432-006-0092-x>
- Dahl WJ, Stewart ML (2015) Position of the academy of nutrition and dietetics: health implications of dietary fiber. *J Acad Nutr Diet* 115(11):1861–1870. <https://doi.org/10.1016/j.jand.2015.09.003>
- Day L, Gomez J, Oiseth SK, Gidley MJ, Williams BA (2012) Faster fermentation of cooked carrot cell clusters compared to cell wall fragments in vitro by porcine feces. *J Agric Food Chem* 60(12):3282–3290. <https://doi.org/10.1021/Jf204974s>
- Dhital S, Ghanendra G, Free W (2018) Dietary fibre regulations: is it time for (A)us to innovate? *Food Aust* 70(3):26–28
- Duncan SH, Barcenilla A, Stewart CS, Pryde SE, Flint HJ (2002) Acetate utilization and butyryl coenzyme A (CoA): acetate-CoA transferase in butyrate-producing bacteria from the human large intestine. *Appl Environ Microbiol* 68(10):5186–5190. <https://doi.org/10.1128/aem.68.10.5186-5190.2002>
- Duncan SH, Louis P, Thomson JM, Flint HJ (2009) The role of pH in determining the species composition of the human colonic microbiota. *Environ Microbiol* 11(8):2112–2122. <https://doi.org/10.1111/j.1462-2920.2009.01931.x>
- Ellis PR, Ren YJ, Jenkins DJ (2004) Role of cell walls in the bioaccessibility of lipids in almond seeds. *Am J Clin Nutr* 80(3):604–613. <https://doi.org/10.1093/ajcn/80.3.604>
- Ferreira-Lazarte A, Kachrimanidou V, Villamiel M, Rastall RA, Moreno FJ (2018) In vitro fermentation properties of pectins and enzymatic-modified pectins obtained from different renewable bioresources. *Carbohydr Polym* 199:482–491. <https://doi.org/10.1016/j.carbpol.2018.07.041>
- Ford AC, Moayyedi P, Lacy BE, Lembo AJ, Saito YA, Schiller LR, Soffer EE, Spiegel BMR, Quigley EMM (2014) American College of Gastroenterology monograph on the management of irritable bowel syndrome and chronic idiopathic constipation. *Am J Gastroenterol* 109(S1):S2–S26. <https://doi.org/10.1038/ajg.2014.187>
- Furet JPKLC, Tap J et al (2010) Differential adaptation of human gut microbiota to bariatric surgery-induced weight loss: links with metabolic and low-grade inflammation markers. *Diabetes Metab* 59(12):3049–3057
- Gartaula G, Dhital S, Netzel G, Flanagan BM, Yakubov GE, Beahan CT, Collins HM, Burton RA, Bacic A, Gidley MJ (2018) Quantitative structural organisation model for wheat endosperm cell walls: cellulose as an important constituent. *Carbohydr Polym* 196:199–208. <https://doi.org/10.1016/j.carbpol.2018.05.041>
- Gidley MJ (2013) Hydrocolloids in the digestive tract and related health implications. *Curr Opin Colloid Interface Sci* 18(4):371–378. <https://doi.org/10.1016/j.cocis.2013.04.003>

- Gidley MJ, Yakubov GE (2019) Functional categorisation of dietary fibre in foods: beyond 'soluble' vs 'insoluble'. *Trends Food Sci Technol* 86:563–568. <https://doi.org/10.1016/j.tifs.2018.12.006>
- Hamaker BR, Tuncil YE (2014) A perspective on the complexity of dietary fiber structures and their potential effect on the gut microbiota. *J Mol Biol* 426(23):3838–3850. <https://doi.org/10.1016/j.jmb.2014.07.028>
- Hipsley (1953) Dietary "fibre" and pregnancy toxæmia. *Br Med J* 2:420–422. <https://doi.org/10.1136/bmj.2.4833.420>
- Hu J-L, Nie S-P, Li C, Xie M-Y (2013) In vitro fermentation of polysaccharide from the seeds of *Plantago asiatica* L. by human fecal microbiota. *Food Hydrocoll* 33(2):384–392. <https://doi.org/10.1016/j.foodhyd.2013.04.006>
- Hughes SA, Shewry PR, Gibson GR, McCleary BV, Rastall RA (2008) In vitro fermentation of oat and barley derived beta-glucans by human fecal microbiota. *FEMS Microbiol Ecol* 64(3):482–493. <https://doi.org/10.1111/j.1574-6941.2008.00478.x>
- Innami S, Shimizu J, Kudoh K (2000) Dietary fiber and gastrointestinal functions. In: Nishinari K (ed) *Hydrocolloids*. Elsevier Science, Amsterdam, pp 383–392. <https://doi.org/10.1016/B978-044450178-3/50109-8>
- Jiao J, Xu JY, Zhang W, Han S, Qin LQ (2015) Effect of dietary fiber on circulating C-reactive protein in overweight and obese adults: a meta-analysis of randomized controlled trials. *Int J Food Sci Nutr* 66(1):114–119. <https://doi.org/10.3109/09637486.2014.959898>
- Jonathan MC, van den Borne JJGC, van Wiechen P, Souza da Silva C, Schols HA, Gruppen H (2012) In vitro fermentation of 12 dietary fibres by faecal inoculum from pigs and humans. *Food Chem* 133(3):889–897. <https://doi.org/10.1016/j.foodchem.2012.01.110>
- Kiriya S, Ebihara K, Ikegami S (2006) Searching for the definition, terminology and classification of dietary fiber and the new proposal from Japan. *J Jpn Assoc Diet Fiber Res* 10(1):11–24
- Larsen N, Vogensen FK, van den Berg FW, Nielsen DS, Andreasen AS, Pedersen BK, Al-Soud WA, Sorensen SJ, Hansen LH, Jakobsen M (2010) Gut microbiota in human adults with type 2 diabetes differs from non-diabetic adults. *PLoS One* 5(2):e9085. <https://doi.org/10.1371/journal.pone.0009085>
- Leach JD (2007) Evolutionary perspective on dietary intake of fibre and colorectal cancer. *Eur J Clin Nutr* 61:140–142. <https://doi.org/10.1038/sj.ejcn.1602486>
- Li W, Wang K, Sun Y, Ye H, Hu B, Zeng X (2015) Influences of structures of galactooligosaccharides and fructooligosaccharides on the fermentation in vitro by human intestinal microbiota. *J Funct Foods* 13:158–168. <https://doi.org/10.1016/j.jff.2014.12.044>
- Lipkin M, Reddy B, Newmark H, Lamprecht SA (1999) Dietary factors in human colorectal cancer. *Annu Rev Nutr* 19:545–586. <https://doi.org/10.1146/annurev.nutr.19.1.545>
- Liu X, Wu Y, Li F, Zhang D (2015) Dietary fiber intake reduces risk of inflammatory bowel disease: result from a meta-analysis. *Nutr Res* 35(9):753–758. <https://doi.org/10.1016/j.nutres.2015.05.021>
- Louis P, Hold GL, Flint HJ (2014) The gut microbiota, bacterial metabolites and colorectal cancer. *Nat Rev Microbiol* 12(10):661–672. <https://doi.org/10.1038/nrmicro3344>
- Lovell RM, Ford AC (2012) Effect of gender on prevalence of irritable bowel syndrome in the community: systematic review and meta-analysis. *Am J Gastroenterol* 107(7):991–1000. <https://doi.org/10.1038/ajg.2012.131>
- Mackie A, Rigby N, Harvey P, Bajka B (2016) Increasing dietary oat fibre decreases the permeability of intestinal mucus. *J Funct Foods* 26:418–427. <https://doi.org/10.1016/j.jff.2016.08.018>
- Makki K, Deehan EC, Walter J, Backhed F (2018) The impact of dietary fiber on gut microbiota in host health and disease. *Cell Host Microbe* 23(6):705–715. <https://doi.org/10.1016/j.chom.2018.05.012>
- Martínez I, Stegen JC, Maldonado-Gómez MX, Eren AM, Siba PM, Greenhill AR, Walter J (2015) The gut microbiota of rural Papua New Guineans: composition, diversity patterns, and ecological processes. *Cell Rep* 11:527–538. <https://doi.org/10.1016/j.celrep.2015.03.049>

- Miquel S, Martin R, Rossi O, Bermudez-Humaran LG, Chatel JM, Sokol H, Thomas M, Wells JM, Langella P (2013) Faecalibacterium prausnitzii and human intestinal health. *Curr Opin Microbiol* 16(3):255–261. <https://doi.org/10.1016/j.mib.2013.06.003>
- Moreno-Indias I, Cardona F, Tinahones FJ, Queipo-Ortuno MI (2014) Impact of the gut microbiota on the development of obesity and type 2 diabetes mellitus. *Front Microbiol* 5:190. <https://doi.org/10.3389/fmicb.2014.00190>
- Mudgil D, Barak S (2013) Composition, properties and health benefits of indigestible carbohydrate polymers as dietary fiber: a review. *Int J Biol Macromol* 61:1–6. <https://doi.org/10.1016/j.ijbiomac.2013.06.044>
- Nagarajan N, Morden A, Bischof D, King EA, Kosztowski M, Wick EC, Stein EM (2015) The role of fiber supplementation in the treatment of irritable bowel syndrome: a systematic review and meta-analysis. *Eur J Gastroenterol Hepatol* 27(9):1002–1010. <https://doi.org/10.1097/MEG.0000000000000425>
- Oakenfull D, Cho SS, Dreher ML (2001) Physicochemical properties of dietary fiber: overview. *Handb Diet Fiber* 199:195–206
- Plongbunjong V, Graudist P, Knudsen KEB, Wichienchot S (2017) Starch-based carbohydrates display the bifidogenic and butyrogenic properties in pH-controlled fecal fermentation. *Int J Food Sci Technol* 52(12):2647–2653. <https://doi.org/10.1111/ijfs.13553>
- Redgwell RJ, Fischer M (2005) Dietary fiber as a versatile food component: an industrial perspective. *Mol Nutr Food Res* 49:521–535. <https://doi.org/10.1002/mnfr.200500028>
- Rose DJ, Venema K, Keshavarzian A, Hamaker BR (2010) Starch-entrapped microspheres show a beneficial fermentation profile and decrease in potentially harmful bacteria during in vitro fermentation in faecal microbiota obtained from patients with inflammatory bowel disease. *Br J Nutr* 103(10):1514–1524. <https://doi.org/10.1017/s0007114509993515>
- Rumpagaporn P, Reuhs BL, Kaur A, Patterson JA, Keshavarzian A, Hamaker BR (2015) Structural features of soluble cereal arabinoxylan fibers associated with a slow rate of in vitro fermentation by human fecal microbiota. *Carbohydr Polym* 130:191–197. <https://doi.org/10.1016/j.carbpol.2015.04.041>
- Sluijs I, Forouhi NG, Beulens JW, van der Schouw YT, Agnoli C, Arriola L, Balkau B, Barricarte A, Boeing H, Bueno-de-Mesquita HB, Clavel-Chapelon F, Crowe FL, de Lauzon-Guillain B, Drogan D, Franks PW, Gavrila D, Gonzalez C, Halkjaer J, Kaaks R, Moskal A, Nilsson P, Overvad K, Palli D, Panico S, Quiros JR, Ricceri F, Rinaldi S, Rolandsson O, Sacerdote C, Sanchez MJ, Slimani N, Spijkerman AM, Teucher B, Tjonneland A, Tormo MJ, Tumino R, van der AD, Sharp SJ, Langenberg C, Feskens EJ, Riboli E, Wareham NJ, InterAct C (2012) The amount and type of dairy product intake and incident type 2 diabetes: results from the EPIC-InterAct study. *Am J Clin Nutr* 96(2):382–390. <https://doi.org/10.3945/ajcn.111.021907>
- Sonnenburg ED, Smits SA, Tikhonov M, Higginbottom SK, Wingreen NS, Sonnenburg JL (2016) Diet-induced extinctions in the gut microbiota compound over generations. *Nature* 529:212–215. <https://doi.org/10.1038/nature16504>
- Tack J, Muller-Lissner S, Stanghellini V, Boeckxstaens G, Kamm MA, Simren M, Galmiche JP, Fried M (2011) Diagnosis and treatment of chronic constipation—a European perspective. *Neurogastroenterol Motil* 23(8):697–710. <https://doi.org/10.1111/j.1365-2982.2011.01709.x>
- Taghipoor M, Barles G, Georgelin C, Licois JR, Lescoat P (2014) Digestion modeling in the small intestine: impact of dietary fiber. *Math Biosci* 258:101–112. <https://doi.org/10.1016/j.mbs.2014.09.011>
- Tan J, McKenzie C, Potamitis M, Thorburn AN, Mackay CR, Macia L (2014) The role of short-chain fatty acids in health and disease. *Adv Immunol* 121:91–119. <https://doi.org/10.1016/B978-0-12-800100-4.00003-9>
- Tap J, Furet JP, Bensaada M, Philippe C, Roth H, Rabot S, Lakhdari O, Lombard V, Henrissat B, Corthier G, Fontaine E, Doré J, Leclerc M (2015) Gut microbiota richness promotes its stability upon increased dietary fiber intake in healthy adults. *Environ Microbiol* 17:4954–4964. <https://doi.org/10.1111/1462-2920.13006>

- Thompson LU, Maningat CC, Woo K, Seib PA (2011) In vitro digestion of RS4-type resistant wheat and potato starches, and fermentation of indigestible fractions. *Cereal Chem* 88(1):72–79. <https://doi.org/10.1094/cchem-07-10-0098>
- Topping DL, Lockett TJ (2016) Human physiology and health: dietary fiber, short-chain fatty acids, and their impact on gut physiology. Reference module in food sciences. <https://doi.org/10.1016/b978-0-08-100596-5.21016-0>
- Tuncil YE, Nakatsu CH, Kazem AE, Arioglu-Tuncil S, Reuhs B, Martens EC, Hamaker BR (2017) Delayed utilization of some fast-fermenting soluble dietary fibers by human gut microbiota when presented in a mixture. *J Funct Foods* 32:347–357. <https://doi.org/10.1016/j.jff.2017.03.001>
- U.S. Food and Drug Administration (2016) Changes to the nutrition facts label. FDA, Silver Spring, MD. <https://www.fda.gov/Food/GuidanceRegulation/GuidanceDocumentsRegulatoryInformation/LabelingNutrition/ucm385663.htm>
- Van Itallie TB (1978) Dietary fiber and obesity. *Am J Clin Nutr* 31:S43–S52. <https://doi.org/10.1093/ajcn/31.10.S43>
- Walker AW, Duncan SH, McWilliam Leitch EC, Child MW, Flint HJ (2005) pH and peptide supply can radically alter bacterial populations and short-chain fatty acid ratios within microbial communities from the human colon. *Appl Environ Microbiol* 71(7):3692–3700. <https://doi.org/10.1128/AEM.71.7.3692-3700.2005>
- Weitkunat K, Schumann S, Nickel D, Hornemann S, Petzke KJ, Schulze MB, Pfeiffer AF, Klaus S (2017) Odd-chain fatty acids as a biomarker for dietary fiber intake: a novel pathway for endogenous production from propionate. *Am J Clin Nutr* 105(6):1544–1551. <https://doi.org/10.3945/ajcn.117.152702>
- Wilfart A, Montagne L, Simmins H, Noblet J, Milgen J (2007) Digesta transit in different segments of the gastrointestinal tract of pigs as affected by insoluble fibre supplied by wheat bran. *Br J Nutr* 98(1):54–62. <https://doi.org/10.1017/S0007114507682981>
- Williams BA, Mikkelsen D, le Paih L, Gidley MJ (2011a) In vitro fermentation kinetics and end-products of cereal arabinoxylans and (1,3;1,4)-beta-glucans by porcine faces. *J Cereal Sci* 53(1):53–58. <https://doi.org/10.1016/j.jcs.2010.09.003>
- Williams BA, Mikkelsen D, le Paih L, Gidley MJ (2011b) In vitro fermentation kinetics and end-products of cereal arabinoxylans and (1,3;1,4)-beta-glucans by porcine faces. *J Cereal Sci* 53(1):53–58. <https://doi.org/10.1016/j.jcs.2010.09.003>
- Wong JMW, de Souza R, Kendall CWC et al (2006) Colonic health: fermentation and short chain fatty acids. *J Clin Gastroenterol* 40(3):235–243. <https://doi.org/10.1097/00004836-200603000-00015>
- Yang J, Martinez I, Walter J, Keshavarzian A, Rose DJ (2013) In vitro characterization of the impact of selected dietary fibers on fecal microbiota composition and short chain fatty acid production. *Anaerobe* 23:74–81. <https://doi.org/10.1016/j.anaerobe.2013.06.012>
- Younes H, Levrat M-A, Demign C, Rmsy C (1995) Resistant starch is more effective than cholestyramine as a lipid-lowering agent in the rat. *Lipids* 30:847–853. <https://doi.org/10.1007/BF02533961>